Design, Synthesis, and Biological Evaluation of Selective Sphingosine Kinase Inhibitors

Mithun Rajendra Raje

Dissertation submitted to the faculty of the Virginia Polytechnic Institute and State University in partial fulfillment of the requirements for the degree of

Doctor of Philosophy

In

Chemistry

Webster L. Santos, Committee Chair

Paul R. Carlier

Felicia A. Etzkorn

James M. Tanko

(April 13, 2012)

(Blacksburg, VA)

Keywords: Sphingosine-1-phosphate, sphingosine kinase inhibitors, reductive amination, structure-activity relationships, guanidine inhibitors

Design, Synthesis, and Biological Evaluation of Selective Sphingosine Kinase Inhibitors

Mithun Rajendra Raje

ABSTRACT

Sphingosine kinase (SphK) has emerged as an attractive target for cancer therapeutics due to its role in cell proliferation. SphK phosphorylates sphingosine to form sphingosine-1-phosphate (S1P) which has been implicated as a major player in cancer growth and survival. SphK exists as two different isoforms, namely SphK1 and SphK2, which play different roles inside the cell. The dearth of isoenzyme-selective inhibitors has been a stumbling block for probing the exact roles of these two isoforms in disease progression.

This report documents our efforts in developing SphK2-selective inhibitors. We provide the first demonstration of a SphK inhibitor containing a quaternary ammonium salt. We developed highly potent and moderately selective inhibitors that were cell permeable and interfered with S1P signaling inside the cell.

In an effort to improve the selectivity of our inhibitors and enhance their *in vivo* stability, we designed and synthesized second generation inhibitors containing a heteroaromatic linker and a guanidine headgroup. These inhibitors were more potent and selective towards SphK2 and affected S1P signaling in cell cultures and various animal models.

Acknowledgements

I would like to sincerely thank my research advisor Dr. Webster L. Santos for his guidance, support, patience, and inspiration throughout my graduate career. His passion for science and dedication to his work is truly unmatched. His motivational mentorship has helped me become a more proficient chemist. I would also like to gratefully acknowledge the support of my committee members, Dr. Paul Carlier, Dr. Felicia Etzkorn, and Dr. James Tanko. Your suggestions and useful insights over all these years gave me a better understanding of my project.

I would like to express gratitude to the members of my research group during my tenure – Dr. Philippe Bissel, Michael Perfetti, Ken Knott, Jing Sun, David Bryson, Jason Crumpton, Brandon Thorpe, Wes Morris, Dr. Ming Gao, Wenyu Zhang, Xi Guo, Joe Calderone, Leah Heist, Molly Congdon, Jessica Wynn, Amanda Nelson, Julie Ta, and Emily Morris. Your friendship and co-operation made working in the Santos lab fun and enjoyable. I would also like to thank our collaborators at the University of Virginia, Dr. Kevin Lynch and his postdoctoral assistant Dr. Yugesh Kharel, for all the biological work presented in this document.

I thank my friends in Blacksburg and elsewhere for their continued love and support. I would like to single out Kshitish Patankar and Siddhesh Pawar for being great roommates and caring friends over all these years. I would also like to thank John and Ann Hess from the International Friendship Program for their hospitality.

The love and affection of my family has always been a source of inspiration for me. I thank my parents, Mr. Rajendra Raje and Mrs. Shubhada Raje, for always believing in me, encouraging me, and supporting me through all the ups and downs in

life. None of this would have been possible without you. I would also like to thank my brother, Kapil Raje, and his wife, Tejal Raje, for their constant support and love. I also thank my grand-parents for everything they have done for me; even though they are not amongst us today, I am sure they are very proud of my achievements.

Table of Contents

List of figures

List of schemes

List of charts

List of tables

List of Abbreviations

9-BBN = 9-Borabicyclo[3.3.1]nonane

ABC = ATP-binding cassette

Akt = Protein kinase B

ASMase = Acidic sphingomyelinase

BACE = β-site amyloid precursor protein cleaving enzyme

Bcl = B-cell lymphoma

BH3 = Bcl-2 homology 3

cDNA = Complementary DNA

Cer = Ceramide

CerS = Dihydroceramide synthase

CGT = Ceramide galactosyl transferase

CoA = Coenzyme A

DAG = Diacylglycerol

DES = Desaturase

DHCer = Dihydroceramide

DHS = L-*threo*-Dihydrosphingosine

DHS = Dihydrosphingosine

DIBAL-H = Diisobutyl aluminum hydride

DMS = *N*,*N*-Dimethylsphingosine

EGF = Epidermal growth factor

ER = Endoplasmic Reticulum

ERK = Extracellular signal-regulated kinase

ESI = Electrospray ionization

FAB = Fast atom bombardment

FBS = Fetal bovine serum

GalCer = Galactosylceramide

GCS = Glucosyl ceramide synthase

GlcCer = Glucosylceramide

GPCR = G-protein coupled receptor

HDAC = Histone deacetylase

HRP = Horse radish peroxidase

K_i = Inhibition constant

K_m = Michaelis constant

MRM = Multiple reaction monitoring

NF-κB = Nuclear factor kappa-light-chain-enhancer of activated B cells

NSMase = Neutral sphingomyelinase

PAK1 = P21 activated protein kinase 1

PCC = Pyridinium chlorochromate

PDGF = Platelet-derived growth factor

PHB2 = Prohibitin 2

S1P = Sphingosine-1-phosphate

SDS-PAGE = Sodium dodecyl sulfate polyacrylamide gel electrophoresis

siRNA = Small interfering RNA

SM = Sphingomyelin

SMase = Sphingomyelinase

SMS = Sphingomyelin synthase

Sph = Sphingosine

SphK = Sphingosine kinase

SPP = Sphingosine-1-phosphate phosphatase

TBS = Tris-buffered saline

TNF = Tumor necrosis factor

TRAF = Tumor-necrosis factor receptor-associated factor

VEGF = Vascular endothelial growth factor

Chapter 1 Introduction

1.1. Sphingolipids

Sphingolipids constitute a considerable fraction of membrane lipids in all eukaryotes and are vital for eukaryotic life. They are primarily found in the outer leaflet of the plasma membrane. Sphingolipids differ from phospholipids in that they are based on a lipophilic amino alcohol (sphingosine, Figure 1.1) rather than glycerol. A fatty acid chain linked to sphingosine via an amide bond results in the formation of ceramide. Complex sphingolipids can be formed by functionalizing the primary alcohol moiety of ceramide. Recent studies have suggested that sphingolipids are involved in the patho-physiology of several diseases like cancer,[1,2] diabetes,[3] Alzheimer's disease,[4] and autoimmune disorders.[5] Thus, scientific interest in sphingolipids, their metabolism, and their function has grown exponentially in recent years.

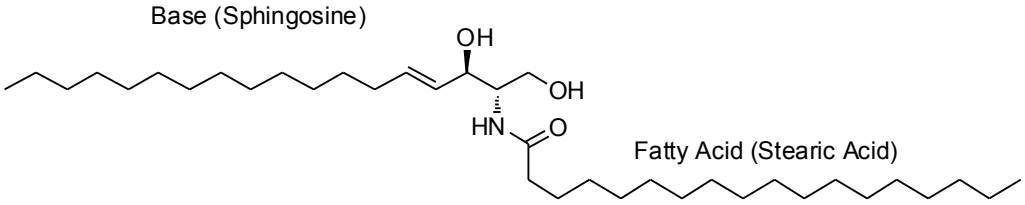

Figure 1.1. Structure of ceramide (Cer)

1.2. Metabolism of sphingolipids

Ceramide (Cer) is the biological building block of sphingolipids and the focal point in several metabolic sphingolipid pathways; among these are the *de novo*, sphingomyelinase, and the endocytic recycling pathways. Cer has been implicated in mediating various cellular processes such as cell cycle arrest and apoptosis. Several factors stimulate the formation of ceramide including tumor necrosis factor-α (TNF- α),[6] phorbol ester,[7] and oxidative stress.[8]

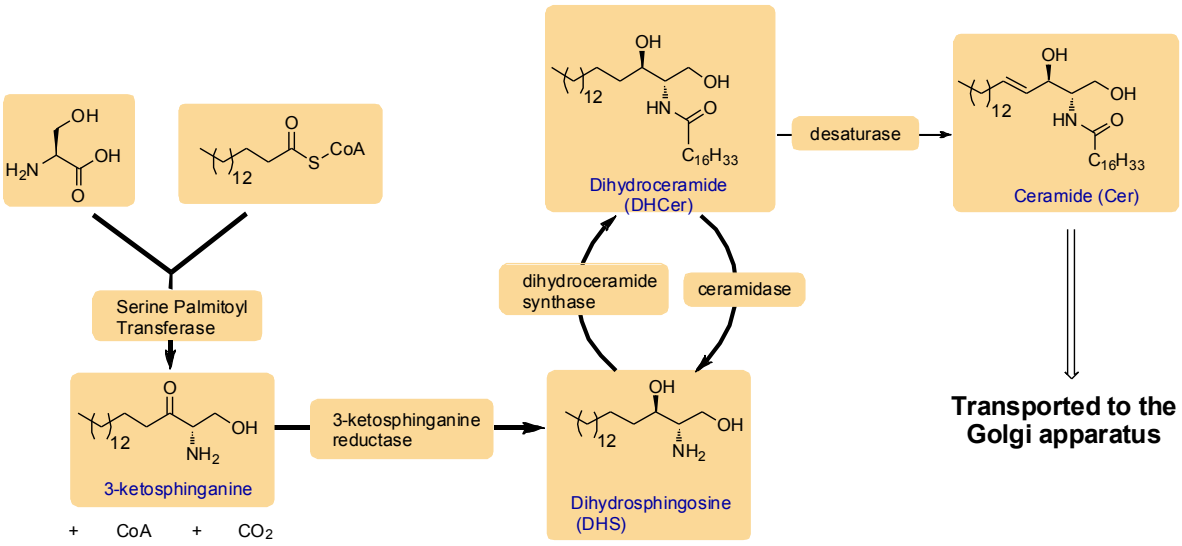

Figure 1.2. *De novo* synthesis of ceramide in the endoplasmic reticulum (ER)

The *de novo* biosynthesis pathway of sphingolipids begins with the condensation of L-serine and palmitoyl-CoA at the cytosolic side of the endoplasmic reticulum (ER) (Figure 1.2). This reaction, catalyzed by the enzyme serine palmitoyl transferase,[9] results in the formation of 3-ketosphinganine. 3-ketosphinganine is then stereoselectively reduced to the D-isomer of dihydrosphingosine (DHS) by the action of 3-keto-sphinganine reductase, which utilizes NADH as a reducing agent. DHS is then *N*-acylated by the action of six different dihydroceramide synthases (CerS1-6)[10,11] to produce dihydroceramide (DHCer). Each CerS utilizes a different acyl CoA and produces various ceramide species; *e.g.*, CerS1 prefers stearoyl CoA and produces C18-ceramide species,[12] CerS2 prefers C20-C26 CoA species,[13] while CerS5 and CerS6 prefer palmitoyl CoA to produce the C16-ceramide species.[14] All CerS are localized to the ER with their catalytic sites facing the cytosol which facilitates the *N*-acylation of newly generated DHS molecules with various fatty acyl CoAs. The key molecule Cer is synthesized by the oxidation of DHCer in the presence of the enzyme desaturase (DES).[15]

DES utilizes molecular oxygen to introduce a hydroxyl group at the C4 position followed by a NADPH-catalyzed dehydration to establish the *trans* 4,5-double bond.[16] This is an important step because Cer, not DHCer, causes apoptosis.[17] Cer, a membrane-bound lipid, has very low solubility in an aqueous environment, and therefore its transport from one membrane to another requires facilitated mechanisms. Cer transport is achieved either by the ceramide transport protein CERT,[18] a cytoplasmic protein with a phosphatidylinositol-4-phosphate-binding domain or by coatomer protein dependent vesicular transport.[19] Both these actions translocate Cer from the ER to the Golgi apparatus, where further metabolism into complex sphingolipids takes place.

Complex sphingolipids are divided into three major groups based on the primary residue attached to their C1-hydroxy. This primary alcoholic moiety in Cer serves as an attachment site for glucose, galactose and phosphocholine to form glucosylceramide (GlcCer), galactosylceramide (GalCer), and sphingomyelin (SM), respectively (Figure 1.3). Ceramide galactosyl transferase (CGT), an ER transmembrane protein,[20] utilizes UDP-galactose and ceramide to form GalCer. Cer gets converted to GlcCer on the cytosolic surface of the cis-Golgi by the enzyme glucosyl ceramide synthase (GCS).[21] GCS, a cis-Golgi transmembrane protein, has its catalytic site facing the cytosol[22] where newly synthesized GlcCer is recognized by the lipid transfer protein four-phosphate-adaptor protein 2 (FAPP2).[23] The most abundant complex sphingolipid in mammalian cells are the sphingomyelin species. SM is essential for the viability of eukaryotic cells in culture. SM is produced from Cer by the action of two different sphingomyelin synthases (SMS). Both SMSs are present in the trans-Golgi with their catalytic sites facing the Golgi lumen.

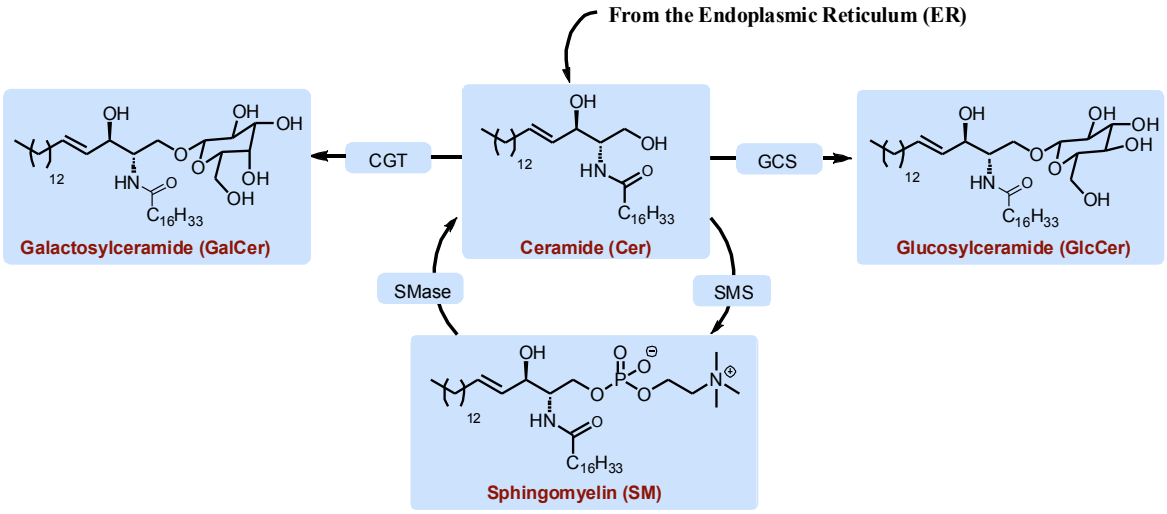

Figure 1.3. Complex sphingolipid synthesis in the Golgi apparatus

The breakdown of SM by hydrolysis of the phosphocholine in the presence of sphingomyelinase (SMase) results in the formation of Cer. There are three major types of SMases characterized by their pH optima as acidic, neutral and alkaline forms. Acidic sphingomyelinase (ASMase) is predominantly a lysosomal protein[24] which metabolizes SM present on endosomal membranes, but can also be secreted in the extracellular space. Neutral sphingomyelinases (NSMase) have diverse subcellular locations including the plasma membrane, ER, Golgi, and the nucleus.[25] Alkaline sphingomyelinase is mainly expressed in the intestinal tract and the bile where it participates in sphingomyelin digestion.[26]

Cer can also be produced by the endocytic recycling pathway, which involves the turnover of membrane sphingolipids in acidic cellular compartments, the late endosomes and the lysosomes, by various enzymes. Sphingosine (Sph) is formed by ceramidase-catalyzed hydrolysis of Cer. Sph undergoes ATP-dependent phosphorylation by sphingosine kinases (SphKs) to form sphingosine-1-phosphate (S1P). S1P can be dephosphorylated back to Sph by two specific S1P phosphatases (SPP1 and SPP2).[27,28]

These are magnesium-dependent, *N*-ethylmaleimide-insensitive type 2 lipid phosphate phosphohydrolases that reside in the ER. S1P can also be degraded irreversibly by a pyridoxal phosphate-dependent S1P lyase to hexadecenal and phosphoethanolamine. S1P levels in the cell are tightly regulated by the balance between its synthesis and degradation.

S1P, Sph, and Cer are vital regulators of cell survival and apoptosis. S1P and Cer exert opposing effects on cell survival; S1P is anti-apoptotic, but Cer is pro-apoptotic and anti-proliferative. Further, since these metabolites are interconvertible by the action of various enzymes, it has been postulated that the relative ratio of S1P and Cer represents a "sphingolipid rheostat", the position of which determines cell fate.[29]

1.3. Sphingosine kinases (SphKs)

SphKs are a distinct, evolutionarily conserved class of lipid kinase. Two isoforms of SphK, named Lcb4 and Lcb5, were first cloned from the yeast species *Saccharomyces cerevisiae*.[30] The two mammalian isoforms of sphingosine kinase, SphK1 and SphK2, have five conserved domains (C1-C5), a unique catalytic domain contained within C1 to C3 and a conserved ATP binding motif ($SGDGX_{(17-21)}K(R)$) present within C2 (Figure 1.4). SphK2 has four transmembrane domains; whereas SphK1 does not have any. Northern-blot analysis has shown that SphKs have different tissue distributions:[31] SphK1 expression is highest in lung and spleen, whereas SphK2 is most abundant in liver and heart.

SphK1 is primarily a cytosolic enzyme, but its substrate, Sph, is mainly present in plasma membranes. Thus, the translocation of SphK1 to the plasma membrane is an important feature of its activation, which is achieved by post-translational modifications such as phosphorylation, ubiquitination, and palmitoylation.[32] The phorbol ester, phorbol

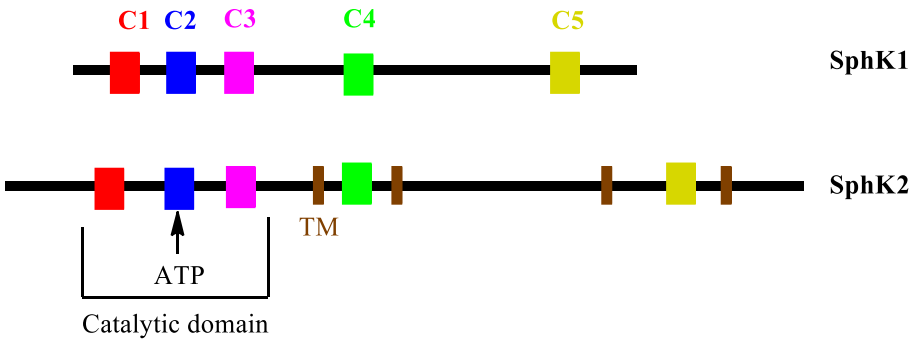

Figure 1.4. Sphingosine kinases

12-myristate 13-acetate (PMA) was shown to induce protein kinase C-mediated phosphorylation of SphK1.[33] Another study showed the phosphorylation of SphK1 at Ser225 catalyzed by ERK2[34] results in its translocation to the plasma membrane. It is worth noting that SphK1 is stimulated by various growth factors; among these are the platelet-derived growth factor (PDGF),[35] vascular endothelial growth factor (VEGF),[36] epidermal growth factor (EGF),[37] and tumor necrosis factor-α (TNF-α).[38,39] There is increasing evidence supporting the role of SphK1 in cancer. For example, increased levels of the SphK1 mRNA transcript and protein have been reported in cancers of the stomach,[40] lung,[41] colon,[42] and non-Hodgkins lymphoma.[43] Recent studies provide clinical evidence for the role of SphK1 in disease progression and reduced survival in patients with gastric cancer,[44] astrocytoma,[45] breast cancer,[46] and glioma.[47]

The role and regulation of SphK2 is much less clearly defined. SphK2 is predominantly localized in the nucleus and at the endoplasmic reticulum.[48,49] However, phosphorylation of SphK2 by protein kinase D results in translocation from the nucleus to the cytoplasm.[50] SphK2 is expected to be pro-apoptotic because of its BH3 domain that interacts with $BclX_L$.[51] However, a recent study suggests an important role for SphK2 in the tumor progression in MCF-7 breast cancer xenografts.[52] Moreover, knockdown of SphK2 in glioblastoma cells inhibits proliferation.[47] These contrasting

results demonstrate the need for a deeper understanding of the role of SphK2 in tumor cell models. The lack of SphK2-selective inhibitors retards detailed scientific studies exploring the role of SphK2 in many diseases. Thus, a major objective of our research is the search for SphK2-selective inhibitors.

1.4. Sphingosine-1-phosphate (S1P)

Sphingosine-1-phosphate (S1P) is produced by phosphorylation of sphingosine with sphingosine kinase. It is a signaling molecule that regulates cell growth,[53] suppresses apoptosis,[29] and controls cell trafficking.[54] S1P levels are tightly controlled by the enzymes involved in its formation (sphingosine kinases and enzymes that produce sphingosine) and by the enzymes involved in its degradation, S1P lyase, two S1P-specific phosphatases and three lipid phosphate phosphatases. It is now known that S1P acts both intracellularly as well as through a family of cell surface receptors.

1.4.1. Intracellular targets of S1P

S1P acts intracellularly to enhance cell proliferation[55] and suppress apoptosis.[56] While early studies suggested that S1P induces calcium release from the ER,[57-59] no intracellular targets were conclusively identified. Recently, however, several intracellular proteins have been recognized as S1P targets.

Histone deacetylase (HDAC) was discovered to be a direct intracellular target of nuclear S1P produced by SphK2.[60] S1P inhibits HDACs 1 and 2 in repressor complexes, increases histone acetylation and enhances gene transcription of *p21* and *c-fos* genes (Figure 1.5). Specific binding of S1P to tumor-necrosis factor receptor-associated factor 2 (TRAF2)[61] stimulates its E3 ligase activity. TRAF2 is a key component in the regulation of NF-κB activation and the anti-apoptotic program initiated by TNF-α.

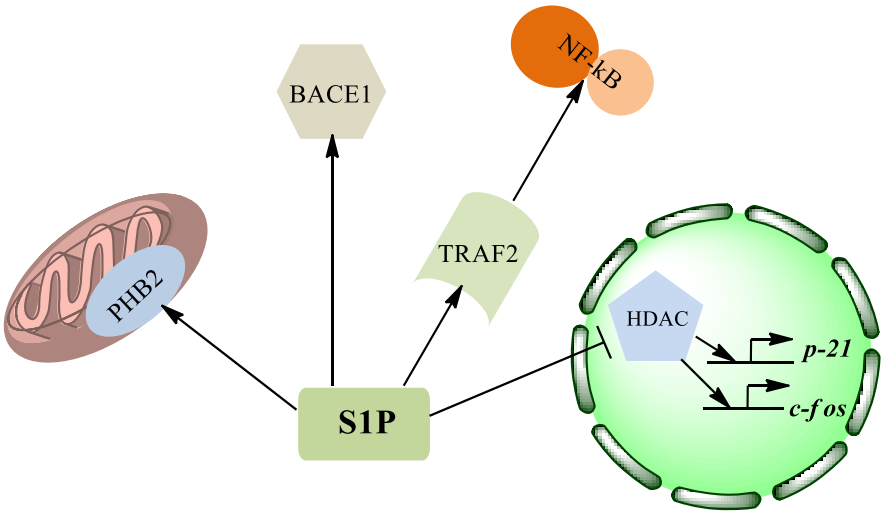

Figure 1.5. Intracellular targets of S1P[3] (Used under fair use, 2012)

Another study showed that the activity of the β-site amyloid precursor protein (APP) cleaving enzyme-1 (BACE1) is modulated by S1P in neurons.[62] A decrease in S1P levels by SphK inhibition or S1P lyase overexpression decreased BACE1 activity. A recent study identified filamin A (FLNa), an actin-cross-linking protein, as a SphK1 interacting protein.[63] It showed that S1P formed by SphK1 directly activated P21 activated protein kinase 1 (PAK1). The study demonstrated that the combined actions of SphK1, FLNa, and PAK1 are essential for cell movement. A recent study also showed that a majority of mitochondrial S1P is produced by SphK2 localized to the mitochondria.[64] Prohibitin 2 (PHB2), a highly conserved mitochondrial protein was shown to bind S1P *in vitro* and *in vivo*.[64] SphK2 knockout mice displayed decreased mitochondrial respiration as a result of abnormal assembly and reduced activity of complex IV of the electron transport chain.[64] This suggested that interaction of S1P with PHB2 is important for mitochondrial respiration.

1.4.2. S1P receptors

S1P acts as a ligand to a family of five G-protein coupled receptors (GPCRs) named $S1P_{1-5}$. S1P regulates a variety of cellular processes through these receptors. These include cell motility,[56,65] invasion,[66] angiogenesis,[67,68] vascular maturation,[69] and lymphocyte trafficking.[70] The affinity constants of S1P for the S1P receptor are mostly in the single digit nanomolar range.[71] The S1P receptors are coupled to various G-proteins that regulate downstream signaling pathways, thus allowing S1P to control diverse physiological processes (Figure 1.6). Several researchers have advocated a functional link between S1P receptors and SphK1, commonly termed "inside-out"signaling.[72] It has been proposed that intracellular S1P, produced by SphK, is released outside of the cell in close proximity to S1P receptors. While the exact mechanism for the release of S1P is not known, some studies suggest that members of the

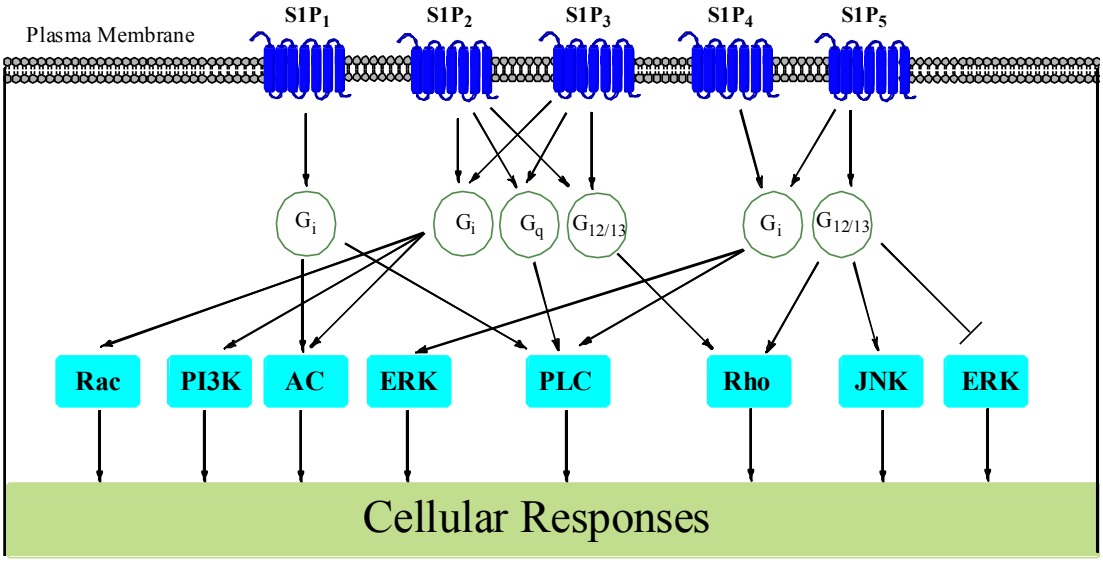

Figure 1.6. S1P is a ligand for five GPCRs

large family of ABC transporters, for example, ABCC1,[73] ABCA1,[74] and ABCG2,[75] might play an important role.

S1P receptors have been implicated in a variety of diseases. These receptors play a crucial role in the trafficking of immune cells; $S1P_1$ activation is important for lymphocytes,[70] $S1P_4$ for neutrophils,[76] and $S1P_5$ for natural killer T cells.[77] S1P receptors are also important in various processes linked to cancer. S1P stimulates the migration of gastric tumor cells through $S1P_3$. On the other hand, S1P binding to $S1P_2$ inhibits cancer cell motility.[78] Thus, the specific effect of S1P is determined by the expression levels of the different receptor subtypes.

1.4.3. S1P and disease

The deregulation of the S1P pathway manifests itself in different ways, *e.g.* overexpression of SphK[40] and altered expression or mutation of S1P receptors.[79] The first observation of the involvement of S1P in cancer was the serum-independent proliferation and increased colony formation and growth of NIH3T3 fibroblasts over-expressing SphK1.[80] These effects were absent for fibroblasts expressing mutant SphK1 and also in the presence of a SphK inhibitor. Recent reports suggest extensive interactions between the signaling pathways of S1P and growth factors implicated in cancer like epidermal growth factor (EGF),[81] heregulin,[63] platelet-derived growth factor (PDGF),[82] and vascular endothelial growth factor (VEGF).[83] Cross-talk with these growth factor receptors regulates processes such as proliferation, migration, and angiogenesis. Thus, dysregulation of S1P signaling has been linked to various diseases and targeting S1P could lead to a new class of therapeutic drugs.

1.5. S1P pathway therapeutics

Various strategies have been developed to limit the effects of S1P signaling in cancer (Figure 1.7). These include: (1) blocking S1P signaling with an S1P receptor antagonist, (2) using an S1P-specific monoclonal antibody as a molecular sponge to deplete S1P from blood and other compartments thereby decreasing its bioavailability at the receptors, (3) synthesizing siRNA that knockdown SphK, and (4) employing sphingosine kinase inhibitors. Although SphK and S1P receptors have been the focus of majority of sphingolipid research, it must be mentioned that the effects of enzymes that remove S1P, S1P phosphatase and S1P lyase, have not been uncovered yet. The role of S1P lyase has not been clearly defined yet. There is very limited evidence for opposing roles for the two S1P phosphatases in cancer.[84,85]

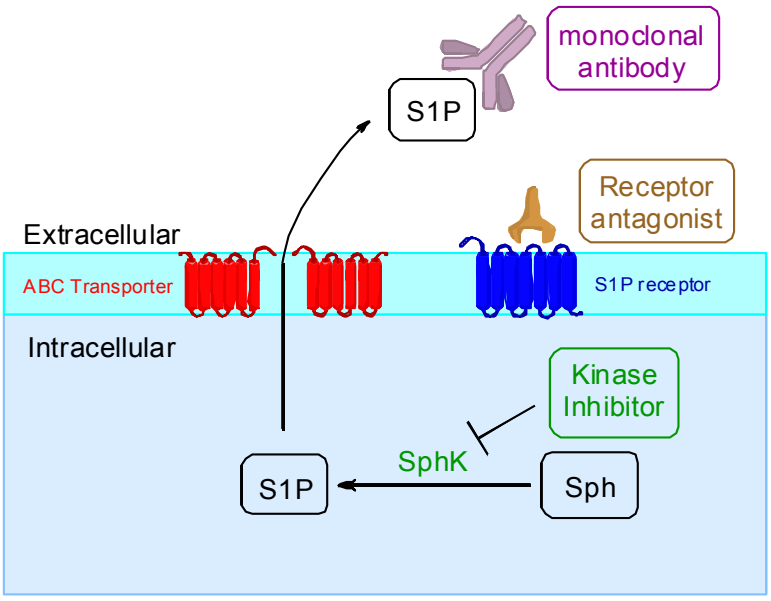

Figure 1.7. Strategies targeting S1P for therapeutics

1.5.1. S1P–specific antibodies

Production of antibodies directed against small (<400 Da) lipids is a difficult and complex process. The process is even more difficult when the immunogen has only one

unique epitope (the polar head group for S1P) which makes generating the antibody response that much more difficult. The process is challenging because of a need for a robust selection assay to quantitatively measure the immune response. An S1P-specific monoclonal antibody has been raised and resulted in decreased tumor progression and, in a few cases, eliminated tumors in mouse xenografts.[86] Use of this antibody *in vitro* reduced S1P-stimulated cell proliferation and blocked the release of pro-angiogenic factors like VEGF and IL-6. Competitive ELISA was used to determine the specificity and sensitivity of the anti-S1P mAb. Anti-angiogenic effects were also observed *in vivo*. Recently, an S1P-specific murine monoclonal antibody, LT1002, was discovered[87] that showed high affinity and specificity for S1P and did not cross-react with other structurally related lipids. A humanized variant of the antibody, LT1009, is currently in Phase I clinical trials.[86]

1.5.2. Small interfering RNA

Specific knockdown of SphK1 by siRNA triggered apoptosis in various tumor cells *in vitro*. Various cancer cells such as leukemia,[88] melanoma,[89] breast,[90] glioblastoma,[47] and prostate[91] displayed increased apoptosis when treated with siRNA by inducing cytochrome *c* release and elevating the levels of ceramide and sphingosine. However, not much attention has been focused on this therapeutic method since it can only be applied for *in vitro* studies.

1.5.3. S1P receptor agonists and antagonists

For a long time, the primary area of research for S1P-receptor targeting therapy was the search for antagonists to $S1P_1$ and $S1P_3$ due to their participation in cell proliferation, migration, invasion, and angiogenesis. These receptors are also involved in growth factor receptor signaling. However, potent antagonists have still not been

discovered. Also, $S1P_1$ is important in many physiological processes such as vascular permeability and lymphocyte migration; any drug candidate must not disturb these vital processes. JTE013, a pyrazolopyridine derivative,[92] is a specific $S1P_2$ receptor antagonist. VPC23019 (Avanti Polar Lipids, Alabaster, AL) is a competitive antagonist at both $S1P_1$ and $S1P_3$ receptors.[93] VPC23019 has been shown to inhibit S1P-induced migration of thyroid[94] and ovarian[95] cancer cells.

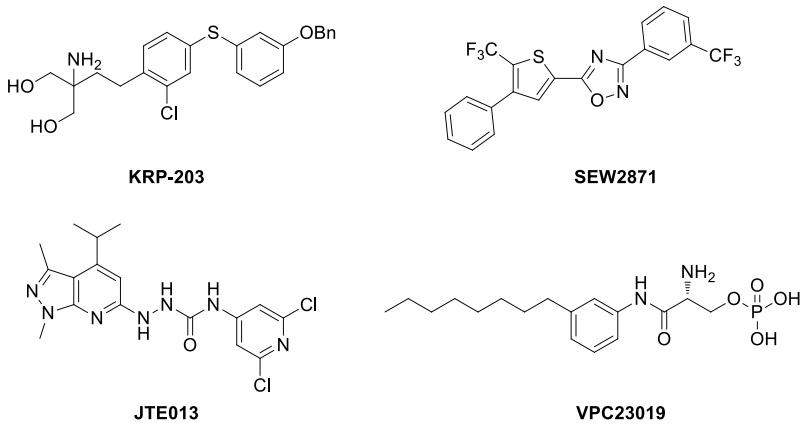

Figure 1.8. Structures of S1P receptor agonists and antagonists

Following the success of FTY720 (*vide infra*), S1P selective agonists gained significance. KRP-203 (Kyorin Pharmaceutical, Tokyo, Japan) was found to be a $S1P_1$ receptor-selective agonist (Figure 1.8).[96] It regulates response of both T-cells and B cells.[97] It has been used in combination with low-dose cyclosporine in a heart transplantation model where it improved allogeneic immune response.[98] SEW2871 (Maybridge, Tintagel, Cornwall, UK) is an $S1P_1$-selective agonist that induces lymphopenia in mice.[99] It works by inducing $S1P_1$ internalization and recycling, unlike FTY720, which causes degradation of the receptor.

1.5.3.1. FTY720

The immunosuppressant FTY720 (Gilenya®) is a sphingosine analog that was approved by the Food and Drug Administration in 2010 for use in treating relapsing-remitting multiple sclerosis (Figure 1.9).[100,101] FTY720 is phosphorylated *in vivo* by SphK2 to FTY720-P,[102] an S1P mimic, which induces internalization and degradation of the $S1P_1$ receptor resulting in prolonged receptor downregulation (Figure 1.10).[103] The resultant absence of an S1P signal modulates immune function by influencing lymphocyte trafficking, specifically by decreasing the egress of lymphocytes from secondary lymphoid tissues.

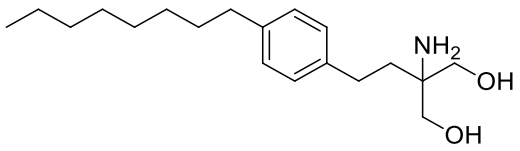

Figure 1.9. FTY720

1.5.4. SphK inhibitors

The sphingolipid rheostat[29] suggests that the dynamic balance between the cellular levels of ceramide and S1P determines cell fate. As a result, the enzymes in the cell that regulate this pathway are potential targets for cancer therapeutics.[104] Since S1P is the proximal effector, sphingosine kinase (SphK) plays a crucial role in the control of this balance. Thus, developing inhibitors of SphK can limit the intracellular action of S1P leading to cell proliferation. The earliest inhibitors of SphK were analogues of sphingosine like L-*threo*-dihydrosphingosine (DHS)[105] and *N*,*N*-dimethylsphingosine (DMS)[106](Figure 1.11). Initial results were encouraging and showed that these inhibitors were very effective at inhibiting the growth of lung and gastric cancer cells[107] and they also decreased lung metathesis of melanoma cells.[108] However, these inhibitors caused

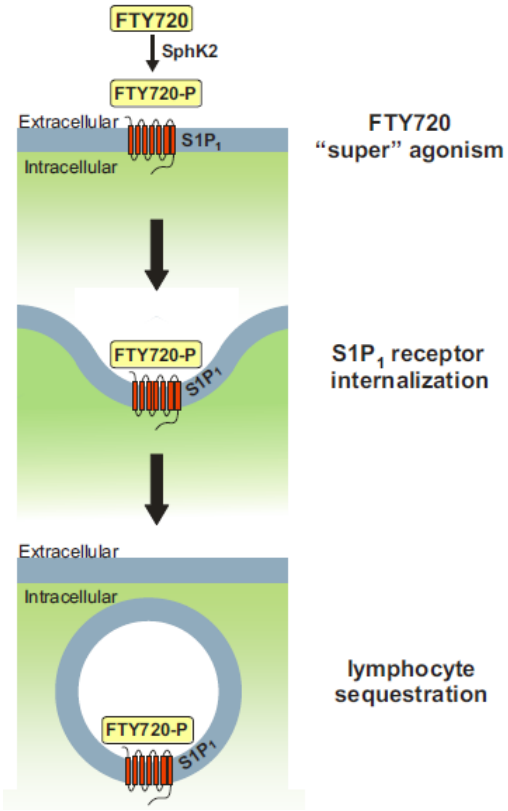

Figure 1.10. Internalization of $S1P_1$ by FTY720-P[72] (Used with permission of American Society for Pharmacology and Experimental Therapeutics, Figure 5, Kazuaki Takabe, Steven W. Paugh, Sheldon Milstien, and Sarah Spiegel, "Inside-Out" Signaling of Sphingosine-1-Phosphate: Therapeutic Targets, *Pharmacol Rev* June 2008, 60, 181-195)

significant hepatotoxicity and hemolysis at higher doses.[109] More importantly, both DHS and DMS are not specific for SphK. Not only do they inhibit both SphK1 and SphK2 equally, but they also inhibit other lipid and protein kinases like ceramide kinase,[110] protein kinase C,[111] sphingosine-dependent protein kinase,[112] casein kinase II[113] and 3-phosphoinositide-dependent kinase.[114]

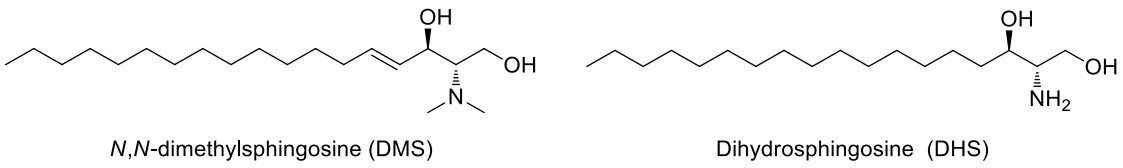

N,*N*-dimethylsphingosine (DMS) Dihydrosphingosine (DHS)

Figure 1.11. Sphingosine analogues as kinase inhibitors

Several natural products were identified in high throughput screening assays as inhibitors of SphK (Figure 1.12). **B-5354a** and **B-5354c** were isolated from a novel marine bacterium, SANK 71896.[115] **B-5354c** is a non-competitive inhibitor with a K_i of 12 μM.[116] It induced caspase-dependent apoptosis in prostate cancer cells by shifting the sphingolipid rheostat toward ceramide. SphK1 inhibition also sensitized prostate cancer cells to chemotherapy-induced apoptosis.[117] **F-12509a** is a natural product obtained from the culture broth of a discomycete, *Trichopezizella barabata*.[118] It is a competitive inhibitor with a K_i of 5 μM. It induced apoptosis in both chemoresistant and chemosensitive HL-60 acute myeloid leukemia cells.[119,120] S-15183a was obtained from the culture broth of a fungus, *Zopfiella inermis*,[121] and was shown to reduce S1P formation in platelets. Although these natural products are moderately potent SphK inhibitors, the specificity of these compounds is uncertain and their large-scale production seems unfeasible.

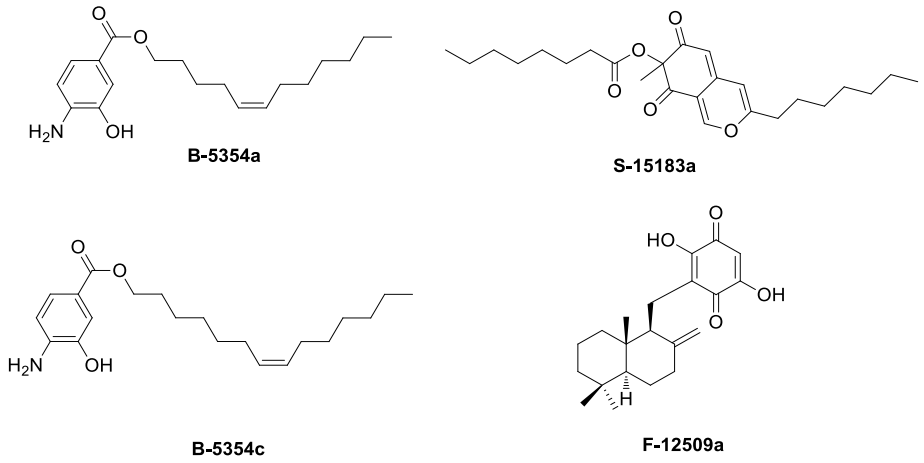

Figure 1.12. Natural product inhibitors of sphingosine kinase

Investigators from the Apogee Biotechnology Company in Hershey, PA tested the viability of developing non-lipid inhibitors of SphK. They developed a medium

throughput assay for recombinant human SphK fused to glutathione *S*-transferase that was used to screen a library of synthetic compounds. A number of novel inhibitors of human SphK were identified and several representative compounds were characterized in detail (Figure 1.13)

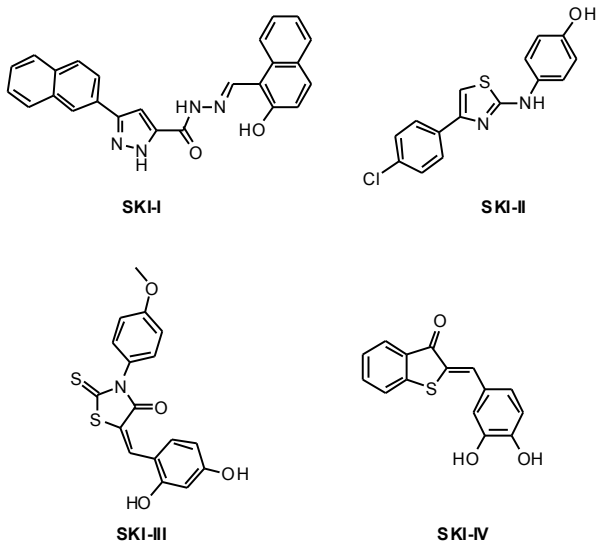

Figure 1.13. Non-lipid inhibitors of sphingosine kinase

SKI-II was the most potent compound isolated (IC_{50}: 0.5 mM for SphK activity). It reduced intracellular S1P, inhibited proliferation and induced apoptosis in various cancer cell lines.[40] *In vivo* studies demonstrated good oral bioavailability and efficient inhibition of tumor growth.[122] It exhibited strong cytotoxicity toward T24 bladder carcinoma cells and MCF-7 breast cancer cells. It was also shown to be active against human prostate cancer cells (PC-3) by reducing the S1P levels.[91]

The need for subtype-selective SphK inhibitors has not gone unnoticed (Figure 1.). SK1-I is a water-soluble, isoenzyme-specific inhibitor of SphK1 that induces apoptosis in human leukemia cells[123] and reduces growth of AML xenograft tumors and glioblastoma xenografts.[124] SphK1 inhibitors based on replacing the aminodiol in

sphingosine by a serine amide (**12aa)** were synthesized[125] and their structure was optimized to increase water solubility and oral availability.[126] The most potent and selective SphK1 inhibitors featured amidine groups (**28**)[127]; these inhibitors significantly reduced endogenous S1P levels in human leukemia U937 cells at nanomolar concentrations.[128]

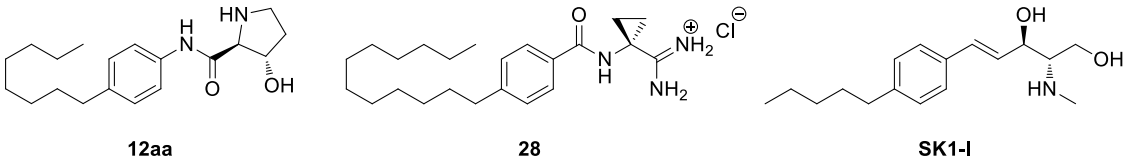

Figure 1.14. SphK1 selective inhibitors

While several studies generated SphK1-selective inhibitors, reports of SphK2-selective compounds are scarce. SphK2-selective inhibitors reported in the literature were obtained either via screening of commercial small molecule libraries (**ABC294640**)[129] or by synthesizing analogues of sphingosine (**SG-12)** (Figure 1.).[130] Recently, the methyl ether of FTY720 (**(*R*)-FTY720-OMe)**[131] was reported as an inhibitor of SphK2 with a K_i of 16.5 μM. Unfortunately, rational design of SphK inhibitors has been hampered by the lack of crystal structure of either protein. While it has been suggested that the C4 domain is involved in specific recognition of Sph via the interaction of the basic amine in sphingosine with the Asp177, rational design of SphK remains a challenge.

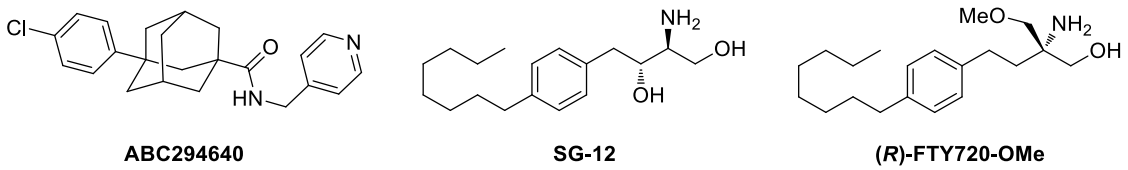

Figure 1.15. SphK2 selective inhibitors

The lack of potent SphK2-selective inhibitors hampers detailed scientific studies exploring the role of SphK2 in many diseases. In addition, poor inhibitor potency has prevented these compounds going into clinical trials.[2] Inhibitors of SphKs with the combination of drug-like properties, potency, and selectivity will be valuable in evaluating these enzymes as therapeutic targets.

1.6. References

1. Pyne, N. J., Pyne, S., Sphingosine-1-phosphate and cancer, *Nat. Rev. Cancer* **2010**, *10*, 489-503.

2. Pyne, S., Bittman, R., Pyne, N. J., Sphingosine kinase inhibitors and cancer: Seeking the golden sword of Hercules, *Cancer Res.* **2011**, *71*, 6576-6582.

3. Maceyka, M., Harikumar, K. B., Milstien, S., Spiegel, S., Sphingosine-1-phosphate signaling and its role in disease, *Trends Cell Biol.* **2012**, *22*, 50-60.

4. He, X., Huang, Y., Li, B., Gong, C.-X., Schuchman, E. H., Deregulation of sphingolipid metabolism in Alzheimer's disease, *Neurobiol. Aging* **2010**, *31*, 398-408.

5. Fyrst, H., Saba, J. D., An update on sphingosine-1-phosphate and other sphingolipid mediators, *Nat. Chem. Biol.* **2010**, *6*, 489-497.

6. Schutze, S., Potthoff, K., Machleidt, T., Berkovic, D., Wiegmann, K., Kronke, M., TNF activates NF-κB by Phosphatidylcholine-specific phospholipase C-induced "acidic" sphingomyelin breakdown, *Cell* **1992**, *71*, 765-776.

7. Garzotto, M., White-Jones, M., Jiang, Y. W., Ehleiter, D., Liao, W. C., Haimovitz-Friedman, A., Fuks, Z., Kolesnick, R., 12-*O*-tetradecanoylphorbol-13-acetate-induced apoptosis in LNCaP cells is mediated through ceramide synthase, *Cancer Res.* **1998**, *58*, 2260-2264.

8. Goldkorn, T., Balaban, N., Shannon, M., Chea, V., Matsukuma, K., Gilchrist, D., Wang, H., Chan, C., H_2O_2 acts on cellular membranes to generate ceramide signaling and initiate apoptosis in tracheobronchial epithelial cells, *J. Cell Sci.* **1998**, *111*, 3209-3220.

9. Futerman, A. H., Stieger, B., Hubbard, A. L., Pagano, R. E., Sphingomyelin synthesis in rat liver occurs predominantly at the cis and medial cisternae of the Golgi apparatus, *J. Biol. Chem.* **1990**, *265*, 8650-8657.

10. Lahiri, S., Lee, H., Mesicek, J., Fuks, Z., Haimovitz-Friedman, A., Kolesnick, R. N., Futerman, A. H., Kinetic characterization of mammalian ceramide synthases:

Determination of K_m values towards sphinganine, *FEBS Lett.* **2007**, *581*, 5289-5294.

11. Pewzner-Jung, Y., Ben-Dor, S., Futerman, A. H., When do Lasses (longevity assurance genes) become CerS (ceramide synthases): Insights into the regulation of ceramide synthesis, *J. Biol. Chem.* **2006**, *281*, 25001-25005.

12. Venkataraman, K., Riebeling, C., Bodennec, J., Riezman, H., Allegood, J. C., Sullard, M. C., Merrill, A. H., Futerman, A. H., Upstream of growth and differentiation factor 1 (*uog1*), a mammalian homolog of the yeast longevity assurance gene 1 (*LAG1*), regulates *N*-stearoyl-sphinganine (C18-(dihydro)ceramide) synthesis in a fumonisin B1-independent manner in mammalian cells, *J. Biol. Chem.* **2002**, *277*, 35642-35649.

13. Laviad, E. L., Albee, L., Pankova-Kholmyansky, I., Epstein, S., Park, H., Merrill, A. H., Futerman, A. H., Characterization of ceramide synthase 2: Tissue distribution, substrate specificity, and inhibition by sphingosine 1-phosphate, *J. Biol. Chem.* **2008**, *283*, 5677-5684.

14. Riebeling, C., Allegood, J. C., Wang, E., Merrill, A. H., Futerman, A. H., Two mammalian longevity assurance gene (*LAG1*) family members, *trh1* and *trh4*, regulate dihydroceramide synthesis using different fatty acyl-CoA donors, *J. Biol. Chem.* **2003**, *278*, 43452-43459.

15. Michel, C., Vanechtendeckert, G., Conversion of dihydroceramide to ceramide occurs at the cytosolic face of the endoplasmic reticulum, *FEBS Lett.* **1997**, *416*, 153-155.

16. Savile, C. K., Fabrias, G., Buist, P. H., Dihydroceramide Δ^4 desaturase initiates substrate oxidation at C-4, *J. Am. Chem. Soc.* **2001**, *123*, 4382-4385.

17. Kolesnick, R., Hannun, Y. A., Ceramide and apoptosis, *Trends Biochem. Sci.* **1999**, *24*, 224-225.

18. Hanada, K., Kumagai, K., Yasuda, S., Miura, Y., Kawano, M., Fukasawa, M., Nishijima, M., Molecular machinery for non-vesicular trafficking of ceramide, *Nature* **2003**, *426*, 803-809.

19. Watson, P., Stephens, D. J., ER to Golgi transport: Form and formation of vesicular and tubular carriers, *Biochim. Biophys. Acta, Mol. Cell Res.* **2005**, *1744*, 304-315.

20. Stahl, N., Jurevics, H., Morell, P., Suzuki, K., Popko, B., Isolation, characterization, and expression of cDNA clones that encode rat UDP-galactose: Ceramide galactosyltransferase, *J. Neurosci. Res.* **1994**, *38*, 234-242.

21. Ichikawa, S., Sakiyama, H., Suzuki, G., Hidari, K., Hirabayashi, Y., Expression cloning of a cDNA for human ceramide glucosyltransferase that catalyzes the first glycosylation step of glycosphingolipid synthesis, *PNAS* **1996**, *93*, 4638-4643.

22. Jeckel, D., Karrenbauer, A., Burger, K. N. J., Vanmeer, G., Wieland, F., Glucosylceramide is synthesized at the cytosolic surface of various Golgi subfractions, *J. Cell Biol.* **1992**, *117*, 259-267.

23. D'Angelo, G., Polishchuk, E., Di Tullio, G., Santoro, M., Di Campli, A., Godi, A., West, G., Bielawski, J., Chuang, C. C., Van Der Spoel, A. C., Platt, F. M., Hannun, Y. A., Polishchuk, R., Mattjus, P., De Matteis, M. A., Glycosphingolipid synthesis requires FAPP2 transfer of glucosylceramide, *Nature* **2007**, *449*, 62-67.

24. Quintern, L. E., Schuchman, E. H., Levran, O., Suchi, M., Ferlinz, K., Reinke, H., Sandhoff, K., Desnick, R. J., Isolation of cDNA clones encoding human acid sphingomyelinase: Occurrence of alternatively processed transcripts, *EMBO J.* **1989**, *8*, 2469-2473.

25. Wu, B. X., Clarke, C. J., Hannun, Y. A., Mammalian neutral sphingomyelinases: Regulation and roles in cell signaling responses, *Neuromol. Med.* **2010**, *12*, 320-330.

26. Duan, R. D., Cheng, Y. J., Hansen, G., Hertervig, E., Liu, J. J., Syk, I., Sjostrom, H., Nilsson, A., Purification, localization, and expression of human intestinal alkaline sphingomyelinase, *J. Lipid Res.* **2003**, *44*, 1241-1250.

27. Le Stunff, H., Peterson, C., Thornton, R., Milstien, S., Mandala, S. M., Spiegel, S., Characterization of murine sphingosine-1-phosphate phosphohydrolase, *J. Biol. Chem.* **2002**, *277*, 8920-8927.

28. Ogawa, C., Kihara, A., Gokoh, M., Igarashi, Y., Identification and characterization of a novel human sphingosine-1-phosphate phosphohydrolase, hSPP2, *J. Biol. Chem.* **2003**, *278*, 1268-1272.

29. Cuvillier, O., Pirianov, G., Kleuser, B., Vanek, P. G., Coso, O. A., Gutkind, J. S., Spiegel, S., Suppression of ceramide-mediated programmed cell death by sphingosine-1-phosphate, *Nature* **1996**, *381*, 800-803.

30. Kohama, T., Olivera, A., Edsall, L., Nagiec, M. M., Dickson, R., Spiegel, S., Molecular cloning and functional characterization of murine sphinogosine kinase, *J. Biol. Chem.* **1998**, *273*, 23722-23728.

31. Liu, H., Chakravarty, D., Maceyka, M., Milstien, S., Spiegel, S., Sphingosine kinases: A novel family of lipid kinases, *Prog. Nucleic Acid Res. Mol. Biol.* **2002**, *71*, 493-511.

32. Kihara, A., Kurotsu, F., Sano, T., Iwaki, S., Igarashi, Y., Long-chain base kinase Lcb4 is anchored to the membrane through its palmitoylation by Akr1, *Mol. Cell. Biol.* **2005**, *25*, 9189-9197.

33. Johnson, K. R., Becker, K. P., Facchinetti, M. M., Hannun, Y. A., Obeid, L. M., PKC-dependent activation of sphingosine kinase 1 and translocation to the plasma membrane: Extracellular release of sphingosine-1-phosphate induced by phorbol 12-myristate 13-acetate (PMA), *J. Biol. Chem.* **2002**, *277*, 35257-35262.

34. Pitson, S. M., Moretti, P. A. B., Zebol, J. R., Lynn, H. E., Xia, P., Vadas, M. A., Wattenberg, B. W., Activation of sphingosine kinase 1 by ERK1/2-mediated phosphorylation, *EMBO J.* **2003**, *22*, 5491-5500.

35. Hobson, J. P., Rosenfeldt, H. M., Barak, L. S., Olivera, A., Poulton, S., Caron, M. G., Milstien, S., Spiegel, S., Role of the sphingosine-1-phosphate receptor Edg-1 in PDGF-induced cell motility, *Science* **2001**, *291*, 1800-1803.

36. Shu, X. D., Wu, W. C., Mosteller, R. D., Broek, D., Sphingosine kinase mediates vascular endothelial growth factor-induced activation of Ras and mitogen-activated protein kinases, *Mol. Cell. Biol.* **2002**, *22*, 7758-7768.

37. Sarkar, S., Maceyka, M., Hait, N. C., Paugh, S. W., Sankala, H., Milstien, S., Spiegel, S., Sphingosine kinase 1 is required for migration, proliferation and survival of MCF-7 human breast cancer cells, *FEBS Lett.* **2005**, *579*, 5313-5317.

38. Xia, P., Wang, L. J., Moretti, P. A. B., Albanese, N., Chai, F. G., Pitson, S. M., D'andrea, R. J., Gamble, J. R., Vadas, M. A., Sphingosine kinase interacts with TRAF2 and dissects tumor necrosis factor-α signaling, *J. Biol. Chem.* **2002**, *277*, 7996-8003.

39. Pettus, B. J., Bielawski, J., Porcelli, A. M., Reames, D. L., Johnson, K. R., Morrow, J., Chalfant, C. E., Obeid, L. M., Hannun, Y. A., The sphingosine kinase 1/sphingosine-1-phosphate pathway mediates cox-2 induction and pge(2) production in response to tnf-alpha, *FASEB J.* **2003**, *17*, 1411-1421.

40. French, K. J., Schrecengost, R. S., Lee, B. D., Zhuang, Y., Smith, S. N., Eberly, J. L., Yun, J. K., Smith, C. D., Discovery and evaluation of inhibitors of human sphingosine kinase, *Cancer Res.* **2003**, *63*, 5962-5969.

41. Johnson, K. R., Johnson, K. Y., Crellin, H. G., Ogretmen, B., Boylan, A. M., Harley, R. A., Obeid, L. M., Immunohistochemical distribution of sphingosine kinase 1 in normal and tumor lung tissue, *J. Histochem. Cytochem.* **2005**, *53*, 1159-1166.

42. Kawamori, T., Kaneshiro, T., Okumura, M., Maalouf, S., Uflacker, A., Bielawski, J., Hannun, Y. A., Obeid, L. M., Role for sphingosine kinase 1 in colon carcinogenesis, *FASEB J.* **2009**, *23*, 405-414.

43. Bayerl, M. G., Bruggeman, R. D., Conroy, E. J., Hengst, J. A., King, T. S., Jimenez, M., Claxton, D. F., Yun, J. K., Sphingosine kinase 1 protein and mRNA are overexpressed in non-Hodgkin lymphomas and are attractive targets for novel pharmacological interventions, *Leuk. Lymphoma* **2008**, *49*, 948-954.

44. Li, W., Yu, C. P., Xia, J. T., Zhang, L., Weng, G. X., Zheng, H. Q., Kong, Q. L., Hu, L. J., Zeng, M. S., Zeng, Y. X., Li, M. F., Li, J., Song, L. B., Sphingosine kinase 1 is associated with gastric cancer progression and poor survival of patients, *Clin. Cancer Res.* **2009**, *15*, 1393-1399.

45. Li, J., Guan, H. Y., Gong, L. Y., Song, L. B., Zhang, N., Wu, J. H., Yuan, J., Zheng, Y. J., Huang, Z. S., Li, M. F., Clinical significance of sphingosine kinase 1 expression in human astrocytomas progression and overall patient survival, *Clin. Cancer Res.* **2008**, *14*, 6996-7003.

46. Ruckäberle, E., Rody, A., Engels, K., Gaetje, R., Von Minckwitz, G., Schiffmann, S., Grosch, S., Geisslinger, G., Holtrich, U., Karn, T., Kaufmann, M., Microarray analysis of altered sphingolipid metabolism reveals prognostic significance of sphingosine kinase 1 in breast cancer, *Breast Cancer Res. Treat.* **2008**, *112*, 41-52.

47. Van Brocklyn, J. R., Jackson, C. A., Pearl, D. K., Kotur, M. S., Snyder, P. J., Prior, T. W., Sphingosine kinase 1 expression correlates with poor survival of patients with glioblastoma multiforme: Roles of sphingosine kinase isoforms in growth of glioblastoma cell lines, *J. Neuropathol. Exp. Neurol.* **2005**, *64*, 695-705.

48. Maceyka, M., Sankala, H., Hait, N. C., Le Stunff, H., Liu, H., Toman, R., Collier, C., Zhang, M., Satin, L. S., Merrill, A. H., Milstien, S., Spiegel, S., SphK1 and SphK2, sphingosine kinase isoenzymes with opposing functions in sphingolipid metabolism, *J. Biol. Chem.* **2005**, *280*, 37118-37129.

49. Igarashi, N., Okada, T., Hayashi, S., Fujita, T., Jahangeer, S., Nakamura, S., Sphingosine kinase 2 is a nuclear protein and inhibits DNA synthesis, *J. Biol. Chem.* **2003**, *278*, 46832-46839.

50. Ding, G., Sonoda, H., Yu, H., Kajimoto, T., Goparaju, S. K., Jahangeer, S., Okada, T., Nakamura, S., Protein kinase D-mediated phosphorylation and nuclear export of sphingosine kinase 2, *J. Biol. Chem.* **2007**, *282*, 27493-27502.

51. Liu, H., Toman, R. E., Goparaju, S. K., Maceyka, M., Nava, V. E., Sankala, H., Payne, S. G., Bektas, M., Ishii, I., Chun, J., Milstien, S., Spiegel, S., Sphingosine kinase type 2 is a putative BH3-only protein that induces apoptosis, *J. Biol. Chem.* **2003**, *278*, 40330-40336.

52. Weigert, A., Schiffmann, S., Sekar, D., Ley, S., Menrad, H., Werno, C., Grosch, S., Geisslinger, G., Brune, B., Sphingosine kinase 2 deficient tumor xenografts

show impaired growth and fail to polarize macrophages towards an anti-inflammatory phenotype, *Int. J. Cancer* **2009**, *125*, 2114-2121.

53. Olivera, A., Spiegel, S., Sphingosine-1-phosphate as 2nd messenger in cell-proliferation induced by PDGF and FCS mitogens, *Nature* **1993**, *365*, 557-560.

54. Spiegel, S., Milstien, S., The outs and the ins of sphingosine-1-phosphate in immunity, *Nat. Rev. Immunol.* **2011**, *11*, 403-415.

55. Van Brocklyn, J. R., Lee, M. J., Menzeleev, R., Olivera, A., Edsall, L., Cuvillier, O., Thomas, D. M., Coopman, P. J. P., Thangada, S., Liu, C. H., Hla, T., Spiegel, S., Dual actions of sphingosine-1-phosphate: Extracellular through the G_i-coupled receptor Edg-1 and intracellular to regulate proliferation and survival, *J. Cell Biol.* **1998**, *142*, 229-240.

56. Rosenfeldt, H. M., Hobson, J. P., Maceyka, M., Olivera, A., Nava, V. E., Milstien, S., Spiegel, S., Edg-1 links the PDGF receptor to Src and focal adhesion kinase activation leading to lamellipodia formation and cell migration, *FASEB J.* **2001**, *15*, 2649-2659.

57. Ghosh, T. K., Bian, J., Gill, D. L., Intracellular calcium release mediated by sphingosine derivatives generated in cells, *Science* **1990**, *248*, 1653-1656.

58. Ghosh, T. K., Bian, J. H., Gill, D. L., Sphingosine 1-phosphate generated in the endoplasmic reticulum membrane activates release of stored calcium, *J. Biol. Chem.* **1994**, *269*, 22628-22635.

59. Mattie, M., Brooker, G., Spiegel, S., Sphingosine-1-phosphate, a putative 2nd messenger, mobilizes calcium from internal stores via an inositol trisphosphate-independent pathway, *J. Biol. Chem.* **1994**, *269*, 3181-3188.

60. Hait, N. C., Allegood, J., Maceyka, M., Strub, G. M., Harikumar, K. B., Singh, S. K., Luo, C., Marmorstein, R., Kordula, T., Milstien, S., Spiegel, S., Regulation of histone acetylation in the nucleus by sphingosine-1-phosphate, *Science* **2009**, *325*, 1254-1257.

61. Alvarez, S. E., Harikumar, K. B., Hait, N. C., Allegood, J., Strub, G. M., Kim, E. Y., Maceyka, M., Jiang, H. L., Luo, C., Kordula, T., Milstien, S., Spiegel, S., Sphingosine-1-phosphate is a missing cofactor for the E3 ubiquitin ligase TRAF2, *Nature* **2010**, *465*, 1084-U149.

62. Takasugi, N., Sasaki, T., Suzuki, K., Osawa, S., Isshiki, H., Hori, Y., Shimada, N., Higo, T., Yokoshima, S., Fukuyama, T., Lee, V. M. Y., Trojanowski, J. Q., Tomita, T., Iwatsubo, T., BACE1 activity is modulated by cell-associated sphingosine-1-phosphate, *J. Neurosci.* **2011**, *31*, 6850-6857.

63. Maceyka, M., Alvarez, S. E., Milstien, S., Spiegel, S., Filamin A links sphingosine kinase 1 and sphingosine-1-phosphate receptor 1 at lamellipodia to orchestrate cell migration, *Mol. Cell. Biol.* **2008**, *28*, 5687-5697.

64. Strub, G. M., Paillard, M., Liang, J., Gomez, L., Allegood, J. C., Hait, N. C., Maceyka, M., Price, M. M., Chen, Q., Simpson, D. C., Kordula, T., Milstien, S., Lesnefsky, E. J., Spiegel, S., Sphingosine-1-phosphate produced by sphingosine kinase 2 in mitochondria interacts with prohibitin 2 to regulate complex IV assembly and respiration, *FASEB J.* **2011**, *25*, 600-612.

65. Lee, M. J., Thangada, S., Paik, J. H., Sapkota, G. P., Ancellin, N., Chae, S. S., Wu, M. T., Morales-Ruiz, M., Sessa, W. C., Alessi, D. R., Hla, T., Akt-mediated phosphorylation of the G protein-coupled receptor Edg-1 is required for endothelial cell chemotaxis, *Mol. Cell* **2001**, *8*, 693-704.

66. Lee, M. J., Thangada, S., Claffey, K. P., Ancellin, N., Liu, C. H., Kluk, M., Volpi, M., Sha'afi, R. I., Hla, T., Vascular endothelial cell adherens junction assembly and morphogenesis induced by sphingosine-1-phosphate, *Cell* **1999**, *99*, 301-312.

67. English, D., Welch, Z., Kovala, A. T., Harvey, K., Volpert, O. V., Brindley, D. N., Garcia, J. G. N., Sphingosine 1-phosphate released from platelets during clotting accounts for the potent endothelial cell chemotactic activity of blood serum and provides a novel link between hemostasis and angiogenesis, *FASEB J.* **2000**, *14*, 2255-2265.

68. Wang, F., Van Brocklyn, J. R., Hobson, J. P., Movafagh, S., Zukowska-Grojec, Z., Milstien, S., Spiegel, S., Sphingosine 1-phosphate stimulates cell migration through a G_i-coupled cell surface receptor: Potential involvement in angiogenesis, *J. Biol. Chem.* **1999**, *274*, 35343-35350.

69. Liu, Y. J., Wada, R., Yamashita, T., Mi, Y. D., Deng, C. X., Hobson, J. P., Rosenfeldt, H. M., Nava, V. E., Chae, S. S., Lee, M. J., Liu, C. H., Hla, T., Spiegel, S., Proia, R. L., Edg-1, the G protein-coupled receptor for sphingosine-1-phosphate, is essential for vascular maturation, *J. Clin. Invest.* **2000**, *106*, 951-961.

70. Schwab, S. R., Cyster, J. G., Finding a way out: Lymphocyte egress from lymphoid organs, *Nat. Immunol.* **2007**, *8*, 1295-1301.

71. Mandala, S., Hajdu, R., Bergstrom, J., Quackenbush, E., Xie, J., Milligan, J., Thornton, R., Shei, G. J., Card, D., Keohane, C., Rosenbach, M., Hale, J., Lynch, C. L., Rupprecht, K., Parsons, W., Rosen, H., Alteration of lymphocyte trafficking by sphingosine-1-phosphate receptor agonists, *Science* **2002**, *296*, 346-349.

72. Takabe, K., Paugh, S. W., Milstien, S., Spiegel, S., "Inside-out" Signaling of sphingosine-1-phosphate: Therapeutic targets, *Pharmacol. Rev.* **2008**, *60*, 181-195.

73. Mitra, P., Oskeritzian, C. A., Payne, S. G., Beaven, M. A., Milstien, S., Spiegel, S., Role of ABCC1 in export of sphingosine-1-phosphate from mast cells, *PNAS* **2006**, *103*, 16394-16399.

74. Sato, K., Malchinkhuu, E., Horiuchi, Y., Mogi, C., Tomura, H., Tosaka, M., Yoshimoto, Y., Kuwabara, A., Okajima, F., Critical role of ABCA1 transporter in sphingosine-1-phosphate release from astrocytes, *J. Neurochem.* **2007**, *103*, 2610-2619.

75. Takabe, K., Kim, R. H., Allegood, J. C., Mitra, P., Ramachandran, S., Nagahashi, M., Harikumar, K. B., Hait, N. C., Milstien, S., Spiegel, S., Estradiol induces export of sphingosine 1-phosphate from breast cancer cells via ABCC1 and ABCG2, *J. Biol. Chem.* **2010**, *285*, 10477-10486.

76. Allende, M. L., Bektas, M., Lee, B. G., Bonifacino, E., Kang, J. M., Tuymetova, G., Chen, W. P., Saba, J. D., Proia, R. L., Sphingosine-1-phosphate lyase deficiency produces a pro-inflammatory response while impairing neutrophil trafficking, *J. Biol. Chem.* **2011**, *286*, 7348-7358.

77. Jenne, C. N., Enders, A., Rivera, R., Watson, S. R., Bankovich, A. J., Pereira, J. P., Xu, Y., Roots, C. M., Beilke, J. N., Banerjee, A., Reiner, S. L., Miller, S. A., Weinmann, A. S., Goodnow, C. C., Lanier, L. L., Cyster, J. G., Chun, J., T-bet-dependent $S1P_5$ expression in NK cells promotes egress from lymph nodes and bone marrow, *J. Exp. Med.* **2009**, *206*, 2469-2481.

78. Yamashita, H., Kitayama, J., Shida, D., Yamaguchi, H., Mori, K., Osada, M., Aoki, S., Yatomi, Y., Takuwa, Y., Nagawa, H., Sphingosine-1-phosphate receptor expression profile in human gastric cancer cells: Differential regulation on the migration and proliferation, *J. Surg. Res.* **2006**, *130*, 80-87.

79. Cattoretti, G., Mandelbaum, J., Lee, N., Chaves, A. H., Mahler, A. M., Chadburn, A., Dalla-Favera, R., Pasqualucci, L., Maclennan, A. J., Targeted disruption of the $S1P_2$ sphingosine-1-phosphate receptor gene leads to diffuse large B-cell lymphoma formation, *Cancer Res.* **2009**, *69*, 8686-8692.

80. Xia, P., Gamble, J. R., Wang, L. J., Pitson, S. M., Moretti, P. A. B., Wattenberg, B. W., D'andrea, R. J., Vadas, M. A., An oncogenic role of sphingosine kinase, *Curr. Biol.* **2000**, *10*, 1527-1530.

81. Sukocheva, O., Wadham, C., Holmes, A., Albanese, N., Verrier, E., Feng, F., Bernal, A., Derian, C. K., Ullrich, A., Vadas, M. A., Xia, P., Estrogen transactivates EGFR via the sphingosine-1-phosphate receptor Edg-3: The role of sphingosine kinase 1, *J. Cell Biol.* **2006**, *173*, 301-310.

82. Baudhuin, L. M., Jiang, Y., Zaslavsky, A., Ishii, I., Chun, J., Xu, Y., $S1P_3$-mediated Akt activation and cross-talk with platelet-derived growth factor receptor (PDGFR), *FASEB J.* **2004**, *18*, 341-343.

83. Wu, W. C., Shu, X. D., Hovsepyan, H., Mosteller, R. D., Broek, D., VEGF receptor expression and signaling in human bladder tumors, *Oncogene* **2003**, *22*, 3361-3370.

84. Johnson, K. R., Johnson, K. Y., Becker, K. P., Bielawski, J., Mao, C. G., Obeid, L. M., Role of human sphingosine-1-phosphate phosphatase 1 in the regulation of intra- and extracellular sphingosine-1-phosphate levels and cell viability, *J. Biol. Chem.* **2003**, *278*, 34541-34547.

85. Mechtcheriakova, D., Wlachos, A., Sobanov, J., Kopp, T., Reuschel, R., Bornancin, F., Cai, R., Zemann, B., Urtz, N., Stingl, G., Zlabinger, G., Woisetschlager, M., Baumruker, T., Billich, A., Sphingosine 1-phosphate phosphatase 2 is induced during inflammatory responses, *Cell. Signal.* **2007**, *19*, 748-760.

86. Visentin, B., Vekich, J. A., Sibbald, B. J., Cavalli, A. L., Moreno, K. M., Matteo, R. G., Garland, W. A., Lu, Y. L., Yu, S. X., Hall, H. S., Kundra, V., Mills, G. B., Sabbadini, R. A., Validation of an anti-sphingosine-1-phosphate antibody as a potential therapeutic in reducing growth, invasion, and angiogenesis in multiple tumor lineages, *Cancer Cell* **2006**, *9*, 225-238.

87. O'Brien, N., Jones, S. T., Williams, D. G., Cunningham, H. B., Moreno, K., Visentin, B., Gentile, A., Vekich, J., Shestowsky, W., Hiraiwa, M., Matteo, R., Cavalli, A., Grotjahn, D., Grant, M., Hansen, G., Campbell, M. A., Sabbadini, R., Production and characterization of monoclonal anti-sphingosine-1-phosphate antibodies, *J. Lipid Res.* **2009**, *50*, 2245-2257.

88. Taha, T. A., Osta, W., Kozhaya, L., Bielawski, J., Johnson, K. R., Gillanders, W. E., Dbaibo, G. S., Hannun, Y. A., Obeid, L. M., Down-regulation of sphingosine kinase 1 by DNA damage: Dependence on proteases and p53, *J. Biol. Chem.* **2004**, *279*, 20546-20554.

89. Bektas, M., Jolly, P. S., Muller, C., Eberle, R., Spiegel, S., Geilen, C. C., Sphingosine kinase activity counteracts ceramide-mediated cell death in human melanoma cells: Role of Bcl-2 expression, *Oncogene* **2005**, *24*, 178-187.

90. Taha, T. A., Kitatani, K., El-Alwani, M., Bielawski, J., Hannun, Y. A., Obeid, L. M., Loss of sphingosine kinase 1 activates the intrinsic pathway of programmed cell death: Modulation of sphingolipid levels and the induction of apoptosis, *FASEB J.* **2006**, *19*, 482-484.

91. Pchejetski, D., Golzio, M., Bonhoure, E., Calvet, C., Doumerc, N., Garcia, V., Mazerolles, C., Rischmann, P., Teissie, J., Malavaud, B., Cuvillier, O., Sphingosine kinase 1 as a chemotherapy sensor in prostate adenocarcinoma cell and mouse models, *Cancer Res.* **2005**, *65*, 11667-11675.

92. Kawasaki, H., Ozawa, K., Yamamoto, K., Pyrazolopyridine compounds and use thereof as drugs. World patent WO0198301, **2001**.

93. Davis, M. D., Clemens, J. J., Macdonald, T. L., Lynch, K. R., Sphingosine-1-phosphate analogs as receptor antagonists, *J. Biol. Chem.* **2005**, *280*, 9833-9841.

94. Balthasar, S., Samulin, J., Ahlgren, H., Bergelin, N., Lundqvist, M., Toescu, E. C., Eggo, M. C., Tornquist, K., Sphingosine-1-phosphate receptor expression profile and regulation of migration in human thyroid cancer cells, *Biochem. J.* **2006**, *398*, 547-556.

95. Park, K. S., Kim, M. K., Lee, H. Y., Kim, S. D., Lee, S. Y., Kim, J. M., Ryu, S. H., Bae, Y. S., S1p stimulates chemotactic migration and invasion in OVCAR3 ovarian cancer cells, *Biochem. Biophys. Res. Commun.* **2007**, *356*, 239-244.

96. Shimizu, H., Takahashi, M., Kaneko, T., Murakami, T., Hakamata, Y., Kudou, S., Kishi, T., Fukuchi, K., Iwanami, S., Kuriyama, K., Yasue, T., Enosawa, S., Matsumoto, K., Takeyoshi, I., Morishita, Y., Kobayashi, E., KRP-203, a novel synthetic immunosuppressant, prolongs graft survival and attenuates chronic rejection in rat skin and heart allografts, *Circulation* **2005**, *111*, 222-229.

97. Mizushima, T., Ito, T., Kishi, D., Kai, Y., Tamagawa, H., Nezu, R., Kiyono, H., Matsuda, H., Therapeutic effects of a new lymphocyte homing reagent FTY720 in interleukin-10 gene-deficient mice with colitis, *Inflamm. Bowel Dis.* **2004**, *10*, 182-192.

98. Suzuki, C., Takahashi, M., Morimoto, H., Izawa, A., Ise, H., Fujishiro, J., Murakami, T., Ishiyama, J., Nakada, A., Nakayama, J., Shimada, K., Ikeda, U., Kobayashi, E., Efficacy of mycophenolic acid combined with KRP-203, a novel immunomodulator, in a rat heart transplantation model, *J. Heart Lung Transplant.* **2006**, *25*, 302-309.

99. Sanna, M. G., Liao, J. Y., Jo, E. J., Alfonso, C., Ahn, M. Y., Peterson, M. S., Webb, B., Lefebvre, S., Chun, J., Gray, N., Rosen, H., Sphingosine-1-phosphate (S1P) receptor subtypes $S1P_1$ and $S1P_3$, respectively, regulate lymphocyte recirculation and heart rate, *J. Biol. Chem.* **2004**, *279*, 13839-13848.

100. Cohen, J. A., Barkhof, F., Comi, G., Hartung, H. P., Khatri, B. O., Montalban, X., Pelletier, J., Capra, R., Gallo, P., Izquierdo, G., Tiel-Wilck, K., De Vera, A., Jin, J., Stites, T., Wu, S., Aradhye, S., Kappos, L., Grp, T. S., Oral fingolimod or intramuscular interferon for relapsing multiple sclerosis, *N. Engl. J. Med.* **2010**, *362*, 402-415.

101. Kappos, L., Radue, E. W., O'connor, P., Polman, C., Hohlfeld, R., Calabresi, P., Selmaj, K., Agoropoulou, C., Leyk, M., Zhang-Auberson, L., Burtin, P., Grp, F. S., A placebo-controlled trial of oral fingolimod in relapsing multiple sclerosis, *N. Engl. J. Med.* **2010**, *362*, 387-401.

102. Sanchez, T., Estrada-Hernandez, T., Paik, J. H., Wu, M. T., Venkataraman, K., Brinkmann, V., Claffey, K., Hla, T., Phosphorylation and action of the

immunomodulator FTY720 inhibits vascular endothelial cell growth factor-induced vascular permeability, *J. Biol. Chem.* **2003**, *278*, 47281-47290.

103. Matloubian, M., Lo, C. G., Cinamon, G., Lesneski, M. J., Xu, Y., Brinkmann, V., Allende, M. L., Proia, R. L., Cyster, J. G., Lymphocyte egress from thymus and peripheral lymphoid organs is dependent on S1P receptor 1, *Nature* **2004**, *427*, 355-360.

104. Spiegel, S., Milstien, S., Sphingosine-1-phosphate: An enigmatic signalling lipid, *Nat. Rev. Mol. Cell Biol.* **2003**, *4*, 397-407.

105. Buehrer, B. M., Bell, R. M., Inhibition of sphingosine kinase *in vitro* and in platelets: Implications for signal transduction pathways, *J. Biol. Chem.* **1992**, *267*, 3154-3159.

106. Yatomi, Y., Ruan, F. Q., Megidish, T., Toyokuni, T., Hakomori, S. I., Igarashi, Y., *N,N*-Dimethylsphingosine inhibition of sphingosine kinase and sphingosine-1-phosphate activity in human platelets, *Biochemistry* **1996**, *35*, 626-633.

107. Endo, K., Igarashi, Y., Nisar, M., Zhou, Q. H., Hakomori, S. I., Cell membrane signaling as target in cancer therapy: Inhibitory effect of *N,N*-dimethyl and *N,N,N*-trimethyl sphingosine derivatives on *in vitro* and *in vivo* growth of human tumor cells in nude mice, *Cancer Res.* **1991**, *51*, 1613-1618.

108. Okoshi, H., Hakomori, S., Nisar, M., Zhou, Q. H., Kimura, S., Tashiro, K., Igarashi, Y., Cell membrane signaling as target in cancer therapy II: Inhibitory effect of *N,N,N*-trimethylsphingosine on metastatic potential of murine B16 melanoma cell line through blocking of tumor cell-dependent platelet aggregation, *Cancer Res.* **1991**, *51*, 6019-6024.

109. Kedderis, L. B., Bozigian, H. P., Kleeman, J. M., Hall, R. L., Palmer, T. E., Harrison, S. D., Susick, R. L., Toxicity of the protein kinase C inhibitor safingol administered alone and in combination with chemotherapeutic agents, *Fundam. Appl. Toxicol.* **1995**, *25*, 201-217.

110. Sugiura, M., Kono, K., Liu, H., Shimizugawa, T., Minekura, H., Spiegel, S., Kohama, T., Ceramide kinase, a novel lipid kinase: Molecular cloning and functional characterization, *J. Biol. Chem.* **2002**, *277*, 23294-23300.

111. Igarashi, Y., Hakomori, S., Toyokuni, T., Dean, B., Fujita, S., Sugimoto, M., Ogawa, T., Elghendy, K., Racker, E., Effect of chemically well-defined sphingosine and its *N*-methyl derivatives on protein kinase C and Src kinase activities, *Biochemistry* **1989**, *28*, 6796-6800.

112. Megidish, T., White, T., Takio, K., Titani, K., Igarashi, Y., Hakomori, S., The signal modulator protein 14-3-3 is a target of sphingosine-dependent or *N,N*-dimethylsphingosine-dependent kinase in 3T3(A31) cells, *Biochem. Biophys. Res. Commun.* **1995**, *216*, 739-747.

113. Mcdonald, O. B., Hannun, Y. A., Reynolds, C. H., Sahyoun, N., Activation of casein kinase-II by sphingosine, *J. Biol. Chem.* **1991**, *266*, 21773-21776.

114. King, C. C., Zenke, F. T., Dawson, P. E., Dutil, E. M., Newton, A. C., Hemmings, B. A., Bokoch, G. M., Sphingosine is a novel activator of 3-phosphoinositide-dependent kinase 1, *J. Biol. Chem.* **2000**, *275*, 18108-18113.

115. Kono, K., Tanaka, M., Mizuno, T., Kodama, K., Ogita, T., Kohama, T., B-5354a, b and c, new sphingosine kinase inhibitors, produced by a marine bacterium: Taxonomy, fermentation, isolation, physico-chemical properties and structure determination, *J. Antibiot. (Tokyo)* **2000**, *53*, 753-758.

116. Kono, K., Tanaka, M., Ogita, T., Kohama, T., Characterization of B-5354c, a new sphingosine kinase inhibitor, produced by a marine bacterium, *J. Antibiot. (Tokyo)* **2000**, *53*, 759-764.

117. Pchejetski, D., Doumerc, N., Golzio, M., Naymark, M., Teissie, J., Kohama, T., Waxman, J., Malavaud, B., Cuvillier, O., Chemosensitizing effects of sphingosine kinase 1 inhibition in prostate cancer cell and animal models, *Mol. Cancer Ther.* **2008**, *7*, 1836-1845.

118. Kono, K., Tanaka, M., Ogita, T., Hosoya, T., Kohama, T., F-12509a, a new sphingosine kinase inhibitor, produced by a discomycete, *J. Antibiot. (Tokyo)* **2000**, *53*, 459-466.

119. Bonhoure, E., Lauret, A., Barnes, D. J., Martin, C., Malavaud, B., Kohama, T., Melo, J. V., Cuvillier, O., Sphingosine kinase 1 is a downstream regulator of imatinib-induced apoptosis in chronic myeloid leukemia cells, *Leukemia* **2008**, *22*, 971-979.

120. Bonhoure, E., Pchejetski, D., Aouali, N., Morjani, H., Levade, T., Kohama, T., Cuvillier, O., Overcoming MDR-associated chemoresistance in HL-60 acute myeloid leukemia cells by targeting sphingosine kinase 1, *Leukemia* **2006**, *20*, 95-102.

121. Kono, K., Tanaka, M., Ono, Y., Hosoya, T., Ogita, T., Kohama, T., S-15183a and b, new sphingosine kinase inhibitors, produced by a fungus, *J. Antibiot. (Tokyo)* **2001**, *54*, 415-420.

122. French, K. J., Upson, J. J., Keller, S. N., Zhuang, Y., Yun, J. K., Smith, C. D., Antitumor activity of sphingosine kinase inhibitors, *J. Pharmacol. Exp. Ther.* **2006**, *318*, 596-603.

123. Paugh, S. W., Paugh, B. S., Rahmani, M., Kapitonov, D., Almenara, J. A., Kordula, T., Milstien, S., Adams, J. K., Zipkin, R. E., Grant, S., Spiegel, S., A selective sphingosine kinase 1 inhibitor integrates multiple molecular therapeutic targets in human leukemia, *Blood* **2008**, *112*, 1382-1391.

124. Kapitonov, D., Allegood, J. C., Mitchell, C., Hait, N. C., Almenara, J. A., Adams, J. K., Zipkin, R. E., Dent, P., Kordula, T., Milstien, S., Spiegel, S., Targeting sphingosine kinase 1 inhibits Akt signaling, induces apoptosis, and suppresses growth of human glioblastoma cells and xenografts, *Cancer Res.* **2009**, *69*, 6915-6923.

125. Xiang, Y., Asmussen, G., Booker, M., Hirth, B., Kane, J. L., Jr., Liao, J., Noson, K. D., Yee, C., Discovery of novel sphingosine kinase 1 inhibitors, *Bioorg. Med. Chem. Lett.* **2009**, *19*, 6119-6121.

126. Xiang, Y. B., Hirth, B., Kane, J. L., Liao, J. K., Noson, K. D., Yee, C., Asmussen, G., Fitzgerald, M., Klaus, C., Booker, M., Discovery of novel sphingosine kinase-1 inhibitors. Part 2, *Bioorg. Med. Chem. Lett.* **2010**, *20*, 4550-4554.

127. Mathews, T. P., Kennedy, A. J., Kharel, Y., Kennedy, P. C., Nicoara, O., Sunkara, M., Morris, A. J., Wamhoff, B. R., Lynch, K. R., Macdonald, T. L., Discovery, biological evaluation, and structure-activity relationship of amidine based sphingosine kinase inhibitors, *J. Med. Chem.* **2010**, *53*, 2766-2778.

128. Kennedy, A. J., Mathews, T. P., Kharel, Y., Field, S. D., Moyer, M. L., East, J. E., Houck, J. D., Lynch, K. R., Macdonald, T. L., Development of amidine-based sphingosine kinase 1 nanomolar inhibitors and reduction of sphingosine-1-phosphate in human leukemia cells, *J. Med. Chem.* **2011**, *54*, 3524-3548.

129. French, K. J., Zhuang, Y., Maines, L. W., Gao, P., Wang, W. X., Beljanski, V., Upson, J. J., Green, C. L., Keller, S. N., Smith, C. D., Pharmacology and antitumor activity of ABC294640, a selective inhibitor of sphingosine kinase 2, *J. Pharmacol. Exp. Ther.* **2010**, *333*, 129-139.

130. Kim, J. W., Kim, Y. W., Inagaki, Y., Hwang, Y. A., Mitsutake, S., Ryu, Y. W., Lee, W. K., Ha, H. J., Park, C. S., Igarashi, Y., Synthesis and evaluation of sphingoid analogs as inhibitors of sphingosine kinases, *Bioorg. Med. Chem.* **2005**, *13*, 3475-3485.

131. Lim, K. G., Sun, C. D., Bittman, R., Pyne, N. J., Pyne, S., (*R*)-FTY720 methyl ether is a specific sphingosine kinase 2 inhibitor: Effect on sphingosine kinase 2 expression in HEK 293 cells and actin rearrangement and survival of MCF-7 breast cancer cells, *Cell. Signal.* **2011**, *23*, 1590-1595.

Chapter 2 Design, synthesis, and biological evaluation of sphingosine kinase inhibitors

Attributions

Chapter 1 summarized published work by other investigators highlighting the importance of targeting S1P and developing SphK inhibitors for potential therapeutic use in various hyperproliferative disease states. This chapter discusses our contributions to this growing pool of inhibitors focusing on isoenzyme-selective SphK inhibitors to define the role of SphK1 and SphK2 more clearly.

This chapter was taken from two articles published in peer-reviewed journals (Raje, M. R.; Knott, K.; Kharel, Y.; Bissel, P.; Lynch, K. R.; Santos, W. L., *Bioorg*. *Med*. *Chem*. **2012**, *20*, 183-194 and Knott, K.; Kharel, Y.; Raje, M. R.; Lynch, K. R.; Santos, W. L., *Bioorg*. *Med*. *Chem*. *Lett*. DOI: 10.1016/j.bmcl.2012.01.050), a manuscript submitted to the Biochemical Journal and another manuscript that is in preparation for submission. The author of this dissertation performed a major portion of the work described in this chapter. He was responsible for all the design, synthesis, and characterization of the inhibitors. He performed the majority of the writing and editing of the manuscript submitted to *Bioorg*. *Med*. *Chem*. and the manuscript in preparation for submission. He also performed substantial amount of editing of the manuscript submitted to *Bioorg*. *Med*. *Chem*. *Lett*. All the biological work described in this chapter was performed by Dr. Yugesh Kharel, a postdoctoral associate in Dr. Kevin Lynch's lab at the University of Virginia. The author was responsible for analyzing and plotting the raw data.

2.1. Design of inhibitors

The design of SphK inhibitors has been hindered by the lack of a crystal structure of the enzyme. Conventional methods of kinase inhibition, such as the use of adenosine analogues to target the ATP binding site, have only been mildly successful. The similarity of the ATP binding site in various related kinases renders such inhibitors non-selective and prone to off-target effects. In the case of SphK, the amino acid sequence of the ATP binding domain of SphK1 and SphK2 is conserved across a wide array of kinases belonging to the diacylglycerol (DAG) family making the ATP-targeting strategy especially unattractive. As a result, ligand-based inhibitor design is the most popular approach for finding new SphK inhibitors.

The emergence of Fingolimod (FTY720) as a potent and orally bioavailable immunomodulatory agent generated immense interest in S1P biology by revealing novel therapeutic targets within the S1P pathway (Figure 2.1). Since then, FTY720 has been

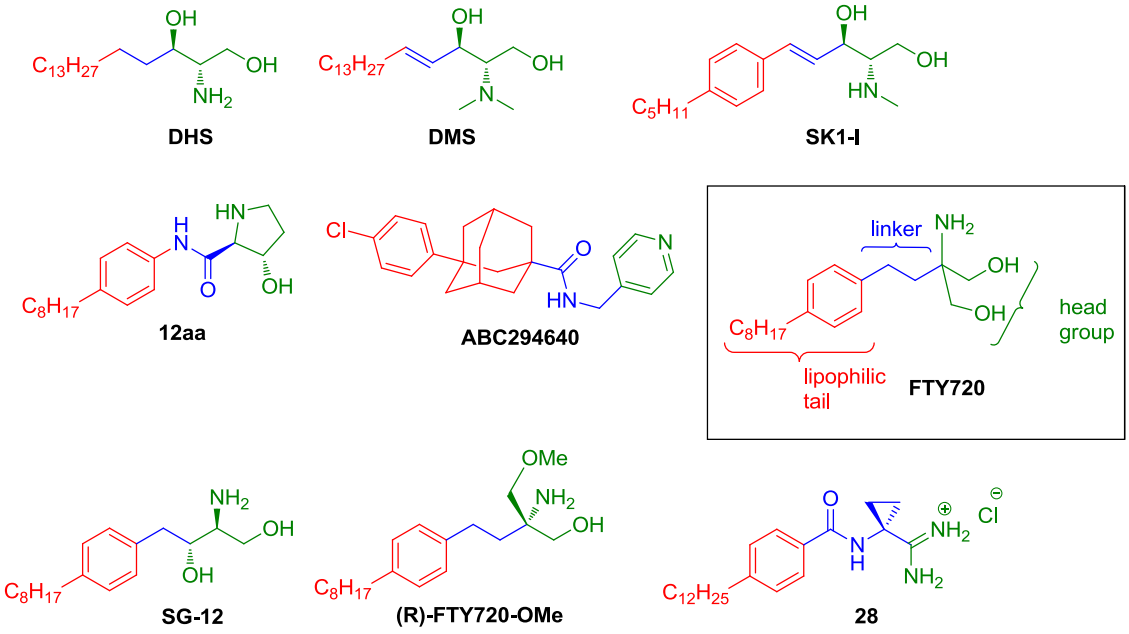

Figure 2.1. Sphingosine kinase inhibitors in the literature

used as the basis for the design of numerous S1P receptor agonists[1] and SphK dual inhibitors.[2] These FTY720 analogues have provided valuable insight into the structural requirements necessary for sphingosine phosphorylation since FTY720 is a SphK2 substrate. Synthesis of conformationally biased analogues[3] indicated that SphK shows a high degree of stereoselectivity in substrate recognition.[4] Careful structural analysis of these inhibitors (Figure 2.1) revealed a highly lipophilic "tail" as a key characteristic feature of SphK inhibitors (shown in red). Also noteworthy is that all inhibitors possessed a polar headgroup (shown in green). The lipophilic tail and the head group were then connected by a "linker" (shown in blue) that was either highly flexible (alkyl linker) or slightly rigid (alkenyl or amide linker). Previous studies[3] by the Macdonald group at the University of Virginia showed that restricting the conformations of the three bonds linking the amino headgroup and the phenyl moiety produced better agonists compared to FTY720 with the flexible linker (Figure 2.2). Thus, in our study, we chose to incorporate a rigid cyclohexyl linker so that the spatial orientation of the head group allows it to better interact with the binding pocket. We planned to employ various surrogate head groups attached to the cyclohexane ring which would interact with the enzyme binding pocket. To avoid the possibility of our inhibitors acting as kinase substrates, we deleted the hydroxyl groups in the FTY720 structure. We also observed that there were a total of 18 carbons from the end of the hydrophobic tail to the head group. This observation

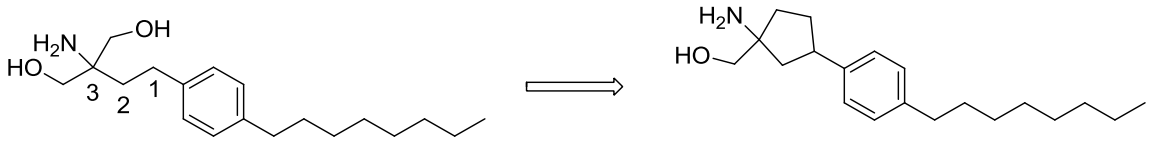

Figure 2.2. Conformational restriction of FTY720

allowed us to fix the length of the hydrocarbon chain to 12 carbons. Looking at the various inhibitors in the literature, we incorporated the (*p*-octyl) phenyl as our hydrophobic tail. These structural modifications provided a template for the synthesis of our inhibitors (Figure 2.3).

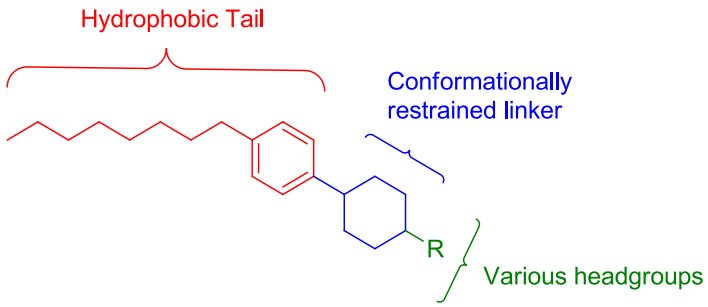

Figure 2.3. Template for inhibitor design

2.2. Synthesis of inhibitors for preliminary screening

After careful scrutiny of various inhibitors reported in the literature, we noticed that all inhibitors possessed a basic amine functionality. Based on this observation, we hypothesized that the presence of an amine head group is vital for our compounds to act as SphK inhibitors. Thus, we examined head groups bearing different functionalities to verify this hypothesis. To generate a library with different headgroups but the same tail and linker, we envisioned a divergent synthesis using substituted cyclohexanone **3** as a key intermediate (Scheme 2.1). This was a good strategy because a ketone functional group is an excellent synthetic handle and can be readily and quickly converted into a range of other moieties.

Thus, lithium-halogen exchange of aryl bromide **1** with *n*-butyllithium followed by reaction with 1,4-cyclohexanedione monoethylene ketal afforded tertiary alcohol **2** in 75% yield. Dehydration, hydrogenation of the resulting alkene and deprotection of the

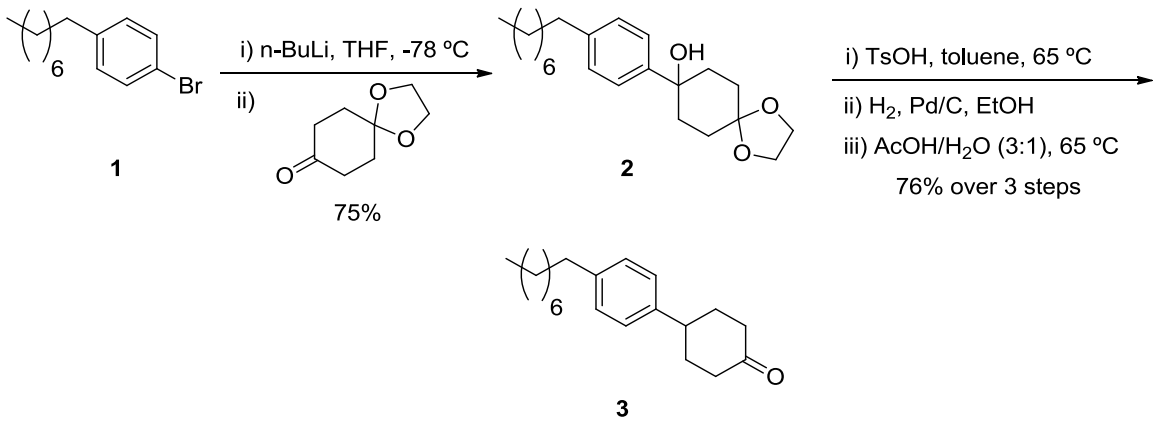

Scheme 2.1. Synthesis of intermediate **3**

spiroketal[5] smoothly provided ketone **3** in 76% yield over 3 steps. Ketone **3** was then converted into compounds **4-9**, each consisting of different functionalities on the cyclohexane ring (Scheme 2.2). A Strecker reaction converted the ketone into the corresponding amino-nitrile **4**. A Horner-Wadsworth-Emmons olefination of **3** generated the α,β-unsaturated ester **5** which was subsequently reduced to allylic alcohol **6** using DIBAL-H. Treatment of **3** with nitromethane and sodium ethoxide afforded the nitro-alcohol **7** while oxime **8** was obtained by condensation of the ketone with hydroxylamine hydrochloride. Sodium borohydride reduction of **3** yielded the *trans* secondary alcohol **9** as the major product. Reductive amination of **3** with benzylamine and lithium borohydride provided the *trans* secondary amine; removal of the benzyl group by catalytic hydrogenation produced the primary amine **10k**. Each of the compounds **4-10k** have different head groups (shown in green) and their inhibition activities would allow us to verify our initial hypothesis.

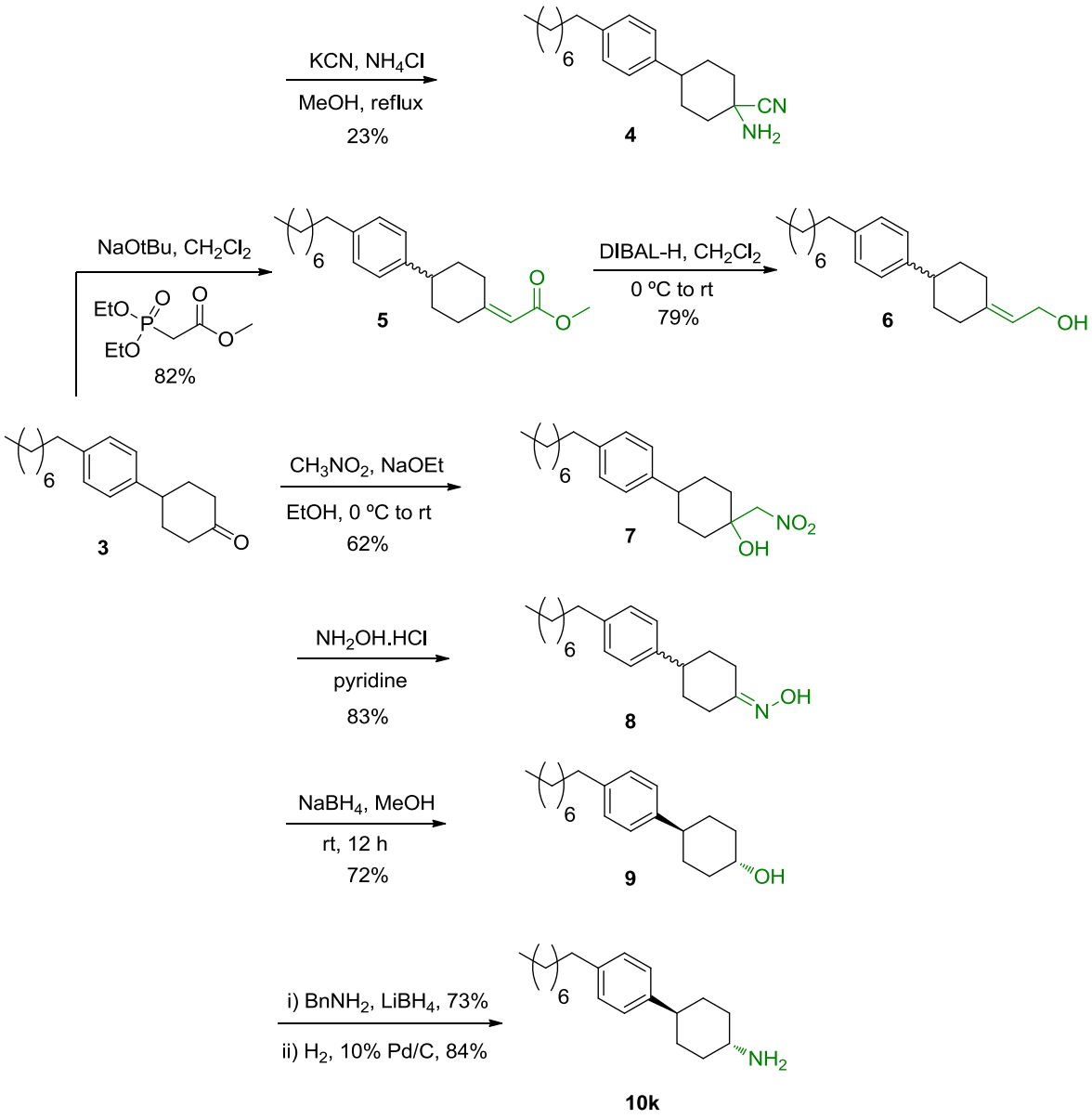

Scheme 2.2. Installation of different headgroups for preliminary screening

2.3. SphK assay

Compounds were evaluated for SphK1 and SphK2 inhibition in the laboratory of our University of Virginia collaborator Professor Kevin Lynch (Department of Pharmacology). Assays were performed by his postdoctoral associate Dr. Yugesh Kharel. The exact conditions for the assay are described in the experimental section

(Chapter 3.3.1). Briefly, human SphK1 and mouse SphK2 cDNAs were used to generate recombinant baculoviruses that encoded the respective proteins. Infection of Sf9 insect cells with the viruses for 72 h resulted in >1000-fold increase in SphK activity in 10,000 x g supernatant fluid from homogenized cell pellets. The infected Sf9 cell extract containing 2-3 μg protein was used as a source of enzyme in the assay. Radiolabeled enzyme products were detected by autoradiography and identified by migration relative to authentic standards. For quantification, the silica gel containing radiolabeled lipid was scraped into a scintillation vial and counted.

2.3.1. Preliminary screening assay

Compounds **4-10k** were tested in an *in vitro* inhibition assay against SphK1 and SphK2 with 5-10 μM sphingosine. The compounds were initially screened at a concentration of 100 μM to identify lead structures that could potentially be improved. Possible inhibitors were defined as those able to inhibit at least 50% at 100 μM concentration. The results of this initial screening are summarized in Chart 2.1.

As shown in the chart, only the primary amine **10k** showed greater than 50% inhibition. All other compounds with different headgroup functionalities showed little or no inhibition. This supports our hypothesis about the requirement of an amine in the headgroup. Encouraged by these results, we decided to investigate the activity of 4-(4-octylphenyl) cyclohexanamine derivatives.

2.4. Stereoselective reductive amination

Keeping in mind the stereoselective kinase recognition,[4] we hypothesized that the biological activity of *cis*/*trans* 4-(4-octylphenyl)cyclohexanamine derivatives would be different because of their spatial orientation. We were thus confronted with the stereoselective synthesis of a series of *N*-alkyl-4-(4-octylphenyl)cyclohexanamines.

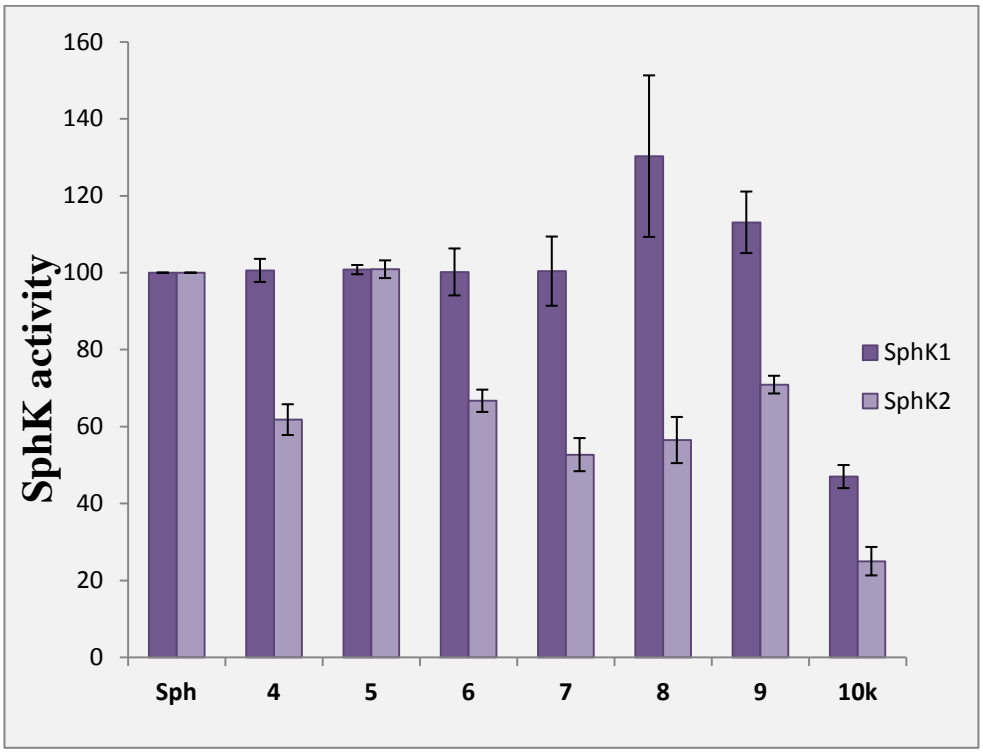

Chart 2.1. Preliminary screening results

The reduction of related cyclohexanones to the corresponding cyclohexanols using metal hydrides has been well-studied.[6,7] Similar principles can be applied to the reduction of cyclic imine derivatives: hindered hydride reagents selectively provide axial amines and small reagents prefer axial attack to provide the more stable equatorial product.[8] Previous stereochemical studies were focused on the effect of the position of substituents on the cyclohexylimines, most notably the conformationally biased 4-*tert*-butyl cyclohexylimine.[9] However, there were no published reports on the stereoselectivity of reductive amination in case of 4-phenylcyclohexylimine, where the substituent preference for equatorial orientation is not as strong. Reductive amination studies using cyclic secondary amines suggested additional effects of nitrogen substituents on the direction of hydride attack.[8] In short, a systematic investigation using

a series of primary amines had not been reported. Furthermore, few studies employed stereoselective reductive amination of 4-substituted cyclohexanones without isolation of the intermediate imine.[10-12] Thus, we investigated whether the identity of the amine group has an effect on the stereoselectivity of the resulting reduction reaction. This was the first systematic reductive amination study of 4-(4-octylphenyl) cyclohexanone with a variety of primary amines to selectively provide either the *cis* or *trans* isomer using various borohydride reducing agents (Scheme 2.3).

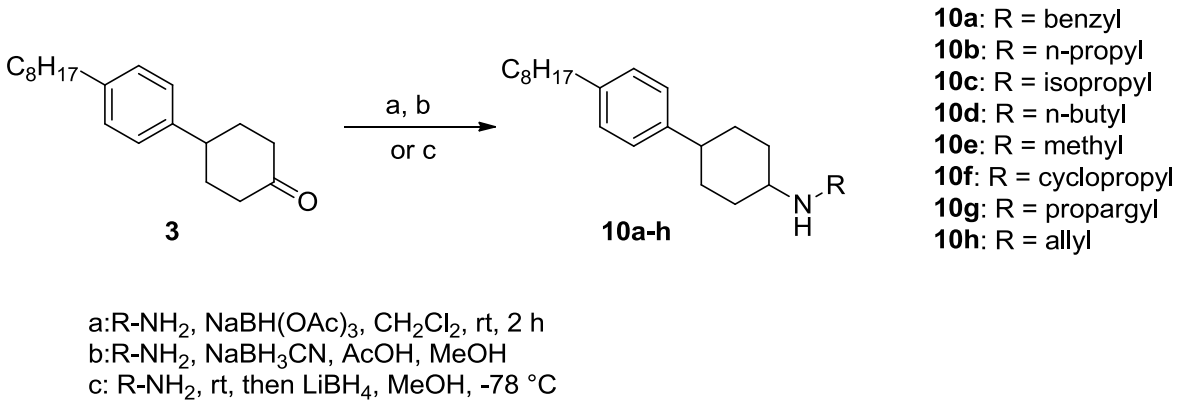

Scheme 2.3. Reductive amination using various reducing agents

In considering reagents for reductive amination, we desired a more convenient "direct" method[13] that did not require the isolation of the imine/iminium salt. Isolation of the iminium salt could be cumbersome and incomplete formation of the imine could lead to a competing ketone reduction depending on the reducing agent used. This was avoided by shifting the equilibrium using excess amine. Thus, cyclohexanone **3** was reacted with various primary amines to form the corresponding imine *in situ*, which was reduced in the presence of borohydride reducing agents to produce *cis*/*trans*-**10**. The results of the reductive amination are summarized in Table 2.1.

Table 2.1. Stereoselectivity of reductive amination reactions

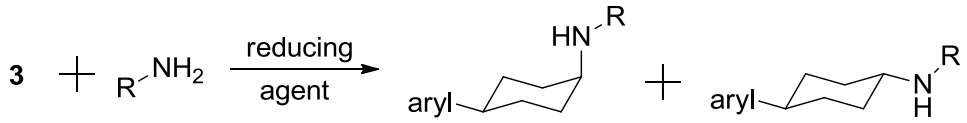

Entry	Amine	*cis*:*trans* ratio[a] (yield, %)		
		$NaBH(OAc)_3$[b]	$NaCNBH_3$[b]	$LiBH_4$[c]
10a	CH_3NH_2	71:29 (77)	34:66 (71)	4:96 (99)
10b	$^{n}PrNH_2$	66:34 (66)	36:64 (69)	8:92 (95)
10c	$^{i}PrNH_2$	69:31 (64)	41:59 (70)	6:94 (97)
10d	$^{n}BuNH_2$	64:36 (68)	39:61 (69)	9:91 (99)
10e	$BnNH_2$	69:31 (74)	21:79 (82)	4:96 (88)
10f	Cyclopropyl amine	70:30 (66)	38:62 (70)	5:95 (97)
10g	Propargyl amine	70:30 (75)	32:68 (67)	4:96 (98)
10h	Allylamine	78:22 (63)	37:63 (64)	5:95 (94)

[a] Ratios determined by GC-MS analysis of crude reaction mixture. [b] Combined isolated yield of *cis* and *trans* products. [c] GC yield.

Sodium triacetoxyborohydride,[14] a sterically hindered hydride reagent, provided modest *cis* selectivity as a result of equatorial hydride attack. The increase in size of the alkyl substituent on the intermediate imine had no effect on the stereoselectivity of the reaction (entries **10a**-**10h**). In general, the *cis* product was favored (about 2:1 over *trans*). In contrast, when the less hindered sodium cyanoborohydride was used, the *trans* product dominated. To further improve the *trans* selectivity of the reaction, we employed lithium borohydride as the reducing agent.[11] Indeed, at –78 °C in methanol, $LiBH_4$ afforded >9:1 ratio of equatorial to axial amine products. Moreover, we did not observe any reduction

of **3** to the corresponding alcohol. With all of the borohydride reducing agents used, to our delight, stereoselectivity of the reductive amination was dictated by reducing agent and tolerated functionalized amines of varying size. $LiBH_4$ was the most selective reagent to produce primarily the *trans* product. Also, the size of the substituent on the nitrogen of the cyclohexylimine had no effect on the stereoselectivity of the reduction. The stereoselectivity of the reductive amination can be explained based on the steric approach control and torsional strain control.[8]

2.4.1. Explanation of stereoselectivity

Equatorial attack in the case of non-bulky hydride donors results in torsional strain as the nitrogen passes through an eclipsed conformation (Figure 2.4A). Torsional strain is avoided in the axial attack since the nitrogen moves away from the equatorial hydrogens (Figure 2.4B). It results in predominant formation of the *trans* product.

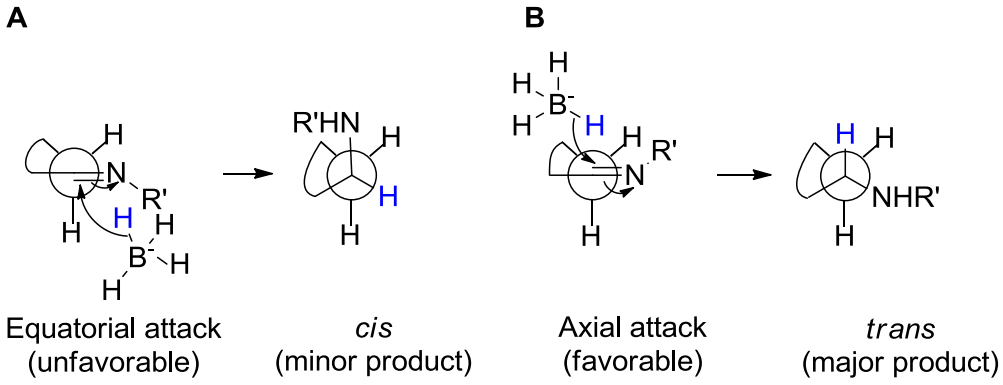

Figure 2.4. Stereoselectivity in reductive amination with non-bulky hydrides

Bulky hydride donors prefer the equatorial direction of approach (Figure 2.5A) compared to the axial direction (Figure 2.5B) to avoid the steric strain between the borohydride reagent and the axial hydrogens. It results in predominant formation of the *cis* product.

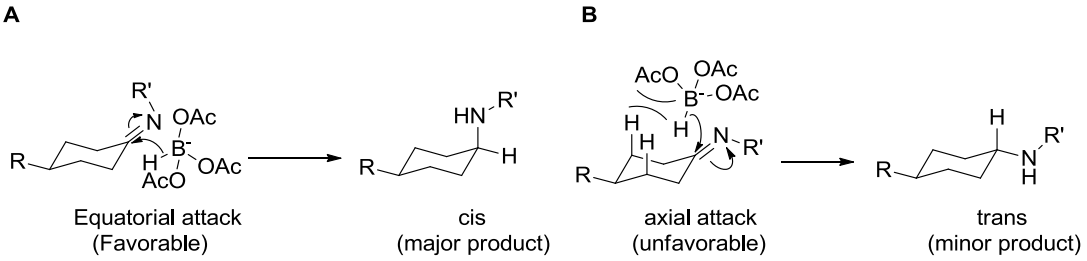

Figure 2.5. Stereoselectivity in reductive amination with sterically hindered hydrides

2.4.2. Identification of *cis* and *trans* isomers

The identity of the *cis* and *trans* isomers was determined by studying the chemical shift and analyzing the splitting pattern of the proton on the carbon bearing the amine group on the cyclohexane ring in the ^{1}H NMR spectrum. The equatorial proton in the *cis* isomer (2.98 ppm) is downfield compared to the axial proton in the *trans* isomer (2.69 ppm) due to magnetic anisotropy. The presence of the equatorial proton within the deshielding cone of the C2—C3 bond causes it to shift downfield (Figure 2.6). The *cis* and *trans* isomers also show distinct splitting patterns in the ^{1}H NMR spectrum. For example, a clearly defined triplet of triplets is observed for *trans*-**10c** (Figure 2.7). This splitting pattern is caused by strong coupling (^3J = 11.8 Hz) of axial H_a to neighboring axial protons and weak coupling (^3J = 3.6 Hz) to neighboring equatorial protons. In contrast, for the *cis*-**10c** isomer, the signal for equatorial H_e is a multiplet as a result of weak equatorial-equatorial and equatorial-axial spin coupling (Figure 2.8).

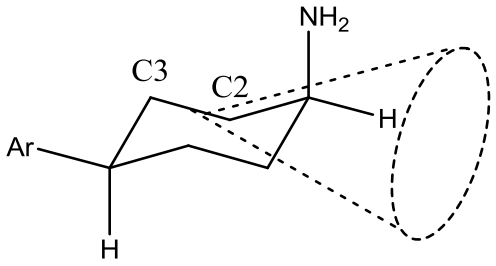

Figure 2.6. Deshielding of equatorial proton in a cyclohexane ring

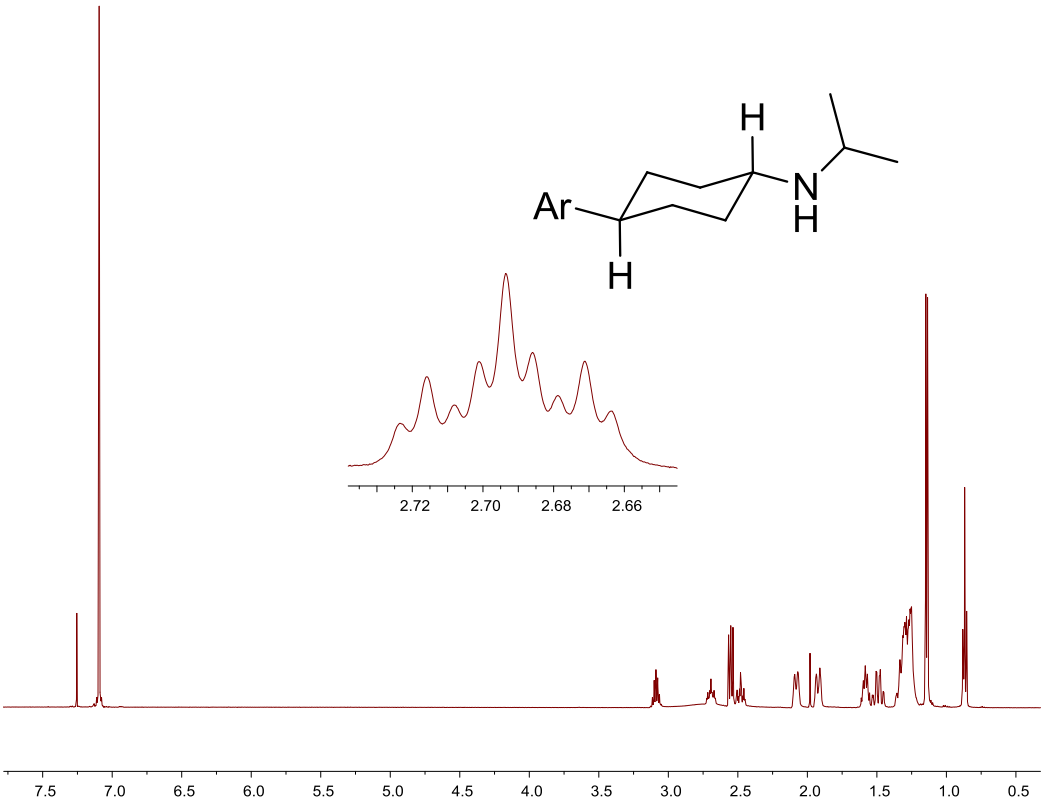

Figure 2.7. ^{1}H NMR spectrum of ***trans*-10c** showing the splitting pattern

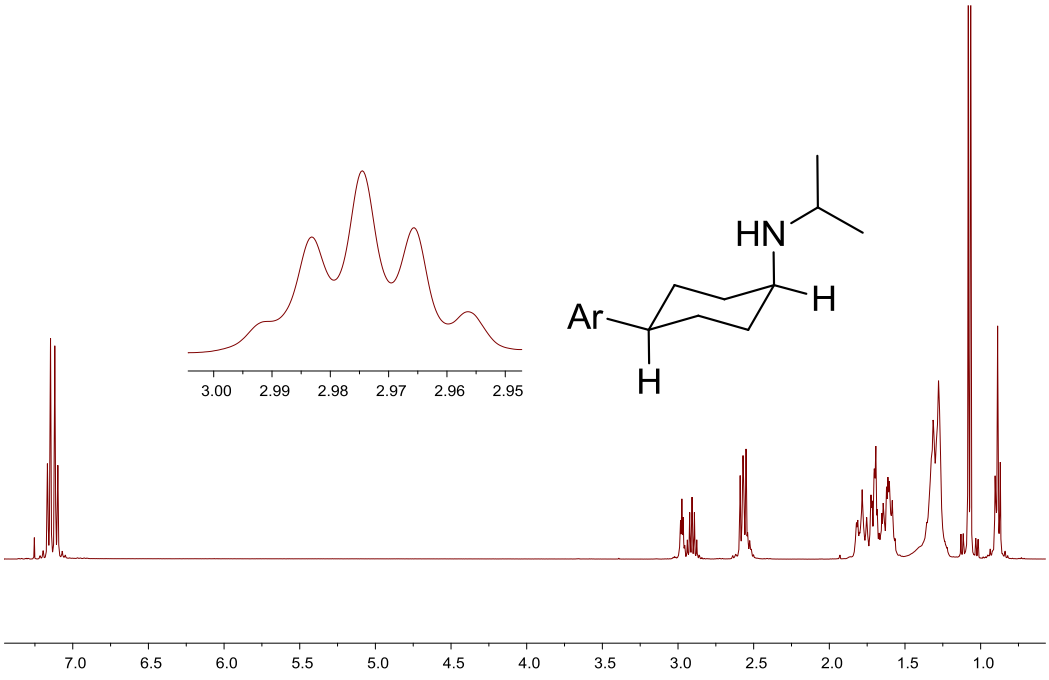

Figure 2.8. ^{1}H NMR spectrum of ***cis*-10c** showing the splitting pattern

2.4.3. GC analysis of reductive amination reactions

The ratio of *cis* and *trans* isomers could not be determined by integration of the ^{1}H NMR peaks due to signal overlap. Hence, GC analysis was used to determine the isomer ratio of the crude product mixture using authentic sample as standard. The *cis* and

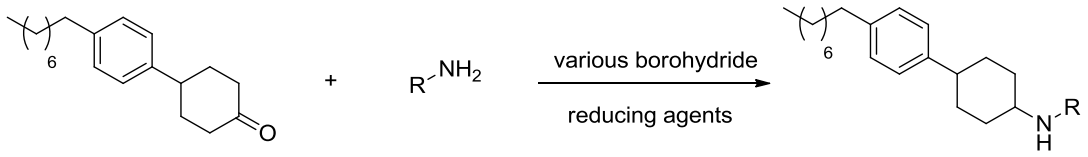

Table 2.2. Retention times for the *cis* and *trans* isomers of various *N*-substituted 4-(4-octylphenyl) cyclohexylamines

R group	Retention time R_t (min)	
	cis	*trans*
Methyl	13.88	14.05
n-Propyl	15.18	15.67
Isopropyl	14.46	14.84
n-Butyl	16.37	17.10
Benzyl	26.11	28.37
Cyclopropyl	14.53	15.12
Propargyl	15.72	16.02
Allyl	15.25	15.68

trans isomers of various *N*-substituted 4-(4-octylphenyl) cyclohexylamines displayed different retention times on the GC (Table 2.2). Thus, injection of the crude reaction mixture provided us the ratio of the two isomers. After the unequivocal identification of isomers based on ^{1}H NMR, the pure isomers were used as standards in the GC to

determine the product ratio. The GC traces of the purified *cis* and *trans* isomers and the crude reaction mixture are depicted in Figure 2.9 and Figure 2.10, respectively.

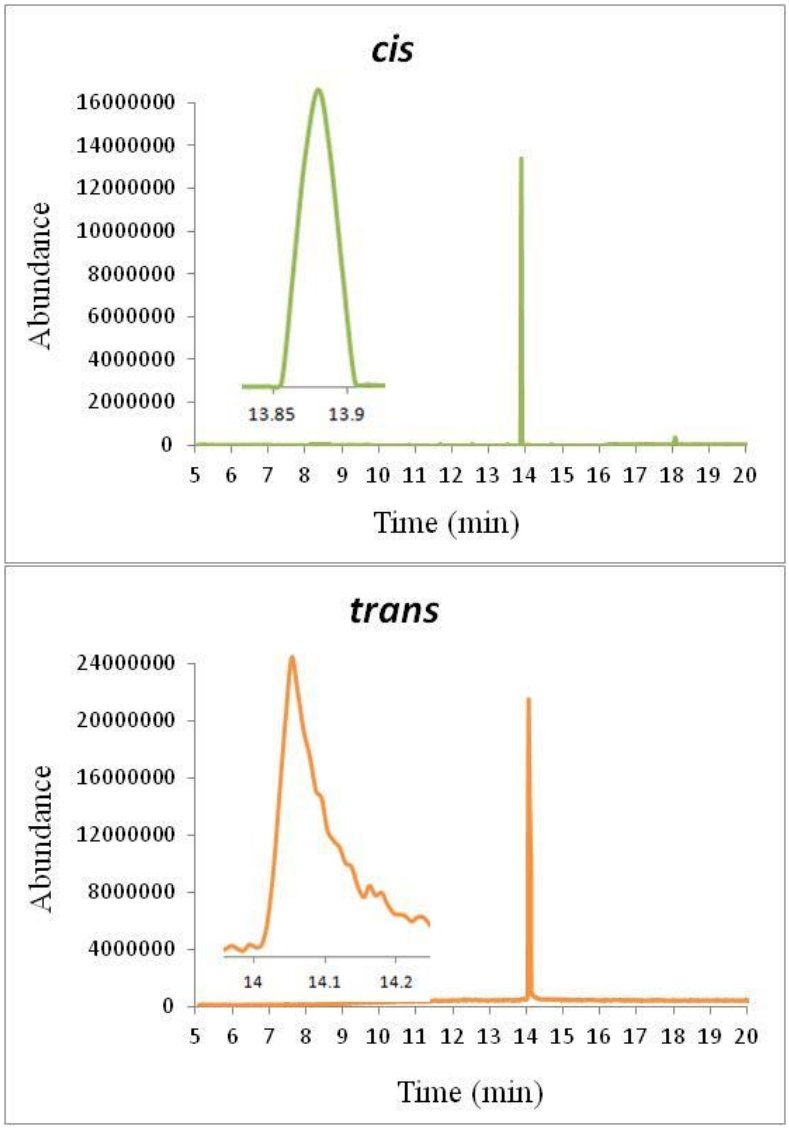

Figure 2.9. GC traces of purified *cis* (top) and *trans* (bottom) isomers

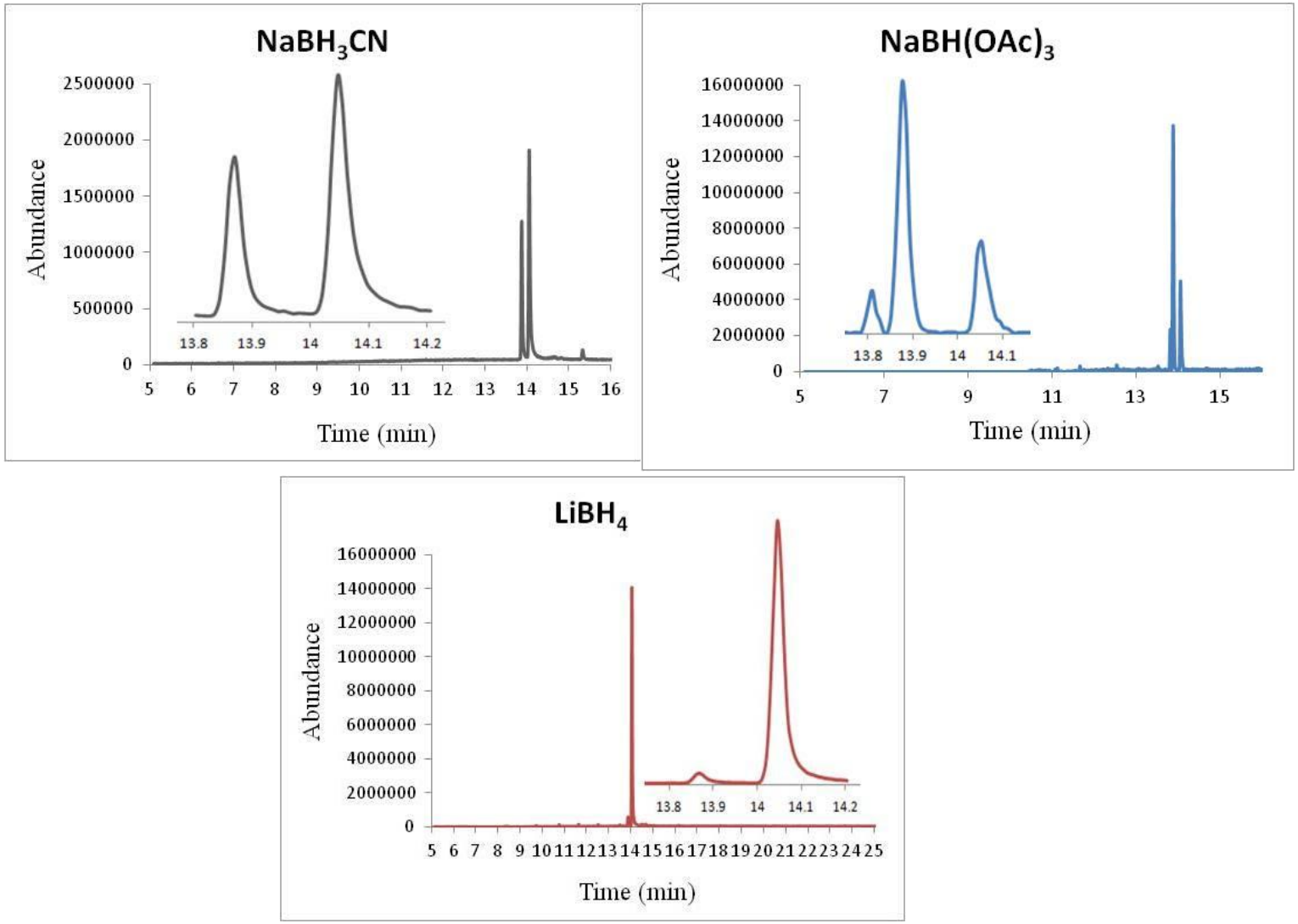

Figure 2.10. GC traces of reductive amination reactions with sodium cyanoborohydride (top left), sodium triacetoxyborohydride (top right), and lithium borohydride (bottom).

2.4.4. Biological evaluation of secondary amines

Secondary amines were synthesized following the procedure outlined in Scheme 2.3 (Figure 2.11). *Cis* and *trans* isomers of each amine were tested separately in the biological assay. The results are displayed in Chart 2.2. The *trans* isomers of secondary amines **10a–d** and **10h** were significantly more potent inhibitors of SphK1 than the corresponding *cis* isomers. In the case of compounds **10e, 10f** and **10g**, both isomers were largely ineffective while for compound **10i**, both isomers were equally effective. Against SphK2, however, different trends were observed. For compounds **10b**, **10d**, and **10h**, the *trans* isomer was significantly more active than the *cis* isomer. However, for compounds **10a**, **10c**, **10e**, and **10i**, both the *cis* and *trans* isomers were equally effective. Interestingly, both isomers of compounds **10f–g** were largely inactive; the origin of the unfavorable interaction with the cyclopropyl and propargyl groups is currently not clear.

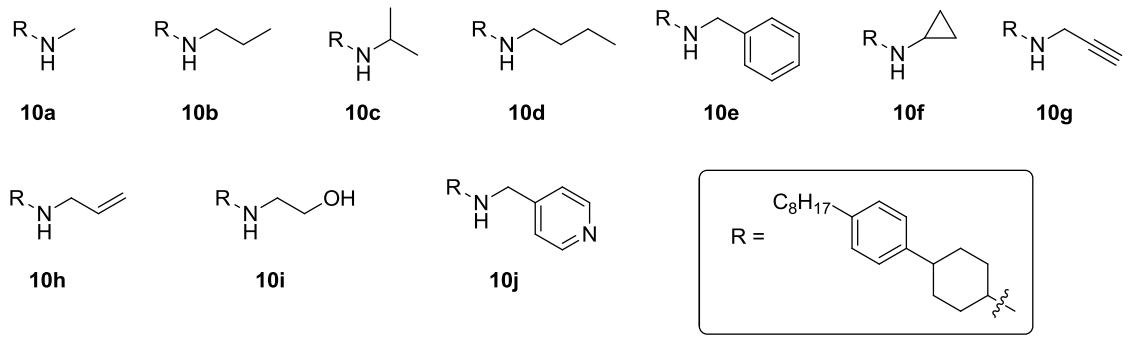

Figure 2.11. Secondary amines synthesized by reductive amination

2.5. Higher order amines

To diversify our inhibitors further, we modified the head group by converting the secondary amines into higher order amines.

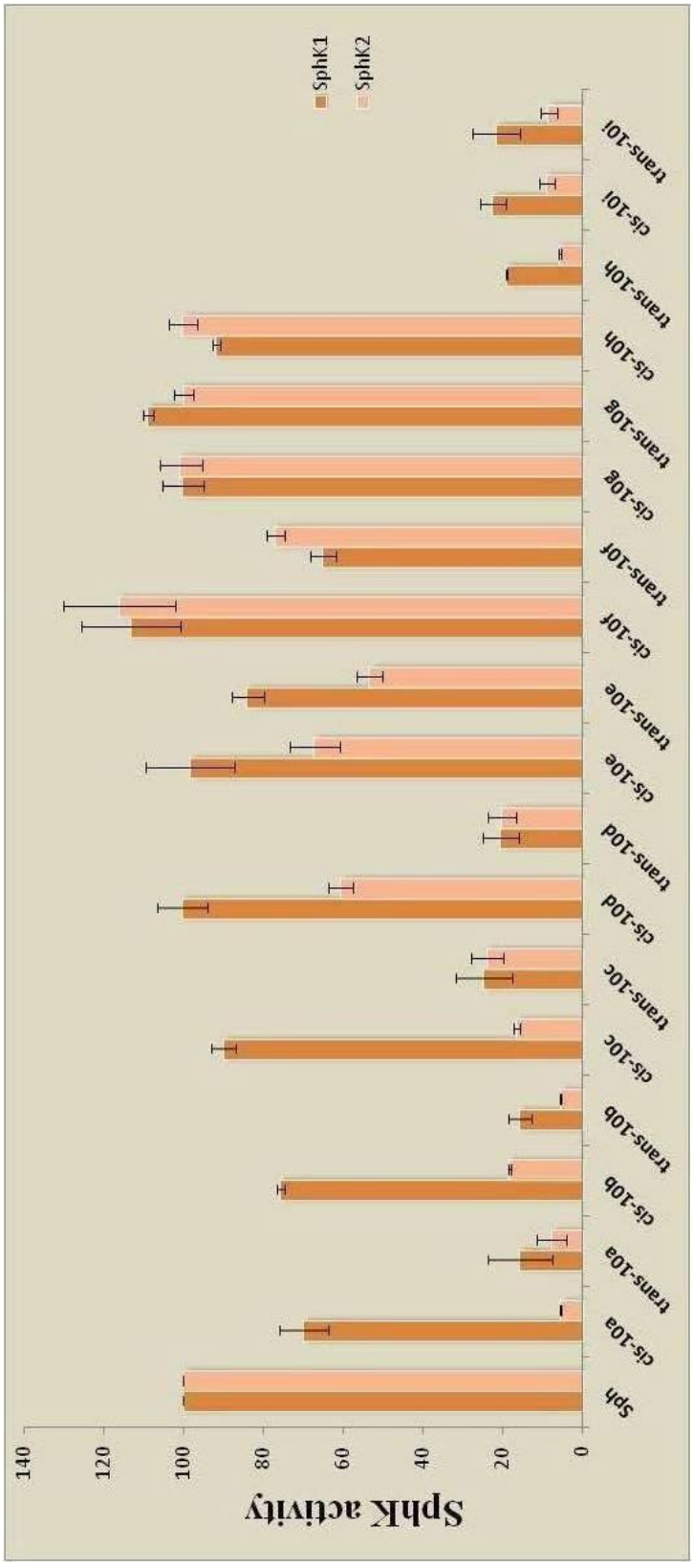

Chart 2.2. Inhibition data for secondary amines

2.5.1. Tertiary amines

Secondary amines **10a-c** were transformed into tertiary methyl amines **11a-c** by an Eschweiler-Clarke reaction (Scheme 2.4).[15] The secondary amine was reacted with paraformaldehyde and formic acid in refluxing methanol to form the methyl tertiary amine. The tertiary amines synthesized were evaluated for their inhibitory activity (Figure 2.12).

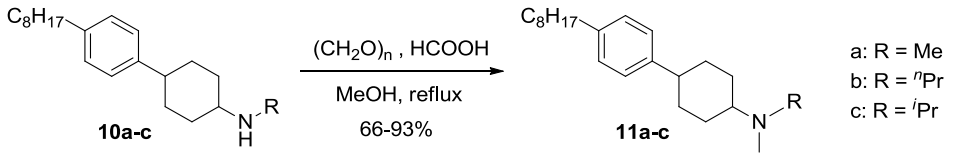

Scheme 2.4. Synthesis of tertiary amines via an Eschweiler-Clarke reaction

The results of the inhibition assay are summarized in Chart 2.3. We compared the activity of the tertiary amines to the corresponding secondary amines. We observed that a majority of tertiary amines **11** were far less active than the secondary amines **10**. A notable exception was *trans*-**11a** being more selective for SphK2 compared to *trans*-**10a**. Since amines are protonated at physiological pH, we hypothesized that the protonated

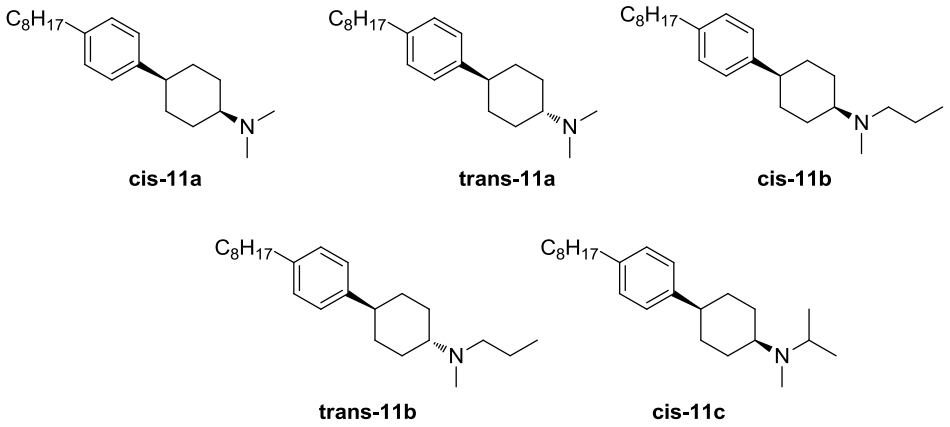

Figure 2.12. Tertiary amines synthesized

amines bind at the enzyme pocket primarily by electrostatic interaction. Conversion of the secondary amine to tertiary amine resulted in reduced basicity causing a decrease in the amount of protonated amine. The lower concentration of the protonated tertiary amine produced diminished interaction with the enzyme binding pocket compared to the secondary amine. As a result, tertiary amines were less active in comparison to the corresponding secondary amines. Due to the reduced activity of tertiary amines, the remaining secondary amines were not converted into tertiary amines.

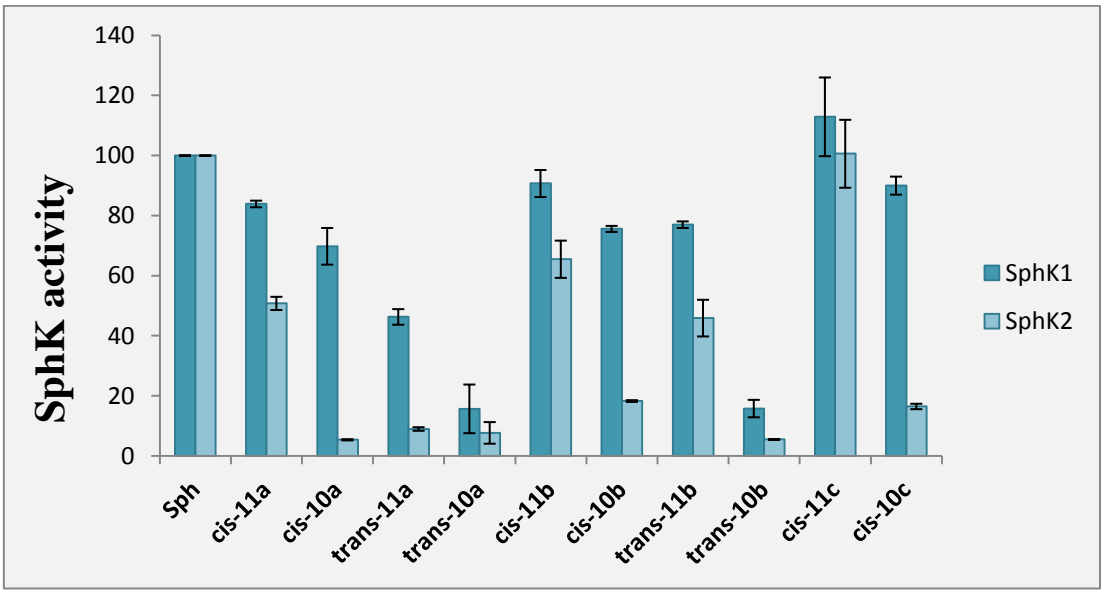

Chart 2.3. Inhibition data for tertiary amines

2.5.2. Quaternary ammonium salts

The tertiary amines **11a-c** were further converted into quaternary ammonium salts **12a-c** (Scheme 2.5). The remaining active secondary amines were converted directly into the quaternary ammonium salts **12e, 12h,** and **12i** by reaction with methyl iodide in the presence of potassium carbonate. These quaternary ammonium salts were discovered to be as effective inhibitors of SphK1/2 as the secondary amines (Figure 2.13). Consistent with the results with secondary amines, *trans* isomers were more potent than *cis* isomers,

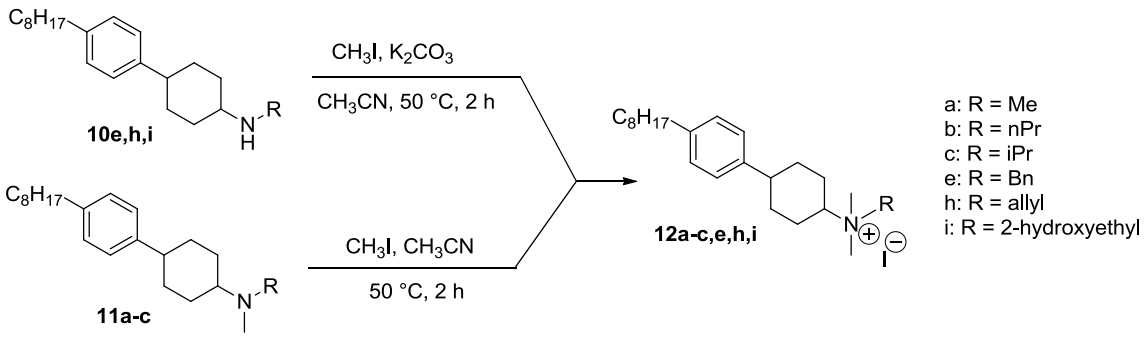

Scheme 2.5. Synthesis of quaternary ammonium salts

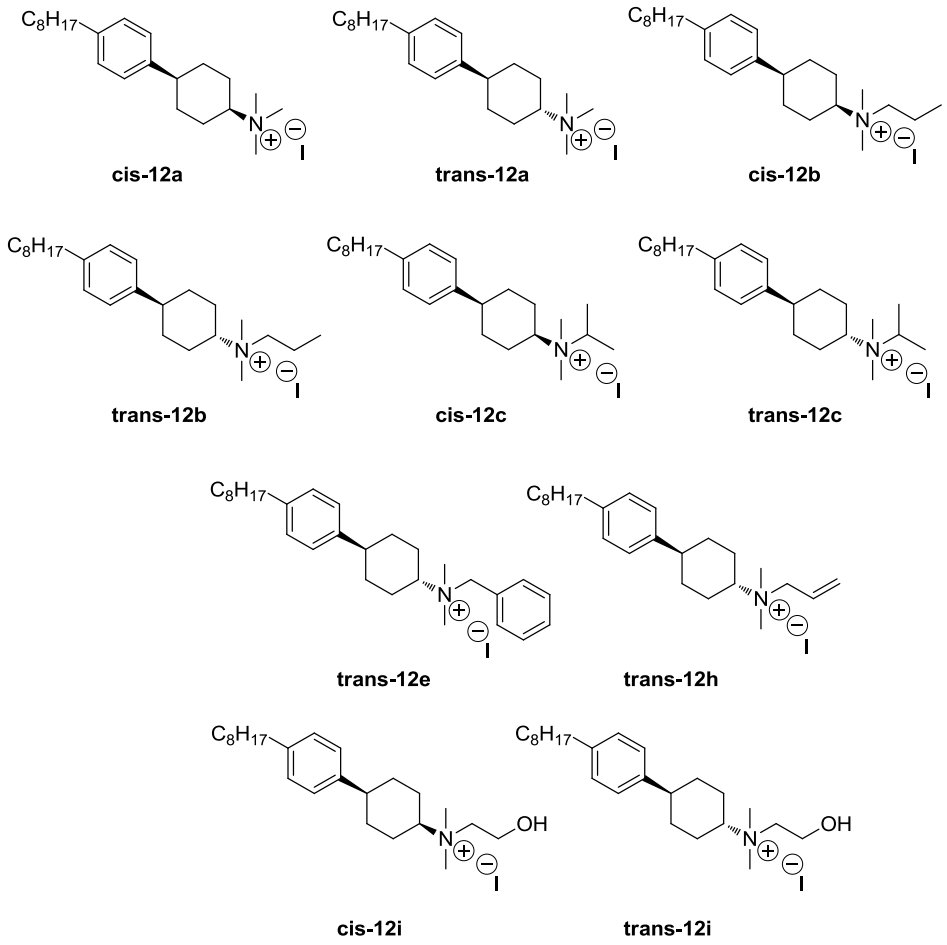

Figure 2.13. Quaternary ammonium salts synthesized

specifically with SphK1 (Chart 2.4). The data indicate that the *cis* isomers are selective towards SphK2, but follow-up assays at 10 μM inhibitor concentration revealed moderate inhibition against SphK2. Because quaternary ammonium salts have the desired water solubility and potential cell permeability, we proceeded to determine inhibition constants for the active quaternary ammonium salts.

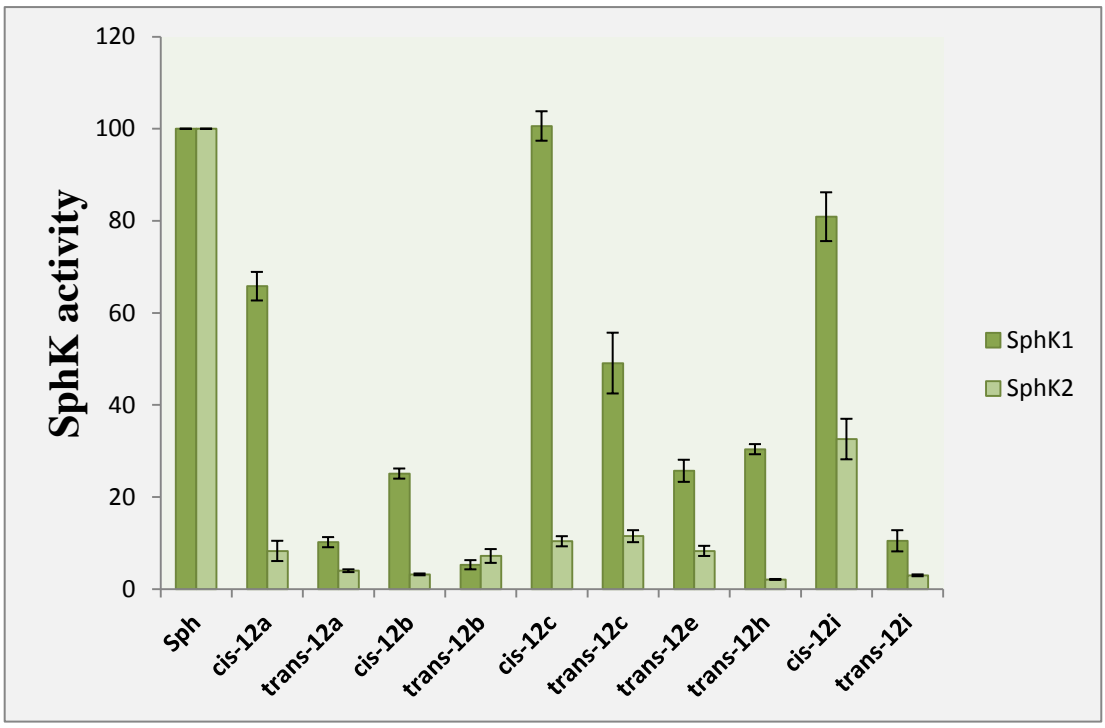

Chart 2.4. Inhibition data for quaternary ammonium salts

2.6. Inhibition constants

The single point assays described previously helped us identify possible inhibitors. To confirm the potencies of select compounds identified as hits, their K_i values were determined. The two kinases SphK1 and SphK2 have different K_m values for sphingosine. For the determination of the K_m for sphingosine, the concentration of ATP was fixed at 250 μM and sphingosine was varied from 0-50 μM. The K_m values were 10 μM and 5 μM for SphK1 and SphK2, respectively, in good agreement with previously

reported values of 5-17 μM for SphK1[16,17] and 3-5 μM for SphK2.[18] Next, the concentration of sphingosine was fixed at the K_m value (i.e., 10 μM for SphK1 and 5 μM for SphK2) and the inhibitor concentration was varied to generate a dose response curve. Then, the ideal inhibitor concentration for determining the K_i value was determined (~50% inhibition near the K_m for sphingosine).

Determination of K_i values typically requires varying substrate concentration at multiple inhibitor concentrations. However, this method is time-consuming, tedious, and requires large quantities of inhibitors. In addition, this method requires the use of pure enzyme which adds to the cost. Therefore, to save time, effort, and money, an alternate method for determining K_i was developed.[19] SphK kinetic constants were obtained by measuring the initial velocity of catalysis (less than 5% of the substrate was consumed) using highly expressed crude enzyme and fitting the data to the Michaelis-Menten equation by non-linear regression using GraphPad Prism 5.01 (GraphPad Software). For competitive inhibitors, which show no change in the V_{max} value on addition of the inhibitor (*e.g.* Figure 2.14B), K_i was calculated using the following equation:[19]

$$K_i = [I]/(K'_m/K_m - 1)$$

where [I] is the concentration of inhibitor; and K'_m and K_m are the Michaelis-Menten constants in presence and absence of inhibitor, respectively. For non-competitive inhibitors, where V_{max} varied upon addition of the inhibitor (*e.g.* Figure 2.14A), K_i was calculated using the following equation:[19]

$$K_i = [I]/(V_{max}/V'_{max} - 1)$$

where V'_{max} and V_{max} are reaction velocities in presence and absence of inhibitors, respectively. The validity of this method was verified when determination of the K_i value

by independent variation of substrate and inhibitor concentration using pure enzyme resulted in no more than 10% variability compared to the method described above.

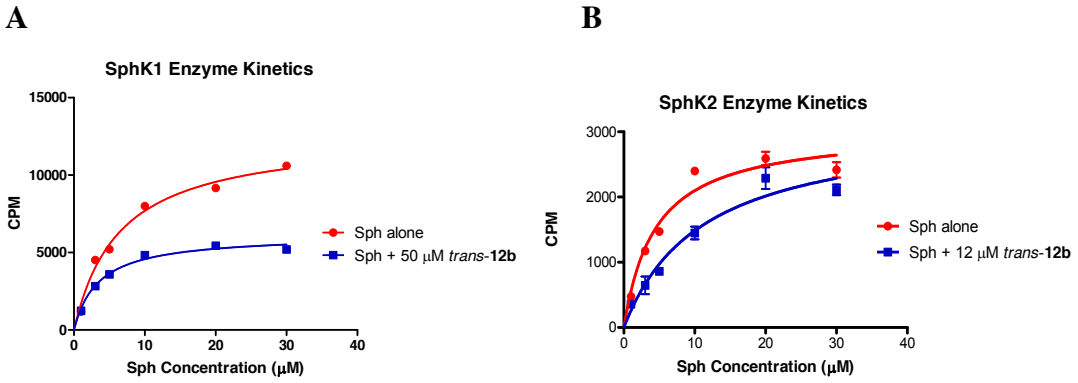

Figure 2.14. Enzyme kinetics for ***trans*-12b**

The K_i values are listed in Table 2.3. Because SphK1/2 have different K_m values (10 and 5 μM, respectively),[16,18] the selectivity ratios were normalized with the respective K_m values. These results suggest that quaternary ammonium salts are more potent and selective towards SphK2 relative to secondary amines (compare entries 1-3 vs. 4-7). Since the inhibitors interact with the binding pocket via an electrostatic interaction, quaternary salts, which carry a full-fledged positive charge, will interact more strongly than secondary amines, which are in equilibrium with the corresponding protonated amine. As the size of substituents on the amine increases, we found that the potency decreases, presumably as a result of increased steric interaction in the enzyme binding pocket. Among the quaternary ammonium salts tested, *trans*-**12a** and *trans*-**12b** are the most potent (K_i = 8 μM) and selective (~fourfold for *trans*-**12a** and threefold for *trans*-**12b**). To the best of our knowledge, this is the first demonstration[20] of a SphK inhibitor scaffold containing a quaternary amine, consistent with the observation that a positive charge is essential in SphK inhibitors.

Table 2.3. K_i values for select compounds

Entry	Compound	K_i (μM)		Selectivity[a]
		SphK1	SphK2	
1	*cis*-**10a**	>100	40 ± 6	-
2	*trans*-**10i**	22 ± 2	38 ± 5	1.23
3	*trans*-**10k**	32 ± 4	29 ± 5	0.55
4	*trans*-**12a**	60 ± 6	8 ± 2	3.75
5	*trans*-**12b**	47 ± 4	8 ± 1	2.94
6	*trans*-**12c**	>100	33 ± 7	-
7	*trans*-**12i**	70 ± 8	14 ± 2	2.5

[a] Selectivity = $(K_i/K_m)^{SphK1}/(K_i/K_m)^{SphK2}$

2.7. Intact cell assay and cell permeability studies

We next investigated the effect of our inhibitors in intact cells. Initially, S1P levels were measured in the presence of *trans*-**12a** and **12b** in U937 cells (human histiocytic leukemia cells) using LC/MS[21] and were found to be unchanged. To confirm SphK2 specific inhibition, exogenous FTY720 was added in these cells and the phosphorylation of FTY720 was monitored with or without compounds in cell extracts using LC/MS (Details of the LC/MS protocol are described in section 3.3.2). Because FTY720 is a specific substrate of SphK2, a decrease in FTY720-P concentration would suggest SphK2-selective inhibition. Gratifyingly, both compounds *trans*-**12a** and *trans*-**12b** significantly suppressed the production of FTY720-P (Figure 2.15A) and exaggerated the accumulation of FTY720 in cells (Figure 2.15B), which suggests that

trans-**12a** and **12b** inhibit SphK2. In addition, S1P-dependent Akt/ERK phosphorylation was also monitored. It was reported recently that treatment with SphK inhibitors resulted in decreased cell survival as a consequence of S1P biosynthesis blockade, a process monitored by the decreased phosphorylation of ERK and Akt.[22,23] When U937 cells were treated with different concentrations of *trans*-**12a** and **12b** for 16 h, a dose-dependent decrease in Akt and ERK phosphorylation was observed (Figure 2.15C). Specifically, both *trans*-**12a** and **12b** quantitatively inhibited ERK phosphorylation; however, *trans*-**12b** appeared to be more potent than *trans*-**12a** as evidenced by the complete

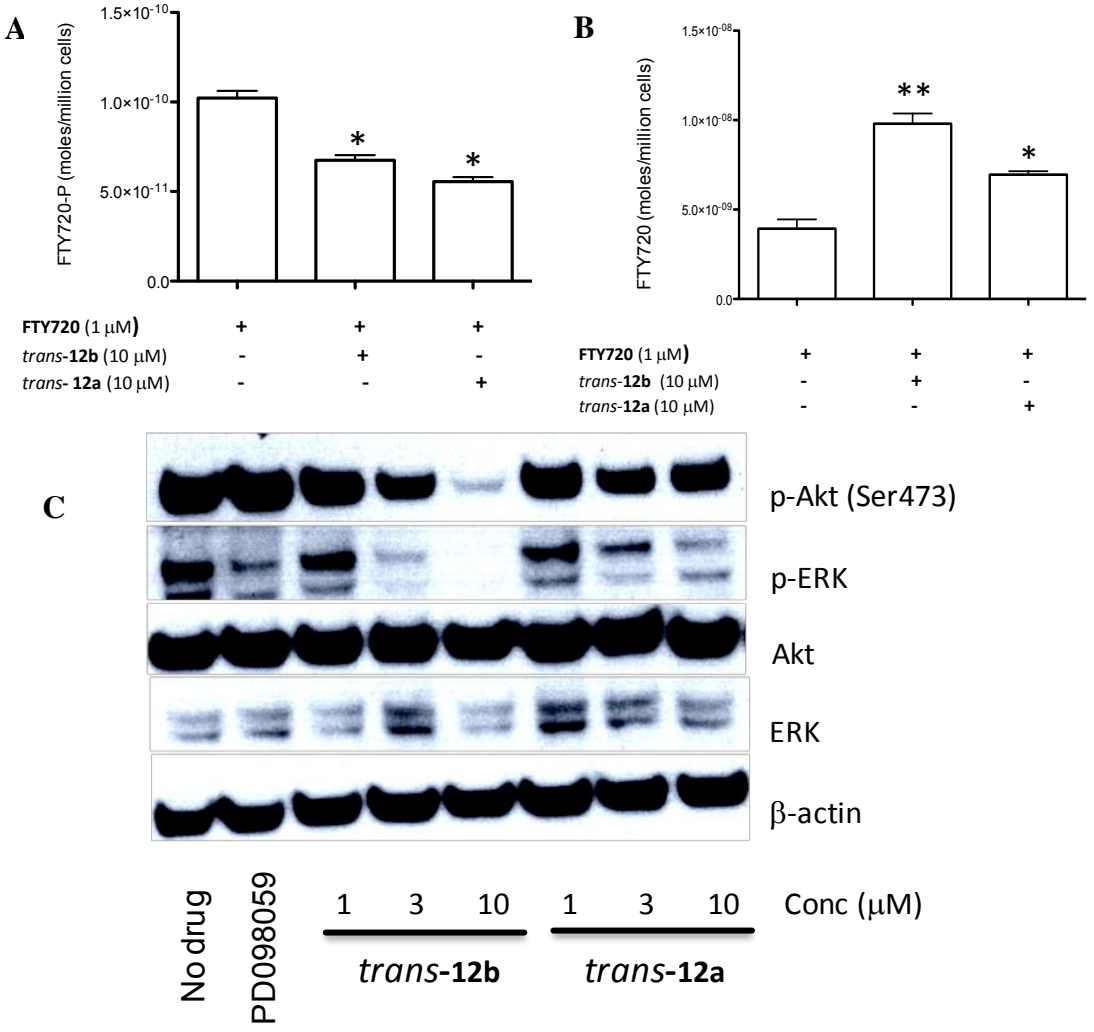

Figure 2.15. SphK2 inhibition in U937 cells.

disappearance of p-Akt band in the Western blot. Collectively, our data suggest that our inhibitors are cell permeable compounds that interfere with S1P signaling.

2.8. Effect of orientation of the head group

To define the structure-activity profile of our inhibitors, we investigated if the spatial orientation of the head group influences the inhibition activity of these compounds. Thus, we synthesized 1,3-disubstituted cyclohexanamine derivatives following the synthetic strategy outlined in Scheme 2.6. Lithium-halogen exchange of aryl bromide **1** with *n*-butyllithium followed by reaction with 3-ethoxy-2-cyclohexen-1-one afforded the α,β-unsaturated ketone **13**. Reduction with hydrogen in the presence of

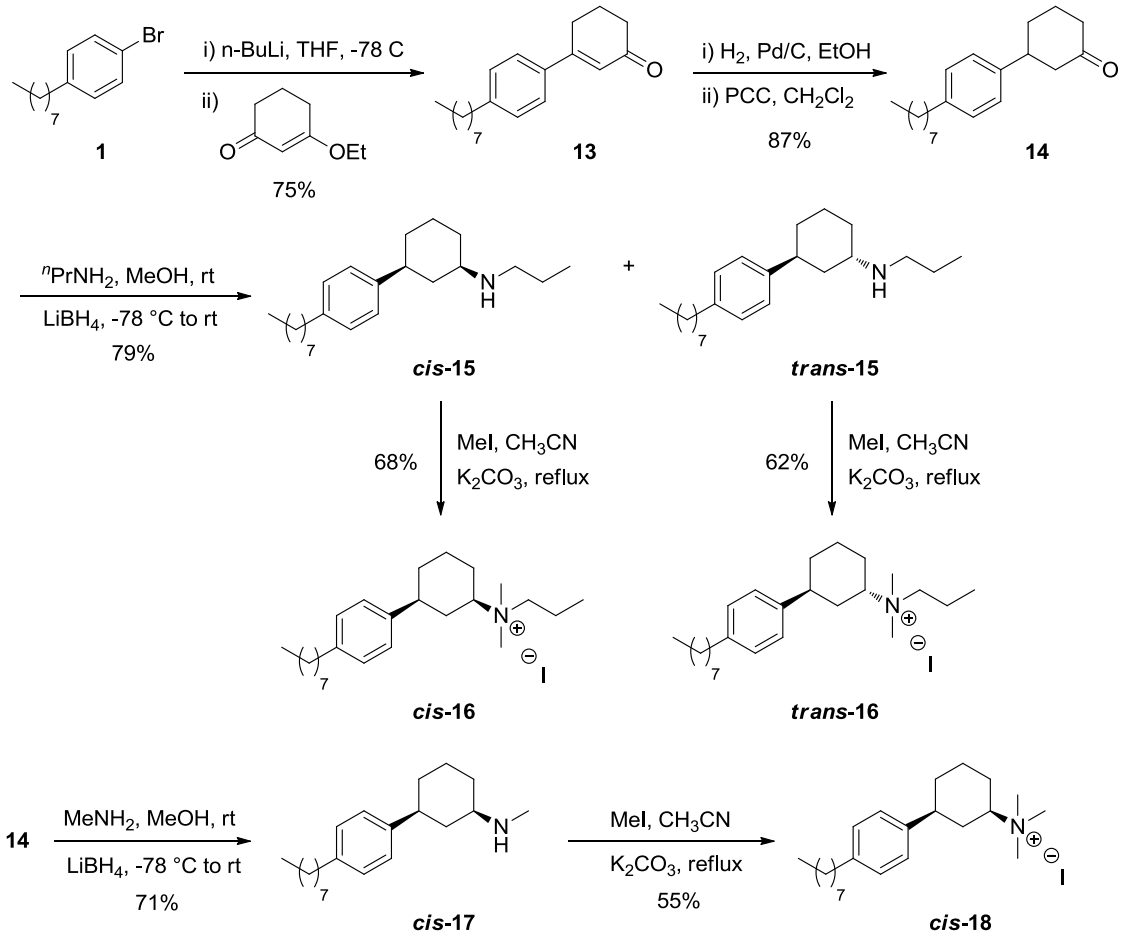

Scheme 2.6. Synthesis of 1,3-disubstituted cyclohexanamines

palladium (10% on carbon) followed by PCC oxidation provided the 3-aryl substituted 1-cyclohexanone **14**. Reductive amination with *n*-propylamine and methylamine using lithium borohydride provided the secondary amines **15** and **17**. In both cases, the *cis* isomer was the major product (83% for *n*-propylamine and 89% for methylamine) while the *trans* isomer was the minor product (17% for *n*-propylamine and 11% for methylamine). In case of methylamine, only the *cis* isomer was isolated. These secondary amines were converted into quaternary ammonium salts **16** and **18** by exhaustive methylation.

The 1,3-substituted quaternary ammonium salts **16** and **18** were assayed for their inhibition activity and compared to the corresponding 1,4-substituted quaternary ammonium salts **12a** and **12b** (Chart 2.5). We observed that **16** and **18** were completely inactive against both SphK1 and SphK2. Thus, the 1,4-orientation on the cyclohexane is the better orientation and affords stronger inhibition.

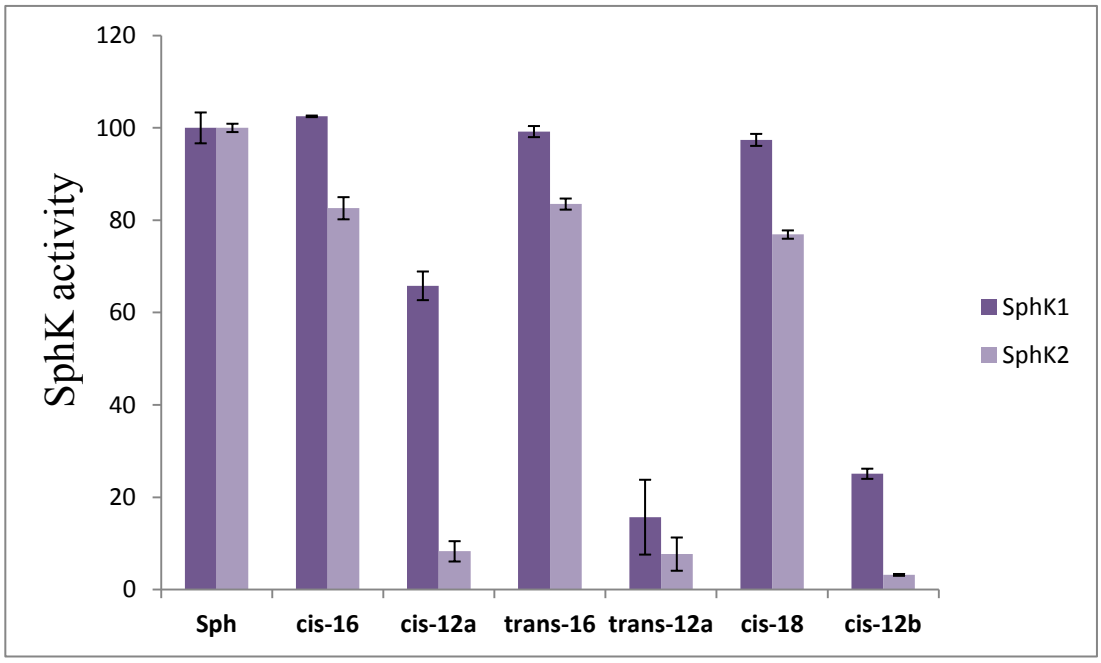

Chart 2.5. Effect of head group orientation on inhibition activity

2.9. Effect of tail length on inhibition activity

To further define the structure-activity profile of our inhibitors, we examined whether the nature and length of the alkyl tail influences SphK isoenzyme selectivity. Hence, we synthesized *trans*-**12b** derivatives with varying linkages and lipid tail length (Figure 2.16). The quaternary ammonium salts with varying alkyl tail lengths were synthesized by Ken Knott in our research group (Figure 2.17) and compound *trans*-**22** with the ether linkage was synthesized by the author (Scheme 2.7).

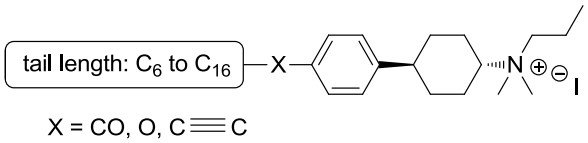

Figure 2.16. Template for inhibitor structures with varying linkages and tail length

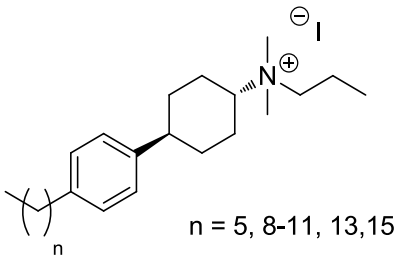

Figure 2.17. Inhibitors with varying tail lengths

Heptyl bromide was first converted to the iodide using the Finkelstein reaction and then reacted with 4-(4-hydroxyphenyl)cyclohexanone **19** to afford cyclohexanone **20**, which was then transformed to the quaternary ammonium salt *trans*-**22** by the reductive amination and exhaustive methylation protocol as described before.

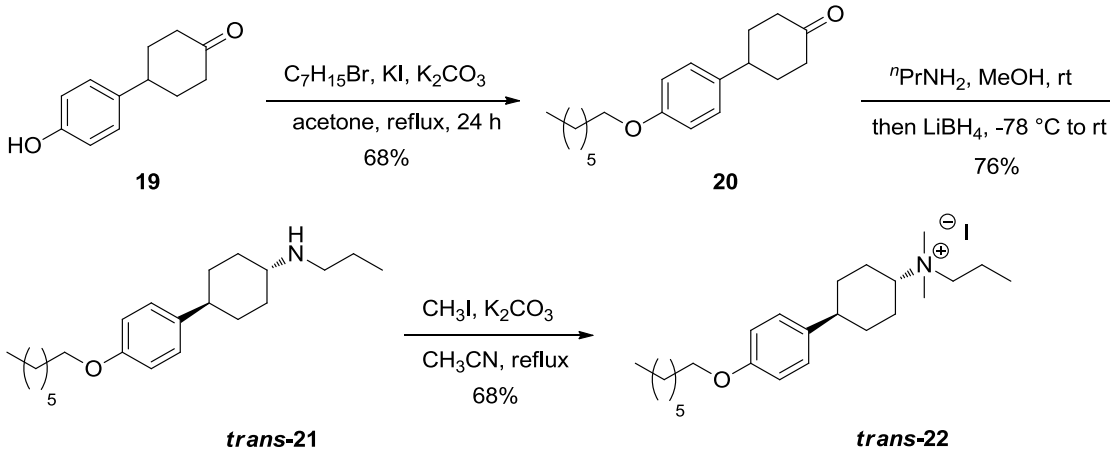

Scheme 2.7. Synthesis of compound with ether tail

Compounds were initially screened at 10 μM to determine which lipid tail linkage—*i.e*., ketone, alkynyl, alkyl or ether—is worth pursuing further. Each of these linkers aimed to probe solubility properties as well as geometry of the group adjacent to the aryl ring. Using a single concentration assay, we were able to screen compounds that were selective toward SphK2. We defined < 40% SphK2 activity as a threshold level that is sufficiently stringent to generate inhibitors in the low μM range. Compounds with the alkynyl chain, the compound with the ether linkage, and compounds containing the alkyl chain were assayed. Since the alkynyl and alkyl chain compounds had similar activities, we investigated only the alkyl chain compounds further. The alkyl chain compounds synthesized by Ken Knott are listed in Figure 2.16. To validate our observations, the K_i values for this series of compounds were determined (Chart 2.6).

The data showed that these compounds inhibited both SphK1 and SphK2 and the compound bearing the C14 chain (**C14**, n=13) and the C8 chain (*trans*-**12b**) were the best inhibitors in the series. Because the K_m values of SphK1 (10 μM) and SphK2 (5 μM) are different, the inhibitory activities at each enzyme were normalized by the K_m to compare

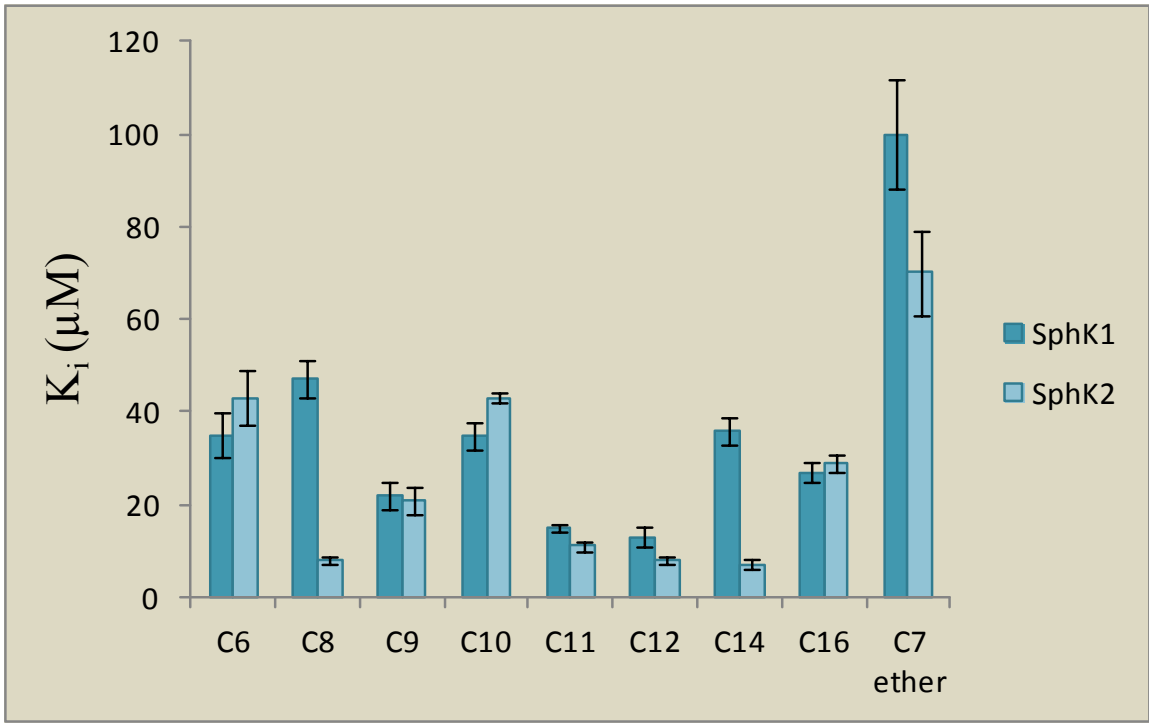

Chart 2.6. Inhibition constants of inhibitors with various tail lengths

the selectivity. Only **C14** and **C8** (*trans*-**12b**) showed selectivity toward SphK2 while the rest were non-selective (Chart 2.7). These compounds are approximately threefold selective for SphK2 over SphK1. Although there is a difference of six methylene units between *trans*-**12b** and **C14,** their selectivity and affinities are identical. We hypothesized that *trans*-**12b** and the **C14** compound could be binding at different locations on the enzyme. Although the selectivity observed here appears to be modest, it is not surprising because SphK2 is thought to be more substrate sensitive; it has a different K_m for Sph. Thus, we demonstrated that the 'tail' can impart SphK2 selectivity.[24]

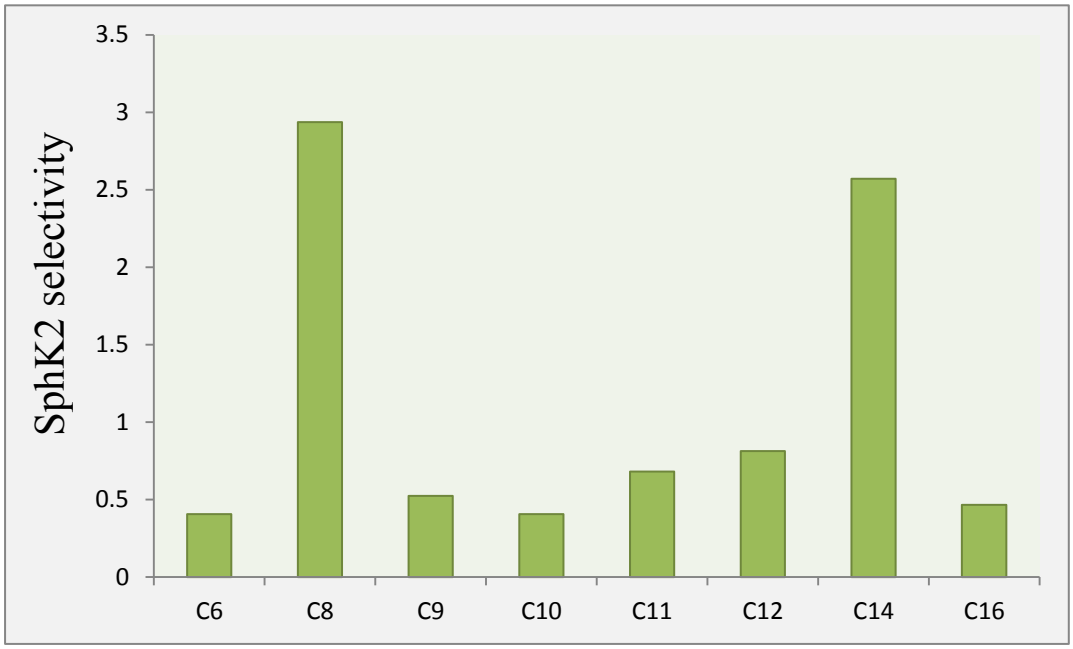

Chart 2.7. SphK2 selectivity for inhibitors with various tail lengths

2.10. Design of second generation inhibitors

The previous discussion detailed our efforts to synthesize SphK2-selective inhibitors that led to the identification of quaternary ammonium salts that were fairly potent and moderately selective inhibitors.[20] The inhibition data validated our hypothesis that a positive charge is an important contributor to an ionic interaction between the inhibitor and a SphK residue. In an effort to explore the structure-activity relationship study of the headgroup in our inhibitors, we decided to replace the quaternary ammonium group in *trans*-**12b** with another unit capable of engaging in ionic interactions. We focused our attention on the guanidine group since it has been used in various therapeutic drugs.[25] Recently, sphingosine kinase inhibitors containing the guanidine group have also been reported.[26] We also wanted to address the issue of our inhibitor selectivity. We hypothesized that the moderate selectivity of our inhibitors was the result of a lack of functional groups (other than the polar headgroup) that can have strong interactions with

the enzyme binding pocket. One of the ways to overcome this problem is the incorporation of heteroatoms that can participate in hydrogen bonding. The oxadiazole ring has been used before for the synthesis of dual SphK inhibitors.[4] Thus, in our second generation inhibitors, we introduced a potential selectivity enhancing moiety replacing the cyclohexane ring with a heteroaromatic 1,2,4-oxadiazole ring (Figure 2.18). Care was taken that the distance between the end of the hydrophobic tail and the positive charge in the head group was kept similar to our first generation inhibitors. These structural modifications provided us with a template for the synthesis of our second generation inhibitors.

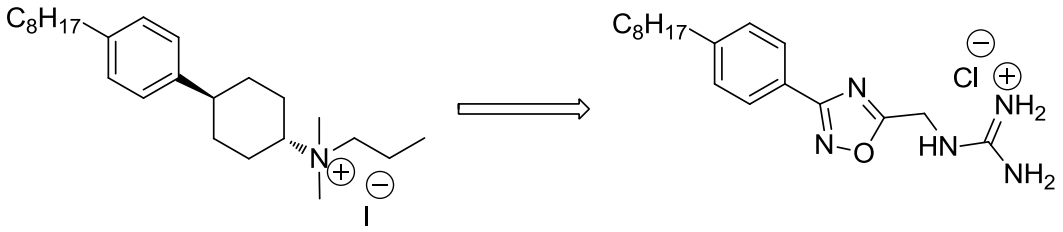

Figure 2.18. Design of second generation inhibitors

2.11. Synthesis of second generation inhibitors

Retrosynthetic analysis indicated that the 1,2,4-oxadiazole moiety can be accessed from an amidoxime and a carboxylic acid (Figure 2.19). The installation of the guanidine group requires the presence of a free amino group which can be introduced as part of the carboxylic acid compound. Thus, we used a combination of amidoxime and amino acids to construct the 1,2,4-oxadiazoles. Use of amino acids also allows easy diversification due to ready availability of various amino acids. An array of substituents with varying characteristics can be installed around the guanidine head group and would serve to elucidate the SAR around that moiety.

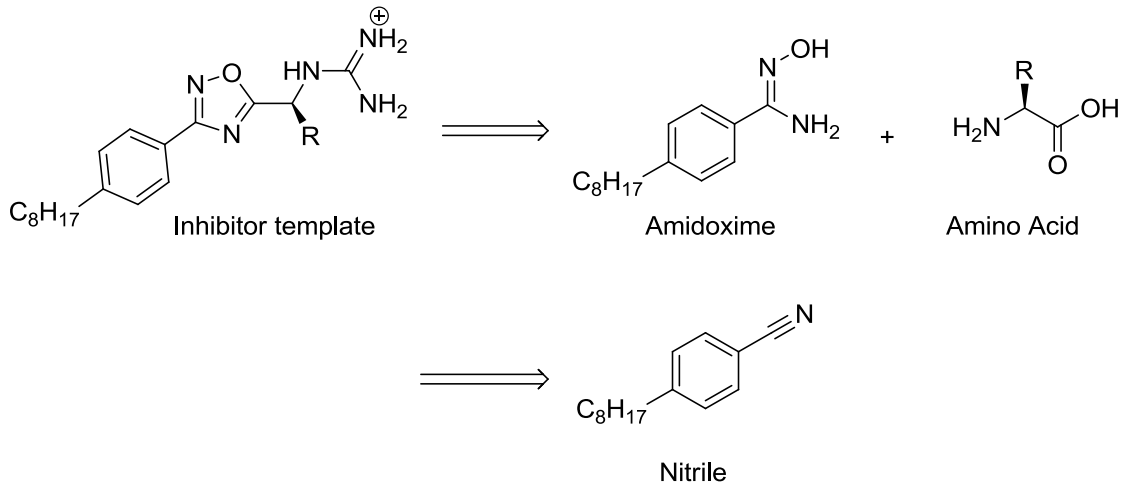

Figure 2.19. Retrosynthetic analysis for second generation inhibitors

The first step was the synthesis of aryl nitrile that could be converted to the amidoxime. Two reactions were attempted for the conversion of the aryl bromide into the aryl nitrile (Scheme 2.8). The Rosenmund-von Braun reaction utilizing copper cyanide[27] resulted in 46% yield while the palladium catalyzed cyanation with potassium ferrocyanide[28] provided a meager yield of 27%. Since such low yields on the first step of the synthesis were unacceptable, we decided to change the synthetic route. Instead of introducing the nitrile group by a cyanation reaction, we began with 4-iodobenzonitrile and installed the octyl chain with a palladium catalyzed cross-coupling (Scheme 2.9).

A Suzuki-Miyaura cross-coupling between 4-iodobenzonitrile and the organoborane product of 1-octene and 9-BBN[29] resulted in a good yield of 4-octylbenzonitrile (**23**). Aryl nitrile **23** was subsequently converted into amidoxime **24** by reaction with hydroxylamine hydrochloride and triethylamine in refluxing ethanol.[30] The amidoxime was reacted with various Boc-protected amino acids (glycine, valine and alanine) in the presence of HCTU to afford the 1,2,4-oxadiazole (**26**) in decent yields.

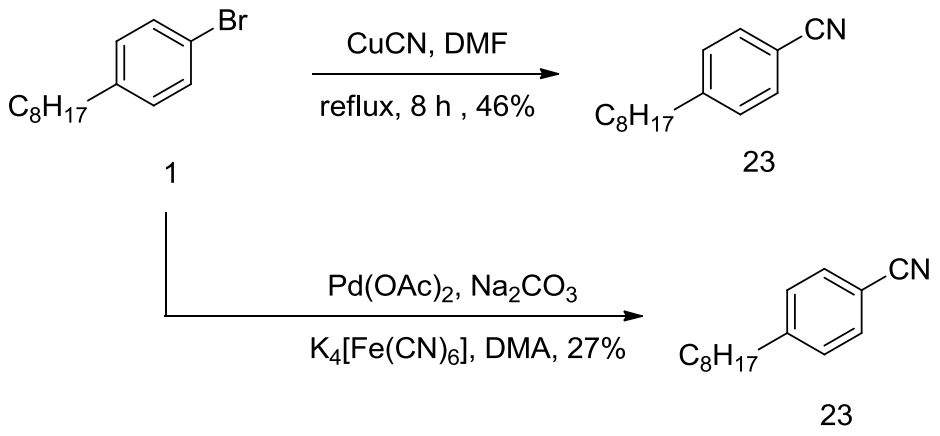

Scheme 2.8. Attempted syntheses of aryl nitrile **23**

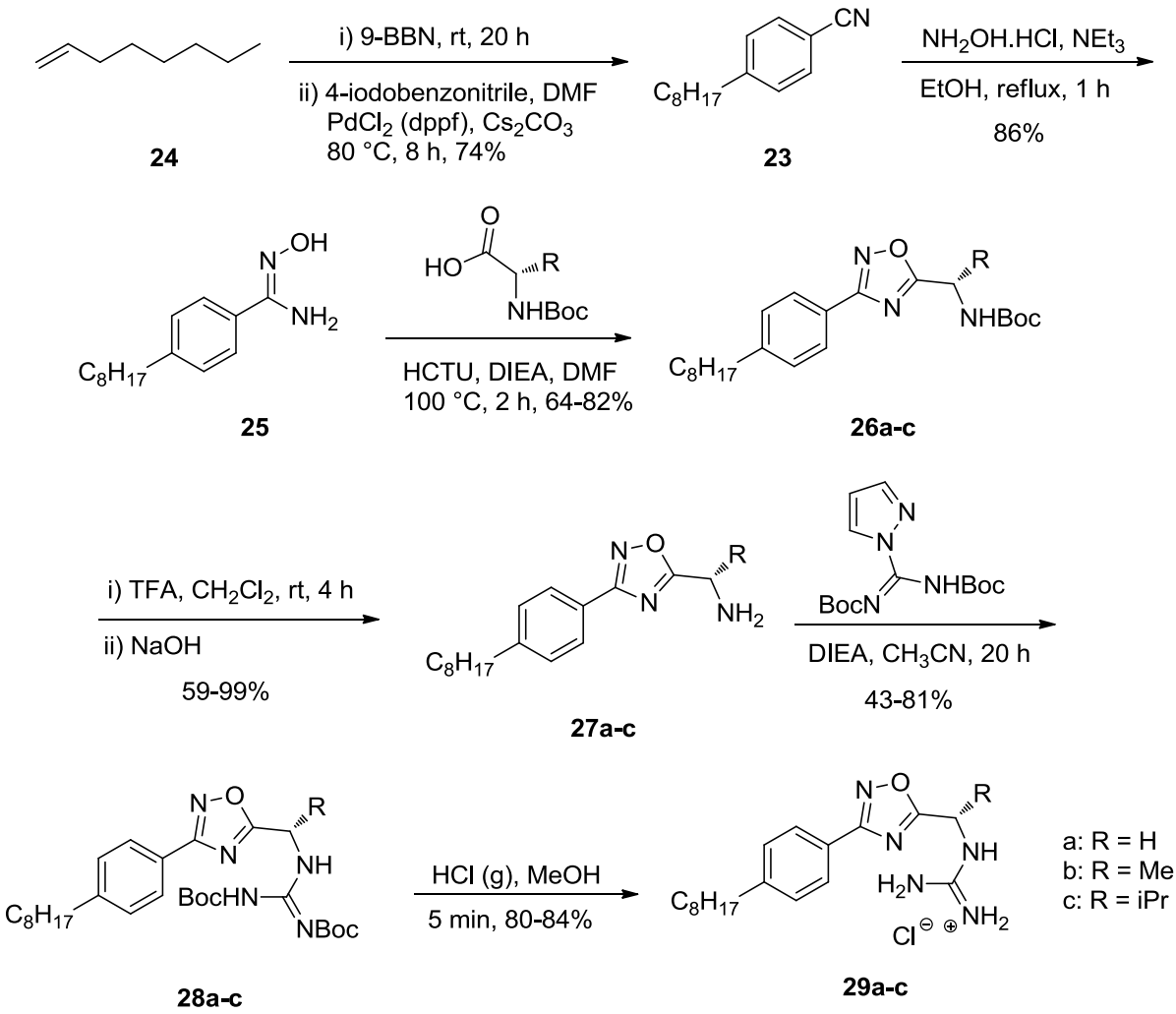

Scheme 2.9. Synthesis of guanidine-based inhibitors **29a-c**

Deprotection of the Boc group with trifluoroacetic acid in dichloromethane, followed by reaction with N,N'-di-Boc-1H-pyrazole-1-carboxamidine provided compound **28**. The final guanidine inhibitors were obtained by deprotection of the Boc groups using HCl gas in methanol. The same synthetic protocol was used for the synthesis of proline and hydroxy-proline derivatives (Scheme 2.10).

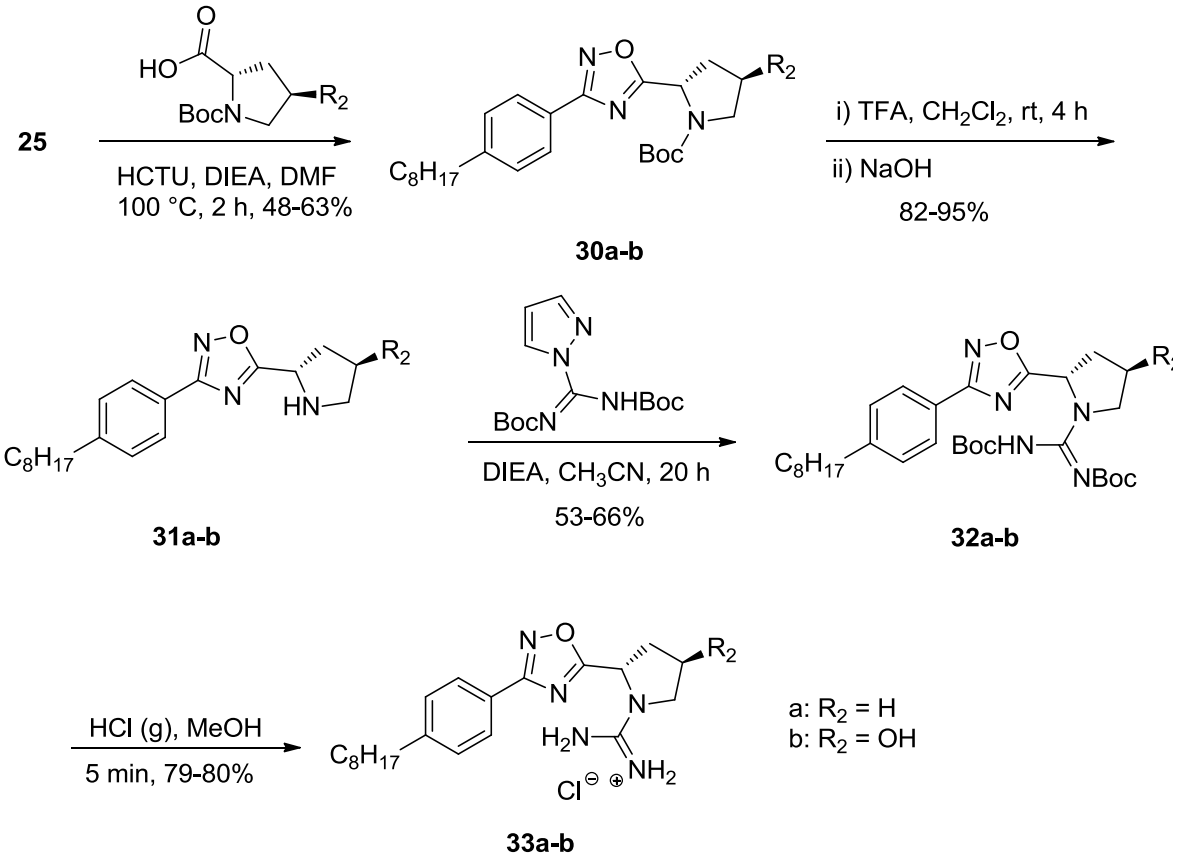

Scheme 2.10. Synthesis of guanidine-based inhibitors **33a-b**

2.12. Biological evaluation of second generation inhibitors

The guanidine compounds **29a-c** and **33a-b** were evaluated for their activity against both SphK1 and SphK2 using the assay described in Section 2.3 (Figure 2.20). The compounds were assayed at an inhibitor concentration of 10 μM and 1 μM. The

results of these assays are displayed in Chart 2.8 and Chart 2.9, respectively. At 10 μM inhibitor concentration, compounds **29a-29c** exhibited ~50% inhibition level for SphK1 and ~40% inhibition level for SphK2 making them moderately potent and largely non-selective. However, compounds **33a-33b** containing the pyrrolidine guanidine moiety displayed better potency and selectivity for SphK2. A follow-up assay with 1 μM inhibitor concentration revealed **33a** as a more potent inhibitor of SphK2 compared to **33b** (~50% inhibition). Encouraged by these results, the inhibition constants for **33a** were determined by the method outlined in Section 2.6. The inhibition constants were 1.3 ± 0.4 μM for SphK2 and 13 ± 1.2 μM for SphK1 making it 5-fold selective for SphK2 after adjusting for the different K_m values. Since **33a** was the most active guanidine inhibitor, further *in vitro* and *in vivo* biological studies were carried out with this compound, which will henceforth be referred to by our internal name **BD10.** A comparison of *trans*-**12b** and **BD10** reveals that the structural changes incorporated in the 2nd generation of inhibitors afforded more potent and selective inhibitors (Table 2.4).

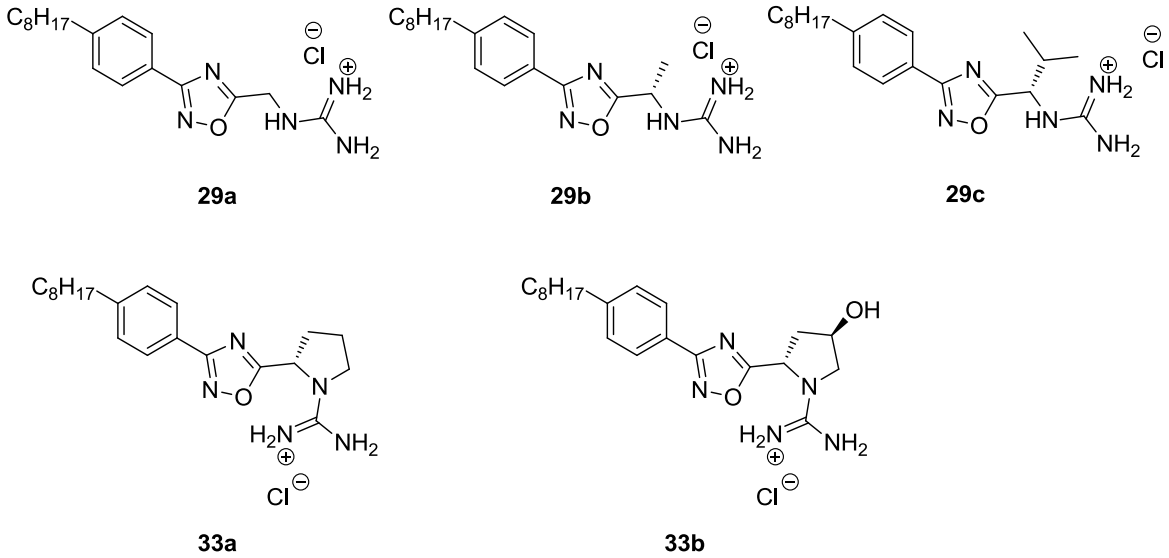

Figure 2.20. Guanidine inhibitors synthesized

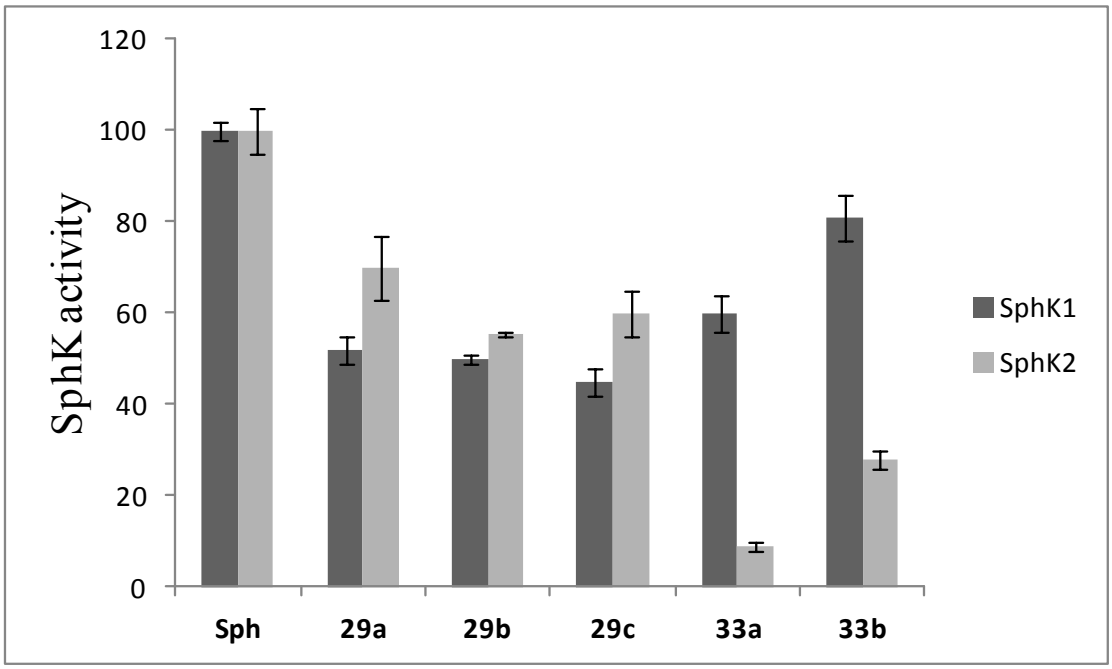

Chart 2.8. Inhibition assay of guanidine compounds at 10 μM

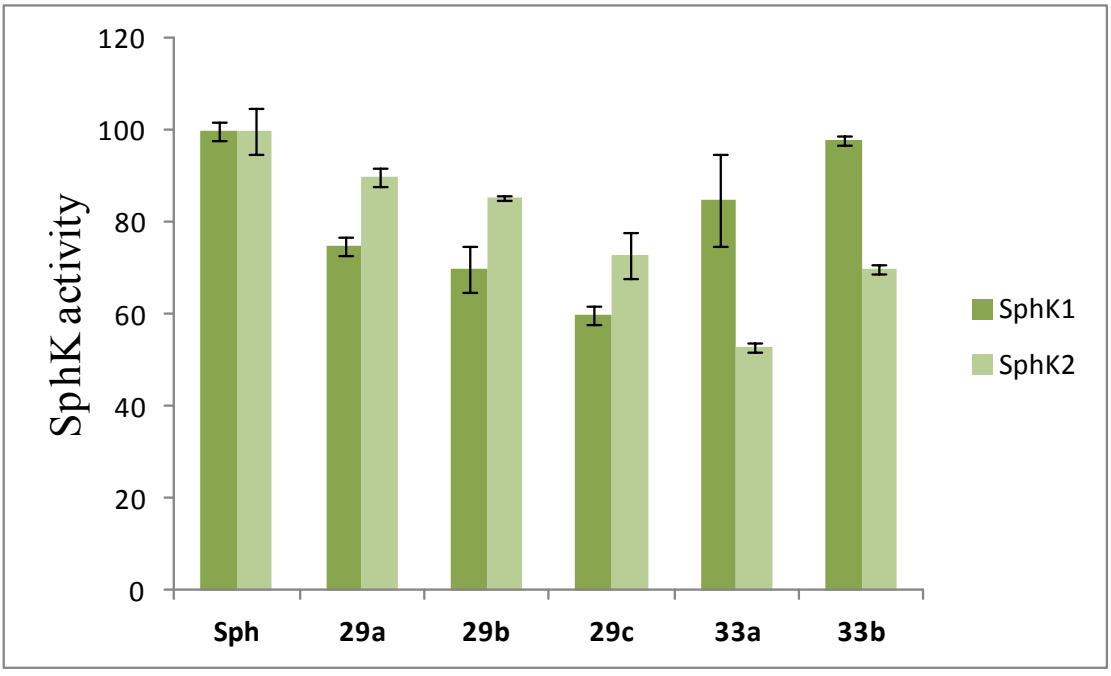

Chart 2.9. Inhibition assay of guanidine compounds at 1 μM

Table 2.4. K_i comparison of 1st and 2nd generation inhibitors

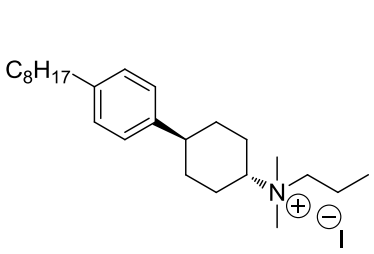

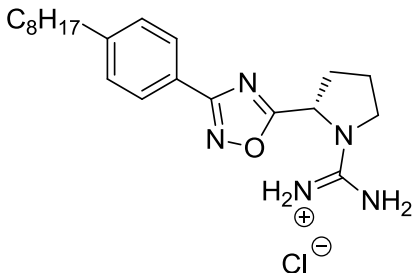

K_i SphK1 (μM)	47 ± 4	13 ± 1.2
K_i SphK2 (μM)	8 ± 1	1.3 ± 0.4

2.12.1. Evaluation of BD10 in cultured cells

We next investigated whether **BD10** was capable of penetrating cells and inhibiting SphK therein. We chose two model systems for the evaluation of the inhibitor. Human monocyte U937 cells were used to monitor SphK1 inhibition since these cells display a high level of SphK1 and SphK2 activity. Also, the U937 cell line has been used in previous studies with SphK1 inhibitors.[31] This would enable us to compare the inhibitor effects. Thus, U937 cells were treated with various concentrations of **BD10** and the accumulation of cell-associated Sph, S1P, and **BD10** was measured. As depicted in Figure 2.21A, treatment of cultures with **BD10** for two hours resulted in diminished S1P in a drug-concentration dependent manner. Correspondingly, a rise in sphingosine levels was detected (Figure 2.21B). **BD10** levels in the cultured cells showed an increase with increase in concentration thus proving that it is capable of penetrating cells (Figure 2.22).

The observed decrease in S1P level as a result of SphK inhibition is most probably due to diminished synthesis. However, the possibility of elevated degradation or increased export of S1P cannot be ruled out. To distinguish between these scenarios,

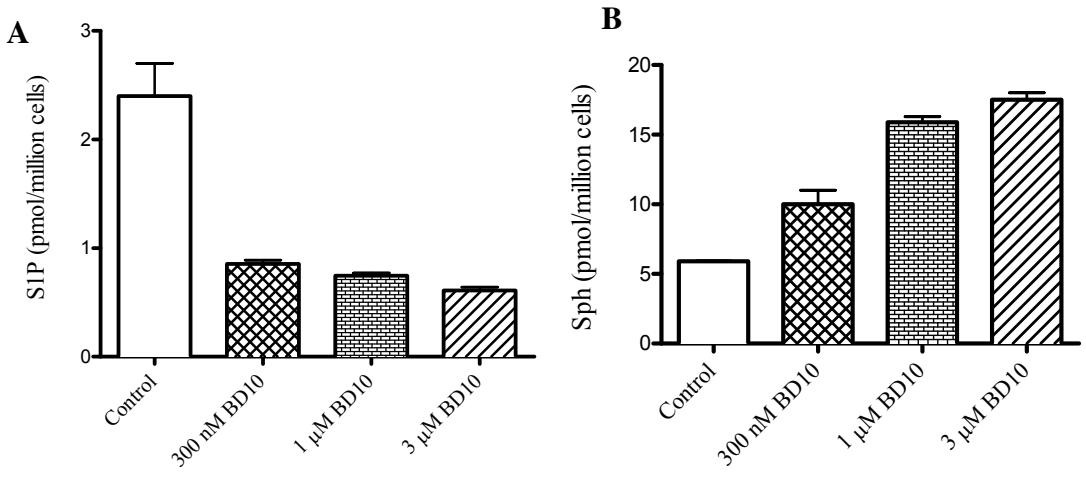

Figure 2.21. S1P and Sph levels in U937 cells

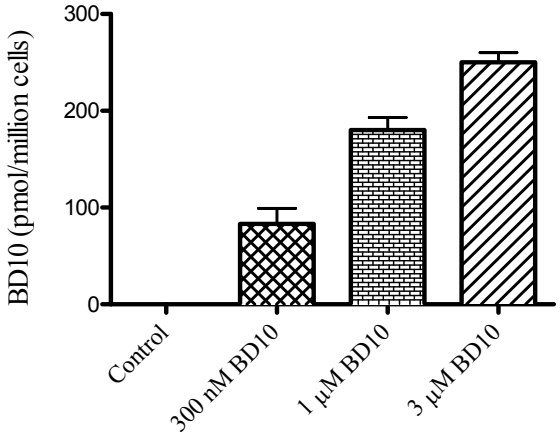

Figure 2.22. BD10 levels in U937 cells

FTY720, a SphK2-selective substrate, was added and the effect of **BD10** on FTY720-P levels was measured. Cells supplied with exogenous FTY720 (1 μM) exhibited a pronounced increase in FTY720 and FTY720-P levels (Figure 2.23). FTY720-P levels decreased in a concentration-dependent manner on addition of **BD10** (Figure 2.23A) and we observed a corresponding increase in FTY720 levels (Figure 2.23B). Therefore, the

decrease in S1P levels on addition of **BD10** in U937 culture cells is due in part to inhibition of S1P synthesis.

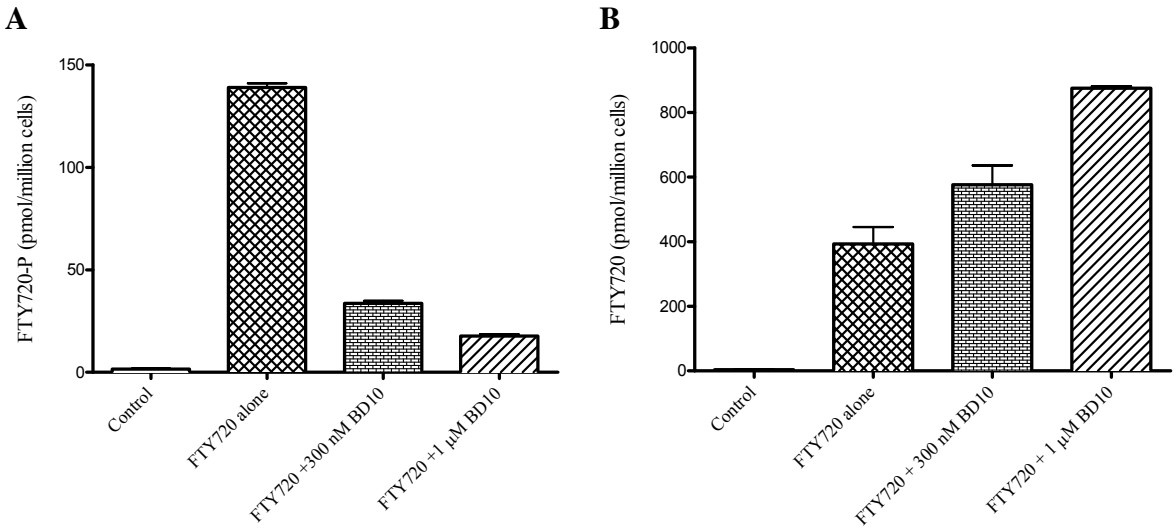

Figure 2.23. FTY720-P and FTY720 levels in U937 cells

2.12.2. *In vivo* evaluation of BD10

Next, we determined whether **BD10** blocked SphK *in vivo*. Thus, the levels of sphingolipids in the blood of mice that were injected intraperitoneally with **BD10** (10 mg/kg) were measured at various times after the injection. Surprisingly, in the wild type mice, we observed elevated levels of S1P for up to two hours after injection (Figure 2.24). This rapid increase in S1P levels in response to SphK inhibition by **BD10** *in vivo* is intriguing. It is in sharp contrast to a SphK1 selective inhibitor that caused a reduction in S1P levels.[21] An obvious idea is that SphK1 is somehow upregulated in response to lack of SphK2 activity. This is not entirely unprecedented. A recent study[32] showed that specific knockdown of SphK1 by siRNA did not influence the expression levels of SphK2 mRNA in A498 cells. However, knockdown of SphK2 significantly affected the expression levels of mRNA and enzymatic activity of SphK1 resulting in increased S1P

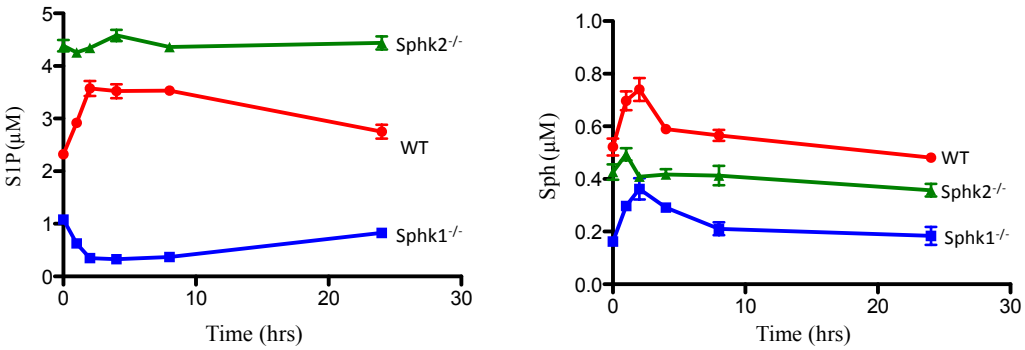

Figure 2.24. S1P and Sph levels in the blood of mice

levels. Consistent with recent observations,[33,34] our results support the idea of non-redundancy in the cellular functions of SphK1 and SphK2. It is possible that the opposing effects of SphK1 and SphK2 knockdown are a result of their different cellular localizations.

To evaluate our target specificity, *in vivo* studies were conducted with SphK1$^{-/-}$ and SphK2$^{-/-}$ mice. In the case of SphK1$^{-/-}$ mice, we observed a decrease in blood S1P levels while for SphK2$^{-/-}$ mice, no noticeable change was observed in the S1P levels. This shows that although **BD10** is only 5-fold selective towards SphK2, it does not inhibit SphK1 *in vivo*. It also suggests that at this dose, BD10 is covering its target (SphK2) and that the decrease in S1P levels is due to SphK2 inhibition rather than through interaction with another target. In wild type and SphK1$^{-/-}$ mice, the changes in blood S1P persisted for at least 12 hours. Consistent with this effect, circulating **BD10** levels remained elevated with a $T_{1/2}$ of 4-5 hours (Figure 2.25). This was an improvement on previous SphK1 inhibitors that were cleared from the bloodstream in just one hour.[21] Our work will now allow us to test whether inhibiting SphK2 in animal models of disease will lead to anti-proliferative therapy.

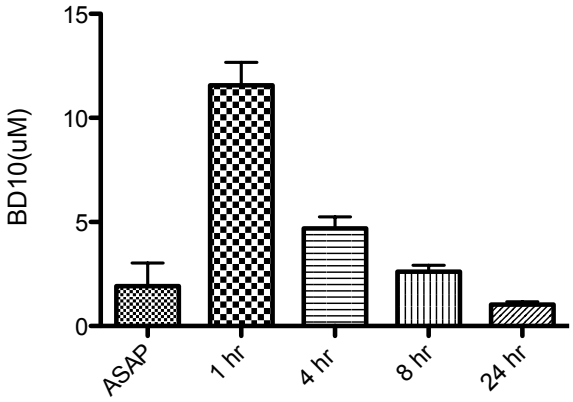

Figure 2.25. BD10 levels in WT mice whole blood

2.13. Conclusions

We discovered a novel scaffold that afforded compounds with low micromolar inhibitory activities that are moderately SphK2 selective. In general, *trans* isomers bearing small quaternary ammonium salts are good SphK2 inhibitors. The consistent increase in inhibitory activity upon exhaustive methylation of the secondary amines suggests that electrostatic interactions contribute significantly to the affinities of these compounds. We also demonstrated that *trans*-**12a** and **12b** inhibited Akt/ERK phosphorylation suggesting that these compounds inhibit the SphK-dependent phosphorylation cascade. Further, we also illustrated that the "tail" can impart SphK2 selectivity. Modification of the head group orientation proved that the 1,4-disubstituted quaternary ammonium salts possessed the best spatial orientation to interact with the binding pocket of the enzyme.

The latter half of the chapter describes SAR explorations of our second generation sphingosine kinase inhibitors. Replacement of the quaternary ammonium headgroup with a guanidine group and the cyclohexyl linker with a 1,2,4-oxadiazole moiety

provided a new scaffold. The second generation inhibitors were more potent and selective. Most notably, **BD10**, an inhibitor containing a pyrrolidine unit possessed a K_i value of 1.3 μM for SphK2. **BD10** decreased S1P levels in cultured U937 cells yet increased S1P levels in wild type mice.

2.14. References

1. Clemens, J. J., Davis, M. D., Lynch, K. R., Macdonald, T. L., Synthesis of 4(5)-phenylimidazole-based analogues of sphingosine-1-phosphate and FTY720: Discovery of potent $S1P_1$ receptor agonists, *Bioorg*. *Med*. *Chem*. *Lett*. **2005**, *15*, 3568-3572.

2. Mathews, T. P., Kennedy, A. J., Kharel, Y., Kennedy, P. C., Nicoara, O., Sunkara, M., Morris, A. J., Wamhoff, B. R., Lynch, K. R., Macdonald, T. L., Discovery, biological evaluation, and structure-activity relationship of amidine based sphingosine kinase inhibitors, *J*. *Med*. *Chem*. **2010**, *53*, 2766-2778.

3. Zhu, R., Snyder, A. H., Kharel, Y., Schaffter, L., Sun, Q., Kennedy, P. C., Lynch, K. R., Macdonald, T. L., Asymmetric synthesis of conformationally constrained fingolimod analogues - discovery of an orally active sphingosine-1-phosphate receptor type-1 agonist and receptor type-3 antagonist, *J*. *Med*. *Chem*. **2007**, *50*, 6428-6435.

4. Foss, F. W., Mathews, T. P., Kharel, Y., Kennedy, P. C., Snyder, A. H., Davis, M. D., Lynch, K. R., Macdonald, T. L., Synthesis and biological evaluation of sphingosine kinase substrates as sphingosine-1-phosphate receptor prodrugs, *Bioorg*. *Med*. *Chem*. **2009**, *17*, 6123-6136.

5. Chu, X. J., Bartkovitz, D., Danho, W., Swistok, J., Cheung, A. W. H., Kurylko, G., Rowan, K., Yeon, M., Franco, L., Qi, L. D., Chen, L., Yagaloff, K., Discovery of 1-amino-4-phenylcyclohexane-1-carboxylic acid and its influence on agonist selectivity between human melanocortin-4 and-1 receptors in linear pentapeptides, *Bioorg*. *Med*. *Chem*. *Lett*. **2005**, *15*, 4910-4914.

6. Eliel, E. L., Senda, Y., Reduction with metal hydrides-XIX, *Tetrahedron* **1970**, *26*, 2411-2428.

7. Wigfield, D. C., Stereochemistry and mechanism of ketone reductions by hydride reagents, *Tetrahedron* **1979**, *35*, 449-462.

8. Hutchins, R. O., Su, W. Y., Sivakumar, R., Cistone, F., Stercho, Y. P., Stereoselective reductions of substituted cyclohexyl and cyclopentyl carbon-nitrogen pi-systems with hydride reagents, *J*. *Org*. *Chem*. **1983**, *48*, 3412-3422.

9. Wrobel, J. E., Ganem, B., A general, highly stereoselective synthesis of amines, *Tetrahedron Lett*. **1981**, *22*, 3447-3450.

10. Mcgill, J. M., Labell, E. S., Williams, M., Hydride reagents for stereoselective reductive amination. An improved preparation of 3-endo-tropanamine, *Tetrahedron Lett*. **1996**, *37*, 3977-3980.

11. Cabral, S., Hulin, B., Kawai, M., Lithium borohydride: A reagent of choice for the selective reductive amination of cyclohexanones, *Tetrahedron Lett*. **2007**, *48*, 7134-7136.

12. Julian, L. D., Wang, Z. W., Bostick, T., Caille, S., Choi, R., Degraffenreid, M., Di, Y. M., He, X., Hungate, R. W., Jaen, J. C., Liu, J. S., Monshouwer, M., Mcminn, D., Rew, Y., Sudom, A., Sun, D. Q., Tu, H., Ursu, S., Walker, N., Yan, X. L., Ye, Q. P., Powers, J. P., Discovery of novel, potent benzamide inhibitors of 11 β-hydroxysteroid dehydrogenase type 1 (11 β-HSD1) exhibiting oral activity in an enzyme inhibition *ex vivo* model, *J*. *Med*. *Chem*. **2008**, *51*, 3953-3960.

13. Abdelmagid, A. F., Carson, K. G., Harris, B. D., Maryanoff, C. A., Shah, R. D., Reductive amination of aldehydes and ketones with sodium triacetoxyborohydride. Studies on direct and indirect reductive amination procedures, *J*. *Org*. *Chem*. **1996**, *61*, 3849-3862.

14. Abdelmagid, A. F., Maryanoff, C. A., Carson, K. G., Reductive amination of aldehydes and ketones by using sodium triacetoxyborohydride, *Tetrahedron Lett*. **1990**, *31*, 5595-5598.

15. Cobb, A. J. A., Marson, C. M., Asymmetric synthesis using catalysts containing multiple stereogenic centres and a *trans*-1,2-diaminocyclohexane core; reversal of predominant enantioselectivity upon *N*-alkylation, *Tetrahedron* **2005**, *61*, 1269-1279.

16. Olivera, A., Kohama, T., Tu, Z. X., Milstien, S., Spiegel, S., Purification and characterization of rat kidney sphingosine kinase, *J*. *Biol*. *Chem*. **1998**, *273*, 12576-12583.

17. Pitson, S. M., D'andrea, R. J., Vandeleur, L., Moretti, P. A. B., Xia, P., Gamble, J. R., Vadas, M. A., Wattenberg, B. W., Human sphingosine kinase: Purification, molecular cloning and characterization of the native and recombinant enzymes, *Biochem*. *J*. **2000**, *350*, 429-441.

18. Liu, H., Sugiura, M., Nava, V. E., Edsall, L. C., Kono, K., Poulton, S., Milstien, S., Kohama, T., Spiegel, S., Molecular cloning and functional characterization of a novel mammalian sphingosine kinase type 2 isoform, *J*. *Biol*. *Chem*. **2000**, *275*, 19513-19520.

19. Kharel, Y., Mathews, T. P., Kennedy, A. J., Houck, J. D., Macdonald, T. L., Lynch, K. R., A rapid assay for assessment of sphingosine kinase inhibitors and substrates, *Anal*. *Biochem*. **2011**, *411*, 230-235.

20. Raje, M. R., Knott, K., Kharel, Y., Bissel, P., Lynch, K. R., Santos, W. L., Design, synthesis and biological activity of sphingosine kinase 2 selective inhibitors, *Bioorg*. *Med*. *Chem*. **2012**, *20*, 183-194.

21. Kharel, Y., Mathews, T. P., Gellett, A. M., Tomsig, J. L., Kennedy, P. C., Moyer, M. L., Macdonald, T. L., Lynch, K. R., Sphingosine kinase type 1 inhibition reveals rapid turnover of circulating sphingosine-1-phosphate, *Biochem*. *J*. **2011**, *440*, 345-353.

22. Morales-Ruiz, M., Lee, M. J., Zollner, S., Gratton, J. P., Scotland, R., Shiojima, I., Walsh, K., Hla, T., Sessa, W. C., Sphingosine-1-phosphate activates Akt, nitric oxide production, and chemotaxis through a G_i protein/phosphoinositide 3-kinase pathway in endothelial cells, *J*. *Biol*. *Chem*. **2001**, *276*, 19672-19677.

23. Van Brocklyn, J. R., Letterle, C. A., Snyder, P. J., Prior, T. W., Sphingosine-1-phosphate stimulates human glioma cell proliferation through G_i-coupled receptors: Role of ERK MAP kinase and phosphatidylinositol 3-kinase β, *Cancer Lett*. **2002**, *181*, 195-204.

24. Knott, K., Kharel, Y., Raje, M. R., Lynch, K. R., Santos, W. L., Effect of alkyl chain length on sphingosine kinase 2 selectivity, *Bioorg*. *Med*. *Chem*. *Lett*. http://dx.doi.org/10.1016/j.bmcl.2012.01.050

25. Saczewski, F., Balewski, L., Biological activities of guanidine compounds, *Expert Opin*. *Ther*. *Pat*. **2009**, *19*, 1417-1448.

26. Sharma, A. K., Sphingo-guanidines and their use as inhibitors of sphingosine kinase, *Expert Opin*. *Ther*. *Pat*. **2011**, *21*, 807-812.

27. Friedman, L., Shechter, H., Dimethylformamide as a useful solvent in preparing nitriles from aryl halides and cuprous cyanide; improved isolation techniques, *J*. *Org*. *Chem*. **1961**, *26*, 2522-2524.

28. Weissman, S. A., Zewge, D., Chen, C., Ligand-free palladium-catalyzed cyanation of aryl halides, *J*. *Org*. *Chem*. **2005**, *70*, 1508-1510.

29. Miyaura, N., Ishiyama, T., Sasaki, H., Ishikawa, M., Sato, M., Suzuki, A., Palladium-catalyzed inter- and intramolecular cross-coupling reactions of B-alkyl-9-borabicyclo[3.3.1]nonane derivatives with 1-halo-1-alkenes or haloarenes. Syntheses of functionalized alkenes, arenes, and cycloalkenes via a hydroboration-coupling sequence, *J*. *Am*. *Chem*. *Soc*. **1989**, *111*, 314-321.

30. Li, Z., Chen, W., Hale, J. J., Lynch, C. L., Mills, S. G., Hajdu, R., Keohane, C. A., Rosenbach, M. J., Milligan, J. A., Shei, G.-J., Chrebet, G., Parent, S. A.,

Bergstrom, J., Card, D., Forrest, M., Quackenbush, E. J., Wickham, L. A., Vargas, H., Evans, R. M., Rosen, H., Mandala, S., Discovery of potent 3,5-diphenyl-1,2,4-oxadiazole sphingosine-1-phosphate-1 ($S1P_1$) receptor agonists with exceptional selectivity against $S1P_2$ and $S1P_3$, *J*. *Med*. *Chem*. **2005**, *48*, 6169-6173.

31. Paugh, S. W., Paugh, B. S., Rahmani, M., Kapitonov, D., Almenara, J. A., Kordula, T., Milstien, S., Adams, J. K., Zipkin, R. E., Grant, S., Spiegel, S., A selective sphingosine kinase 1 inhibitor integrates multiple molecular therapeutic targets in human leukemia, *Blood* **2008**, *112*, 1382-1391.

32. Gao, P., Smith, C. D., Ablation of sphingosine kinase 2 inhibits tumor cell proliferation and migration, *Mol*. *Cancer Res*. **2011**, *9*, 1509-1519.

33. Van Brocklyn, J. R., Jackson, C. A., Pearl, D. K., Kotur, M. S., Snyder, P. J., Prior, T. W., Sphingosine kinase 1 expression correlates with poor survival of patients with glioblastoma multiforme: Roles of sphingosine kinase isoforms in growth of glioblastoma cell lines, *J*. *Neuropathol*. *Exp*. *Neurol*. **2005**, *64*, 695-705.

34. Weigert, A., Schiffmann, S., Sekar, D., Ley, S., Menrad, H., Werno, C., Grosch, S., Geisslinger, G., Brune, B., Sphingosine kinase 2 deficient tumor xenografts show impaired growth and fail to polarize macrophages towards an anti-inflammatory phenotype, *Int*. *J*. *Cancer* **2009**, *125*, 2114-2121.

Chapter 3 Experimental

3.1. General

Melting points were recorded using a Büchi B-540 melting point instrument and are uncorrected. ^{1}H NMR spectra were recorded on a JEOL EclipsePlus-500 (500 MHz) or a Varian Inova-400 (400 MHz) spectrometer. Chemical shifts are reported in ppm from tetramethylsilane with the solvent resonance as an internal standard ($CDCl_3$: 7.26 ppm). Data are reported as follows: chemical shift, multiplicity (s = singlet, d = doublet, t = triplet, q = quartet, br = broad, m = multiplet), coupling constants (Hz), and integration. ^{13}C NMR spectra were recorded on an EclipsePlus-500 (126 MHz) spectrometer or a Varian Inova-400 (101 MHz) spectrometer with complete proton decoupling. Chemical shifts are reported in ppm with the solvent resonance as the internal standard ($CDCl_3$: 77.16 ppm). Low resolution mass spectrometry (ESI-MS) was performed on a Thermo Instrument TSQ triple quadrupole mass spectrometer (Thermo Finnigan, San Jose, CA, USA), equipped with an ESI source, which was used in the positive ion mode. High resolution mass spectroscopy (HRMS) was performed on an Agilent 6220 LC/MS time-of-flight mass spectrometer using either electrospray ionization (ESI) or fast atom bombardment (FAB). Column chromatography was performed either on a CombiFlash® Rf automated chromatography or by either using flash grade silica gel (SiO_2, 32–63 μm) or neutral, activated, Brockmann I aluminum oxide (Al_2O_3, ~150 mesh, 58 Å). Thin layer chromatography (TLC) was performed either on EMD silica gel 60 F_{254} plates or EMD aluminum oxide 60 F_{254} neutral plates. All reactions were conducted in oven or flame dried glassware under an inert atmosphere of nitrogen using magnetic stirring. Solvents were dried using the PureSolv™ solvent

purification system. All other chemical reagents were purchased from commercial sources and were used without further purification.

3.2. Synthetic procedures

General procedure A: Reductive amination with sodium triacetoxyborohydride

Primary amine (1.1 equiv) was added to a solution of **3** (1 equiv) in CH_2Cl_2 and the solution stirred for 5 min. Sodium triacetoxyborohydride (1.4 equiv) was added and the mixture was stirred for 1 h. The reaction mixture was diluted by the addition of saturated $NaHCO_3$ and stirred for an additional 10 min. It was then partitioned between water and CH_2Cl_2. The aqueous layer was extracted 3 times with CH_2Cl_2 and the combined organic layers were washed with brine, dried with sodium sulfate and filtered. The organic solvent was removed by evaporation under reduced pressure and the crude product was purified by column chromatography on neutral alumina.

General procedure B: Reductive amination with sodium cyanoborohydride

Primary amine (1.1 equiv) was added to a solution of **3** (1 equiv) in MeOH at 0 °C. After 15 min., sodium cyanoborohydride (0.7 equiv) and acetic acid (1.2 equiv) were added and the mixture was warmed to rt. After 12 h, the solution was evaporated under reduced pressure, saturated $NaHCO_3$ was added and the mixture extracted with EtOAc. The organic phase was washed with brine, dried with sodium sulfate, and concentrated on a rotary evaporator. The crude product was purified by column chromatography on neutral alumina.

General procedure C: Reductive amination with lithium borohydride

Primary amine (3 equiv) was added to a solution of 3 (1 equiv) in methanol. The mixture was stirred for 1 h at rt, cooled to -78 °C, and treated with a 2 M solution of lithium borohydride in THF (1.1 equiv). After stirring at -78 °C for 1 h, the mixture was

slowly warmed to rt and stirred for 16 h. It was quenched by slow addition of a saturated solution of $NaHCO_3$. The resulting mixture was partitioned between EtOAc and water. The aqueous layer was extracted with EtOAc and the combined organic phases washed with brine, dried over sodium sulfate, filtered, and concentrated. The crude product was purified by column chromatography on neutral alumina.

General procedure D: Eschweiler–Clarke methylation of secondary amines

Formic acid (4 equiv) was added to a solution of secondary amine (1 equiv) and paraformaldehyde (4 equiv) in methanol at rt. The reaction mixture was refluxed for 6 h. After cooling to rt, it was partitioned between ether and water. 10% NaOH was added to the aqueous layer until the pH is ~12. The basic aqueous layer was then extracted 3 times with ether. The combined organic extracts were washed with brine, dried with sodium sulfate and the solvent removed by evaporation under reduced pressure. The product was purified by column chromatography on neutral alumina.

General procedure E: Synthesis of quaternary ammonium salts from tertiary amines.

Methyl iodide (10 equiv) was added to a solution of the tertiary amine (1 equiv) in acetonitrile. The reaction mixture was refluxed for 2 h. The organic solvent was evaporated under reduced pressure and the residue dissolved in diethyl ether. The precipitate was collected by filtration and washed 3 times with diethyl ether to give the pure quaternary ammonium salt.

General procedure F: Synthesis of quaternary ammonium salts from secondary amines.

Methyl iodide (10 equiv) was added to a solution of the secondary amine (1 equiv) and K_2CO_3 (3 equiv) in acetonitrile. The reaction mixture was refluxed for 2 h. The organic solvent was evaporated under reduced pressure and the residue dissolved in diethyl ether. The precipitate was collected by filtration and washed 3 times with diethyl ether. The precipitate was dissolved in $CHCl_3$, the inorganic precipitates filtered and the filtrate concentrated under reduced pressure to give the pure quaternary ammonium salt.

General procedure G: Synthesis of 1,2,4-oxadiazole

DIEA (1.8 equiv) was added to a solution of **25** (1 equiv) and the appropriate Boc-protected amino acid (1.2 equiv) in DMF (0.2 M solution). HCTU (1.2 equiv) was then added to the resulting mixture at rt and stirred at 100 ^oC for 3 h. At this time, TLC showed complete conversion of starting material. The solution was partitioned between ethyl acetate and water. The organic layer was washed several times with a sat. LiBr. The aqueous solution was then extracted with ethyl acetate and the combined organic layers were washed with sat. $NaHCO_3$ and brine, dried over Na_2SO_4 and concentrated under reduced pressure. The residue was purified by column chromatography on silica gel (85/15 hexanes/EtOAc) to give the products**.**

General procedure H: Boc deprotection using trifluoroacetic acid

Trifluoroacetic acid (15 equiv) was added to a solution of Boc-protected amine (1 equiv) in CH_2Cl_2 (0.2 M solution). The reaction mixture was then stirred at rt for 3 h. At this time, TLC showed complete conversion of starting material. The organic solvent was removed under reduced pressure. The resulting residue was partitioned between

diethyl ether and water. The aqueous solution was adjusted to pH 14 by adding 10% NaOH solution. The solution was then extracted with ether and the combined organic layers were washed with brine, dried over Na_2SO_4, filtered and concentrated under reduced pressure to provide the products.

General procedure I: Guanylation of amines

DIEA (3 equiv) was added to a solution of free amine (1 equiv) and N,N'-Di-Boc-1H-pyrazole-1-carboxamidine (0.9 equiv) in acetonitrile (0.2 M solution). The reaction mixture was then stirred at rt for 1-3 days. The organic solvent was removed under reduced pressure. The residue was purified by column chromatography on silica gel (85/15 hexanes/EtOAc) to give the product.

General procedure J: Boc deprotection using HCl (g)

Hydrogen chloride gas was passed through a solution of diBoc-protected guanidine dissolved in methanol (0.2 M solution) for 5 min. The organic solvent was then removed under reduced pressure. The residue was washed with diethyl ether to give the product as a white solid.

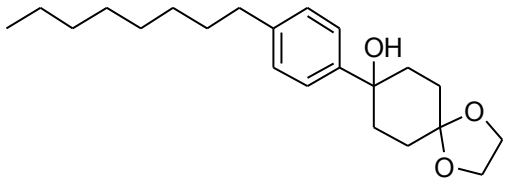

8-(4-Octylphenyl)-1,4-dioxaspiro[4.5]decan-8-ol (2). To a solution of 1-bromo-4-octylbenzene (1 g, 3.60 mmol) in 25 mL THF at -78 °C, *n*-butyllithium (2.5 M in hexanes, 1.96 mL, 4.32 mmol) was added and the solution stirred for 10 min. Then, a solution of 1,4-dioxaspiro[4.5]decan-8-one (0.696 g, 4.32 mmol) in 10 mL THF was added dropwise at -78 °C. The reaction was stirred for 2 h at -78 °C, warmed to 0 °C and

quenched with dropwise addition of a saturated solution of NH_4Cl. The reaction mixture was partitioned between water and EtOAc. The aqueous phase was extracted with EtOAc and the combined organic phases were washed with brine, dried over anhydrous sodium sulfate and concentrated on a rotary evaporator. The resulting residue was purified by column chromatography over silica gel (95/5 dichloromethane/acetone) to give the title compound (0.96 g, 75%) as a white solid, mp 52 °C; ^{1}H NMR (400 MHz, $CDCl_3$) δ 7.44–7.40 (m, 2H), 7.18–7.13 (m, 2H), 4.03–3.93 (m, 4H), 2.67–2.54 (m, 2H), 2.22–2.04 (m, 4H), 1.85–1.77 (m, 2H), 1.72–1.55 (m, 5H), 1.40–1.20 (m, 10H), 0.87 (t, *J* = 7.1 Hz, 3H); ^{13}C NMR (101 MHz, $CDCl_3$) δ 145.7, 141.6, 128.2, 124.4, 108.5, 72.2, 64.3, 64.2, 36.6, 35.5, 31.9, 31.5, 30.8, 29.5, 29.4, 29.3, 22.7, 14.1; HRMS (FAB+) *m/z* calcd for $C_{22}H_{33}O_2$ $[M\text{-}OH]^+$ 329.2481, found 329.24603.

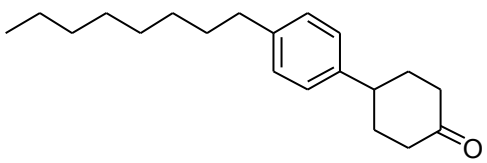

4-(4-Octylphenyl)cyclohexanone (3). *p*-Toluenesulfonic acid monohydrate (0.106 g, 0.556 mmol) was added to a solution of **2** (1.96 g, 5.66 mmol) in toluene (40 mL) and the reaction mixture was heated at 65 °C for 1 h. Toluene was evaporated under reduced pressure to give a pink oil which was dissolved in EtOAc. It was washed with $NaHCO_3$, brine, dried under sodium sulfate, and the solution concentrated on a rotary evaporator. The resulting oil was dissolved in ethanol and transferred to a 2-neck flask equipped with a magnetic stirrer. 10% Pd on activated carbon (10 mol %) was added and the reaction run under H_2 gas for 20 h. Pd/C was filtered through a plug of celite and the filtrate concentrated on a rotary evaporator. Acetic acid (45 mL) and water (15 mL) was added to the resulting oil and the solution heated at 65 °C for 2 h. The reaction mixture was

cooled to rt and partitioned between hexanes and water. The aqueous layer was extracted with hexanes and the combined organic extracts washed with $NaHCO_3$, brine, and dried with sodium sulfate. The organic solvents were evaporated under reduced pressure and the resulting oil purified by column chromatography over silica gel (90/10 hexanes/EtOAc) to give the title compound (1.24 g, 76%) as a white solid, mp 36.0–37.0 °C; ^{1}H NMR (500 MHz, $CDCl_3$) δ 7.18–7.10 (m, 4H), 2.99 (tt, *J* = 3.0 Hz, 12.0 Hz, 1H), 2.62–2.43 (m, 6H), 2.26–2.16 (m, 2H), 1.99–1.86 (m, 2H), 1.65–1.53 (m, 2H), 1.36–1.20 (m, 10H), 0.87 (t, *J* = 6.8 Hz, 3H); ^{13}C NMR (101 MHz, $CDCl_3$) δ 211.3, 141.9, 141.2, 128.6, 126.5, 42.4, 41.4, 35.6, 34.1, 31.9, 31.5, 29.5, 29.4, 29.3, 22.7, 14.1; HRMS (FAB+) *m/z* calcd for $C_{20}H_{30}O$ $[M+H]^+$ 287.2375, found 287.23669.

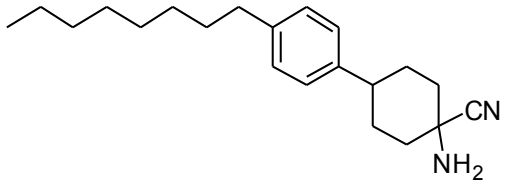

1**-Amino-4-(4-octylphenyl)cyclohexanecarbonitrile (4).** A solution of potassium cyanide (0.091 g, 1.396 mmol) and ammonium chloride (0.021 g, 0.394 mmol) in water (2.5 mL) was added to a solution of **3** (0.1 g, 0.349 mmol) in methanol (2.5 ml). The mixture was stirred overnight at 60 °C. After cooling to rt, the mixture was diluted with water and extracted with EtOAc. The organic layer was washed with brine, dried with sodium sulfate and evaporated under reduced pressure. The residue obtained was purified by column chromatography on silica gel (90/10 EtOAc/hexanes) to give the title compound as a colorless oil; ^{1}H NMR (500 MHz, $CDCl_3$) δ 7.16–7.09 (m, 4H), 2.58–2.54 (m, 2H), 2.48 (tt, *J* = 3.6 Hz, 12.3 Hz, 1H), 2.18–2.12 (m, 2H), 1.98–1.78 (m, 6H), 1.67–1.61 (m, 2H), 1.61–1.56 (m, 2H), 1.35–1.21 (m, 10H), 0.87 (t, *J* = 7.0 Hz, 3H); ^{13}C NMR

(101 MHz, $CDCl_3$) δ 142.5, 141.1, 128.4, 126.6, 123.7, 51.5, 42.6, 38.3, 35.5, 31.9, 31.5, 30.7, 29.4, 29.4, 29.2, 22.6, 13.9.

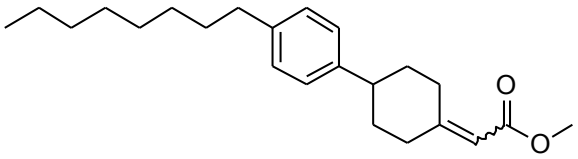

Methyl 2-(4-(4-octylphenyl)cyclohexylidene)acetate (5). To a solution of methyl diethylphosphonoacetate (0.33 mL, 1.745 mmol) in CH_2Cl_2 (5 mL) at -78 °C was added sodium tert-butoxide (0.138 g, 1.396 mmol) over a period of 15 min. The reaction mixture was stirred for 1 h at -78 °C. Then, a solution of **3** (0.2 g, 0.698 mmol) in CH_2Cl_2 (2 mL) was added dropwise. The solution was allowed to warm to rt and then stirred overnight. The reaction was quenched by the addition of saturated NH_4Cl. The reaction mixture was partitioned between CH_2Cl_2 and water and the aqueous layer extracted with CH_2Cl_2. The combined organic layers were washed with saturated $NaHCO_3$, brine, dried over sodium sulfate and filtered. The filtrate was concentrated on a rotary evaporator and the residue was purified by column chromatography over silica gel (95/5 hexanes/EtOAc, R_f = 0.38) to give the title compound (0.195 g, 82%) as a white solid, mp 39.1–40.0 °C; ^{1}H NMR (500 MHz, $CDCl_3$) δ 7.11 (s, 4H), 5.69 (s, 1H), 4.02–3.93 (m, 1H), 3.71 (s, 3H), 2.77 (tt, *J* = 3.8 Hz, 11.9 Hz, 1H), 2.57 (t, *J* = 7.9 Hz, 2H), 2.44–2.31 (m, 2H), 2.11–2.00 (m, 3H), 1.69–1.55 (m, 4H), 1.37–1.22 (m, 10H), 0.89 (t, *J* = 7.0 Hz, 3H); ^{13}C NMR (101 MHz, $CDCl_3$) δ 167.4, 162.6, 143.3, 141.0, 128.6, 126.8, 113.4, 51.1, 43.9, 38.0, 35.9, 35.8, 35.1, 32.1, 31.8, 29.8, 29.7, 29.6, 29.5, 22.9, 14.3; ESI-MS *m/z* calcd for $C_{23}H_{34}O_2$ $[M+H]^+$ 343.26, found 343.30.

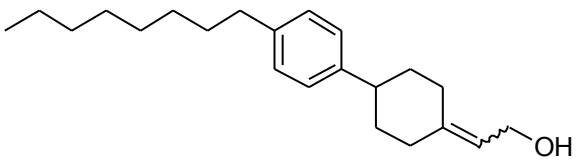

2-(4-(4-Octylphenyl)cyclohexylidene)ethanol (6). Diisobutylaluminum hydride (1 M in toluene, 2.2 mL, 2.2 mmol) was added dropwise to a solution of **5** (0.247 g, 0.721 mmol) in CH_2Cl_2 (7.2 mL) at 0 °C. The solution was allowed to warm to rt and stirred for 1 h. The solution was diluted with careful dropwise addition of 0.09 mL water, 0.14 mL 10% NaOH and then 0.22 mL water and stirred for 30 min. The resulting precipitate was filtered through a plug of celite and the filtrate was washed with brine solution and dried with sodium sulfate. Evaporation of the organic solvent gave a residue which was purified by column chromatography on silica gel (75/25 hexanes/EtOAc, R_f = 0.32) to give the title compound (0.179 g, 79%) as a white solid, mp 36.7–37.4 °C; ^{1}H NMR (500 MHz, $CDCl_3$) δ 7.10 (s, 4H), 5.44 (t, *J* = 7.1 Hz, 1H), 4.18 (d, *J* = 7.1 Hz, 2H), 2.79–2.73 (m, 1H), 2.68 (tt, *J* = 3.5 Hz, 12.2 Hz, 1H), 2.58–2.53 (m, 2H), 2.39–2.29 (m, 1H), 2.27–2.18 (m, 1H), 2.03–1.88 (m, 3H), 1.63–1.41 (m, 4H), 1.36–1.21 (m, 11H), 0.87 (t, *J* = 7.0 Hz, 3H); ^{13}C NMR (101 MHz, $CDCl_3$) δ 143.8, 143.2, 140.6, 128.3, 126.6, 120.9, 58.7, 44.1, 36.8, 35.6, 35.5, 35.1, 31.9, 31.5, 29.5, 29.4, 29.3, 28.6, 22.7, 14.1; HRMS (FAB+) *m/z* calcd for $C_{22}H_{33}$ $[M\text{-}OH]^+$ 297.25823, found 297.25844.

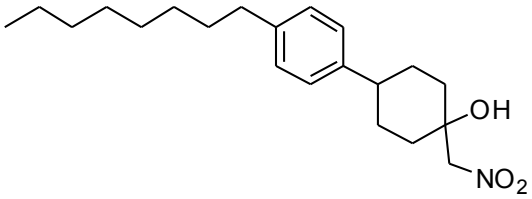

1-(Nitromethyl)-4-(4-octylphenyl)cyclohexanol (7). Nitromethane (0.37 mL, 6.98 mmol) was added to a solution of 3 (0.4 g, 1.396 mmol) in ethanol (8 mL). The mixture cooled to 0 °C and sodium ethoxide (0.114 g, 1.676 mmol) dissolved in ethanol (4 mL)

was added dropwise. The mixture was warmed to rt and stirred for 4 h. It was quenched by the addition of saturated NH_4Cl. It was then partitioned between EtOAc and water. The aqueous layer was extracted with EtOAc and the combined organic extracts were washed with brine and dried with sodium sulfate. The organic solvents were evaporated under reduced pressure and the resulting residue purified by column chromatography over silica gel (75/25 hexanes/EtOAc, $R_f = 0.37$) to give the title compound (0.3 g, 62%) as a white solid, mp 45.8–46.5 °C; ^{1}H NMR (500 MHz, $CDCl_3$) δ 7.12 (s, 4H), 4.68 (s, 2H), 3.09 (s, 1H), 2.62 (tt, *J* = 3.0 Hz, 12.5 Hz, 1H), 2.57 (t, *J* = 7.5 Hz, 2H), 2.01–1.90 (m, 4H), 1.77 (td, *J* = 3.7 Hz, 13.4 Hz, 2H), 1.63–1.49 (m, 4H), 1.37–1.21 (m, 10H), 0.87 (t, *J* = 7.0 Hz, 3H); ^{13}C NMR (101 MHz, $CDCl_3$) δ 142.2, 141.1, 128.5, 126.5, 81.3, 71.2, 42.2, 35.9, 35.5, 31.9, 31.5, 30.5, 29.4, 29.4, 29.2, 22.6, 14.1.

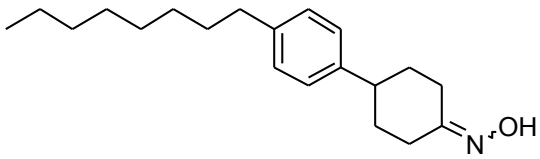

4-(4-Octylphenyl)cyclohexanone oxime (8). Hydroxylamine hydrochloride (72.8 mg, 1.047 mmol) was added to a solution of **3** (100 mg, 0.349 mmol) in pyridine (1 mL) and the resulting solution was heated at 80 °C for 24 h. Pyridine was evaporated under reduced pressure and the resulting residue was dissolved in EtOAc. It was washed with $NaHCO_3$, brine, dried over sodium sulfate and filtered. The resulting solution was concentrated on a rotary evaporator to give the title compound (87 mg, 83%) as a white solid, mp 69.2–70.3 °C; ^{1}H NMR (400 MHz, $CDCl_3$) δ 8.35 (br s, 1H), 7.04 (s, 4H), 3.44–3.36 (m, 1H), 2.68 (tt, *J* = 3.3 Hz, 12.1 Hz, 1H), 2.53–2.42 (m, 3H), 2.19 (td, *J* = 4.7 Hz, 13.6 Hz, 1H), 2.05–1.93 (m, 2H), 1.81 (td, *J* = 5.2 Hz, 13.9 Hz, 1H), 1.68–1.47 (m, 4H), 1.30–1.14 (m, 10H), 0.80 (t, *J* = 6.9 Hz, 3H); ^{13}C NMR (101 MHz, $CDCl_3$) δ 159.9,

142.8, 140.9, 128.5, 126.5, 43.3, 35.6, 34.1, 33.0, 32.0, 31.9, 31.5, 29.5, 29.4, 29.3, 24.2, 22.7, 14.2; HRMS (FAB+) *m/z* calcd for $C_{20}H_{32}NO$ $[M+H]^+$ 302.2484, found 302.2457.

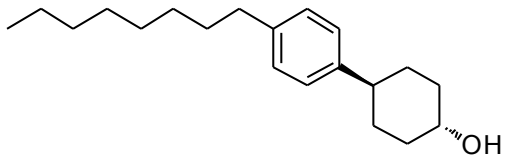

(1*r*,4*r*)-4-(4-Octylphenyl)cyclohexanol (9). Sodium borohydride (0.031 g, 0.826 mmol) was added to a solution of **3** (0.1 g, 0.349 mmol) in methanol (2 mL) at 0 °C. The reaction was warmed to rt and stirred overnight. The solvent was removed by evaporation under reduced pressure and water was added to the resulting residue. The aqueous phase was extracted three times with EtOAc and the combined organic extracts were washed with brine and dried over sodium sulfate. The solvent was evaporated under reduced pressure and the resulting residue was purified by column chromatography on silica gel (50/50 hexanes/EtOAc) to give the title compound (0.073 mg, 72% yield) as a white solid; ^{1}H NMR (500 MHz, $CDCl_3$) δ 7.10 (s, 4H), 3.72-3.65 (m, 1H), 2.58–2.53 (m, 2H), 2.46 (tt, *J* = 3.5 Hz, 12.2 Hz, 1H), 2.12–2.06 (m, 2H), 1.95–1.89 (m, 2H), 1.62–1.22 (m, 16H), 0.87 (t, *J* = 7.5 Hz, 3H); ^{13}C NMR (126 MHz, $CDCl_3$) δ 143.8, 140.8, 128.4, 126.7, 70.8, 43.1, 36.1, 35.6, 32.6, 32.0, 31.6, 29.6, 29.5, 29.4, 22.8, 14.2; HRMS (FAB+) *m/z* calcd for $C_{20}H_{32}O$ $[M-OH]^+$ 288.2453, found 288.2457.

Compounds **10a-10i** were synthesized by both general procedures A and B. General procedure C was used to only calculate the *cis*/*trans* ratio of compounds **10a-10h** using GC.

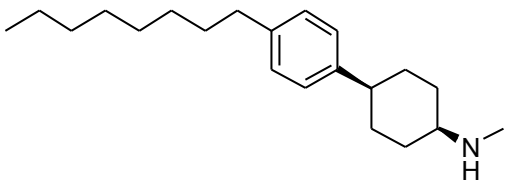

(1*s*,4*s*)-*N*-Methyl-4-(4-octylphenyl)cyclohexanamine (*cis*-10a). Colorless oil; ^{1}H NMR (400 MHz, $CDCl_3$) δ 7.18–7.13 (m, 2H), 7.13–7.07 (m, 2H), 2.79–2.74 (m, 1H), 2.59–2.48 (m, 3H), 2.43 (s, 3H), 1.89–1.71 (m, 4H), 1.68–1.55 (m, 6H), 1.37–1.20 (m, 11H), 0.88 (t, J = 6.9 Hz, 3H); ^{13}C NMR (101 MHz, $CDCl_3$) δ 144.5, 140.3, 128.2, 126.7, 53.8, 43.4, 35.6, 34.2, 31.9, 31.6, 30.1, 29.5, 29.4, 29.3, 28.3, 22.7, 14.1; HRMS (FAB+) *m/z* calcd for $C_{21}H_{36}N$ $[M+H]^+$ 302.2848, found 302.2838.

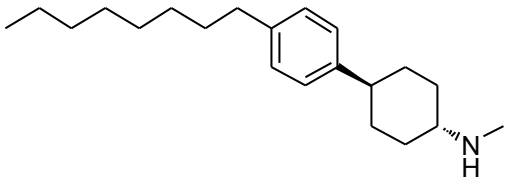

(1*r*,4*r*)-*N*-Methyl-4-(4-octylphenyl)cyclohexanamine (*trans*-10a). Yellow oil; ^{1}H NMR (500 MHz, $CDCl_3$) δ 7.16–7.05 (m, 4H), 2.58–2.52 (m, 2H), 2.51–2.36 (m, 5H), 2.10–2.02 (m, 2H), 1.96–1.88 (m, 2H), 1.65–1.54 (m, 3H), 1.54–1.44 (m, 2H), 1.34–1.17 (m, 12H), 0.87 (t, J = 7.0 Hz, 3H); ^{13}C NMR (126 MHz, $CDCl_3$) δ 144.4, 140.6, 128.4, 126.7, 58.6, 43.8, 35.7, 33.8, 33.5, 33.1, 32.0, 31.6, 29.6, 29.5, 29.4, 22.8, 14.2; HRMS (FAB+) *m/z* calcd for $C_{21}H_{36}N$ $[M+H]^+$ 302.2848, found 302.2838.

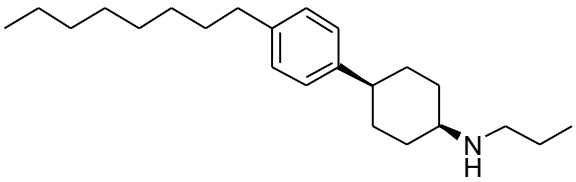

(1*s*,4*s*)-4-(4-Octylphenyl)-*N*-propylcyclohexanamine (*cis*-10b). Colorless oil; ^{1}H NMR (400 MHz, $CDCl_3$) δ 7.17–7.12 (m, 2H), 7.12–7.07 (m, 2H), 2.88–2.82 (m, 1H), 2.59–2.49 (m, 5H), 1.85–1.72 (m, 4H), 1.69–1.46 (m, 8H), 1.37–1.19 (m, 10H), 0.94 (t, J = 7.3 Hz, 3H), 0.88 (t, J = 7.1 Hz, 3H); ^{13}C NMR (101 MHz, $CDCl_3$) δ 144.5, 140.3, 128.2, 126.7, 51.8, 49.3, 43.1, 35.6, 31. 9, 31.6, 30.5, 29.5, 29.4, 29.3, 23.6, 22.7, 14.1, 11.9; HRMS (ESI+) *m/z* calcd for $C_{23}H_{39}N$ $[M+H]^+$ 330.3155, found 330.3126.

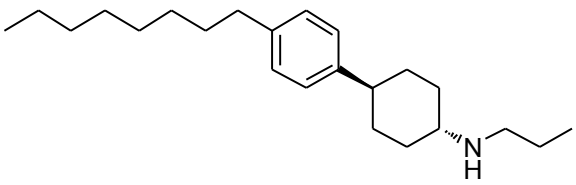

(1*r*,4*r*)-4-(4-Octylphenyl)-*N*-propylcyclohexanamine (*trans*-10b). Colorless oil; ^{1}H NMR (400 MHz, $CDCl_3$) δ 7.14–7.07 (m, 4H), 2.67–2.41 (m, 6H), 2.09–2.00 (m, 2H), 1.96–1.87 (m, 2H), 1.65–1.42 (m, 6H), 1.38–1.17 (m, 13H), 0.93 (t, *J* = 7.4 Hz, 3H), 0.88 (t, *J* = 6.9 Hz, 3H); ^{13}C NMR (101 MHz, $CDCl_3$) δ 144.3, 140.5, 128.3, 126.6, 56.8, 49.2, 43.7, 35.6, 33.9, 33.1, 31.9, 31.5, 29.5, 29.4, 29.3, 23.6, 22.7, 14.1, 11.9; HRMS (ESI+) *m/z* calcd for $C_{23}H_{39}N$ $[M+H]^+$ 330.3155, found 330.3153.

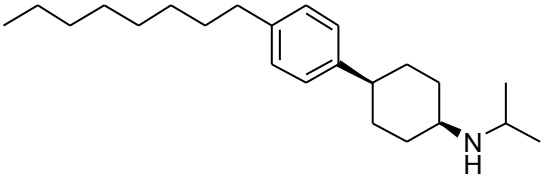

(1*s*,4*s*)-*N*-Isopropyl-4-(4-octylphenyl)cyclohexanamine (*cis*-10c). Colorless oil; ^{1}H NMR (400 MHz, $CDCl_3$) δ 7.23–7.04 (m, 4H), 3.01–2.95 (m, 1H), 2.95–2.87 (m, 1H), 2.65–2.50 (m, 3H), 1.86–1.55 (m, 10H), 1.46–1.21 (m, 11H), 1.08 (d, *J* = 7.5 Hz, 6H), 0.89 (t, *J* = 6.8 Hz, 3H); ^{13}C NMR (101 MHz, $CDCl_3$) δ 144.5, 140.6, 128.5, 126.9, 48.6, 45.1, 43.1, 35.8, 32.2, 31.8, 30.7, 29.8, 29.7, 29.5, 28.5, 23.6, 22.9, 14.4; ESI-MS *m/z* calcd for $C_{23}H_{39}N$ $[M+H]^+$ 330.31, found 330.30.

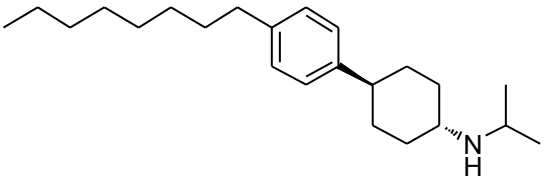

(1*r*,4*r*)-*N*-Isopropyl-4-(4-octylphenyl)cyclohexanamine (*trans*-10c). White solid, mp 41.5–42.5 °C; ^{1}H NMR (500 MHz, $CDCl_3$) δ 7.13–7.07 (m, 4H), 3.14–3.04 (m, 1H), 2.69 (tt, *J* = 3.9 Hz, 11.3 Hz, 1H), 2.55 (t, *J* = 8.0 Hz, 2H), 2.48 (tt, *J* = 3.5 Hz, 12.5 Hz, 1H),

2.12–2.03 (m, 2H), 1.98 (br s, 1H), 1.96–1.88 (m, 2H), 1.62–1.55 (m, 2H), 1.49 (qd, J = 3.0 Hz, 12.5 Hz, 2H), 1.37–1.20 (m, 12H), 1.14 (d, J = 6.3 Hz, 6H), 0.87 (t, J = 6.9 Hz, 3H); ^{13}C NMR (126 MHz, $CDCl_3$) δ 144.1, 140.7, 128.4, 126.7, 53.5, 45.3, 43.5, 35.6, 33.5, 33.2, 32.0, 31.6, 29.6, 29.5, 29.3, 22.8, 14.2; ESI-MS m/z calcd for $C_{23}H_{39}N$ $[M+H]^+$ 330.31, found 330.28; HRMS (ESI+) *m/z* calcd for $C_{23}H_{39}N$ $[M+H]^+$ 330.3155, found 330.3168.

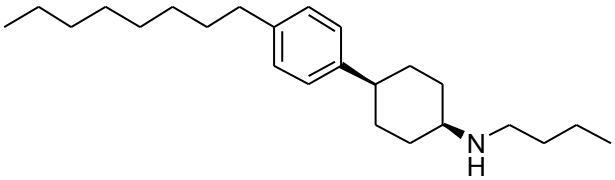

(1*s*,4*s*)-*N*-Butyl-4-(4-octylphenyl)cyclohexanamine (*cis*-10d). Colorless oil; ^{1}H NMR (500 MHz, $CDCl_3$) δ 7.22–7.05 (m, 4H), 2.91–2.85 (m, 1H), 2.69–2.47 (m, 5H), 1.90–1.73 (m, 4H), 1.73–1.57 (m, 6H), 1.56–1.21 (m, 15H), 1.04–0.81 (m, 6H); ^{13}C NMR (126 MHz, $CDCl_3$) δ 144.7, 140.5, 128.5, 127.0, 52.1, 47.3, 43.3, 35.8, 32.8, 32.2, 31.8, 30.7, 29.8, 29.7, 29.5, 28.5, 22.9, 20.9, 14.4, 14.3; ESI-MS *m/z* calcd for $C_{24}H_{41}N$ $[M+H]^+$ 344.32, found 344.30.

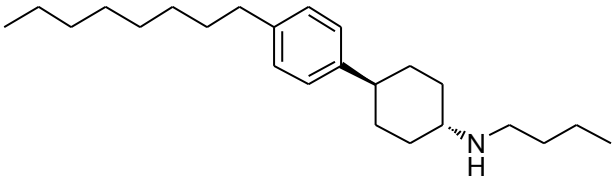

(1*r*,4*r*)-*N*-Butyl-4-(4-octylphenyl)cyclohexanamine (*trans*-10d). Yellow oil; ^{1}H NMR (400 MHz, $CDCl_3$) δ 7.18–7.05 (m, 4H), 2.69–2.63 (m, 2H), 2.60–2.43 (m, 4H), 2.09–2.00 (m, 2H), 1.95–1.88 (m, 2H), 1.64–1.44 (m, 6H), 1.42–1.18 (m, 14H), 0.93 (t, J = 7.3 Hz, 3H), 0.88 (t, J = 6.8 Hz, 3H); ^{13}C NMR (101 MHz, $CDCl_3$) δ 144.3, 140.5, 128.3, 126.6, 56.9, 47.0, 43.7, 35.6, 34.0, 33.1, 32.7, 31.9, 31.6, 29.5, 29.4, 29.3, 22.7, 20.6, 14.1, 14.0; ESI-MS *m/z* calcd for $C_{24}H_{41}N$ $[M+H]^+$ 344.32, found 344.30.

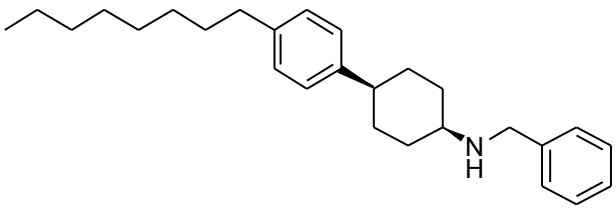

(1*s*,4*s*)-*N*-Benzyl-4-(4-octylphenyl)cyclohexanamine (*cis*-10e). Yellow oil; ^{1}H NMR (500 MHz, $CDCl_3$) δ 7.39–7.31 (m, 4H), 7.27–7.23 (m, 1H), 7.17–7.14 (m, 2H), 7.12–7.08 (m, 2H), 3.80 (s, 2H), 2.96–2.91 (m, 1H), 2.59–2.50 (m, 3H), 1.92–1.81 (m, 4H), 1.68–1.56 (m, 6H), 1.48 (br s, 1H), 1.37–1.22 (m, 10H), 0.88 (t, J = 7.0 Hz, 3H); ^{13}C NMR (126 MHz, $CDCl_3$) δ 144.7, 141.3, 140.4, 128.5, 128.3, 128.2, 126.9, 126.8, 51.4, 51.2, 43.4, 35.7, 32.0, 31.7, 30.6, 29.6, 29.5, 29.4, 28.3, 22.8, 14.2; ESI-MS *m/z* calcd for $C_{27}H_{39}N$ $[M+H]^+$ 378.31, found 378.25; HRMS (ESI+) *m/z* calcd for $C_{27}H_{40}N$ $[M+H]^+$ 378.3155, found 378.3168.

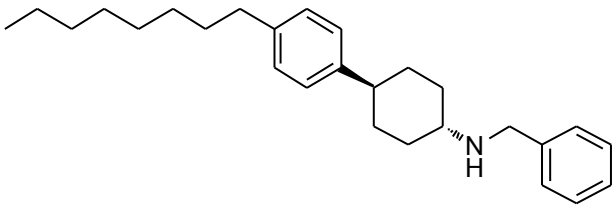

(1*r*,4*r*)-*N*-Benzyl-4-(4-octylphenyl)cyclohexanamine (*trans*-10e). White solid, mp 41.5–42.5 °C; ^{1}H NMR (400 MHz, $CDCl_3$) δ 7.36–7.31 (m, 4H), 7.27–7.23 (m, 1H), 7.13–7.06 (m, 4H), 3.85 (s, 2H), 2.60–2.52 (m, 3H), 2.48 (tt, J = 3.0 Hz, 12.0 Hz, 1H), 2.11–2.04 (m, 2H), 1.94–1.87 (m, 2H), 1.62–1.41 (m, 6H), 1.33–1.23 (m, 11H), 0.87 (t, J = 7.0 Hz, 3H); ^{13}C NMR (101 MHz, $CDCl_3$) δ 144.3, 140.9, 140.5, 128.4, 128.3, 128.1, 126.6, 56.1, 51.2, 43.7, 35.6, 33.8, 33.1, 31.9, 31.5, 29.5, 29.4, 29.3, 22.7, 14.1; ESI-MS *m/z* calcd for $C_{27}H_{39}N$ $[M+H]^+$ 378.31, found 378.25; HRMS (ESI+) *m/z* calcd for $C_{27}H_{40}N$ $[M+H]^+$ 378.3155, found 378.3169.

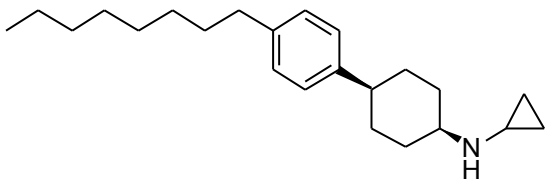

(1*s*,4*s*)-*N*-Cyclopropyl-4-(4-octylphenyl)cyclohexanamine (*cis*-10f). Colorless oil; ^{1}H NMR (500 MHz, $CDCl_3$) δ 7.16–7.07 (m, 4H), 3.02–2.97 (m, 1H), 2.58–2.49 (m, 3H), 2.14–2.08 (m, 1H), 1.92–1.84 (m, 2H), 1.80–1.70 (m, 2H), 1.67–1.55 (m, 7H), 1.35–1.21 (m, 10H), 0.87 (t, J = 6.8 Hz, 3H), 0.46–0.40 (m, 2H), 0.40–0.32 (m, 2H); ^{13}C NMR (126 MHz, $CDCl_3$) δ 144.7, 140.4, 128.3, 126.8, 52.3, 43.3, 35.6, 32.0, 31.6, 30.8, 29.6, 29.5, 29.4, 28.7, 28.5, 22.8, 14.2, 6.4; ESI-MS *m/z* calcd for $C_{23}H_{37}N$ $[M+H]^+$ 328.29, found 328.32.

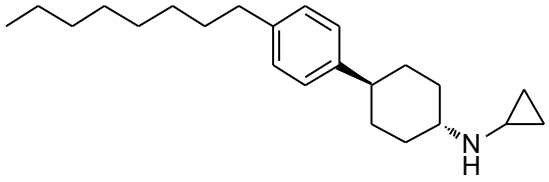

(1*r*,4*r*)-*N*-Cyclopropyl-4-(4-octylphenyl)cyclohexanamine (*trans*-10f). Yellow oil; ^{1}H NMR (500 MHz, $CDCl_3$) δ 7.15–7.08 (m, 4H), 2.66 (tt, J = 4.0 Hz, 11.5 Hz, 1H), 2.57 (t, J = 7.5 Hz, 2H), 2.47 (tt, J = 3.5 Hz, 12.0 Hz, 1H), 2.19–2.10 (m, 3H), 1.95–1.89 (m, 2H), 1.68–1.47 (m, 5H), 1.38–1.19 (m, 12H), 0.89 (t, J = 7.0 Hz, 3H), 0.49–0.42 (m, 2H), 0.41–0.34 (m, 2H); ^{13}C NMR (126 MHz, $CDCl_3$) δ 144.4, 140.6, 128.4, 126.8, 57.6, 43.9, 35.7, 34.3, 33.3, 32.0, 31.6, 29.6, 29.5, 29.4, 28.5, 22.8, 14.2, 6.6; ESI-MS *m/z* calcd for $C_{23}H_{37}N$ $[M+H]^+$ 328.29, found 328.33.

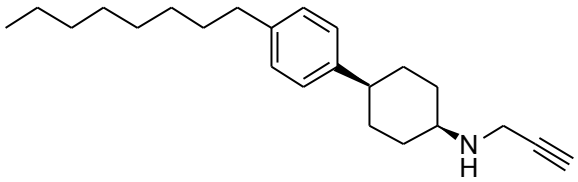

(1*s*,4*s*)-*N*-(Prop-2-ynyl)-4-(4-octylphenyl)cyclohexanamine (*cis*-10g). Colorless oil; ^{1}H NMR (500 MHz, $CDCl_3$) δ 7.19–7.15 (m, 2H), 7.14–7.09 (m, 2H), 3.47 (d, *J* = 2.4 Hz, 2H), 3.16–3.10 (m, 1H), 2.61–2.50 (m, 3H), 2.22 (t, *J* = 2.4 Hz, 1H), 1.90–1.77 (m, 4H), 1.70–1.58 (m, 6H), 1.38–1.22 (m, 10H), 1.12 (br s, 1H), 0.90 (t, *J* = 7.0 Hz, 3H); ^{13}C NMR (126 MHz, $CDCl_3$) δ 144.6, 140.4, 128.3, 126.8, 82.9, 71.0, 50.2, 43.6, 35.8, 35.7, 32.0, 31.7, 30.4, 29.6, 29.5, 29.4, 28.3, 22.7, 14.2; ESI-MS *m/z* calcd for $C_{23}H_{35}N$ $[M+H]^+$ 326.28, found 326.27.

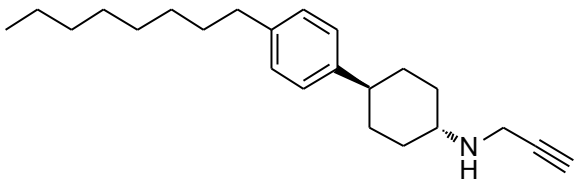

(1*r*,4*r*)-*N*-(Prop-2-ynyl)-4-(4-octylphenyl)cyclohexanamine (*trans*-10g). White solid, mp 48.1–49.1 °C; ^{1}H NMR (500 MHz, $CDCl_3$) δ 7.16–7.09 (m, 4H), 3.50 (d, *J* = 2.4 Hz, 2H), 2.75 (tt, *J* = 3.4 Hz, 11.6 Hz, 1H), 2.56 (t, *J* = 8.0 Hz, 2H), 2.48 (tt, *J* = 3.0 Hz, 12.0 Hz, 1H), 2.22 (t, *J* = 2.4 Hz, 1H), 2.05–1.98 (m, 2H), 1.96–1.89 (m, 2H), 1.63–1.48 (m, 4H), 1.37–1.20 (m, 13H), 0.88 (t, *J* = 7.0 Hz, 3H); ^{13}C NMR (126 MHz, $CDCl_3$) δ 144.3, 140.7, 128.3, 126.7, 82.6, 71.4, 55.0, 43.6, 35.7, 35.4, 33.4, 32.9, 32.0, 31.6, 29.6, 29.5, 29.4, 22.7, 14.1; ESI-MS *m/z* calcd for $C_{23}H_{35}N$ $[M+H]^+$ 326.28, found 326.27.

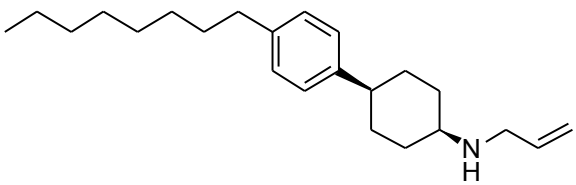

(1*s*,4*s*)-*N*-Allyl-4-(4-octylphenyl)cyclohexanamine (*cis*-10h). Colorless oil; ^{1}H NMR (500 MHz, $CDCl_3$) δ 7.17–7.14 (m, 2H), 7.12–7.09 (m, 2H), 6.02–5.90 (m, 1H), 5.20 (dq, *J* = 1.7 Hz, 17.2 Hz, 1H), 5.09 (dq, *J* = 1.6 Hz, 10.0 Hz, 1H), 3.27 (dt, *J* = 1.4 Hz, 6.0 Hz, 2H), 2.95–2.88 (m, 1H), 2.59–2.50 (m, 3H), 1.86–1.75 (m, 4H), 1.70–1.56 (m, 6H), 1.38–

1.21 (m, 11H), 0.88 (t, J = 7.0 Hz, 3H); ^{13}C NMR (126 MHz, $CDCl_3$) δ 144.5, 140.4, 137.7, 128.4, 126.7, 115.5, 51.3, 50.0, 43.2, 35.5, 32.0, 31.7, 30.5, 29.6, 29.5, 29.4, 28.3, 22.7, 14.2; ESI-MS *m/z* calcd for $C_{23}H_{37}N$ $[M+H]^+$ 328.29, found 328.33.

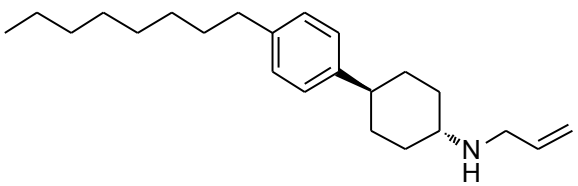

(1*r*,4*r*)-*N*-Allyl-4-(4-octylphenyl)cyclohexanamine (*trans*-10h). Colorless oil; ^{1}H NMR (400 MHz, $CDCl_3$) δ 7.17–7.05 (m, 4H), 6.01–5.87 (m, 1H), 5.19 (dq, J = 1.6 Hz, 17.2 Hz, 1H), 5.12–5.07 (m, 1H), 3.32 (dt, J = 1.3 Hz, 6.0 Hz, 2H), 2.61–2.42 (m, 4H), 2.10–2.00 (m, 2H), 1.96–1.86 (m, 2H), 1.63–1.44 (m, 4H), 1.38–1.17 (m, 13H), 0.87 (t, J = 6.9 Hz, 3H); ^{13}C NMR (126 MHz, $CDCl_3$) δ 144.4, 140.6, 137.4, 128.4, 126.7, 115.7, 56.2, 49.8, 43.8, 35.7, 34.0, 33.2, 32.0, 31.6, 29.6, 29.5, 29.4, 22.8, 14.2; HRMS (FAB+) *m/z* calcd for $C_{23}H_{37}N$ $[M+H]^+$ 328.2999, found 328.3001.

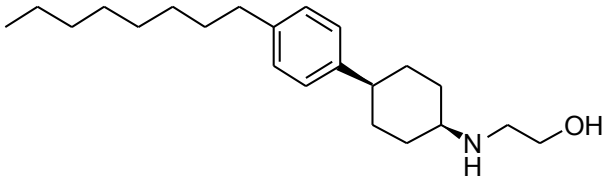

2-(((1*s*,4*s*)-4-(4-Octylphenyl)cyclohexyl)amino)ethanol (*cis*-10i). This compound was synthesized by general procedure A; 76% yield, colorless oil; ^{1}H NMR (400 MHz, $CDCl_3$) δ 7.16–7.12 (m, 2H), 7.12–7.08 (m, 2H), 3.69– 3.59 (m, 2H), 2.93–2.85 (m, 1H), 2.83–2.73 (m, 2H), 2.59–2.48 (m, 3H), 2.12 (br s, 2H), 1.84–1.53 (m, 10H), 1.39–1.18 (m, 10H), 0.87 (t, J = 6.9 Hz, 3H); ^{13}C NMR (101 MHz, $CDCl_3$) δ 144.3, 140.4, 128.3, 126.6, 61.3, 51.5, 48.5, 43.1, 35.5, 31.9, 31.6, 30.6, 29.5, 29.4, 29.3, 28.2, 22.7, 14.1; ESI-MS *m/z* calcd for $C_{22}H_{38}NO$ $[M+H]^+$ 332.29, found 332.30.

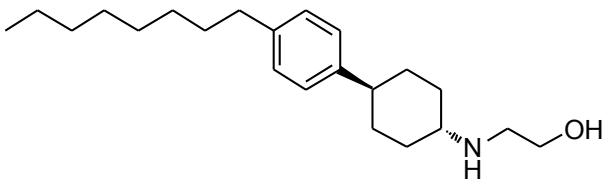

2-((1*r*,4*r*)-4-(4-Octylphenyl)cyclohexylamino)ethanol (*trans*-10i). This compound was synthesized by general procedure B; 53% yield, white solid, mp 79.3–80.0 °C; ^{1}H NMR (500 MHz, $CDCl_3$) δ 7.12–7.07 (m, 4H), 3.65 (t, *J* = 5.0 Hz, 2H), 2.83 (t, *J* = 5.0 Hz, 2H), 2.57–2.47 (m, 4H), 2.08–2.04 (m, 2H), 1.94–1.90 (m, 2H), 1.61–1.43 (m, 4H), 1.35–1.18 (m, 12H), 0.87 (t, *J* = 7.0 Hz, 3H); ^{13}C NMR (126 MHz, $CDCl_3$) δ 144.2, 140.7, 128.4, 126.7, 61.5, 56.5, 48.3, 43.7, 35.6, 34.2, 33.2, 32.0, 31.6, 29.6, 29.5, 29.3, 22.8, 14.2; HRMS (FAB+) *m/z* calcd for $C_{22}H_{38}NO$ $[M+H]^+$ 332.2953, found 332.2972.

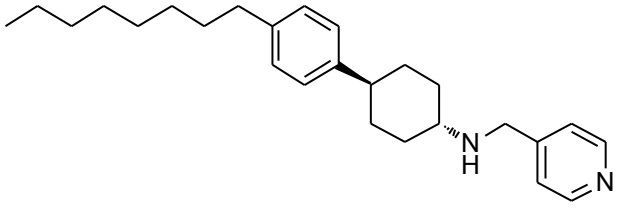

(1*r*,4*r*)-4-(4-Octylphenyl)-*N*-(pyridin-4-ylmethyl) cyclohexanamine (*trans*-10j). This compound was prepared using general procedure C; 20% yield; white solid; ^{1}H NMR (400 MHz, $CDCl_3$) δ 8.58–8.53 (m, 2H), 7.31–7.27 (m, 2H), 7.10 (s, 4H), 3.88 (s, 2H), 2.59–2.43 (m, 4H), 2.12–2.04 (m, 2H), 1.96–1.88 (m, 2H), 1.64–1.55 (m, 2H), 1.55–1.42 (m, 2H), 1.39–1.21 (m, 13H), 0.88 (t, *J* = 6.8 Hz, 3H); ^{13}C NMR (101 MHz, $CDCl_3$) δ 150.1, 149.8, 144.1, 140.6, 128.3, 126.6, 122.9, 56.2, 49.9, 43.6, 35.6, 33.9, 33.0, 31.9, 31.5, 29.5, 29.4, 29.3, 22.7, 14.1.

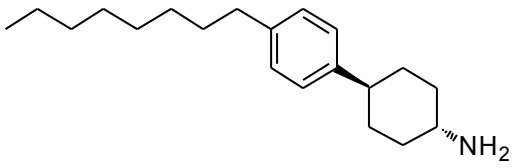

(1*r*,4*r*)-4-(4-Octylphenyl)cyclohexanamine (*trans*-10k). A solution of *trans*-**10e** (80 mg, 0.212 mmol) was dissolved in 2 mL ethanol. Palladium (10 mol%) was added to the solution. A balloon of H_2 gas was attached to the round bottom flask and the solution stirred under H_2 for 20 h. The solution was then filtered through a plug of celite and the resulting filtrate evaporated under reduced pressure to give the title compound as a white solid (50 mg, 84% yield); ^{1}H NMR (500 MHz, $CDCl_3$) δ 7.10 (s, 4H), 2.77–2.69 (m, 1H), 2.55 (t, *J* = 7.5 Hz, 2H), 2.44 (tt, *J* = 3.4 Hz, 11.6 Hz, 1H), 2.0–1.86 (m, 4H), 1.75 (br s, 2H), 1.63–1.45 (m, 4H), 1.39–1.20 (m, 12H), 0.88 (t, *J* = 7.5 Hz, 3H); ^{13}C NMR (126 MHz, $CDCl_3$) δ 143.3, 140.6, 128.7, 128.4, 50.5, 43.3, 37.1, 35.7, 33.3, 32.0, 31.6, 30.8, 29.6, 29.5, 29.4, 22.8, 14.2; HRMS (FAB+) *m/z* calcd for $C_{20}H_{34}N$ $[M+H]^+$ 288.2691, found 288.2680.

Compounds **11a-11c** were synthesized by general procedure D.

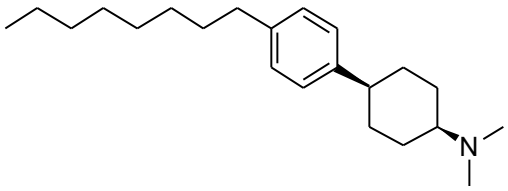

(1*s*,4*s*)-*N*,*N*-Dimethyl-4-(4-octylphenyl)cyclohexanamine (*cis*-11a). 91% Yield, colorless oil; ^{1}H NMR (500 MHz, $CDCl_3$) δ 7.19–7.16 (m, 2H), 7.10–7.07 (m, 2H), 2.65–2.51 (m, 3H), 2.24 (s, 6H), 2.10–2.06 (m, 1H), 1.99–1.86 (m, 4H), 1.65–1.56 (m, 4H), 1.56–1.47 (m, 2H), 1.35–1.22 (m, 10H), 0.87 (t, *J* = 7.0 Hz, 3H); ^{13}C NMR (126 MHz, $CDCl_3$) δ 144.4, 140.3, 128.2, 127.0, 61.1, 43.6, 43.0, 35.6, 32.0, 31.7, 29.6, 29.5, 29.4, 28.9, 28.6, 22.8, 14.2; ESI-MS *m/z* calcd for $C_{22}H_{37}N$ $[M+H]^+$ 316.29, found 316.29.

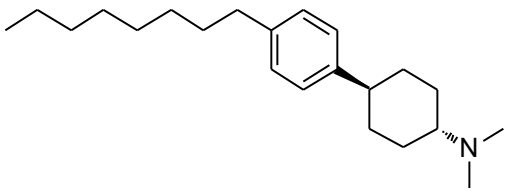

(1*r*,4*r*)-*N*,*N*-Dimethyl-4-(4-octylphenyl)cyclohexanamine (*trans*-11a). 85% Yield, colorless oil; ^{1}H NMR (500 MHz, $CDCl_3$) δ 7.13–7.09 (m, 4H), 2.58–2.54 (t, *J* = 7.5 Hz, 2H), 2.44 (tt, *J* = 3.0 Hz, 11.5 Hz, 1H), 2.32 (s, 6H), 2.25 (tt, *J* = 3.0 Hz, 11.5 Hz, 1H), 2.05–1.94 (m, 4H), 1.63–1.56 (m, 2H), 1.57–1.44 (m, 2H), 1.41–1.22 (m, 12H), 0.88 (t, *J* = 7.5 Hz, 3H); ^{13}C NMR (126 MHz, $CDCl_3$) δ 144.3, 140.6, 128.4, 126.7, 63.5, 43.8, 41.8, 35.7, 33.6, 32.0, 31.6, 29.6, 29.5, 29.4, 29.1, 22.8, 14.2; HRMS (FAB+) *m/z* calcd for $C_{22}H_{37}N$ $[M+H]^+$ 316.3004, found 316.3009.

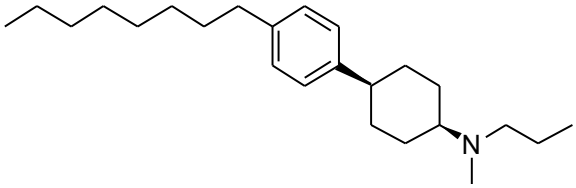

(1*s*,4*s*)-*N*-Methyl-4-(4-octylphenyl)-*N*-propylcyclohexanamine (*cis*-11b). 93% Yield, colorless oil; ^{1}H NMR (400 MHz, $CDCl_3$) δ 7.22–7.16 (m, 2H), 7.13–7.07 (m, 2H), 2.72–2.62 (m, 1H), 2.60–2.52 (m, 2H), 2.45–2.34 (m, 3H), 2.22 (s, 3H), 2.05–1.93 (m, 2H), 1.92–1.81 (m, 2H), 1.66–1.40 (m, 8H), 1.36–1.21 (m, 10H), 0.88 (t, *J* = 7.3 Hz, 6H); ^{13}C NMR (126 MHz, $CDCl_3$) δ 144.2, 140.2, 128.3, 127.1, 58.7, 56.0, 41.9, 38.9, 35.6, 32.0, 31.7, 29.6, 29.5, 29.4, 28.8, 28.1, 22.8, 19.4, 14.2, 12.1; ESI-MS *m/z* calcd for $C_{24}H_{41}N$ $[M+H]^+$ 344.32, found 344.35.

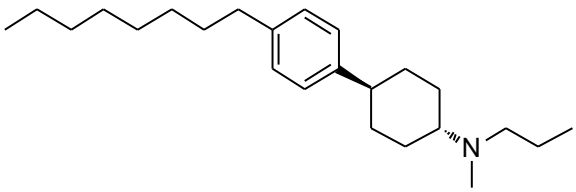

(1*r*,4*r*)-*N*-Methyl-4-(4-octylphenyl)-*N*-propylcyclohexanamine (*trans*-11b). 66% Yield, colorless oil; ^{1}H NMR (500 MHz, $CDCl_3$) δ 7.13–7.07 (m, 4H), 2.58–2.53 (m, 2H), 2.50–2.38 (m, 4H), 2.28 (s, 3H), 1.99–1.90 (m, 4H), 1.62–1.54 (m, 2H), 1.54–1.36 (m, 6H), 1.35–1.21 (m, 10H), 0.92–0.84 (m, 6H); ^{13}C NMR (126 MHz, $CDCl_3$) δ 144.4, 140.6, 128.4, 126.7, 62.3, 56.0, 44.0, 38.1, 35.7, 33.9, 32.0, 31.6, 29.6, 29.5, 29.4, 28.7, 22.8, 21.2, 14.2, 12.1; HRMS (FAB+) *m/z* calcd for $C_{24}H_{41}N$ $[M+H]^+$ 344.3312, found 344.3314.

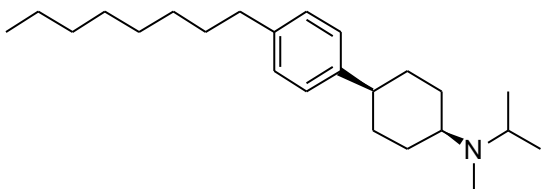

(1*s*,4*s*)-*N*-Isopropyl-*N*-methyl-4-(4-octylphenyl)cyclohexanamine (*cis*-11c). 86% Yield, colorless oil; ^{1}H NMR (400 MHz, $CDCl_3$) δ 7.21–7.15 (m, 2H), 7.14–7.07 (m, 2H), 3.27–3.10 (m, 1H), 2.73–2.52 (m, 4H), 2.14 (s, 3H), 2.05–1.86 (m, 4H), 1.67–1.48 (m, 6H), 1.39–1.19 (m, 10H), 1.01 (d, J = 6.6 Hz, 6H), 0.89 (t, J = 6.8 Hz, 3H); ^{13}C NMR (101 MHz, $CDCl_3$) δ 140.9, 139.0, 129.0, 127.2, 71.7, 63.9, 44.7, 35.6, 34.2, 32.1, 31.7, 29.7, 29.6, 29.5, 29.1, 22.9, 22.4, 17.8, 14.3; ESI-MS *m/z* calcd for $C_{24}H_{41}N$ $[M+H]^+$ 344.32, found 344.32.

Compounds **12a-12c** were synthesized by general procedure E

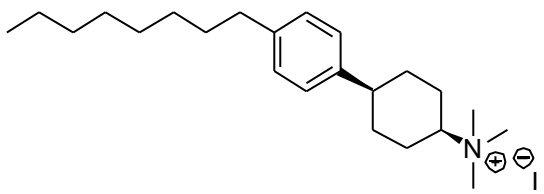

(1*s*,4*s*)-*N*,*N*,*N*-Trimethyl-4-(4-octylphenyl)cyclohexanaminium iodide (*cis*-12a): 69% yield, pink solid, mp 238.4-239.8 °C; ^{1}H NMR (500 MHz, $CDCl_3$) δ 7.22–7.17 (m, 2H), 7.17–7.12 (m, 2H), 4.04 (tt, J = 3.3 Hz, 12.1 Hz, 1H), 3.31 (s, 9H), 3.10 (s, 1H), 2.62–

2.52 (m, 2H), 2.51–2.43 (m, 2H), 2.16–2.00 (m, 4H), 1.69–1.50 (m, 4H), 1.37–1.18 (m, 10H), 0.86 (t, J = 7.0 Hz, 3H); ^{13}C NMR (126 Hz, $CDCl_3$) δ 140.9, 138.7, 128.9, 127.0, 74.6, 51.6, 35.5, 33.8, 32.0, 31.5, 29.6, 29.5, 29.3, 28.5, 22.7, 22.1, 14.2; ESI-MS *m/z* calcd for $C_{25}H_{44}N^+$ 330.32, found 330.31.

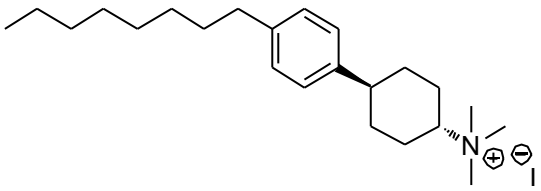

(1*r*,4*r*)-*N*,*N*,*N*-Trimethyl-4-(4-octylphenyl)cyclohexanaminium iodide (*trans*-12a): 72% yield, white solid; ^{1}H NMR (500 MHz, CD_3OD) δ 7.17-7.06 (m, 4H), 3.53 (m, 1H), 3.14 (s, 9H), 2.61-2.51 (m, 3H), 2.40-2.30 (m, 2H), 2.14-2.05 (m, 2H), 1.81-1.52 (m, 6H), 1.37-1.21 (m, 10H), 0.88 (t, J = 7.5 Hz, 3H); ^{13}C NMR (126 MHz, CD_3OD) δ 144.5, 140.8, 128.2, 126.3, 74.1, 50.4, 42.2, 35.2, 32.5, 31.7, 31.4, 29.2, 29.1, 29.0, 26.1, 22.4, 13.1; HRMS (FAB+) *m/z* calcd for $C_{23}H_{40}N^+$ 330.3161, found 330.3168.

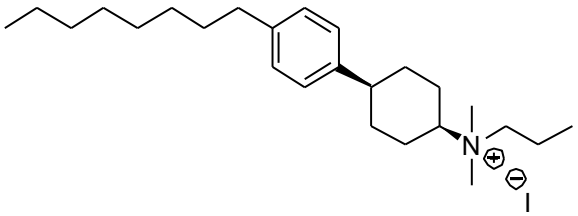

(1*s*,4*s*)-*N*,*N*-Dimethyl-4-(4-octylphenyl)-*N*-propylcyclohexanaminium iodide (*cis*-12b): 68% yield, yellow solid; ^{1}H NMR (400 MHz, $CDCl_3$) δ 7.23–7.18 (m, 2H), 7.17–7.13 (m, 2H), 3.98–3.84 (m, 1H), 3.48–3.39 (m, 2H), 3.21 (s, 6H), 3.12 (m, 1H), 2.61–2.54 (m, 2H), 2.54–2.45 (m, 2H), 2.12–2.00 (m, 4H), 1.90–1.77 (m, 2H), 1.68–1.56 (m, 4H), 1.38–1.19 (m, 10H), 1.04 (t, J = 7.3 Hz, 3H), 0.87 (t, J = 6.9 Hz, 3H); ^{13}C NMR (126 MHz, $CDCl_3$) δ 140.9, 138.6, 128.9, 127.0, 72.7, 64.1, 49.0, 35.5, 33.9, 32.0, 31.5,

29.6, 29.5, 29.4, 28.8, 22.8, 21.9, 16.5, 14.2, 10.9; ESI-MS *m/z* calcd for $C_{25}H_{44}N^+$ 358.35, found 358.34.

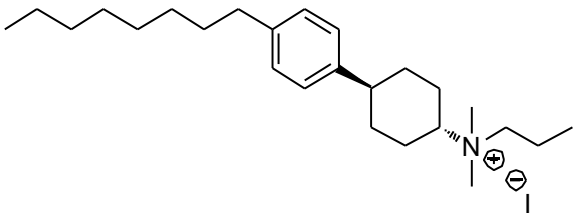

(1*r*,4*r*)-*N*,*N*-Dimethyl-4-(4-octylphenyl)-*N*-propylcyclohexanaminium iodide (*trans*-12b): 71% yield, white solid, mp 162.6-163.7 °C; ^{1}H NMR (400 MHz, $CDCl_3$) δ 7.12–7.05 (m, 4H), 3.77–3.68 (m, 1H), 3.60–3.51 (m, 2H), 3.34 (s, 6H), 2.60–2.50 (m, 3H), 2.37–2.29 (m, 2H), 2.17–2.10 (m, 2H), 1.92–1.80 (m, 2H), 1.78–1.65 (m, 4H), 1.61–1.52 (m, 2H), 1.35–1.20 (m, 10H), 1.07 (t, *J* = 7.3 Hz, 3H), 0.85 (t, *J* = 7.0 Hz, 3H); ^{13}C NMR (126 MHz, $CDCl_3$) δ 141.7, 141.4, 128.6, 126.6, 72.0, 64.5, 49.5, 42.4, 35.6, 32.6, 32.0, 31.6, 29.6, 29.5, 29.3, 26.6, 22.7, 16.5, 14.2, 10.9; ESI-MS *m/z* calcd for $C_{25}H_{44}N^+$ 358.35, found 358.34; HRMS (FAB+) *m/z* calcd for $C_{25}H_{44}N^+$ 358.3463, found 358.3470.

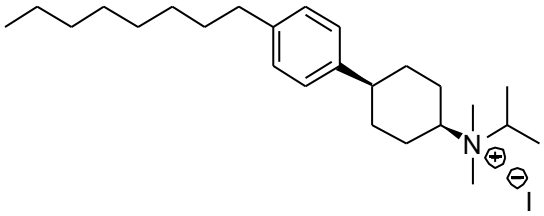

(1*s*,4*s*)-*N*-isopropyl-*N*,*N*-dimethyl-4-(4-octylphenyl)cyclohexanaminium iodide (*cis*-12c): 70% yield, white solid; ^{1}H NMR (500 MHz, $CDCl_3$) δ 7.20-7.07 (m, 4H), 4.06-3.98 (m, 1H), 3.84 (tt, *J* = 3.2 Hz, 11.8 Hz, 1H), 3.14-3.05 (m, 1H), 2.96 (s, 6H), 2.54 (t, *J* = 7.9 Hz, 2H), 2.49-2.42 (m, 2H), 2.17-2.00 (m, 4H), 1.68-1.52 (m, 4H), 1.48 (d, *J* = 6.5 Hz, 6H), 1.34-1.20 (m, 10H), 0.85 (t, *J* = 7.0 Hz, 3H); ^{13}C NMR (101 MHz, $CDCl_3$) δ 140.9, 139.0, 129.0, 127.2, 71.7, 63.9, 44.7, 35.6, 34.2, 32.1, 31.7, 29.7, 29.6, 29.5, 29.1, 22.9, 22.4, 17.8, 14.3; ESI-MS *m/z* calcd for $C_{25}H_{44}N^+$ 358.35, found 358.32.

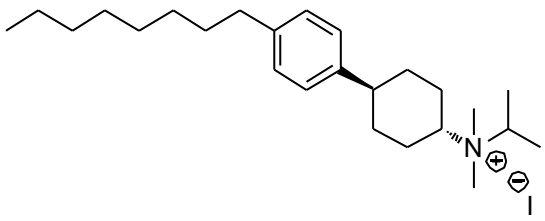

(1*r*,4*r*)-*N*-isopropyl-*N*,*N*-dimethyl-4-(4-octylphenyl)cyclohexanaminium iodide (*trans*-12c): 68% yield, white solid; ^{1}H NMR (400 MHz, $CDCl_3$) δ 7.10 (s, 4H), 4.20-4.08 (m, 1H), 3.72 (tt, *J* = 2.8 Hz, 11.7 Hz, 1H), 3.13 (s, 6H), 2.64-2.52 (m, 3H), 2.45-2.35 (m, 2H), 2.20-2.11 (m, 2H), 1.91-1.66 (m, 4H), 1.65-1.49 (m, 8H), 1.39-1.19 (m, 10H), 0.88 (t, *J* = 6.8 Hz, 3H); ^{13}C NMR (101 MHz, $CDCl_3$) δ 141.6, 141.2, 128.5, 126.5, 71.2, 63.7, 44.7, 42.4, 35.5, 32.7, 31.9, 31.5, 29.5, 29.4, 29.2, 26.8, 22.7, 17.4, 14.1; ESI-MS *m/z* calcd for $C_{25}H_{44}N^+$ 358.35, found 358.32.

Compounds **12e**, **12h**, and **12i** were synthesized by general procedure F.

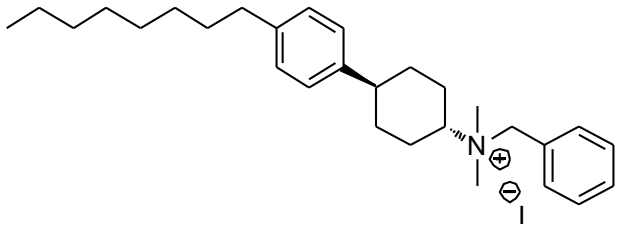

(1*r*,4*r*)-*N*-benzyl-*N*,*N*-dimethyl-4-(4-octylphenyl)cyclohexanaminium iodide (*trans*-12e): 73% yield, white solid, mp 183.9-185.0 ºC; ^{1}H NMR (500 MHz, $CDCl_3$) δ 7.69-7.65 (m, 2H), 7.46-7.38 (m, 3H), 7.08-7.01 (m, 4H), 4.98 (s, 2H), 3.83 (tt, *J* = 2.8 Hz, 12.0 Hz, 1H), 3.20 (s, 6H), 2.59-2.41 (m, 5H), 2.17-2.05 (m, 2H), 1.91-1.76 (m, 2H), 1.67-1.52 (m, 4H), 1.35-1.16 (m, 10H), 0.85 (t, *J* = 7.0 Hz, 3H); ^{13}C NMR (126 MHz, $CDCl_3$) δ 141.7, 141.3, 133.4, 130.9, 129.4, 128.6, 127.3, 126.6, 72.1, 65.1, 47.8, 42.2, 35.6, 32.5, 32.0, 31.6, 29.6, 29.5, 29.3, 27.1, 22.7, 14.2; ESI-MS *m/z* calcd for $C_{29}H_{44}N^+$ 406.35, found 406.31.

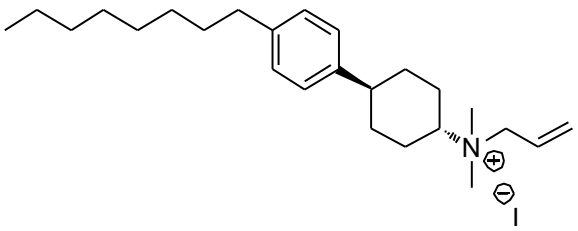

(1*r*,4*r*)-*N*-allyl-*N*,*N*-dimethyl-4-(4-octylphenyl)cyclohexanaminium iodide (*trans*-12h): 72% yield, white solid; ^{1}H NMR (400 MHz, $CDCl_3$) δ 7.10–7.02 (m, 4H), 6.14–5.99 (m, 1H), 5.94–5.86 (m, 1H), 5.78–5.70 (m, 1H), 4.37 (d, J = 7.2 Hz, 2H), 3.65 (tt, J = 3.1 Hz, 12.0 Hz, 1H), 3.30 (s, 6H), 2.61–2.48 (m, 3H), 2.43–2.32 (m, 2H), 2.18–2.08 (m, 2H), 1.87–1.50 (m, 6H), 1.36–1.16 (m, 10H), 0.85 (t, J = 6.9 Hz, 3H); ^{13}C NMR (101 MHz, $CDCl_3$) δ 141.6, 141.2, 130.0, 128.5, 126.5, 124.3, 71.8, 64.7, 48.6, 42.2, 35.5, 32.4, 31.9, 31.5, 29.5, 29.4, 29.2, 26.6, 22.7, 14.1; ESI-MS *m/z* calcd for $C_{25}H_{42}N^+$ 356.35, found 356.32.

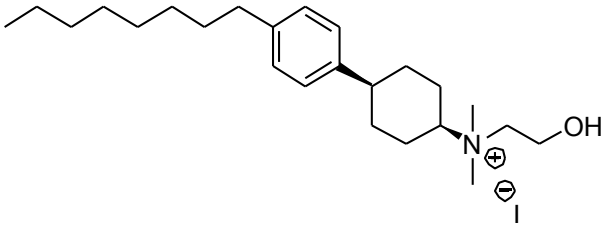

(1*s*,4*s*)-*N*-(2-hydroxyethyl)-*N*,*N*-dimethyl-4-(4-octylphenyl)cyclohexanaminium iodide (*cis*-12i): 52% yield, white solid; ^{1}H NMR (400 MHz, CD_3OD) δ 7.38–7.24 (m, 2H), 7.22–7.07 (m, 2H), 4.09–3.91 (m, 2H), 3.91–3.68 (m, 1H), 3.56–3.43 (m, 2H), 3.15–2.95 (m, 7H), 2.56 (t, J = 7.7 Hz, 2H), 2.53–2.43 (m, 2H), 2.25–2.14 (m, 1H), 2.14–1.91 (m, 3H), 1.80–1.38 (m, 4H), 1.38–1.13 (m, 11H), 0.88 (t, J = 6.6 Hz, 3H); ^{13}C NMR (126 MHz, $CDCl_3$) δ 140.3, 138.7, 128.4, 126.7, 74.0, 63.4, 55.4, 35.0, 33.7, 31.5, 31.2, 29.1, 29.0, 28.9, 28.4, 22.3, 21.4, 13.4; HRMS (FAB+) *m/z* calcd for $C_{24}H_{42}NO^+$ 360.3266, found 360.3273.

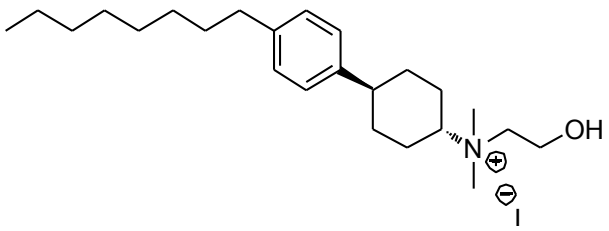

(1*r*,4*r*)-*N*-(2-hydroxyethyl)-*N*,*N*-dimethyl-4-(4-octylphenyl)cyclohexanaminium iodide (*trans*-12i): 39% yield, white solid, mp 153.3-154.2 ºC; ^{1}H NMR (500 MHz, $CDCl_3$) δ 7.11-7.04 (m, 4H), 4.34-4.28 (m, 1H), 4.22-4.16 (m, 2H), 3.95-3.87 (m, 1H), 3.81-3.76 (m, 2H), 3.30 (s, 6H), 2.52 (t, *J* = 7.5 Hz, 2H), 2.42-2.35 (m, 2H), 2.13-2.02 (m, 2H), 1.79-1.65 (m, 4H), 1.60-1.50 (m, 2H), 1.34-1.18 (m, 10H), 0.86 (t, *J* = 7.0 Hz, 3H); ^{13}C NMR (126 MHz, $CDCl_3$) δ 141.8, 141.3, 128.6, 126.7, 73.4, 64.1, 55.9, 50.1, 42.5, 35.6, 32.5, 32.0, 31.6, 29.6, 29.5, 29.4, 26.7, 22.8, 14.2; HRMS (FAB+) *m/z* calcd for $C_{24}H_{42}NO^{+}$ 360.3266, found 360.3259.

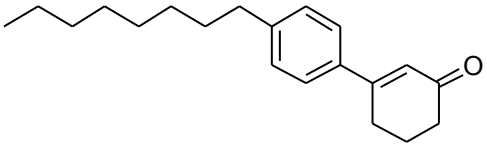

4'-octyl-5,6-dihydro-[1,1'-biphenyl]-3(4H)-one (13). *n*-butyllithium (2.6 M in toluene, 3.5 mL, 8.99 mmol) was added to a solution of 1-bromo-4-octylbenzene (1.75 mL, 7.34 mmol) in THF at -78 °C and the mixture stirred for 20 min. A solution of 3-ethoxycyclohex-2-enone (1.1 mL, 7.49 mmol) in THF was added dropwise and the reaction mixture heated at reflux for 2 h. After cooling to rt, the reaction mixture was acidified with 10% aqueous HCl and stirred for 30 min. It was extracted with three portions of ether. The combined organic extracts were washed with $NaHCO_3$, brine and dried with sodium sulfate. The solvent was evaporated under reduced pressure and the residue purified by column chromatography on silica gel (90/10 hexanes/ethyl acetate) to give the title compound (1.6 g, 5.63 mmol, 75 % yield) as a colorless oil.^{1}H NMR (500

MHz, $CDCl_3$) δ 7.48–7.37 (m, 2H), 7.22–7.13 (m, 2H), 6.39 (s, 1H), 2.76–2.65 (m, 2H), 2.64–2.52 (m, 2H), 2.47–2.37 (m, 2H), 2.15–2.03 (m, 2H), 1.66–1.51 (m, 2H), 1.37–1.15 (m, 10H), 0.85 (t, *J* = 7.0 Hz, 3H); ^{13}C NMR (126 MHz, $CDCl_3$) δ 199.9, 159.7, 145.5, 136.0, 128.9, 126.1, 124.7, 37.4, 35.8, 32.0, 31.4, 29.5, 29.4, 29.3, 28.0, 22.9, 22.8, 14.2.

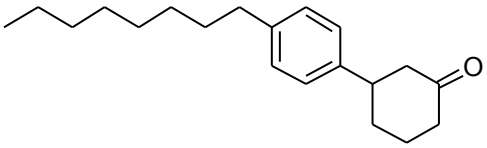

3-(4-octylphenyl)cyclohexanone (14). 10% Pd on activated carbon (0.15 g, 0.14 mmol, 10 mol %) was added to a round bottom flask containing **13** dissolved in ethanol (28 mL) and the reaction was run under H_2 gas for 20 h. Pd/C was filtered through a plug of celite and the filtrate concentrated on a rotary evaporator to provide a colorless oil. The colorless oil was dissolved in CH_2Cl_2. It was added to a round bottom flask containing a finely powdered mixture of pyridinium chlorochromate (2.39 g, 11.1 mmol) and silica gel (1:1) in CH_2Cl_2 (15 mL) and the reaction mixture was stirred for 1 h. It was then diluted with diethyl ether and filtered over a plug of celite. The filtrate was concentrated under vacuum and the residue was diluted with diethyl ether, washed with water, brine, dried over sodium sulfate. After evaporation of the organic solvent under reduced pressure, the resulting residue was purified by column chromatography over silica gel (90/10 hexanes/ethyl acetate) to give the title compound (1.2 g, 4.19 mmol, 75% yield). ^1H NMR (500 MHz, $CDCl_3$) δ 7.20–7.08 (m, 4H), 2.98 (tt, *J* = 11.8, 4.0 Hz, 1H), 2.62–2.41 (m, 5H), 2.41–2.33 (m, 1H), 2.18–2.11 (m, 1H), 2.10–2.03 (m, 1H), 1.89–1.71 (m, 2H), 1.64–1.54 (m, 2H), 1.39–1.19 (m, 10H), 0.88 (t, *J* = 7.2 Hz, 3H); ^{13}C NMR (126 MHz, $CDCl_3$) δ 211.2, 141.7, 141.4, 128.7, 126.5, 49.2, 44.5, 41.3, 35.7, 33.0, 32.0, 31.6, 29.6, 29.5, 29.4, 25.7, 22.8, 14.2.

The following three compounds were synthesized by general procedure C; ratio of *cis* to *trans* isomers for compound **15** was 83:17. Combined % yield of both isomers was 79%. For compound **17,** only the *cis* isomer was isolated.

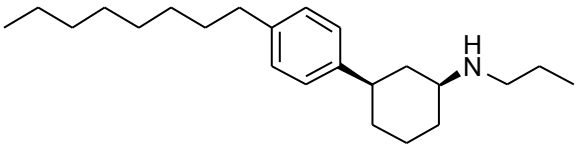

(1*S*,3*R*)-3-(4-octylphenyl)-*N*-propylcyclohexanamine (*cis*-15). Colorless oil, ^{1}H NMR (500 MHz, $CDCl_3$) δ 7.15–7.07 (m, 4H), 2.66–2.50 (m, 6H), 2.15–2.08 (m, 1H), 2.01–1.94 (m, 1H), 1.91–1.81 (m, 2H), 1.64–1.56 (m, 2H), 1.54–1.22 (m, 15H), 1.16–1.06 (m, 1H), 0.95–0.84 (m, 6H); ^{13}C NMR (126 MHz, $CDCl_3$) δ 144.3, 140.6, 128.4, 126.7, 57.4, 49.1, 43.0, 41.5, 35.7, 34.4, 33.5, 32.0, 31.7, 29.6, 29.5, 29.4, 25.4, 23.8, 22.8, 14.2, 12.0; HRMS (ESI+) *m/z* calcd for $C_{23}H_{40}N$ $[M+H]^+$ 330.3155, found 330.3140.

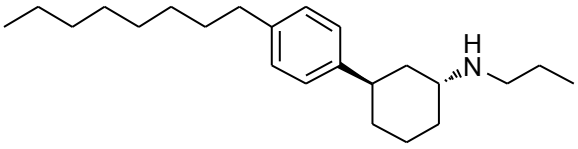

(1*R*,3*R*)-3-(4-octylphenyl)-*N*-propylcyclohexanamine (*trans*-15). Colorless oil; ^{1}H NMR (500 MHz, $CDCl_3$) δ 7.17–7.07 (m, 4H), 3.02–2.95 (m, 1H), 2.89 (tt, *J* = 11.7, 3.4 Hz, 1H), 2.60–2.50 (m, 4H), 1.93–1.81 (m, 2H), 1.78–1.41 (m, 10H), 1.37–1.19 (m, 10H), 0.94 (t, *J* = 7.4 Hz, 3H), 0.88 (t, *J* = 7.0 Hz, 3H); ^{13}C NMR (126 MHz, $CDCl_3$) δ 144.7, 140.4, 128.4, 126.9, 52.7, 49.6, 38.1, 37.2, 35.7, 34.1, 32.0, 31.7, 30.5, 29.6, 29.5, 29.4, 23.6, 22.8, 21.0, 14.2, 12.0; HRMS (ESI+) *m/z* calcd for $C_{23}H_{40}N$ $[M+H]^+$ 330.3155, found 330.3152.

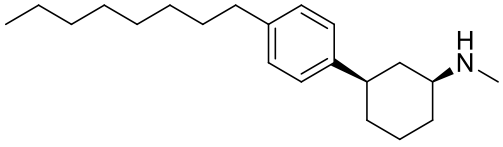

(1*R*,3*R*)-*N*-methyl-3-(4-octylphenyl)cyclohexanamine (*cis*-17). This compound was synthesized by general procedure C; 71% yield; colorless oil; ^{1}H NMR (500 MHz, $CDCl_3$) δ 7.16–7.07 (m, 4H), 2.93–2.83 (m, 2H), 2.56 (t, *J* = 7.7 Hz, 2H), 2.44 (s, 3H), 1.95–1.81 (m, 2H), 1.80–1.41 (m, 8H), 1.38–1.18 (m, 11H), 0.88 (t, *J* = 7.1 Hz, 3H); ^{13}C NMR (126 MHz, $CDCl_3$) δ 144.6, 140.5, 128.4, 126.9, 54.9, 37.7, 37.3, 35.7, 34.3, 34.1, 32.0, 31.7, 29.9, 29.6, 29.5, 29.4, 22.8, 20.9, 14.2.

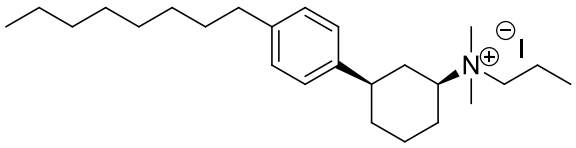

(1*S*,3*R*)-*N*,*N*-dimethyl-3-(4-octylphenyl)-*N*-propylcyclohexanaminium iodide (*cis*-16): This compound was synthesized by general procedure F; 68% yield; white solid; ^{1}H NMR (500 MHz, $CDCl_3$) δ 7.15 (d, *J* = 8.1 Hz, 2H), 7.09 (d, *J* = 8.1 Hz, 2H), 3.98–3.88 (m, 1H), 3.55–3.35 (m, 2H), 3.26 (d, *J* = 13.6 Hz, 6H), 2.88–2.75 (m, 1H), 2.57–2.47 (m, 2H), 2.34–2.25 (m, 1H), 2.23–2.16 (m, 1H), 2.13–2.04 (m, 1H), 1.93–1.37 (m, 9H), 1.33–1.17 (m, 10H), 1.01 (t, *J* = 7.3 Hz, 3H), 0.84 (t, *J* = 6.9 Hz, 3H); ^{13}C NMR (126 MHz, $CDCl_3$) δ 141.7, 141.6, 128.8, 126.8, 72.1, 64.3, 49.4, 49.3, 42.7, 35.6, 33.9, 32.5, 32.0, 31.6, 29.5, 29.4, 29.3, 26.0, 24.8, 22.7, 16.6, 14.2, 10.9; HRMS (ESI+) *m/z* calcd for $C_{25}H_{44}N^{+}$ 358.3468, found 358.3452.

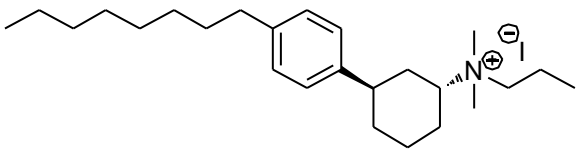

(1*R*,3*R*)-*N*,*N*-dimethyl-3-(4-octylphenyl)-*N*-propylcyclohexanaminium iodide (*trans*-16): This compound was synthesized by general procedure F; 62% yield; white solid; ^{1}H NMR (500 MHz, $CDCl_3$) δ 7.17 (d, *J* = 7.9 Hz, 2H), 7.11 (d, *J* = 8.2 Hz, 2H), 3.60–3.49

(m, 2H), 3.49–3.41 (m, 1H), 3.23 (d, J = 5.2 Hz, 6H), 3.10–3.00 (m, 1H), 2.67–2.58 (m, 1H), 2.58–2.47 (m, 2H), 2.28–2.20 (m, 1H), 2.19–2.04 (m, 2H), 1.99–1.90 (m, 1H), 1.79–1.66 (m, 3H), 1.59–1.47 (m, 3H), 1.44–1.34 (m, 1H), 1.31–1.16 (m, 10H), 0.94 (t, J = 7.3 Hz, 3H), 0.83 (t, J = 7.0 Hz, 3H); ^{13}C NMR (126 MHz, $CDCl_3$) δ 141.3, 138.4, 129.0, 126.9, 68.1, 64.4, 49.7, 49.2, 36.5, 35.4, 31.9, 31.8, 31.5, 29.5, 29.4, 29.3, 26.8, 26.7, 22.7, 21.5, 15.9, 14.2, 10.6; HRMS (ESI+) *m/z* calcd for $C_{25}H_{44}N^+$ 358.3468, found 358.3456.

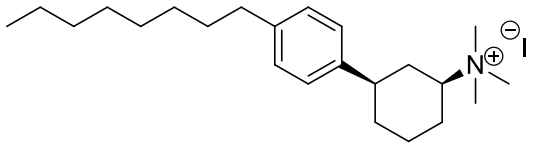

(1*S*,3*R*)-*N*,*N*,*N*-trimethyl-3-(4-octylphenyl)cyclohexanaminium iodide (*cis*-18): This compound was synthesized by general procedure F; 55% yield; white solid; ^{1}H NMR (500 MHz, $CDCl_3$) δ 7.23–7.12 (m, 4H), 3.53–3.46 (m, 1H), 3.35 (s, 9H), 3.18–3.08 (m, 1H), 2.81–2.73 (m, 1H), 2.55 (t, J = 8.2 Hz, 2H), 2.34–2.19 (m, 2H), 2.08–2.00 (m, 1H), 1.98–1.92 (m, 1H), 1.79–1.63 (m, 3H), 1.62–1.53 (m, 2H), 1.36–1.19 (m, 10H), 0.86 (t, J = 7.0 Hz, 3H); ^{13}C NMR (126 MHz, $CDCl_3$) δ 141.4, 138.0, 129.2, 126.8, 71.7, 51.5, 36.4, 35.5, 32.0, 31.5, 31.3, 29.6, 29.5, 29.4, 27.3, 26.8, 22.8, 21.0, 14.2; HRMS (ESI+) *m/z* calcd for $C_{23}H_{40}N^+$ 330.3155, found 330.3128.

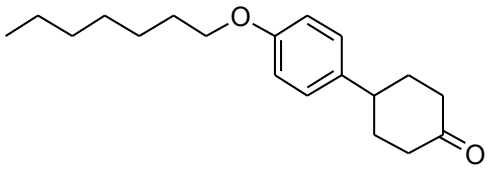

4-(4-(heptyloxy)phenyl)cyclohexanone (20). K_2CO_3 (2.19 g, 15.83 mmol) and KI (0.09 g, 0.528 mmol) were added to a solution of **19** (1 g, 5.28 mmol) and 1-bromoheptane (0.9 mL, 5.81 mmol) in acetone (26 mL). The reaction mixture was refluxed for 24 h and

then filtered to remove all insoluble solids. The filtrate was concentrated under reduced pressure and the resulting residue was purified by column chromatography over silica gel (10% EtOAc in hexanes) to give the title compound (1.0 g, 68% yield) as a white solid, mp 55.7-56.1 °C; ^{1}H NMR (400 MHz, $CDCl_3$) δ 7.17–7.11 (m, 2H), 6.88–6.82 (m, 2H), 3.93 (t, *J* = 6.6 Hz, 2H), 2.97 (tt, *J* = 12.0 Hz, 3.3 Hz, 1H), 2.55–2.42 (m, 4H), 2.23–2.14 (m, 2H), 1.97–1.83 (m, 2H), 1.81–1.72 (m, 2H), 1.50–1.24 (m, 8H), 0.89 (t, *J* = 6.7 Hz, 3H); ^{13}C NMR (101 MHz, $CDCl_3$) δ 211.2, 157.8, 136.6, 127.5, 114.5, 68.0, 41.9, 41.4, 34.2, 31.8, 29.3, 29.1, 26.0, 22.6, 14.1; HRMS (ESI+) *m/z* calcd for $C_{19}H_{28}O_2$ $[M+H]^+$ 288.2089, found 288.2081.

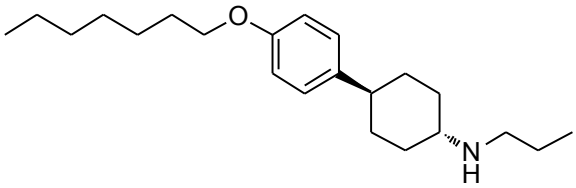

(1*r*,4*r*)-4-(4-(heptyloxy)phenyl)-*N*-propylcyclohexanamine (21). This compound was synthesized by general procedure C. It was purified by column chromatography (100% EtOAc) on neutral alumina; 76%yield; colorless oil; ^{1}H NMR (400 MHz, $CDCl_3$) δ 7.13–7.08 (m, 2H), 6.84–6.79 (m, 2H), 3.92 (t, *J* = 6.6 Hz, 2H), 2.63 (t, *J* = 6.1 Hz, 2H), 2.55–2.40 (m, 2H), 2.10–2.00 (m, 2H), 1.94–1.86 (m, 2H), 1.81–1.71 (m, 2H), 1.58–1.18 (m, 15H), 0.93 (t, *J* = 7.4 Hz, 3H), 0.88 (t, *J* = 6.8 Hz, 3H); ^{13}C NMR (101 MHz, $CDCl_3$) δ 157.3, 139.1, 127.5, 114.2, 67.9, 56.8, 49.1, 43.2, 33.8, 33.3, 31.8, 29.3, 29.1, 26.0, 23.5, 22.6, 14.1, 11.9.

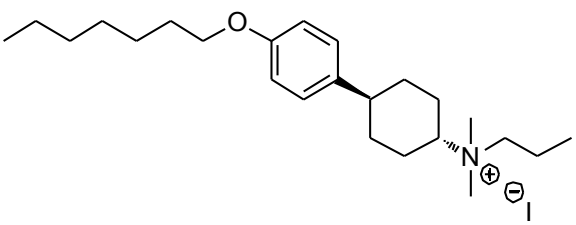

(1*r*,4*r*)-4-(4-(heptyloxy)phenyl)-N,N-dimethyl-*N*-propylcyclohexanaminium iodide (22). This compound was synthesized by general procedure F; 68% yield; white solid; ^{1}H NMR (400 MHz, $CDCl_3$) δ 7.08–6.98 (m, 2H), 6.81–6.72 (m, 2H), 3.85 (t, *J* = 6.6 Hz, 2H), 3.75–3.63 (m, 1H), 3.55–3.47 (m, 2H), 3.28 (s, 6H), 2.52–2.40 (m, 1H), 2.32–2.21 (m, 2H), 2.13–2.02 (m, 2H), 1.86–1.76 (m, 2H), 1.76–1.57 (m, 6H), 1.42–1.32 (m, 2H), 1.32–1.20 (m, 6H), 1.03 (t, *J* = 7.3 Hz, 3H), 0.82 (t, *J* = 6.9 Hz, 3H); ^{13}C NMR (101 MHz, $CDCl_3$) δ 157.9, 136.1, 127.5, 114.5, 71.9, 68.0, 64.4, 49.2, 41.9, 32.6, 31.8, 29.3, 29.1, 26.5, 26.0, 22.6, 16.4, 14.1, 10.8; HRMS (ESI+) *m/z* calcd for $C_{24}H_{42}NO^+$ 360.3266, found 360.3273.

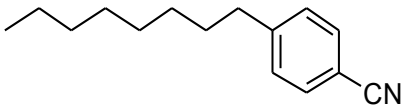

4-Octylbenzonitrile (23): Oct-1-ene (3 mL, 19.2 mmol) was added to a round bottom flask containing THF (8 mL). 9-BBN (42 mL, 21.0 mmol) was added as a 0.5 M solution in THF and the solution stirred overnight at rt. To the above borane solution was added a solution of 4-iodobenzonitrile (4 g, 17.5 mmol) in DMF (50 mL). The reaction mixture was degassed for 10 min by bubbling N_2 through the solution. Cs_2CO_3 (11.4 g, 34.9 mmol) and $PdCl_2$(dppf) (383 mg, 0.52 mmol) were added together. The reaction mixture was stirred at 70 ^{o}C for 10 h. It was poured into a solution of LiBr and extracted three times with hexanes. The combined organic extracts were washed with brine, dried over Na_2SO_4 and concentrated under reduced pressure. The resulting residue was purified by column chromatography over silica gel (95/5 EtOAc/hexanes) to give the title compound (2.3 g, 62%) as a colorless oil. ^{1}H NMR (500 MHz, $CDCl_3$) δ 7.54 (d, *J* = 8.1 Hz, 2H), 7.26 (d, *J* = 8.1 Hz, 2H), 2.64 (t, *J* = 7.8 Hz, 2H), 1.69–1.53 (m, 2H), 1.36–1.18 (m, 10H),

0.86 (t, J = 6.9 Hz, 3H); ^{13}C NMR (126 MHz, $CDCl_3$) δ 148.7, 132.2, 129.3, 119.3, 109.6, 36.2, 32.0, 31.1, 29.5, 29.3, 29.2, 22.7, 14.2.

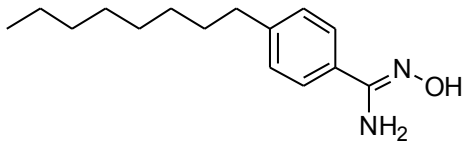

(*Z*)-*N*'-Hydroxy-4-octylbenzimidamide (25): Triethylamine (3.9 mL, 27.8 mmol) and hydroxylamine hydrochloride (1.7 g, 24.5 mmol) were added to a solution of **23** (2.4 g, 11.1 mmol) in 95% ethanol (30 mL). The reaction mixture was refluxed for 2 h. The organic solvent was removed under reduced pressure and the residue was purified by column chromatography on silica gel (65/35 hexanes/EtOAc) to give the title compound (2.5 g, 92%) as a white solid. ^{1}H NMR (500 MHz, $CDCl_3$) δ 9.32 (br s, 1H), 7.54 (d, J = 8.1 Hz, 2H), 7.19 (d, J = 8.0 Hz, 2H), 4.95 (br s, 2H), 2.61 (t, J = 7.8 Hz, 2H), 1.66–1.55 (m, 2H), 1.38–1.18 (m, 10H), 0.89 (t, J = 6.9 Hz, 3H); ^{13}C NMR (126 MHz, $CDCl_3$) δ 152.8, 145.2, 129.8, 128.8, 125.9, 35.9, 32.0, 31.4, 29.6, 29.4, 29.3, 22.8, 14.2.

Compounds **26a**-**26c** and **30a**-**30b** were synthesized according to general procedure G.

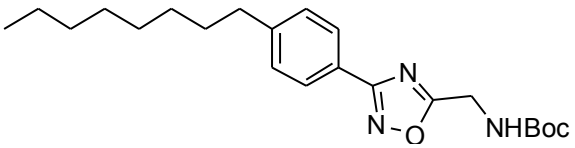

Tert-butyl ((3-(4-octylphenyl)-1,2,4-oxadiazol-5-yl)methyl)carbamate (26a): 64% yield, yellow oil; ^{1}H NMR (500 MHz, $CDCl_3$) δ 7.95 (d, J = 8.1 Hz, 2H), 7.26 (d, J = 8.0 Hz, 2H), 5.38 (br s, 1H), 4.61 (d, J = 5.2 Hz, 2H), 2.64 (t, J = 8.4 Hz, 2H), 1.66–1.56 (m, 2H), 1.46 (s, 9H), 1.36–1.19 (m, 10H), 0.86 (t, J = 6.9 Hz, 3H); ^{13}C NMR (126 MHz, $CDCl_3$) δ 176.4, 168.5, 155.6, 146.8, 129.0, 127.5, 123.9, 80.7, 37.3, 36.0, 32.0, 31.3, 29.5, 29.4, 29.3, 28.4, 22.7, 14.2.

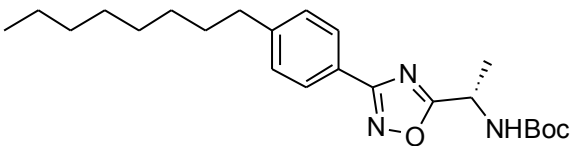

(*S*)-Tert-butyl (1-(3-(4-octylphenyl)-1,2,4-oxadiazol-5-yl)ethyl)carbamate (26b): 82% yield, yellow oil; ^{1}H NMR (500 MHz, $CDCl_3$) δ 7.96 (d, *J* = 8.0 Hz, 2H), 7.26 (d, *J* = 8.0 Hz, 2H), 5.29 (br s, 1H), 5.22–5.03 (m, 1H), 2.64 (t, *J* = 8.0 Hz, 2H), 1.68–1.53 (m, 5H), 1.45 (s, 9H), 1.36–1.17 (m, 10H), 0.86 (t, *J* = 7.1 Hz, 3H); ^{13}C NMR (126 MHz, $CDCl_3$) δ 180.0, 168.4, 154.9, 146.7, 129.0, 127.5, 124.0, 80.5, 44.3, 36.0, 31.9, 31.3, 29.5, 29.3, 29.3, 28.4, 22.7, 20.2, 14.2.

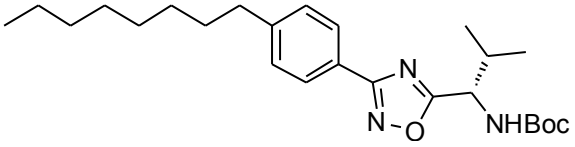

(*S*)-Tert-butyl (2-methyl-1-(3-(4-octylphenyl)-1,2,4-oxadiazol-5-yl)propyl)carbamate (26c): 77% yield, yellow oil; ^{1}H NMR (500 MHz, $CDCl_3$) δ 7.97 (d, *J* = 8.1 Hz, 2H), 7.27 (d, *J* = 8.1 Hz, 2H), 5.28–5.17 (m, 1H), 5.01–4.92 (m, 1H), 2.68–2.60 (m, 2H), 2.33–2.17 (m, 1H), 1.67–1.53 (m, 2H), 1.45 (s, 9H), 1.34–1.16 (m, 10H), 0.98 (d, *J* = 6.8 Hz, 6H), 0.87 (t, *J* = 6.9 Hz, 3H); ^{13}C NMR (126 MHz, $CDCl_3$) δ 178.9, 168.3, 155.4, 146.7, 129.0, 127.5, 124.1, 80.4, 53.7, 36.0, 32.9, 31.9, 31.3, 29.5, 29.3, 28.4, 22.7, 18.7, 18.0, 14.2.

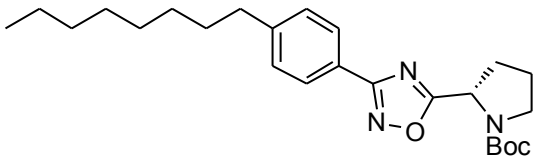

(*S*)-Tert-butyl 2-(3-(4-octylphenyl)-1,2,4-oxadiazol-5-yl)pyrrolidine-1-carboxylate (30a): 48% yield, yellow oil; ^{1}H NMR (500 MHz, $CDCl_3$) δ 7.96 (d, *J* = 7.8 Hz, 2H), 7.33–7.18 (m, 2H), 5.21–5.14 (m, 1H, minor rotamer), 5.07–5.01 (m, 1H, major rotamer),

3.75–3.67 (m, 1H, major rotamer), 3.67–3.61 (m, 1H, minor rotamer), 3.59–3.50 (m, 1H, major rotamer), 3.50–3.41 (m, 1H, minor rotamer), 2.66–2.58 (m, 2H), 2.44–2.25 (m, 1H), 2.20–2.05 (m, 2H), 2.05–1.89 (m, 1H), 1.68–1.54 (m, 2H), 1.44 (s, 3H), 1.37–1.16 (m, 16H), 0.85 (t, J = 6.8 Hz, 3H); ^{13}C NMR (126 MHz, $CDCl_3$, rotamers) δ 180.5 (major), 180.1 (minor), 168.5 (major), 154.3 (minor), 153.6 (major), 146.7 (major), 146.4 (minor), 129.0 (major), 128.9 (minor), 127.5 (minor), 127.5 (major), 124.4 (minor), 124.2 (major), 80.5 (major), 80.4 (minor), 53.9 (major), 46.7 (minor), 46.4 (major), 36.0 (major), 32.5 (major), 32.0 (major), 31.6 (minor), 31.3 (major), 29.5 (major), 29.3 (major), 29.2 (major), 28.5 (minor), 28.2 (major), 24.4 (minor), 23.8 (major), 22.7 (major), 14.2 (major).

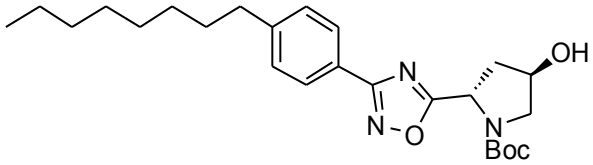

(2*S*,4*R*)-Tert-butyl 4-hydroxy-2-(3-(4-octylphenyl)-1,2,4-oxadiazol-5-yl)pyrrolidine-1-carboxylate (30b): 63% yield, yellow oil; ^{1}H NMR (500 MHz, $CDCl_3$) δ 7.99 (d, J = 7.9 Hz, 2H), 7.31 (d, J = 7.9 Hz, 2H), 5.42–5.30 (m, 1H, minor rotamer), 5.20 (m, 1H, major rotamer), 4.74–4.56 (m, 1H), 3.89–3.79 (m, 1H), 3.77–3.69 (m, 1H, major rotamer), 3.64–3.53 (m, 1H, minor rotamer), 2.74–2.61 (m, 2H), 2.59–2.40 (m, 1H), 2.38–2.28 (m, 1H), 1.74–1.58 (m, 2H), 1.56–1.16 (m, 19H), 0.90 (t, J = 7.0 Hz, 3H); ^{13}C NMR (126 MHz, $CDCl_3$, rotamers) δ 180.3 (major), 168.5 (major), 153.8 (major), 146.7 (major), 146.5 (minor), 129.0 (major), 128.8 (minor), 127.4 (major), 125.8 (minor), 123.9 (major), 81.0 (major), 80.8 (minor), 69.9 (minor), 69.3 (major), 54.8 (major), 52.6 (major), 40.9 (major), 40.2 (minor), 36.0 (major), 31.9 (major), 31.2 (major), 29.4

(major), 29.3 (major), 29.2 (major), 28.3 (minor), 28.1 (major), 22.7 (major), 14.1 (major).

Compounds **27a-27c** and **31a-31b** were synthesized according to general procedure H.

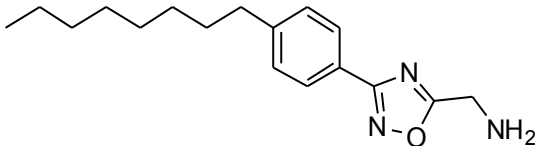

(3-(4-Octylphenyl)-1,2,4-oxadiazol-5-yl)methanamine (27a): 99% yield, yellow solid; ^{1}H NMR (500 MHz, CD_3OD) δ 8.08–7.92 (m, 2H), 7.34 (d, J = 8.4 Hz, 2H), 4.86 (br s, 2H), 4.59 (s, 2H), 2.70–2.62 (m, 2H), 1.70–1.57 (m, 2H), 1.37–1.20 (m, 10H), 0.88 (t, J = 7.0 Hz, 3H); ^{13}C NMR (126 MHz, CD_3OD) δ 173.1, 168.5, 147.2, 128.9, 127.2, 123.4, 35.6, 34.9, 31.7, 31.1, 29.2, 29.1, 29.0, 22.4, 13.1.

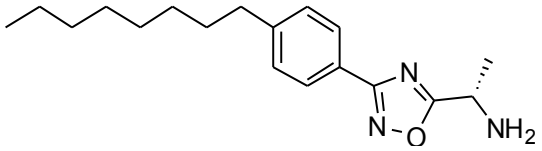

(*S*)-1-(3-(4-Octylphenyl)-1,2,4-oxadiazol-5-yl)ethanamine (27b): 89% yield, yellow solid; ^{1}H NMR (500 MHz, $CDCl_3$) δ 8.06 – 7.89 (m, 2H), 7.35–7.19 (m, 2H), 4.33 (q, J = 6.9 Hz, 1H), 2.70–2.55 (m, 2H), 1.81 (br s, 2H), 1.66–1.52 (m, 5H), 1.36–1.17 (m, 10H), 0.86 (t, J = 7.0 Hz, 3H); ^{13}C NMR (126 MHz, $CDCl_3$) δ 183.0, 168.3, 146.6, 129.0, 127.5, 124.2, 45.0, 36.0, 32.0, 31.3, 29.5, 29.4, 29.3, 22.7, 21.8, 14.2.

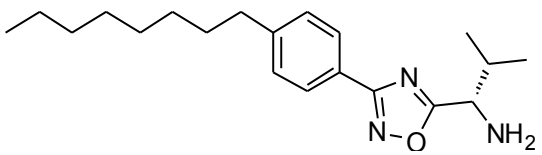

(*S*)-2-Methyl-1-(3-(4-octylphenyl)-1,2,4-oxadiazol-5-yl)propan-1-amine (27c): 59% yield, yellow solid; ^{1}H NMR (500 MHz, $CDCl_3$) δ 8.01–7.92 (m, 2H), 7.30–7.19 (m, 2H), 4.00 (d, *J* = 5.8 Hz, 1H), 2.61 (t, *J* = 8.0 Hz, 2H), 2.23–2.11 (m, 1H), 1.73 (br s, 2H), 1.66–1.53 (m, 2H), 1.38–1.16 (m, 10H), 1.03–0.91 (m, 6H), 0.85 (t, *J* = 7.0 Hz, 3H); ^{13}C NMR (126 MHz, $CDCl_3$) δ 182.2, 168.1, 146.6, 129.0, 127.5, 124.2, 55.1, 36.0, 33.6, 31.9, 31.3, 29.5, 29.3, 22.7, 19.0, 17.9, 14.2.

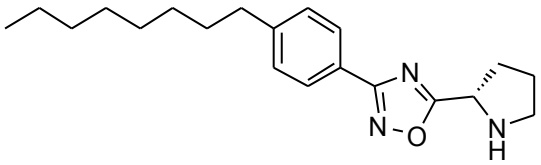

(*S*)-3-(4-Octylphenyl)-5-(pyrrolidin-2-yl)-1,2,4-oxadiazole (31a): 82% yield, yellow solid; ^{1}H NMR (500 MHz, $CDCl_3$) δ 8.01–7.87 (m, 2H), 7.25–7.18 (m, 2H), 4.46 (dd, *J* = 8.3, 5.6 Hz, 1H), 3.20–3.09 (m, 1H), 3.09–2.94 (m, 1H), 2.60 (t, *J* = 8.0 Hz, 2H), 2.34 (br s, 1H), 2.29–2.17 (m, 1H), 2.14–2.00 (m, 1H), 1.96–1.76 (m, 2H), 1.65–1.51 (m, 2H), 1.34–1.13 (m, 10H), 0.83 (t, *J* = 7.0 Hz, 3H); ^{13}C NMR (126 MHz, $CDCl_3$) δ 181.9, 168.2, 146.5, 128.9, 127.5, 124.2, 54.4, 46.9, 36.0, 31.9, 31.3, 31.2, 29.5, 29.3, 29.3, 25.4, 22.7, 14.2; HRMS (ESI+) *m/z* calcd for $C_{20}H_{30}N_3O$ $[M+H]^+$ 328.2389, found 328.2354.

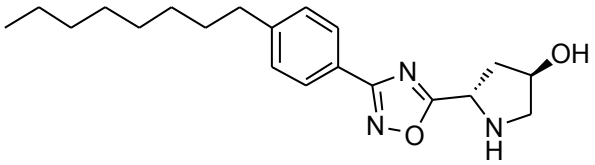

(3*R*,5*S*)-5-(3-(4-Octylphenyl)-1,2,4-oxadiazol-5-yl)pyrrolidin-3-ol (31b): 95% yield, yellow solid; ^{1}H NMR (500 MHz, $CDCl_3$) δ 7.89 (d, *J* = 8.2 Hz, 2H), 7.19 (d, *J* = 8.2 Hz, 2H), 4.79–4.63 (m, 1H), 4.57–4.43 (m, 1H), 3.22–3.10 (m, 1H), 3.08–2.95 (m, 1H), 2.77 (br s, 2H), 2.56 (t, *J* = 7.7 Hz, 2H), 2.35–2.18 (m, 2H), 1.63–1.48 (m, 2H), 1.33–1.10 (m,

10H), 0.80 (t, J = 6.9 Hz, 3H); ^{13}C NMR (126 MHz, $CDCl_3$) δ 181.3, 168.3, 146.6, 128.9, 127.4, 124.0, 72.2, 55.4, 53.0, 40.7, 36.0, 31.9, 31.2, 29.4, 29.3, 29.2, 22.7, 14.1.

Compounds **28a-28c** and **32a-32b** were synthesized according to general procedure I.

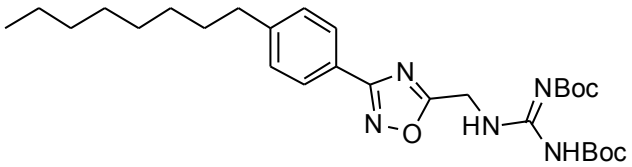

Tert-butyl *N*-[[(tert-butoxy)carbonyl]amino({[3-(4-octylphenyl)-1,2,4-oxadiazol-5-yl]methyl}amino)methylidene]carbamate (28a): 78% yield, yellow oil; ^{1}H NMR (500 MHz, $CDCl_3$) δ 11.47 (br s, 1H), 8.99 (t, J = 5.3 Hz, 1H), 7.99–7.95 (m, 2H), 7.28 (d, J = 8.0 Hz, 2H), 4.95 (d, J = 5.3 Hz, 2H), 2.64 (t, J = 7.7 Hz, 2H), 1.67–1.58 (m, 2H), 1.52 (s, 9H), 1.49 (s, 9H), 1.35–1.19 (m, 10H), 0.86 (t, J = 6.3 Hz, 3H); ^{13}C NMR (126 MHz, $CDCl_3$) δ 175.4, 168.5, 163.2, 156.3, 153.1, 146.8, 129.0, 127.6, 123.8, 83.8, 79.9, 37.3, 36.1, 31.9, 31.3, 29.5, 29.3, 29.3, 28.3, 28.1, 22.7, 14.2.

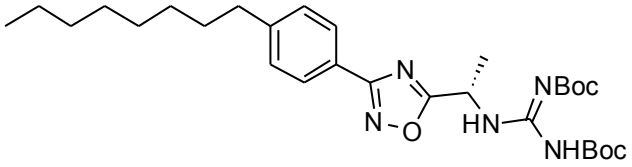

Tert-butyl *N*-[[(tert-butoxy)carbonyl]amino({[(1*S*)-1-[3-(4-octylphenyl)-1,2,4-oxadiazol-5-yl]ethyl]amino})methylidene]carbamate (28b): 81% yield, yellow solid; ^{1}H NMR (500 MHz, $CDCl_3$) δ 11.50 (br s, 1H), 8.97 (d, J = 8.1 Hz, 1H), 8.00–7.92 (m, 2H), 7.30–7.23 (m, 2H), 5.82–5.72 (m, 1H), 2.70–2.55 (m, 2H), 1.71–1.36 (m, 5H), 1.51 (s, 9H), 1.47 (s, 9H), 1.36–1.10 (m, 10H), 0.86 (t, J = 7.0 Hz, 3H); ^{13}C NMR (126 MHz, $CDCl_3$) δ 179.2, 168.5, 163.4, 155.7, 153.1, 146.7, 129.0, 127.6, 124.0, 83.7, 79.7, 43.8, 36.0, 32.0, 31.3, 29.5, 29.3, 28.3, 28.2, 22.7, 20.1, 14.2.

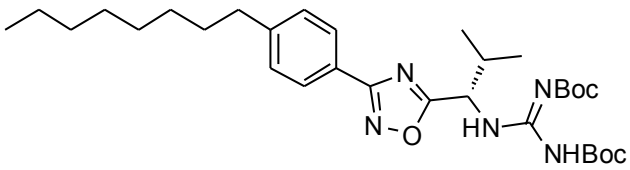

Tert-butyl *N*-[[(tert-butoxy)carbonyl]amino({[(1*S*)-2-methyl-1-[3-(4-octylphenyl)-1,2,4-oxadiazol-5-yl]propyl]amino})methylidene]carbamate (28c): 43% yield, yellow solid; ^{1}H NMR (500 MHz, $CDCl_3$) δ 11.51 (br s, 1H), 9.05 (d, *J* = 8.5 Hz, 1H), 7.98 (d, *J* = 7.3 Hz, 2H), 7.26 (d, *J* = 7.6 Hz, 2H), 5.59–5.55 (m, 1H), 2.64 (t, *J* = 7.6 Hz, 2H), 2.43–2.35 (m, 1H), 1.66–1.57 (m, 2H), 1.52 (s, 9H), 1.44 (s, 9H), 1.34–1.19 (m, 10H), 1.05–0.99 (m, 6H), 0.86 (t, *J* = 6.5 Hz, 3H); ^{13}C NMR (126 MHz, $CDCl_3$) δ 178.2, 168.3, 163.4, 156.3, 153.2, 146.6, 129.0, 127.6, 124.2, 83.6, 79.6, 53.1, 36.0, 32.4, 31.9, 31.3, 29.5, 29.3, 29.3, 28.3, 28.2, 22.7, 18.6, 18.1, 14.2.

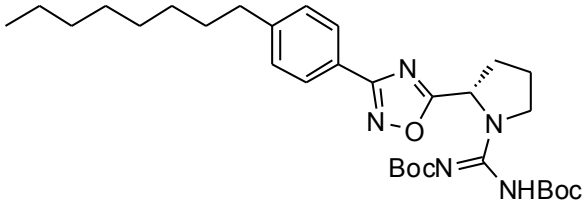

(*S*)-Tert-butyl (((tert-butoxycarbonyl)imino)(2-(3-(4-octylphenyl)-1,2,4-oxadiazol-5-yl)pyrrolidin-1-yl)methyl)carbamate (32a): 66% yield, yellow solid; ^{1}H NMR (500 MHz, $CDCl_3$) δ 7.96 (d, *J* = 8.2 Hz, 2H), 7.26 (d, *J* = 8.0 Hz, 2H), 5.62–5.54 (m, 1H), 3.93–3.83 (m, 1H), 3.83–3.71 (m, 1H), 2.64 (t, *J* = 7.9 Hz, 2H), 2.48–2.36 (m, 1H), 2.30–2.09 (m, 2H), 2.08–1.98 (m, 1H), 1.95–1.86 (m, 1H), 1.67–1.57 (m, 2H), 1.54–1.18 (m, 28H), 0.86 (t, *J* = 7.0 Hz, 3H); ^{13}C NMR (101 MHz, $CDCl_3$) δ 178.7, 168.3, 161.9, 153.5, 150.3, 146.5, 128.8, 127.4, 123.9, 82.2, 79.5, 55.3, 49.4, 35.9, 31.8, 31.2, 29.4, 29.2, 28.1, 23.9, 22.6, 14.1; HRMS (ESI+) *m/z* calcd for $C_{31}H_{48}N_5O_5$ $[M+H]^+$ 570.3655, found 570.3605.

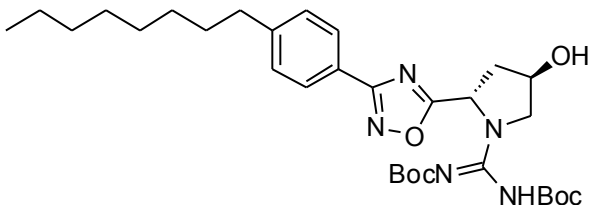

Tert-butyl (((tert-butoxycarbonyl)imino)((2*S*,4*R*)-4-hydroxy-2-(3-(4-octylphenyl)-1,2,4-oxadiazol-5-yl)pyrrolidin-1-yl)methyl)carbamate (32b): 53% yield, yellow solid; ^{1}H NMR (500 MHz, $CDCl_3$) δ 7.99 (d, *J* = 8.3 Hz, 2H), 7.29 (d, *J* = 8.3 Hz, 2H), 5.83 (t, *J* = 8.2 Hz, 1H), 4.72–4.59 (m, 1H), 4.05 (dd, *J* = 12.5, 3.5 Hz, 1H), 3.85–3.69 (m, 1H), 2.67 (t, *J* = 7.6 Hz, 2H), 2.63–2.53 (m, 1H), 2.45–2.32 (m, 1H), 1.74–1.60 (m, 2H), 1.47 (s, 18H), 1.39–1.24 (m, 10H), 0.90 (t, *J* = 7.0 Hz, 3H); ^{13}C NMR (126 MHz,) δ 178.5, 168.5, 154.1, 146.6, 128.9, 127.5, 124.0, 69.3, 58.0, 53.7, 40.0, 36.0, 31.9, 31.2, 29.7, 29.4, 29.2, 28.1, 22.7, 14.1.

Compounds **29a-29c** and **33a-33b** were synthesized according to general procedure J.

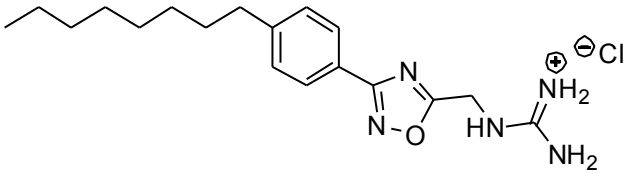

Amino(((3-(4-octylphenyl)-1,2,4-oxadiazol-5-yl)methyl)amino)methaniminium chloride (29a): 84% yield, white solid; ^{1}H NMR (500 MHz, CD_3OD) δ 7.96 (d, *J* = 8.2 Hz, 2H), 7.33 (d, *J* = 8.2 Hz, 2H), 4.84 (s, 2H), 2.67 (t, *J* = 7.6 Hz, 2H), 1.71–1.54 (m, 2H), 1.38–1.19 (m, 10H), 0.88 (t, *J* = 7.0 Hz, 3H); ^{13}C NMR (126 MHz, CD_3OD) δ 175.5, 168.4, 158.1, 147.0, 128.8, 127.1, 123.7, 37.4, 35.5, 31.7, 31.1, 29.2, 29.1, 29.0, 22.4, 13.1; HRMS (ESI+) *m/z* calcd for $C_{18}H_{28}N_5O$ $[M+H]^+$ 330.2294, found 330.2269.

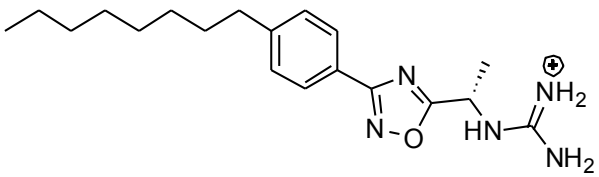

(*S*)-Amino((1-(3-(4-octylphenyl)-1,2,4-oxadiazol-5-yl)ethyl)amino)methaniminium chloride (29b): 82% yield, white solid; ^{1}H NMR (500 MHz, CD_3OD) δ 7.96 (d, *J* = 8.1 Hz, 2H), 7.32 (d, *J* = 8.0 Hz, 2H), 5.28–5.14 (m, 1H), 2.75–2.56 (m, 2H), 1.75 (d, *J* = 6.9 Hz, 3H), 1.68–1.56 (m, 2H), 1.39–1.17 (m, 10H), 0.88 (t, *J* = 6.8 Hz, 3H); ^{13}C NMR (126 MHz, CD_3OD) δ 178.5, 168.4, 157.3, 147.0, 128.8, 127.1, 123.8, 45.2, 35.6, 31.7, 31.1, 29.2, 29.1, 29.0, 22.4, 18.0, 13.1; HRMS (ESI+) *m/z* calcd for $C_{19}H_{30}N_5O$ $[M+H]^+$ 344.2450, found 344.2407.

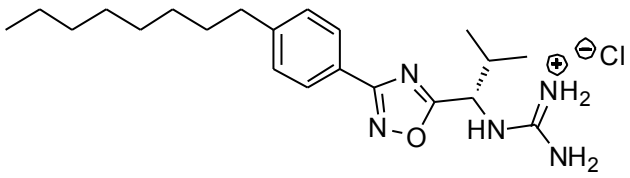

(*S*)-Amino((2-methyl-1-(3-(4-octylphenyl)-1,2,4-oxadiazol-5-yl)propyl)amino)methaniminium chloride (29c): 80% yield, white solid; ^{1}H NMR (500 MHz, CD_3OD) δ 7.96 (d, *J* = 8.1 Hz, 2H), 7.32 (d, *J* = 8.0 Hz, 2H), 5.08–4.99 (m, 1H), 2.65 (t, *J* = 7.9 Hz, 2H), 2.51–2.40 (m, 1H), 1.68–1.56 (m, 2H), 1.38–1.19 (m, 10H), 1.07 (dd, *J* = 15.1, 6.8 Hz, 6H), 0.87 (t, *J* = 6.8 Hz, 3H); ^{13}C NMR (126 MHz, CD_3OD) δ 177.4, 168.4, 157.9, 147.0, 128.9, 127.1, 123.7, 54.7, 35.6, 32.4, 31.7, 31.1, 29.2, 29.1, 29.0, 22.4, 17.6, 16.9, 13.1; HRMS (ESI+) *m/z* calcd for $C_{21}H_{34}N_5O$ $[M+H]^+$ 372.2763, found 372.2773.

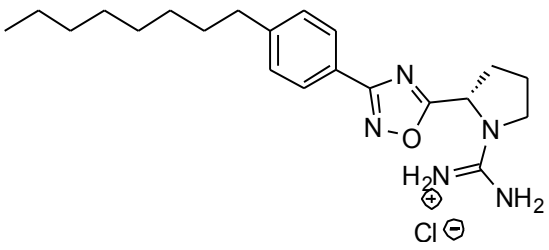

(*S*)-Amino(2-(3-(4-octylphenyl)-1,2,4-oxadiazol-5-yl)pyrrolidin-1-yl)methaniminium chloride (33a): 80% yield, white solid; ^{1}H NMR (500 MHz, CD_3OD) δ 7.94 (d, *J* = 8.2 Hz, 2H), 7.33 (d, *J* = 8.2 Hz, 2H), 5.50–5.38 (m, 1H), 3.80–3.70 (m, 1H), 3.67–3.54 (m, 1H), 2.70–2.39 (m, 4H), 2.28–2.16 (m, 1H), 2.16–1.98 (m, 1H), 1.70–1.55 (m, 2H), 1.39–1.15 (m, 10H), 0.88 (t, *J* = 6.9 Hz, 3H); ^{13}C NMR (126 MHz, CD3OD) δ 177.5, 168.4, 155.8, 147.0, 128.8, 127.1, 123.6, 55.1, 35.5, 31.7, 31.4, 31.1, 29.2, 29.0, 28.9, 23.0, 22.4, 13.1; HRMS (ESI+) *m/z* calcd for $C_{21}H_{32}N_5O$ $[M+H]^+$ 370.2601, found 370.2607.

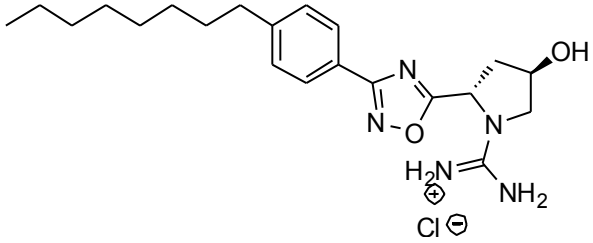

Amino((2*S*,4*R*)-4-hydroxy-2-(3-(4-octylphenyl)-1,2,4-oxadiazol-5-yl)pyrrolidin-1-yl)methaniminium chloride (33b): 79% yield, white solid; ^{1}H NMR (500 MHz, CD_3OD) δ 8.01–7.93 (m, 2H), 7.41–7.31 (m, 2H), 5.66–5.54 (m, 1H), 4.67–4.58 (m, 1H), 3.96–3.85 (m, 1H), 3.65–3.58 (m, 1H), 2.74–2.61 (m, 3H), 2.58–2.49 (m, 1H), 1.73–1.61 (m, 2H), 1.42–1.24 (m, 10H), 0.91 (t, *J* = 7.0 Hz, 3H); ^{13}C NMR (126 MHz, CD_3OD) δ 178.9, 169.8, 157.7, 148.4, 130.2, 128.4, 124.9, 69.8, 57.1, 54.9, 41.1, 36.9, 33.0, 32.4, 30.5, 30.4, 30.3, 23.7, 14.5; HRMS (ESI+) *m/z* calcd for $C_{21}H_{32}N_5O_2$ $[M+H]^+$ 386.2556, found 386.2596.

3.2.1. GC analysis of reductive amination reactions

Gas chromatography/Mass spectrometry (GC/MS) analyses were performed on a Hewlett Packard 6890 Series GC system coupled to a HP 5973 Mass Selective Detector. The column was an Agilent DB-5MS with a length of 60 m, internal diameter of 260 μm, and film thickness of 0.26 μm. The crude reaction mixture after reductive amination was analyzed by GC. The general method consisted of a splitless injection, holding the oven temperature at 180 °C for 5 minutes, ramping the temperature at a rate of 25 °C/min to 290 °C, and holding for an additional 20 minutes. The total run time was 29.40 minutes. For compound **10e** (reductive amination with benzylamine), a modified method was used. Oven temperature was held at 180 °C for 5 min, the temperature was increased at a rate of 30 °C/min to 290 °C, and the oven held at that temperature for an additional 30 min. The total run time was 38.67 min.

3.3. Biological procedures

3.3.1. SphK assay

Human SphK1 and mouse SphK2 cDNAs were used to generate recombinant baculoviruses that encoded the respective proteins. Infection of Sf9 insect cells with the viruses for 72 h resulted in >1000-fold increase in SphK activity in 10,000 x g supernatant fluid from homogenized cell pellets. The infected Sf9 cell extract containing 2-3 μg protein was used as a source of enzyme in the assay. SphK activity was measured in kinase buffer that consisted of the following ingredients: 20 mM Tris-Cl (pH 7.4), 1 mM 2-mercaptoethanol, 1 mM EDTA, 5 mM sodium orthovanadate, 40 mM β-glycerophosphate, 15 mM NaF, 1 mM phenylmethylsulfonyl fluoride, 10 mM $MgCl_2$, 0.5 mM 4-deoxypyridoxine, 10% glycerol, and 0.01 mg/mL each leupeptin, aprotinin, and

soybean trypsin inhibitor. To determine the fractional activity of SphK1 *versus* SphK2, the buffer was supplemented with either 0.5% Triton X-100 or 1 M KCl, respectively.

Substrate (D-*erythro*-sphingosine, 5 μM), [γ^{32}P] ATP (10 μM, specific activity = 8.3 Ci/mmol), and Sf9 insect cell extract (0.02–0.03 mg of total protein) was added to the buffer solution. After 30 min at 37 °C, the reaction mixture was extracted with 2 volumes of $CHCl_3$/MeOH/HCl (100:200:1), and the components in the organic phase were separated by thin layer chromatography using a ^{n}BuOH/CH_3COOH/H_2O (3:1:1) solvent system. Radiolabeled enzyme products were detected by autoradiography and identified by migration relative to authentic standards. For quantification, the silica gel containing radiolabeled lipid was scraped into a scintillation vial and counted.

3.3.2. LC/MS protocol

Analyses were performed by Liquid Chromatography/ESI Mass Spectrometry (LC/MS) using a triple quadrupole mass spectrometer (Sciex 4000 Q-Trap) coupled to a Shimadzu LC-20AD LC system. A binary solvent gradient with a flow rate of 1 mL/min was used to separate FTY720 and FTY720-P by reverse phase chromatography using a Supelco Discovery C18 column (50 mm × 2.1 mm, 5 μm bead size). Mobile phase A consisted of water:methanol:formic acid (79:20:1) while mobile phase B was methanol:formic acid (99:1). The run started with 100% A for 0.5 min. Solvent B was then increased linearly to 100% B in 5.1 min. and held at 100% for 4.3 min. The column was finally re-equilibrated to 100% A for 1 min. Natural sphingolipids were detected using multiple reaction monitoring (MRM) methods previously described[1] as follows: C17S1P (366.4 → 250.4); FTY720 (308.4 → 255.1); FTY720-P (388.4 → 255.1); C17sphingosine (286.4 → 250.3); C17S1P and C17sphingosine were used as the internal

standards. All analytes were analyzed simultaneously using the aforementioned MRMs. Voltages (DP, EP, CE and CXP) for C17S1P and C17sphingosine were: 35, 10, 25, 6 and 156, 10, 25, 14 volts, respectively. Retention times for all analytes under our experimental conditions were between 5.1 and 5.6 min. Quantification was carried out by measuring peak areas using commercial software (Analyst 1.5.1).

3.3.3. Western blot analysis

Cultured U937 cells were incubated with various concentrations of inhibitor for the times indicated (usually 2 h). After incubation, cells were washed with phosphate-buffered saline and lysed using a Dounce homogenizer. Equal amounts of protein were resolved by SDS-PAGE analysis using 10% polyacrylamide gels and resolved proteins transferred to a nitrocellulose membrane. Membranes were blocked with 5% non-fat milk in Tris-buffered saline (TBS, pH 7.4) containing 0.1% Tween 20 for 1 h at room temperature. After rinsing, membranes were incubated with antibodies (diluted 1:1000 in TBS) against ERK, p-ERK, Akt, p-Akt, and β-actin for 1 h. After washing three times in TBS buffer, the nitrocellulose membrane was incubated with a 1:2000 dilution (in TBS) of HRP-conjugated anti-IgG antibody. Detection was accomplished by chemiluminesence using a commercial kit (Perkin Elmer Western Lightning).

3.3.4. *In vitro* evaluation of BD10

U937 cells were grown in RPMI 1640 medium supplemented with L-glutamate, 10% FBS (fetal bovine serum) and penicillin/streptomycin at 37 °C in an atmosphere containing 5% CO_2. At 24 h before adding inhibitors, the growth medium was replaced with medium containing 0.5% or 2% FBS. Cultured U937 cells were exposed to different concentrations of **BD10** (300 nm, 1 μM, and 3 μM). After a 2 h period of

exposure, cells were harvested, lysed and the amounts of sphingolipids and **BD10** in the lysates were measured by LC–MS as described above.

3.3.5. *In vivo* evaluation of BD10

Groups of 8-12 weeks old C57BL/6J mice (wild type, SphK1$^{-/-}$ or SphK2$^{-/-}$) were anaesthetized with methoxyflurane and injected intraperitoneally with **BD10** (10 mg/kg) and/or an equal volume of vehicle. The vehicle was a 2% solution of hydroxypropyl-*β*-cyclodextrin (Cargill Cavitron 82004) in water. After injection, animals were lightly anaesthetized and bled from the retro-orbital sinus at the specified time points (initial time points were 1–2 min after dosing). Blood was extracted immediately by following the procedure described below. Whole blood (20 μL) was mixed with 2 mL of a 3:1 methanol/chloroform mixture and transferred to a capped glass vial. To this suspension was added 10 μL of internal standard solution containing 1 μM C17 S1P and 1 μM C17 Sph. The mixture was homogenized in a bath sonicator for 10 min and incubated at 48 °C for 16 h. The mixture was then cooled to ambient temperature (22 °C) and mixed with 200 μL of 1 M KOH in methanol. The samples were again sonicated and incubated at 37 °C for 2 h. After this time, the samples were neutralized through the addition of 20 μL of acetic acid and transferred to 2 mL microcentrifuge tubes. Samples were then centrifuged at 10000 g for 10 min at 4 °C. The supernatant fluid was collected in a separate glass vial and the pellets discarded. The resulting solution was evaporated under a stream of nitrogen gas. Immediately before LC–MS analysis, the material was dissolved in 300 μL of methanol and centrifuged at 12000 g for 12 min at 4 °C. Then 50 μL of the resulting supernatant fluid was analyzed by LC–MS as described above. Animal protocols were approved before experimentation by the University of Virginia's School of Medicine Animal Care and Use Committee.

3.4. References

1. Shaner, R. L., Allegood, J. C., Park, H., Wang, E., Kelly, S., Haynes, C. A., Sullards, M. C., Merrill, A. H., Quantitative analysis of sphingolipids for lipidomics using triple quadrupole and quadrupole linear ion trap mass spectrometers, *J. Lipid Res.* **2009**, *50*, 1692-1707.

Appendix

^{1}H NMR spectrum of **2**

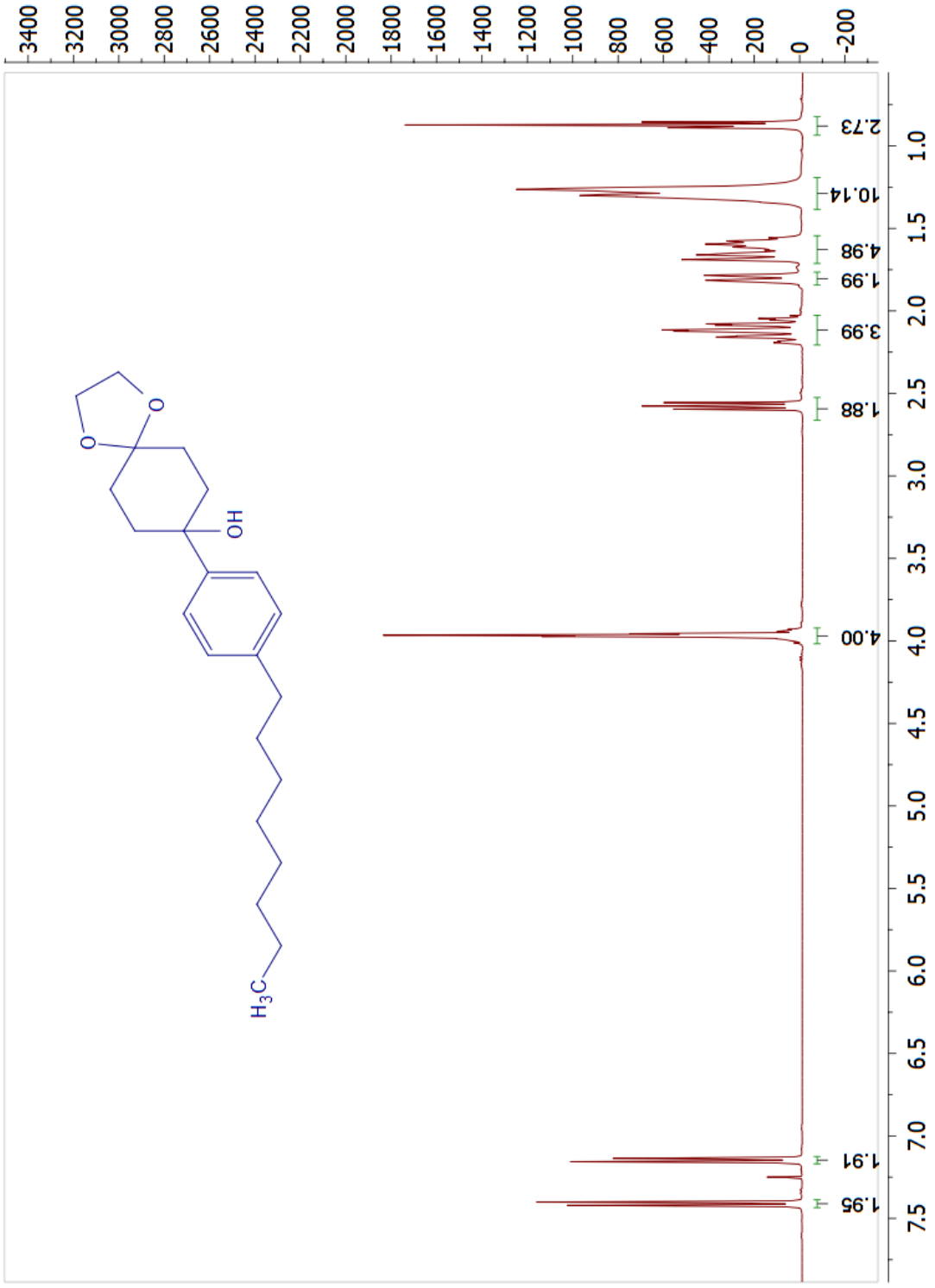

^{13}C NMR spectrum of **2**

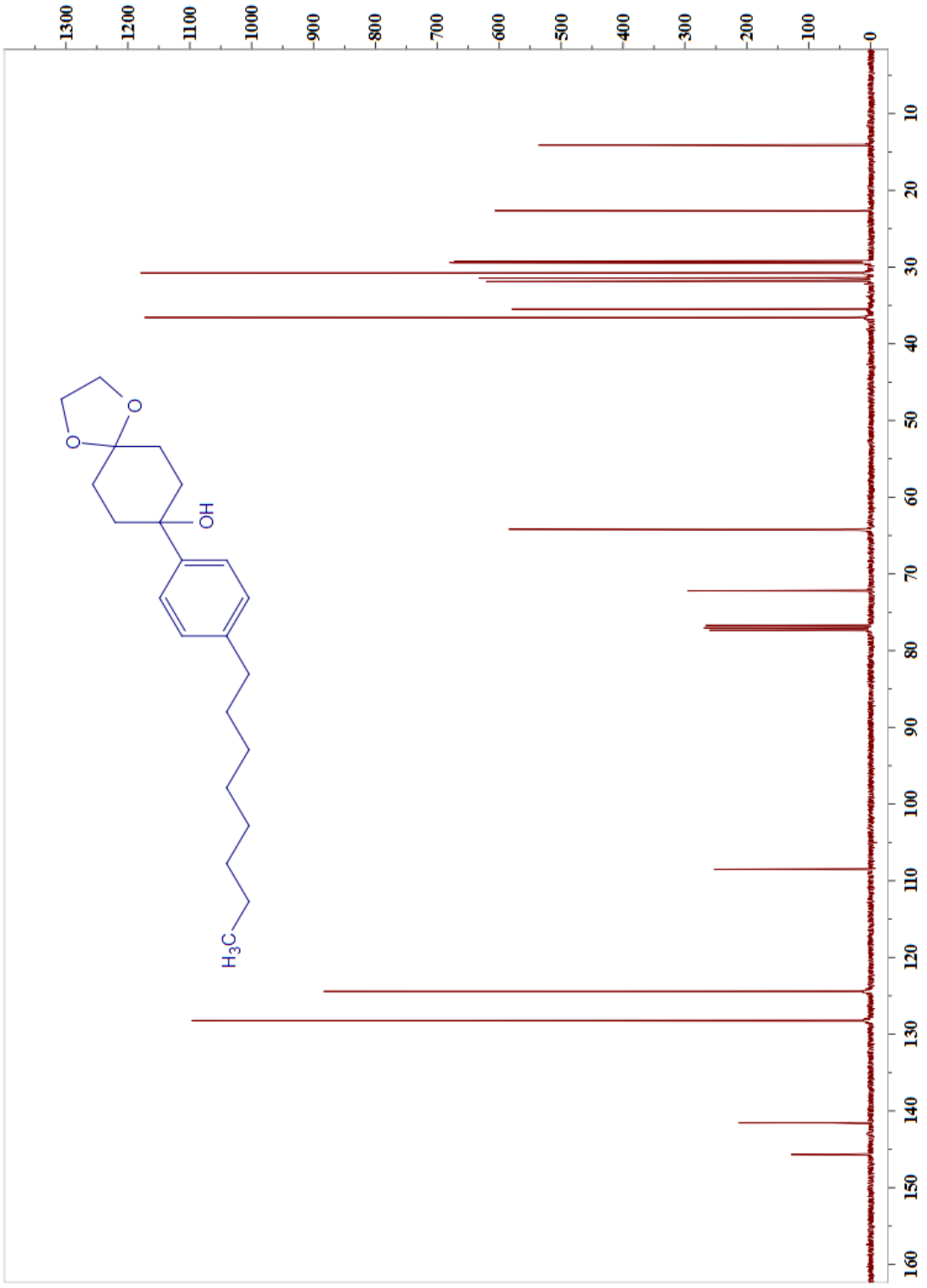

^{1}H NMR spectrum of **3**

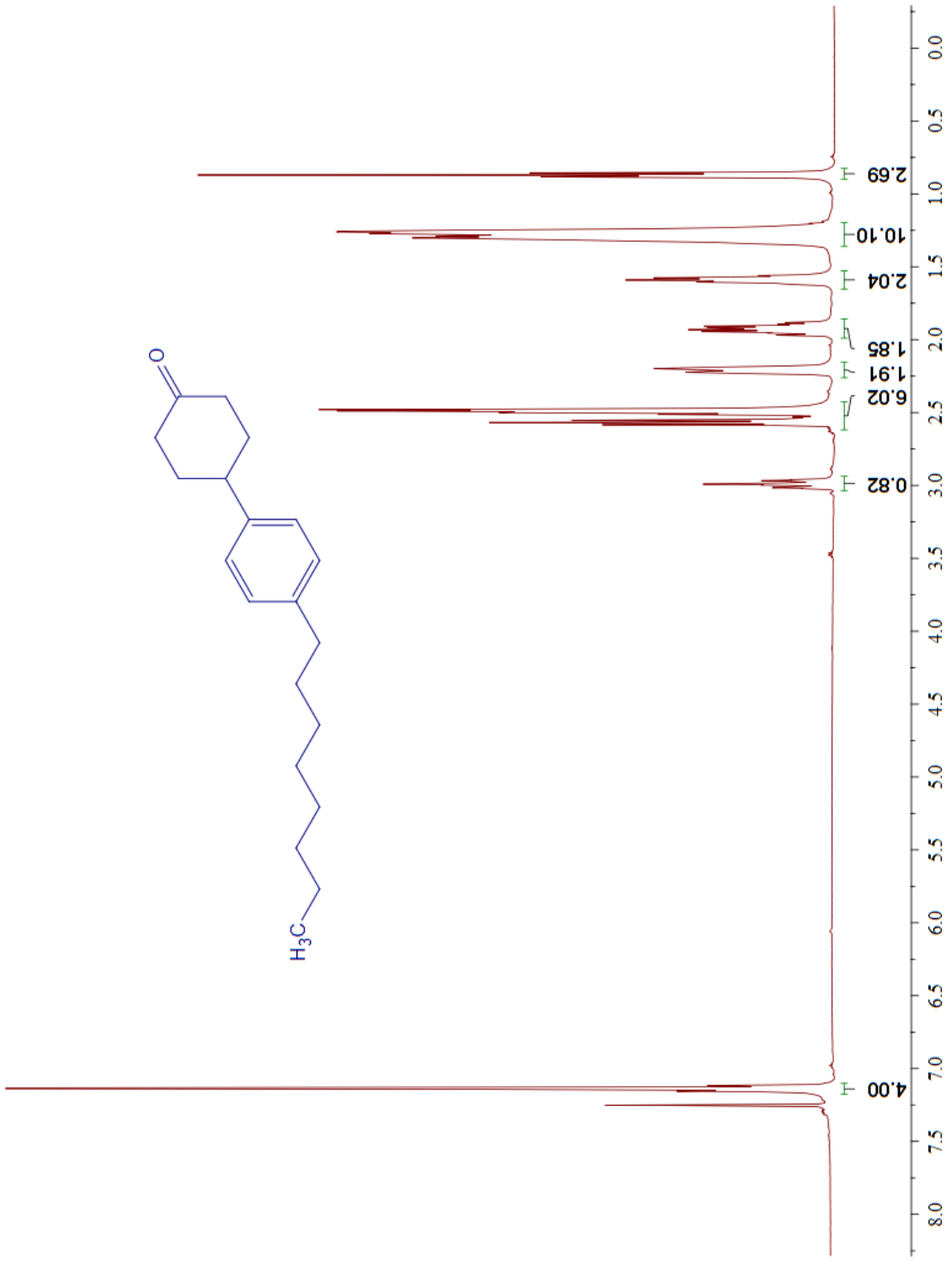

^{13}C NMR spectrum of **3**

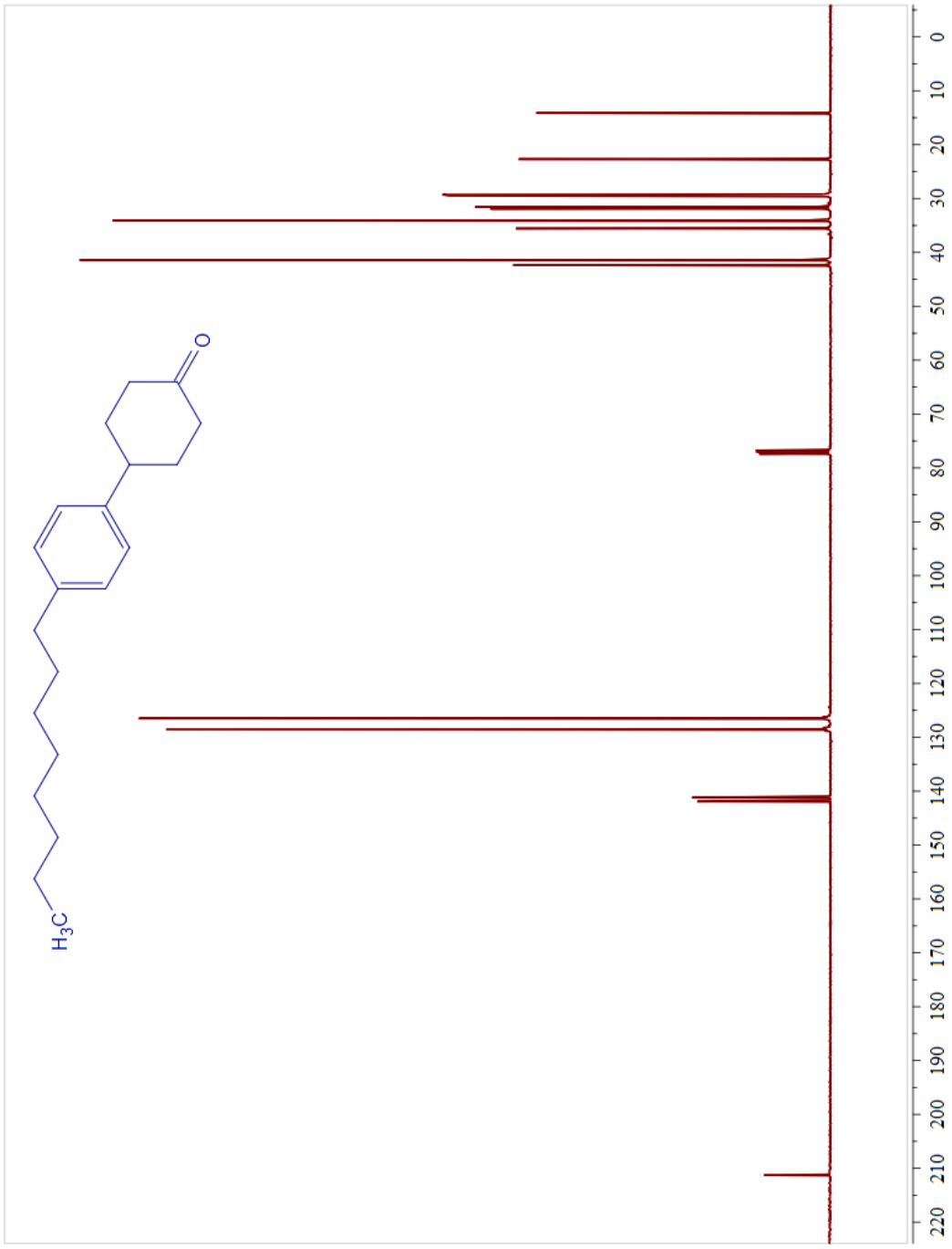

^{1}H NMR spectrum of **4**

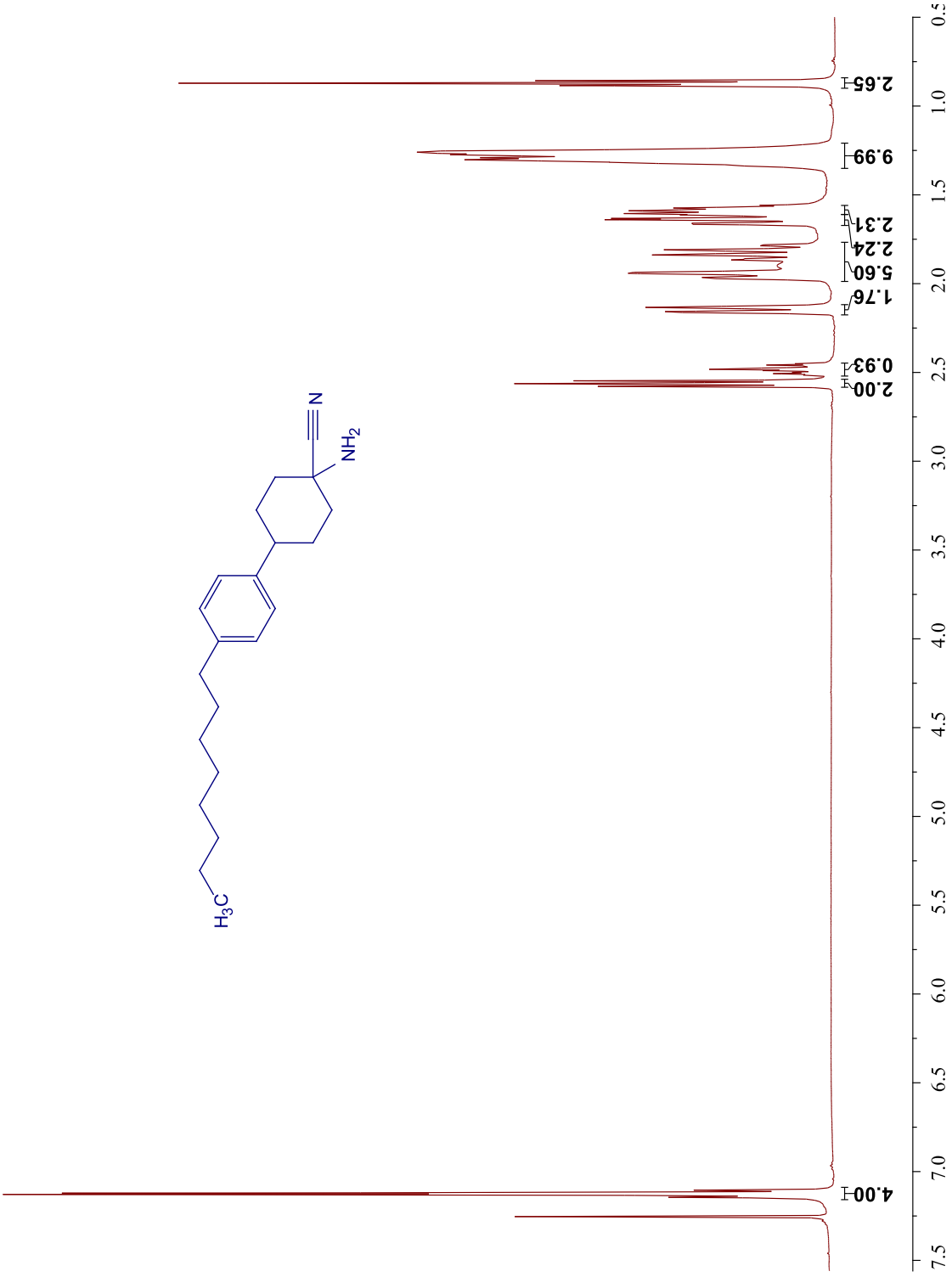

^{13}C NMR spectrum of **4**

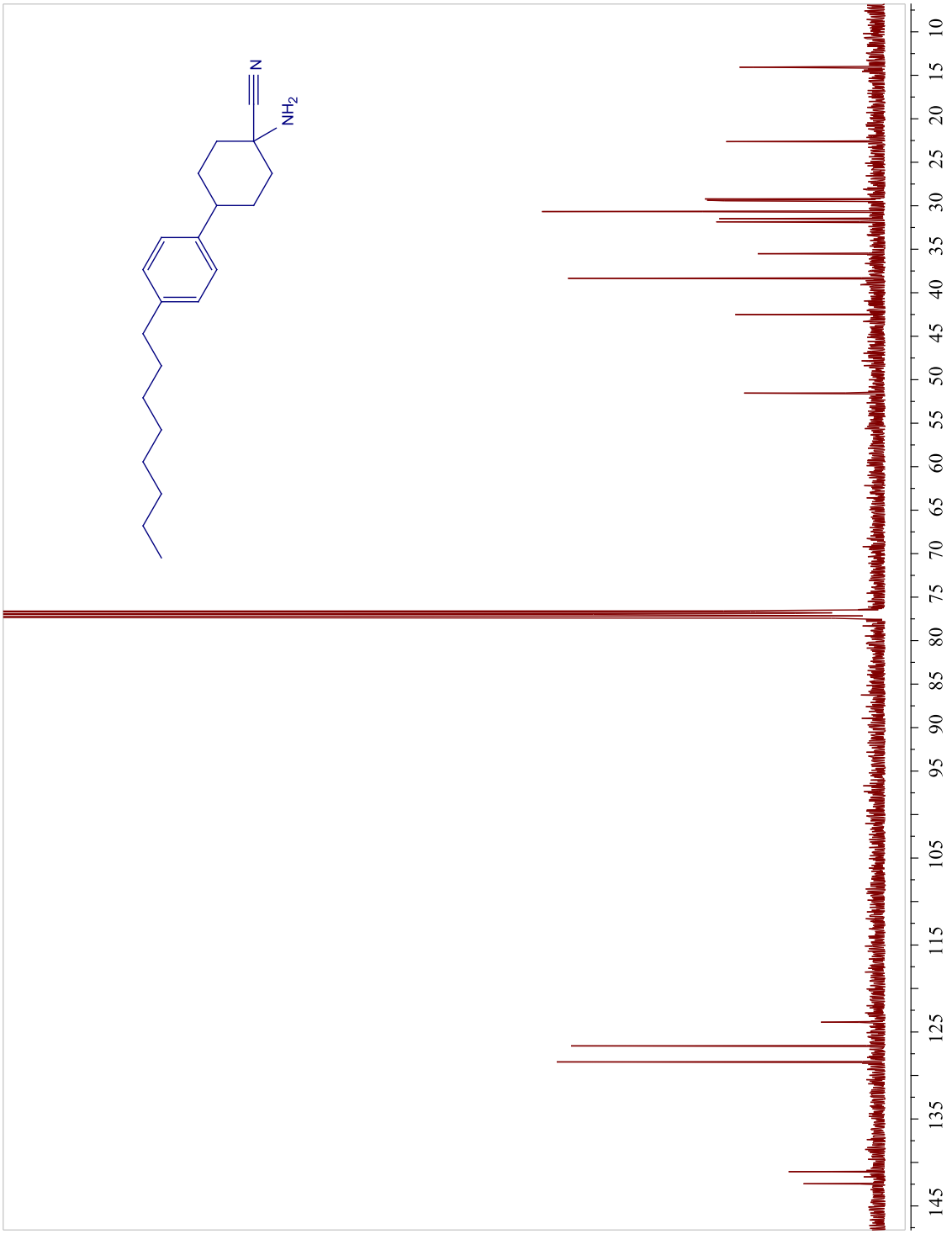

^{1}H NMR spectrum of **5**

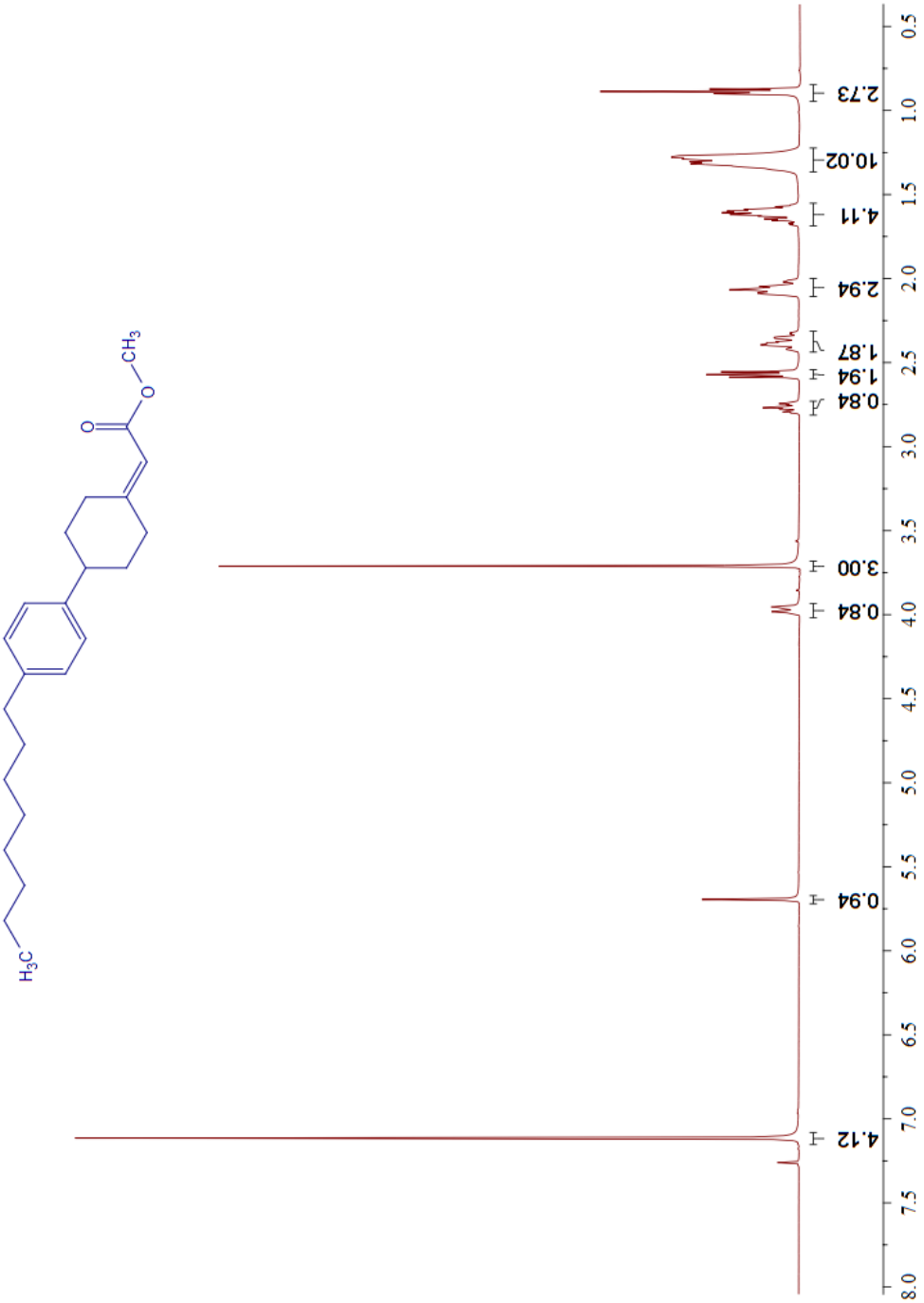

^{13}C NMR spectrum of **5**

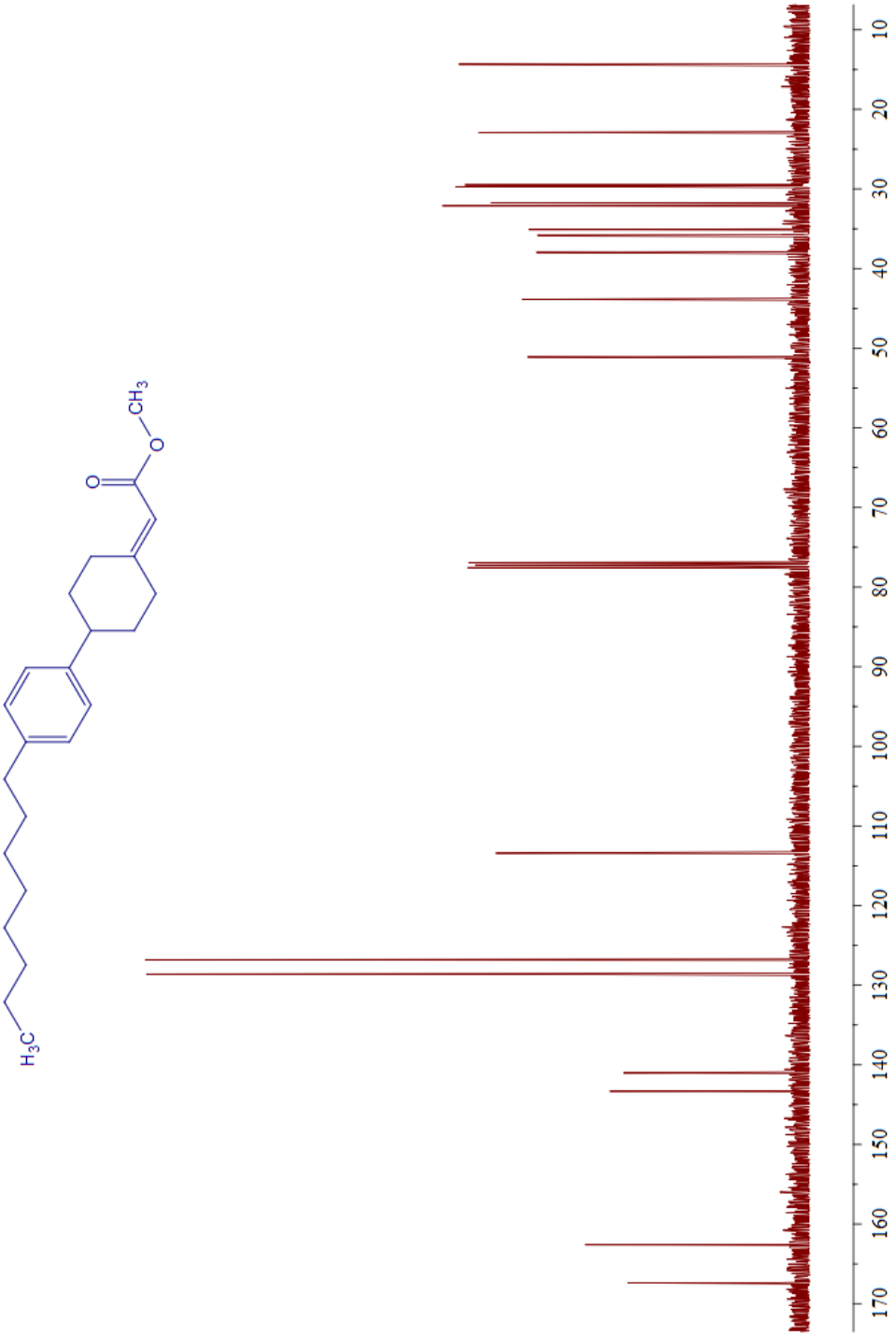

^{1}H NMR spectrum of **6**

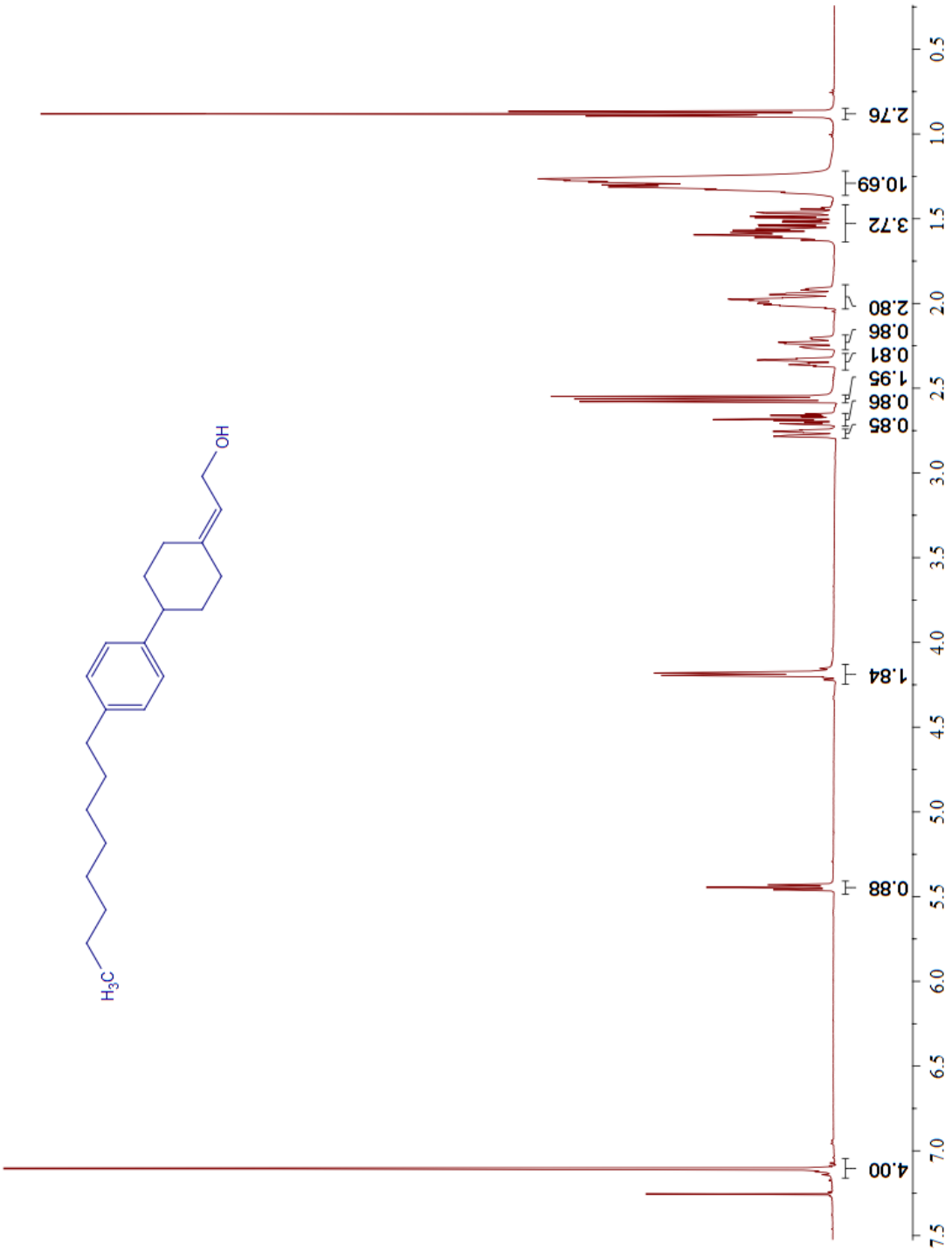

^{13}C NMR spectrum of **6**

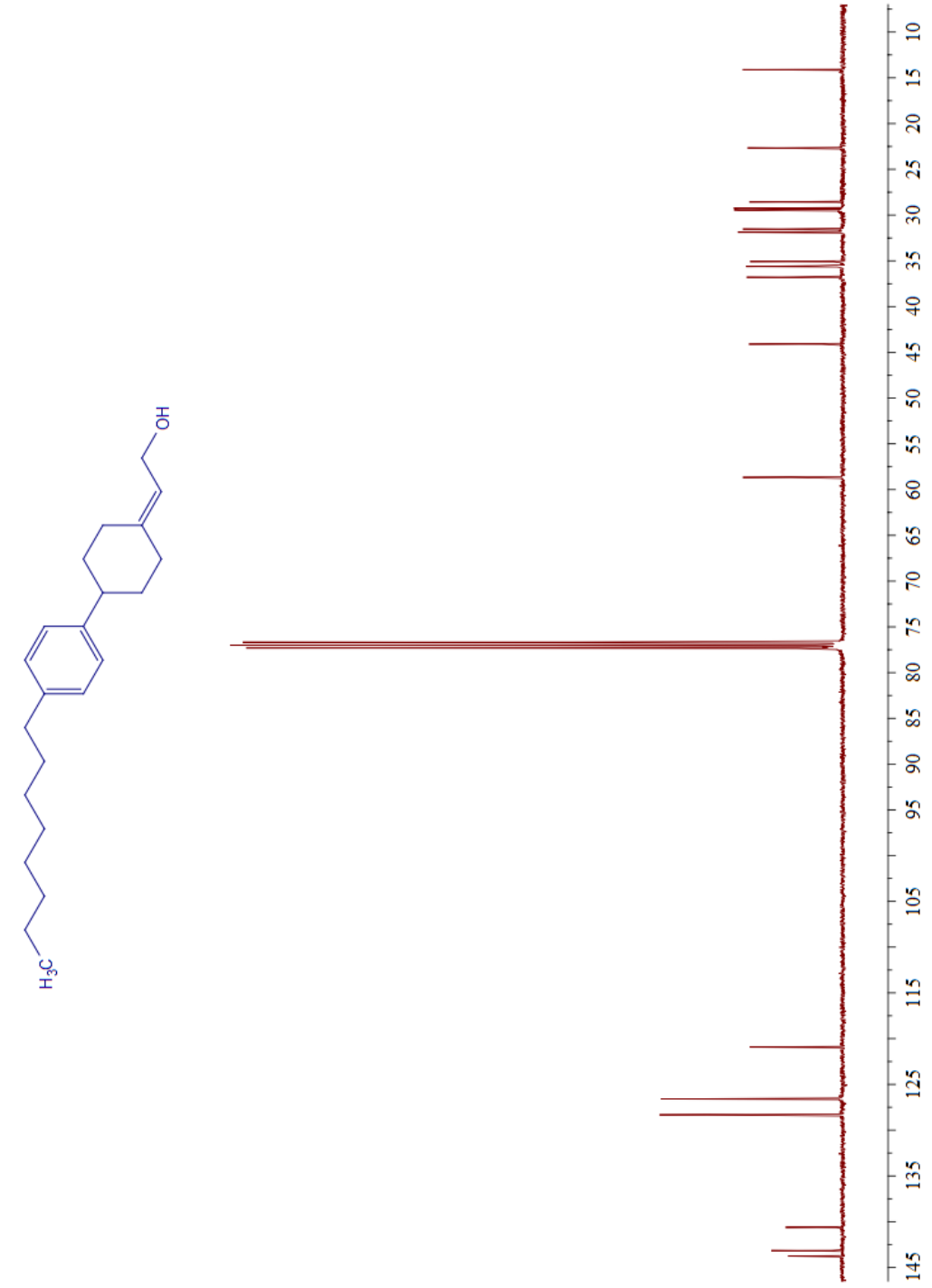

^{1}H NMR spectrum of **7**

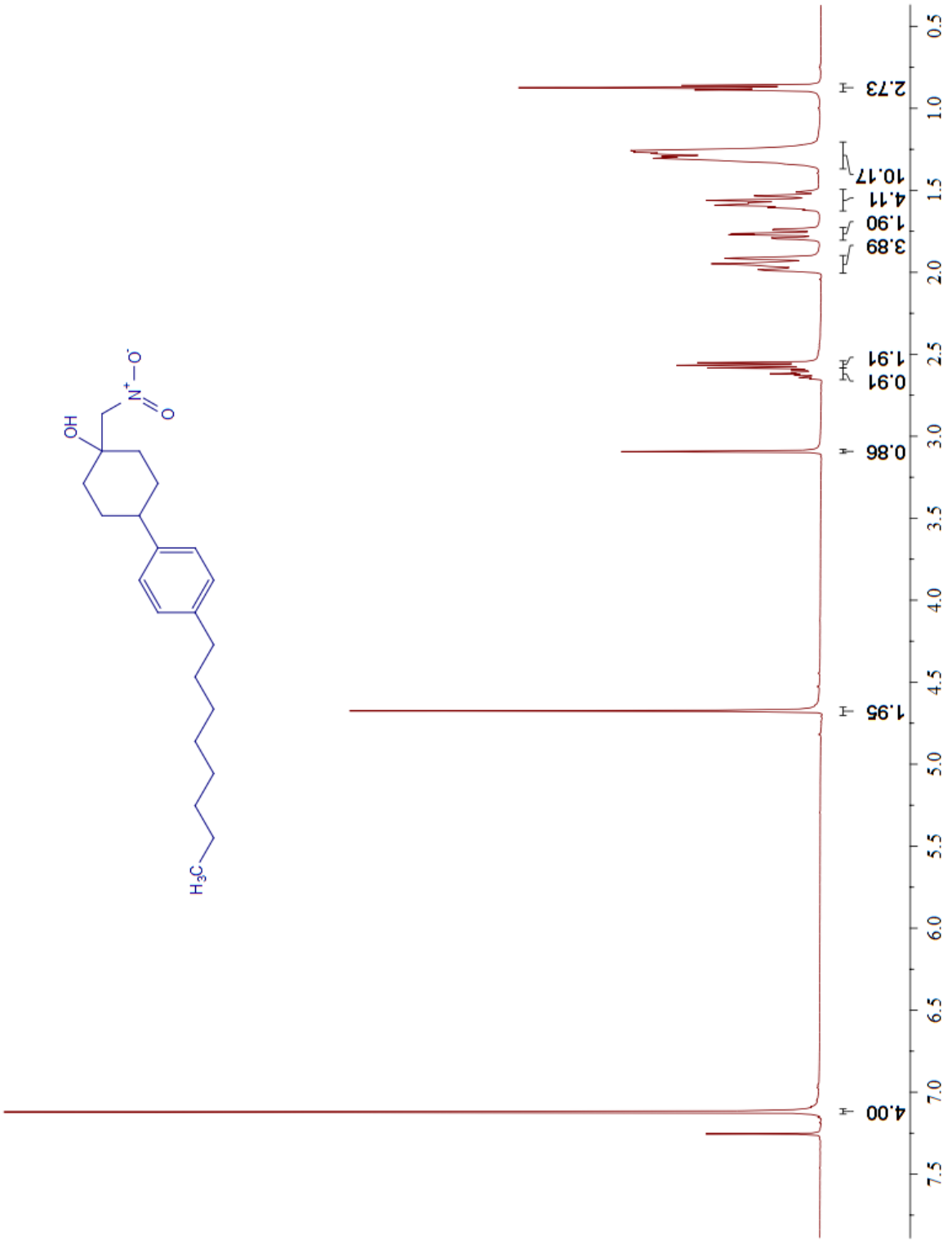

^{13}C NMR spectrum of **7**

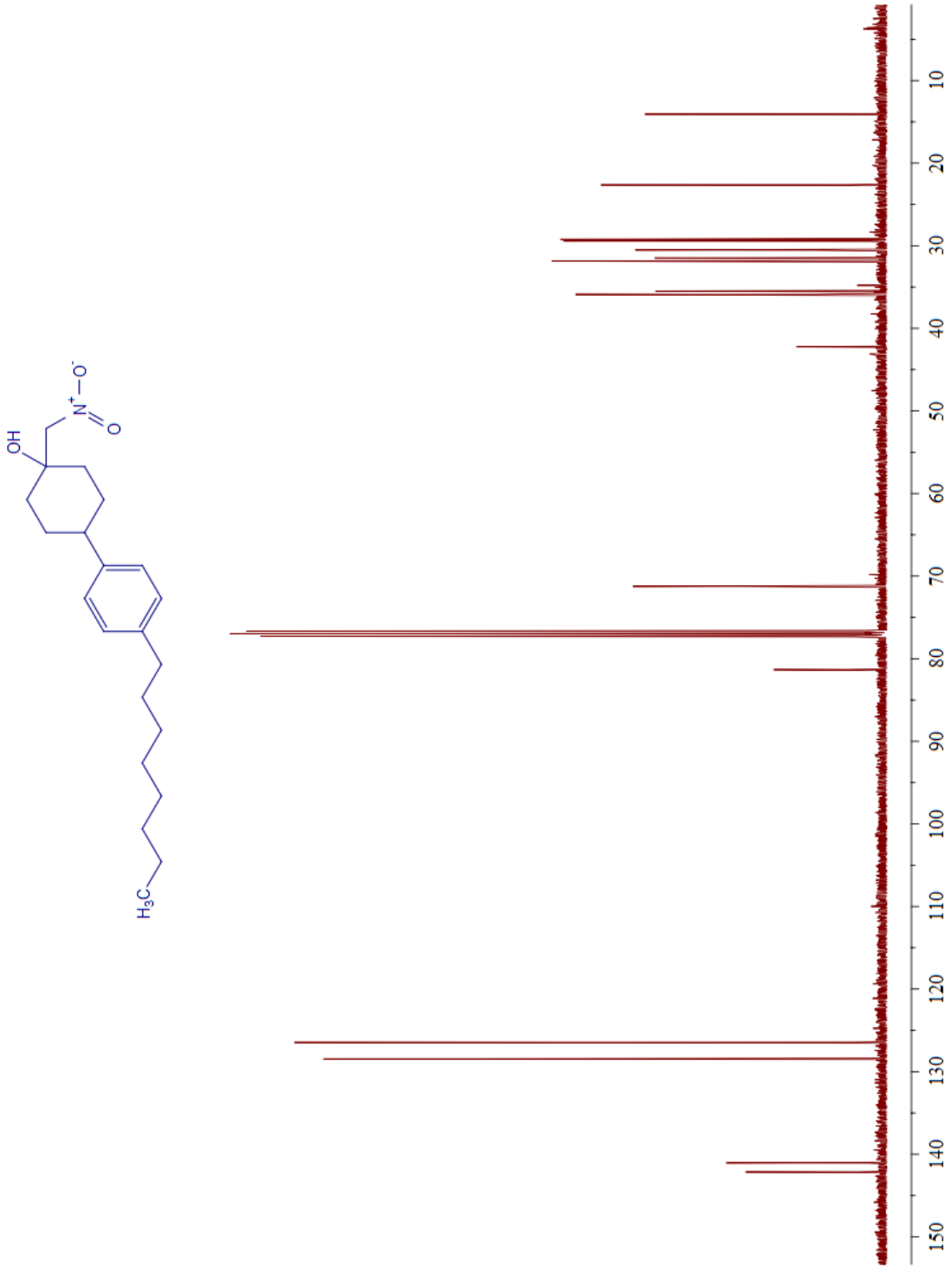

^{1}H NMR spectrum of **8**

^{13}C NMR spectrum of **8**

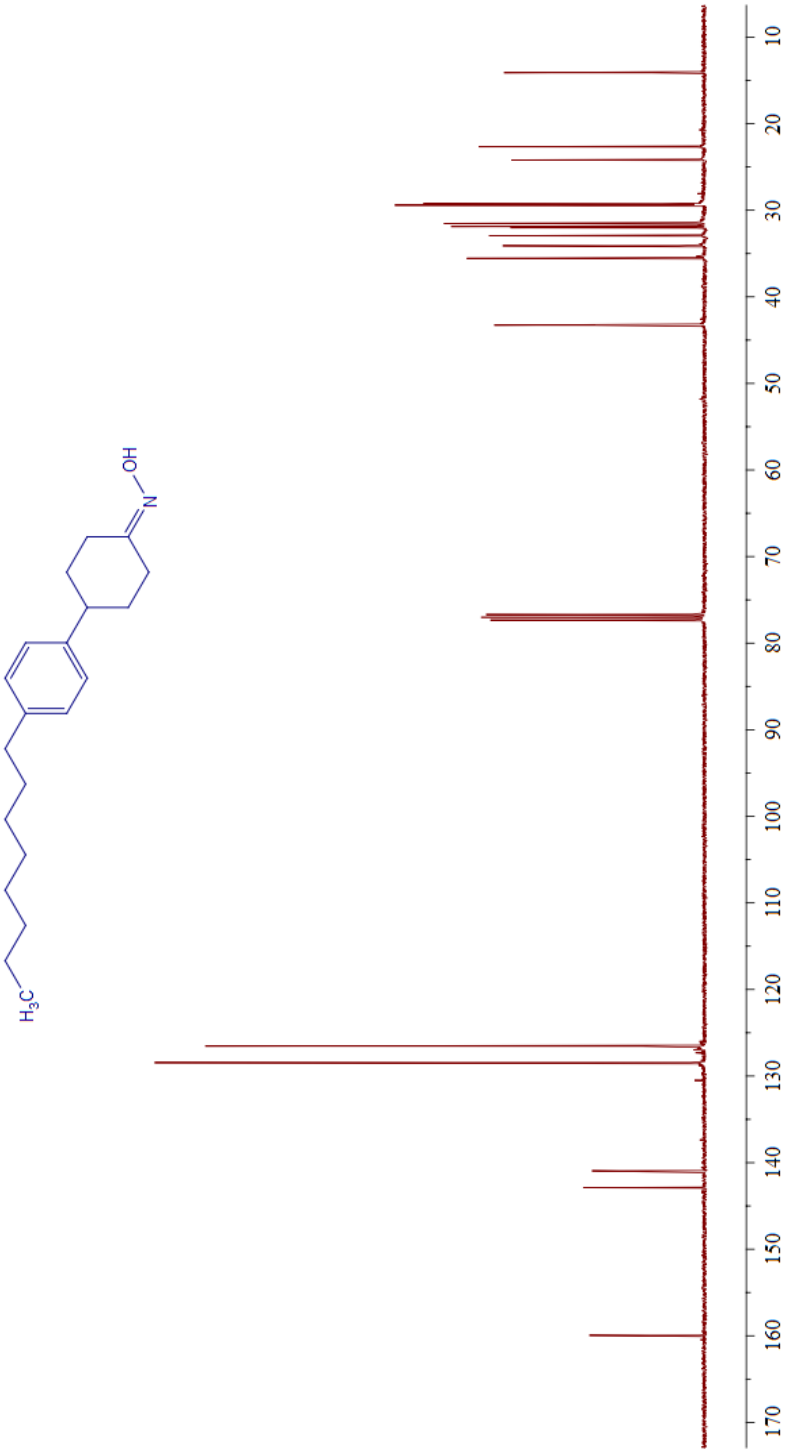

^{1}H NMR spectrum of **9**

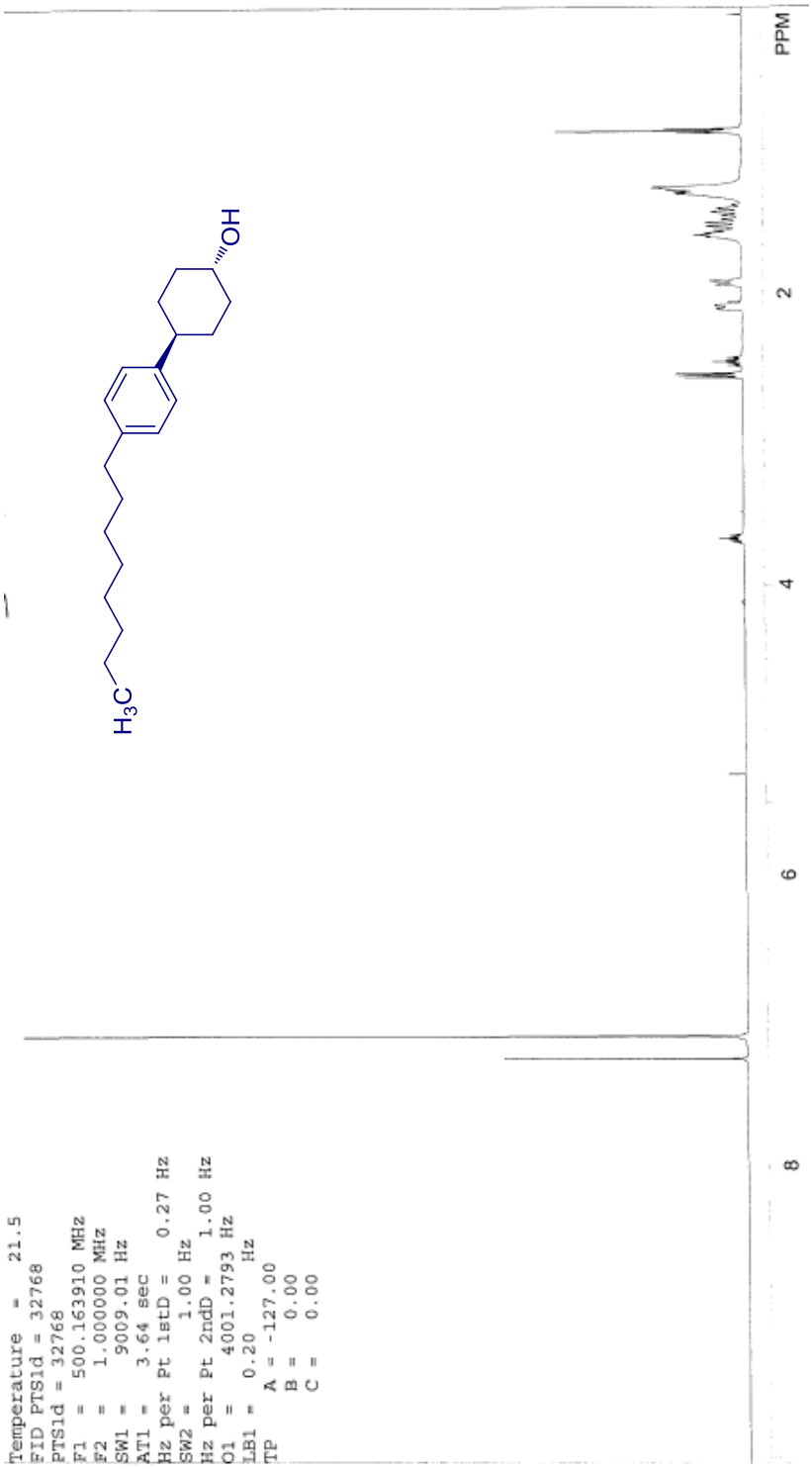

^{13}C NMR spectrum of **9**

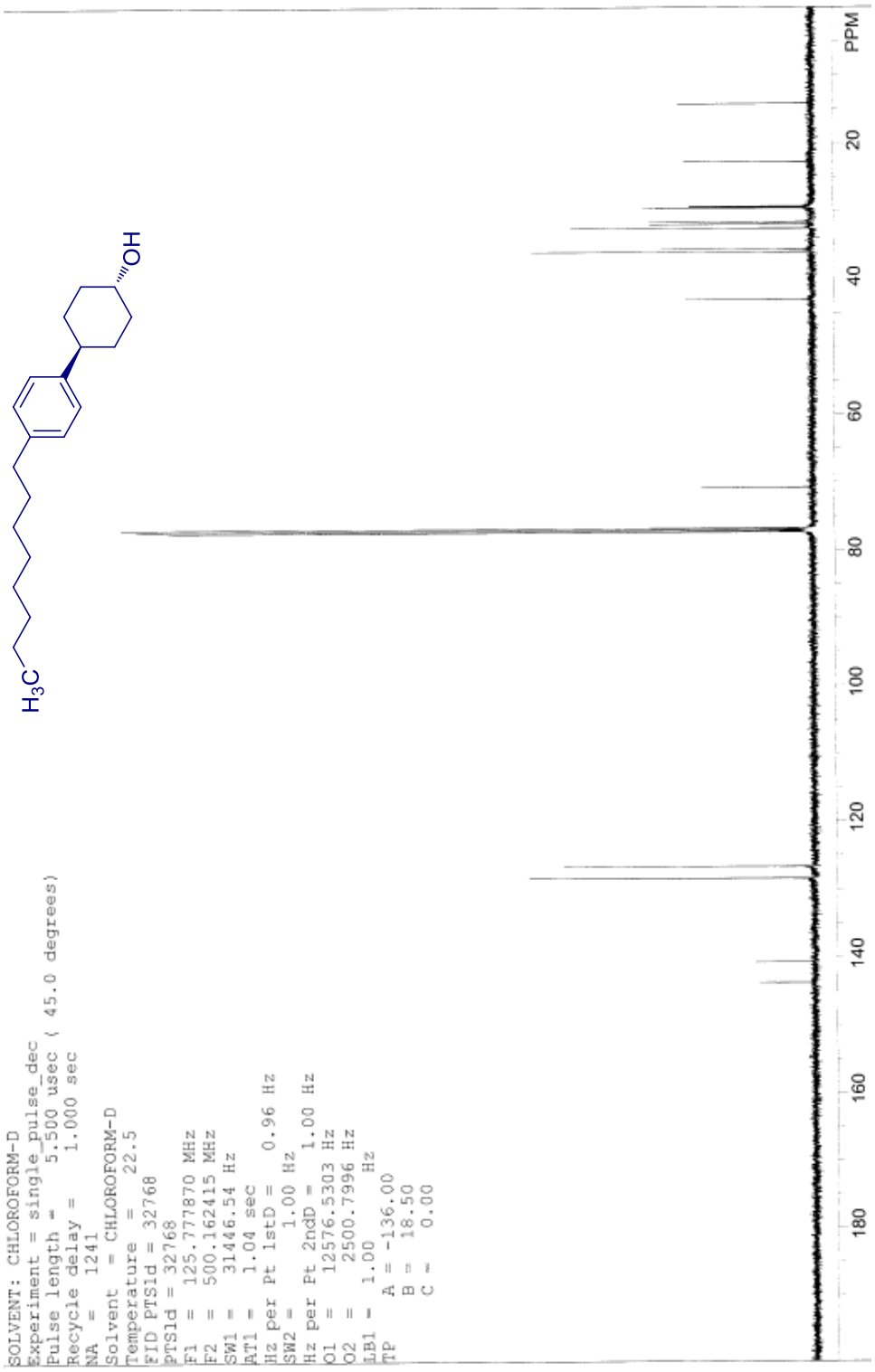

[1]H NMR spectrum of cis-**10a**

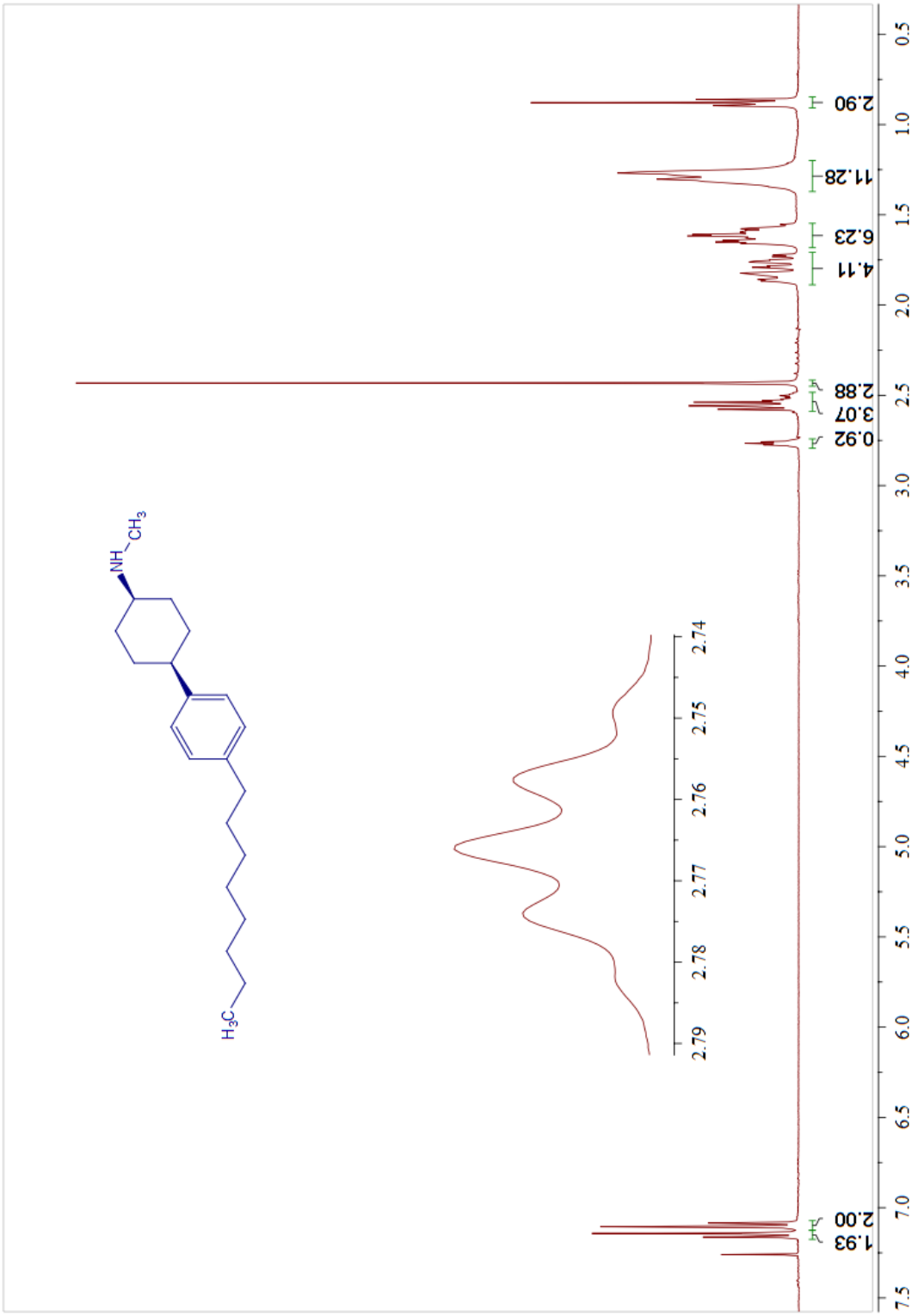

^{13}C NMR spectrum of cis-**10a**

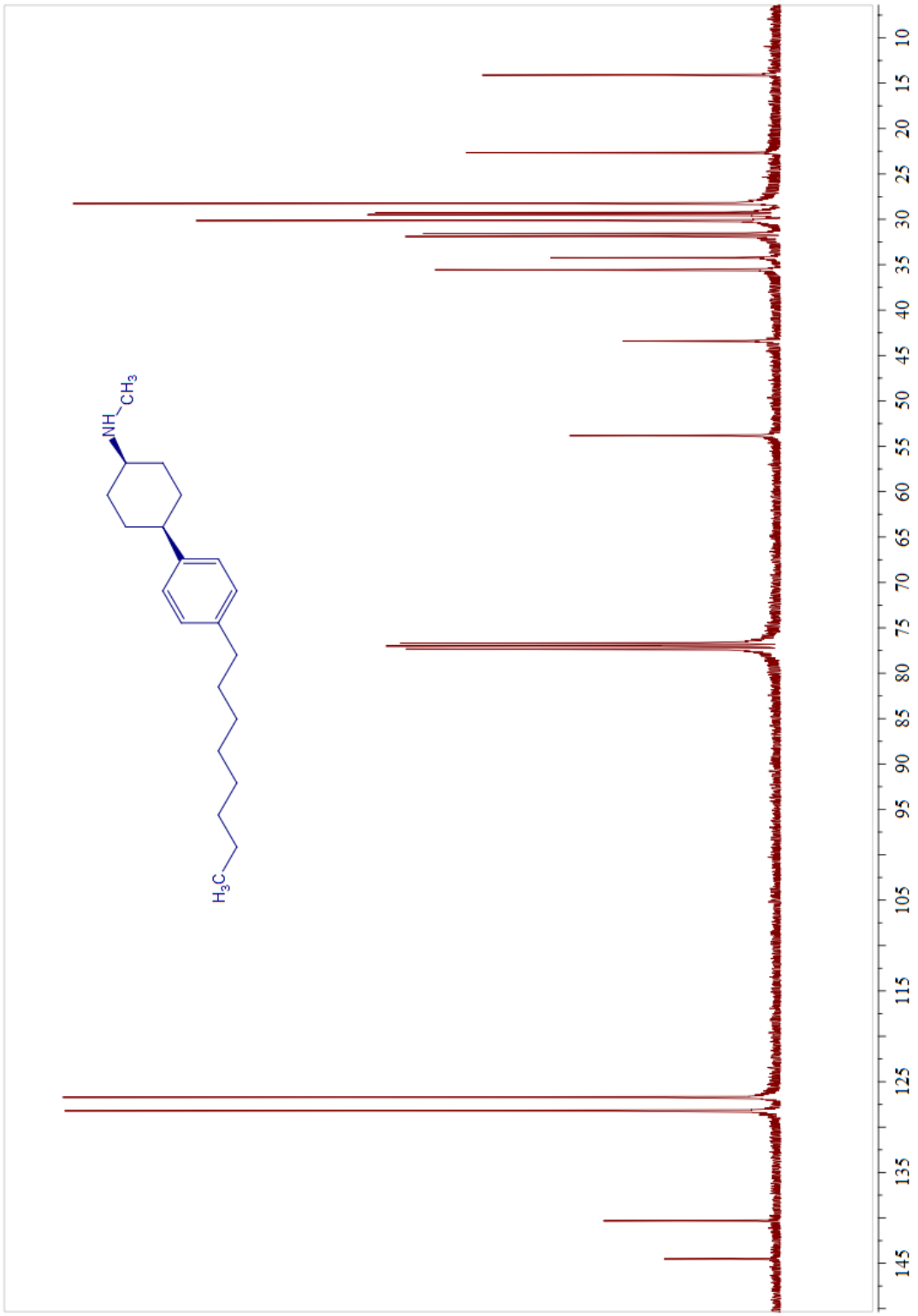

^{1}H NMR spectrum of *trans*-**10a**

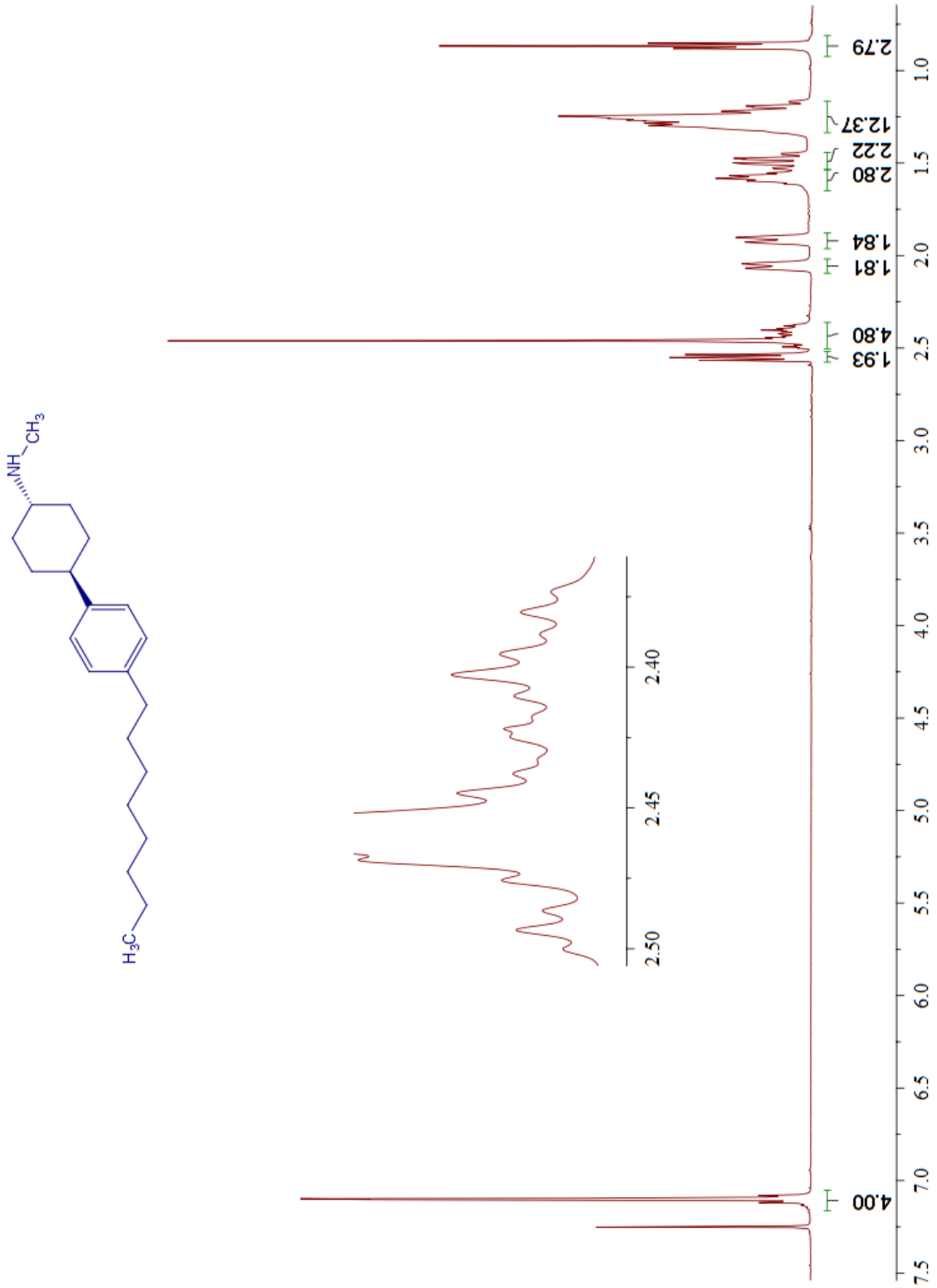

^{13}C NMR spectrum of *trans*-**10a**

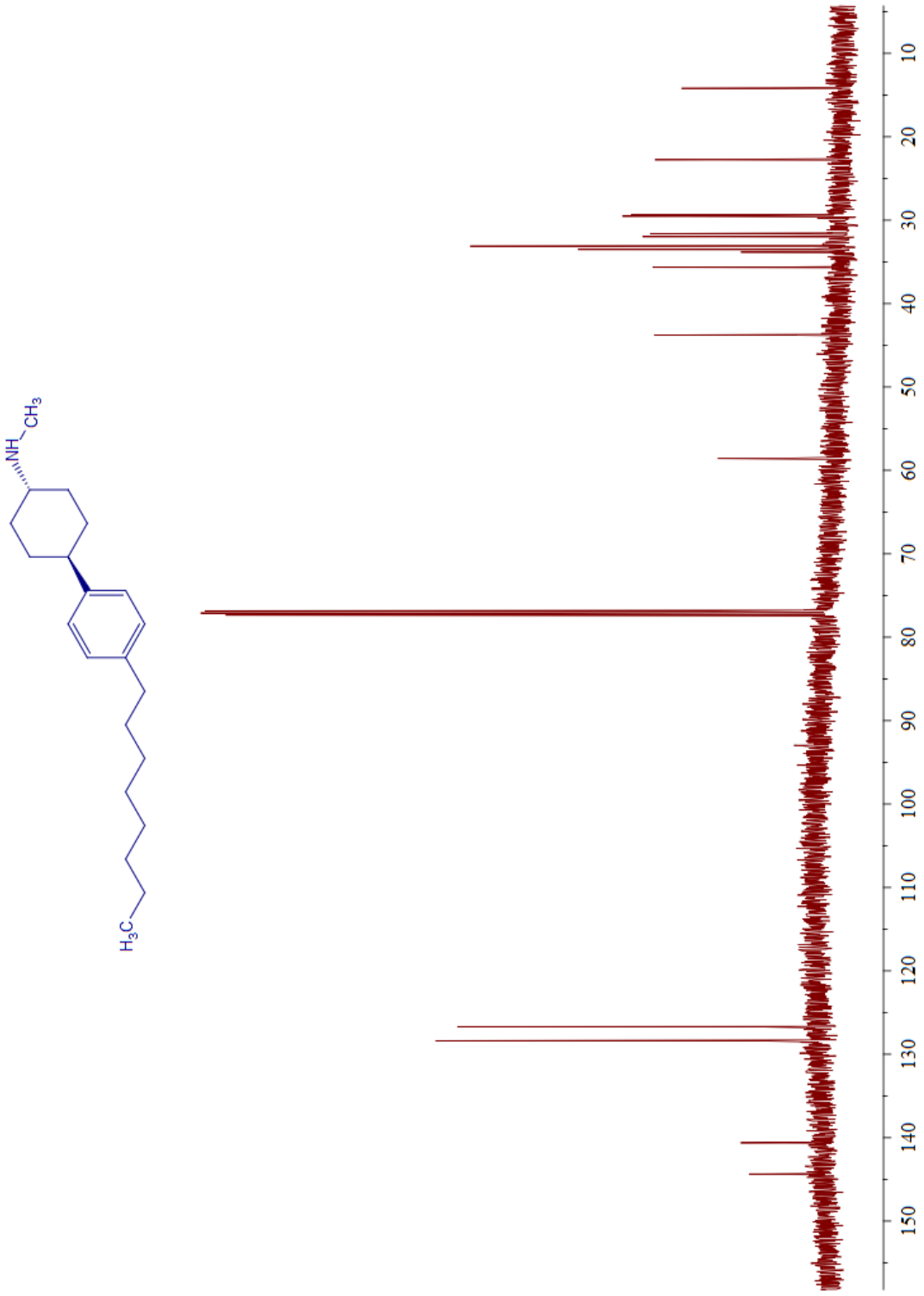

^{1}H NMR spectrum of *cis*-**10b**

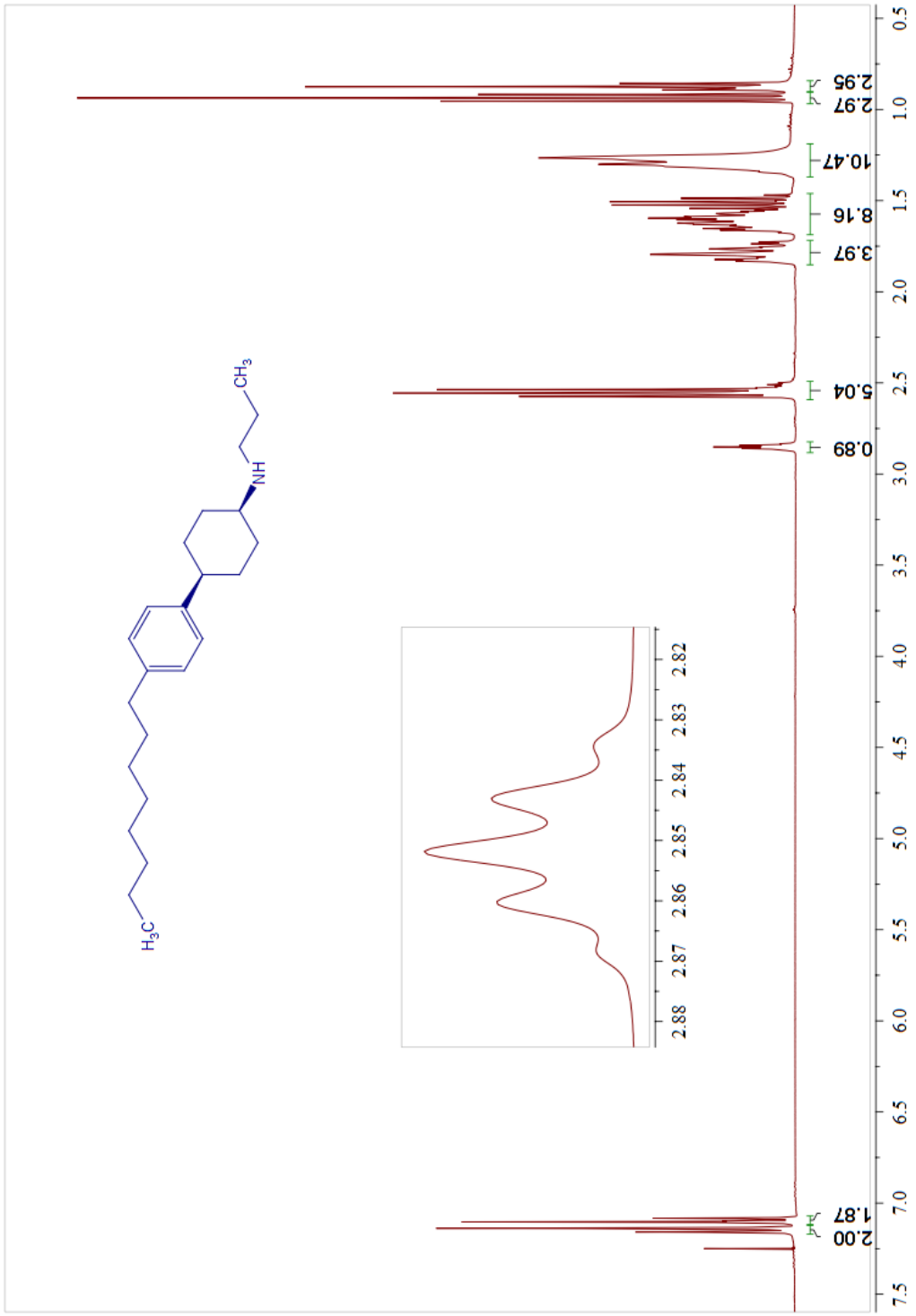

^{13}C NMR spectrum of *cis*-**10b**

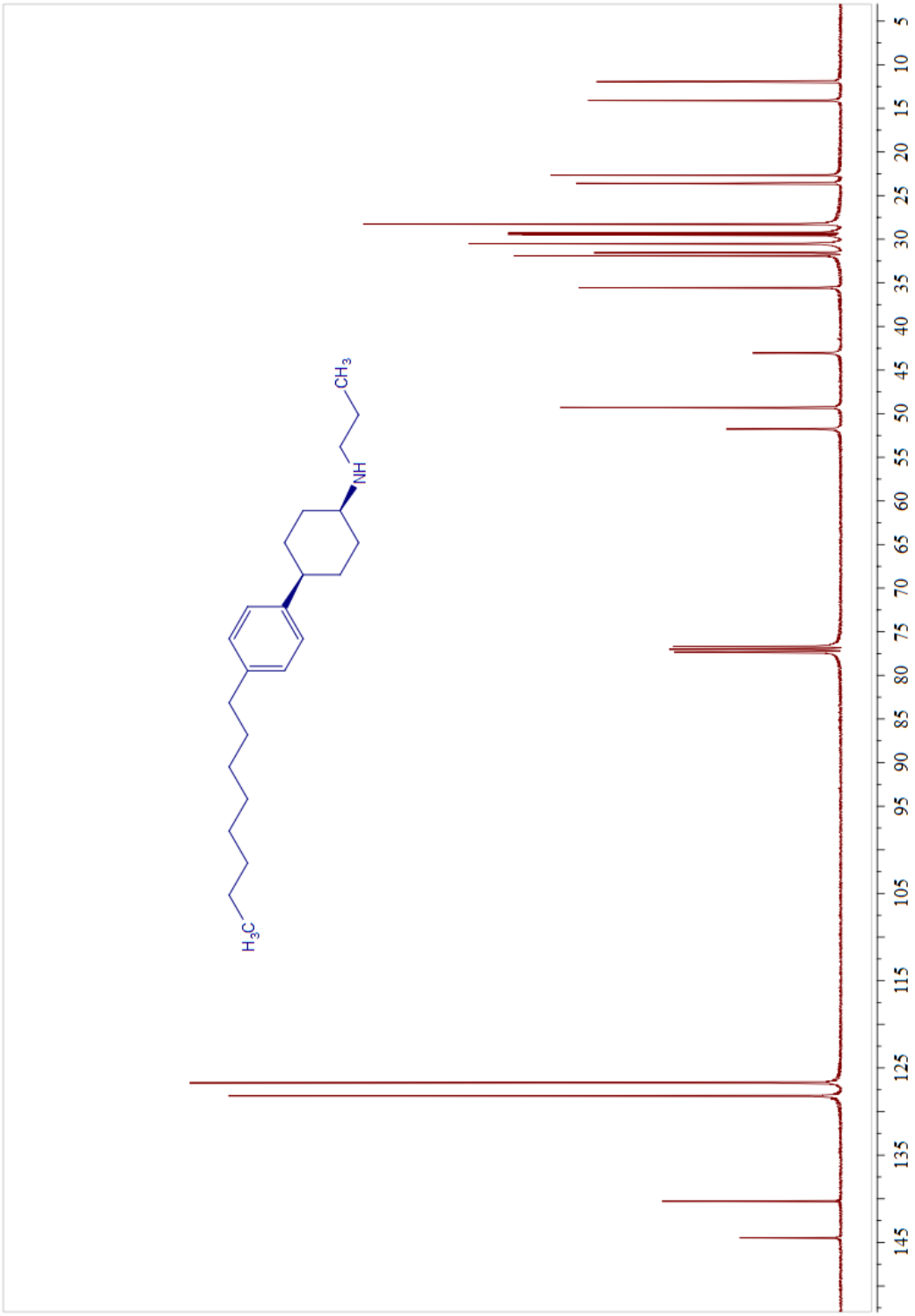

^{1}H NMR spectrum of *trans*-**10b**

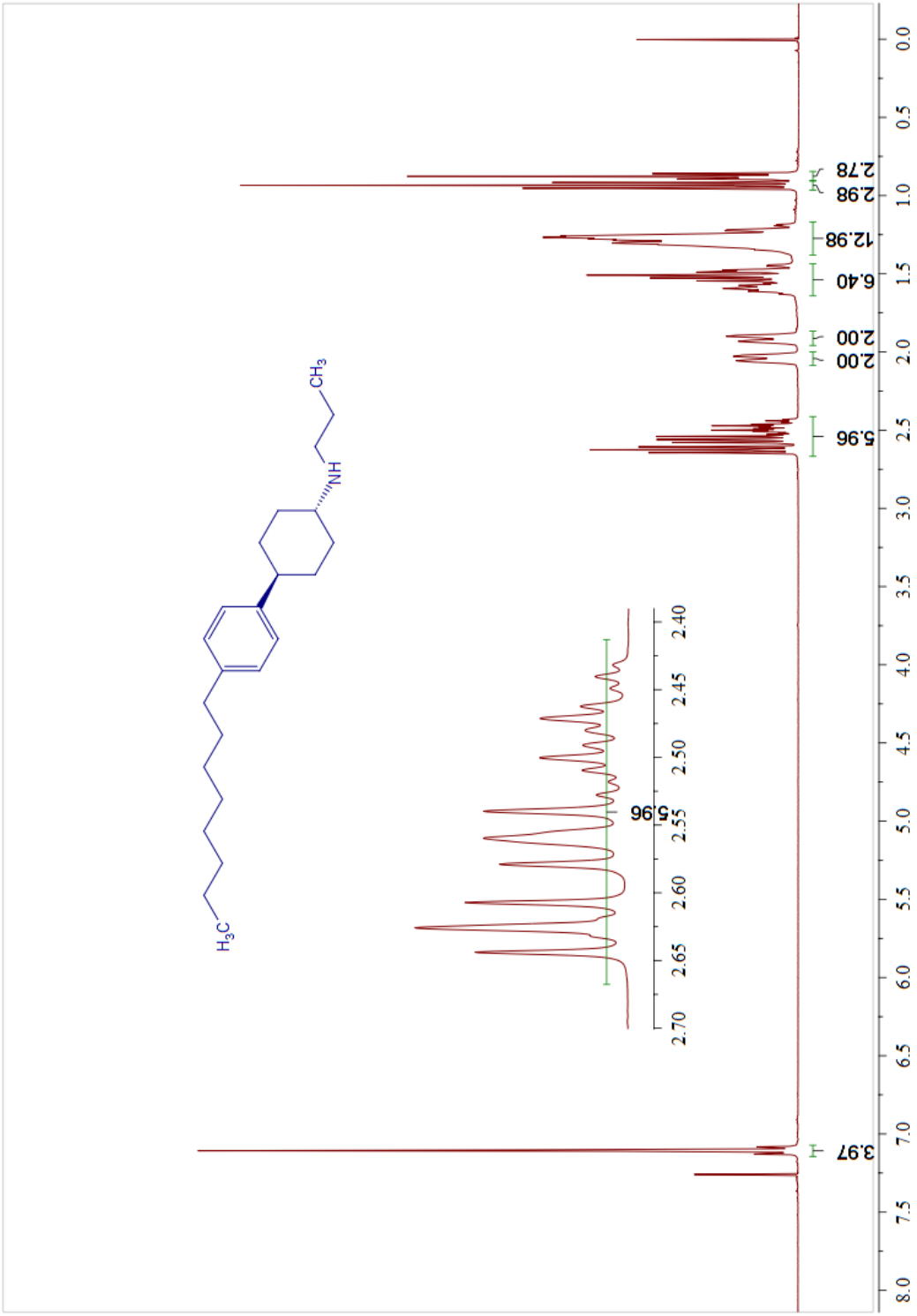

^{13}C NMR spectrum of *trans*-**10b**

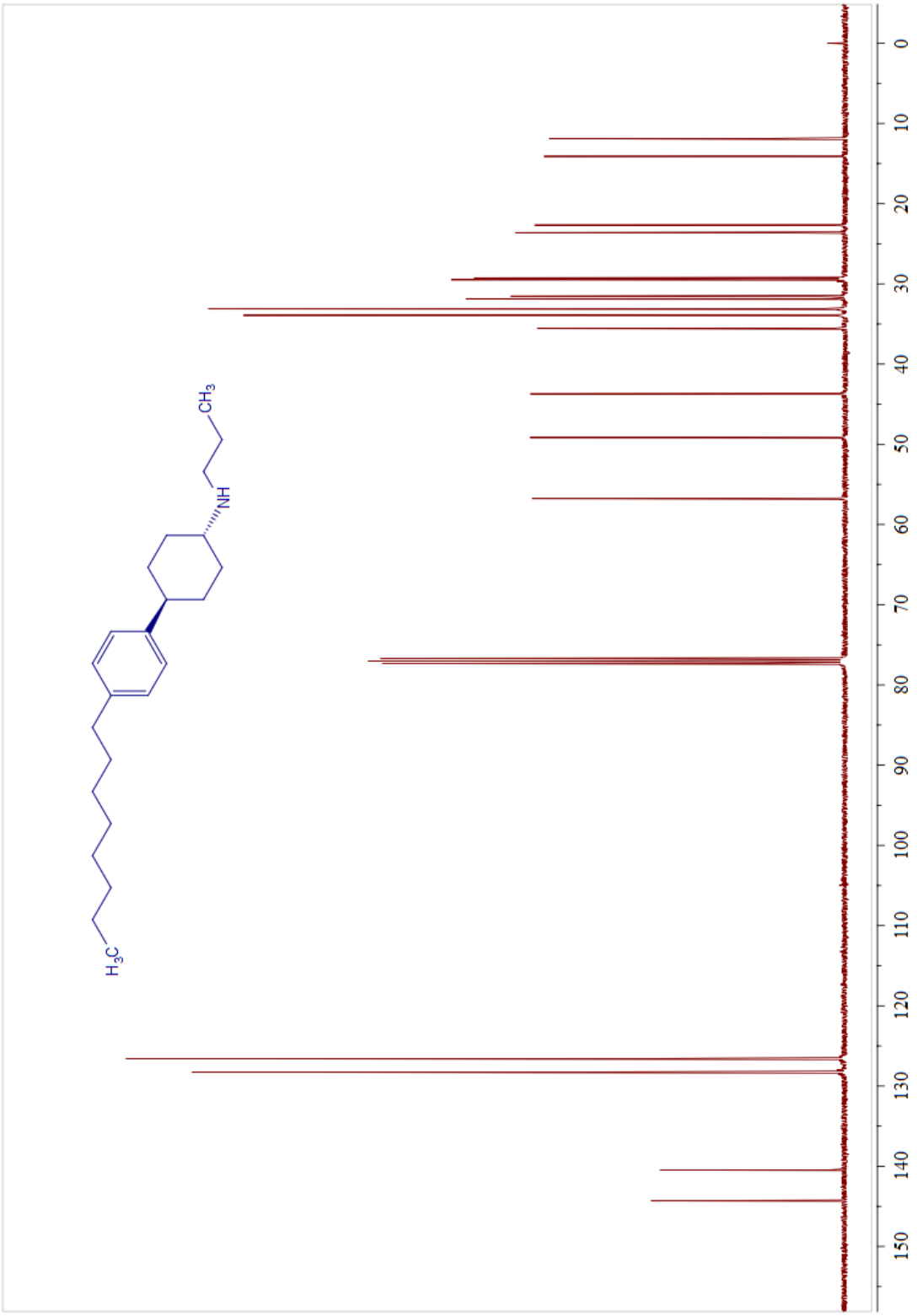

^{1}H NMR spectrum of *cis*-**10c**

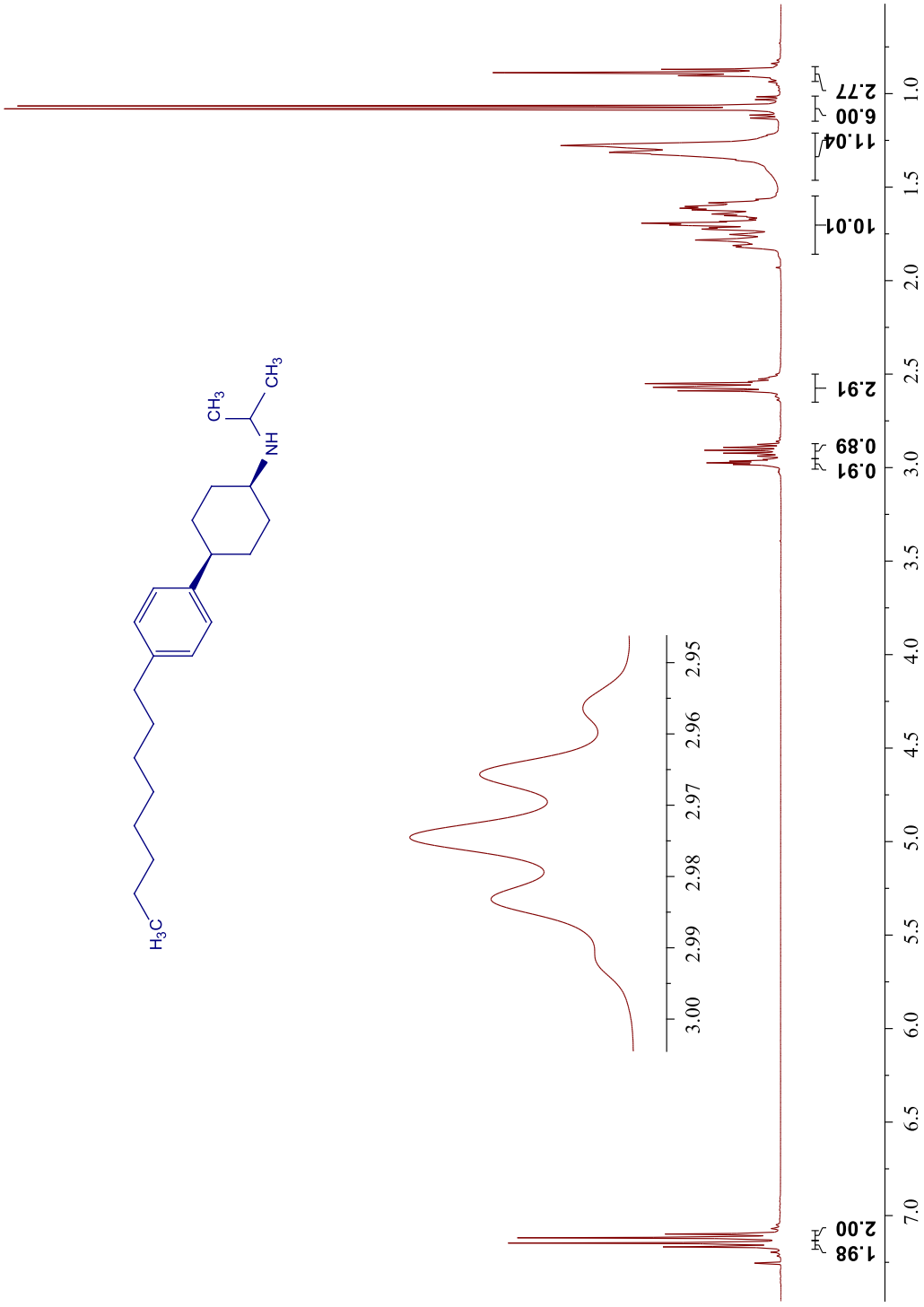

^{13}C NMR spectrum of *cis*-**10c**

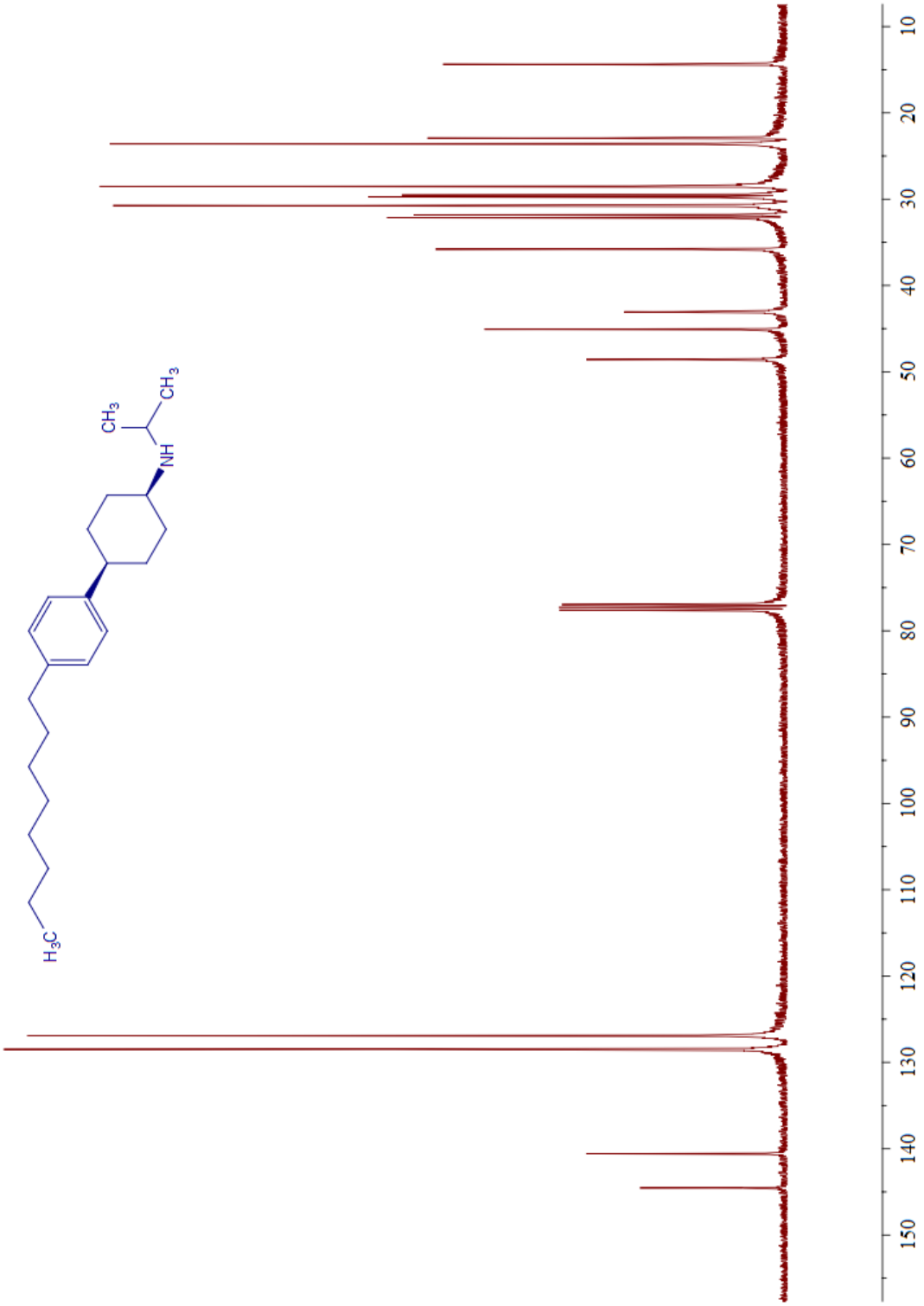

^{1}H NMR spectrum of *trans*-**10c**

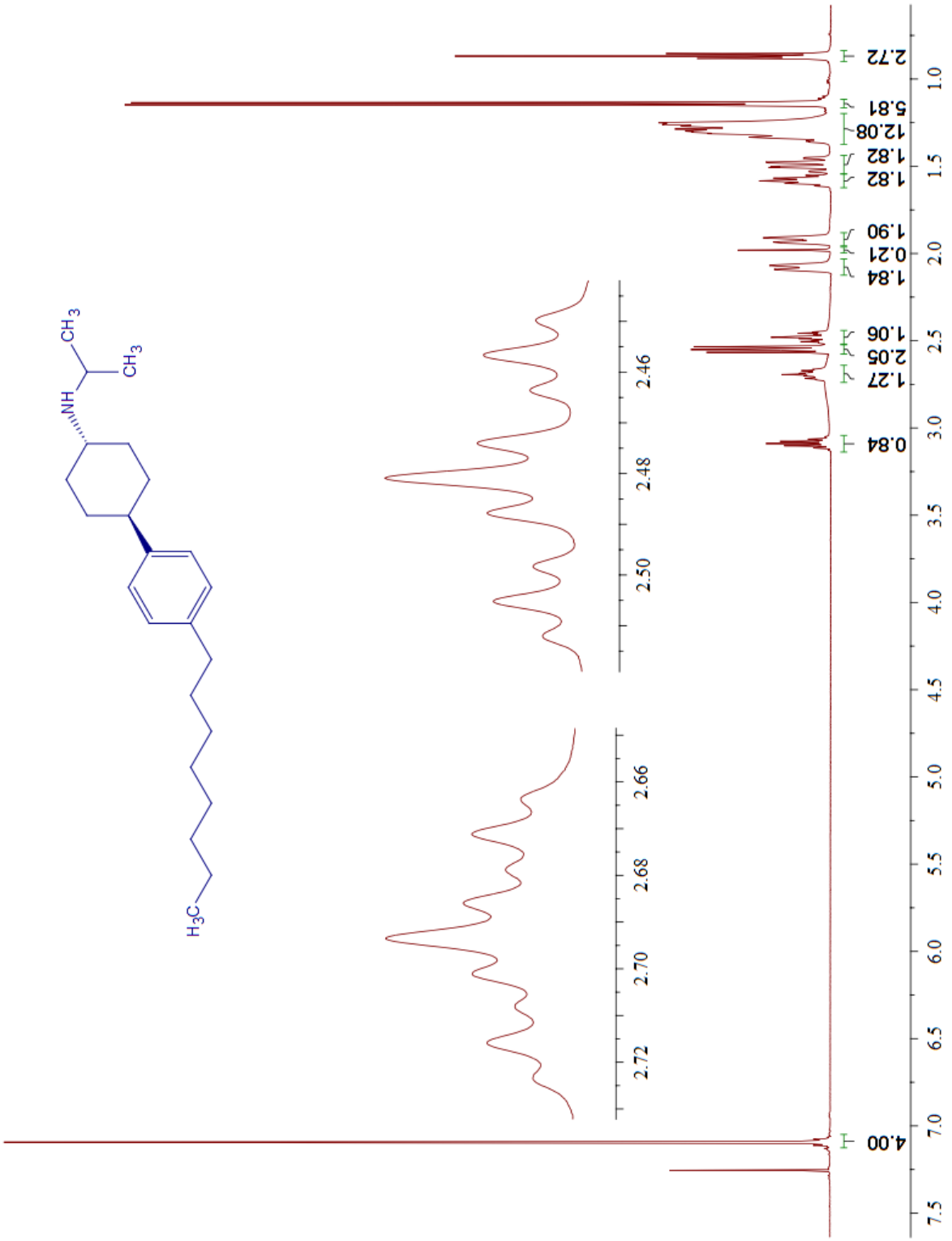

^{13}C NMR spectrum of *trans*-**10c**

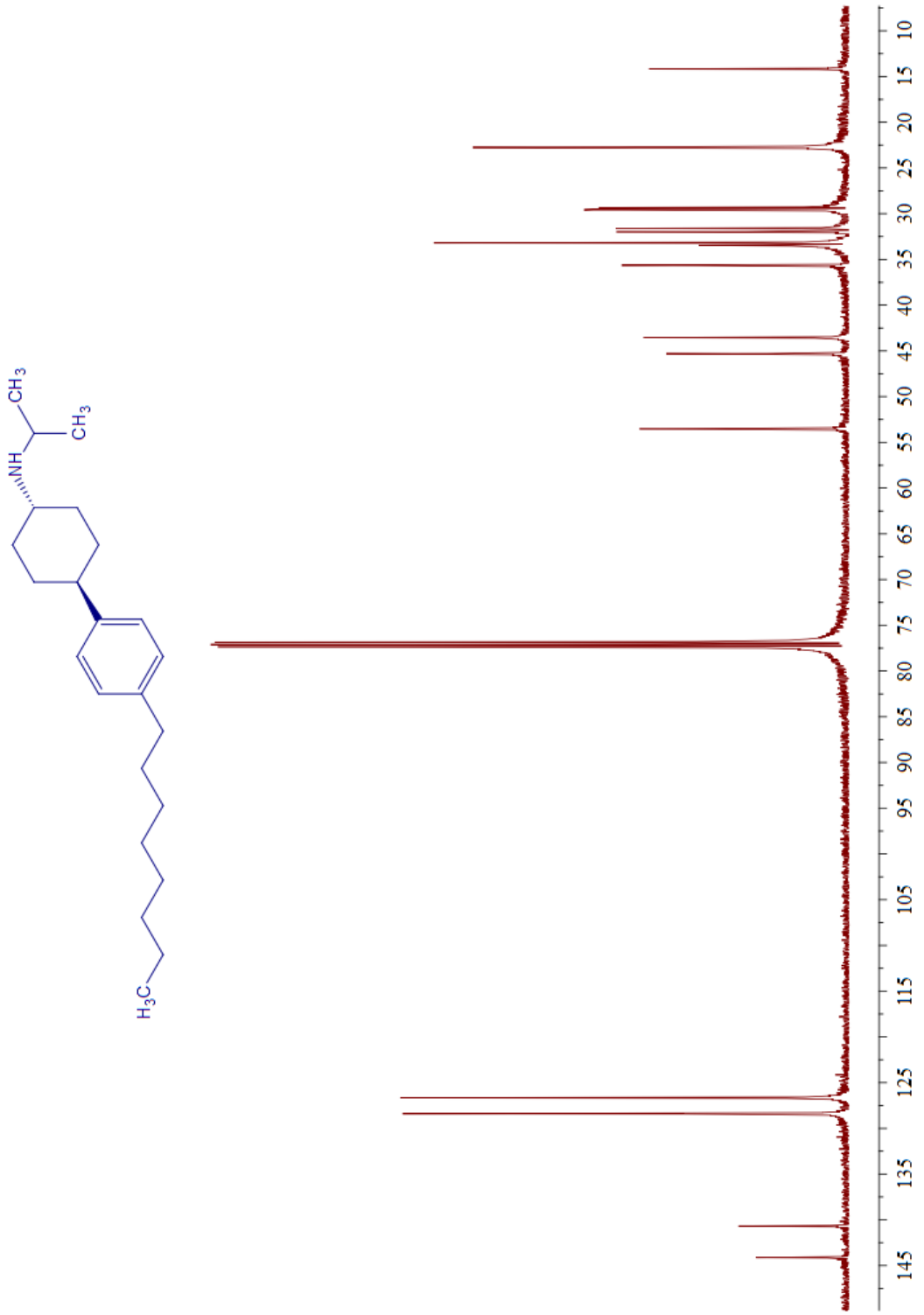

^{1}H NMR spectrum of *cis*-**10d**

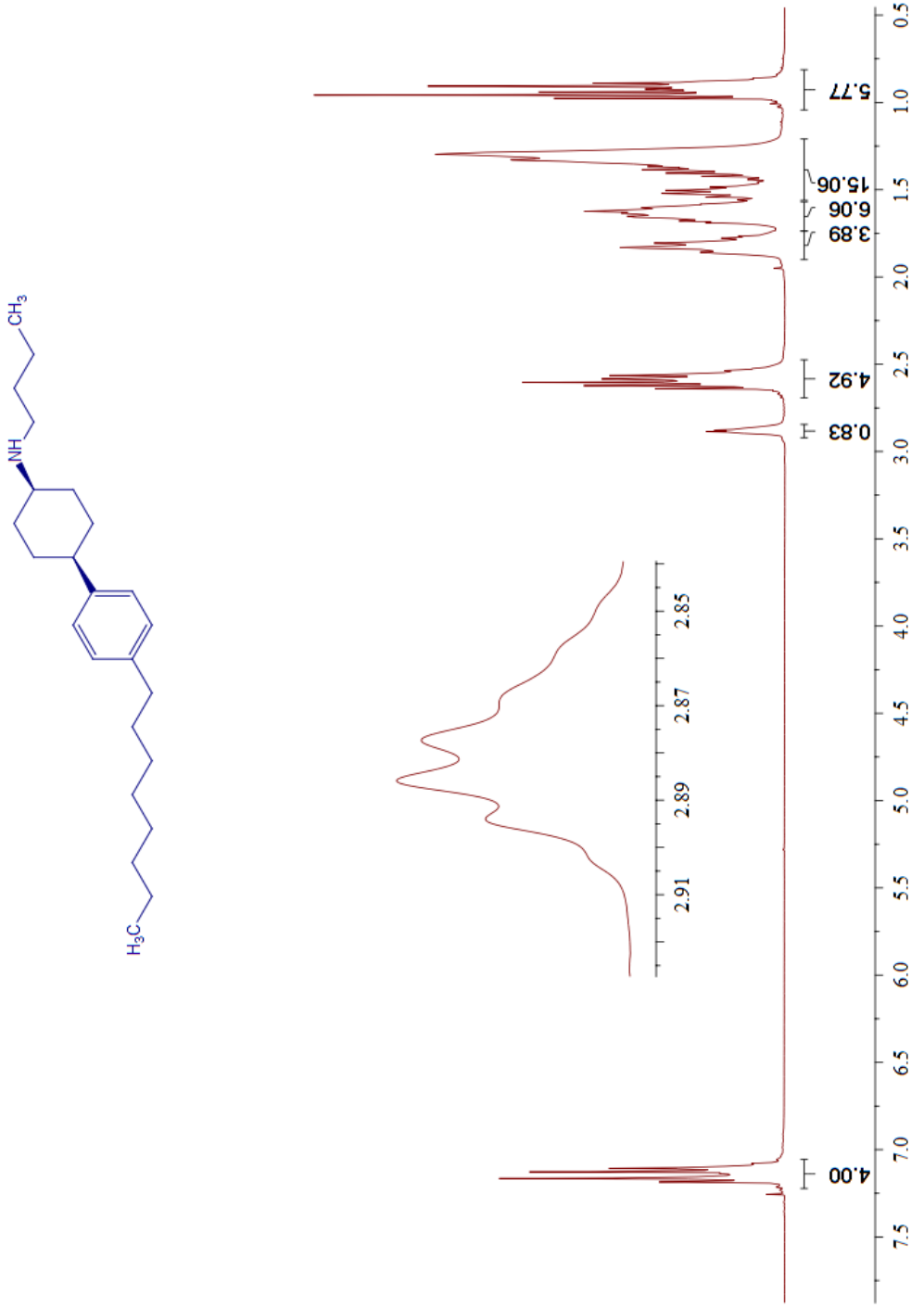

^{13}C NMR spectrum of *cis*-**10d**

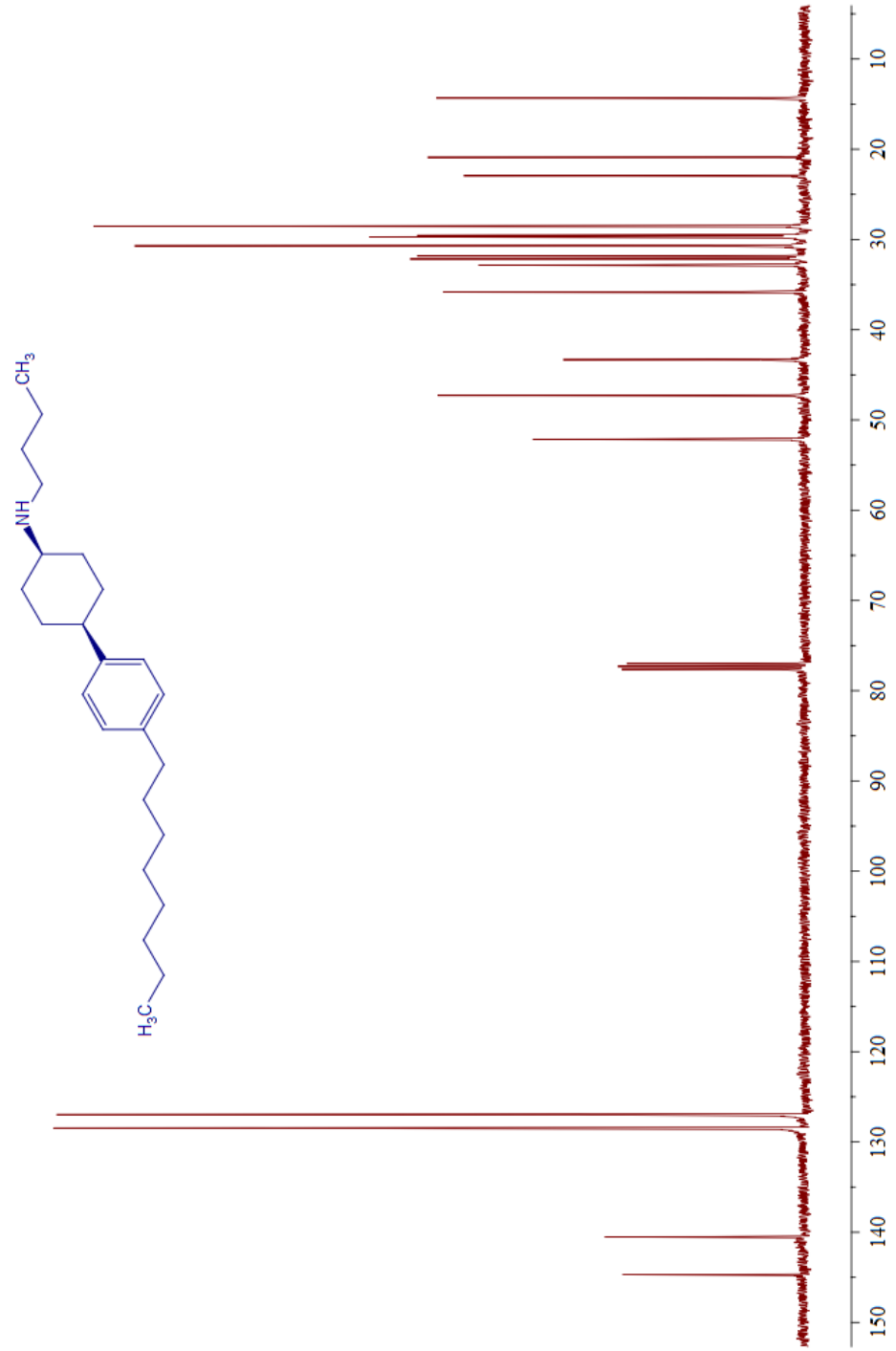

^{1}H NMR spectrum of trans-**10d**

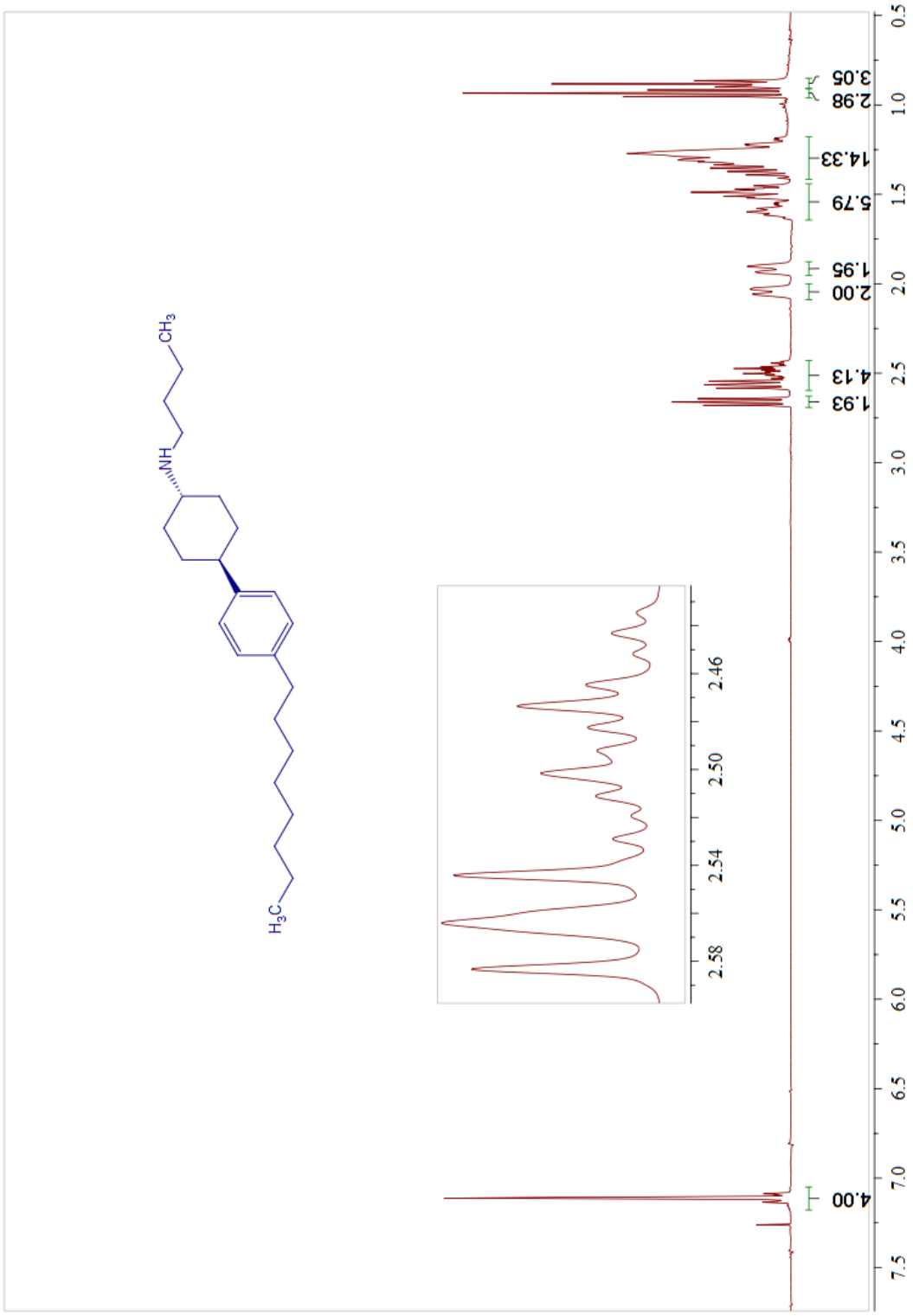

^{13}C NMR spectrum of trans-**10d**

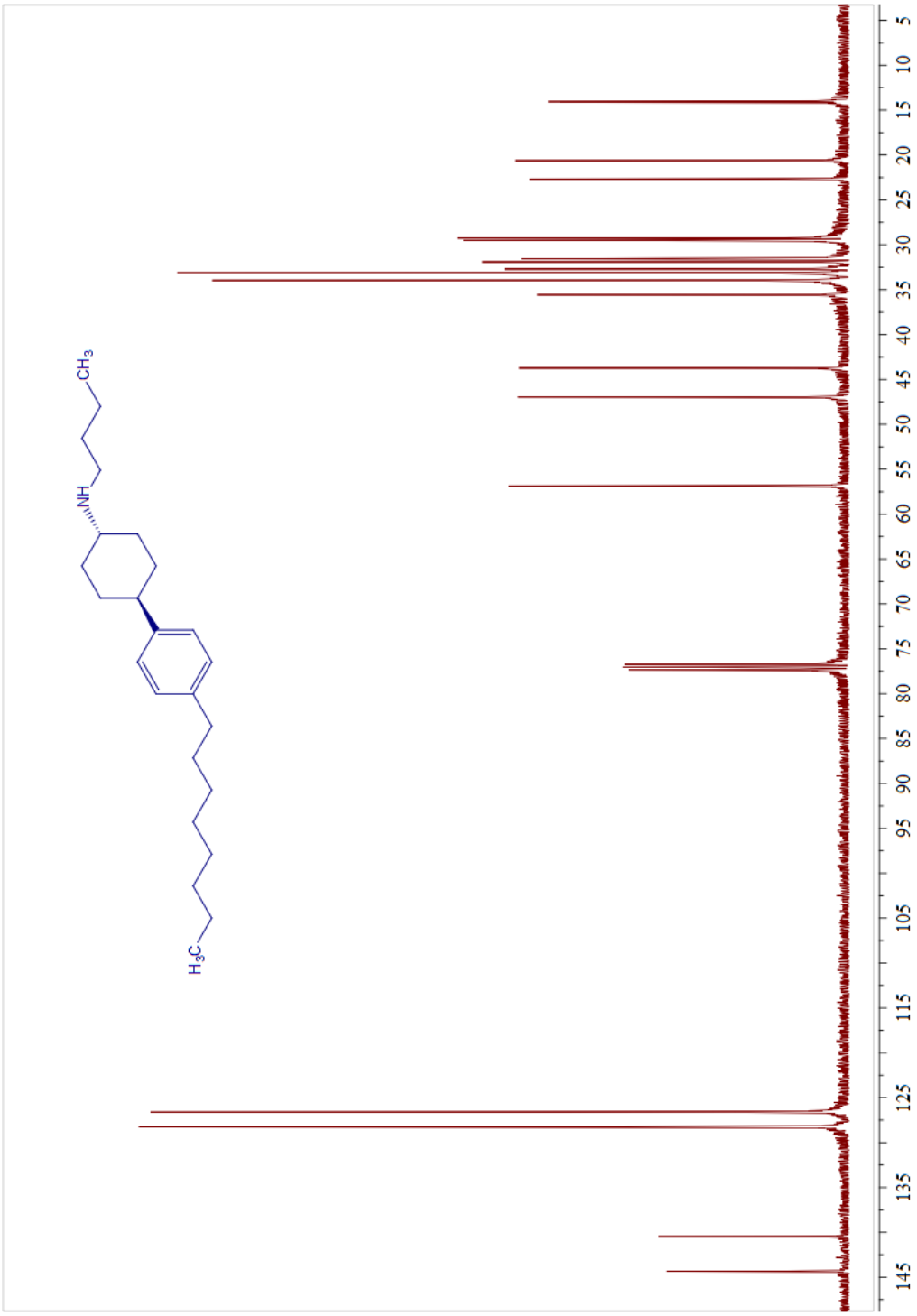

^{1}H NMR spectrum of *cis*-**10e**

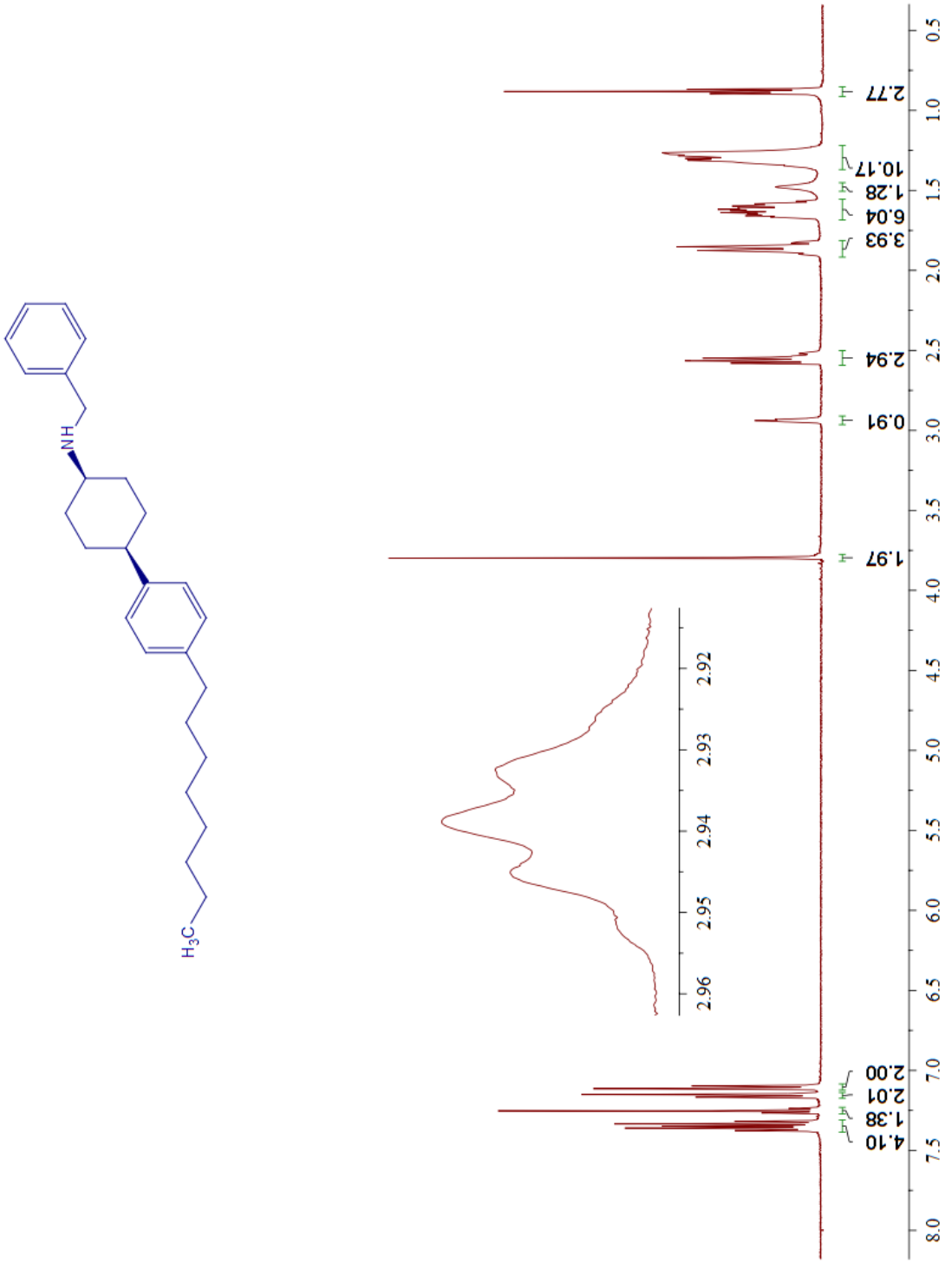

^{13}C NMR spectrum of *cis*-**10e**

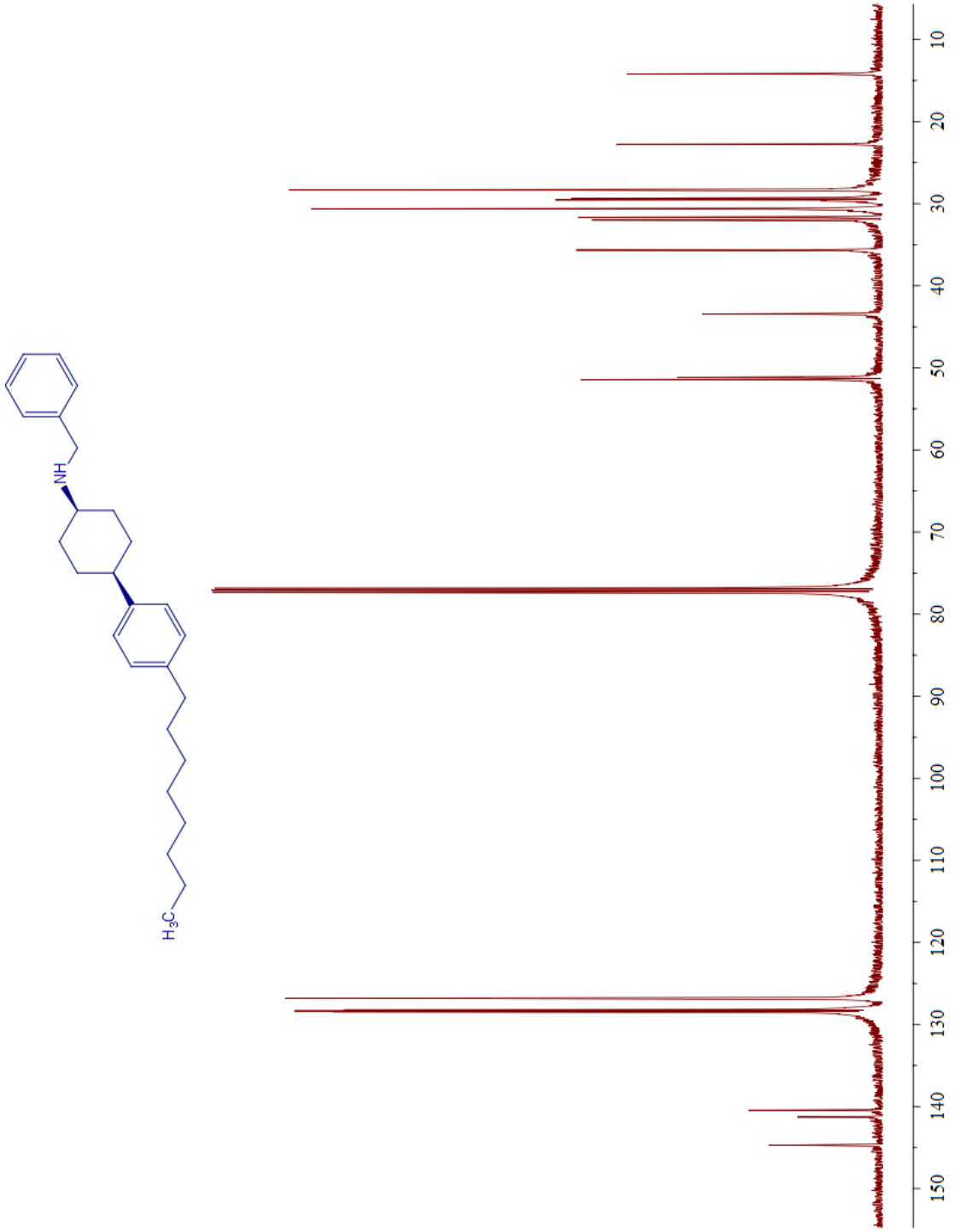

^{1}H NMR spectrum of *trans*-**10e**

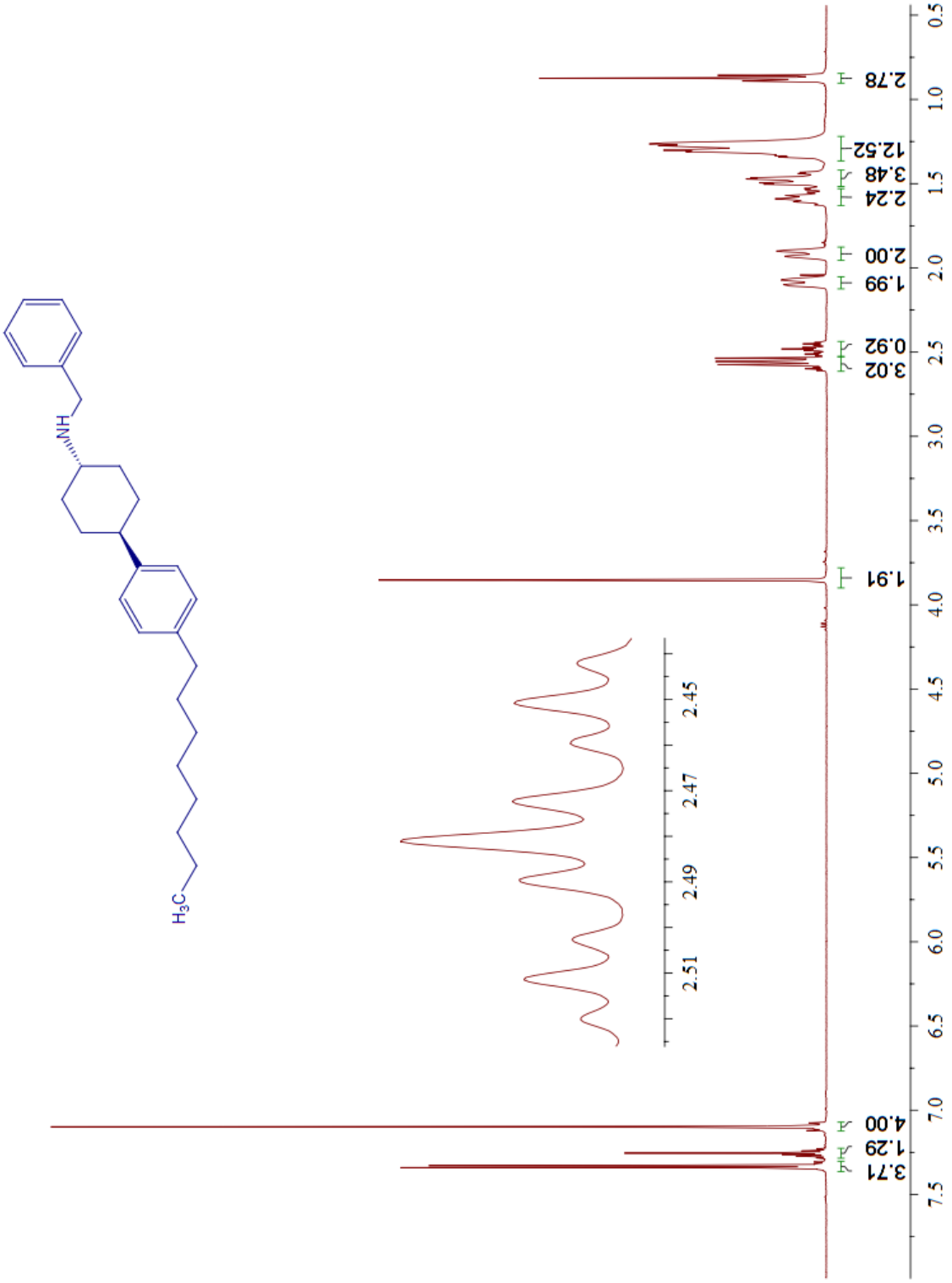

^{13}C NMR spectrum of *trans*-**10e**

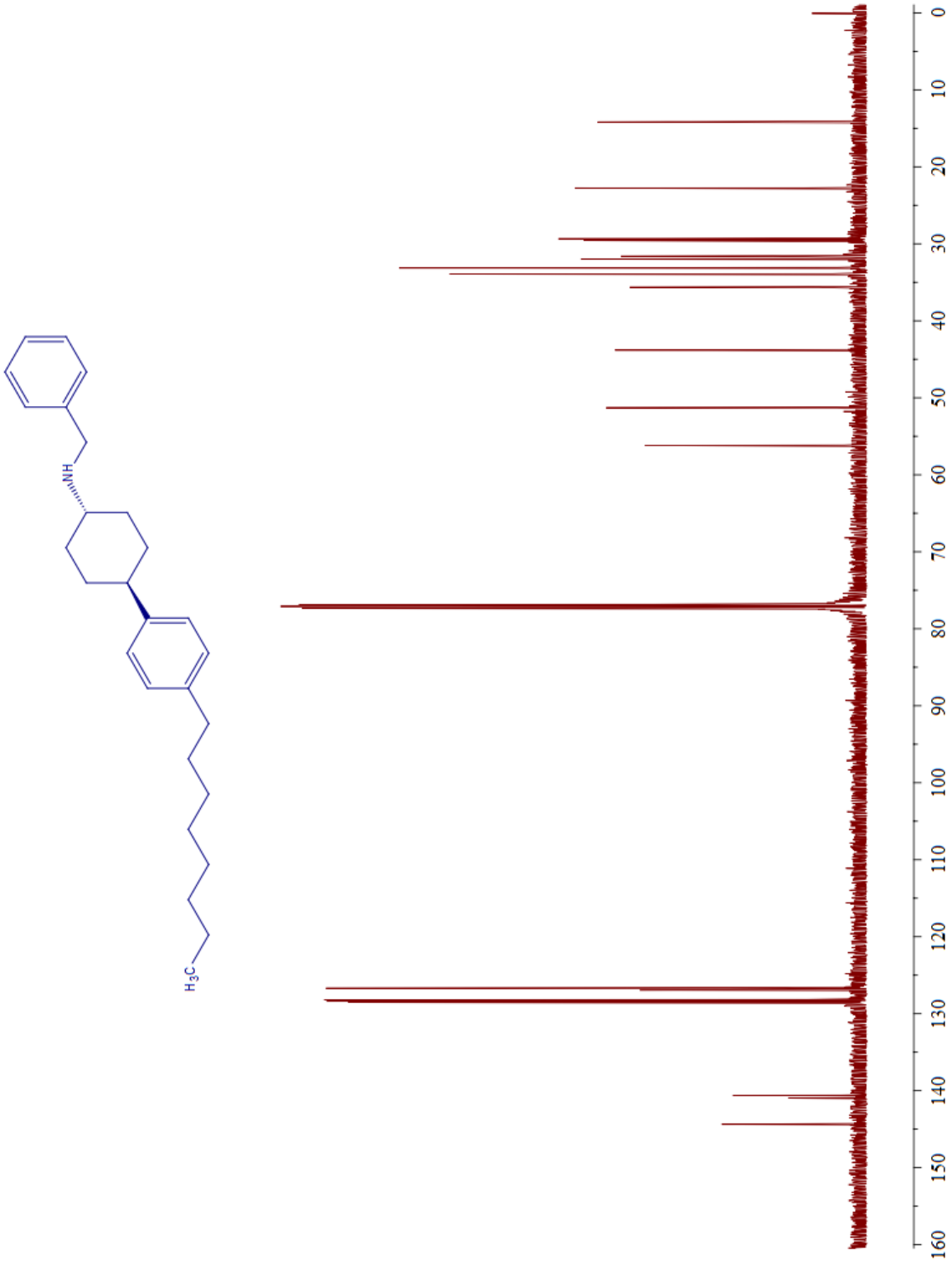

^{1}H NMR spectrum of *cis*-**10f**

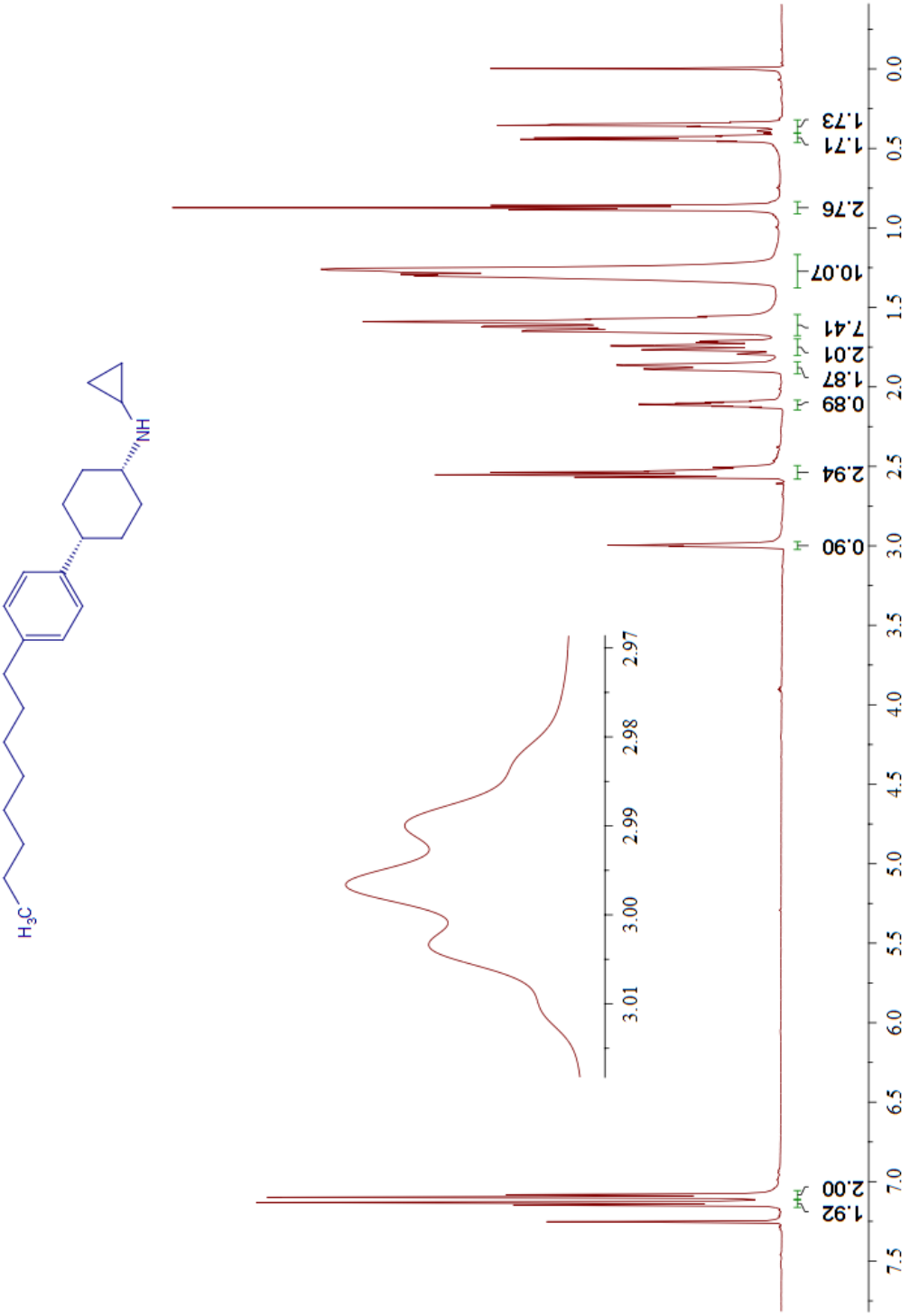

^{13}C NMR spectrum of *cis*-**10f**

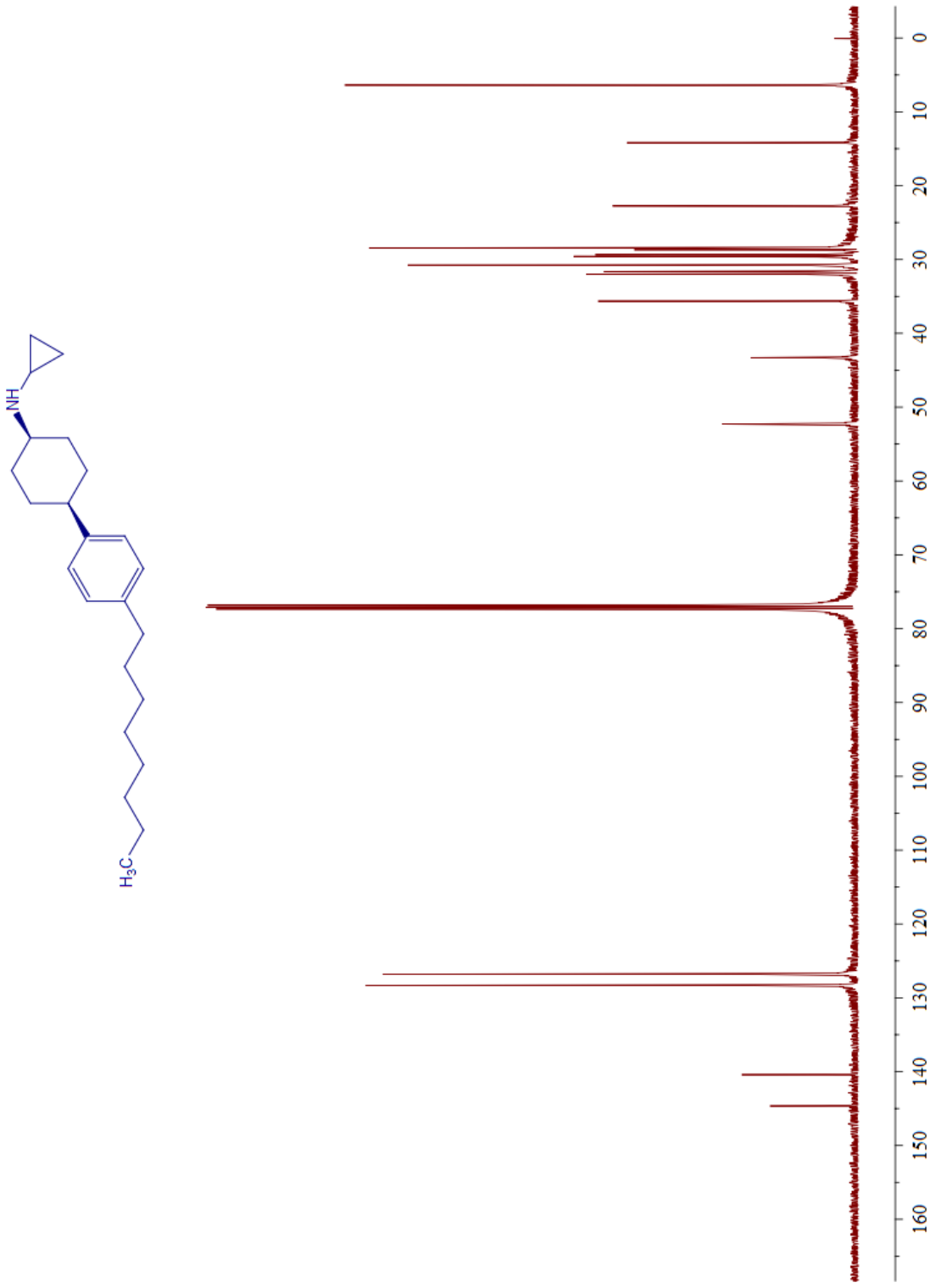

^{1}H NMR spectrum of *trans*-**10f**

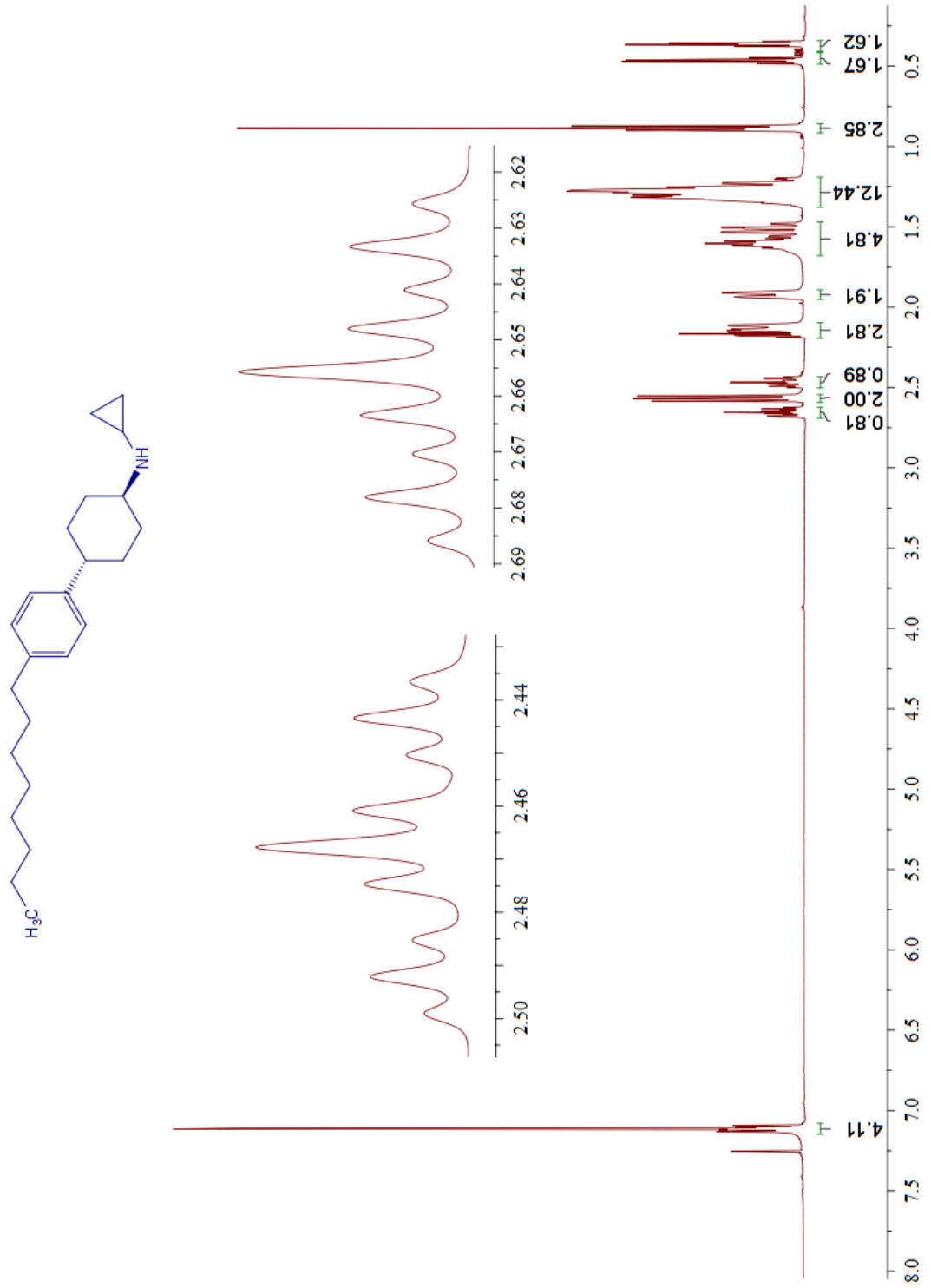

^{13}C NMR spectrum of *trans*-**10f**

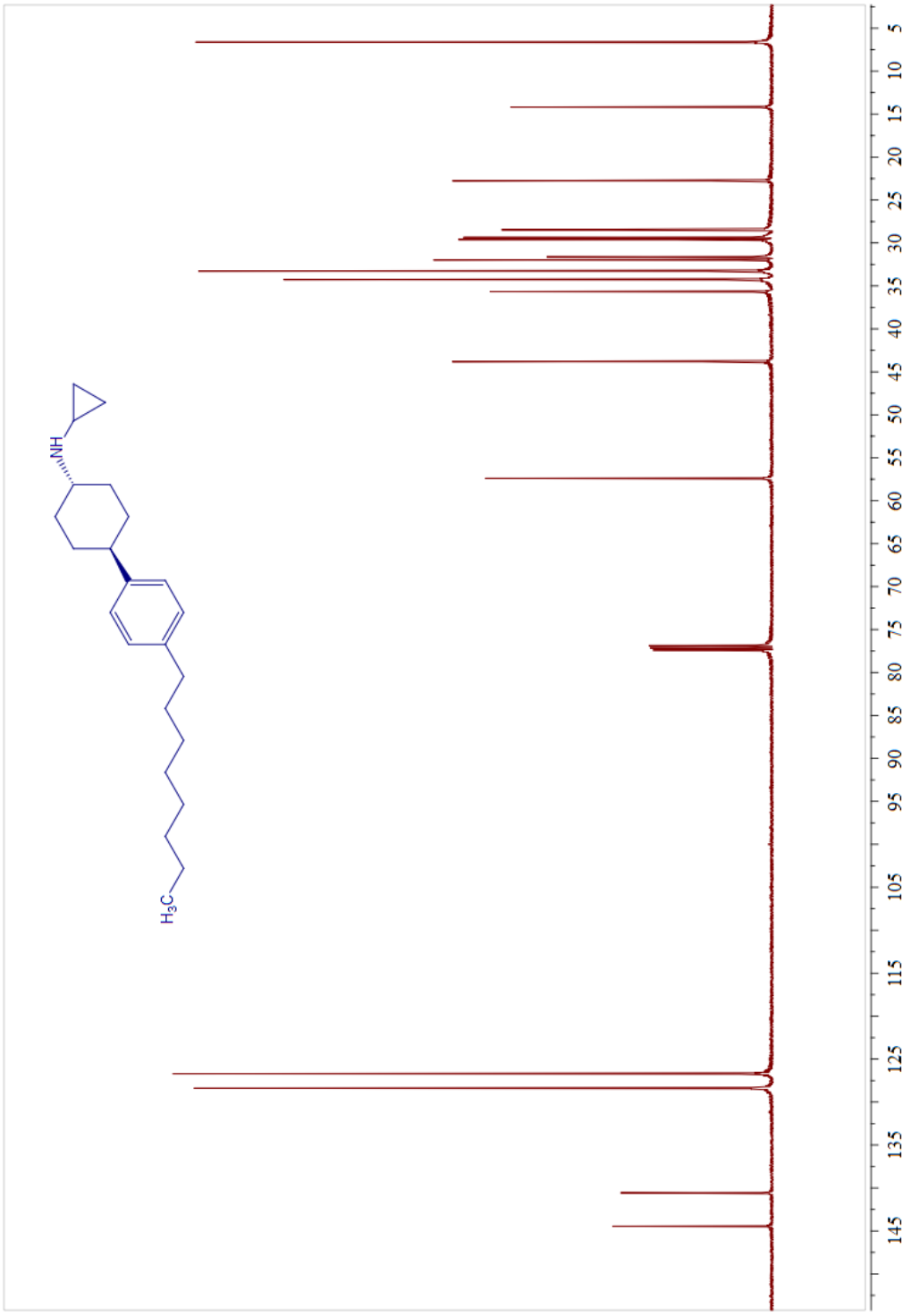

^{1}H NMR spectrum of *cis*-**10g**

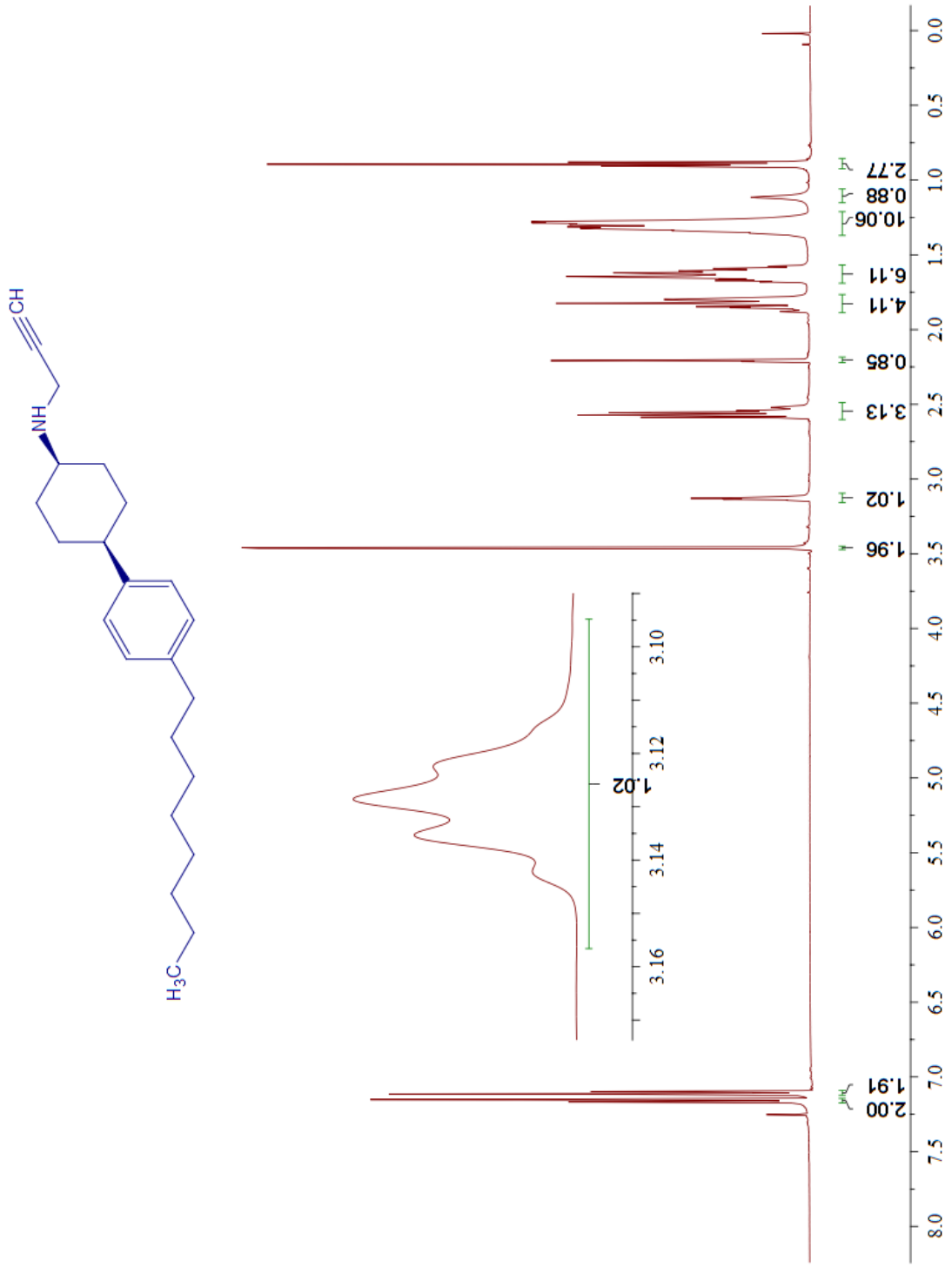

^{13}C NMR spectrum of *cis*-**10g**

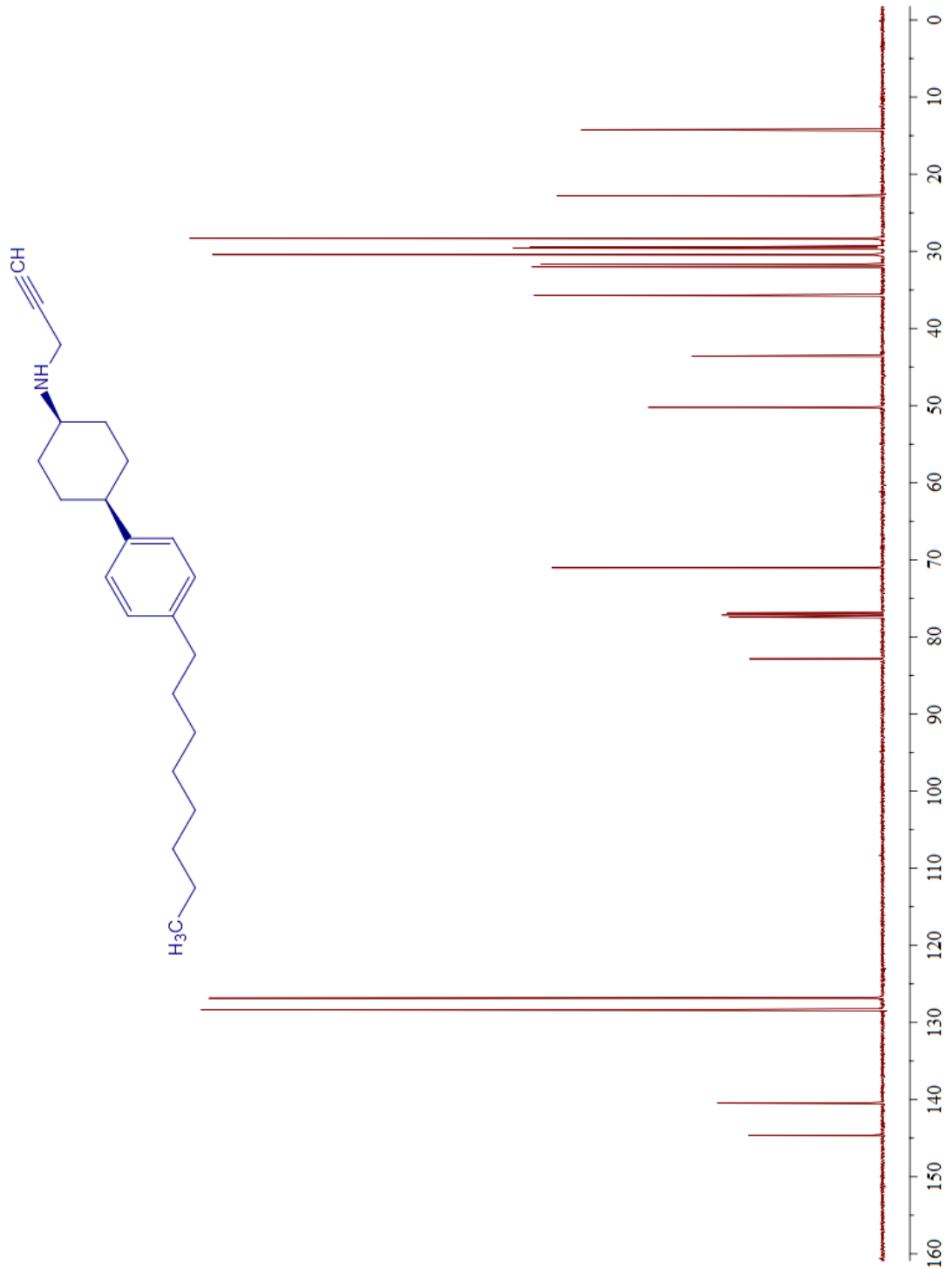

^{1}H NMR spectrum of *trans*-**10g**

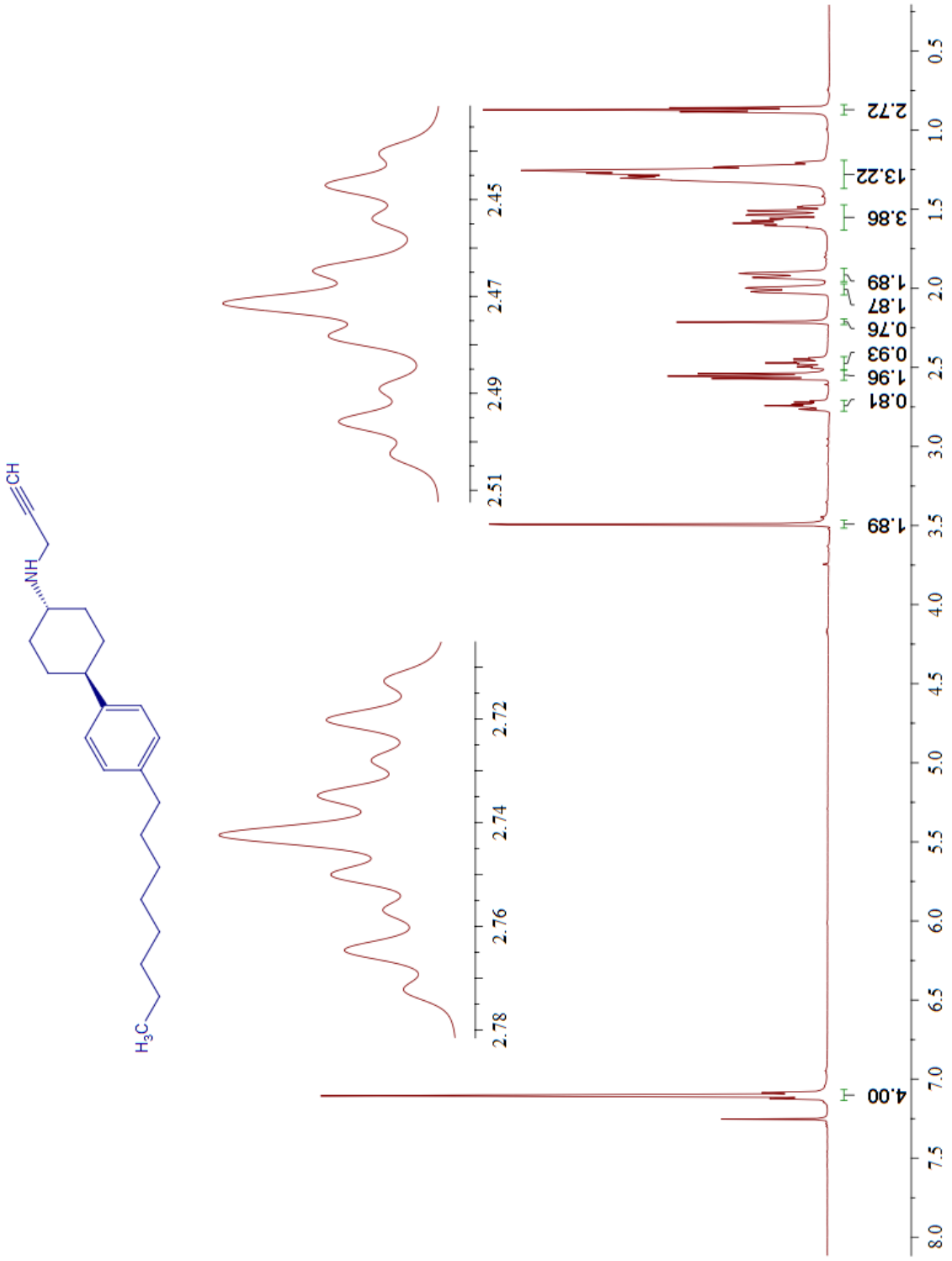

^{13}C NMR spectrum of *trans*-**10g**

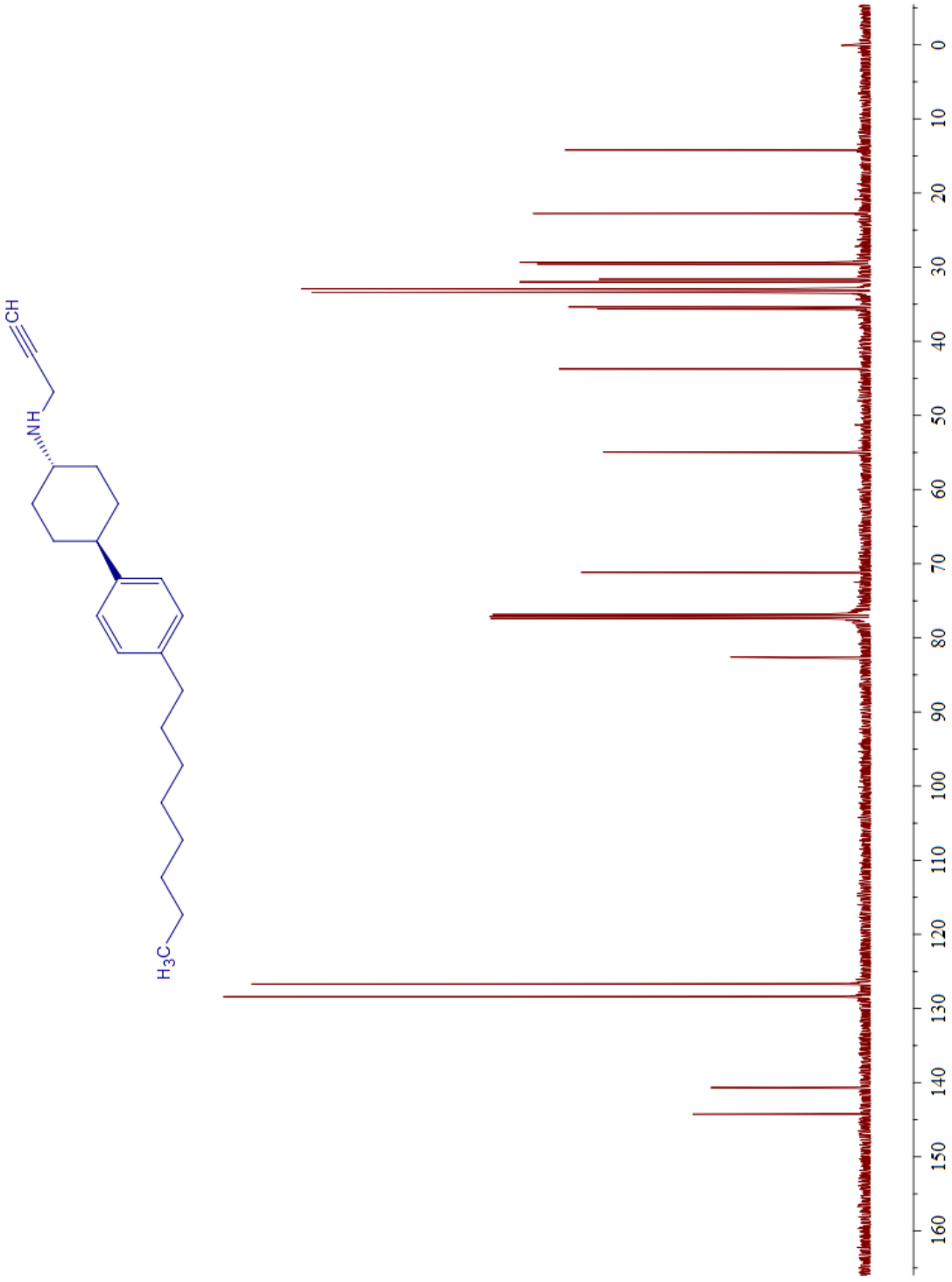

^{1}H NMR spectrum of *cis*-**10h**

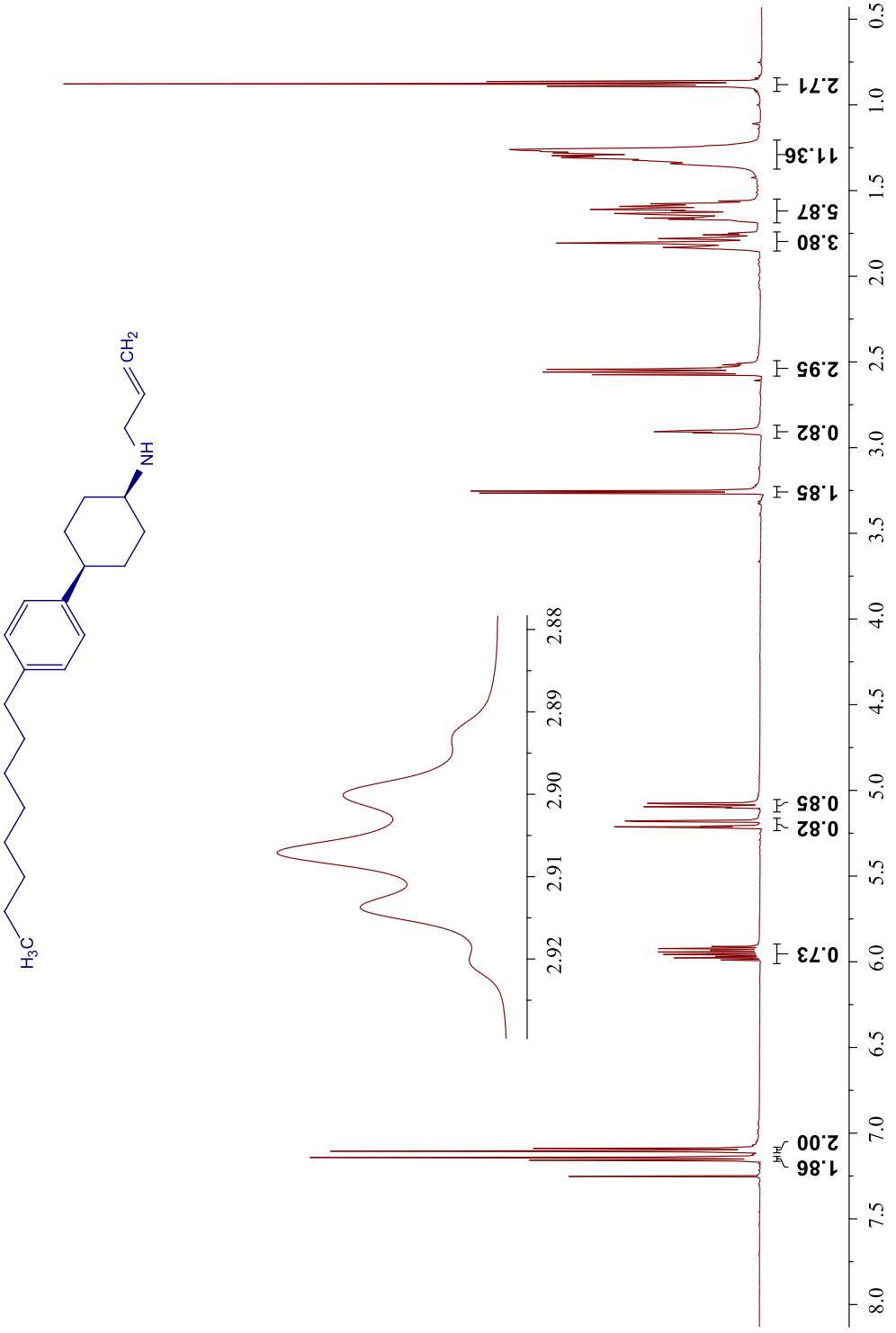

^{13}C NMR spectrum of *cis*-**10h**

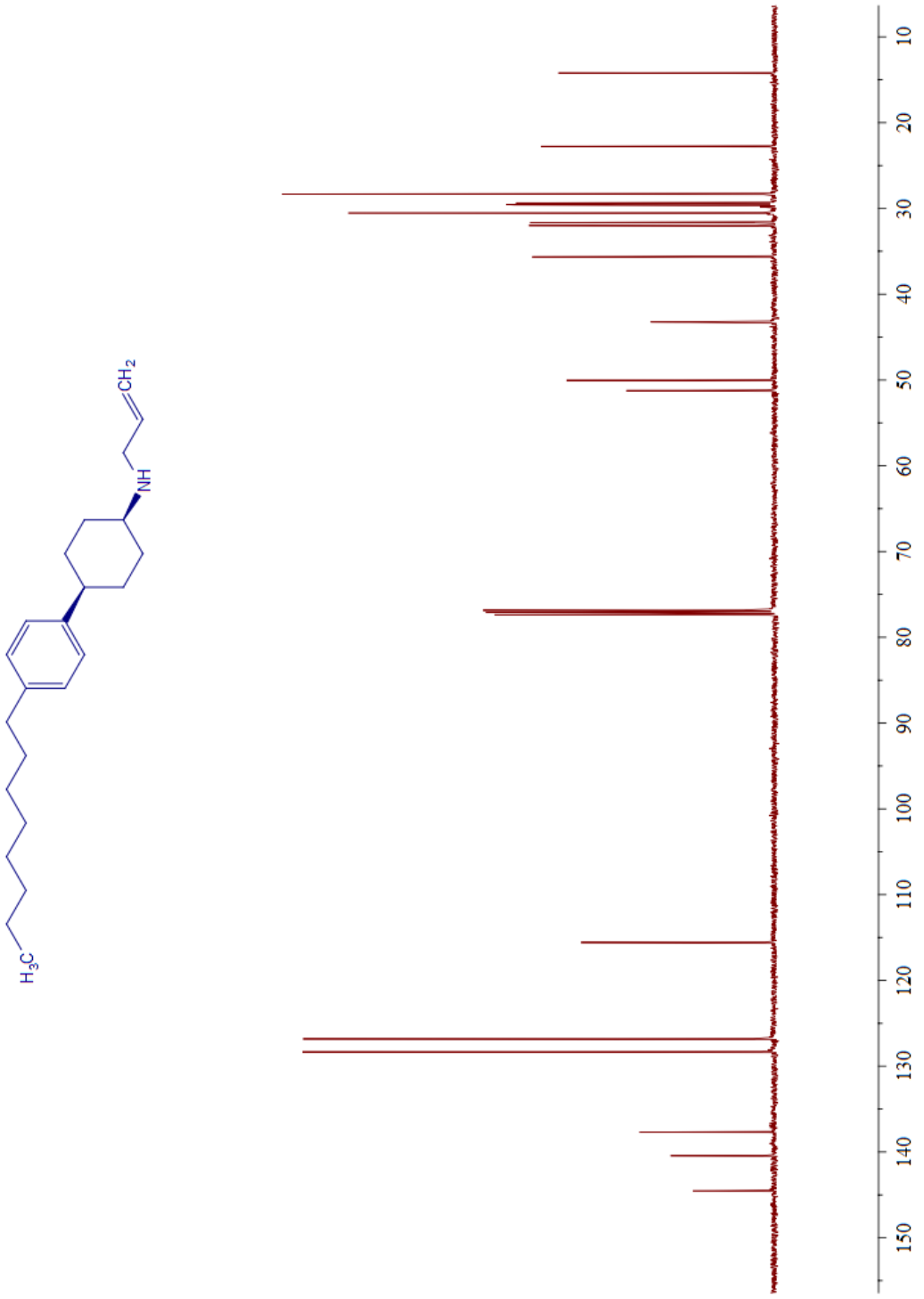

^{1}H NMR spectrum of *trans*-**10h**

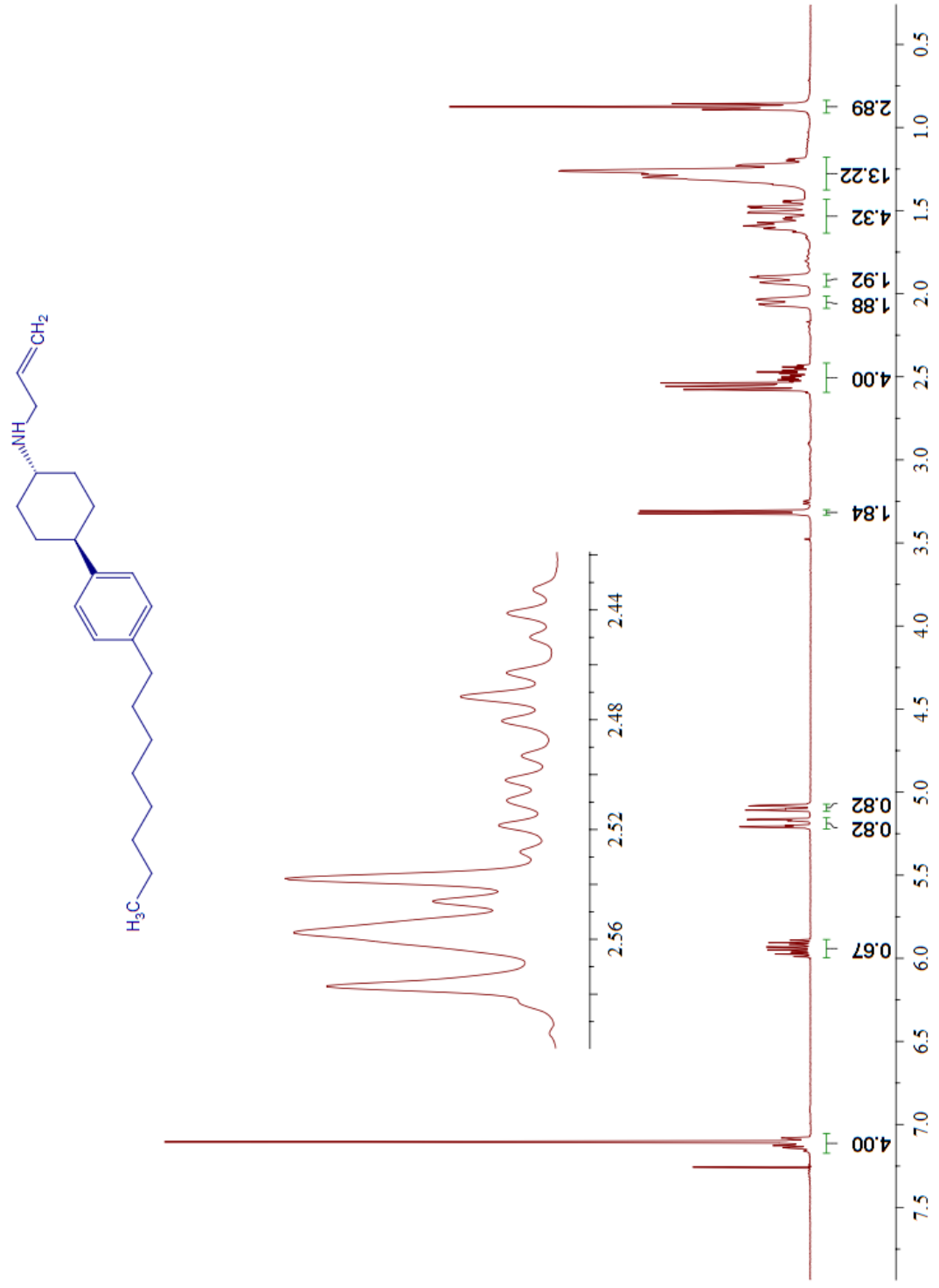

^{13}C NMR spectrum of *trans*-**10h**

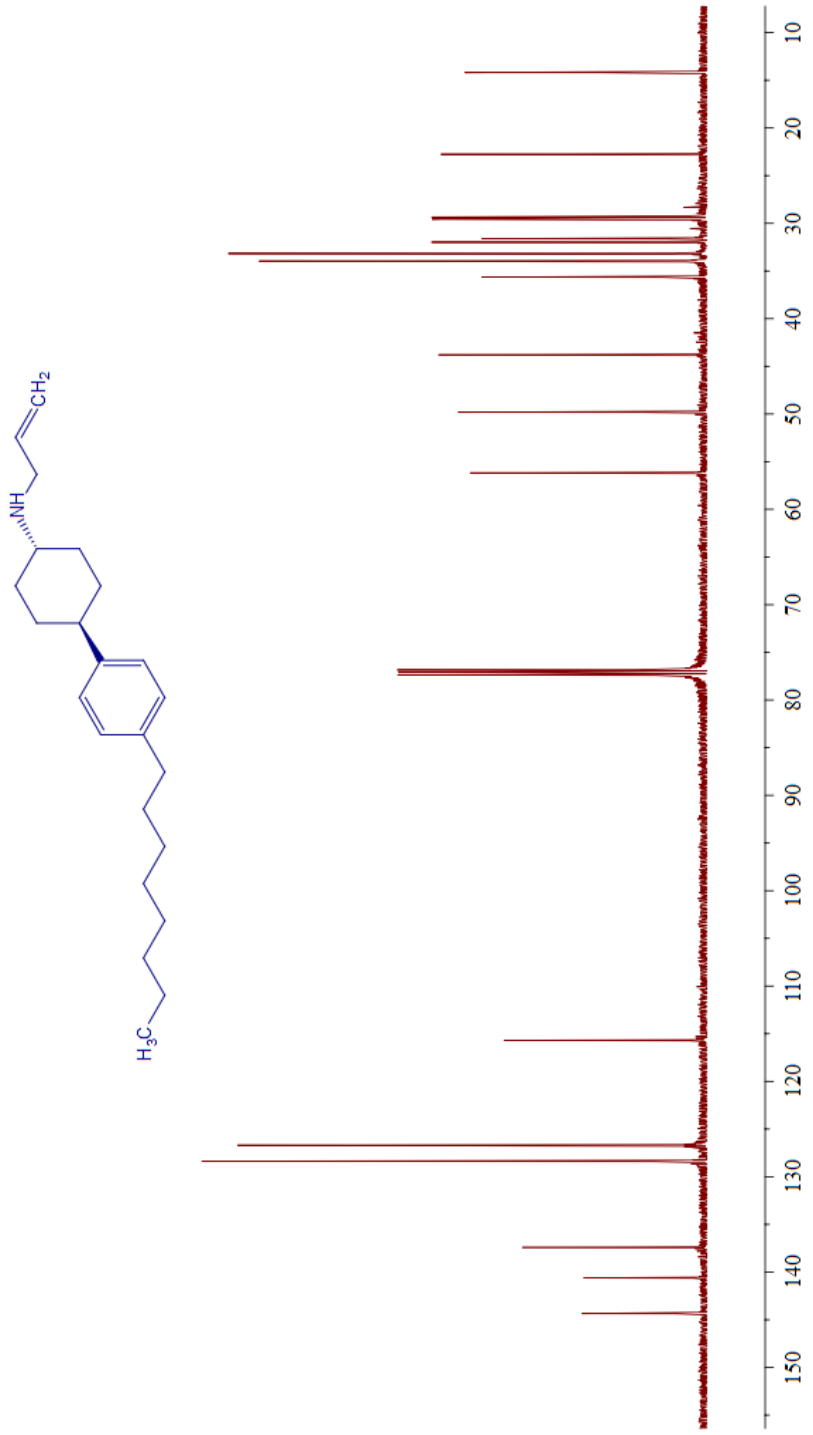

^{1}H NMR spectrum of *cis*-**10i**

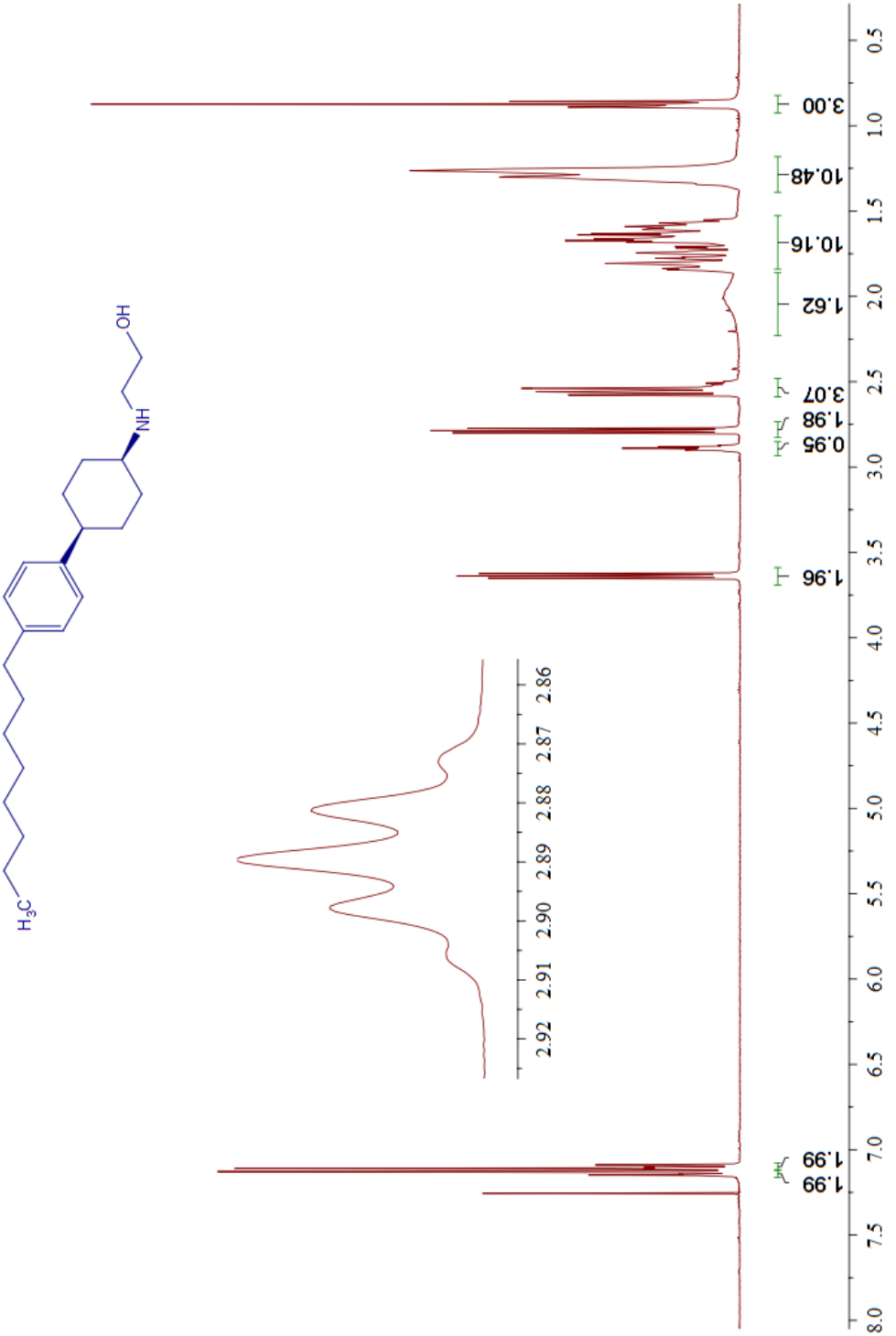

^{13}C NMR spectrum of *cis*-**10i**

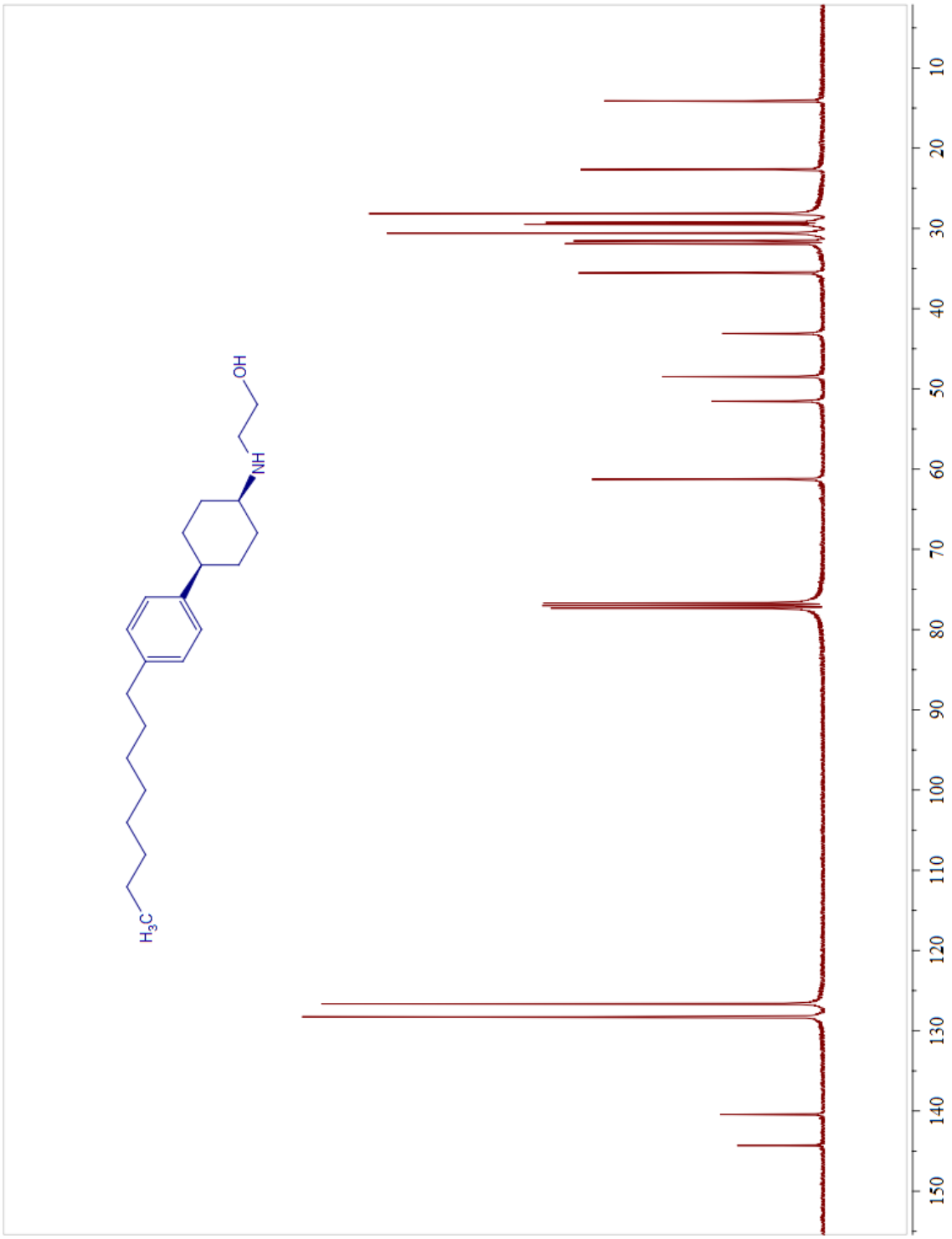

^{1}H NMR spectrum of *trans*-**10i**

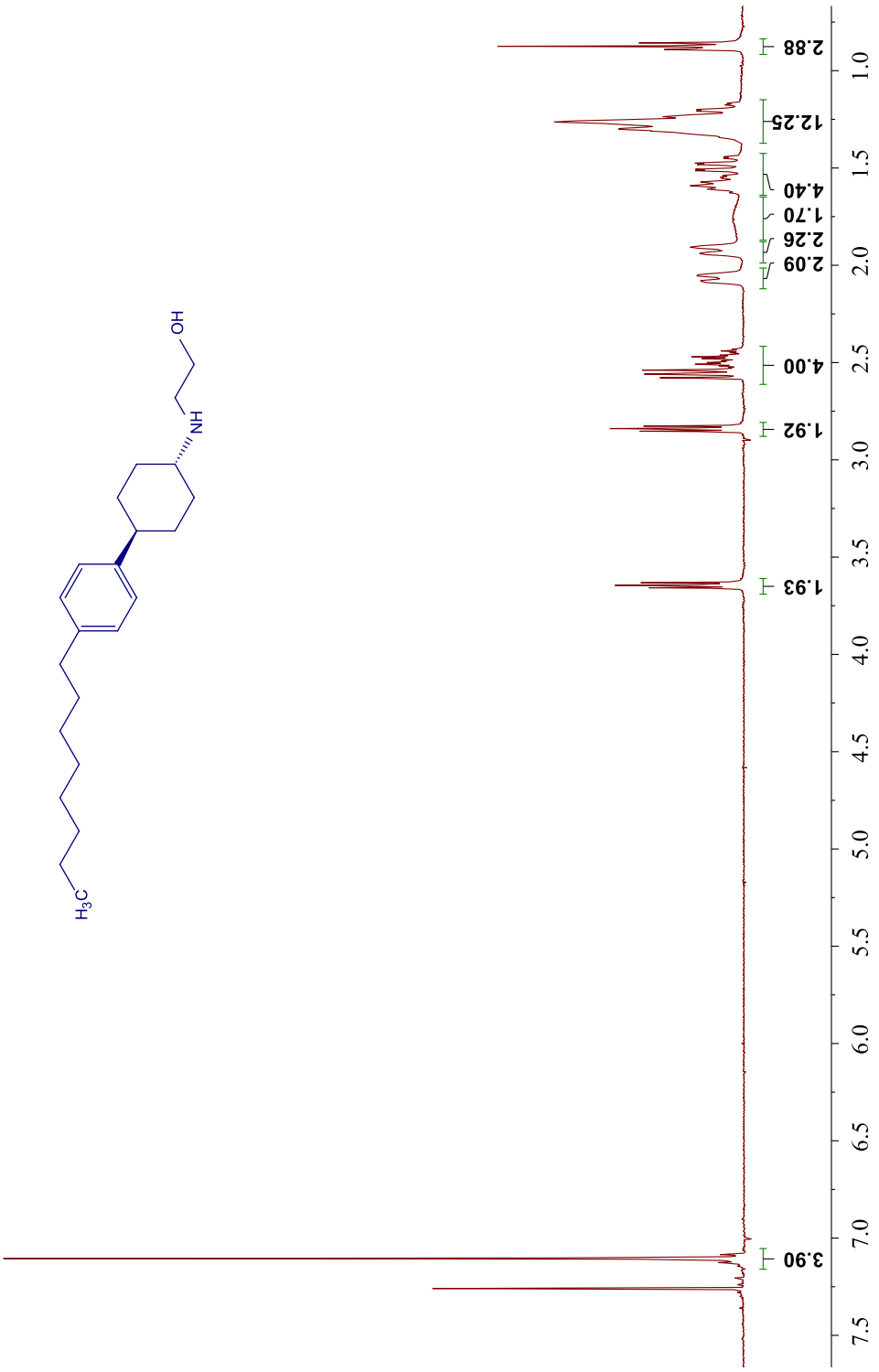

^{13}C NMR spectrum of *trans*-**10i**

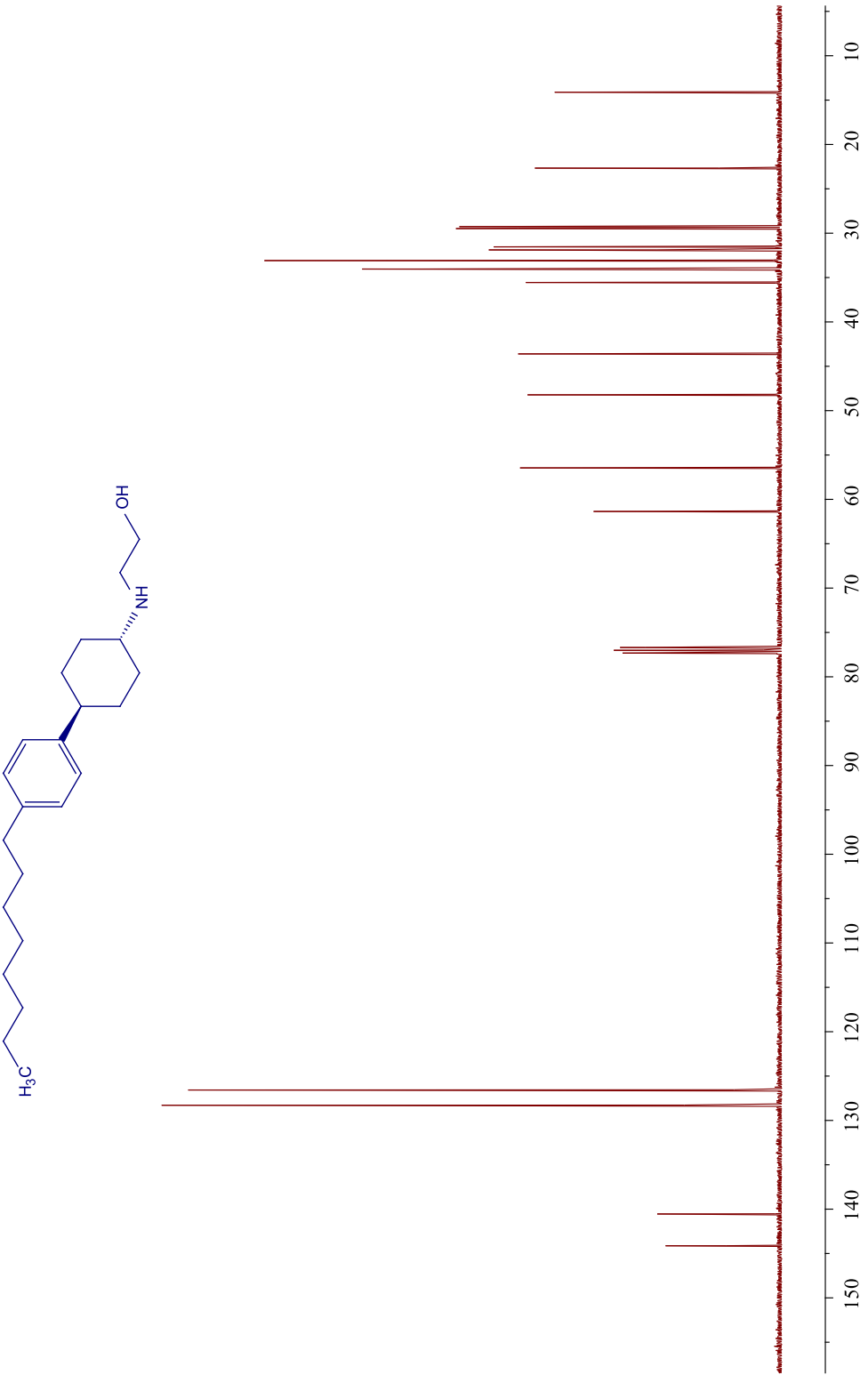

^{1}H NMR spectrum of *trans*-**10j**

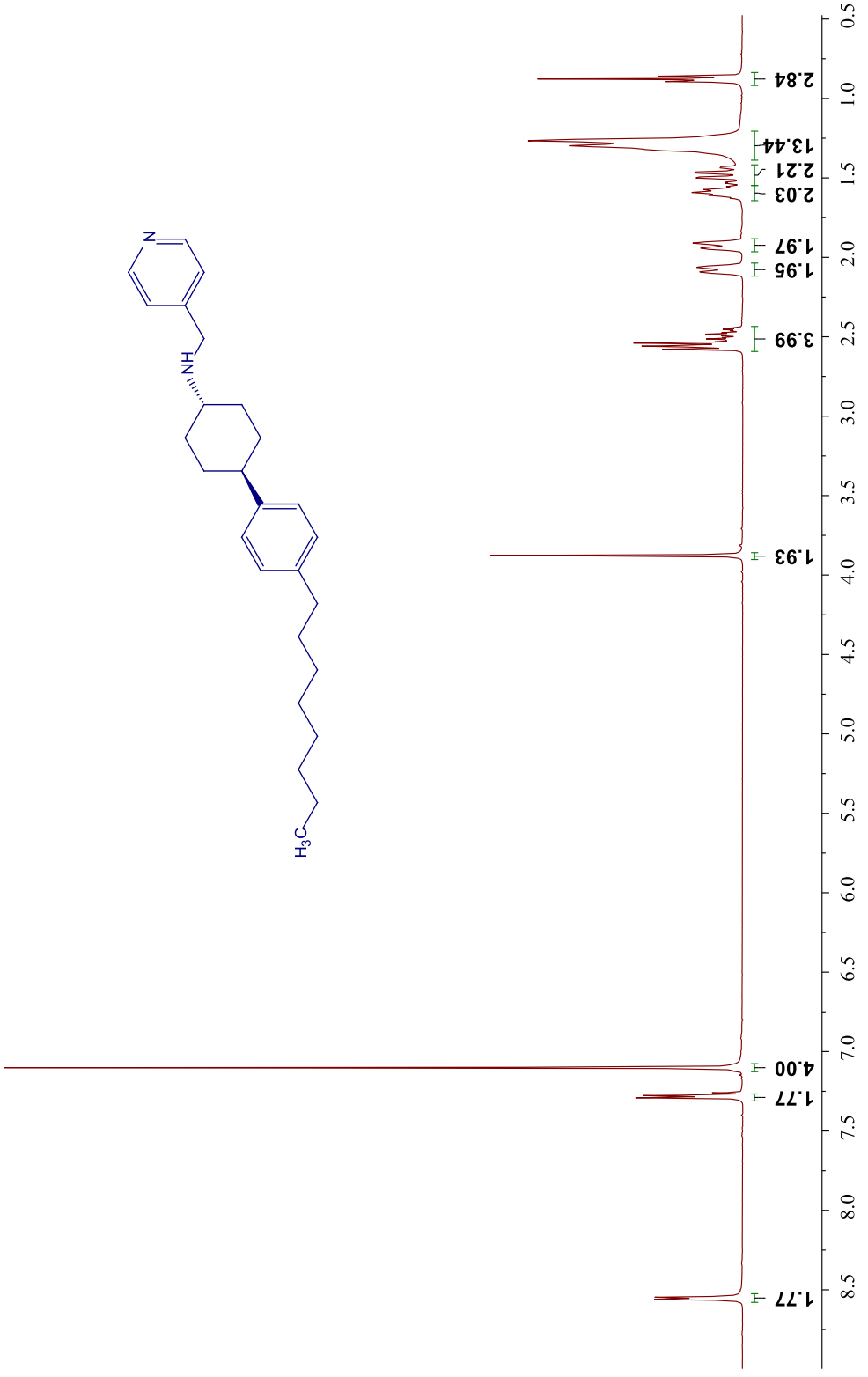

^{13}C NMR spectrum of *trans*-**10j**

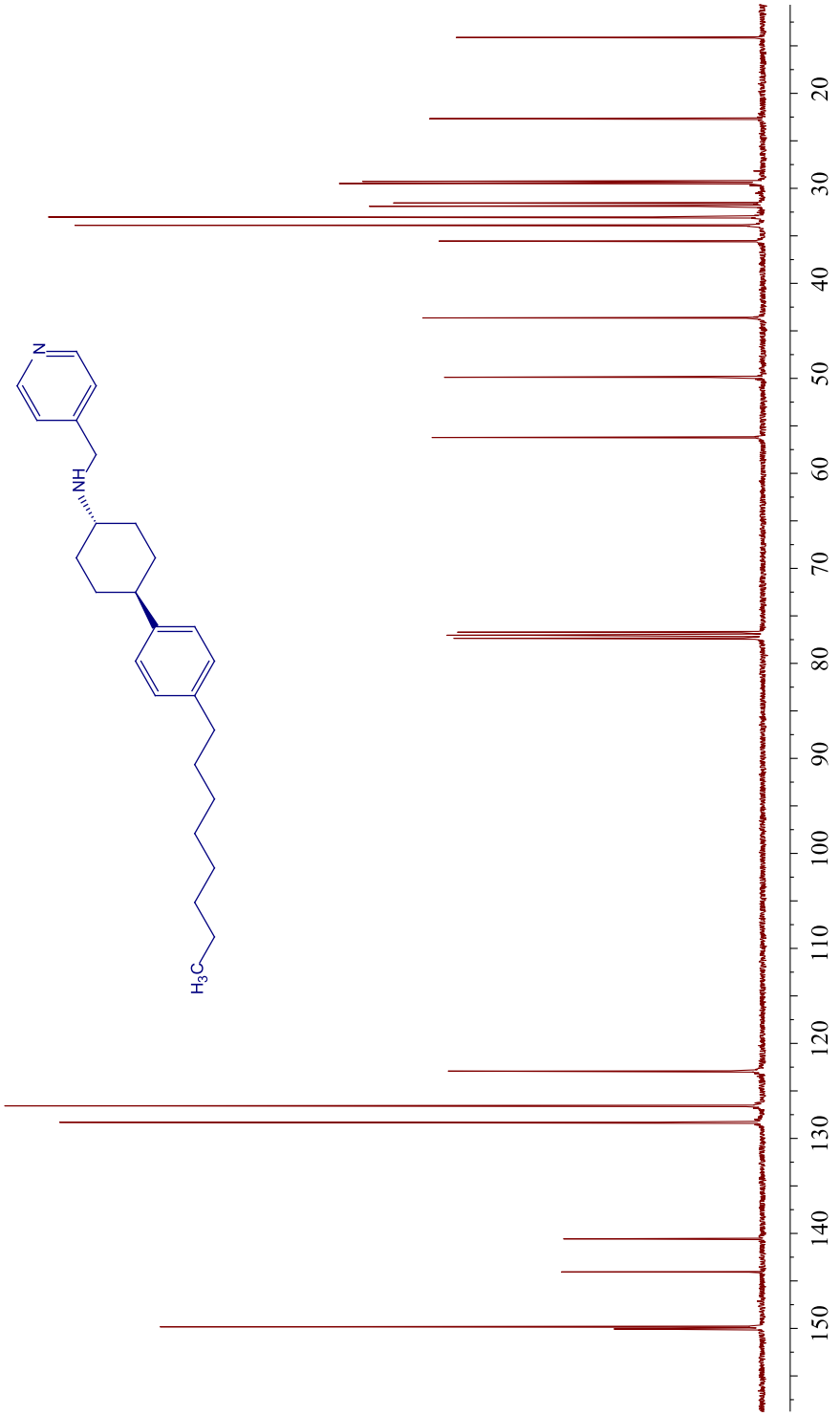

[1]H NMR spectrum of *trans*-**10k**

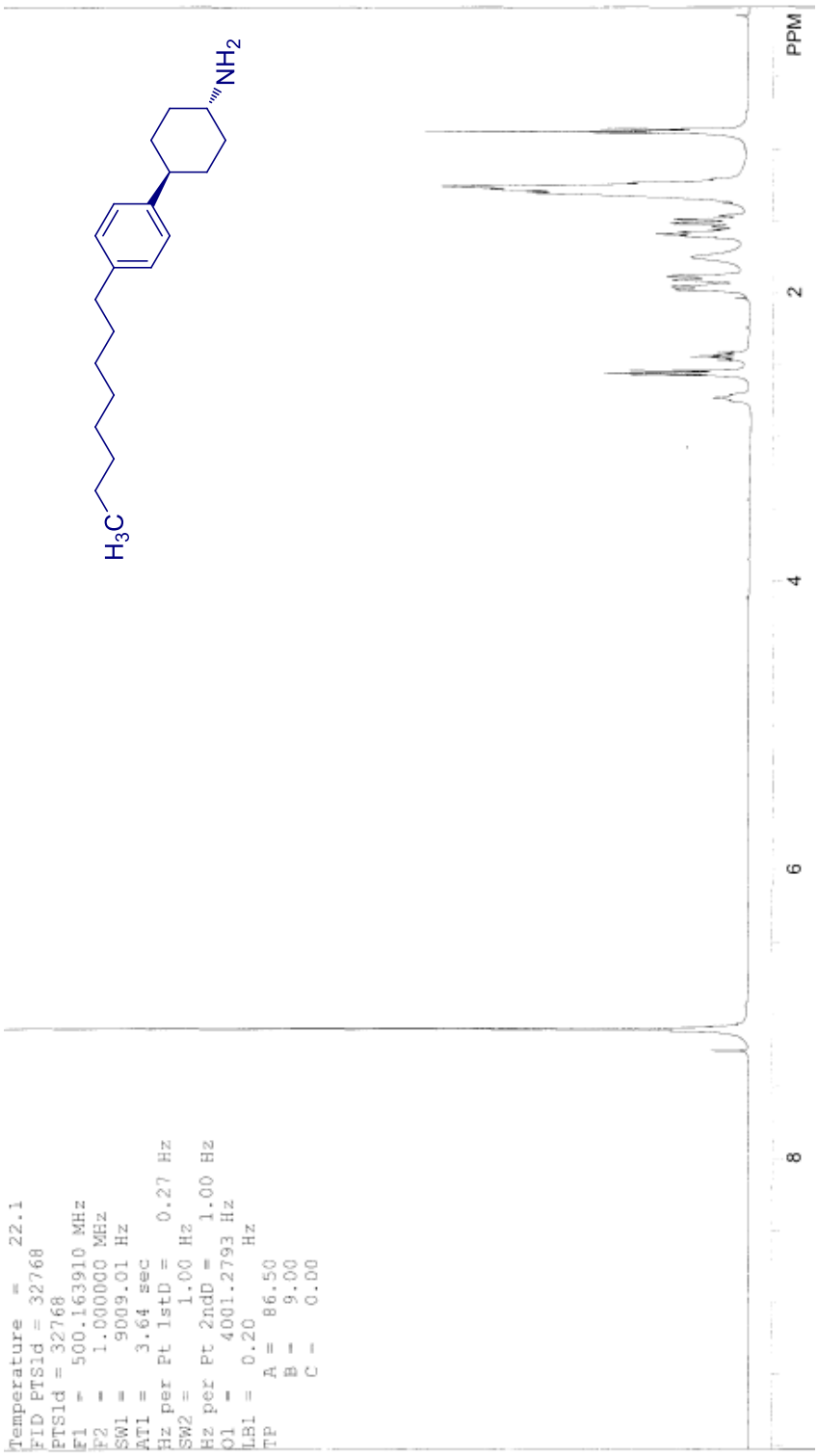

^{13}C NMR spectrum of *trans*-**10k**

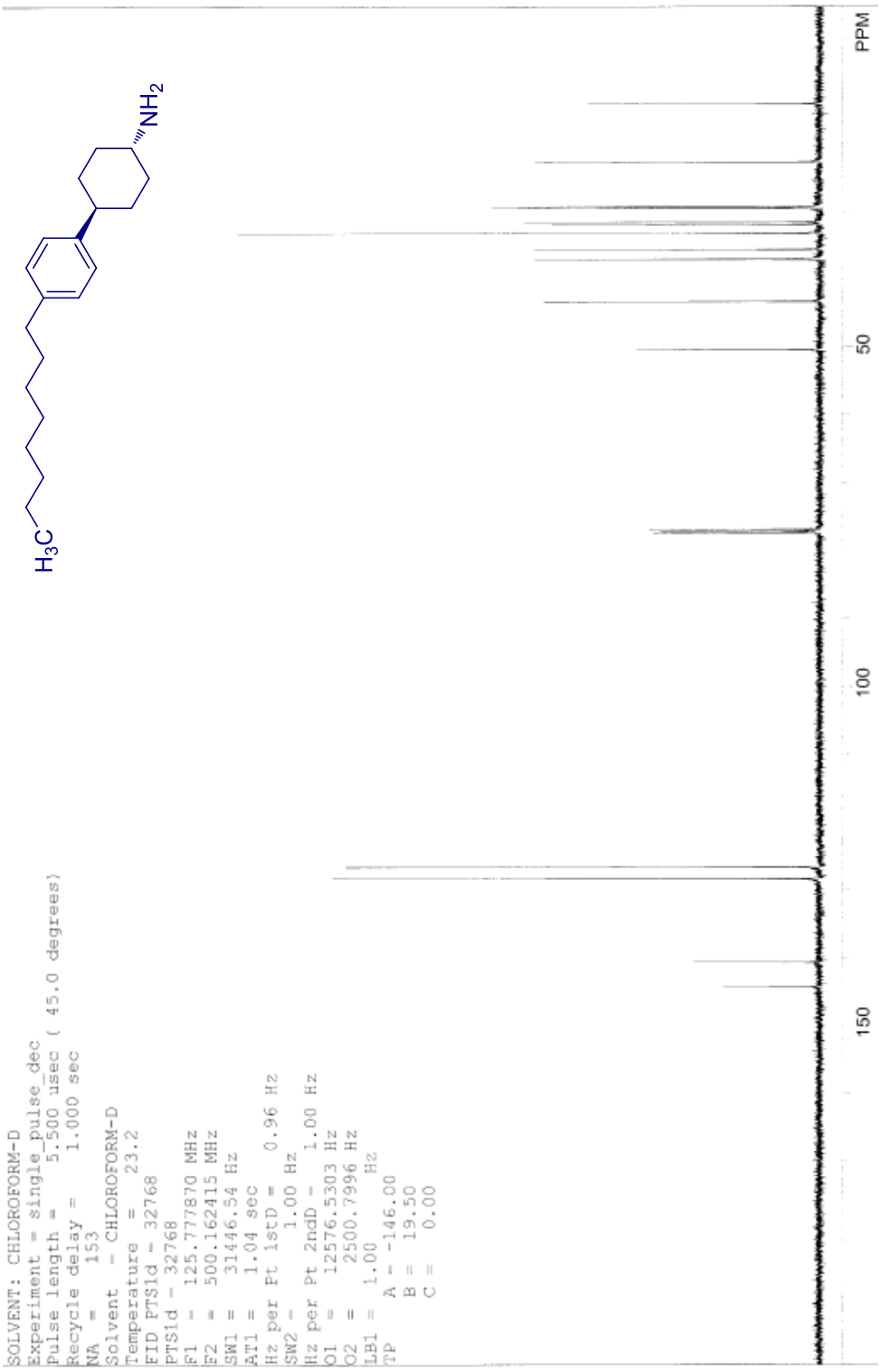

^{1}H NMR spectrum of *cis*-**11a**

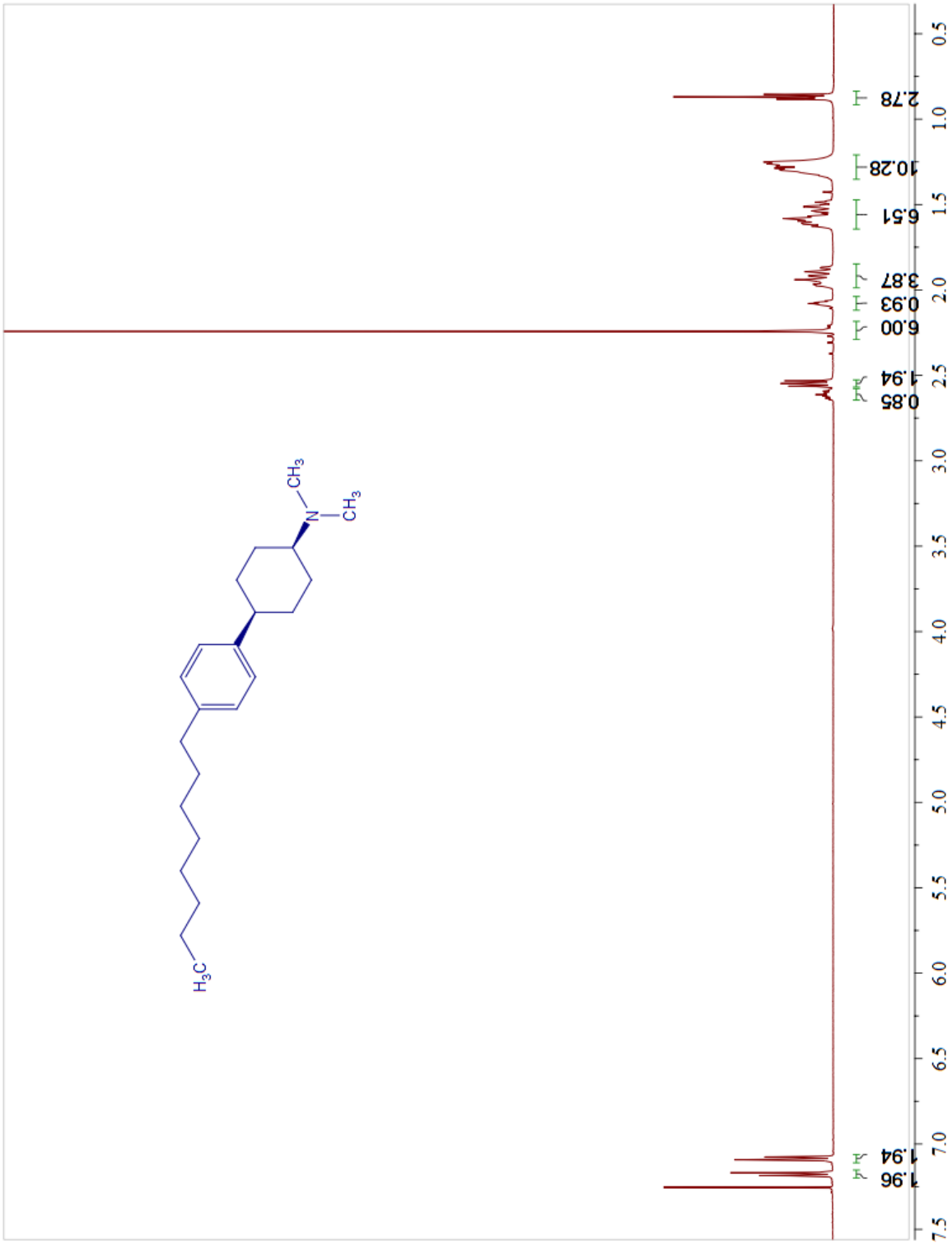

^{13}C NMR spectrum of *cis*-**11a**

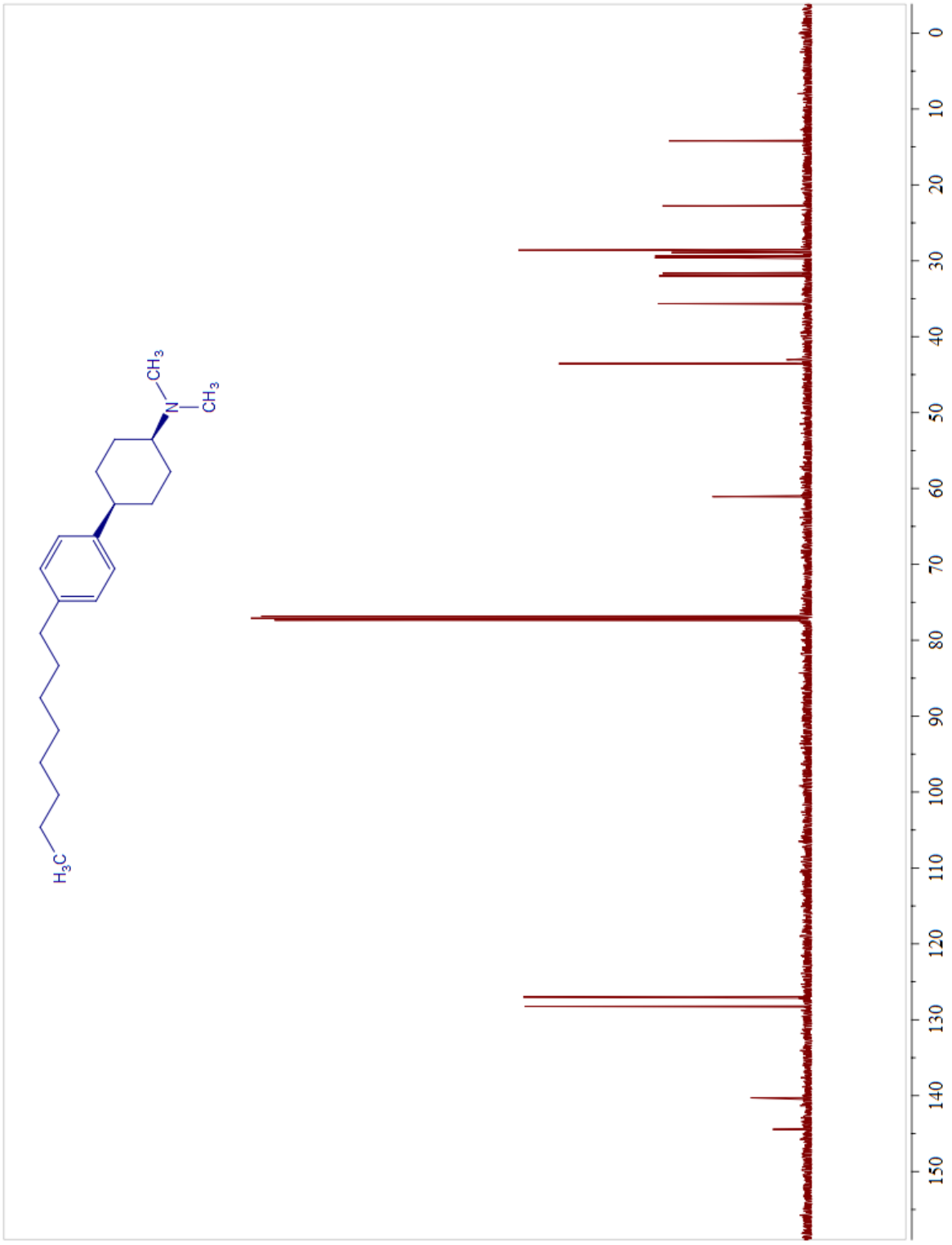

[1]H NMR spectrum of *trans*-**11a**

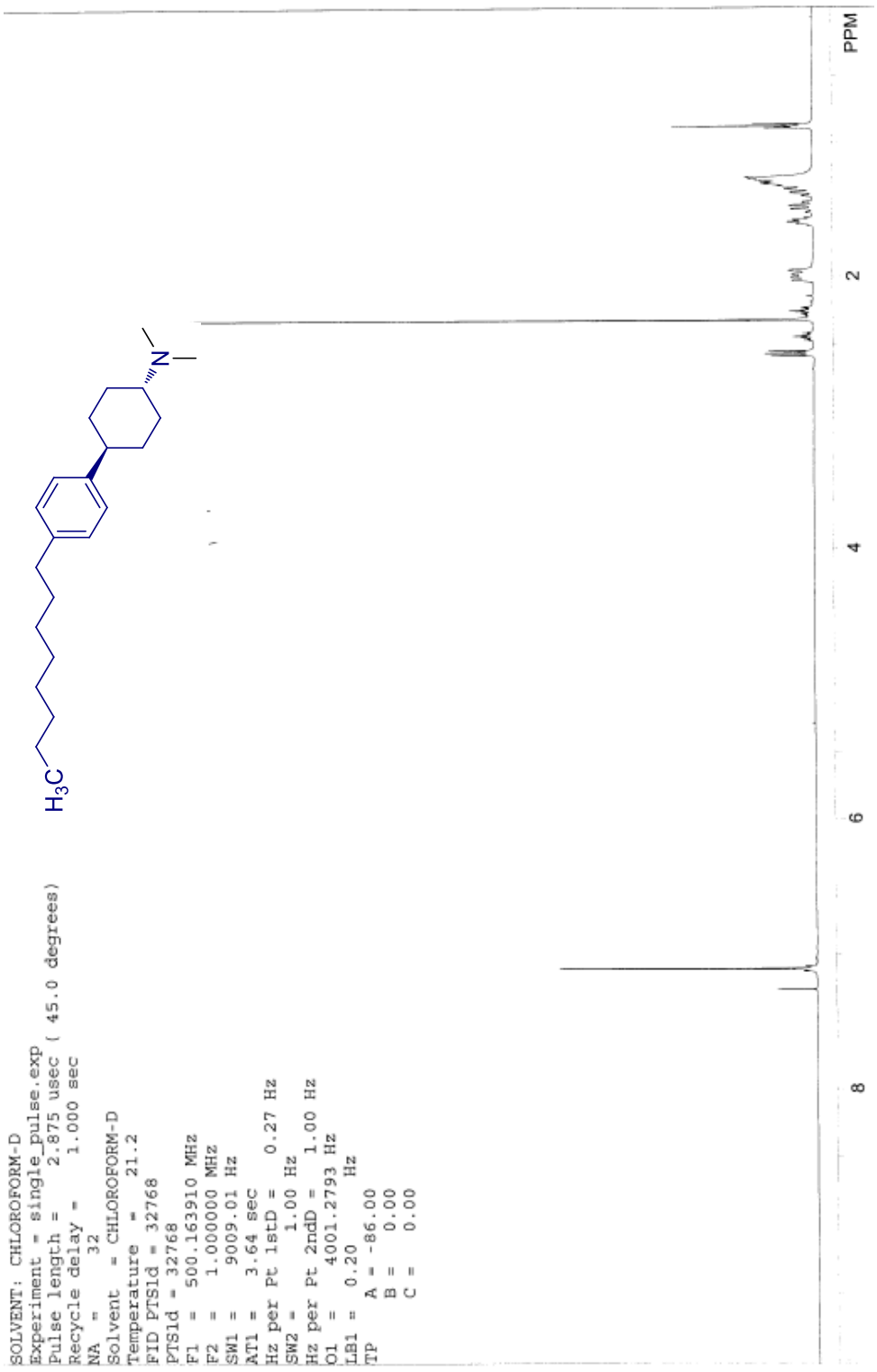

^{13}C NMR spectrum of *trans*-**11a**

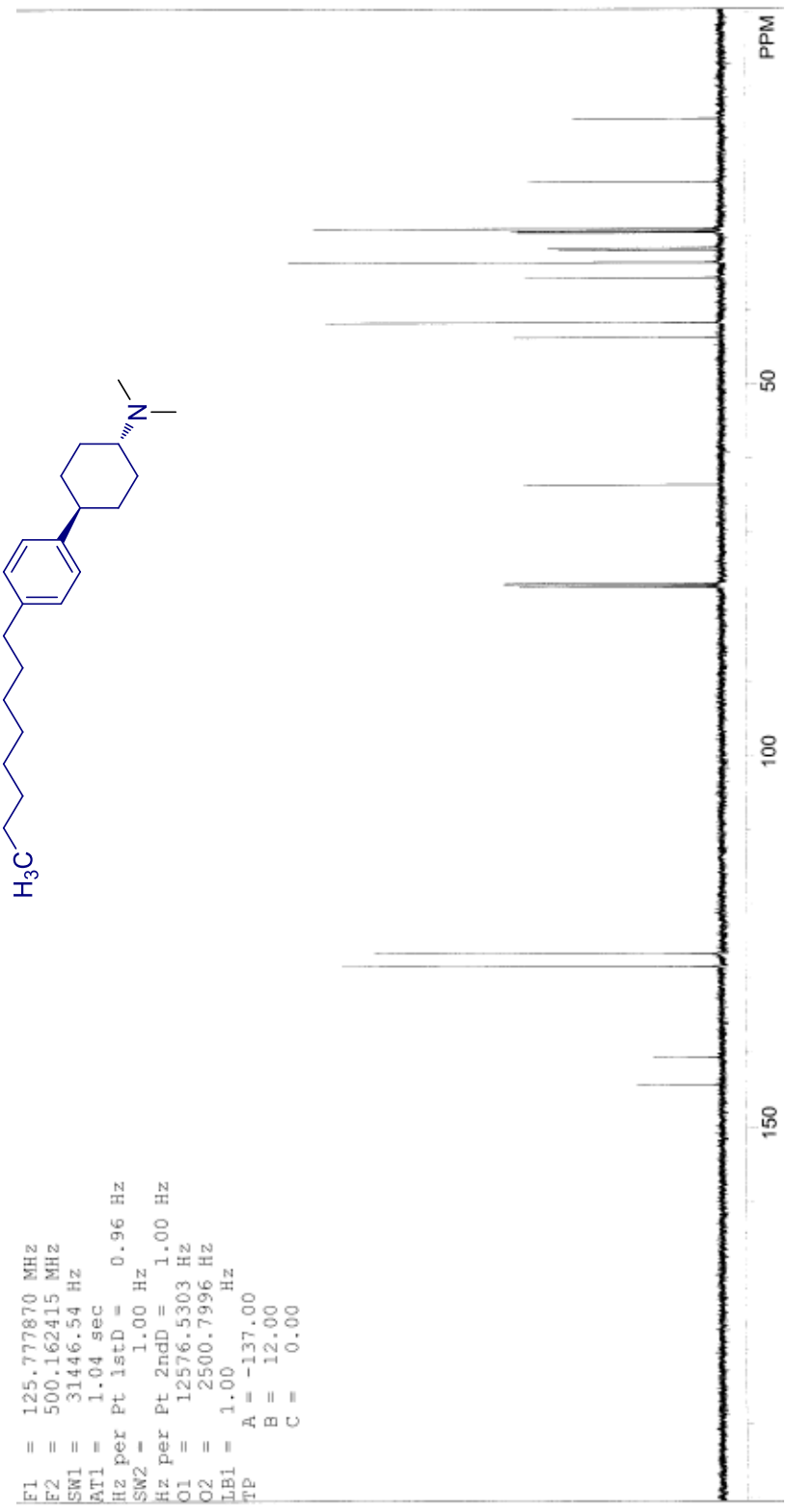

^{1}H NMR spectrum of *cis*-**11b**

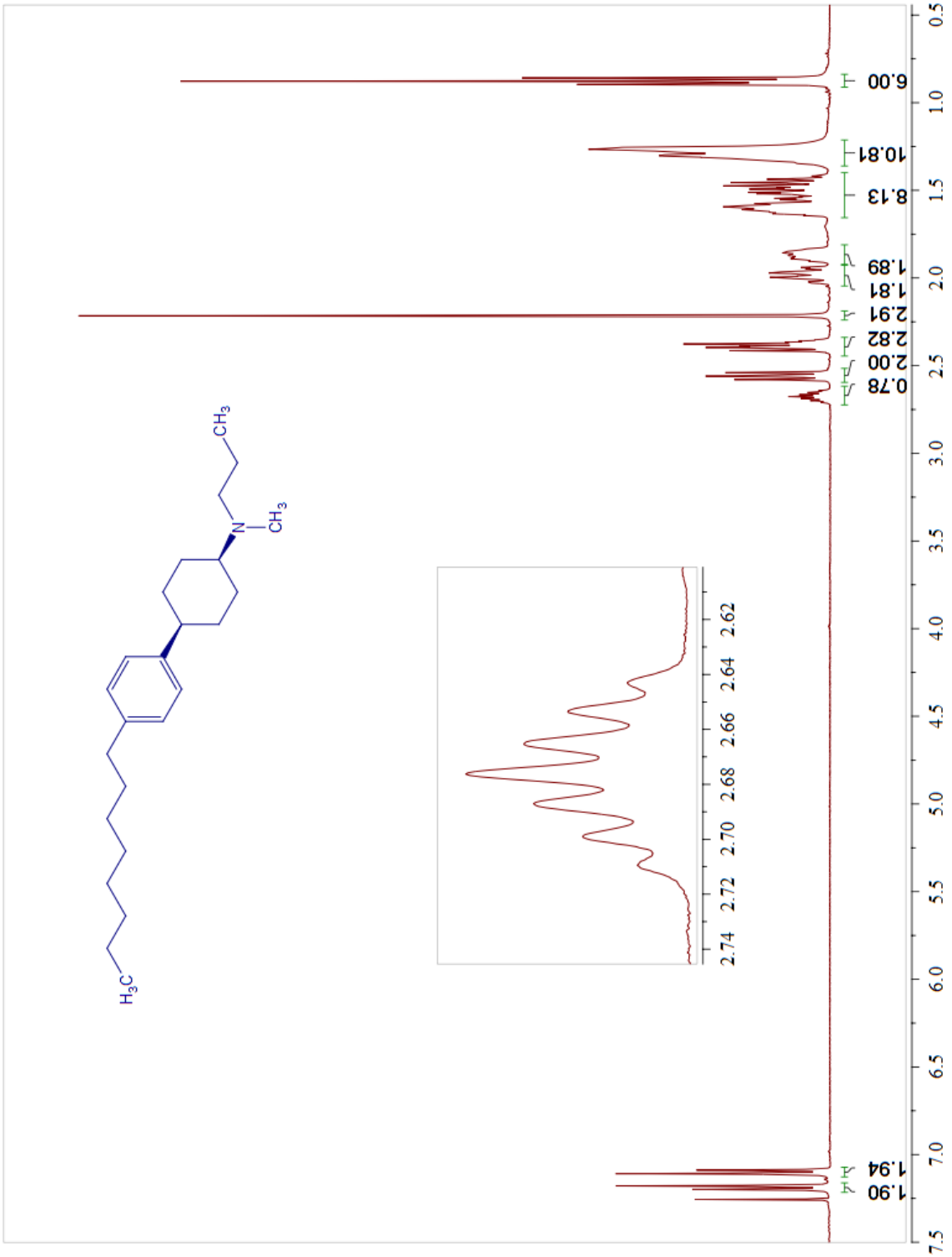

^{13}C NMR spectrum of *cis*-**11b**

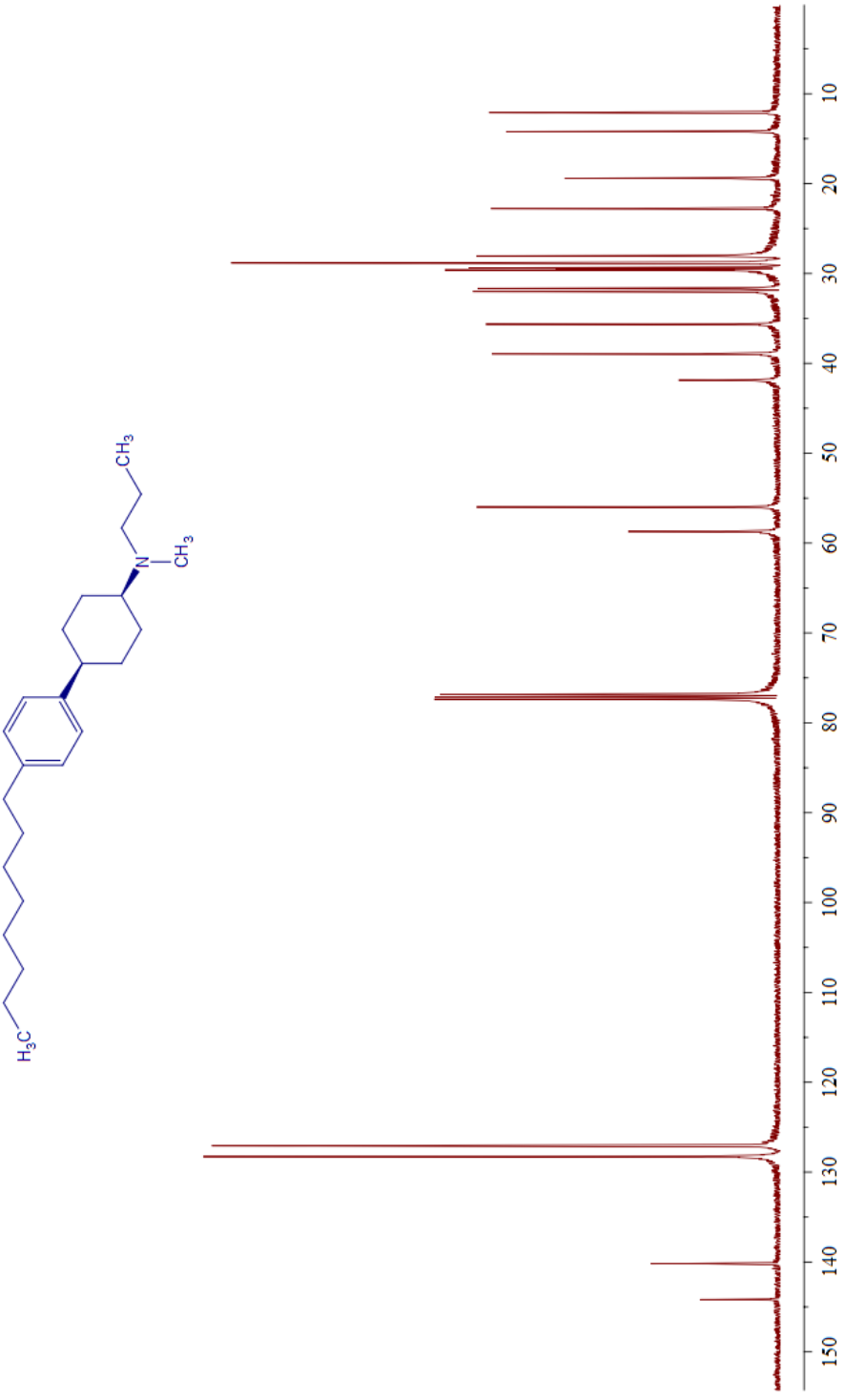

[1]H NMR spectrum of *trans*-**11b**

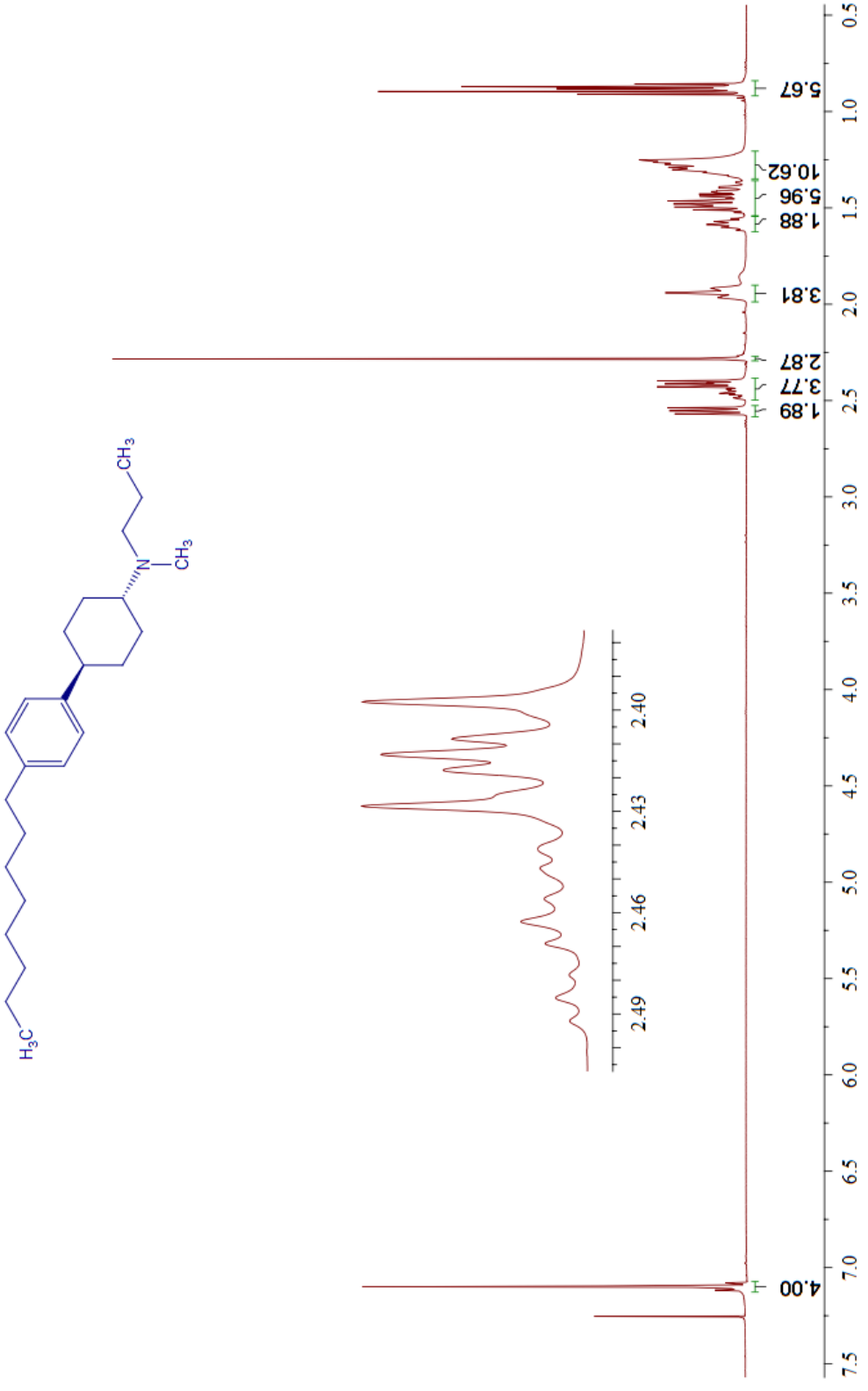

^{13}C NMR spectrum of *trans*-**11b**

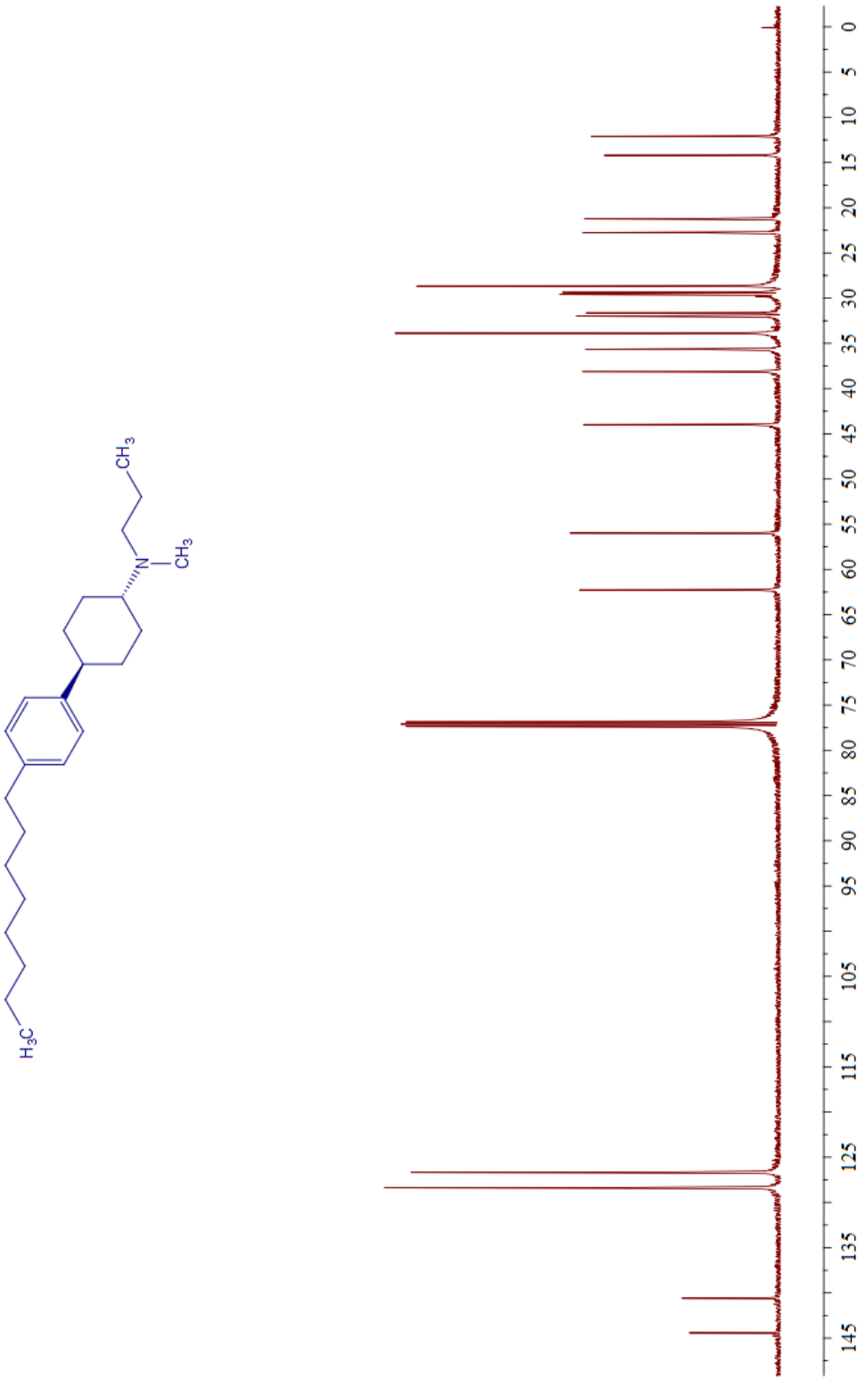

^{1}H NMR spectrum of *cis*-**11c**

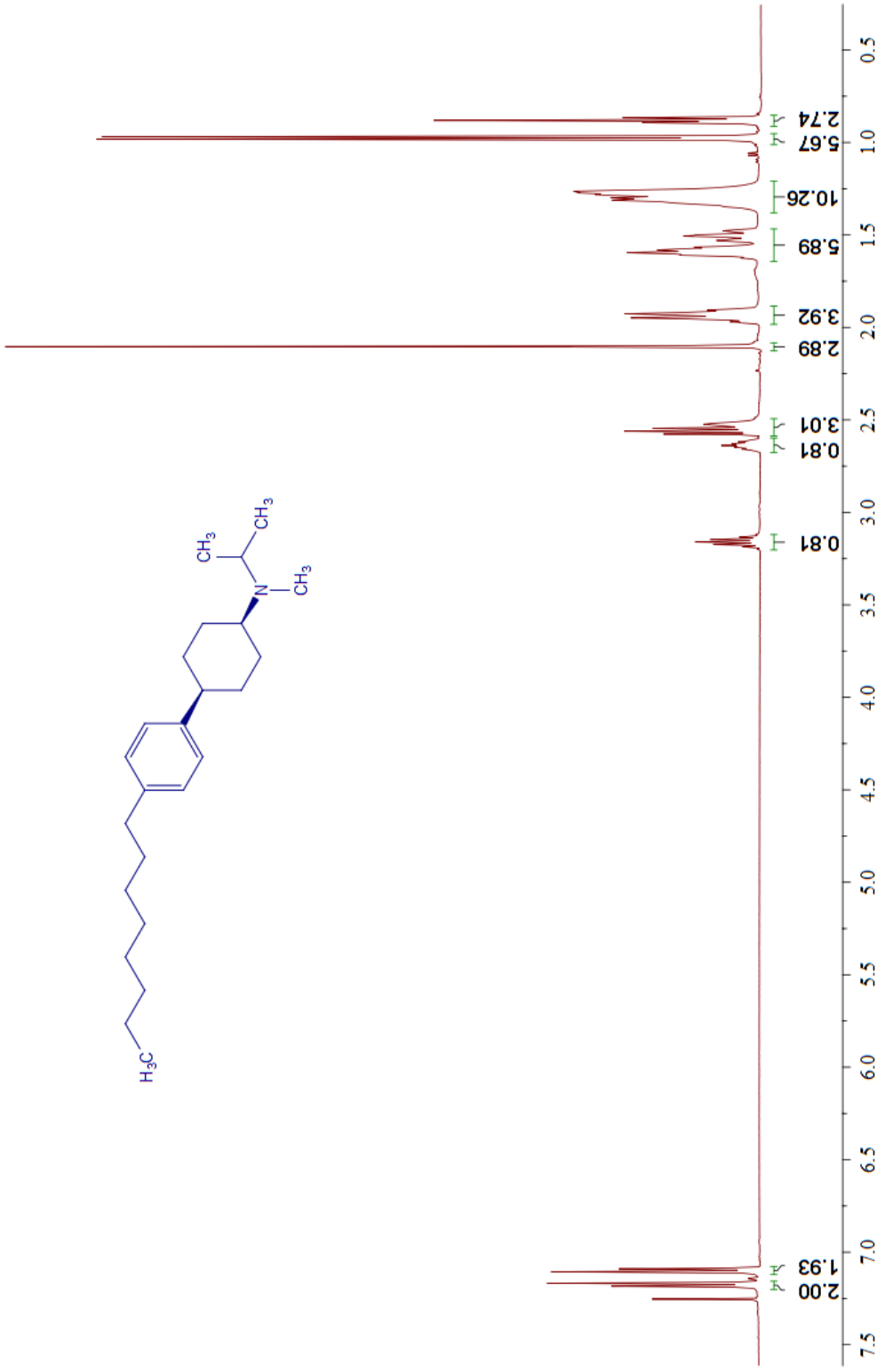

^{13}C NMR spectrum of *cis*-**11c**

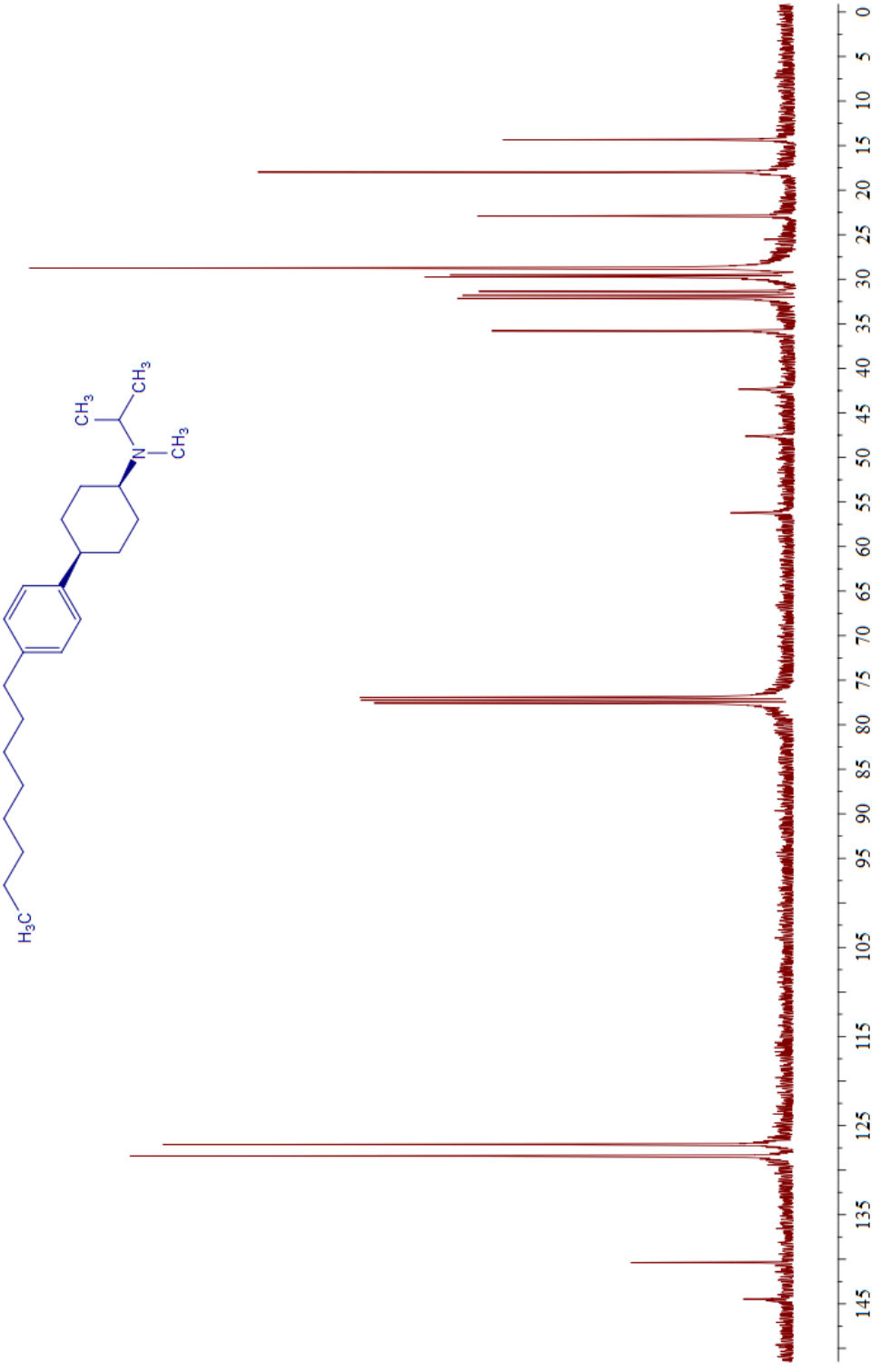

^{1}H NMR spectrum of *cis*-**12a**

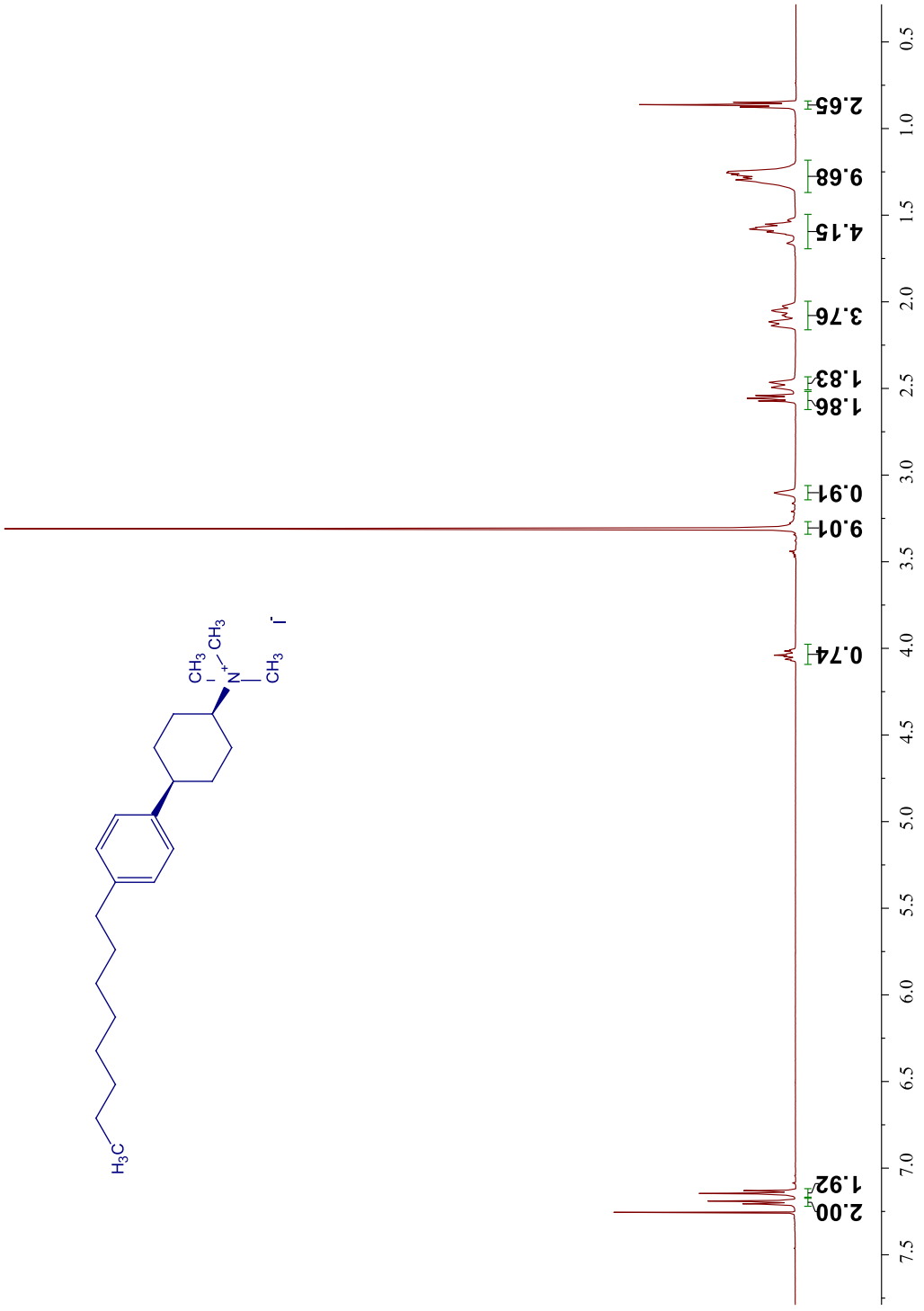

^{13}C NMR spectrum of *cis*-**12a**

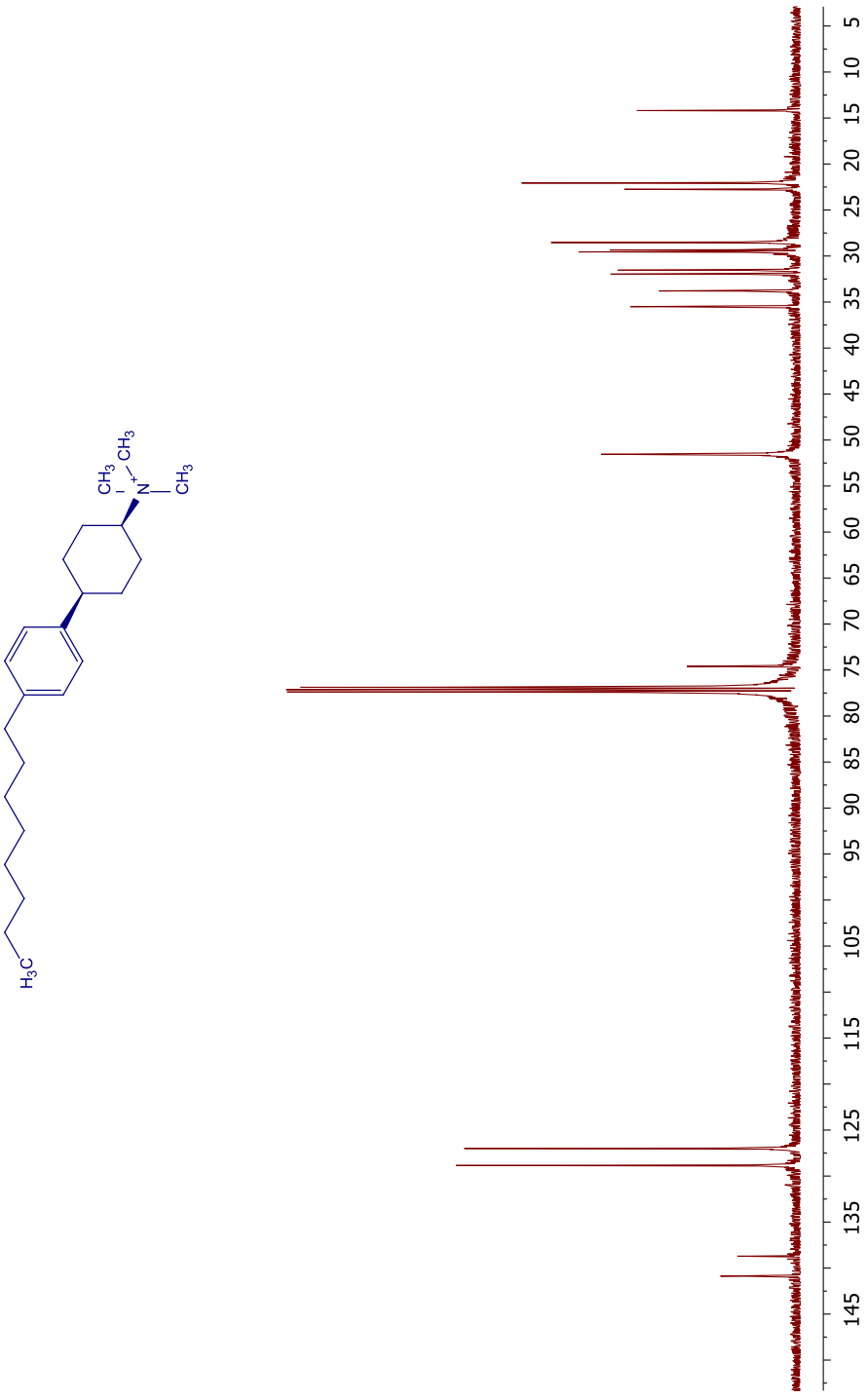

^{1}H NMR spectrum of *trans*-**12a**

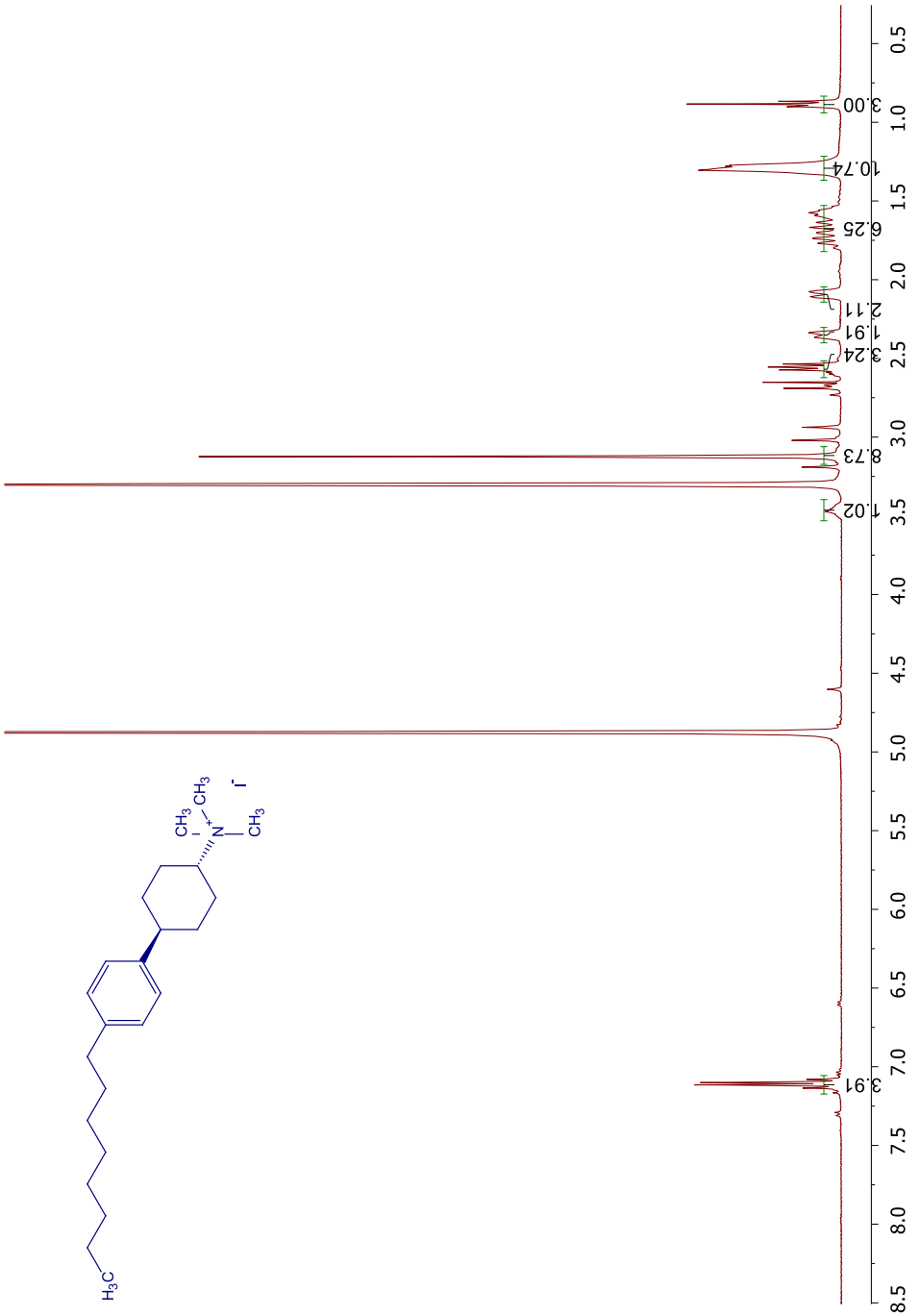

^{13}C NMR spectrum of *trans*-**12a**

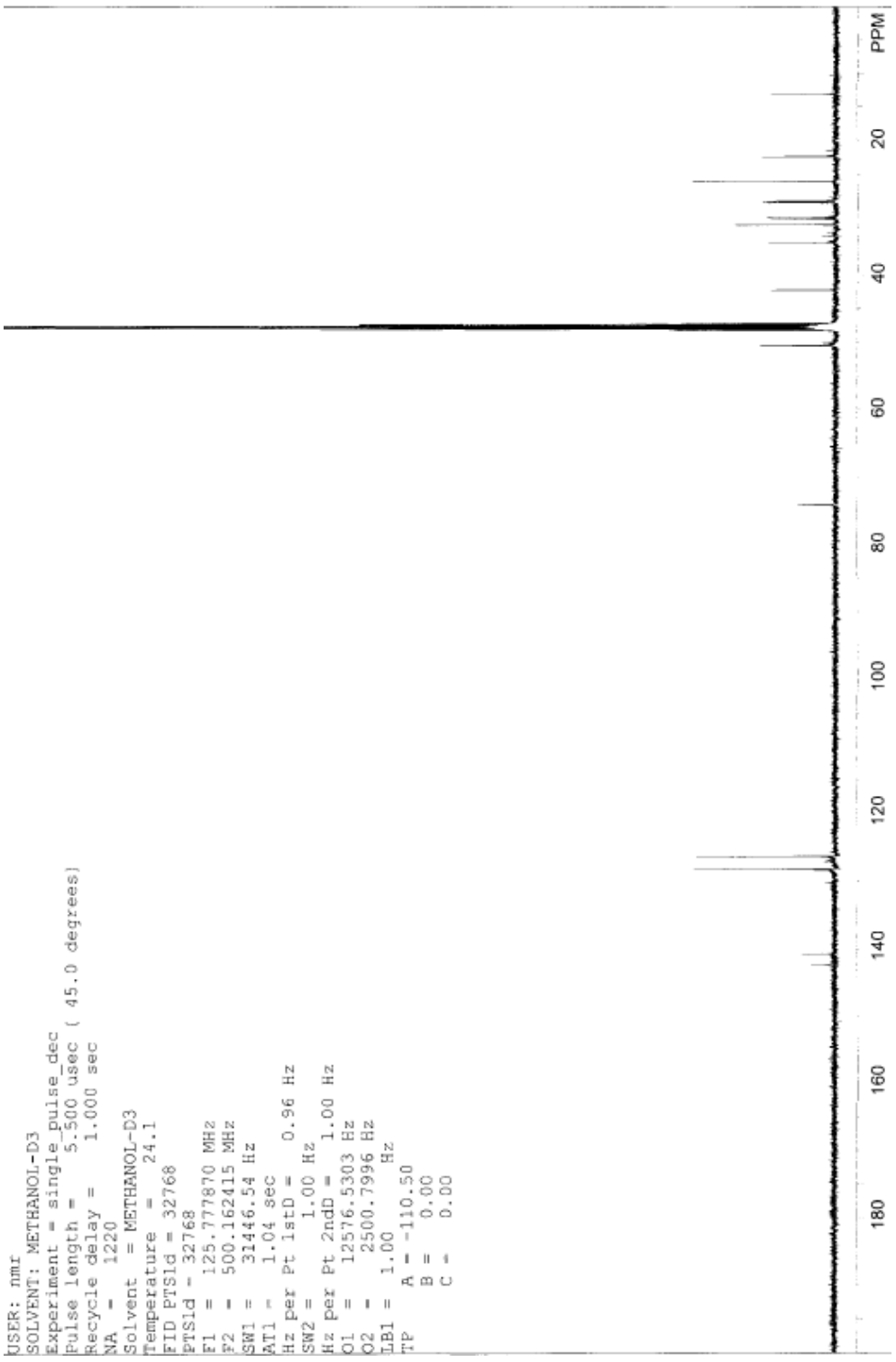

^{1}H NMR spectrum of *cis*-**12b**

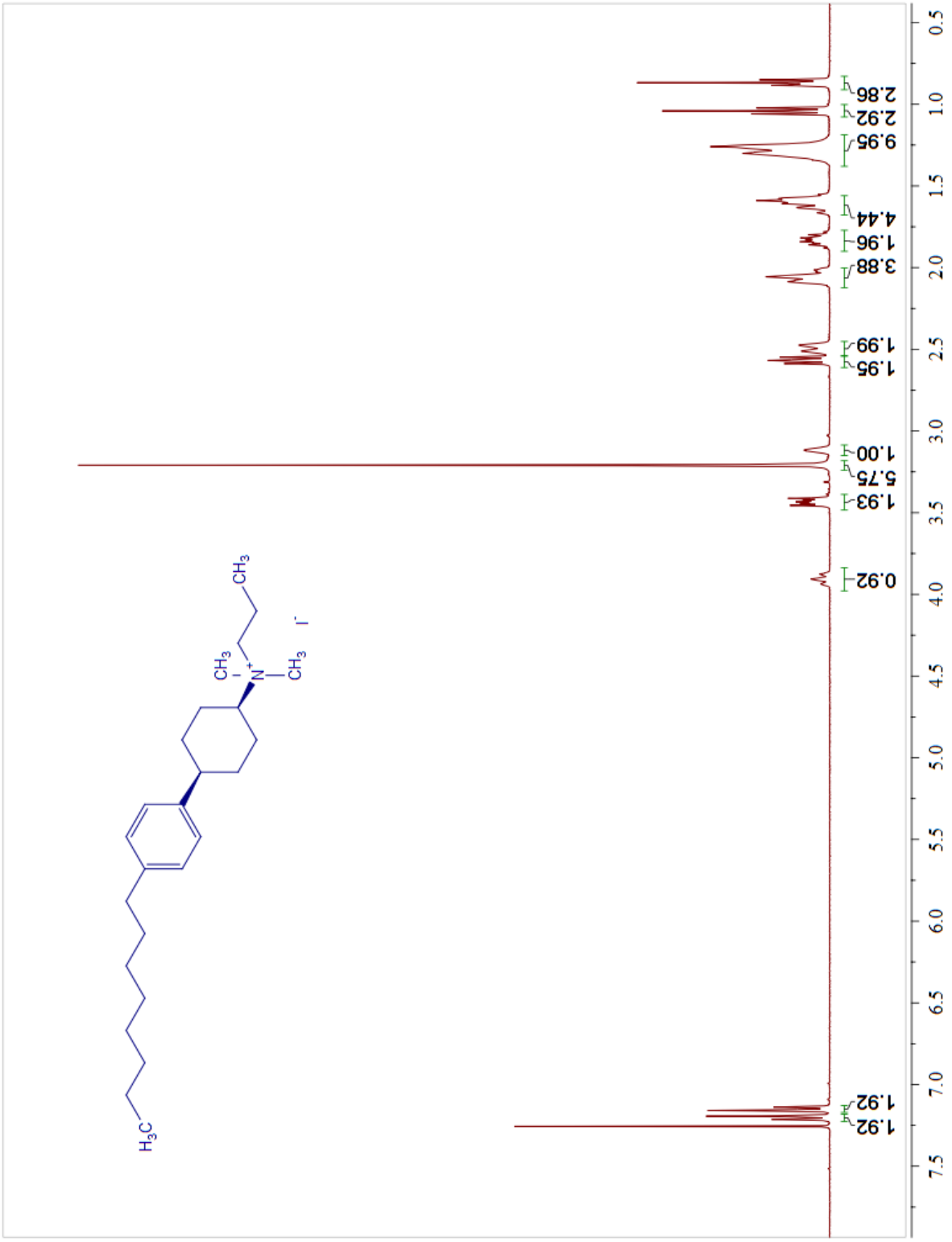

^{13}C NMR spectrum of *cis*-**12b**

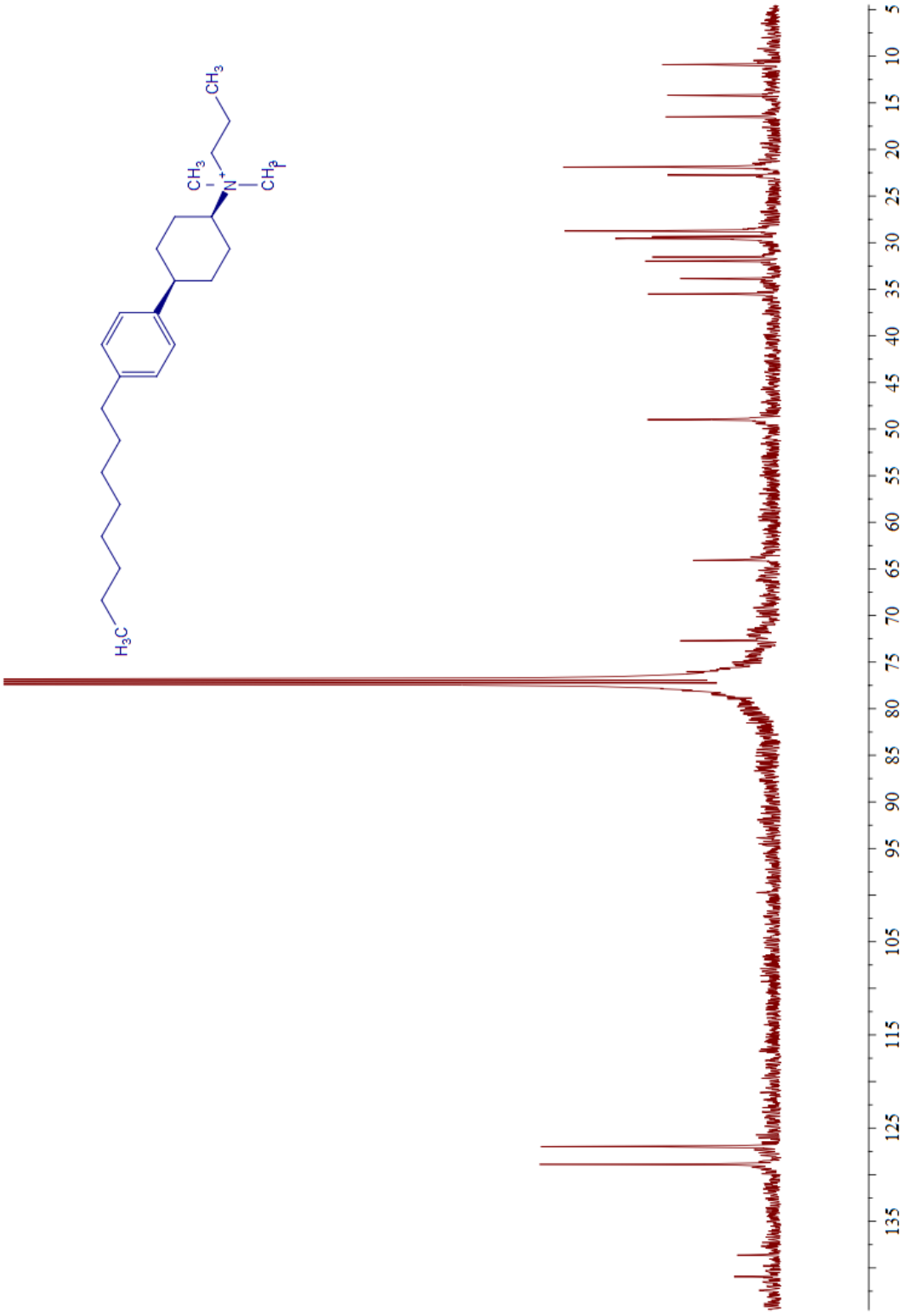

^{1}H NMR spectrum of *trans*-**12b**

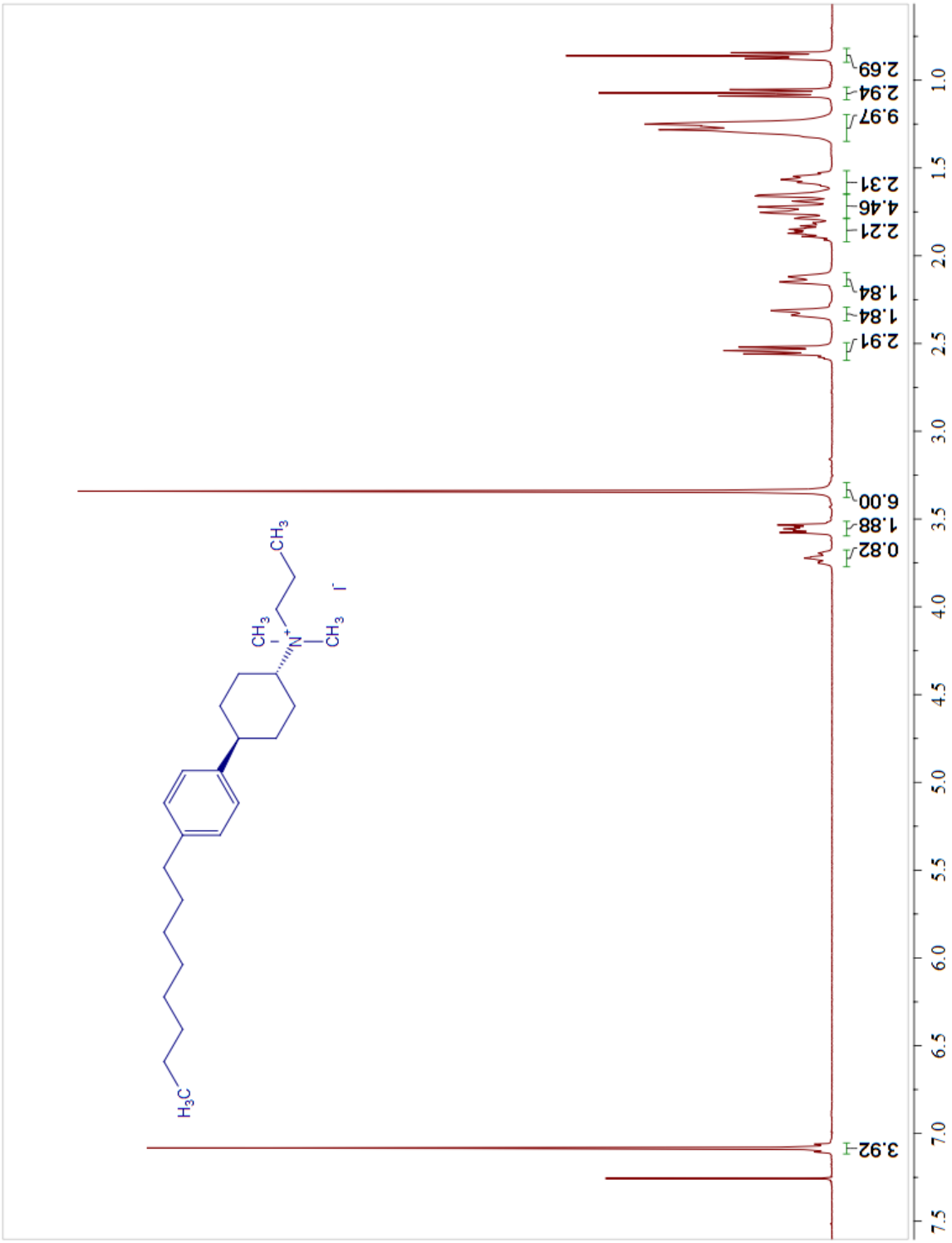

^{13}C NMR spectrum of *trans*-**12b**

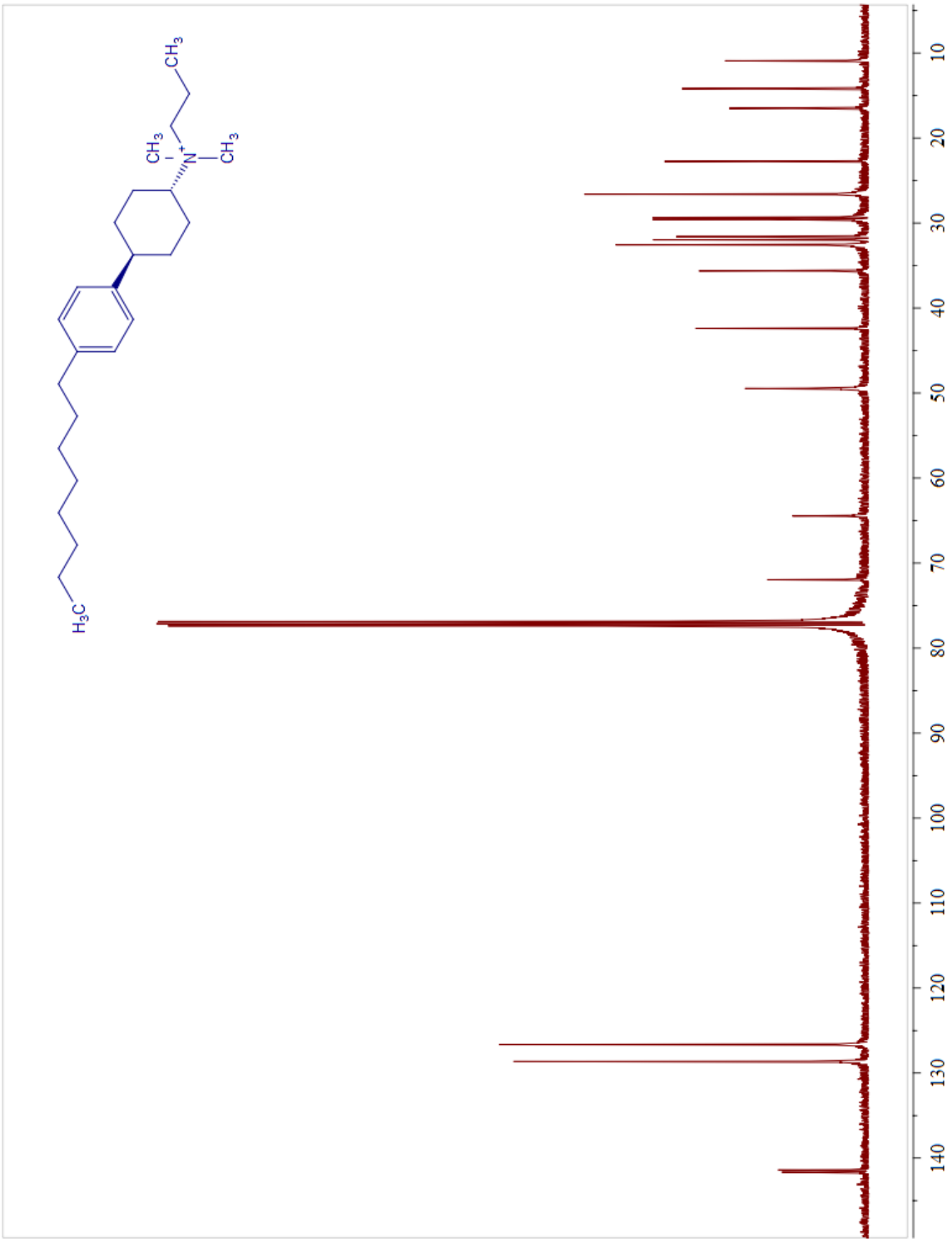

^{1}H NMR spectrum of *cis*-**12c**

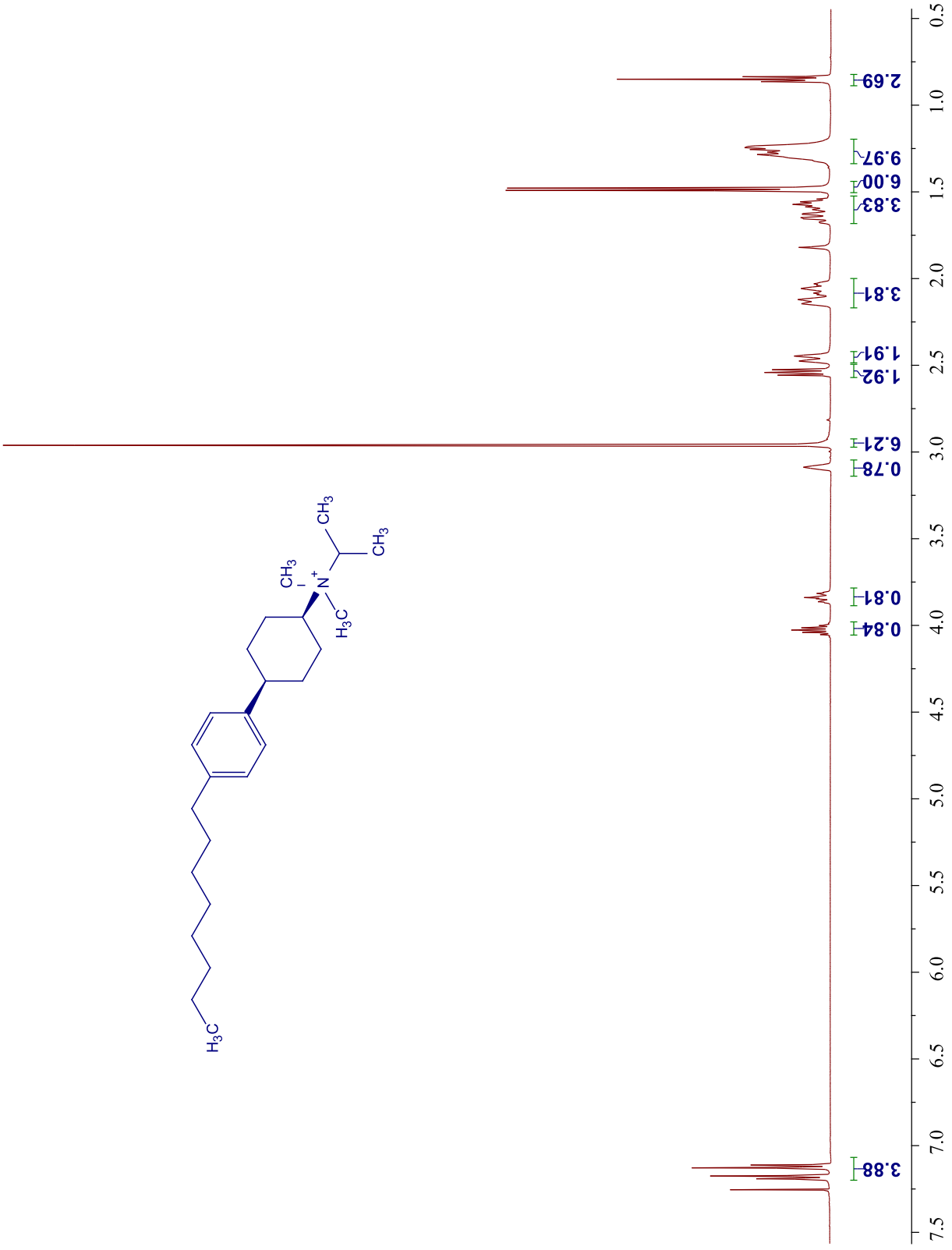

^{13}C NMR spectrum of *cis*-**12c**

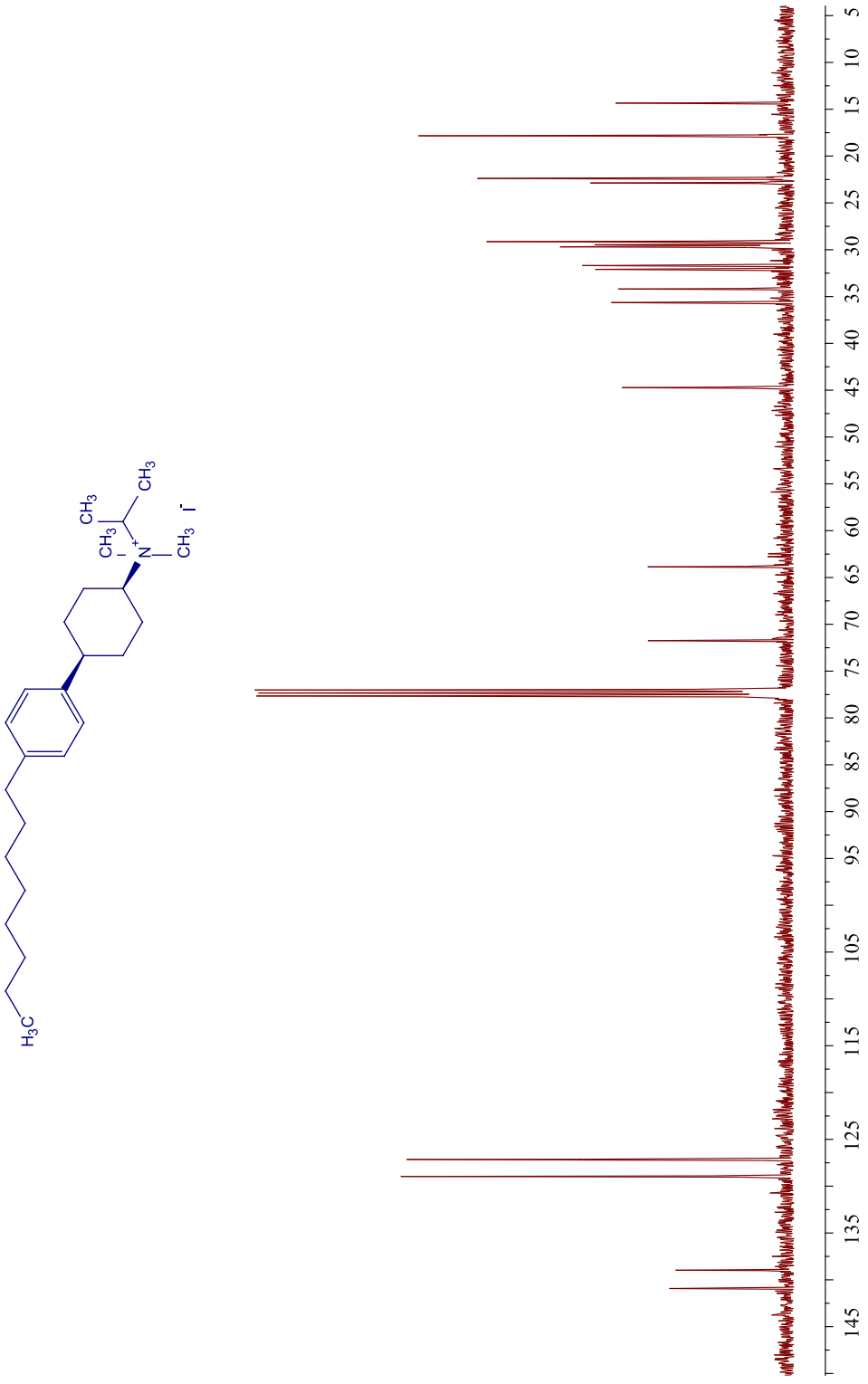

[1]H NMR spectrum of *trans*-**12c**

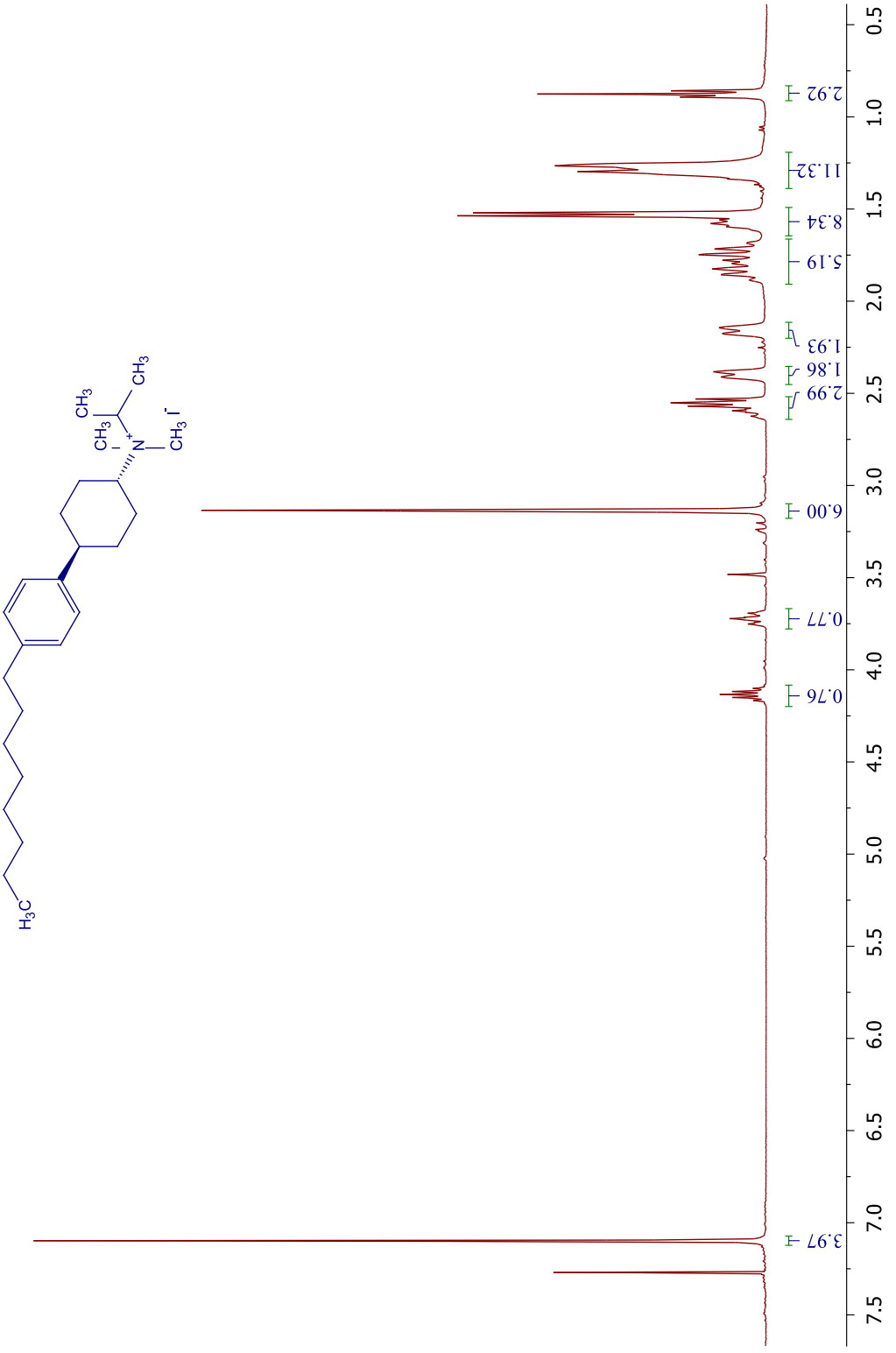

^{13}C NMR spectrum of *trans*-**12c**

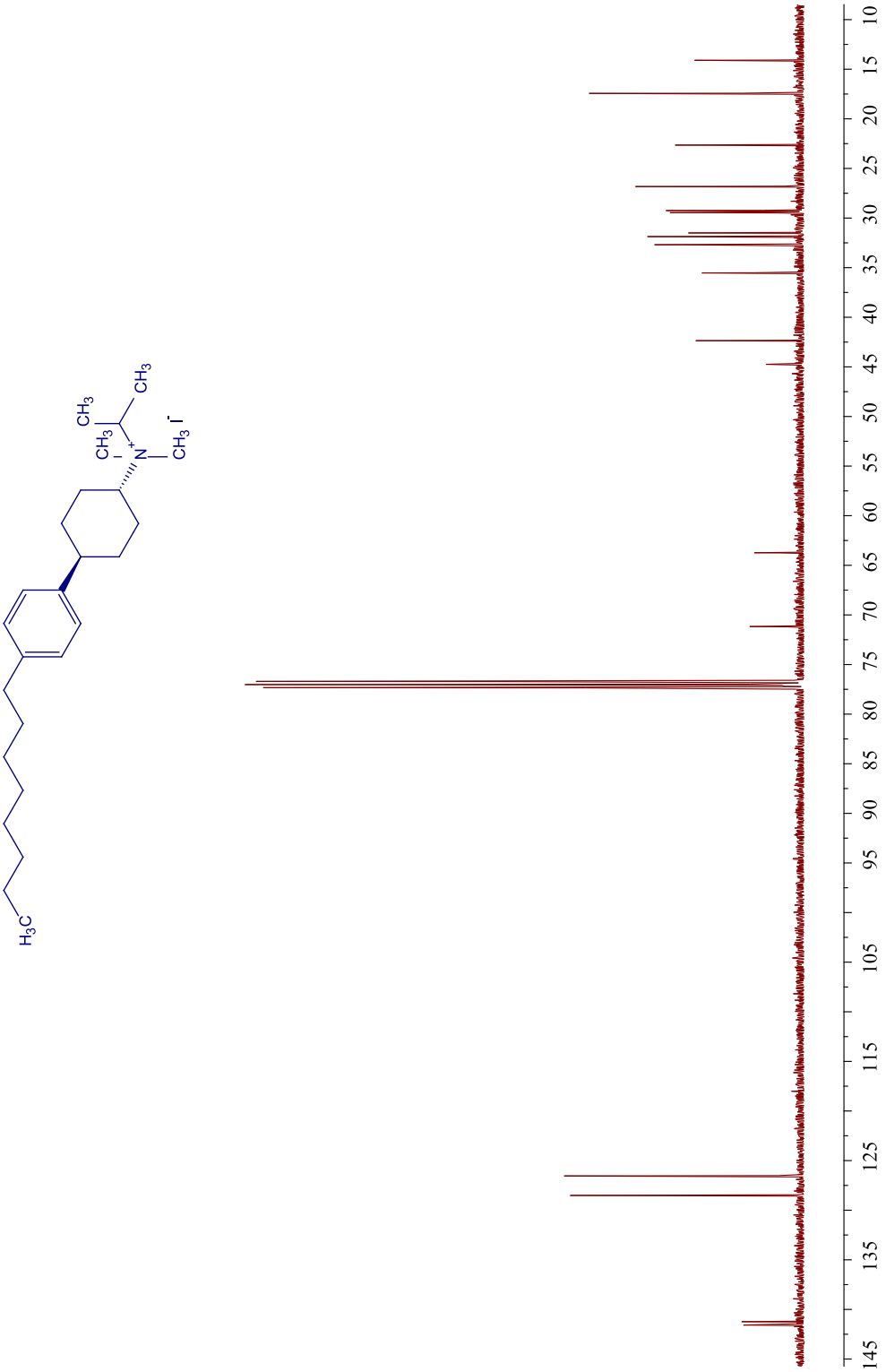

^{1}H NMR spectrum of *trans*-**12e**

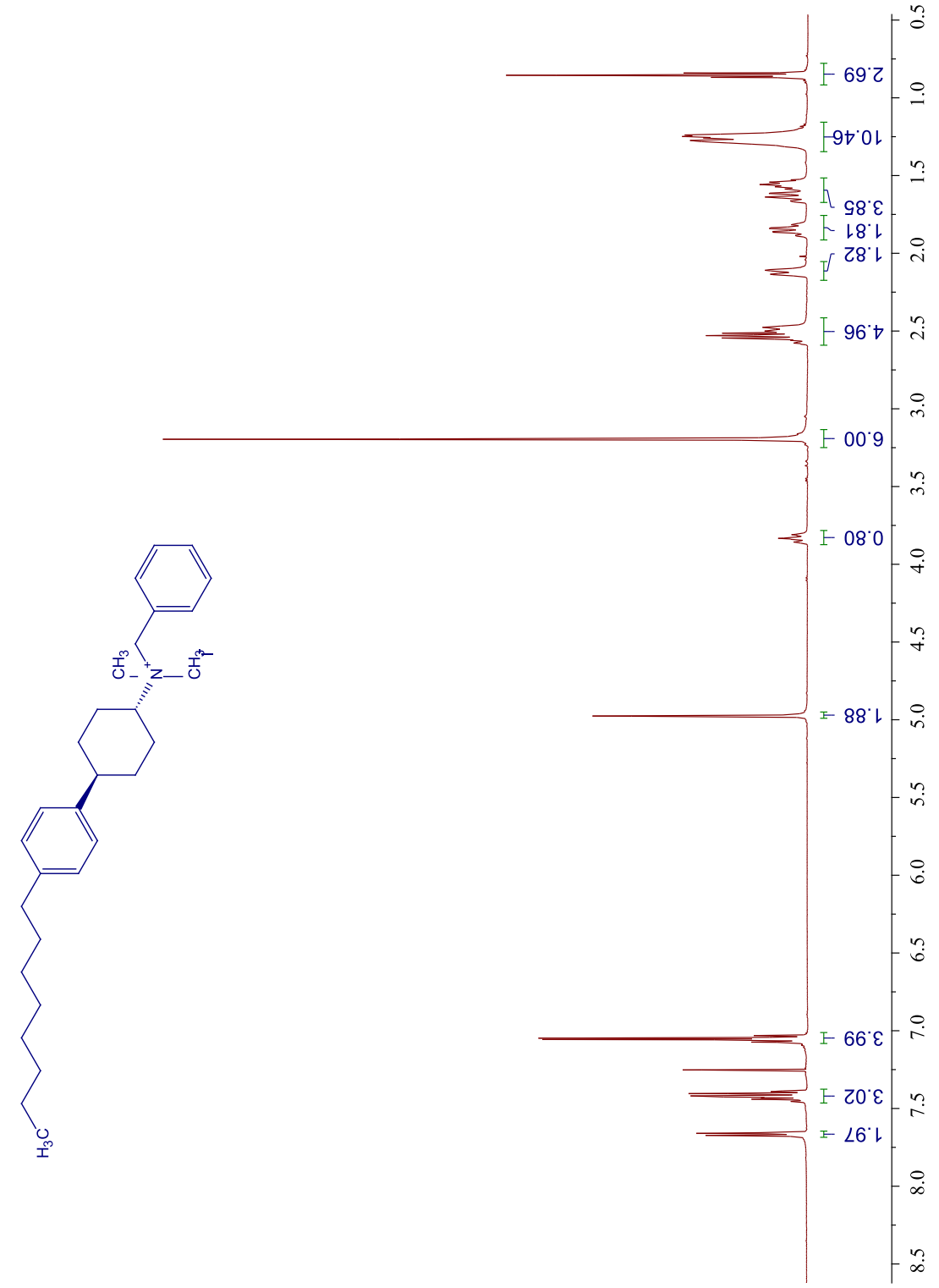

^{13}C NMR spectrum of *trans*-**12e**

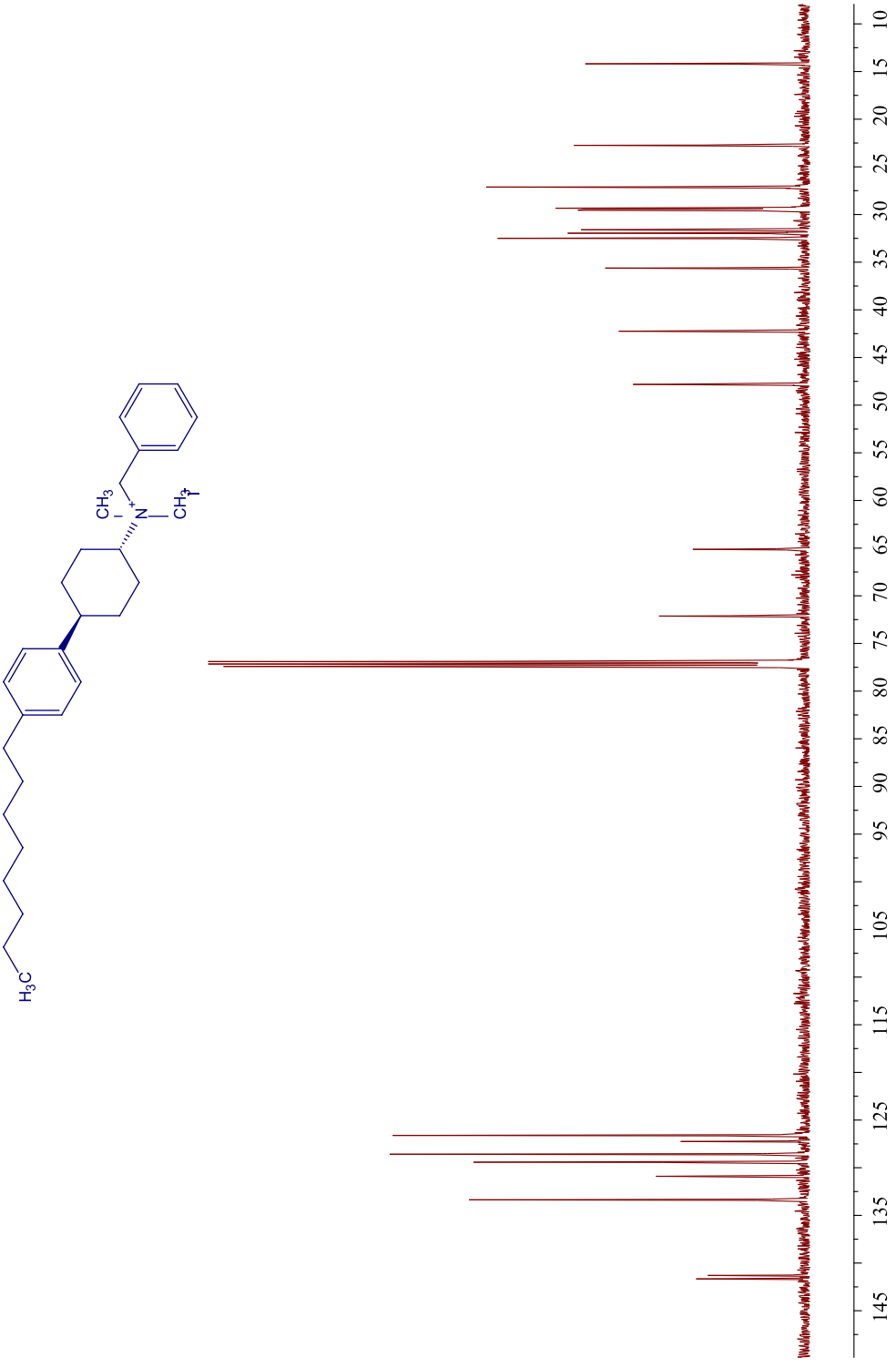

^{1}H NMR spectrum of *trans*-**12h**

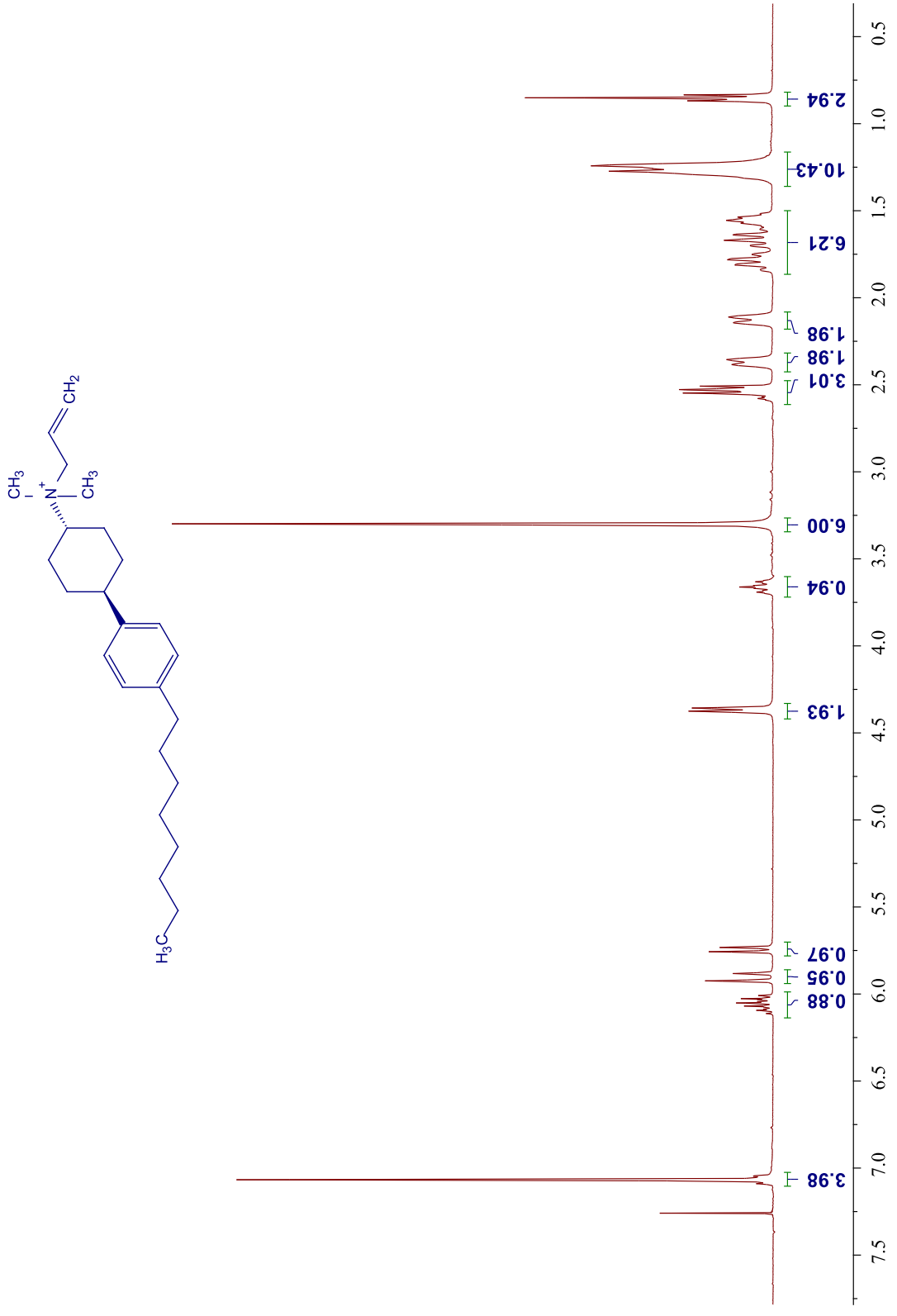

^{13}C NMR spectrum of *trans*-**12h**

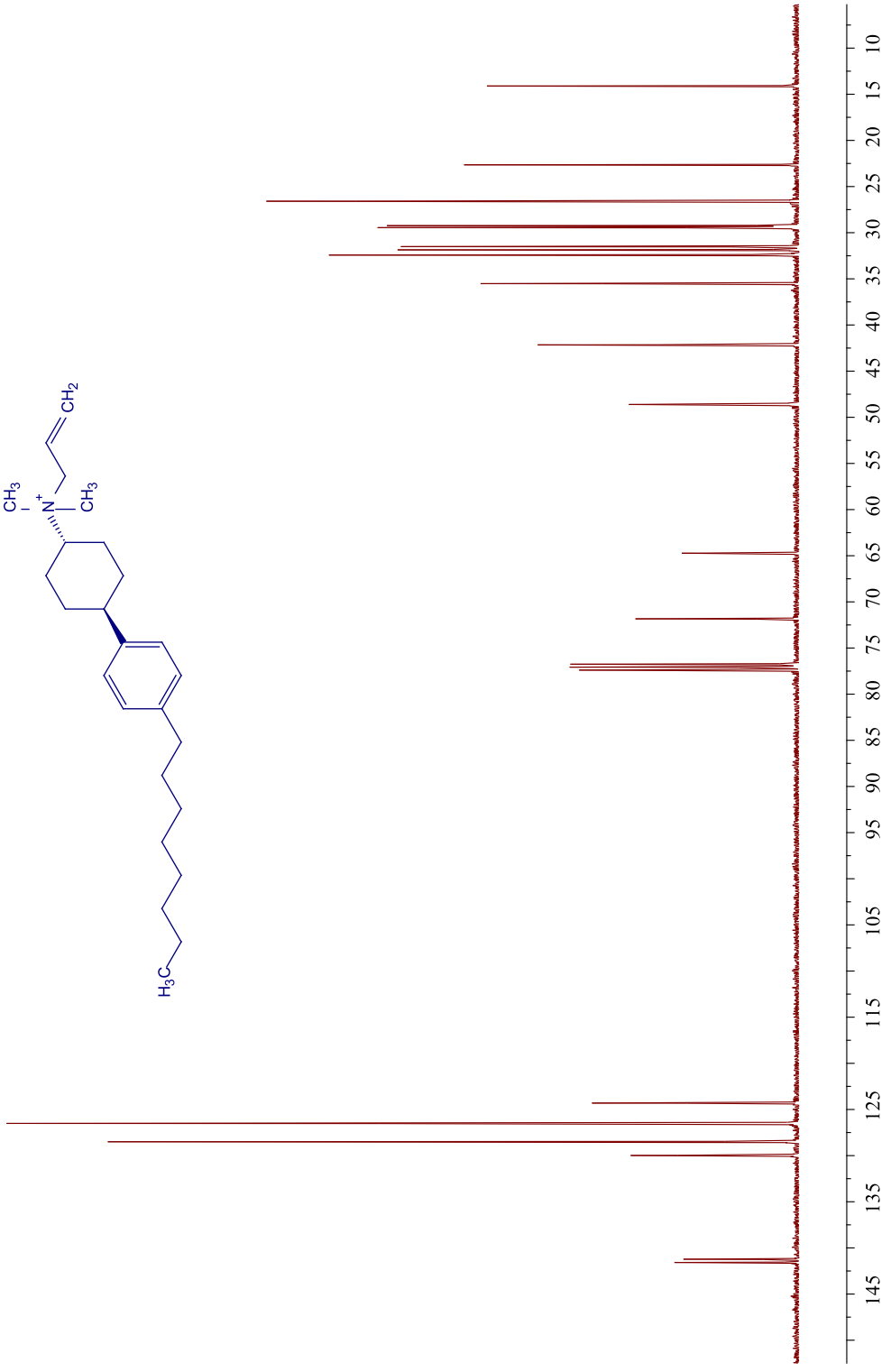

[1]H NMR spectrum of *cis*-**12i**

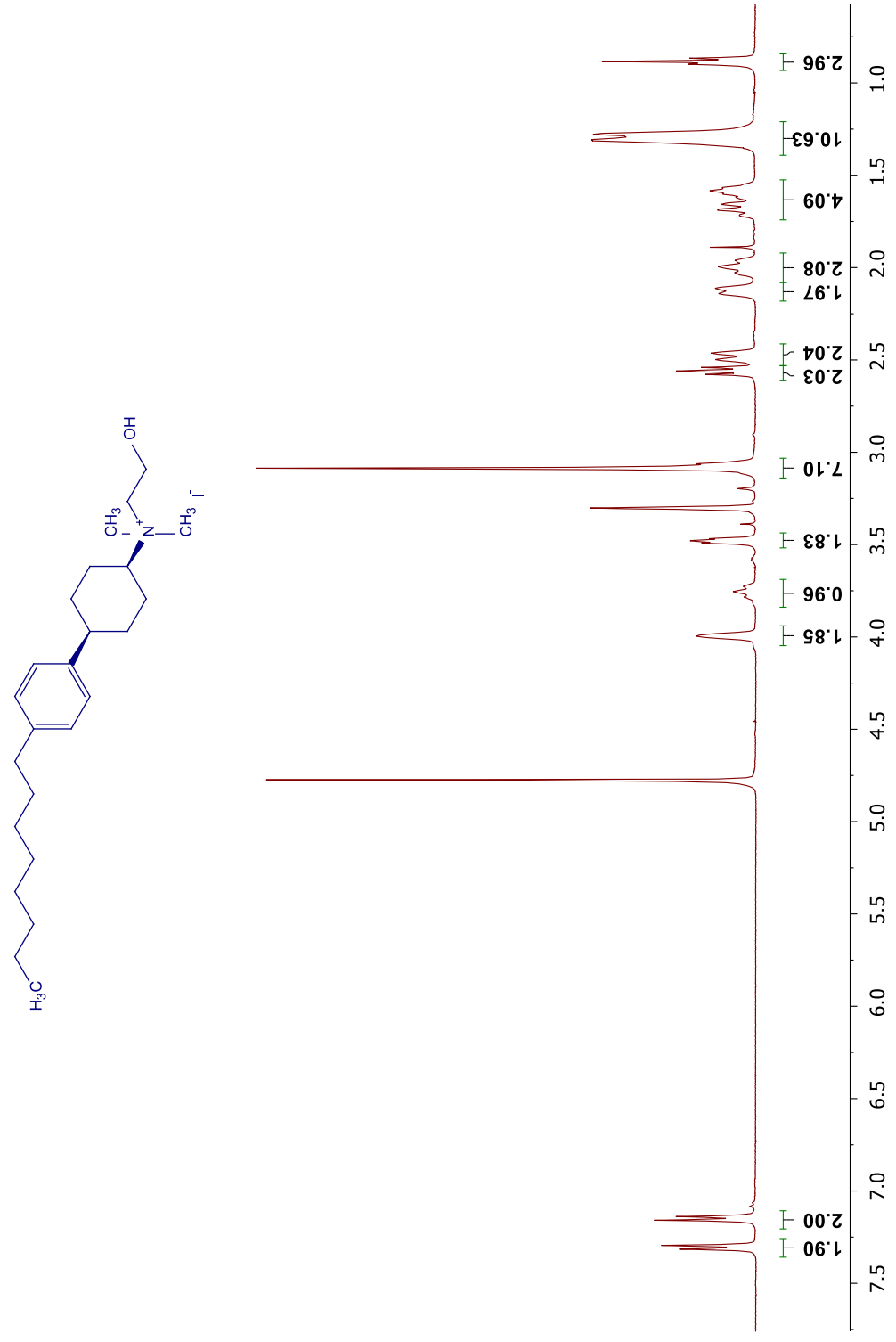

^{13}C NMR spectrum of *cis*-**12i**

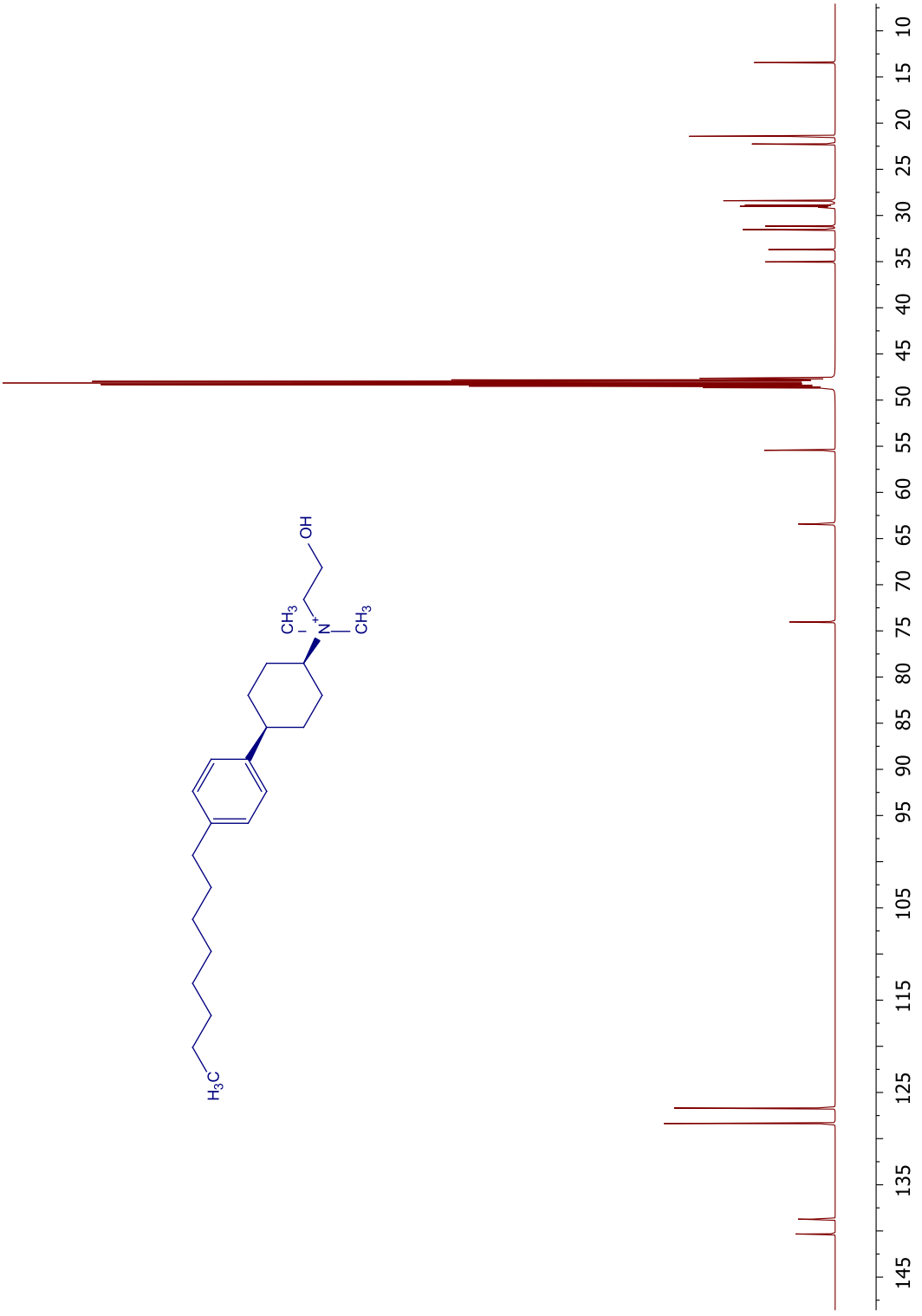

^{1}H NMR spectrum of *trans*-**12i**

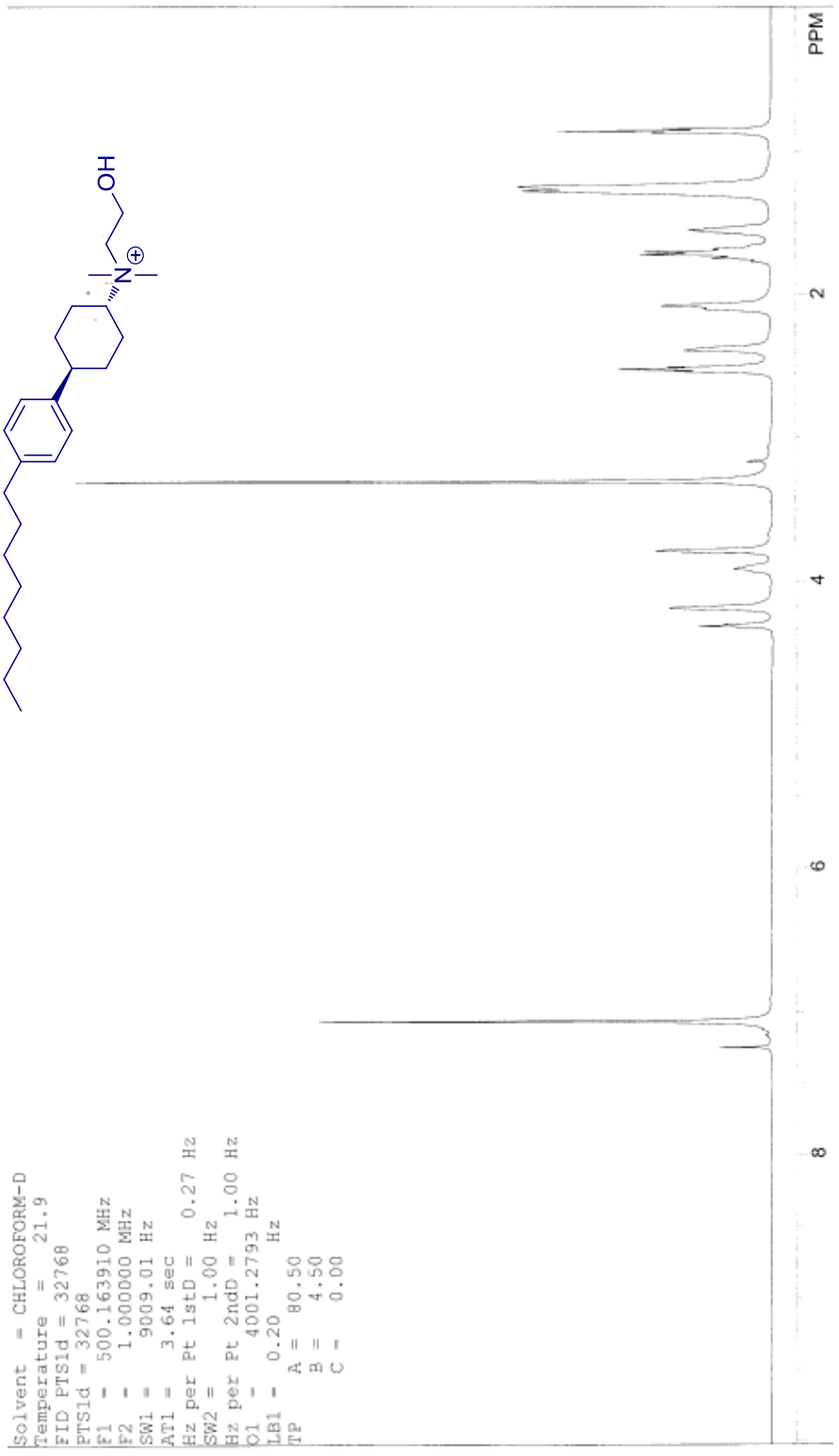

^{13}C NMR spectrum of *trans*-**12i**

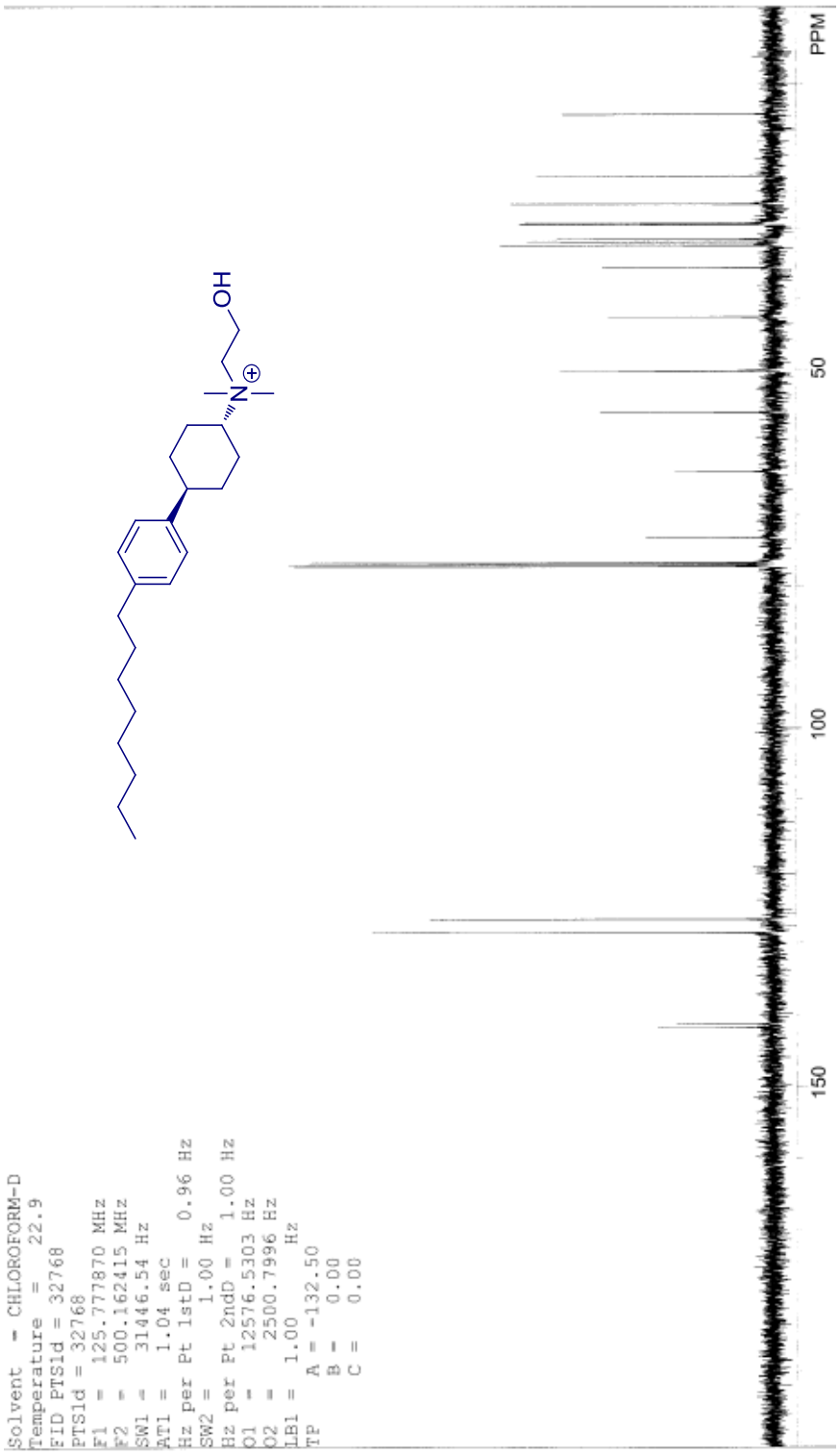

^{1}H NMR spectrum of **13**

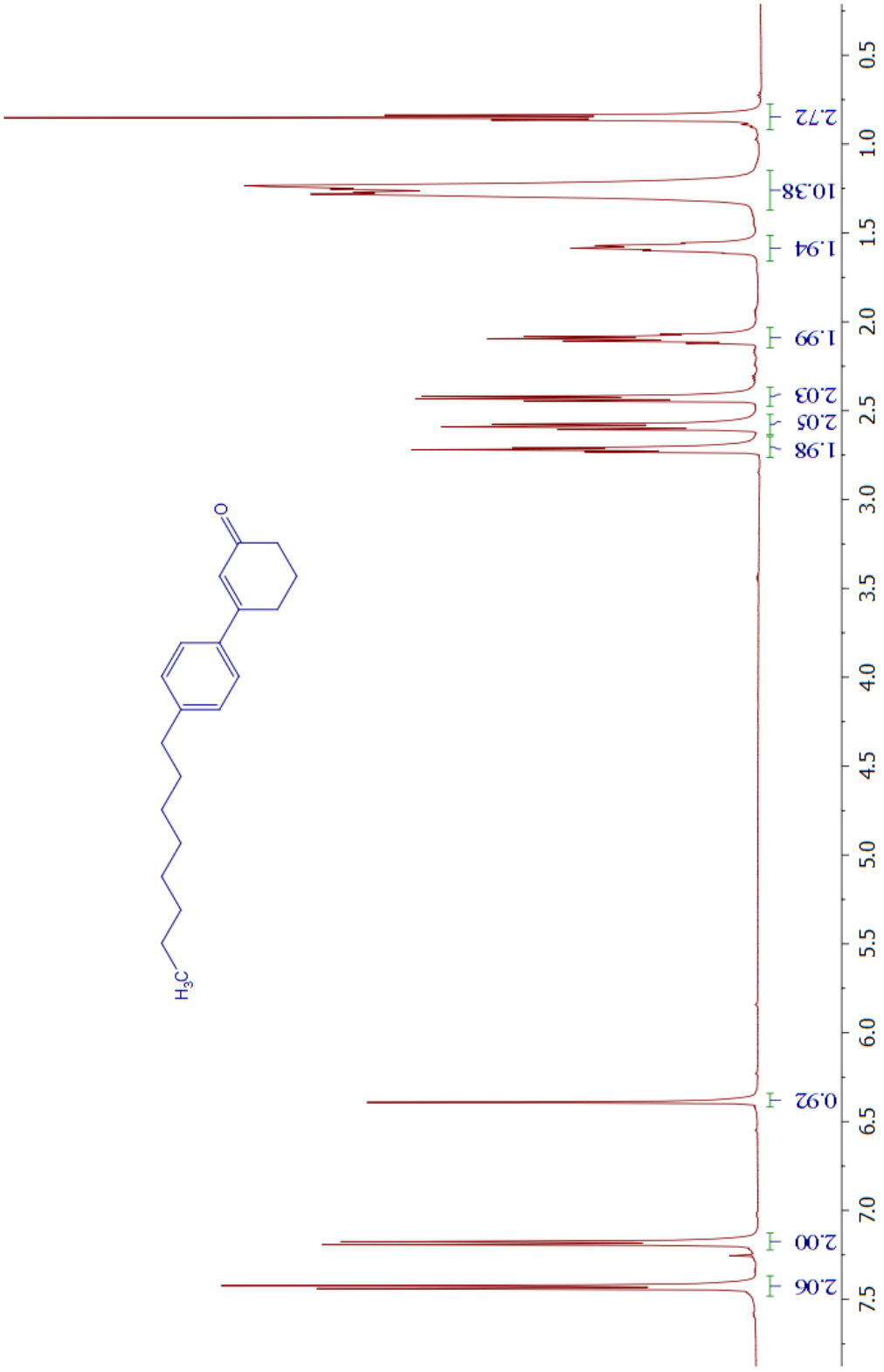

^{13}C NMR spectrum of **13**

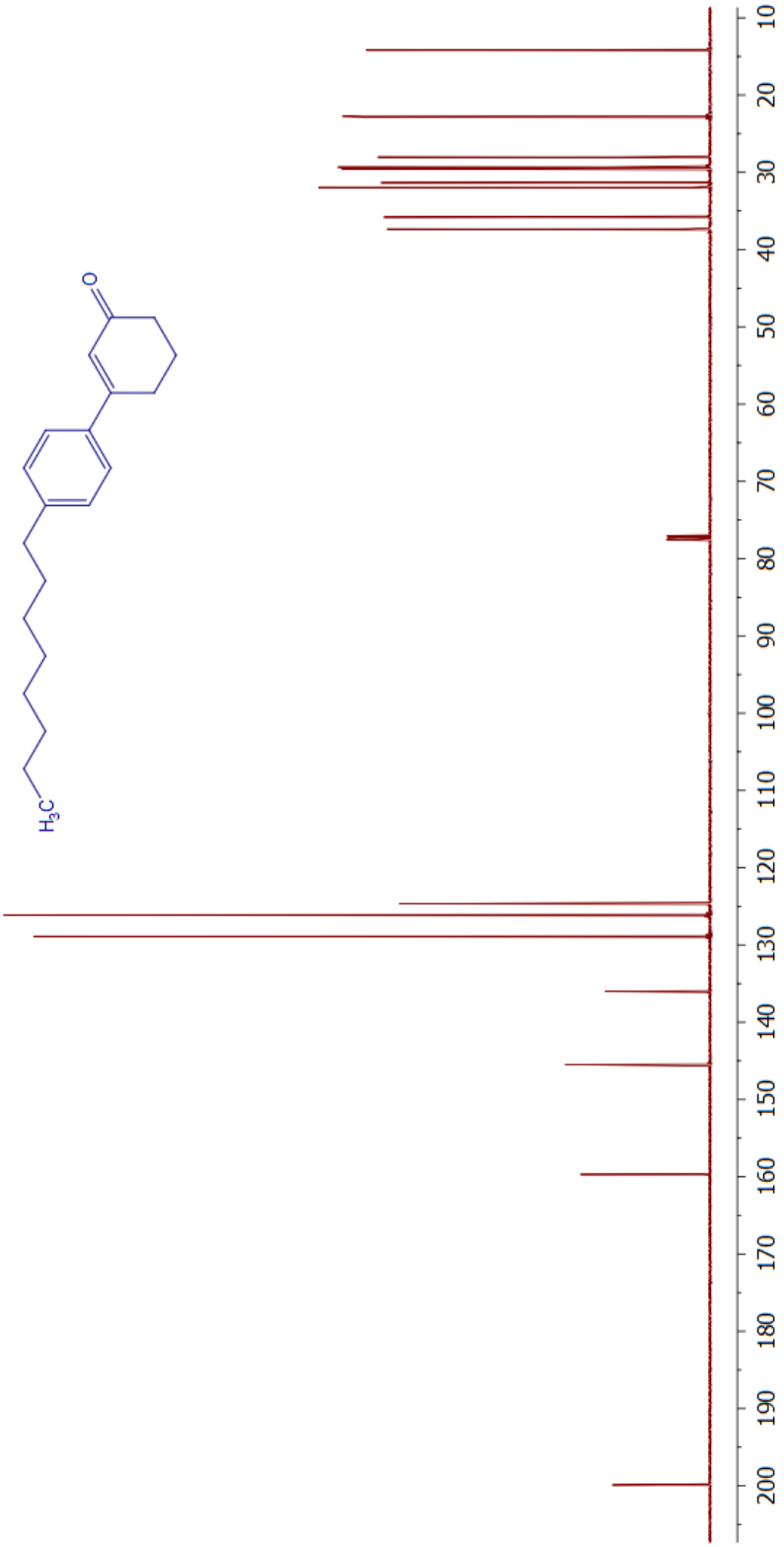

^{1}H NMR spectrum of **14**

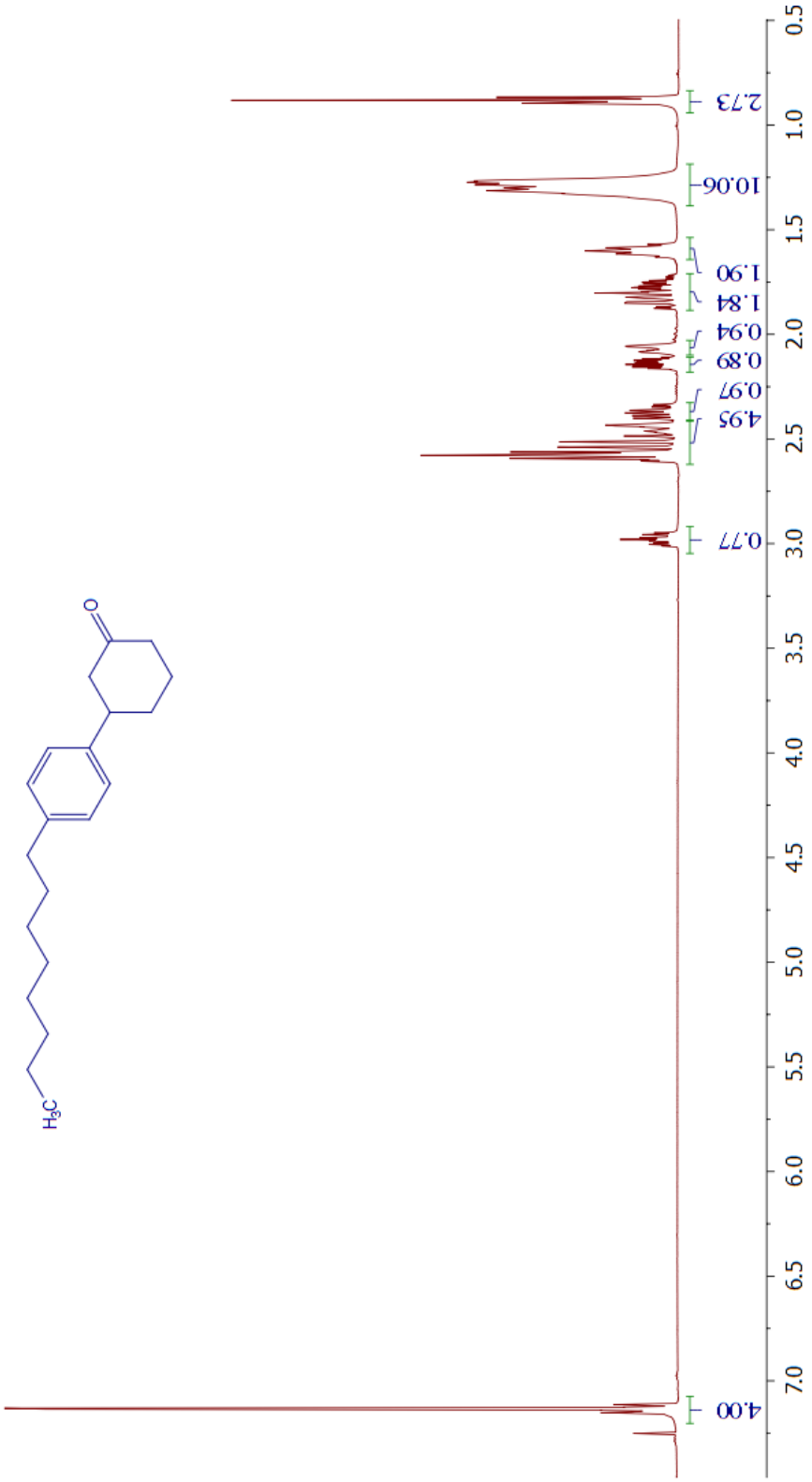

^{13}C NMR spectrum of **14**

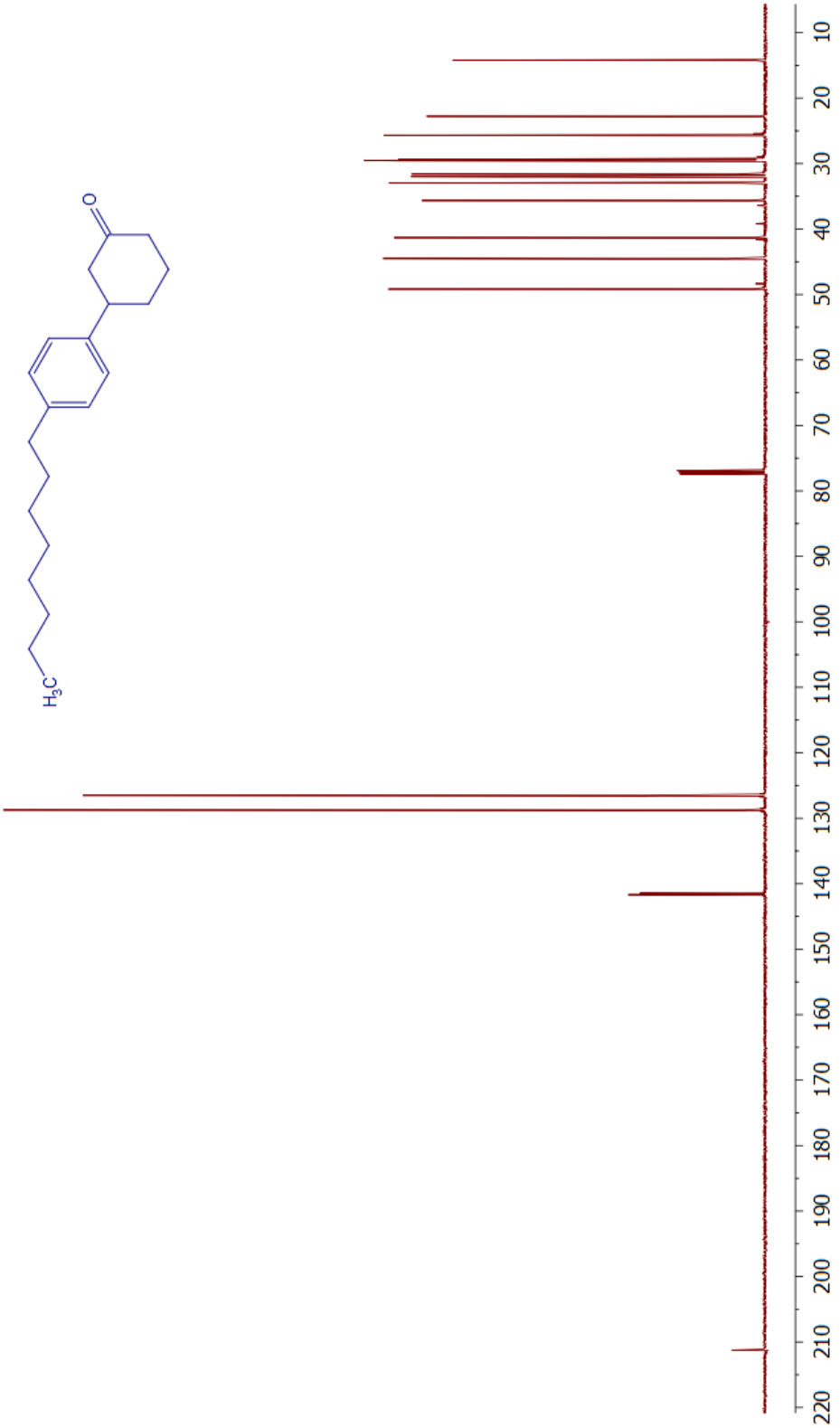

^{1}H NMR spectrum of *cis*-**15**

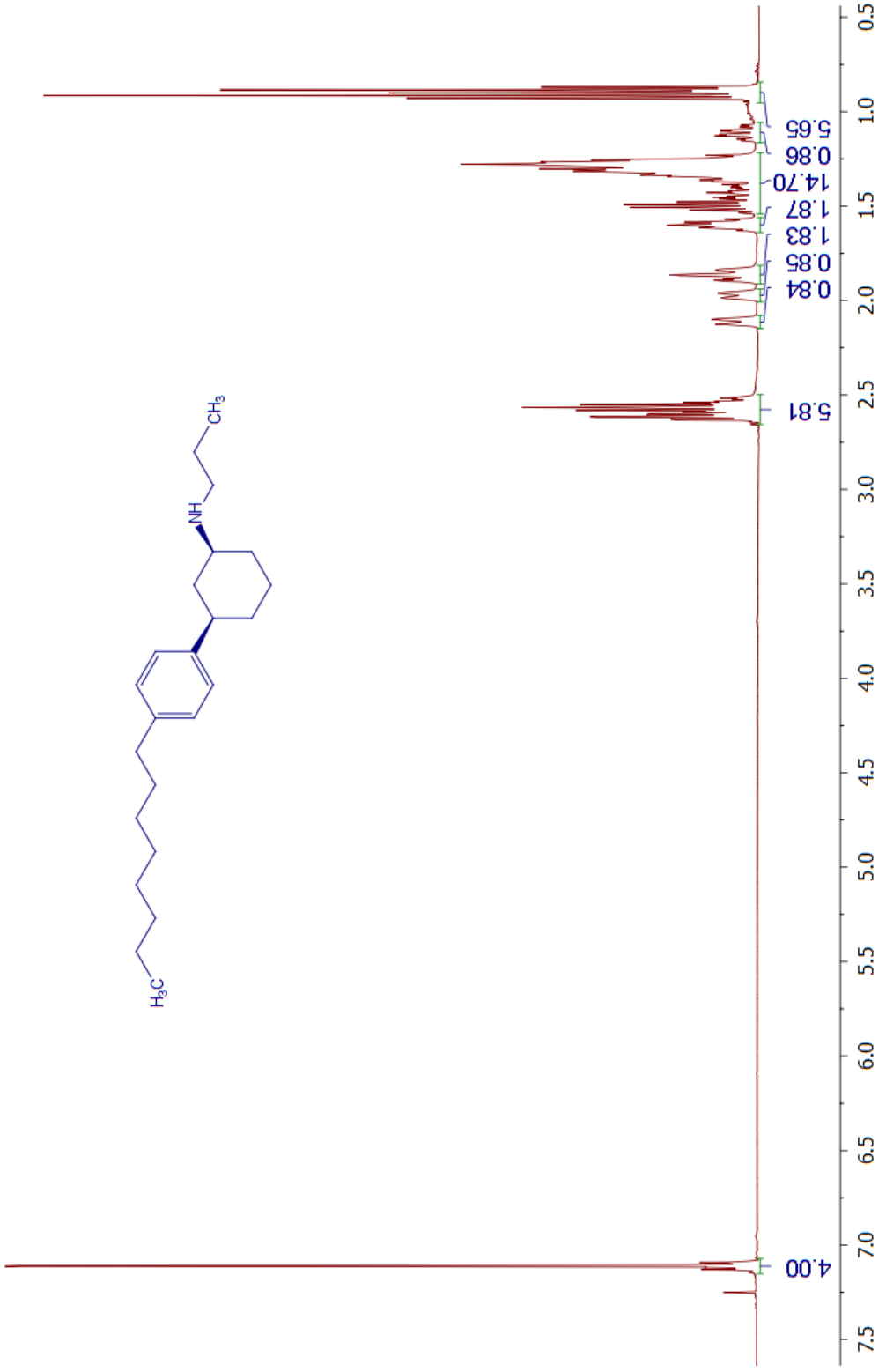

^{13}C NMR spectrum of *cis*-**15**

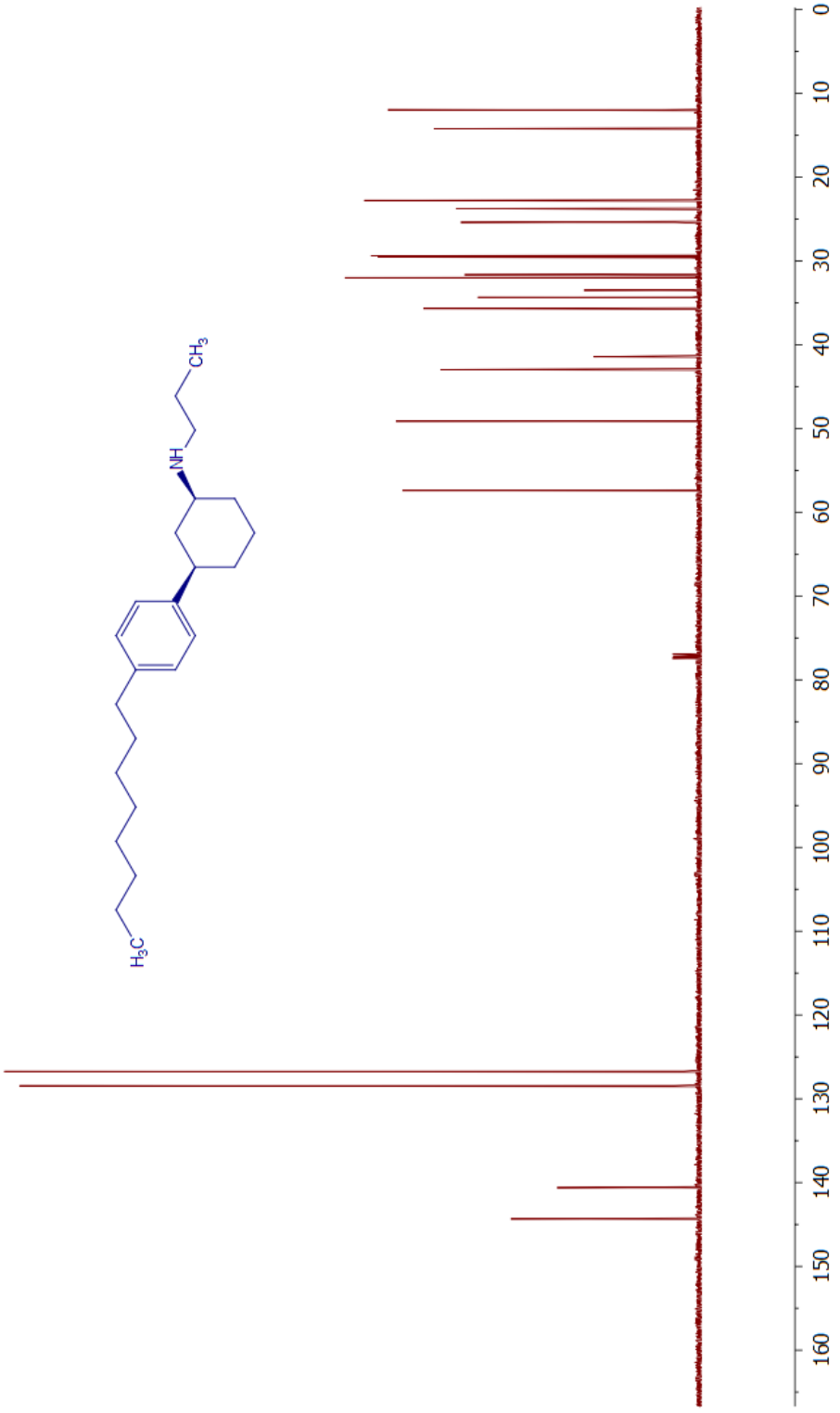

^{1}H NMR spectrum of *trans*-**15**

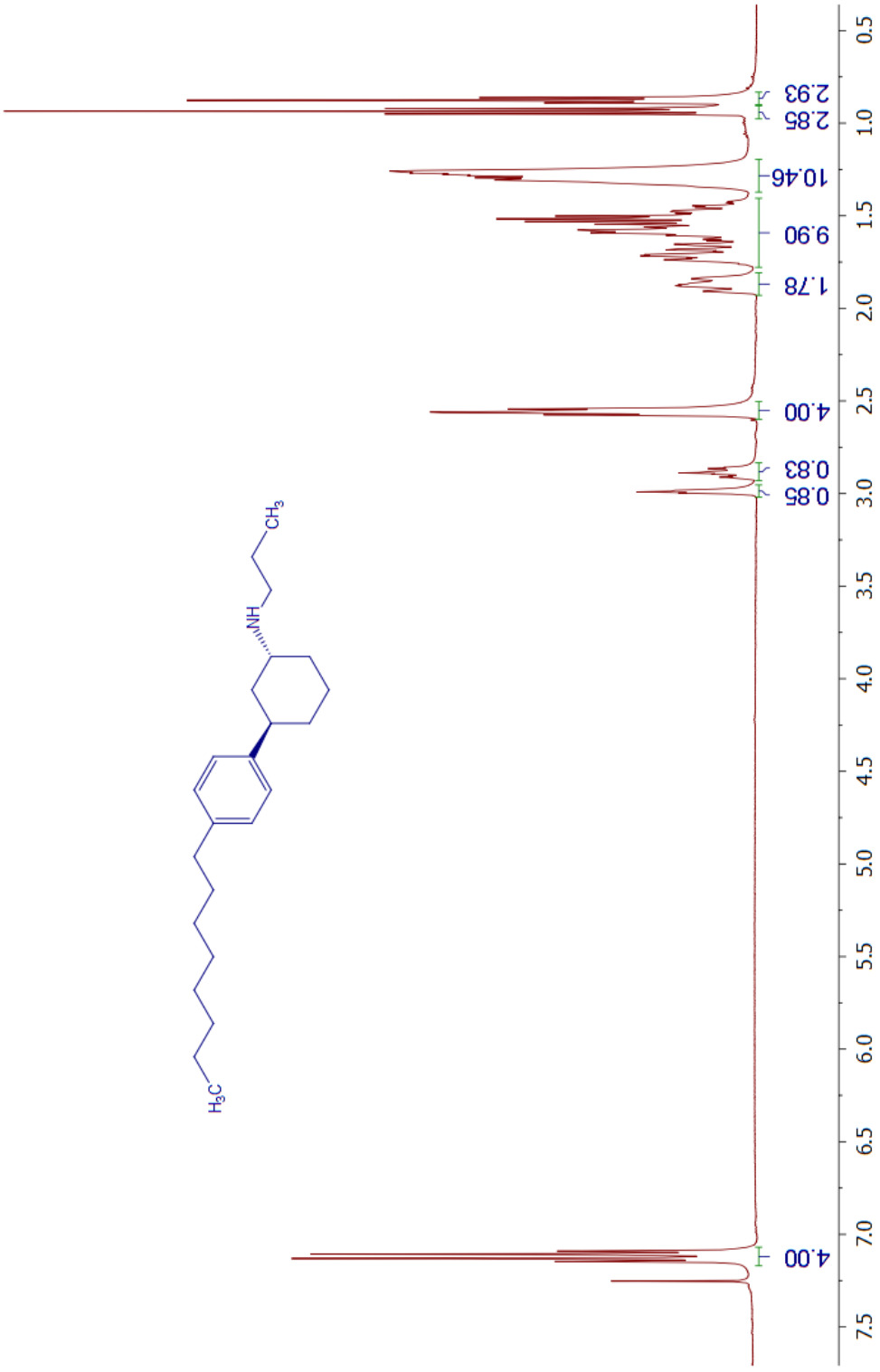

^{13}C NMR spectrum of *trans*-**15**

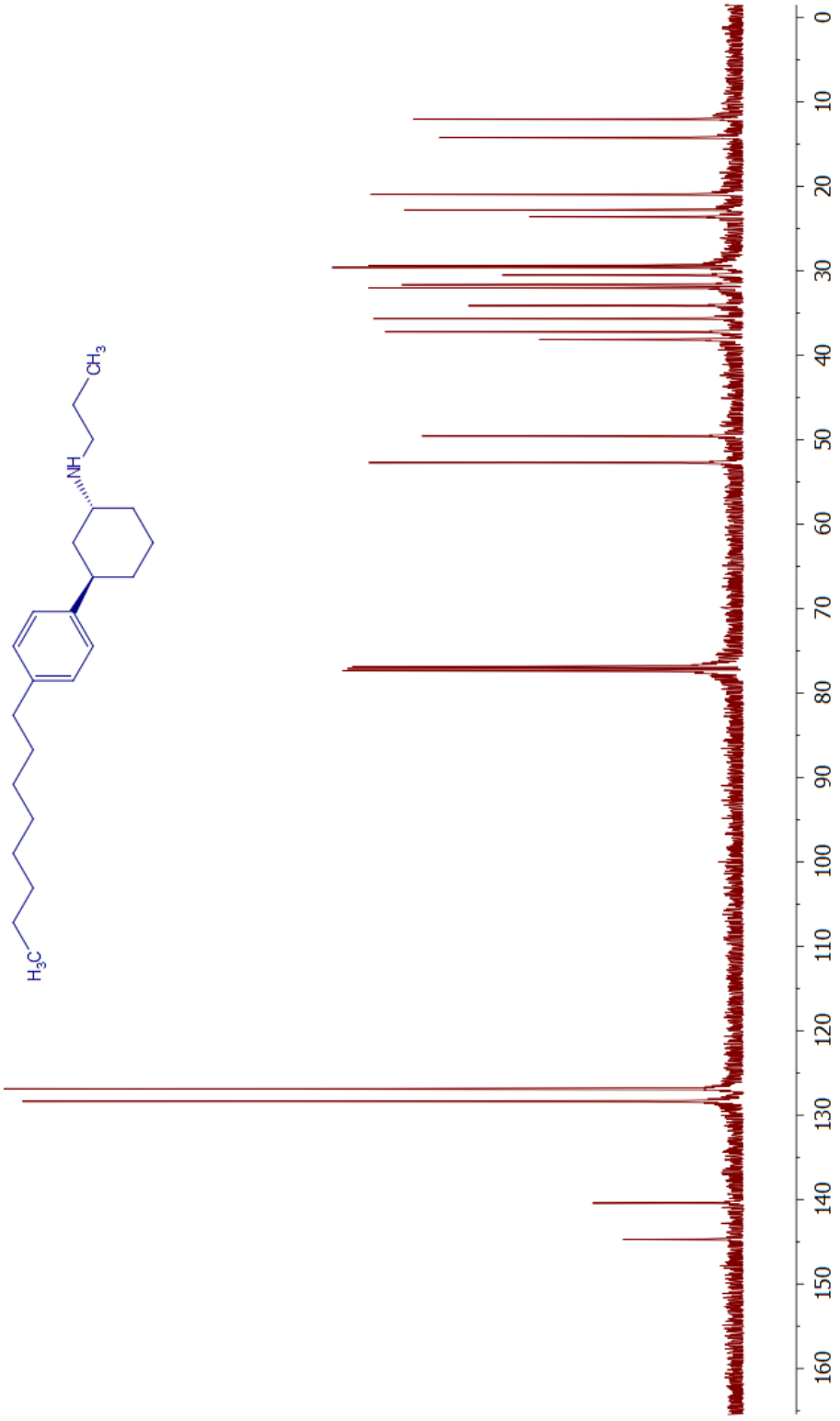

^{1}H NMR spectrum of *cis*-**16**

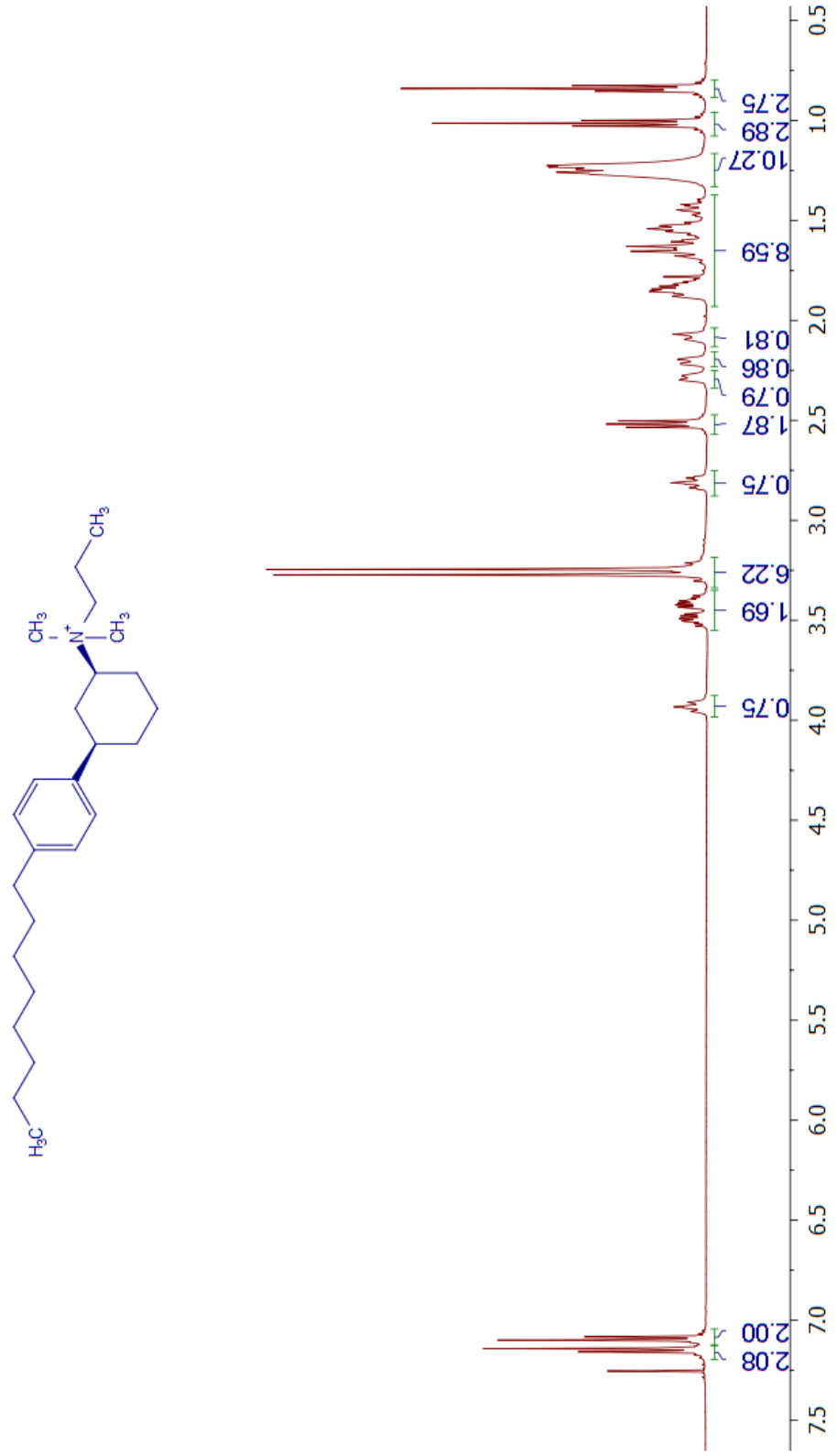

^{13}C NMR spectrum of *cis*-**16**

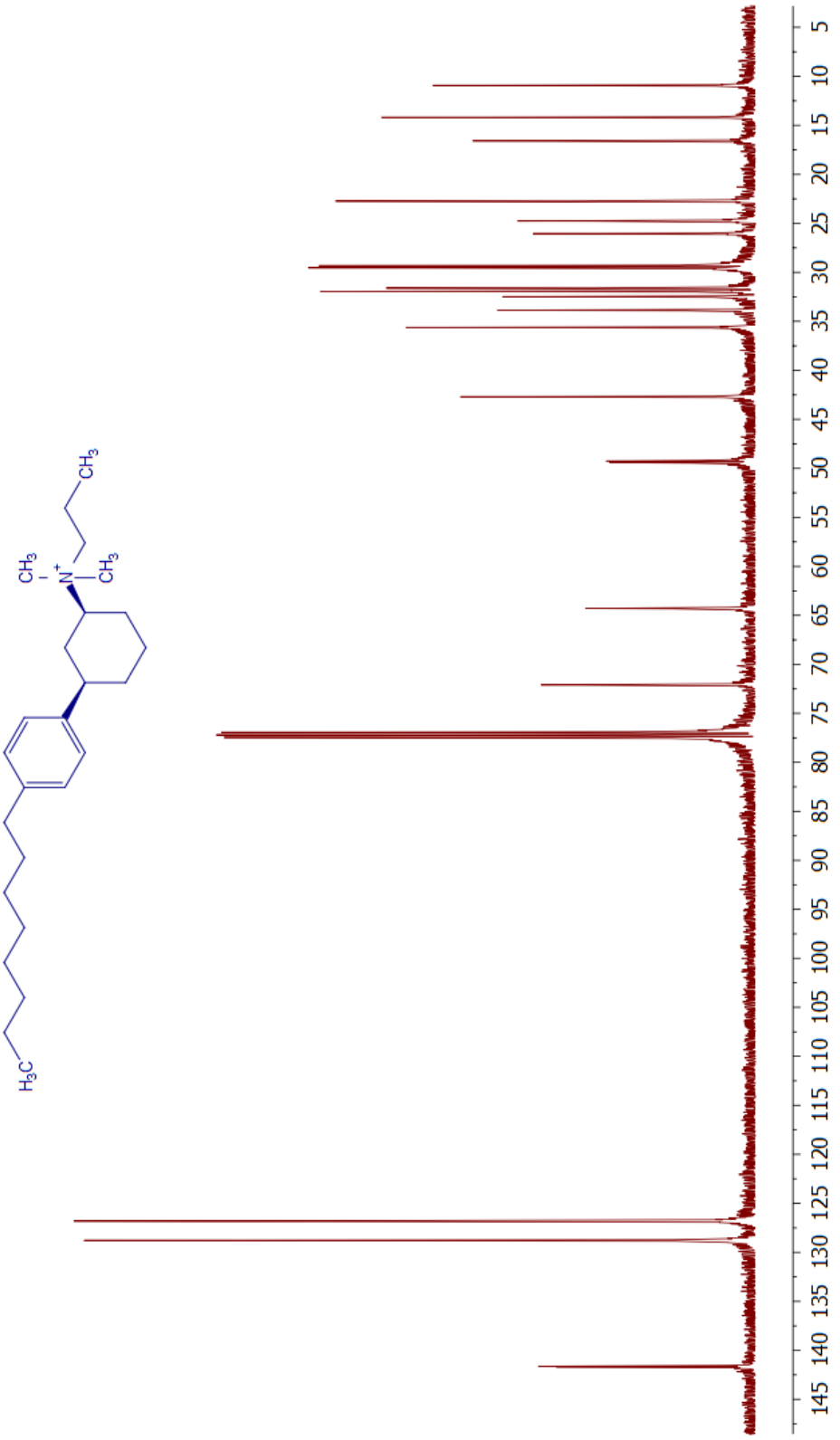

^{1}H NMR spectrum of *trans*-**16**

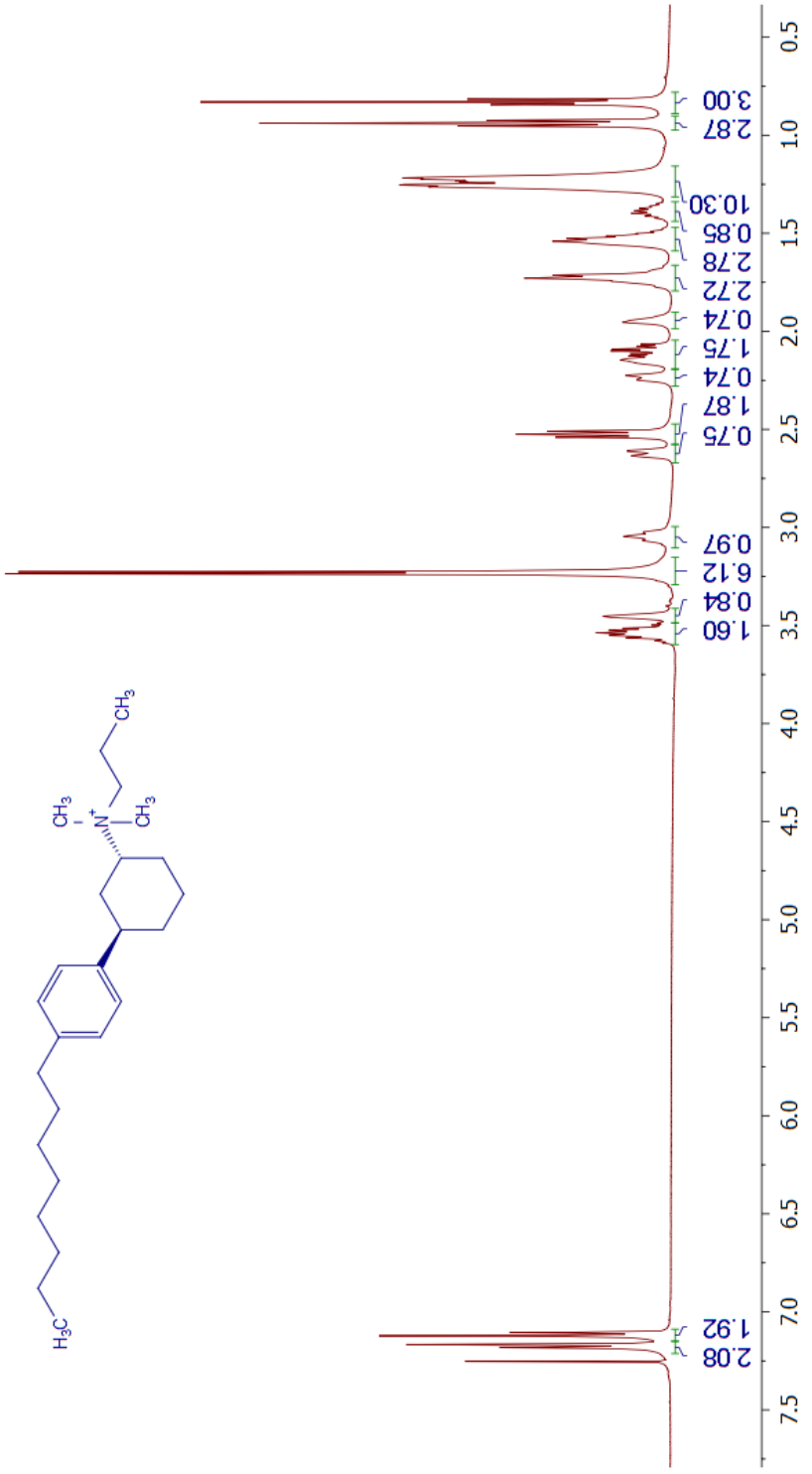

^{13}C NMR spectrum of *trans*-**16**

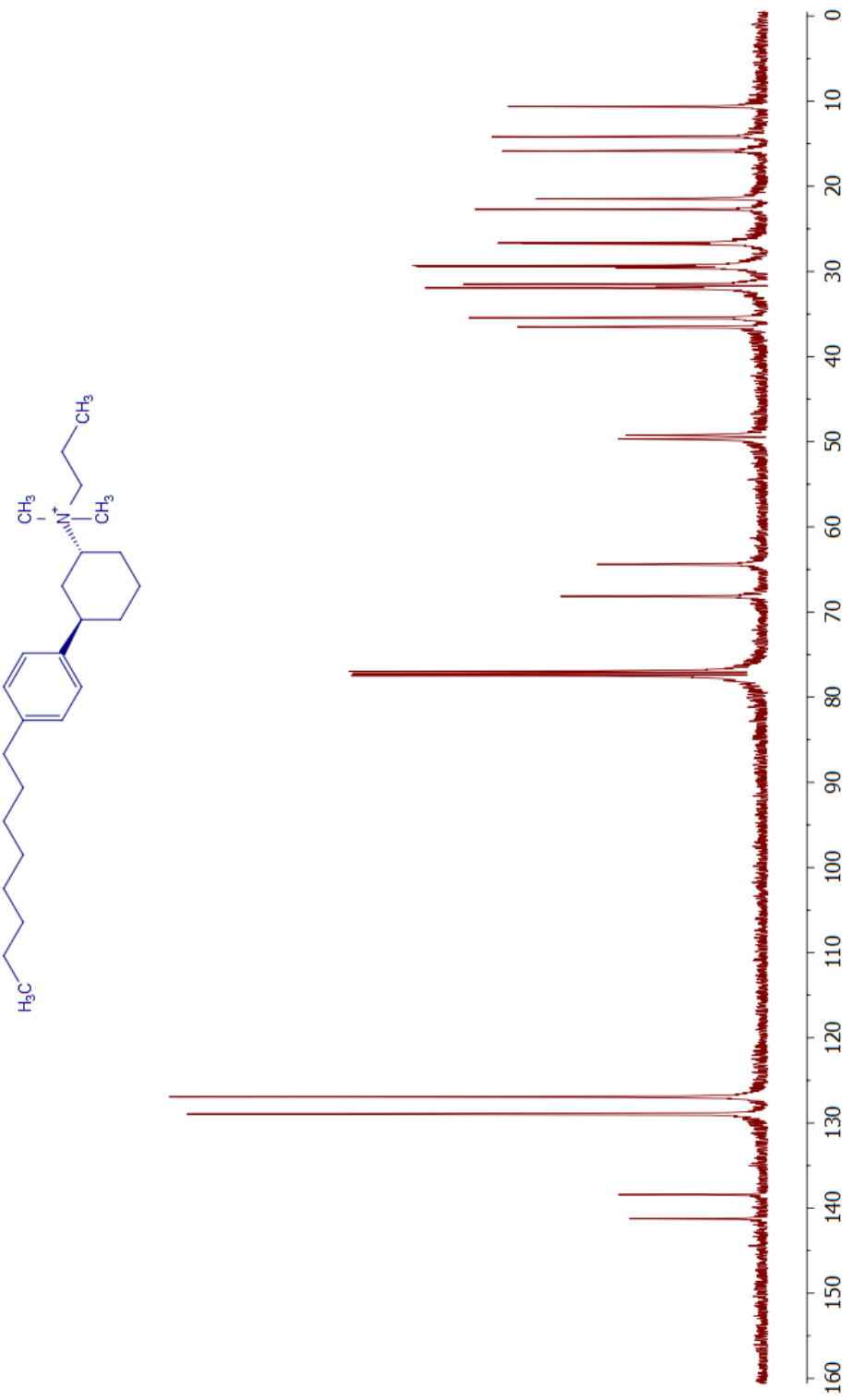

^{1}H NMR spectrum of *cis*-**17**

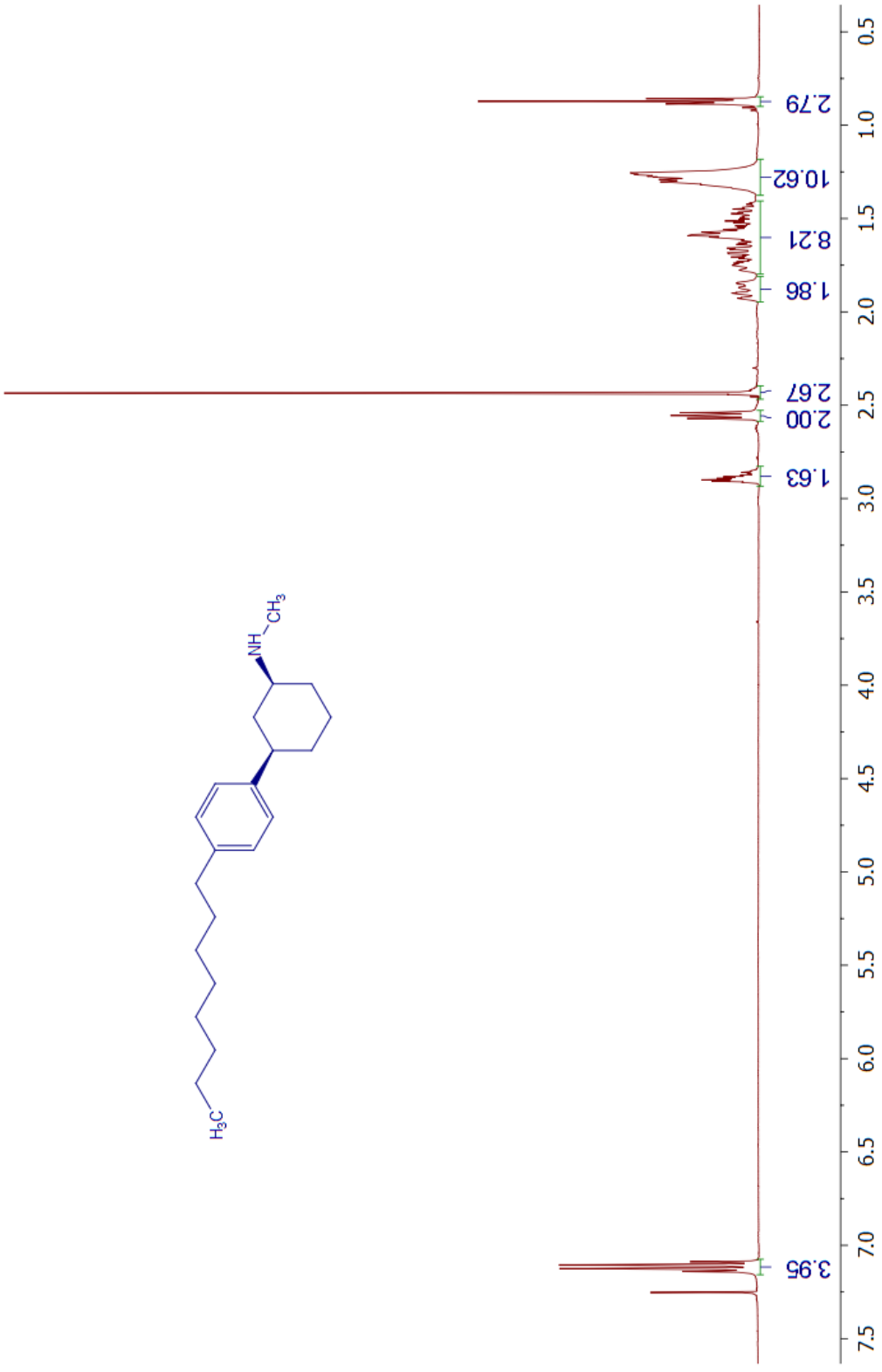

^{13}C NMR spectrum of *cis*-**17**

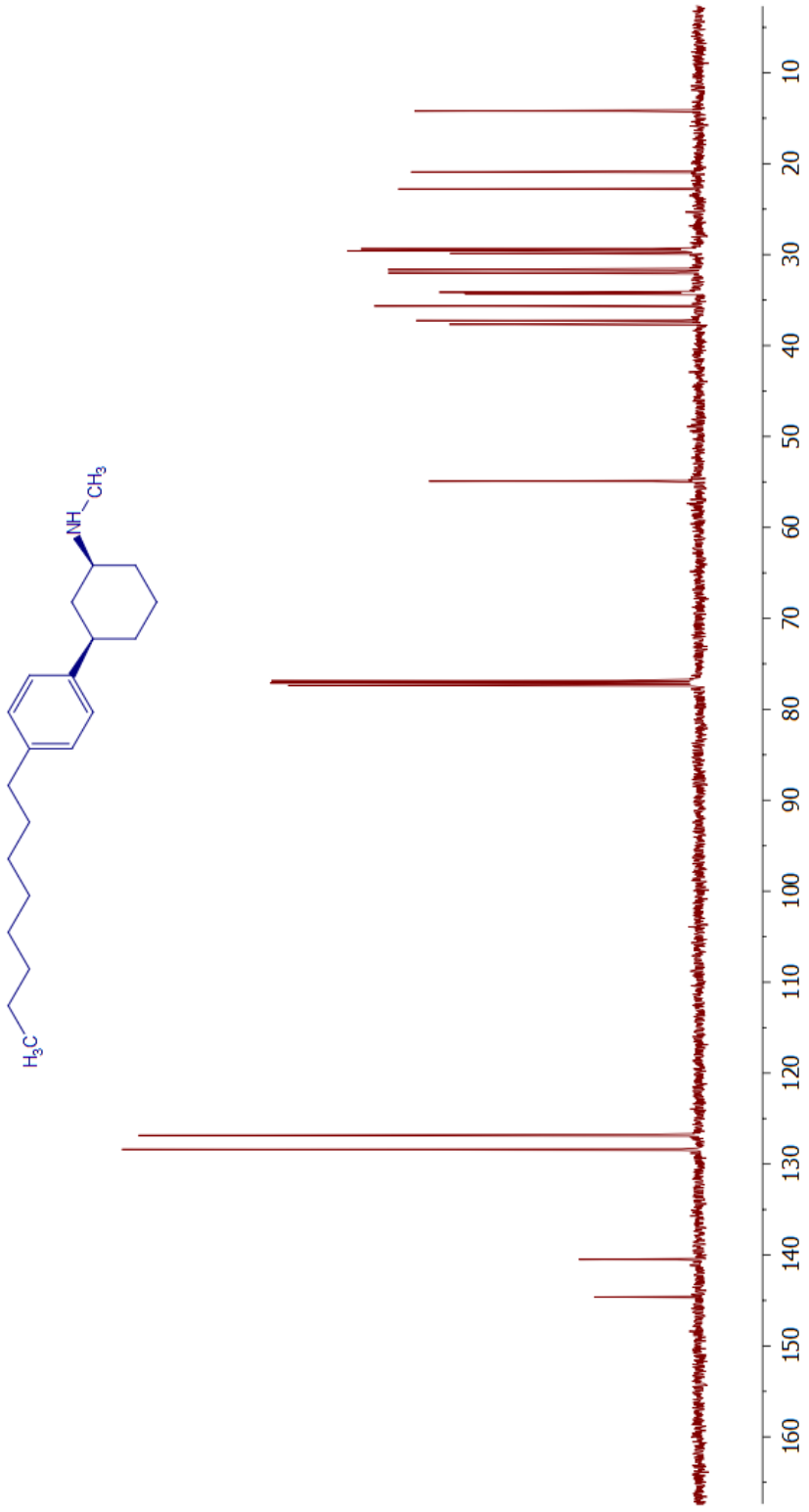

^{1}H NMR spectrum of *cis*-**18**

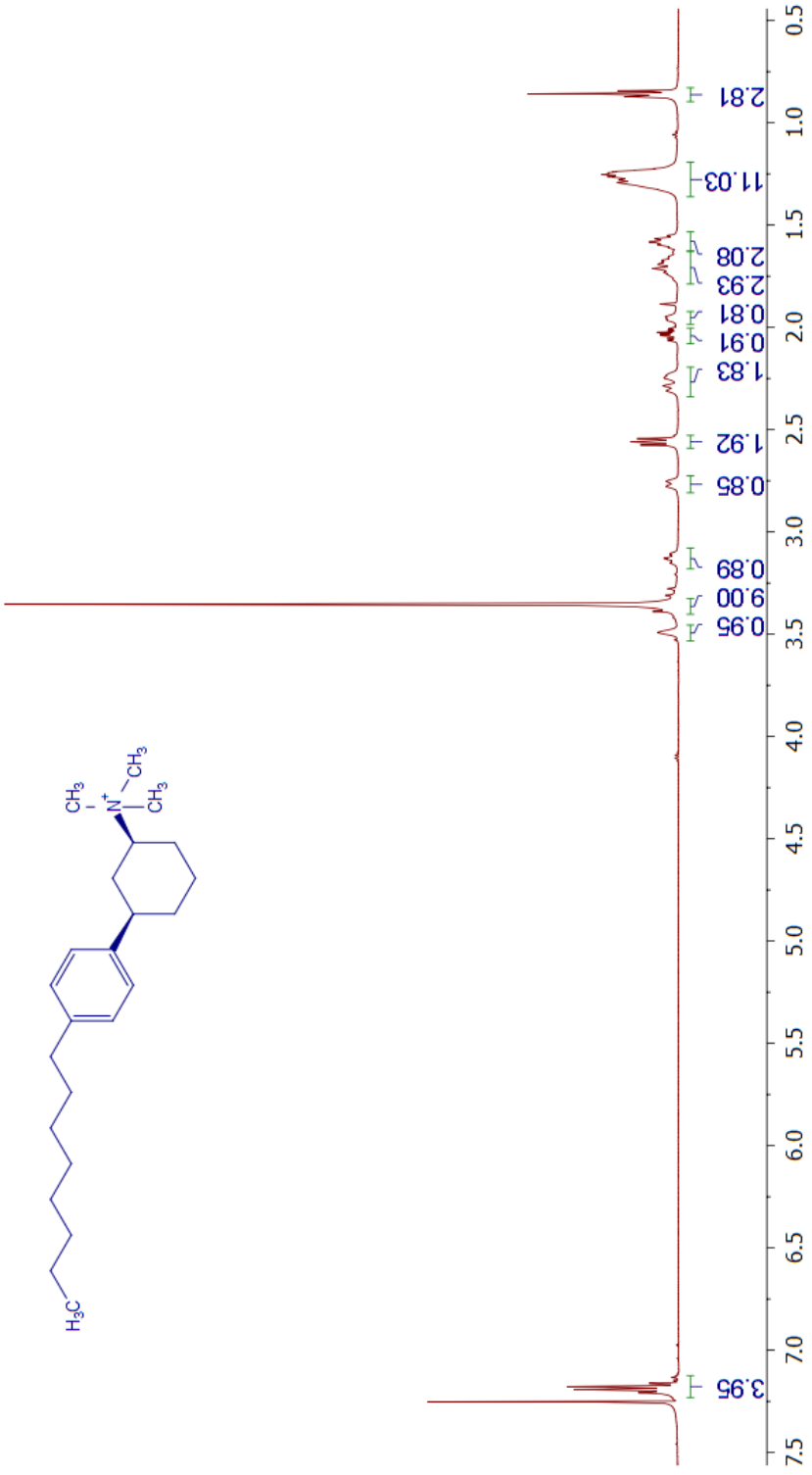

^{13}C NMR spectrum of *cis*-**18**

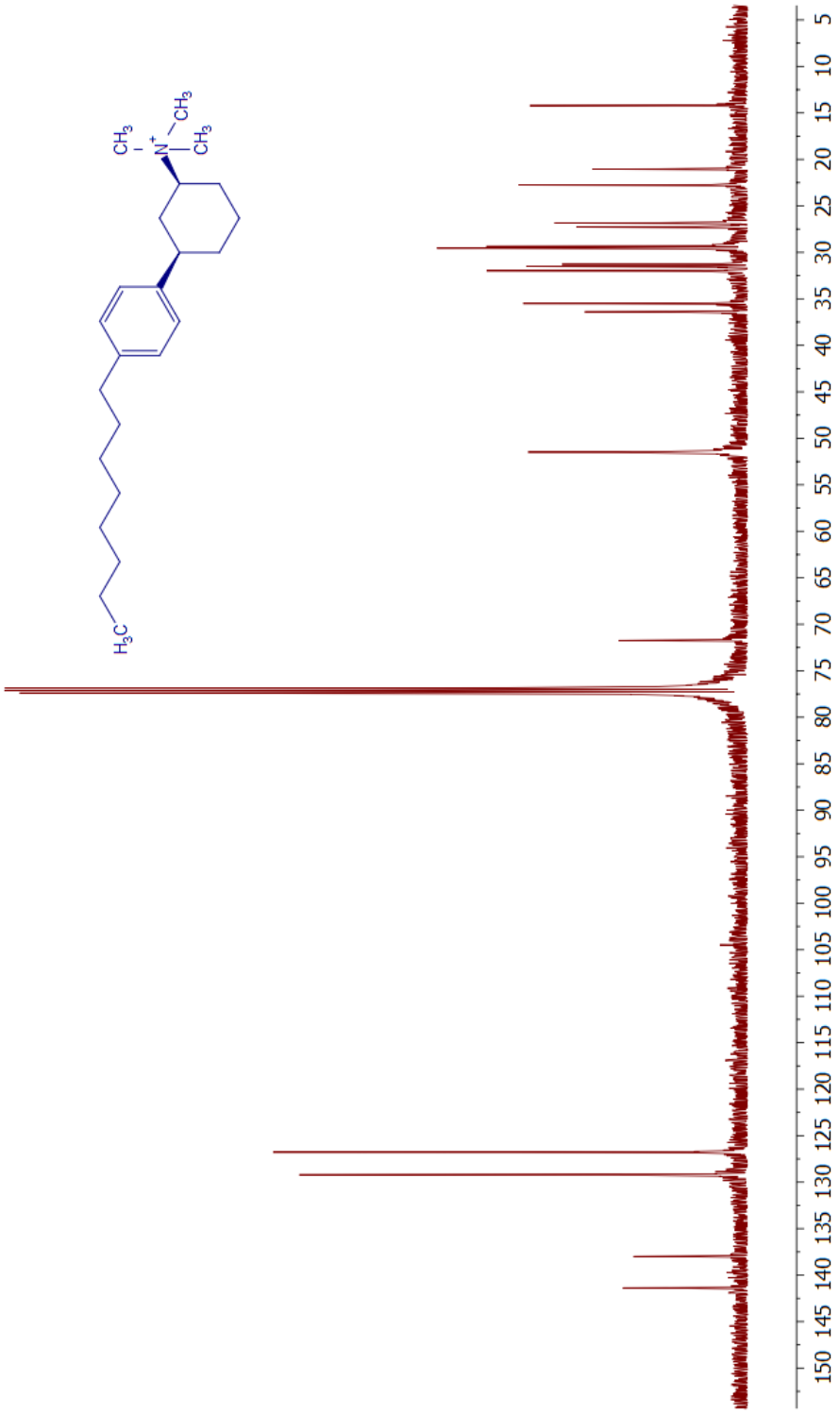

^{1}H NMR spectrum of **20**

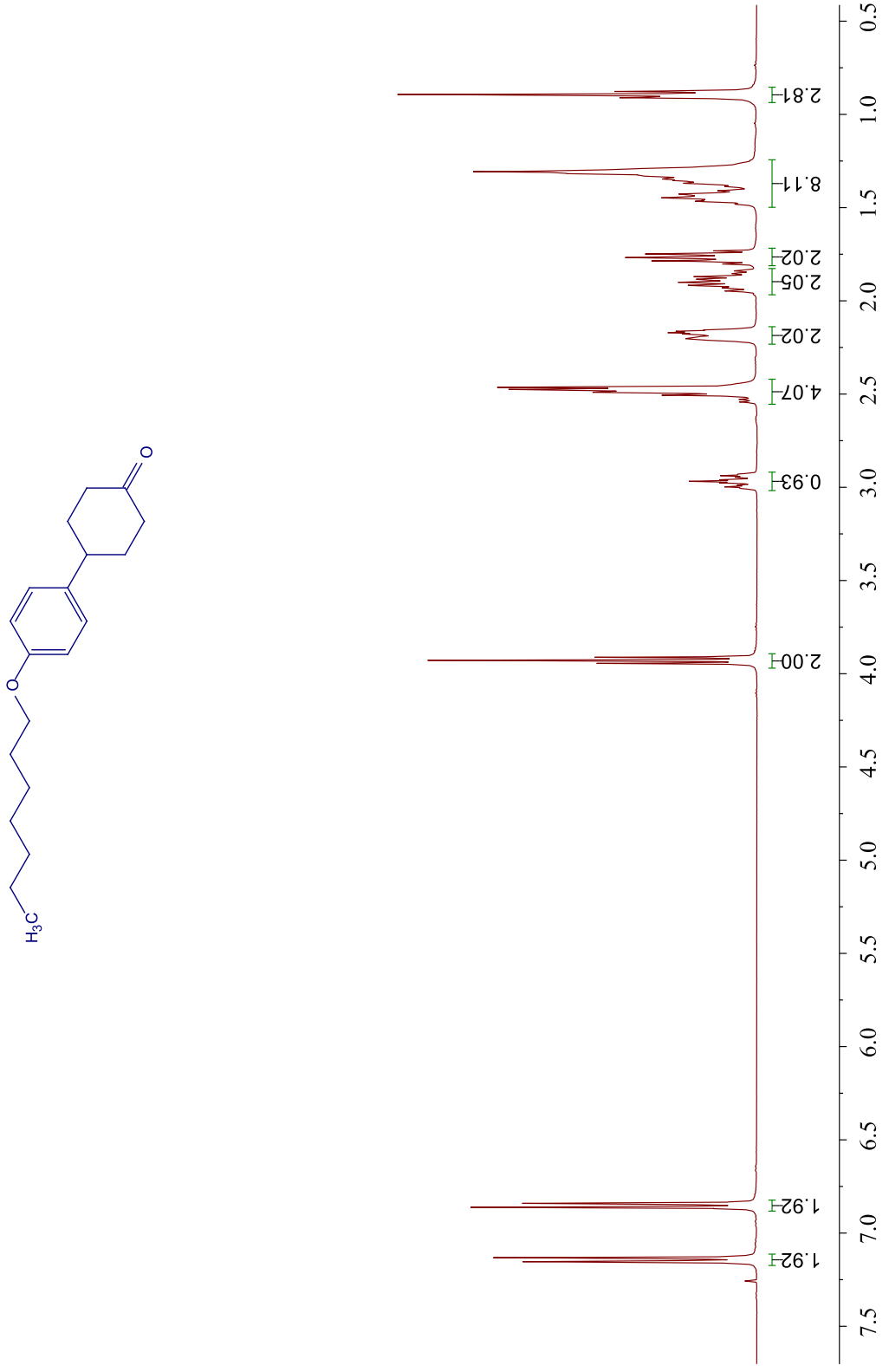

^{13}C NMR spectrum of **20**

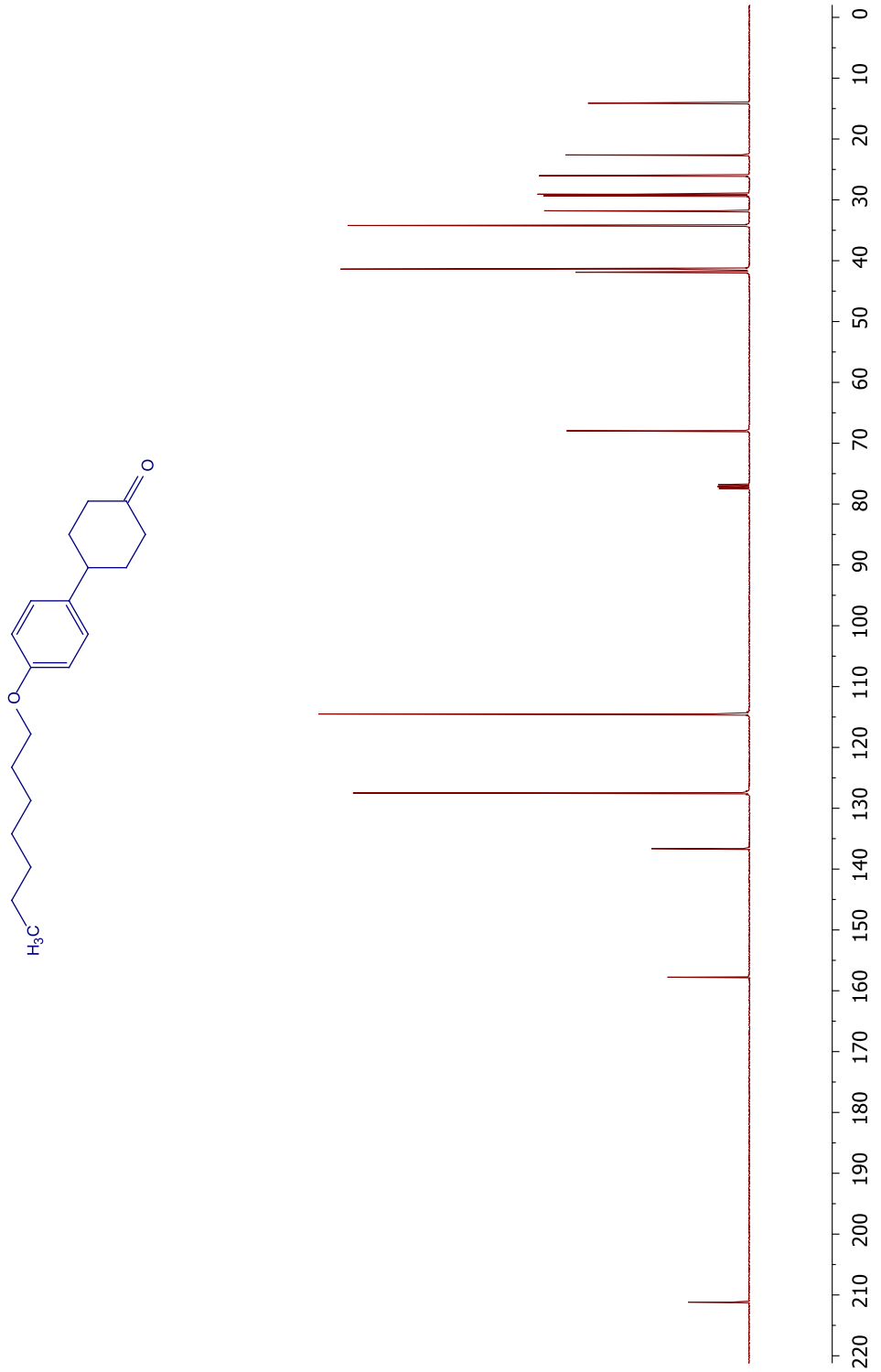

^{1}H NMR spectrum of **21**

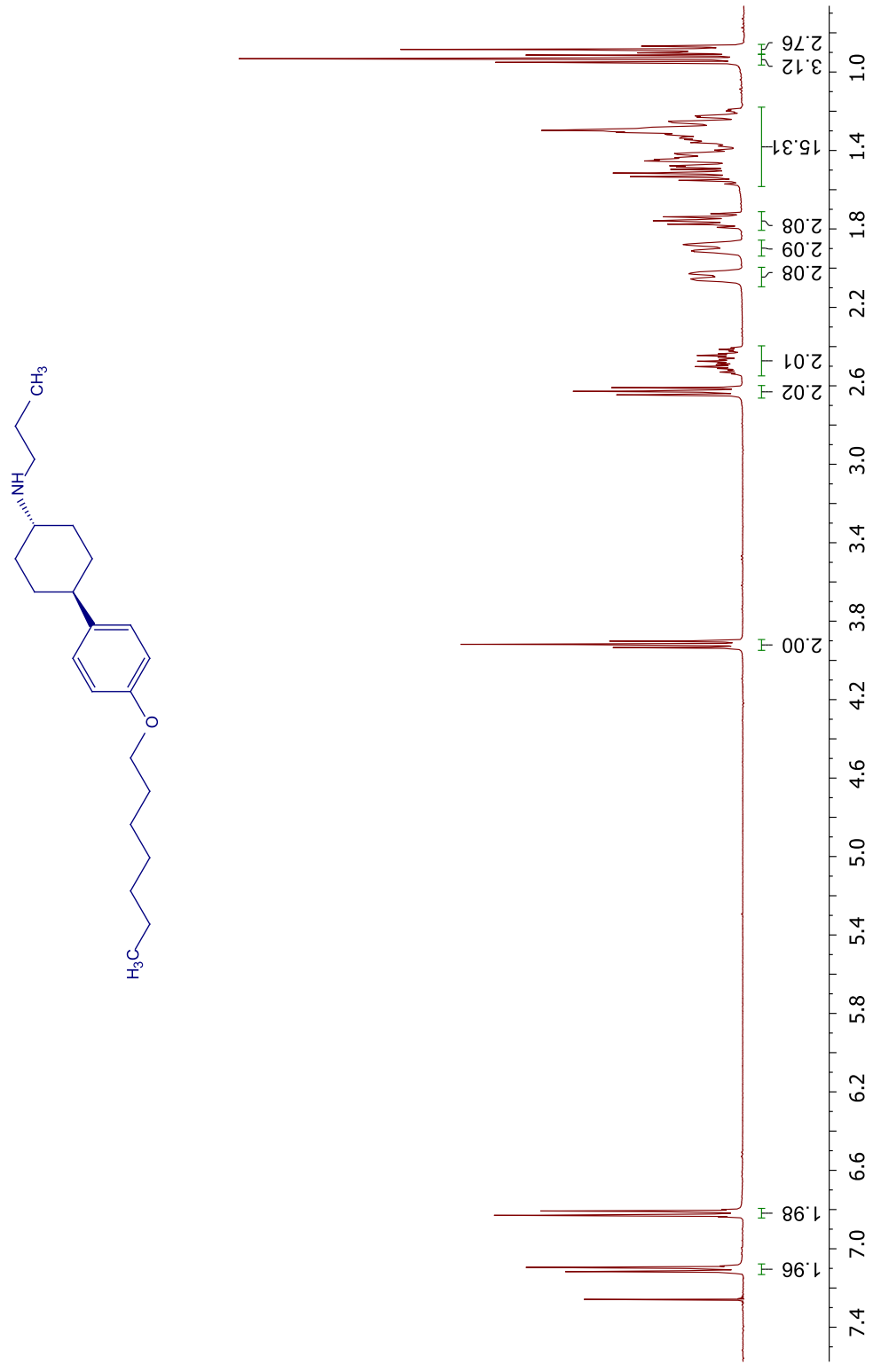

^{13}C NMR spectrum of **21**

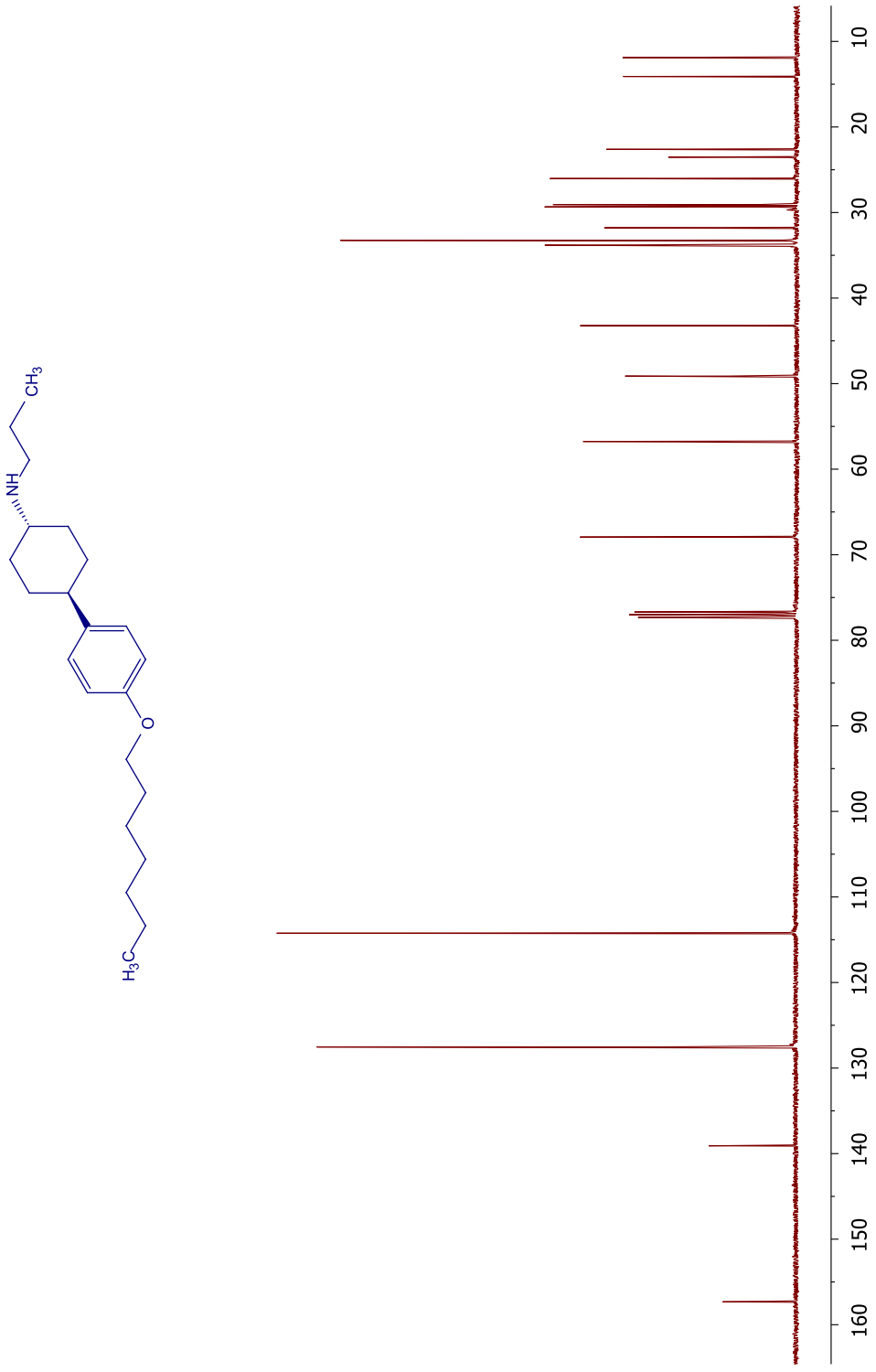

^{1}H NMR spectrum of **22**

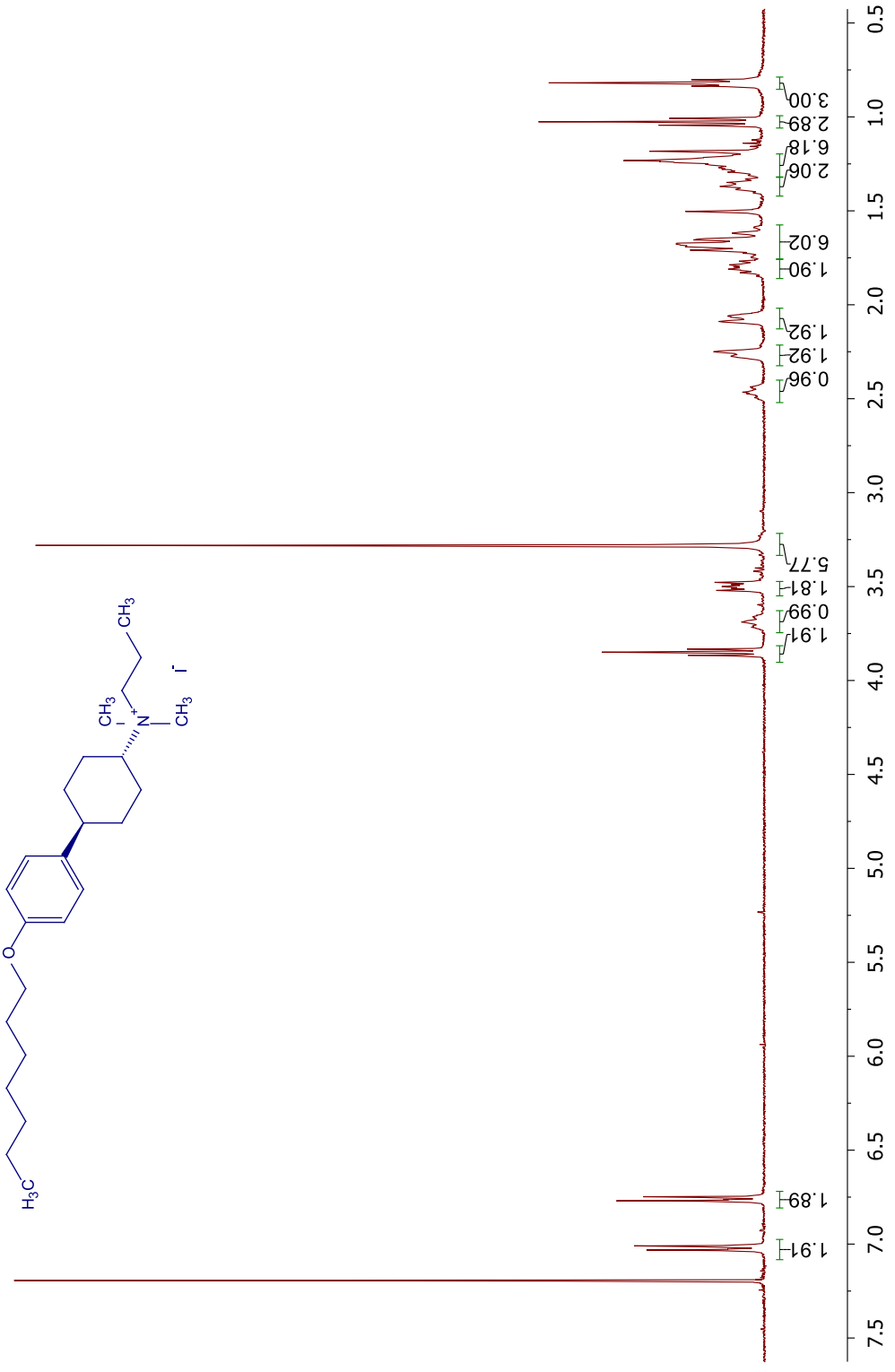

^{13}C NMR spectrum of **22**

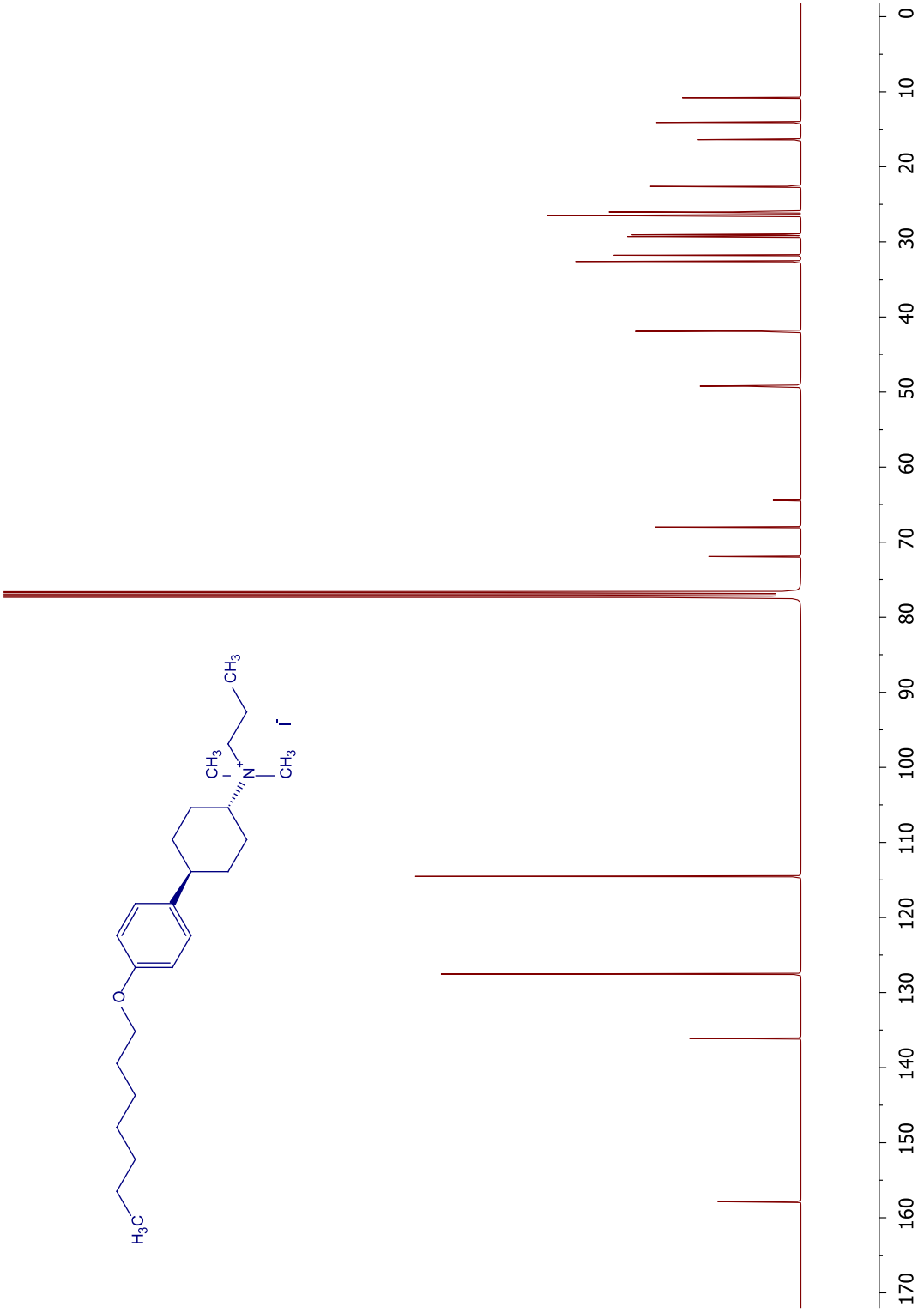

^{1}H NMR spectrum of **23**

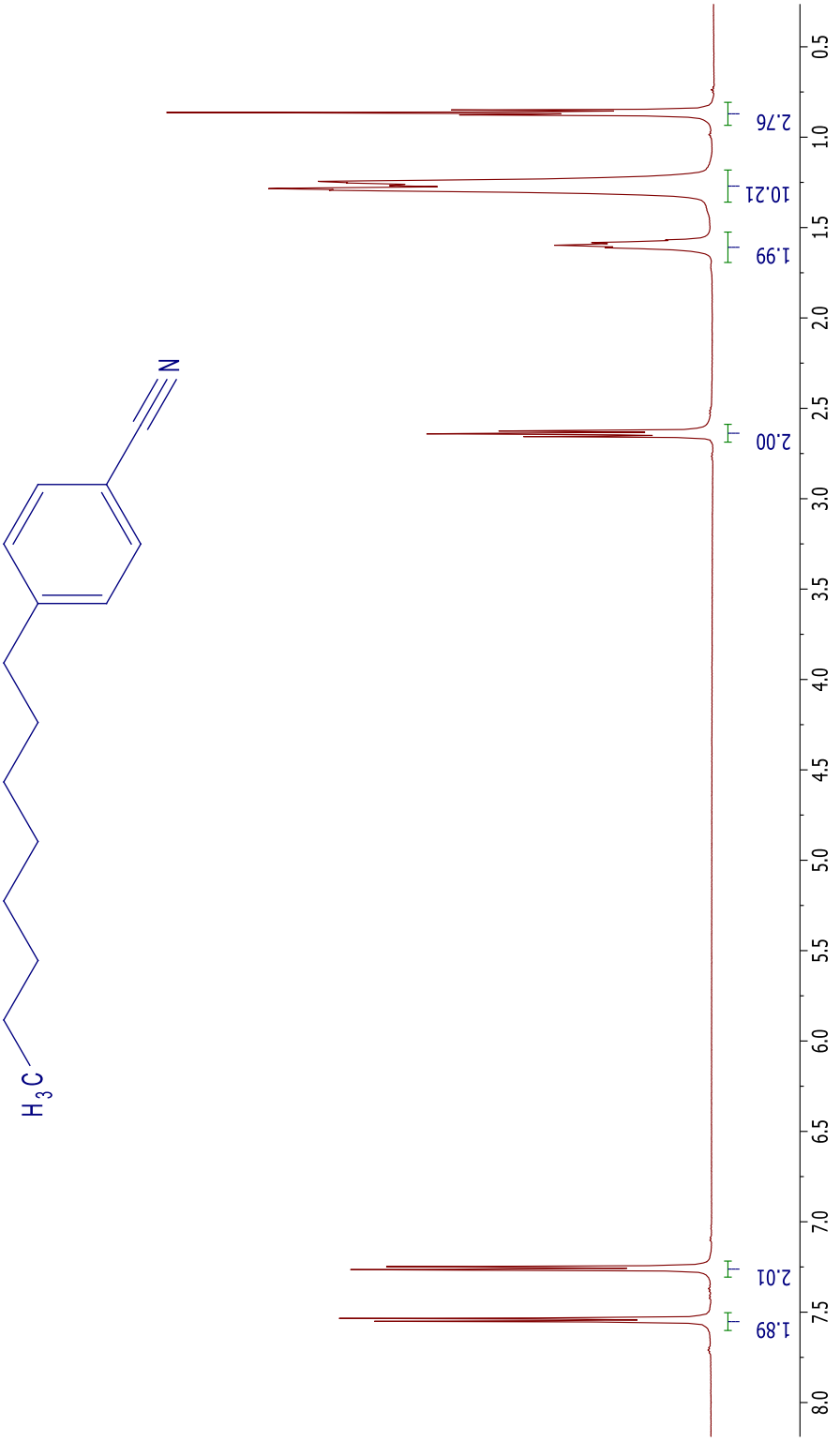

^{13}C NMR spectrum of **23**

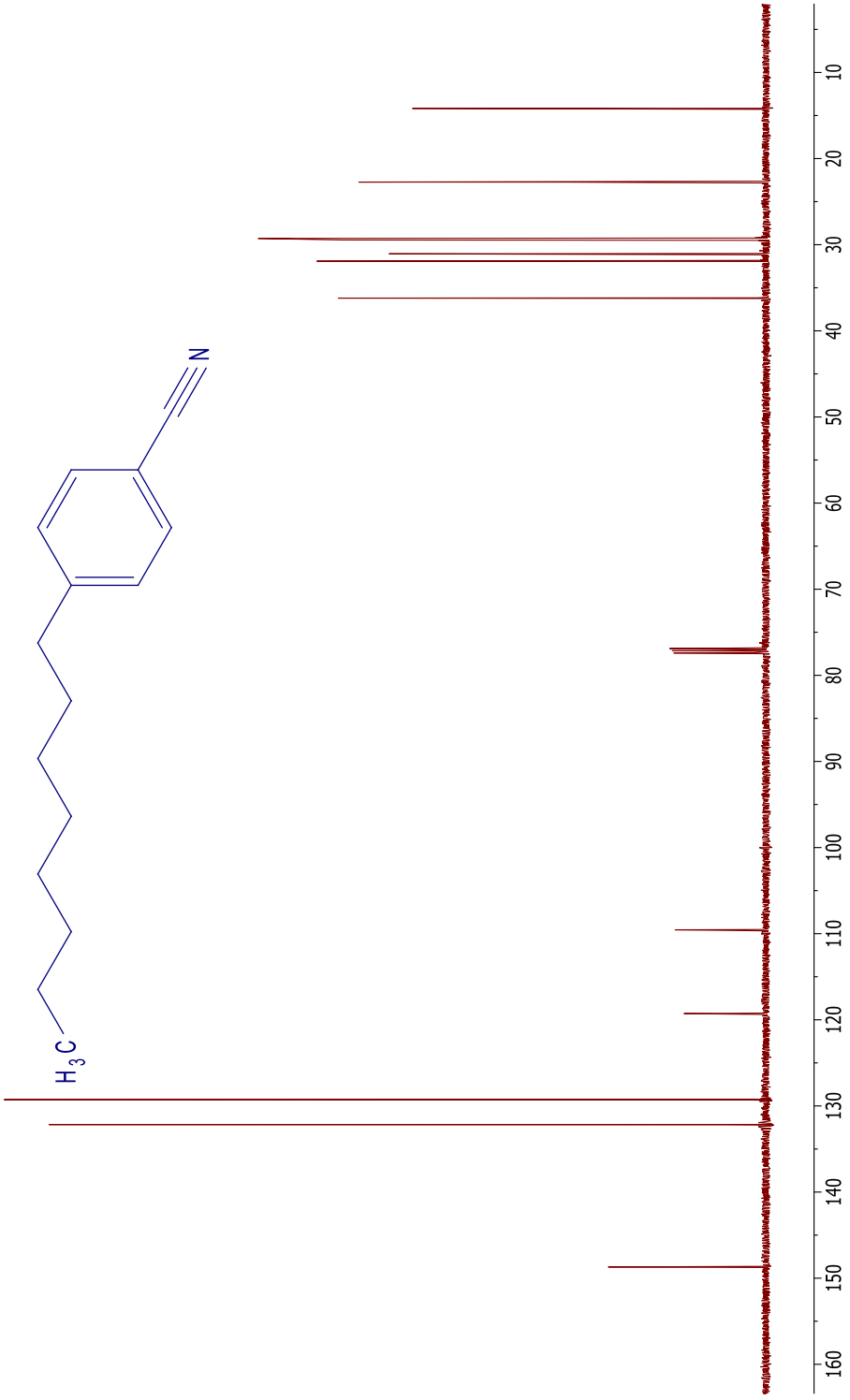

^{1}H NMR spectrum of **25**

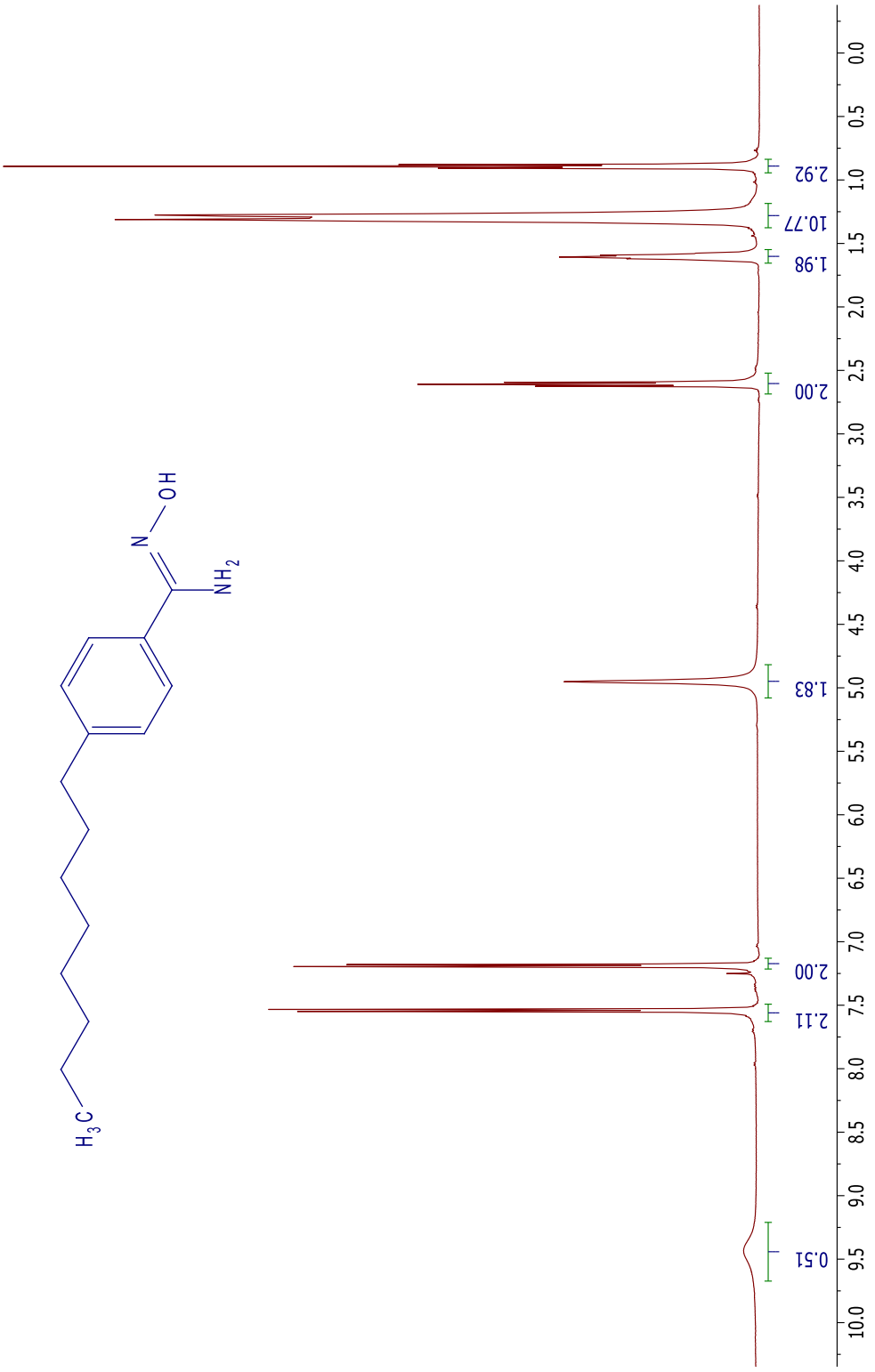

^{13}C NMR spectrum of **25**

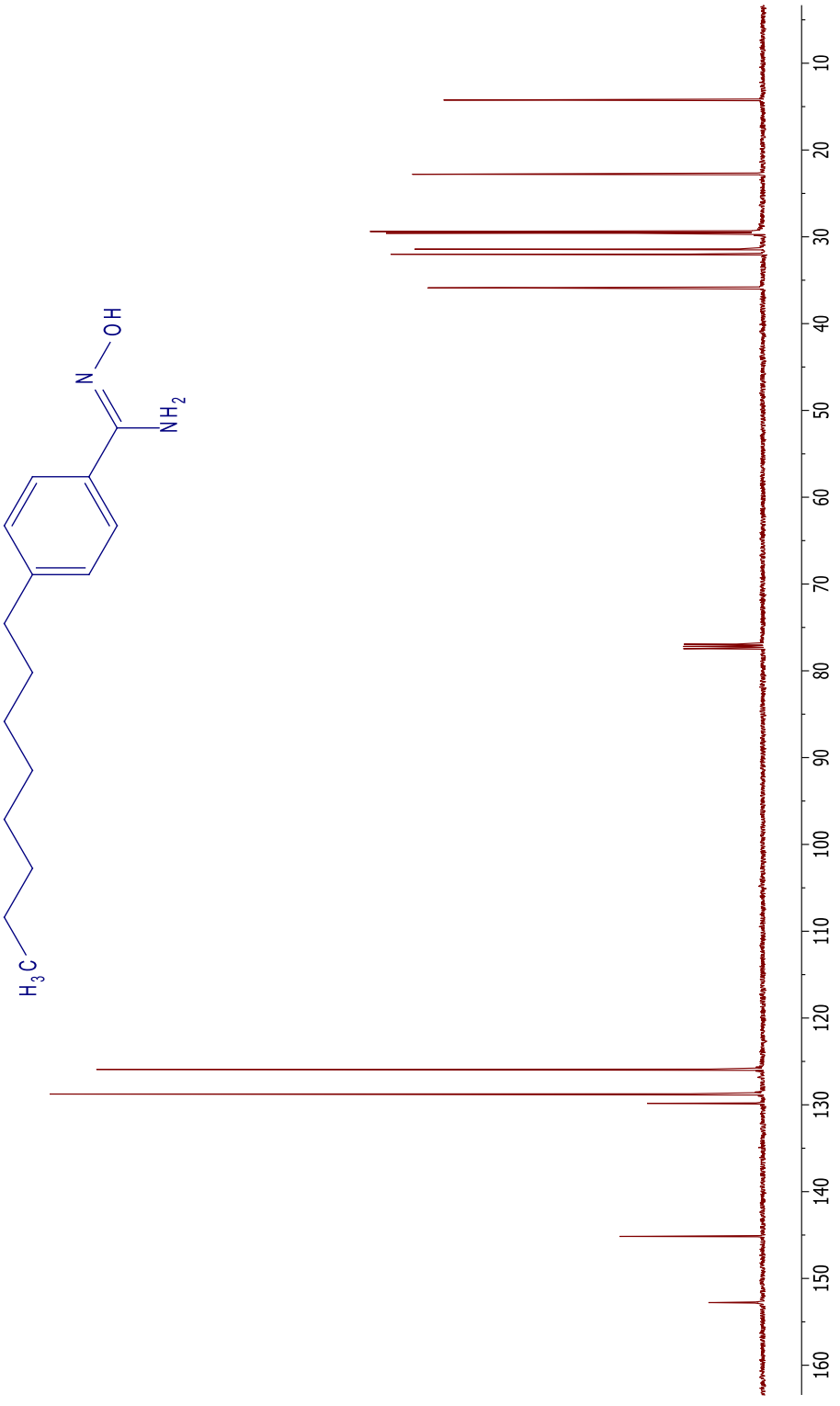

^{1}H NMR spectrum of **26a**

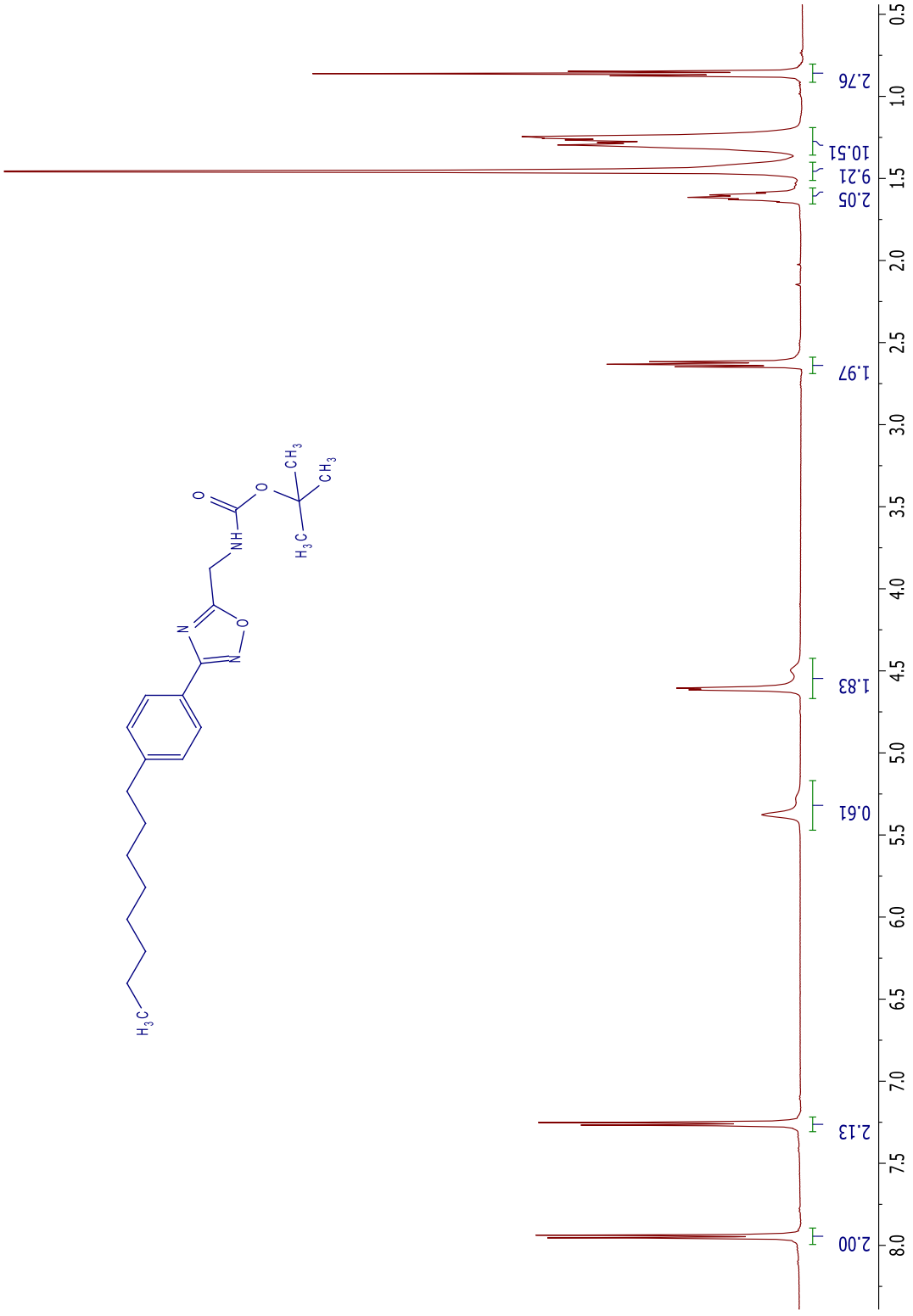

^{13}C NMR spectrum of **26a**

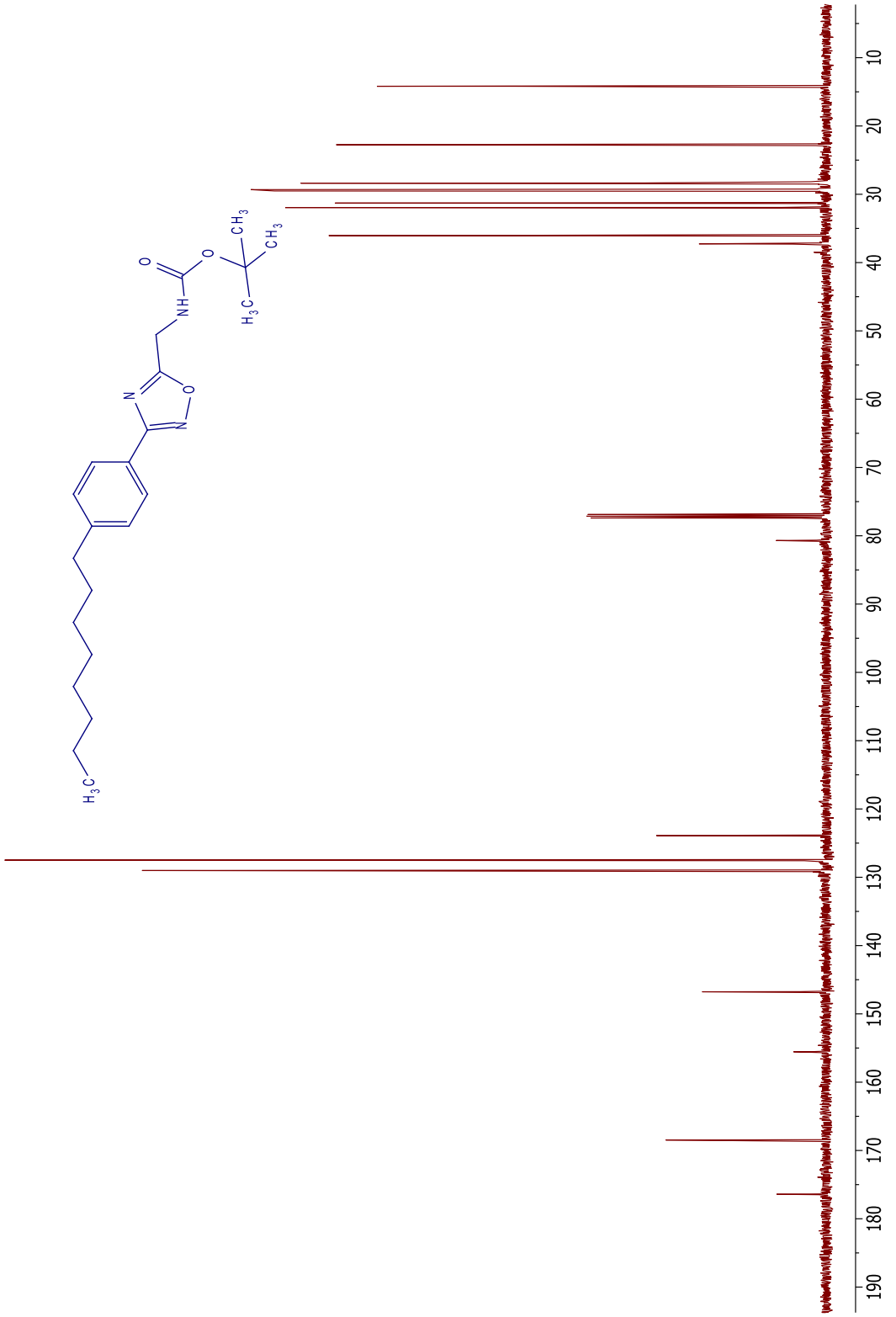

^{1}H NMR spectrum of **26b**

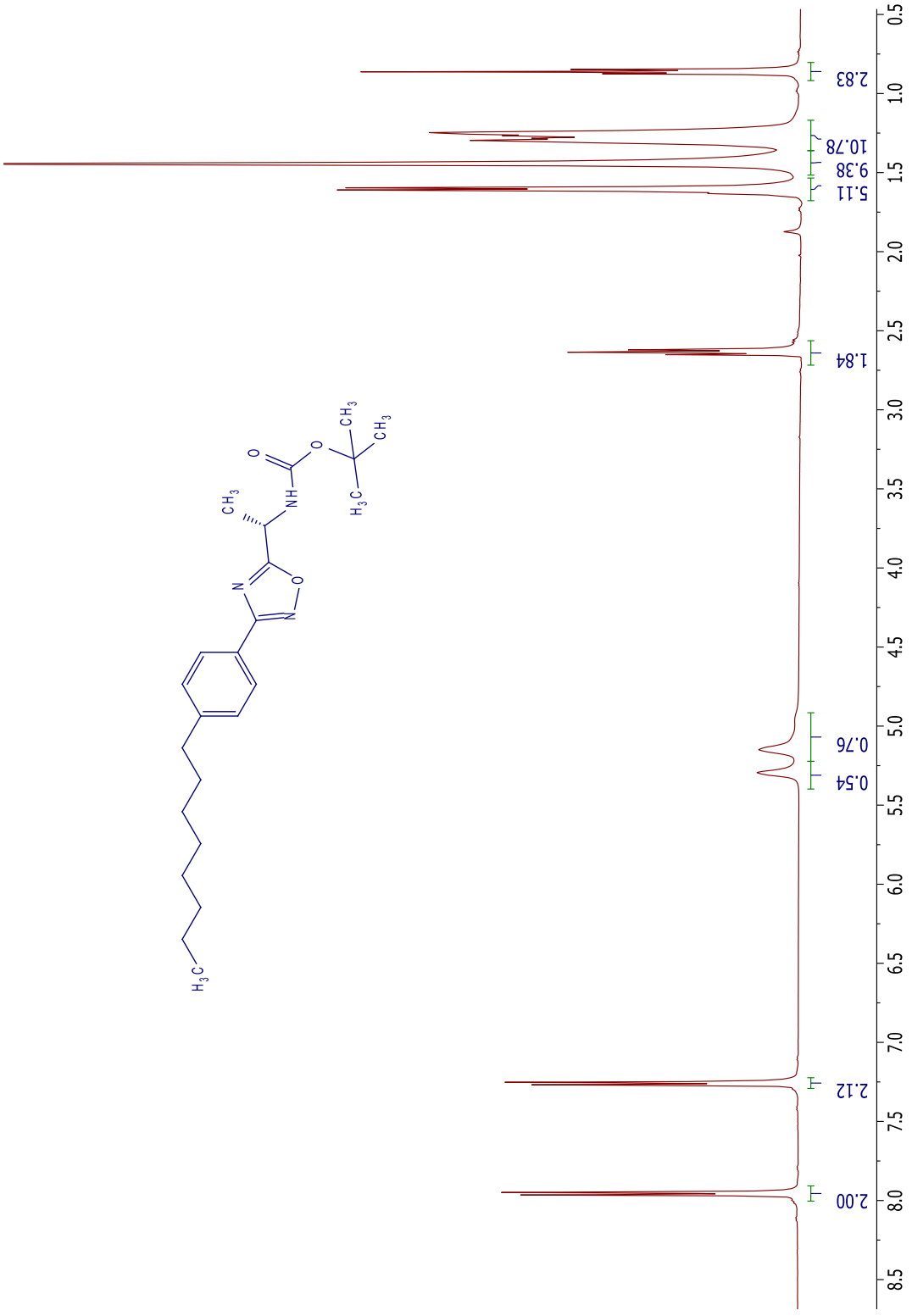

^{13}C NMR spectrum of **26b**

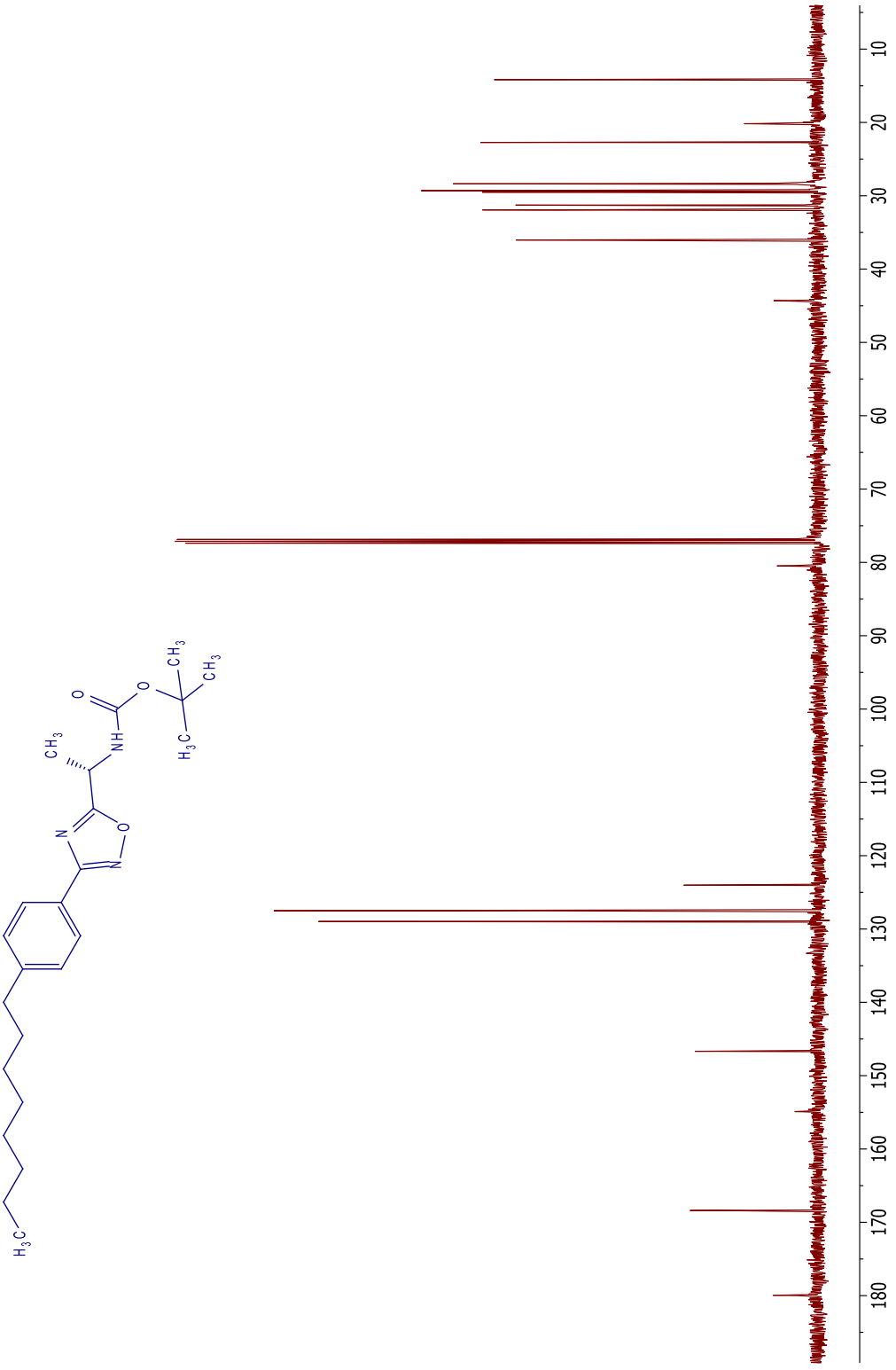

^{1}H NMR spectrum of **26c**

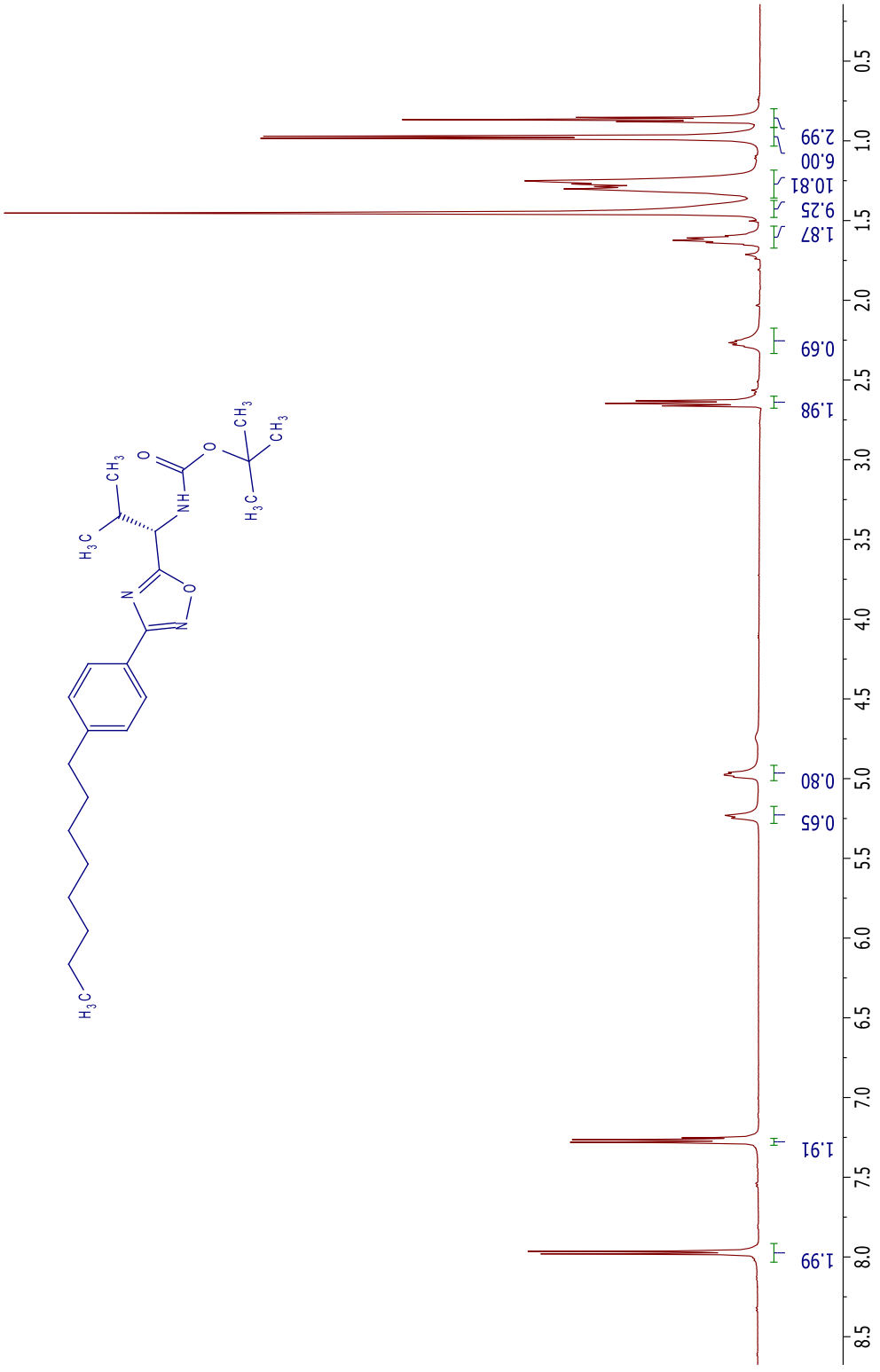

^{13}C NMR spectrum of **26c**

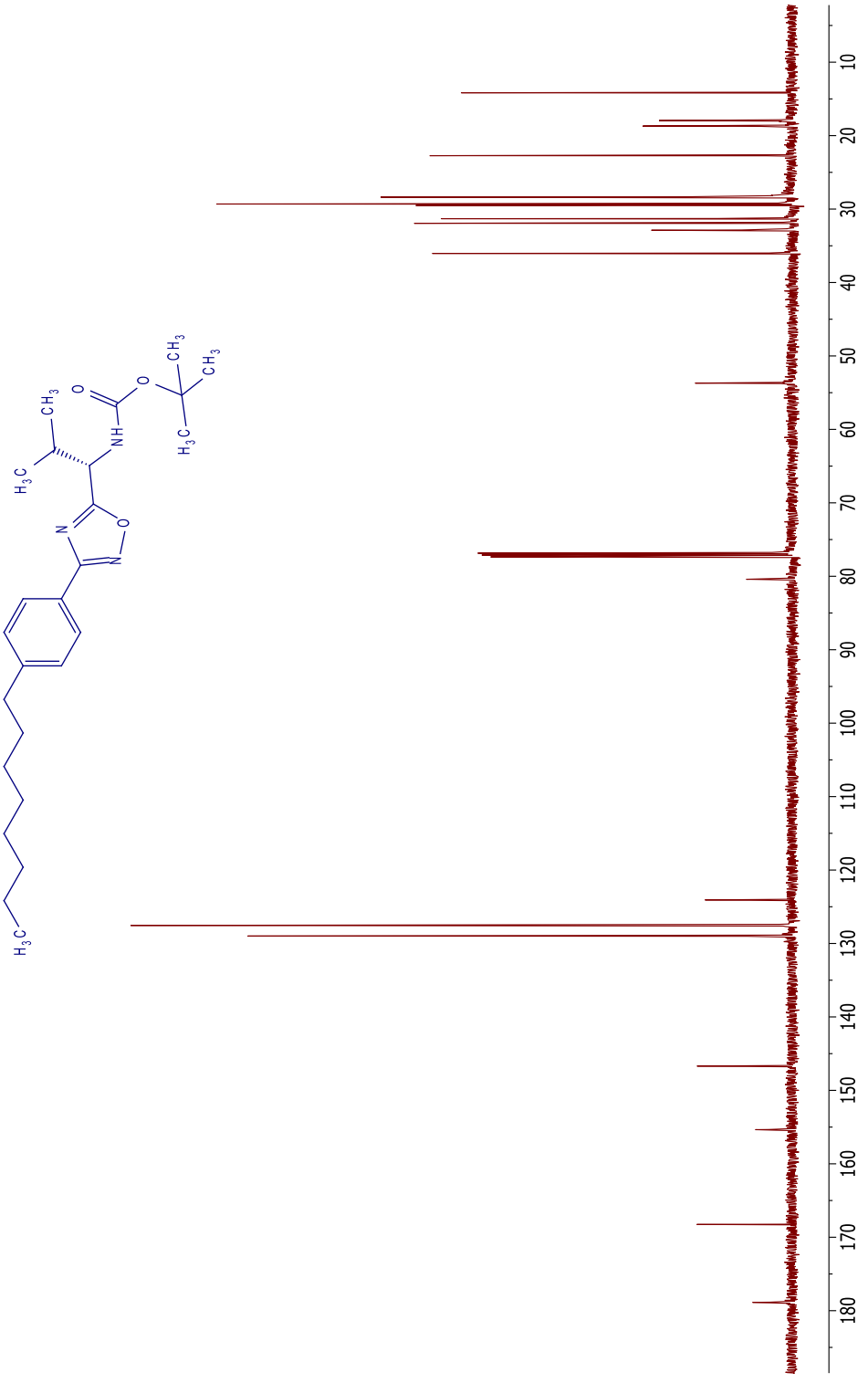

^{1}H NMR spectrum of **30a**

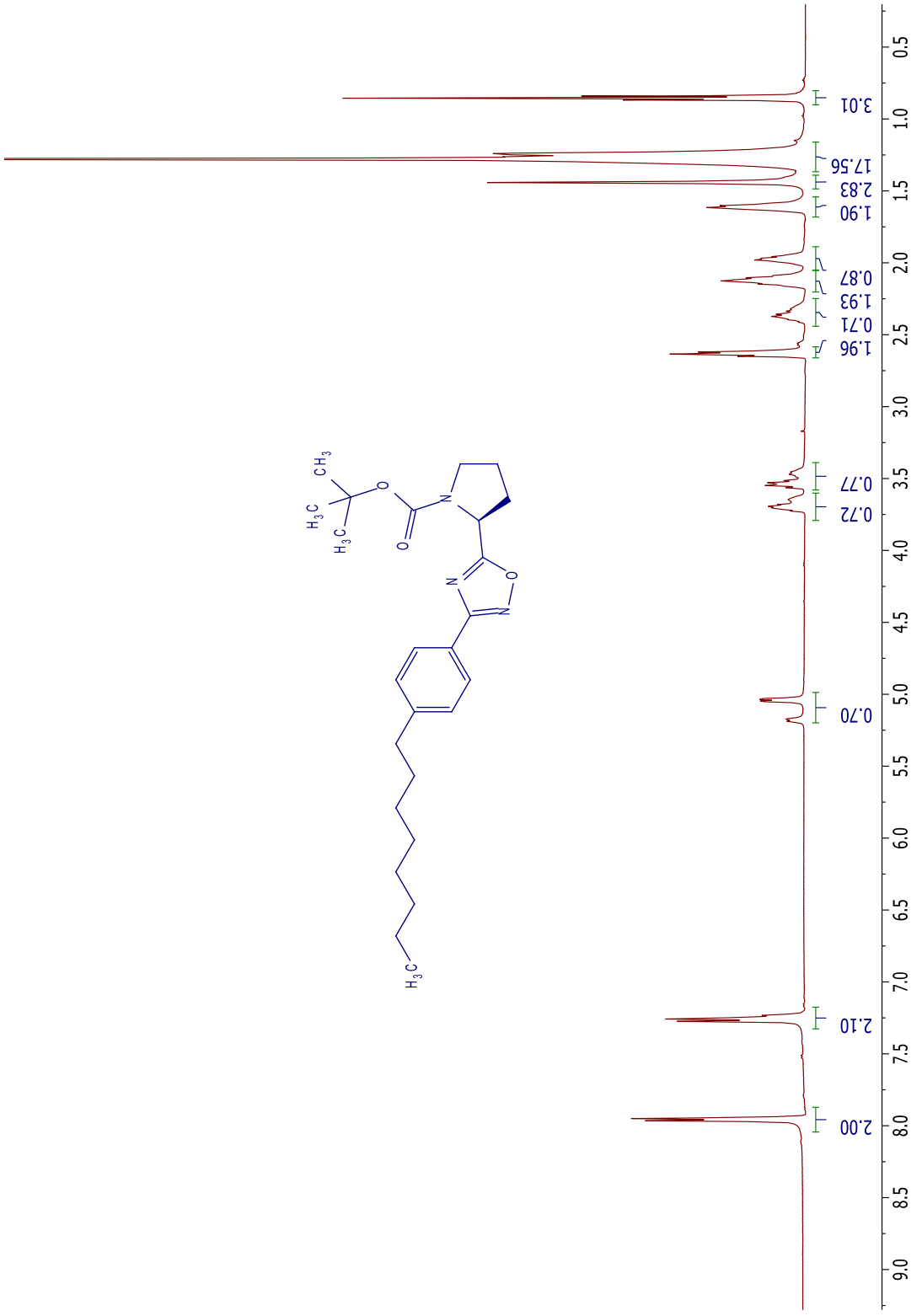

^{13}C NMR spectrum of **30a**

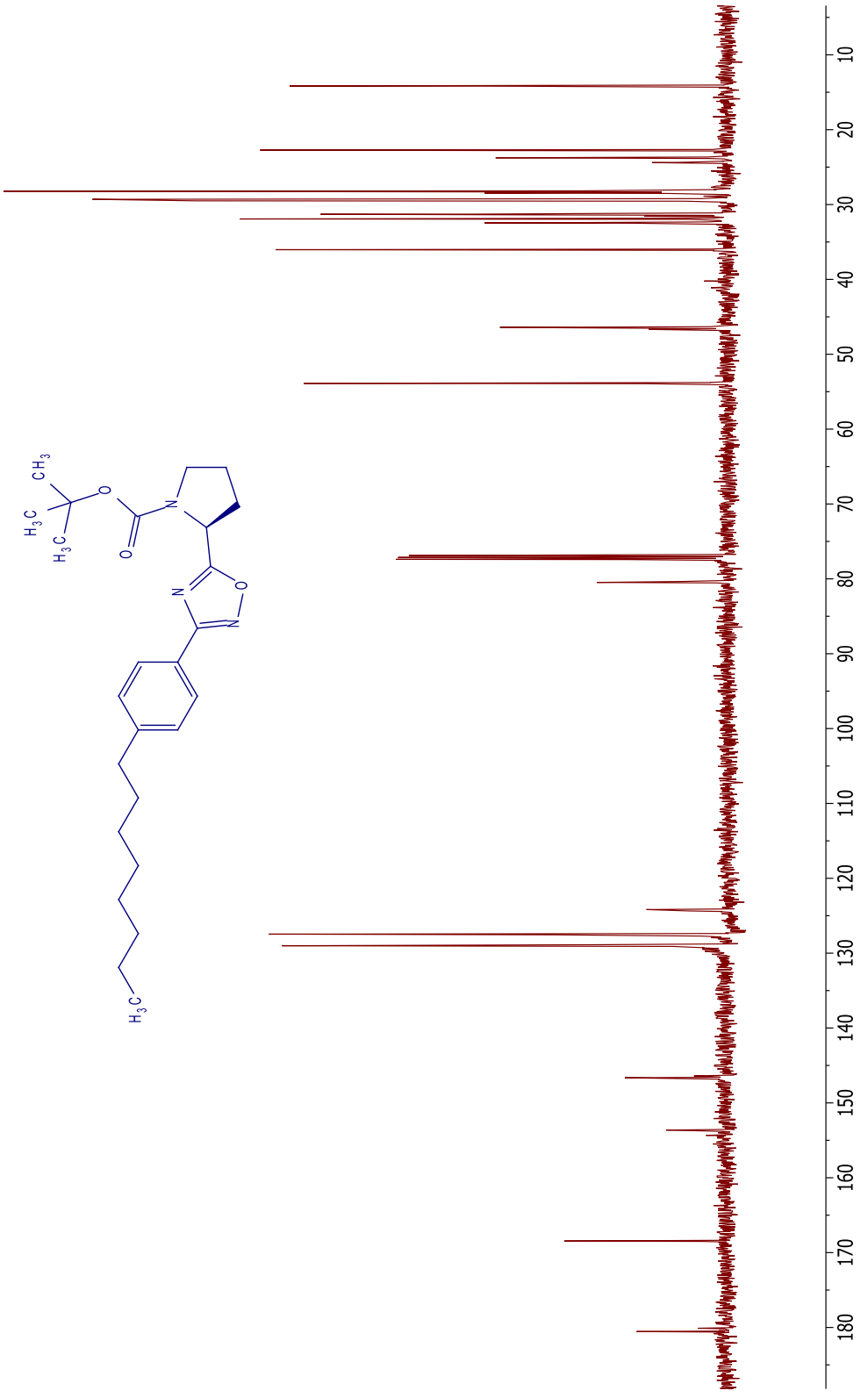

^{1}H NMR spectrum of **30b**

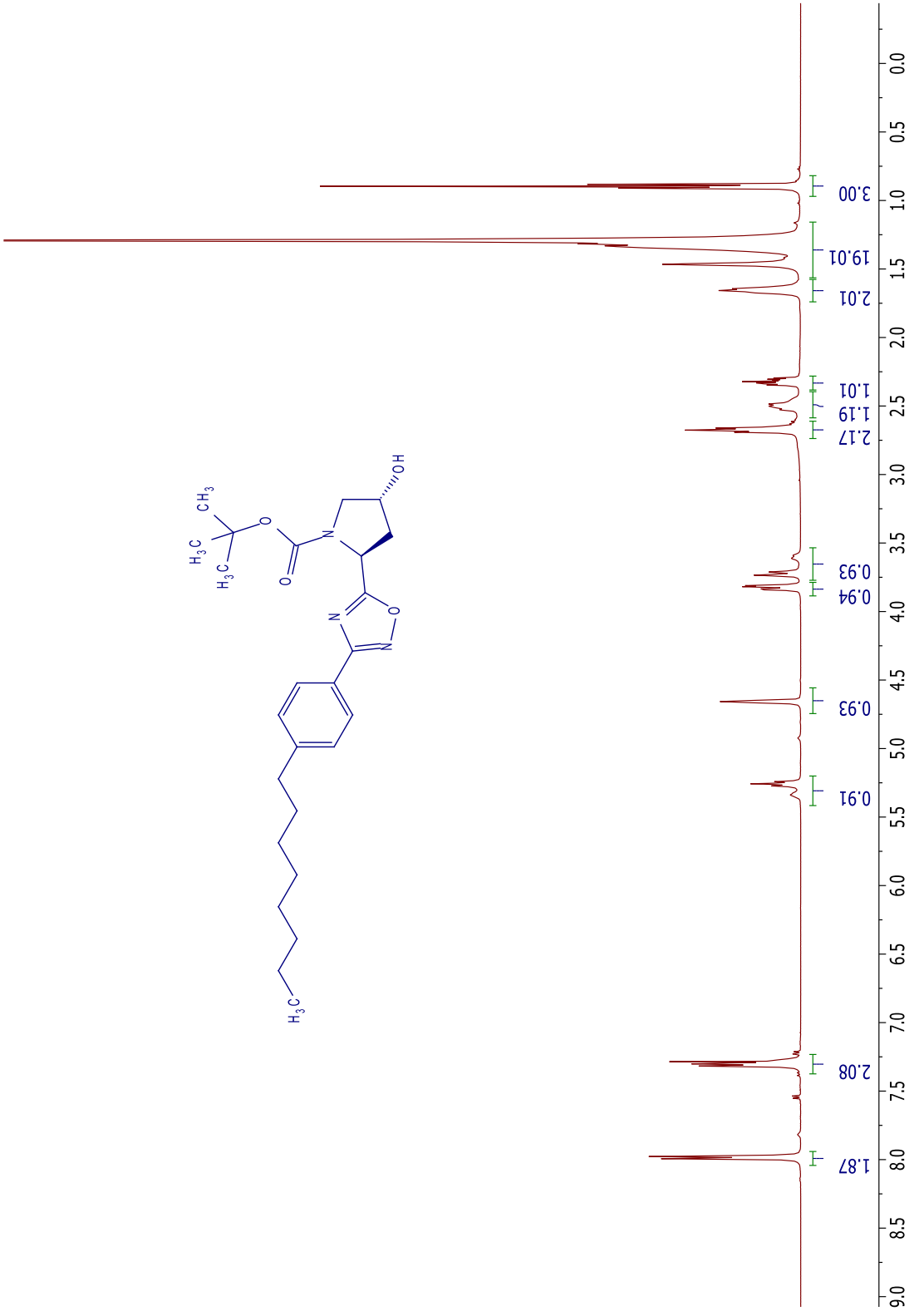

^{13}C NMR spectrum of **30b**

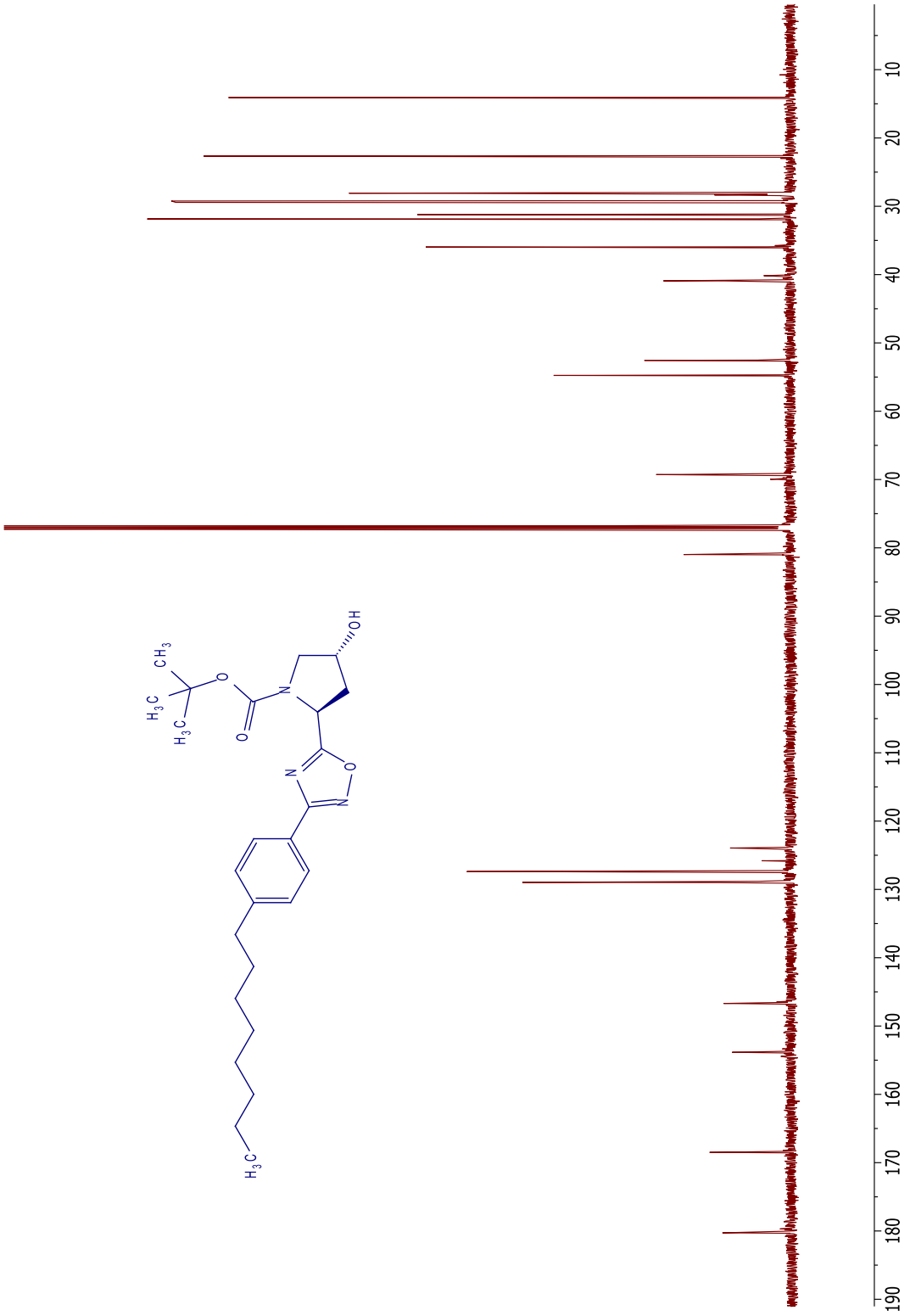

^{1}H NMR spectrum of **27a**

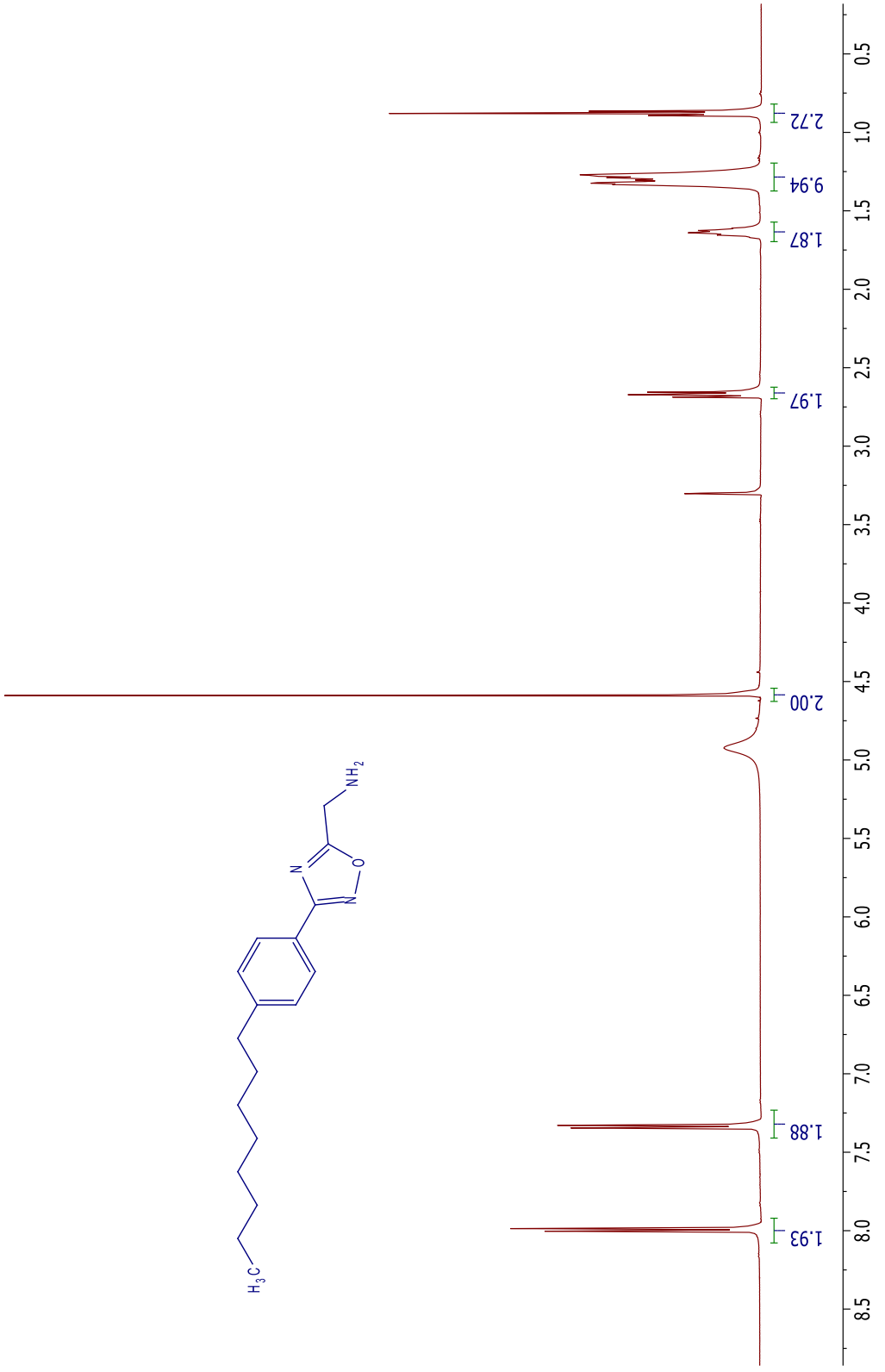

^{13}C NMR spectrum of **27a**

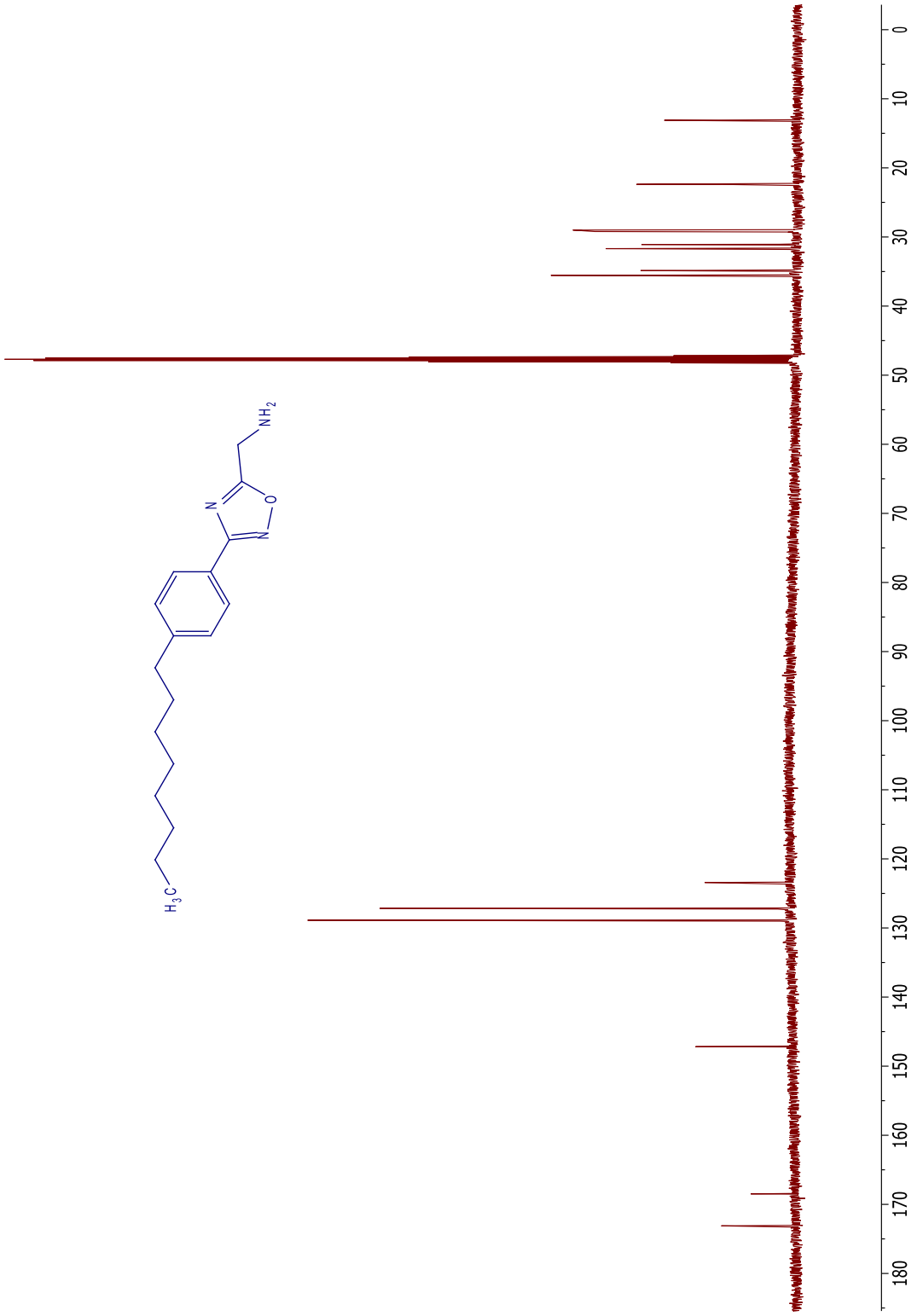

^{1}H NMR spectrum of **27b**

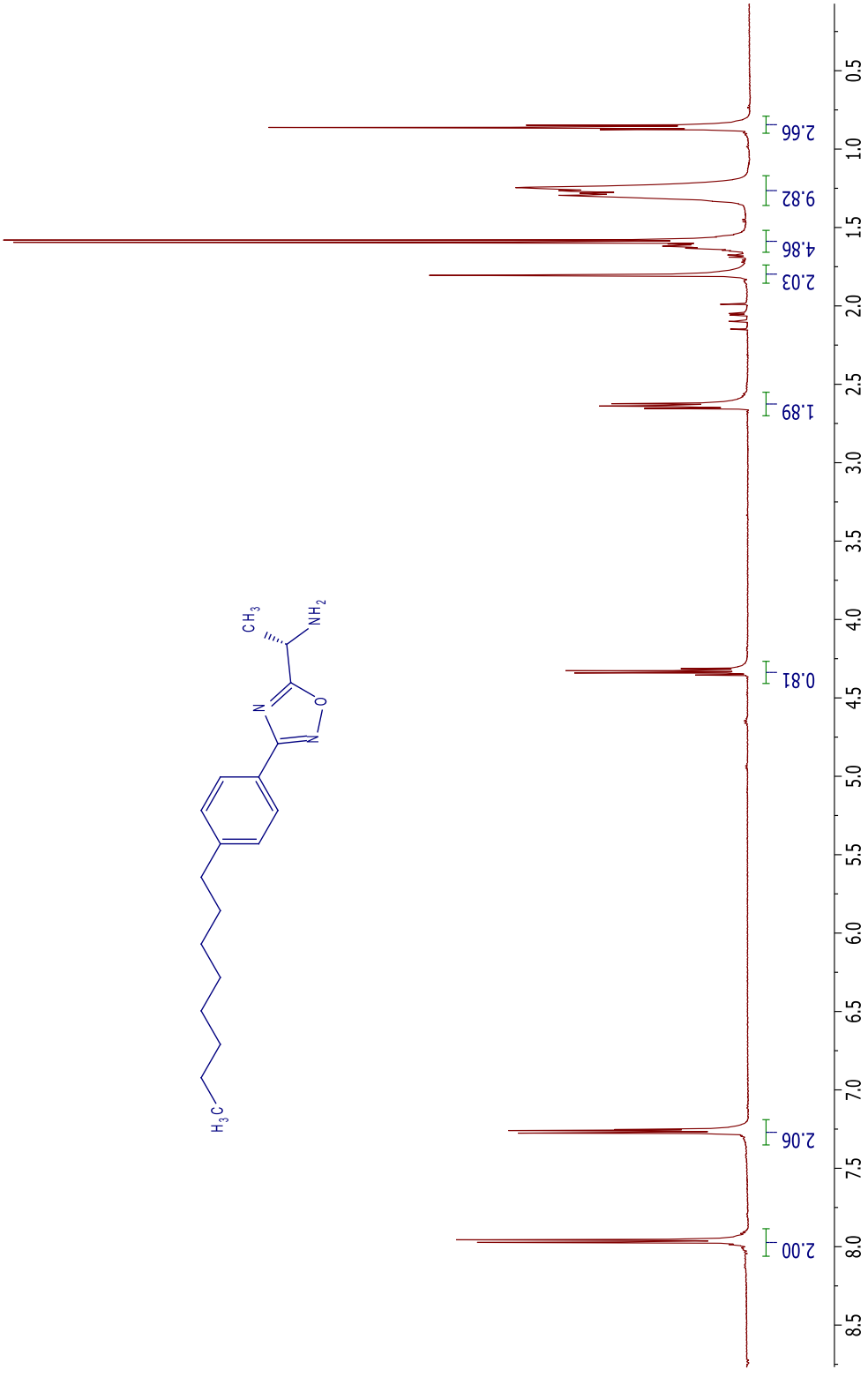

^{13}C NMR spectrum of **27b**

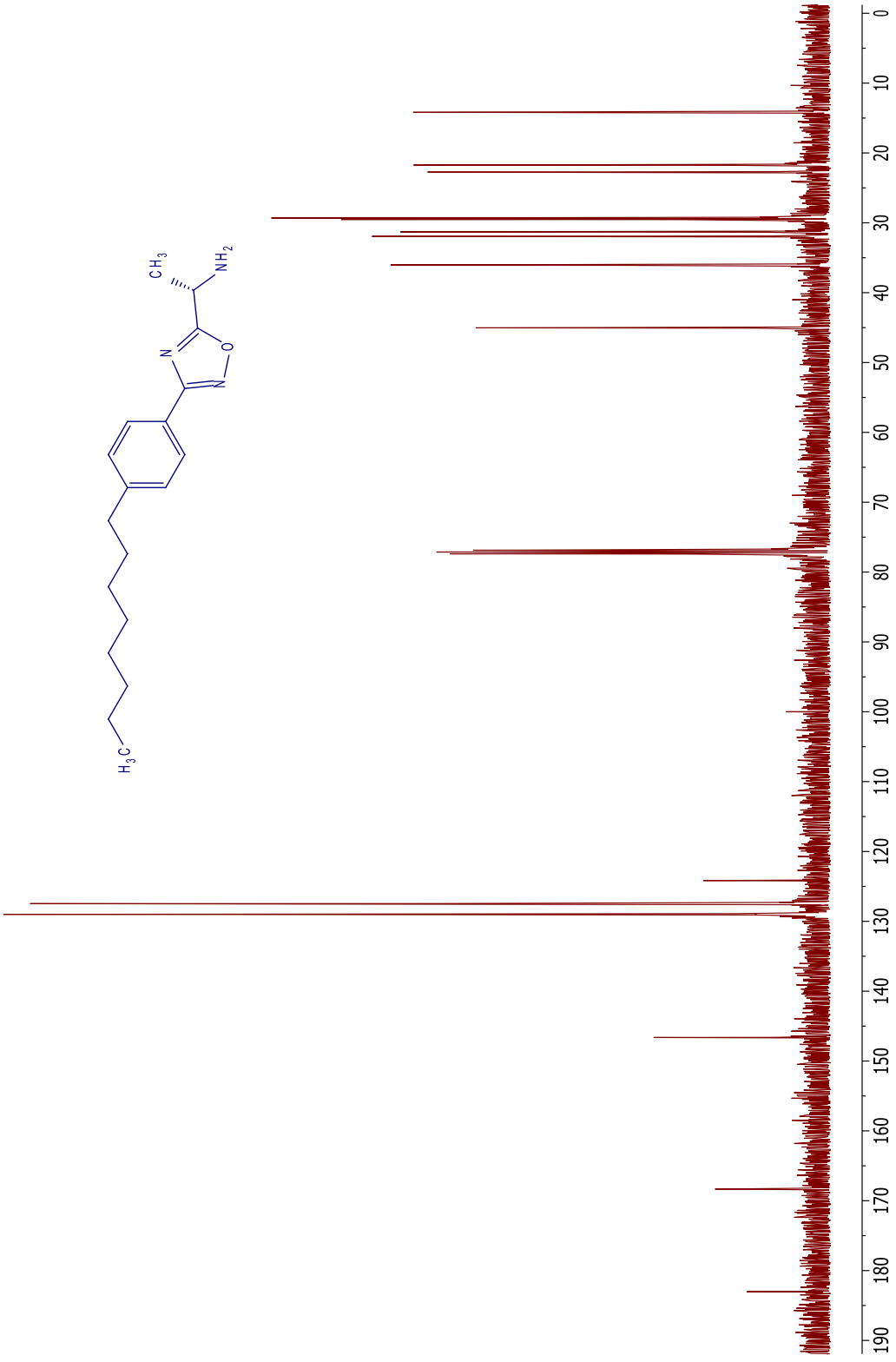

^{1}H NMR spectrum of **27c**

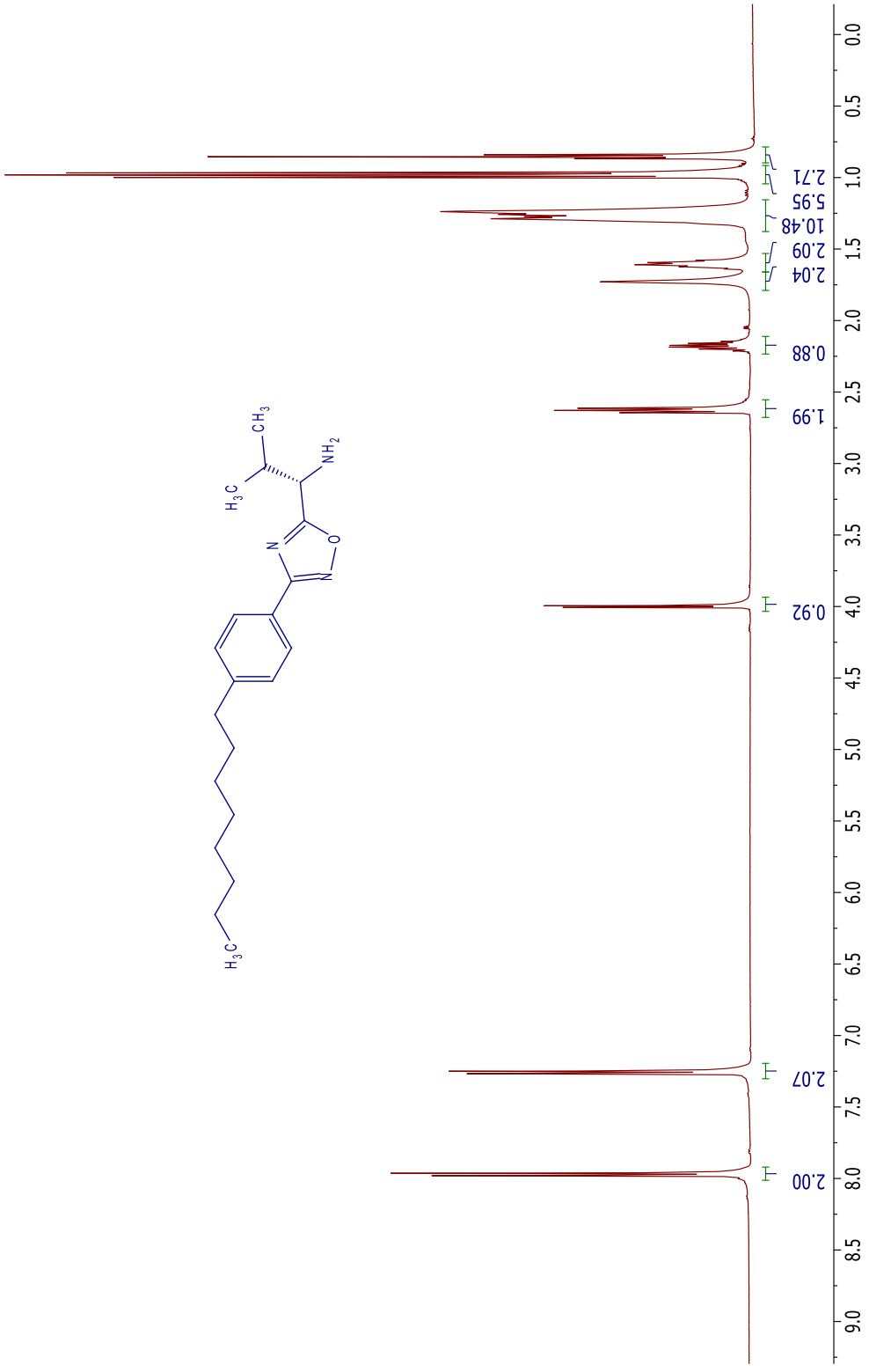

^{13}C NMR spectrum of **27c**

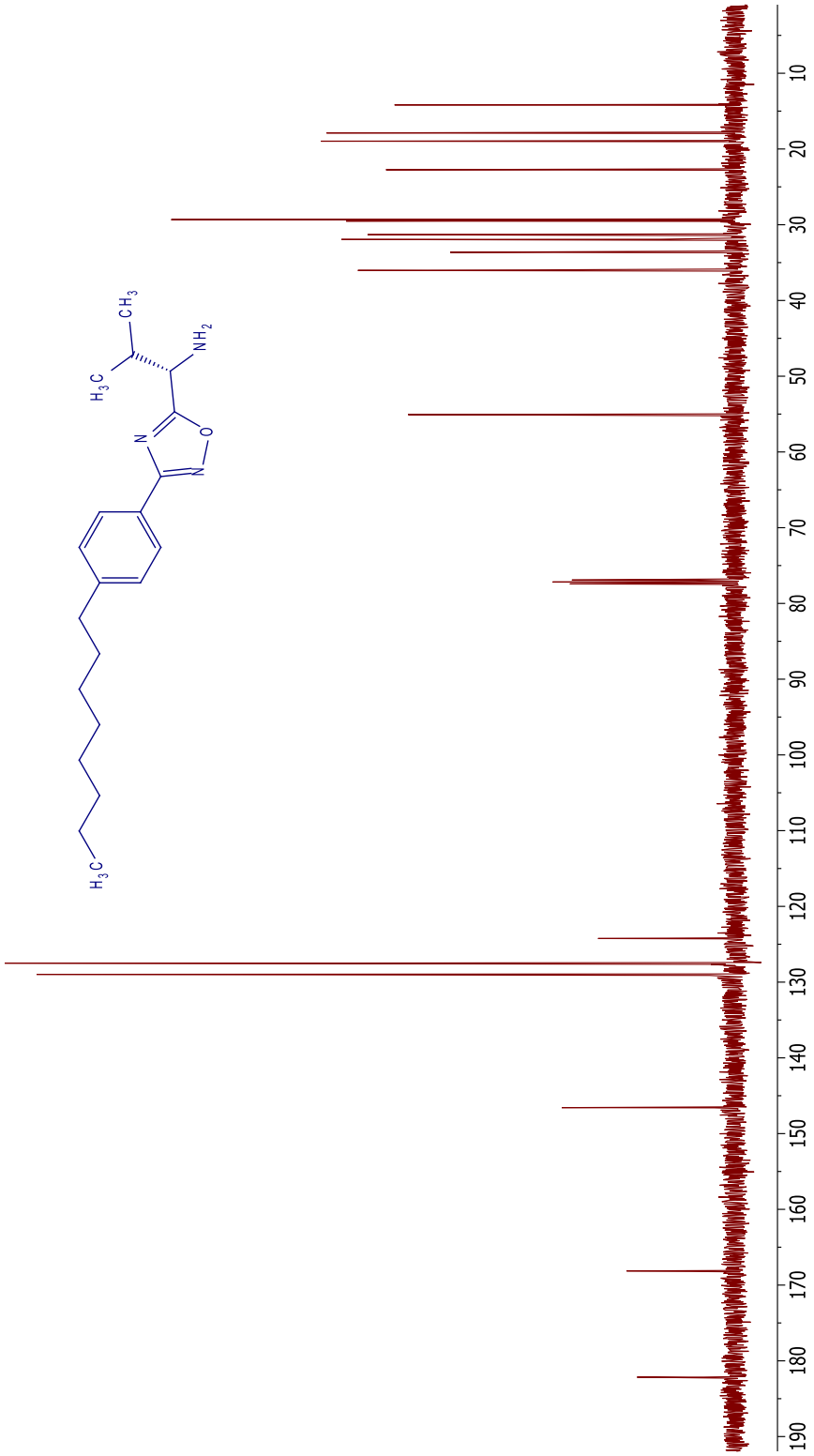

^{1}H NMR spectrum of **31a**

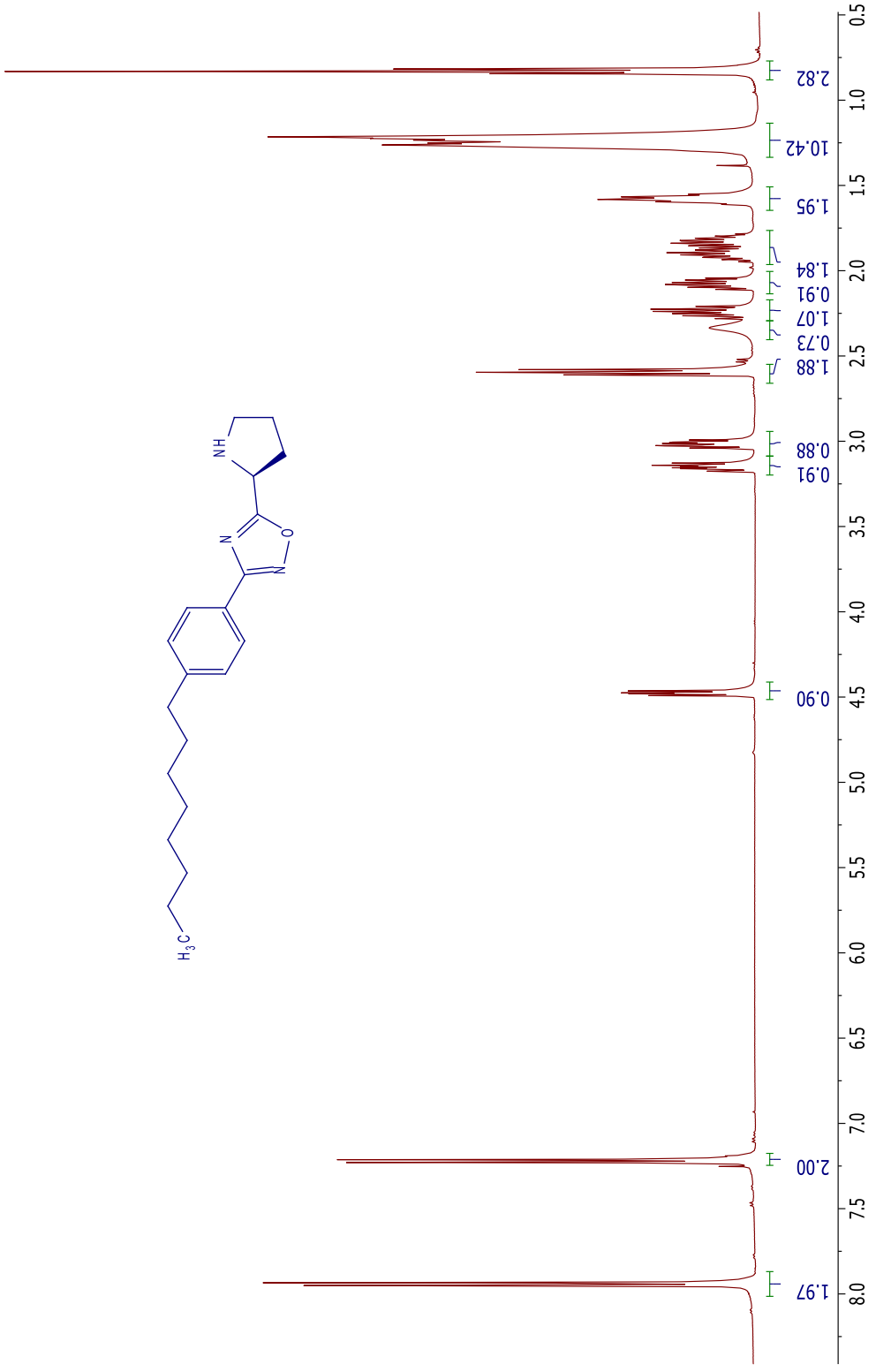

^{13}C NMR spectrum of **31a**

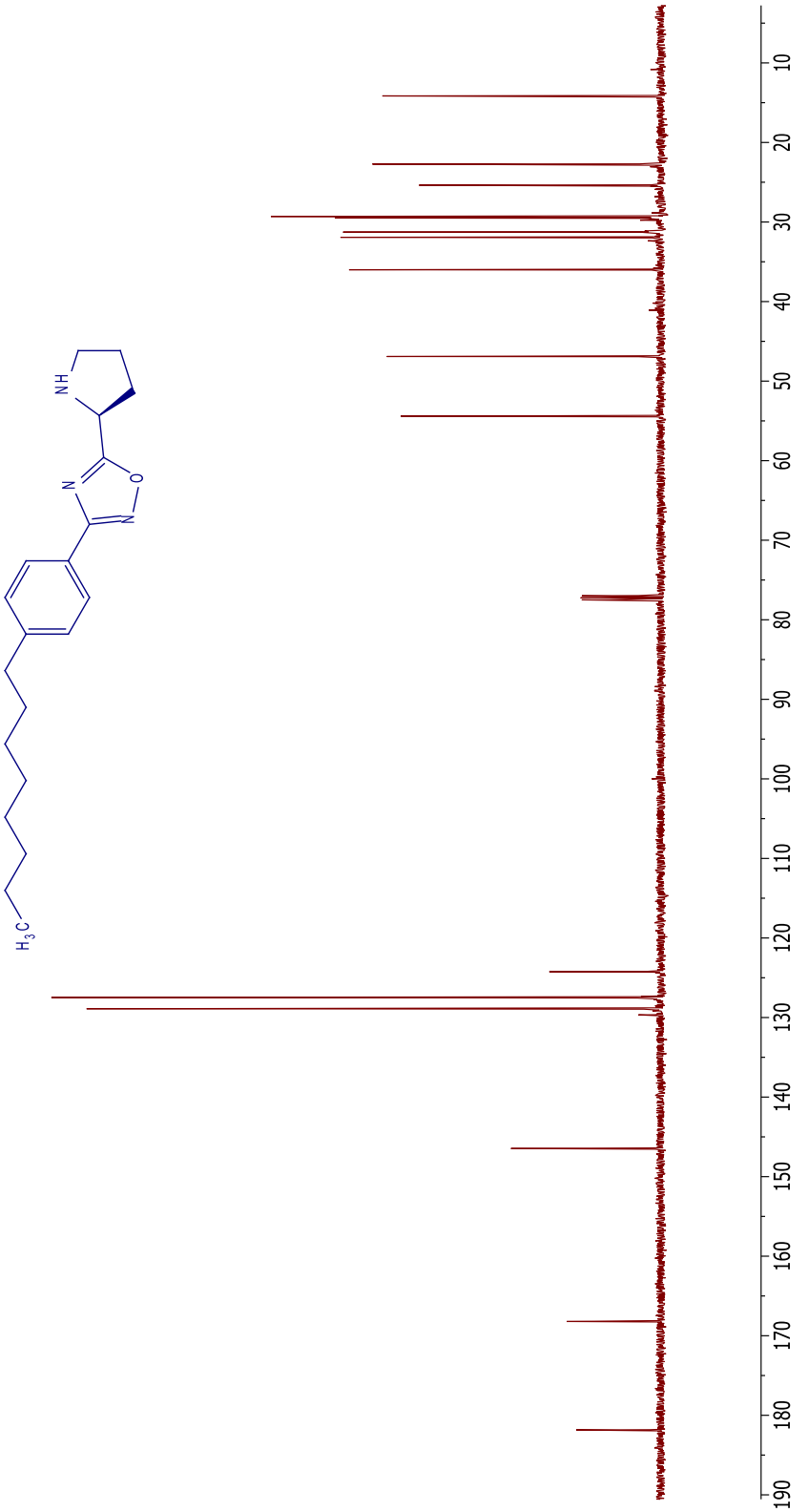

^{1}H NMR spectrum of **31b**

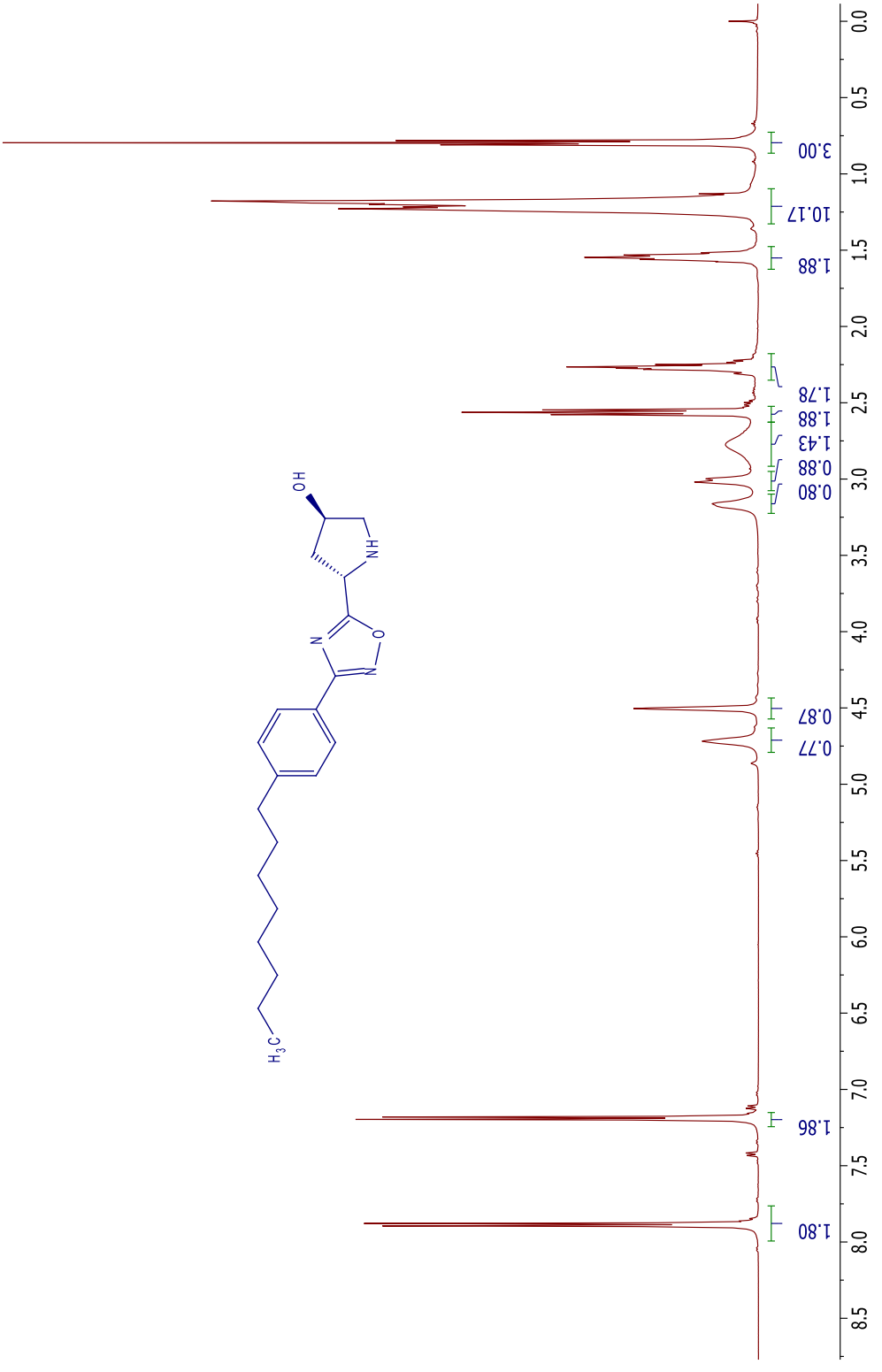

^{13}C NMR spectrum of **31b**

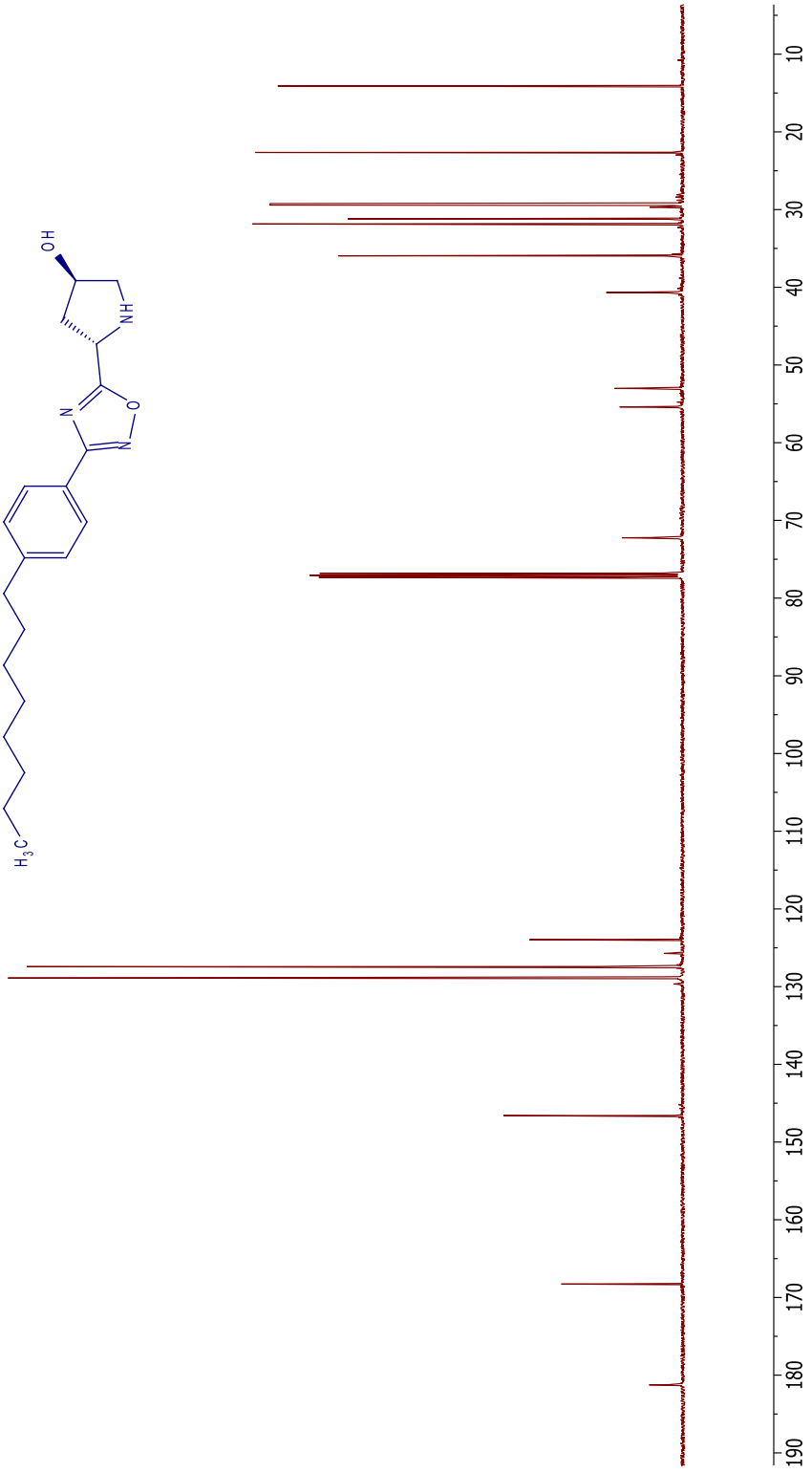

^{1}H NMR spectrum of **28a**

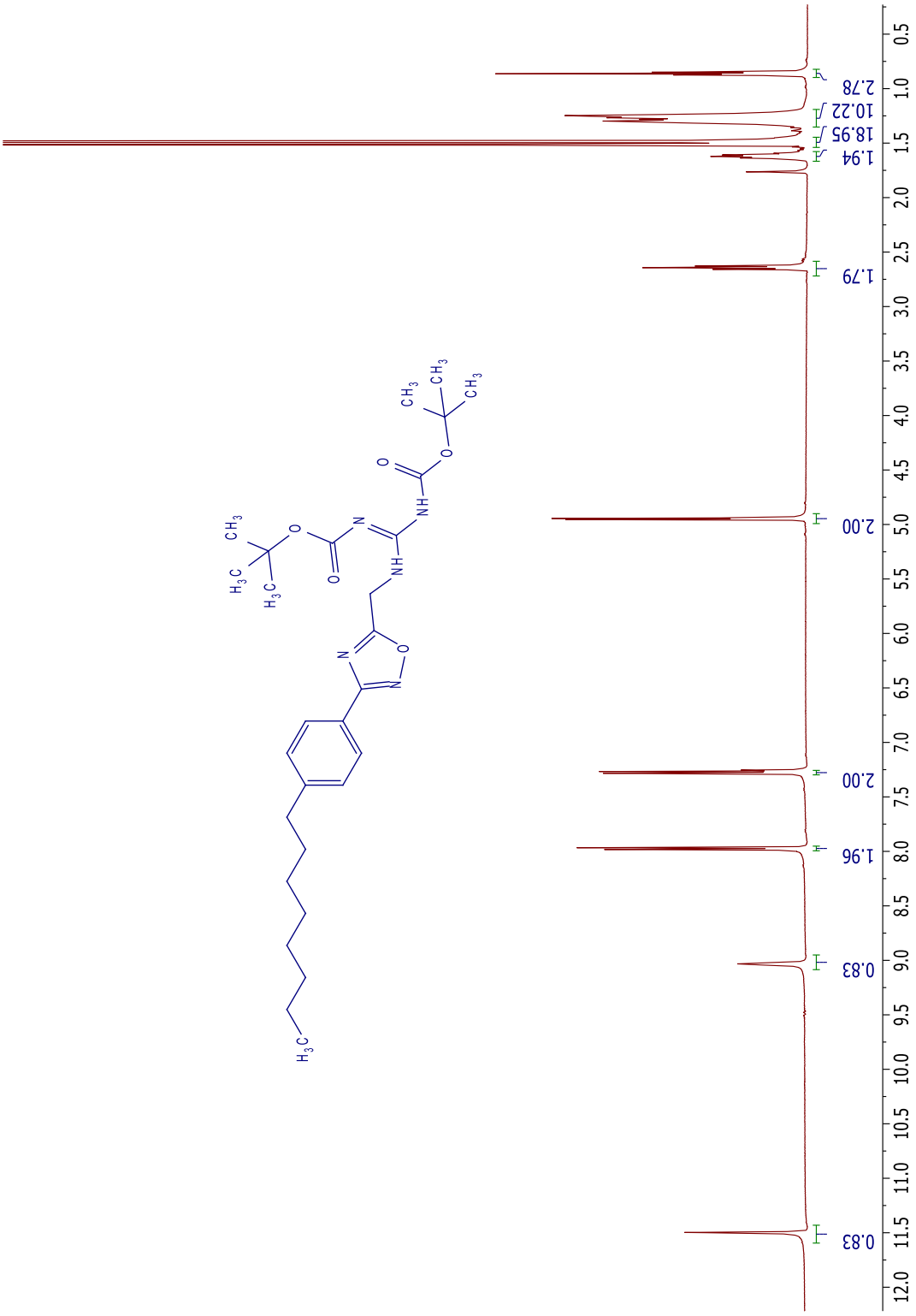

^{13}C NMR spectrum of **28a**

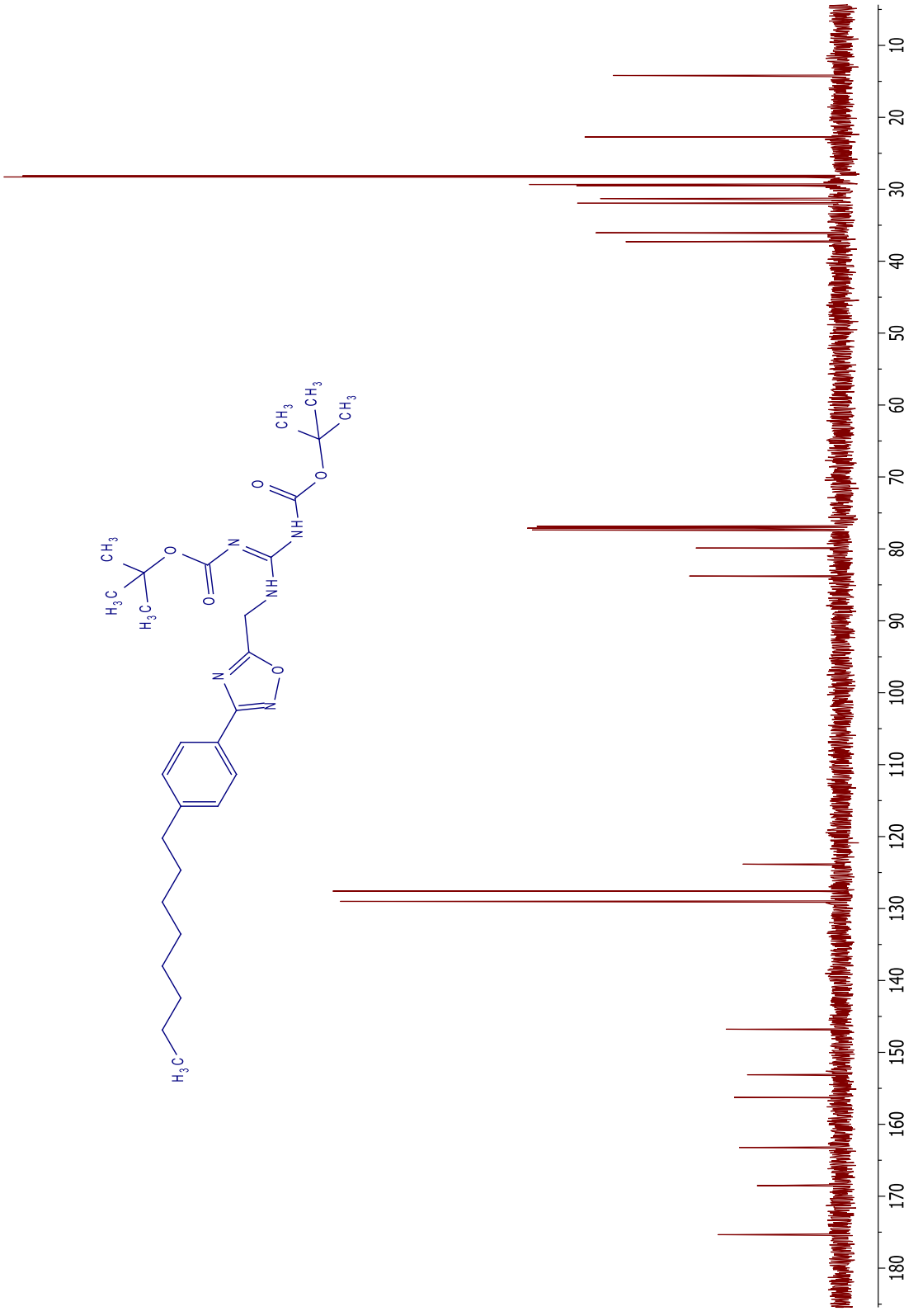

^{1}H NMR spectrum of **28b**

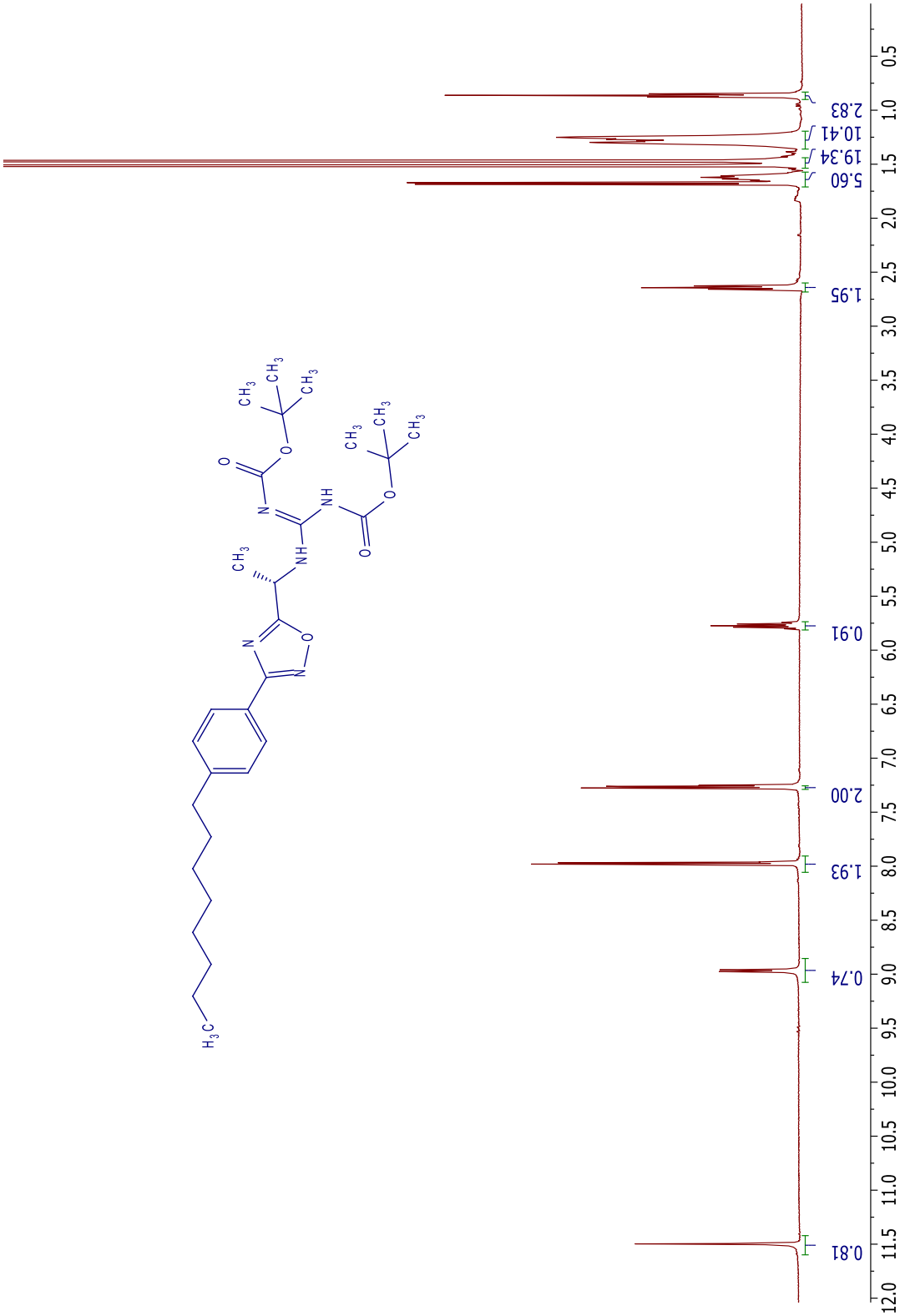

^{13}C NMR spectrum of **28b**

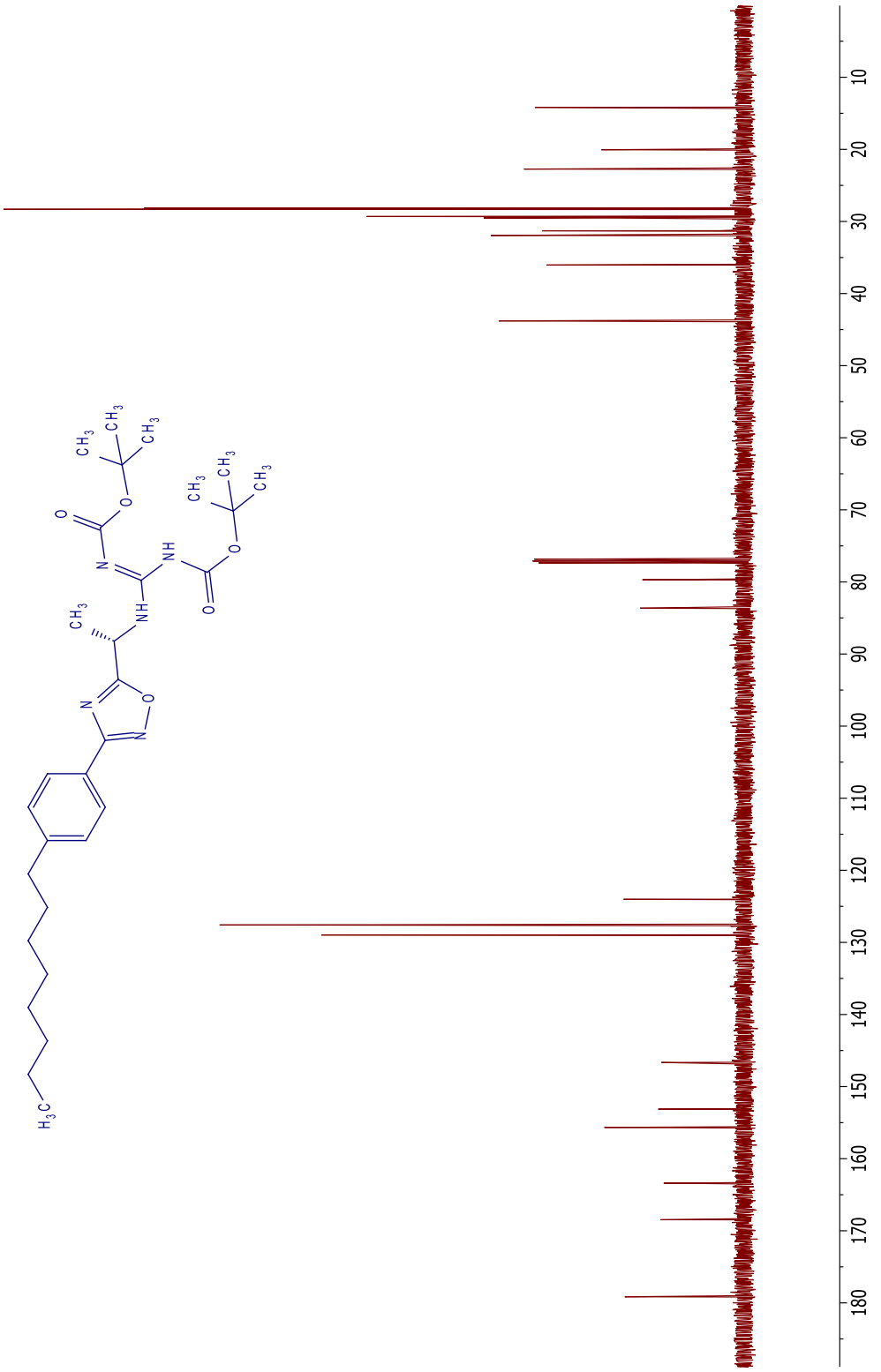

^{1}H NMR spectrum of **28c**

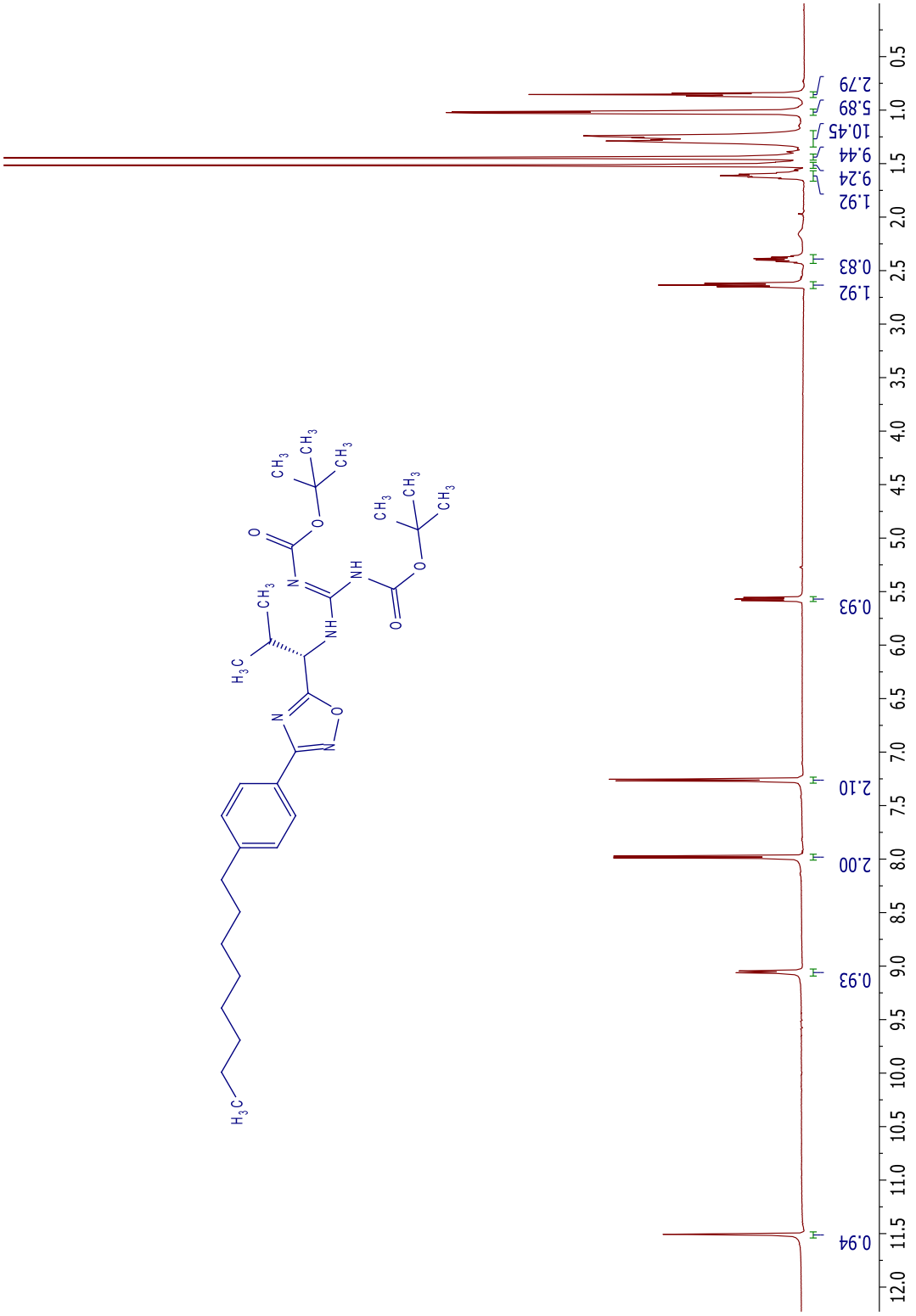

^{13}C NMR spectrum of **28c**

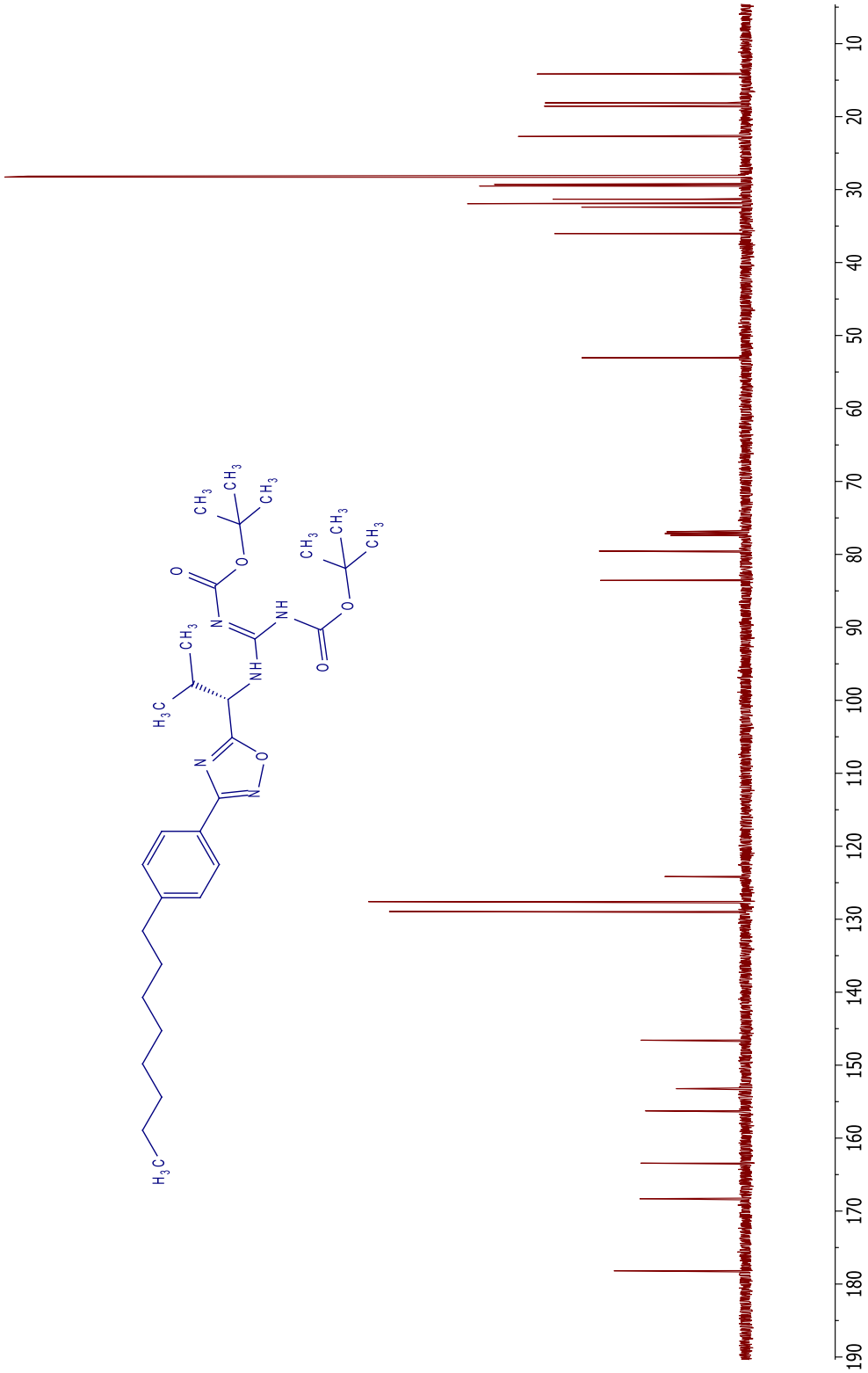

^{1}H NMR spectrum of **32a**

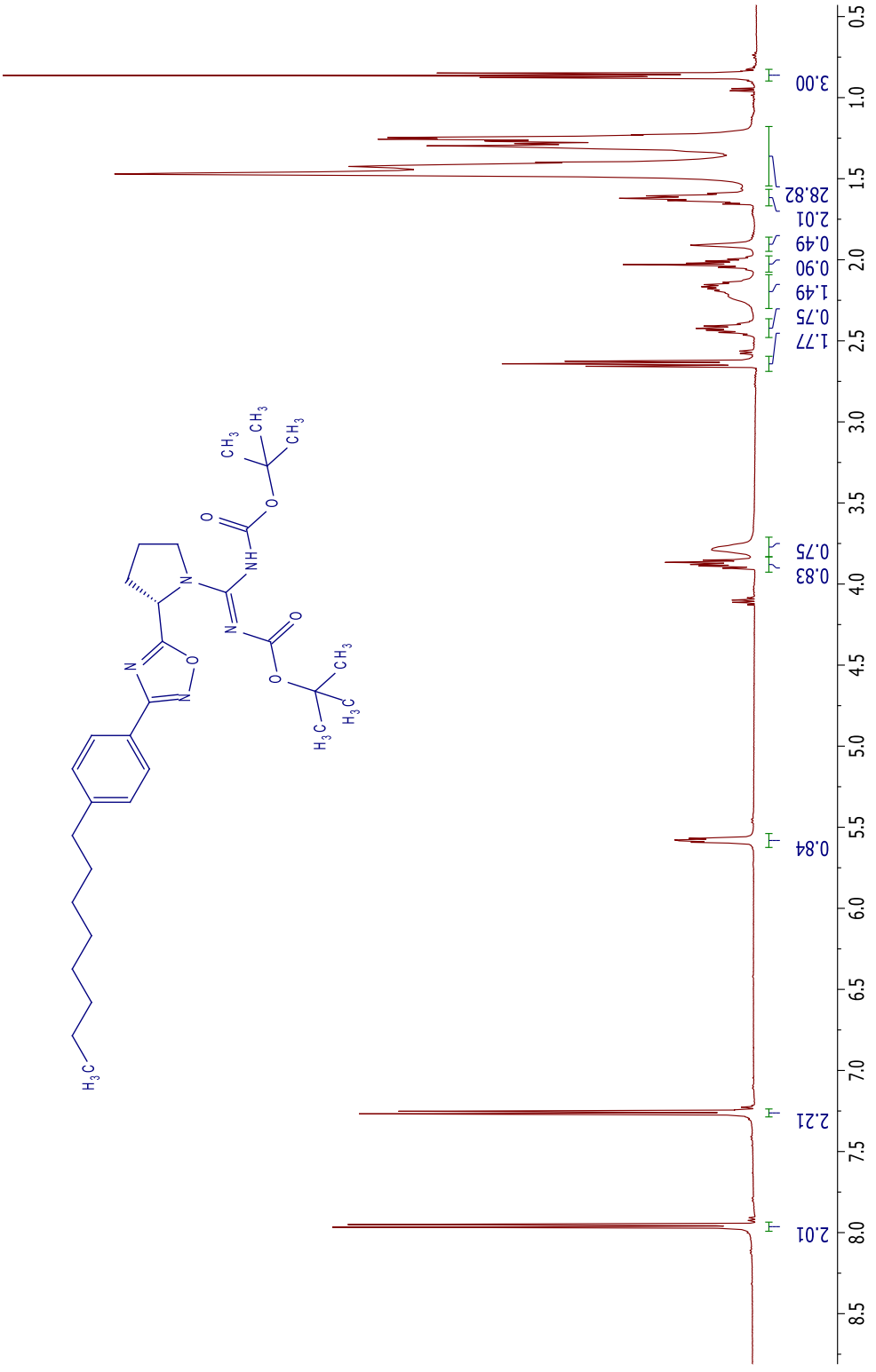

^{13}C NMR spectrum of **32a**

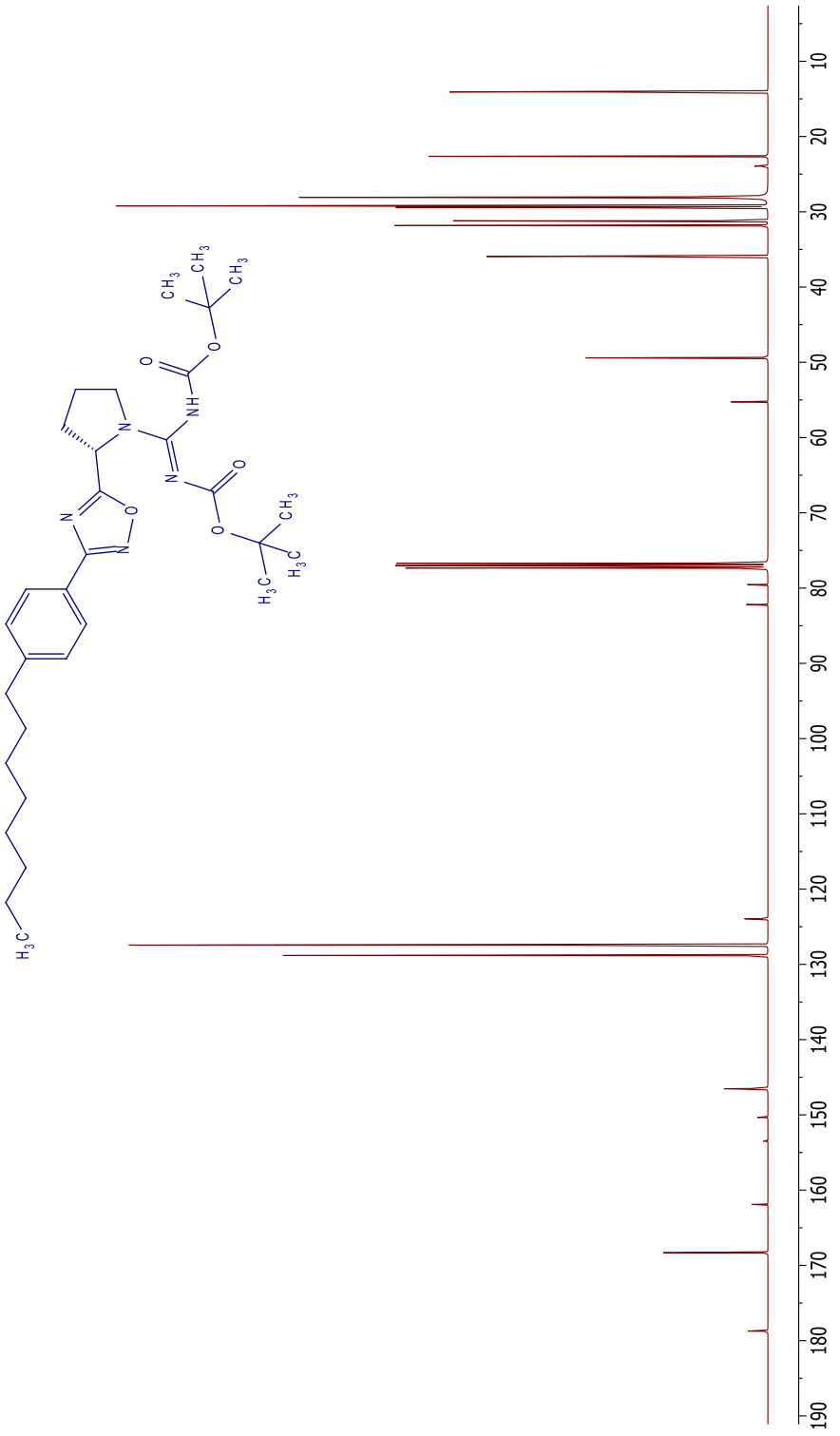

^{1}H NMR spectrum of **32b**

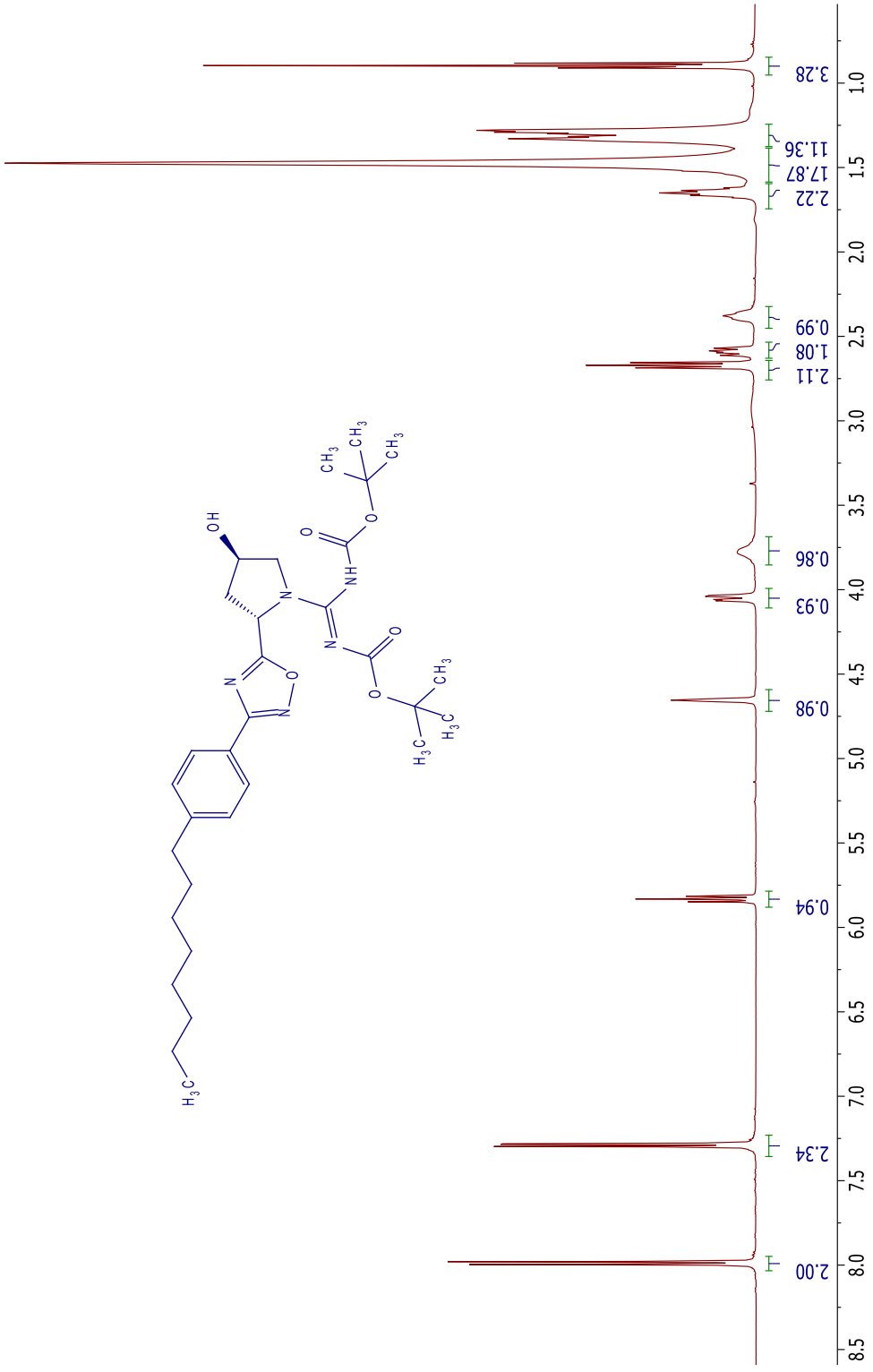

^{13}C NMR spectrum of **32b**

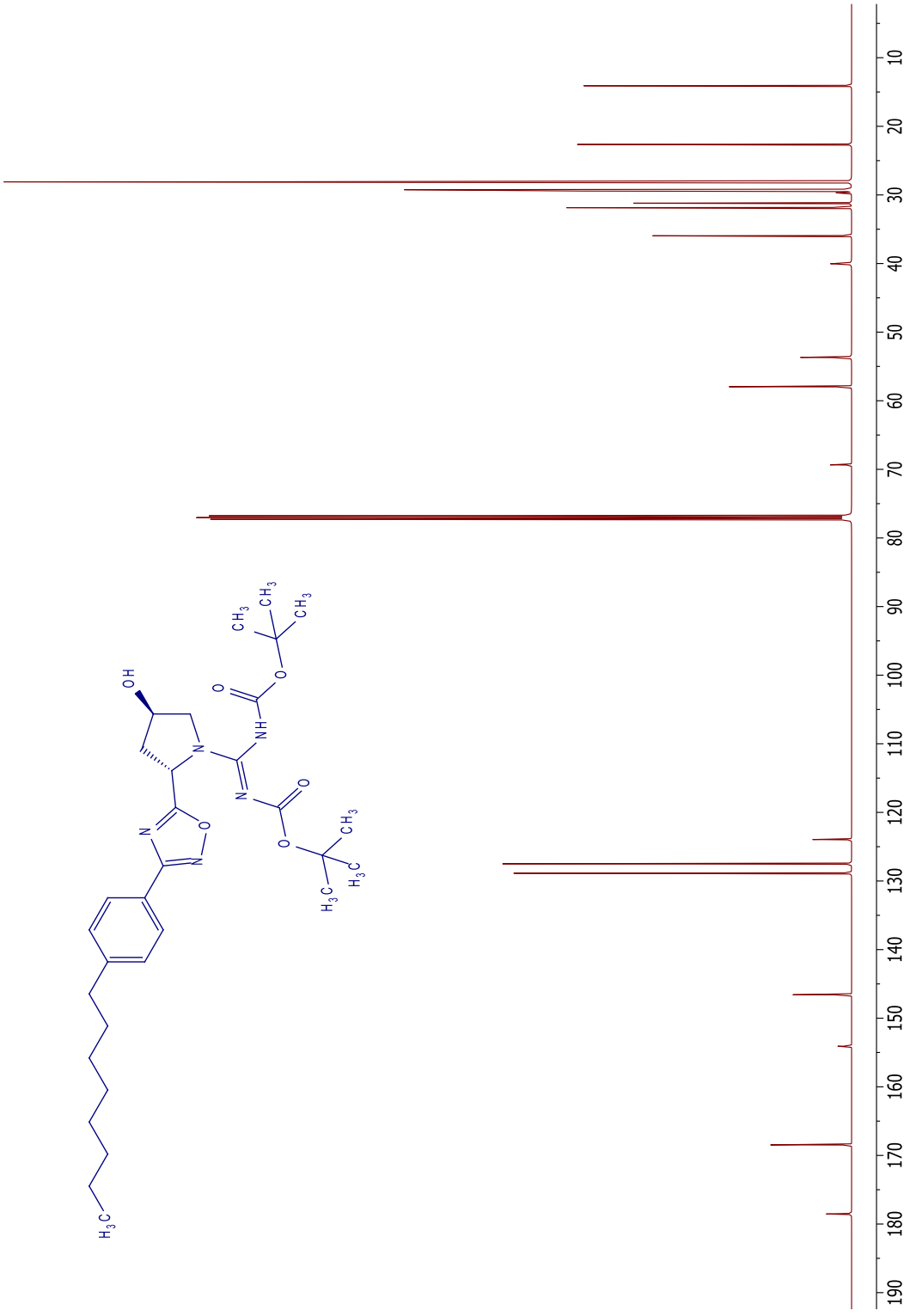

^{1}H NMR spectrum of **29a**

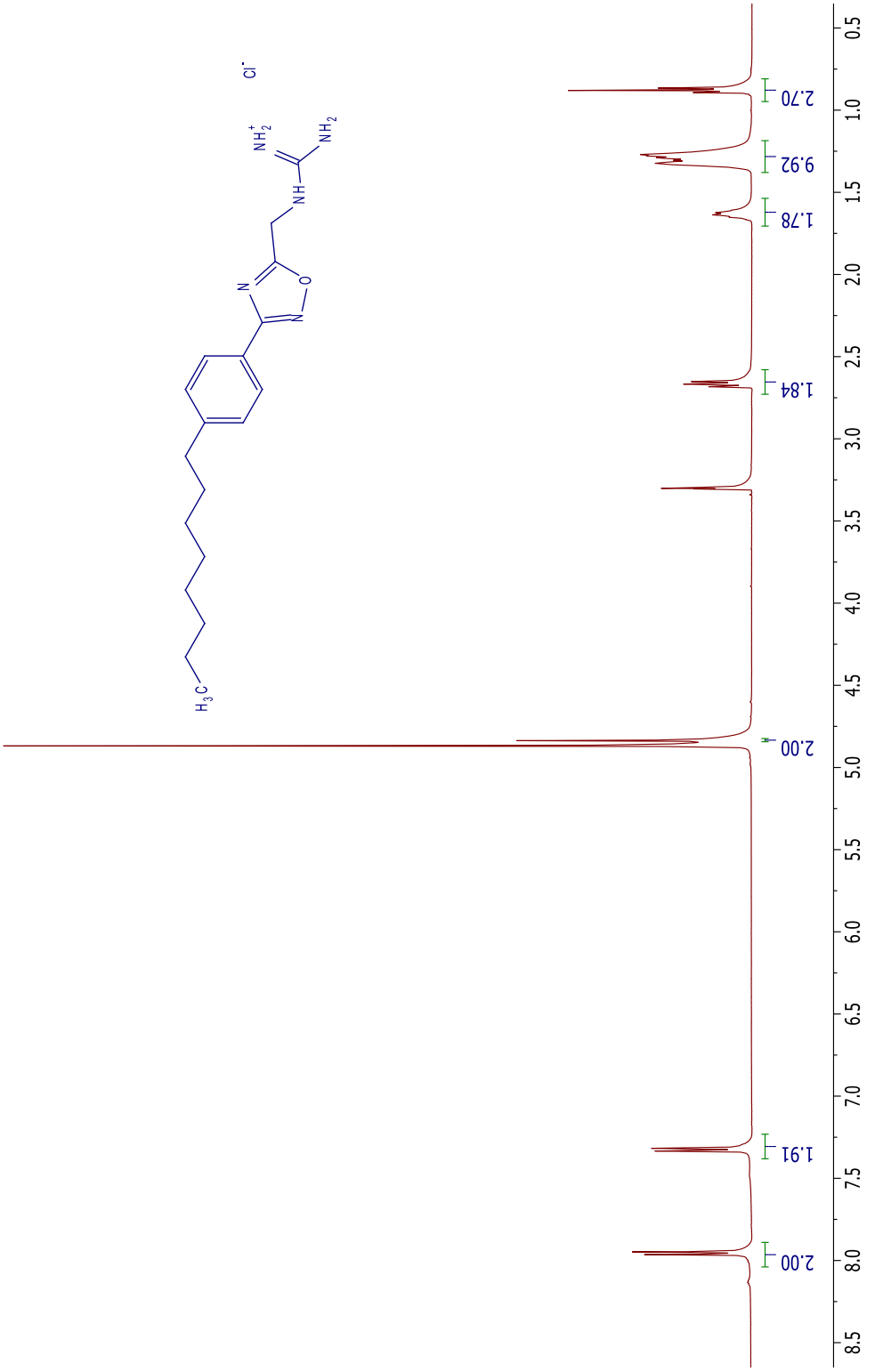

^{13}C NMR spectrum of **29a**

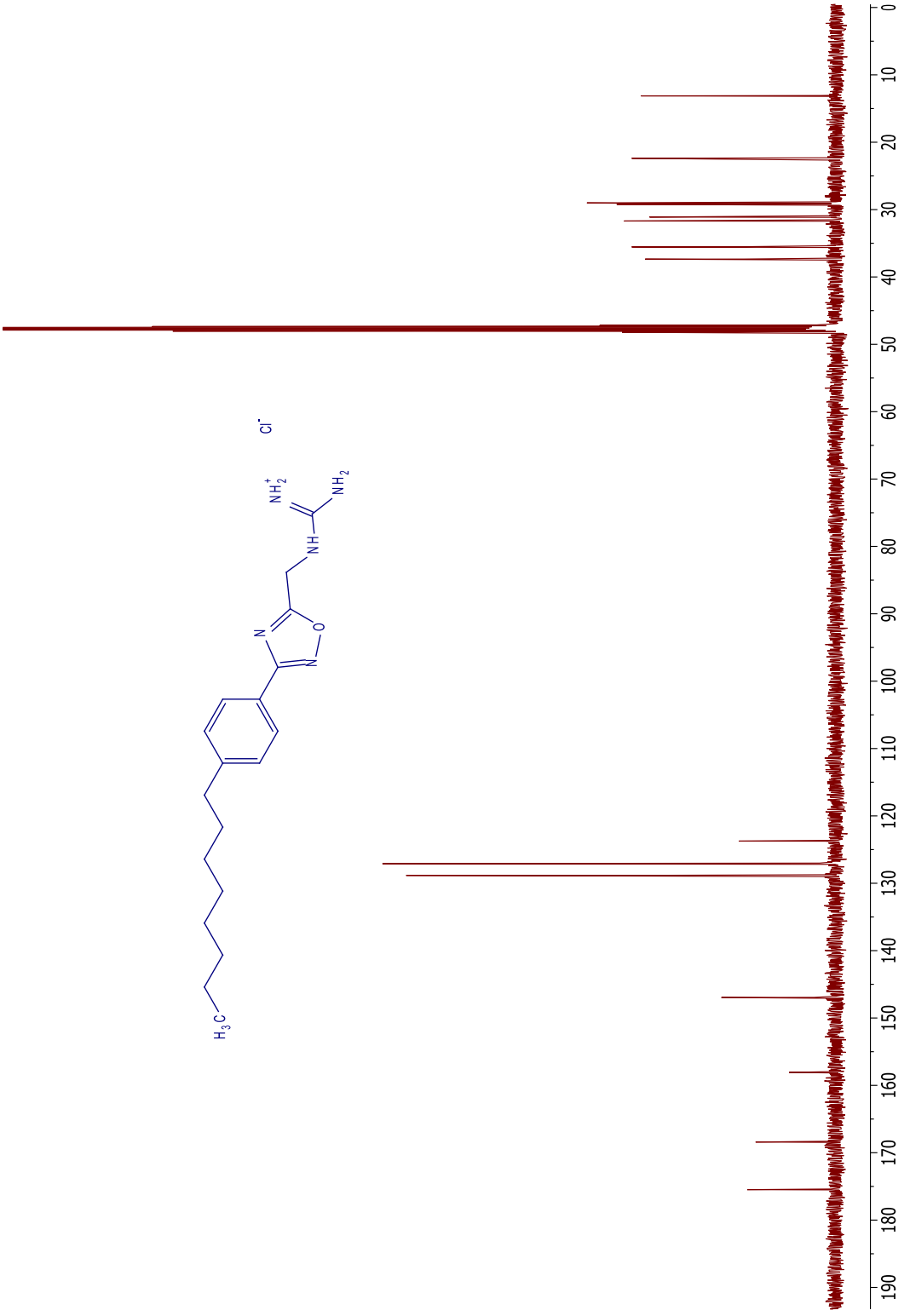

^{1}H NMR spectrum of **29b**

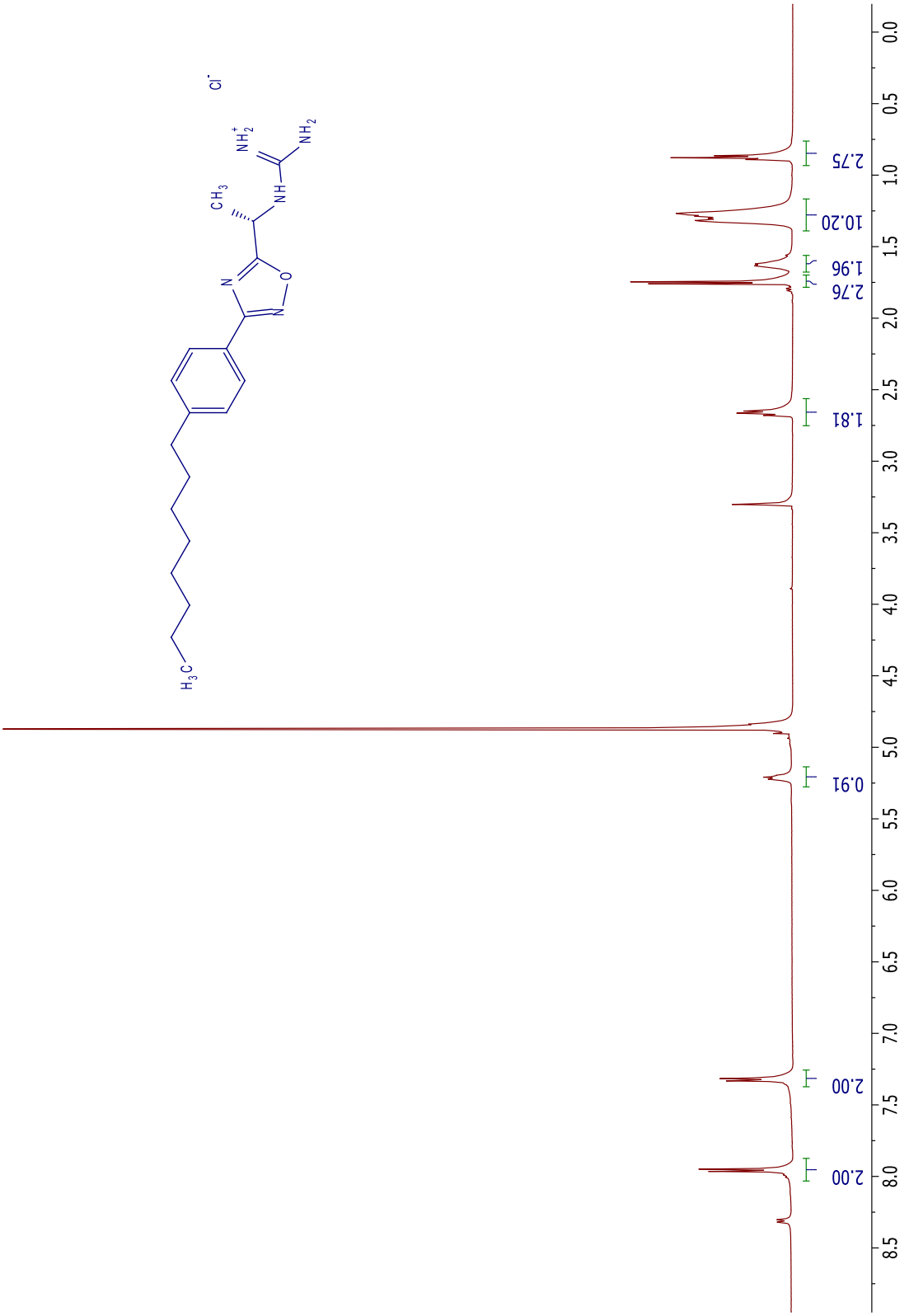

^{13}C NMR spectrum of **29b**

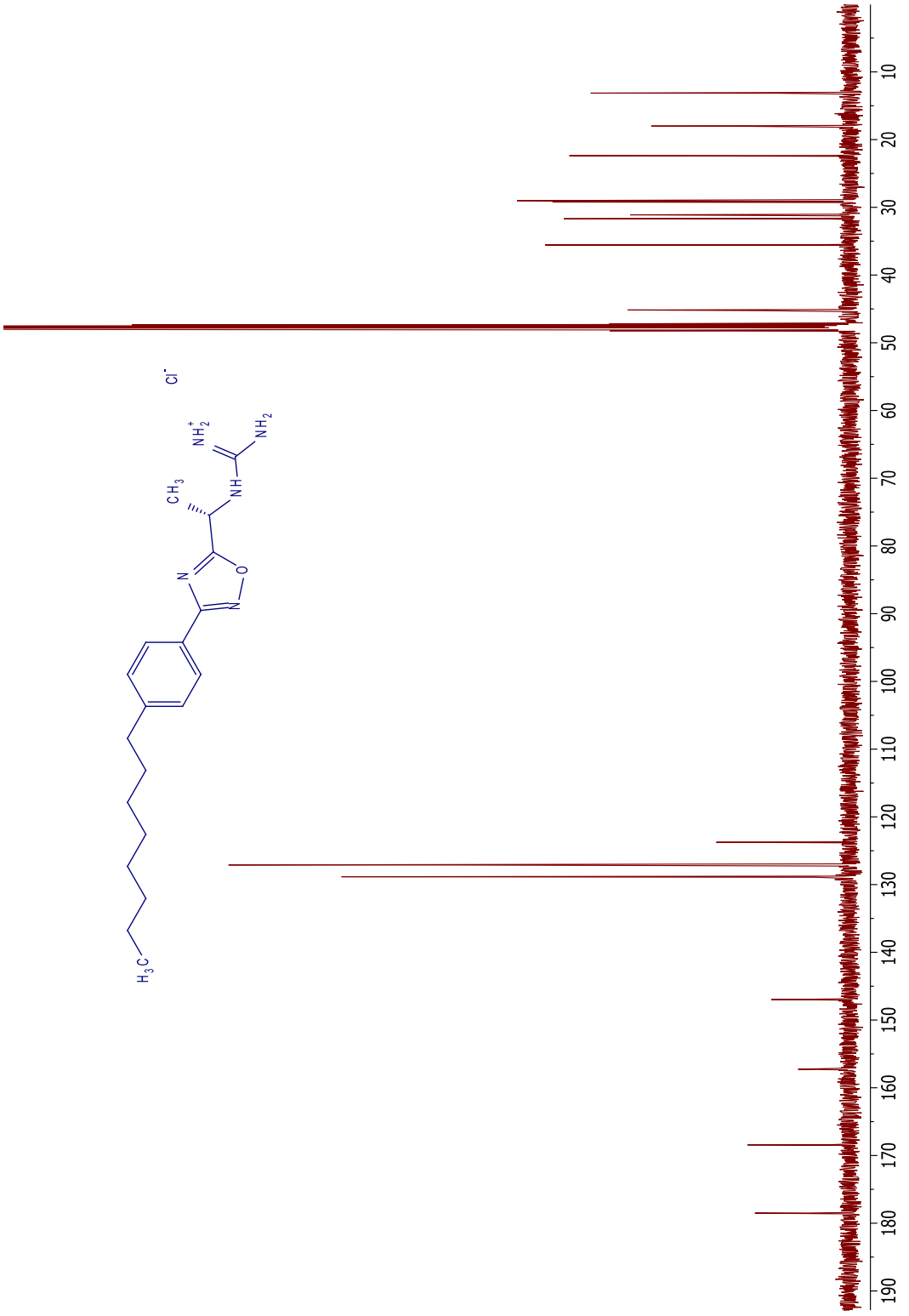

^{1}H NMR spectrum of **29c**

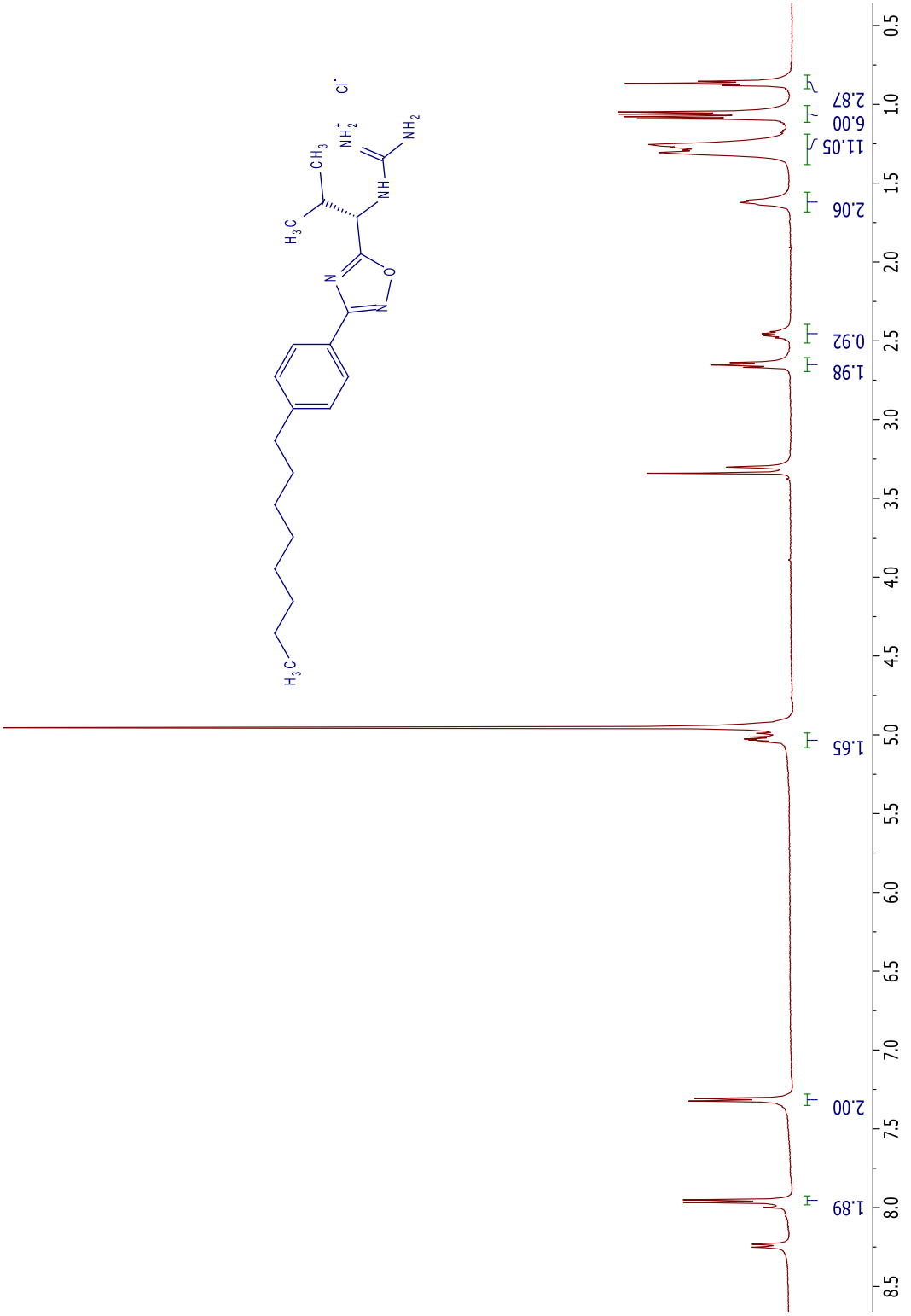

^{13}C NMR spectrum of **29c**

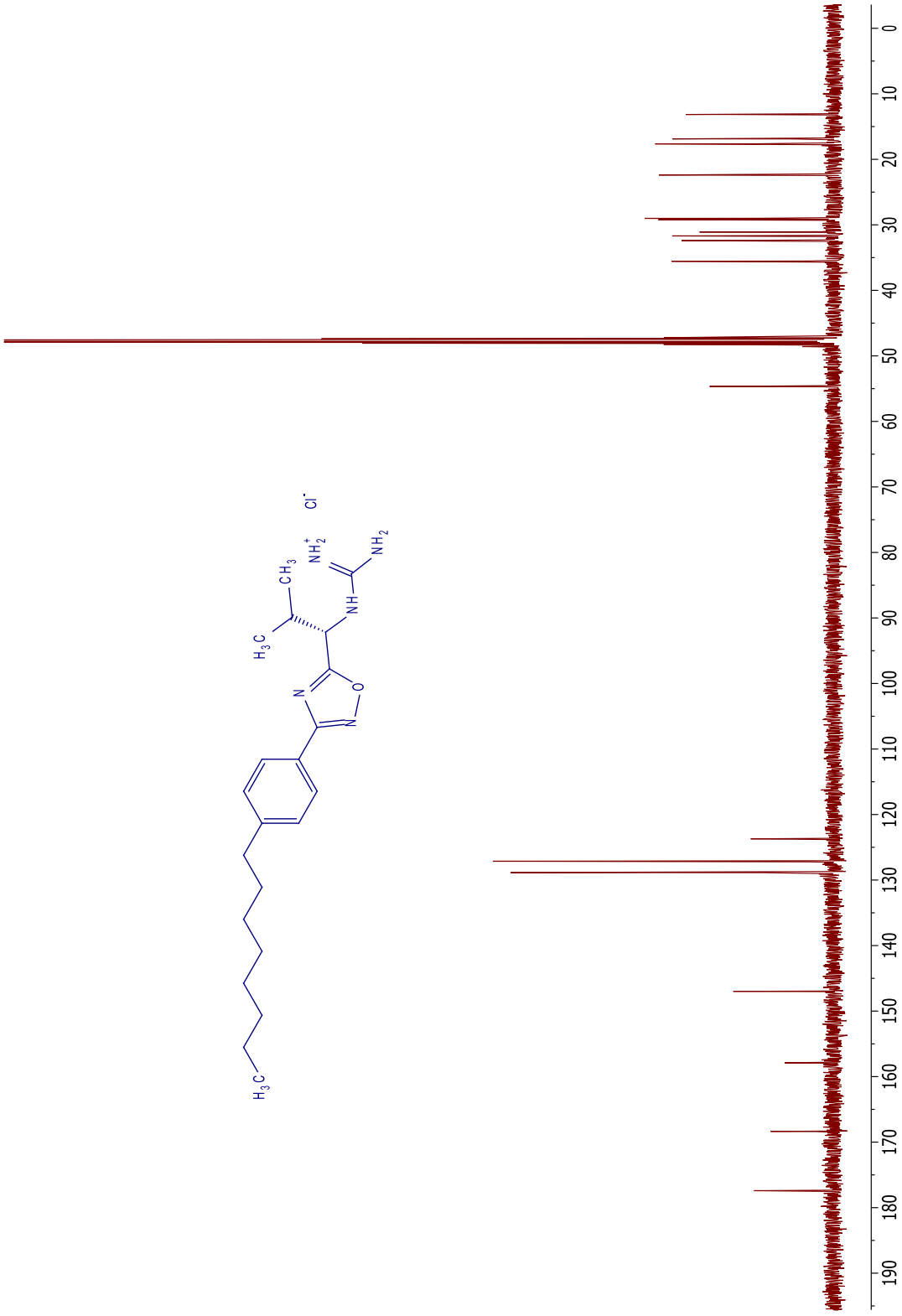

^{1}H NMR spectrum of **33a**

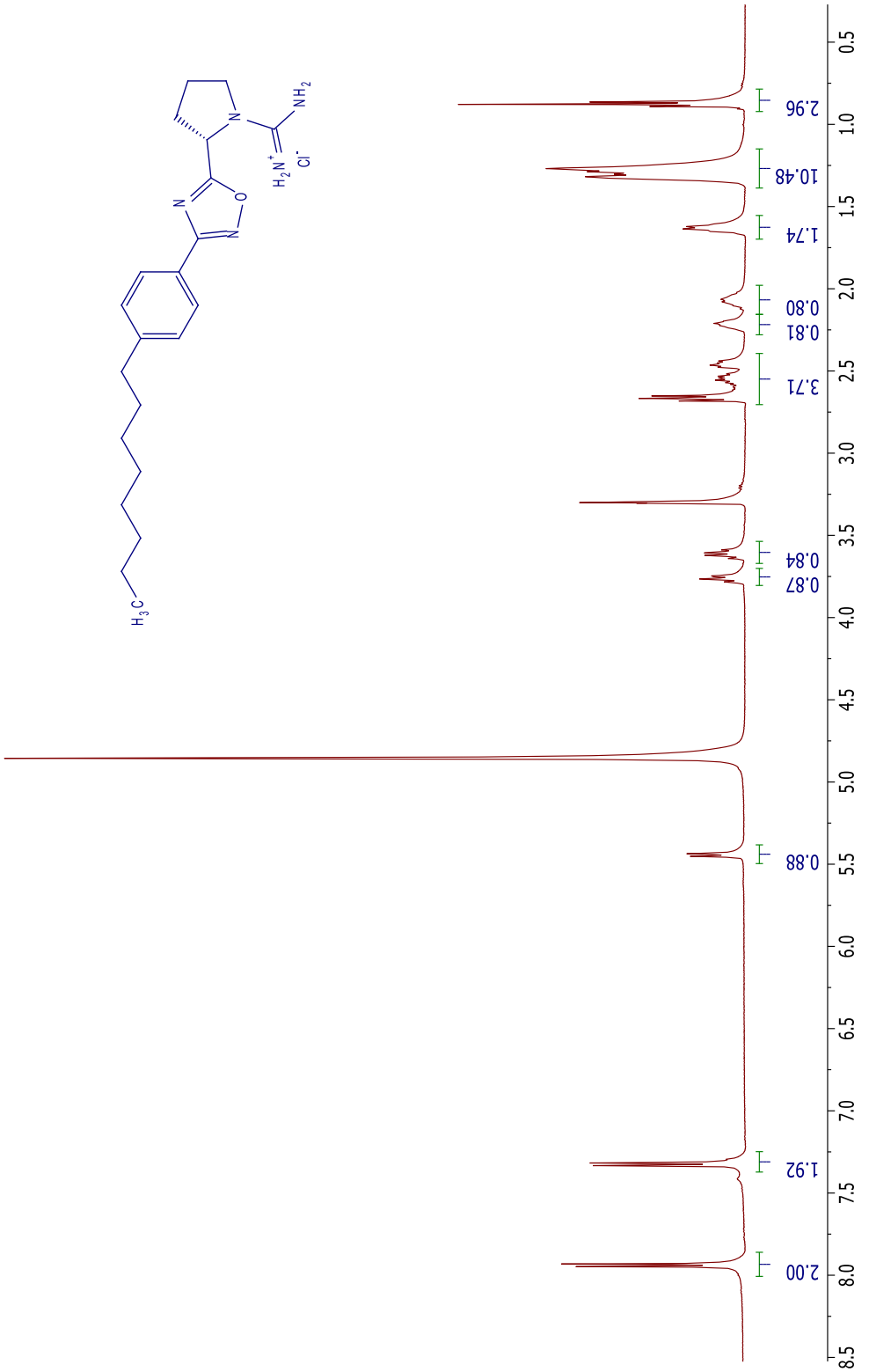

^{13}C NMR spectrum of **33a**

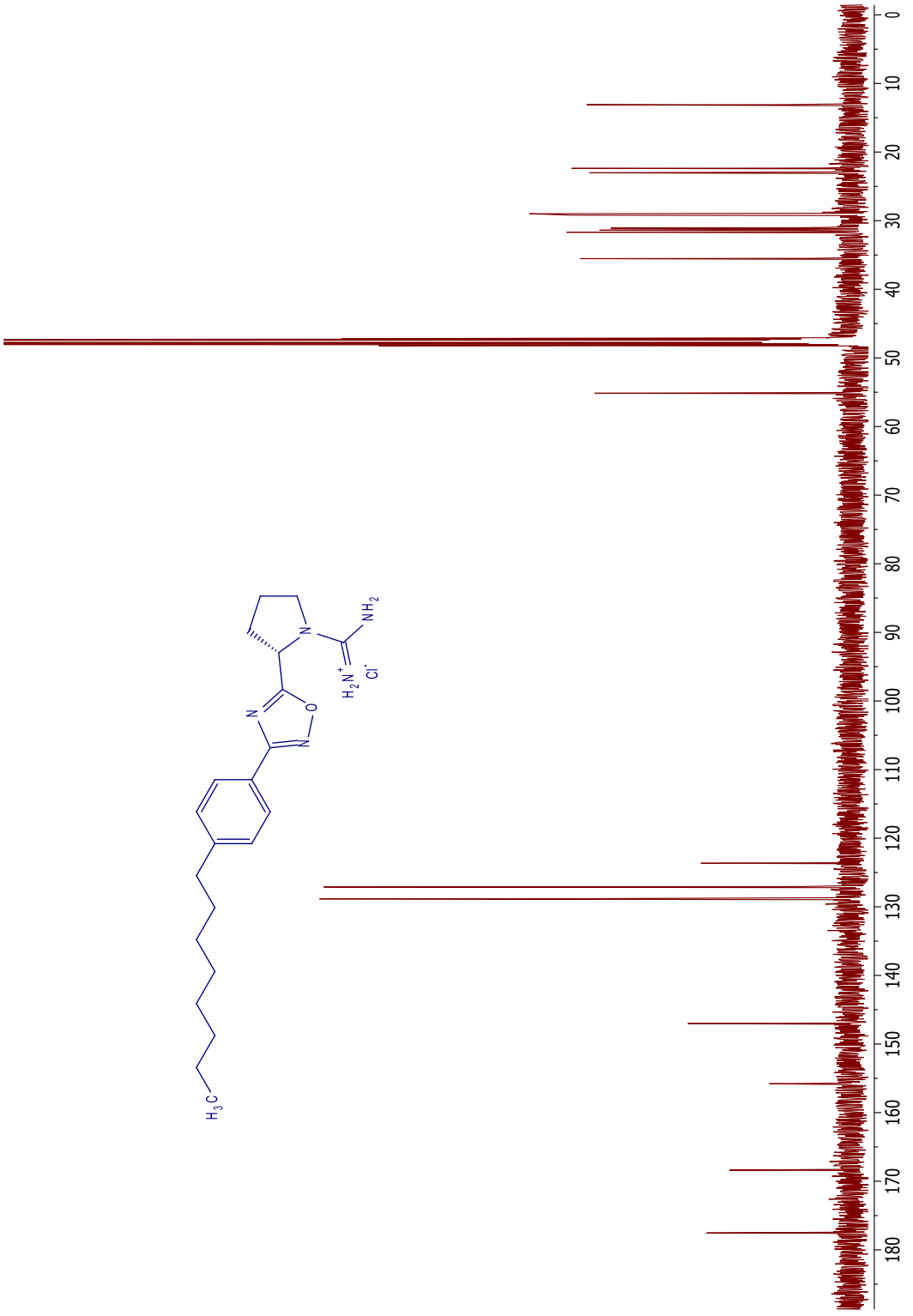

^{1}H NMR spectrum of **33b**

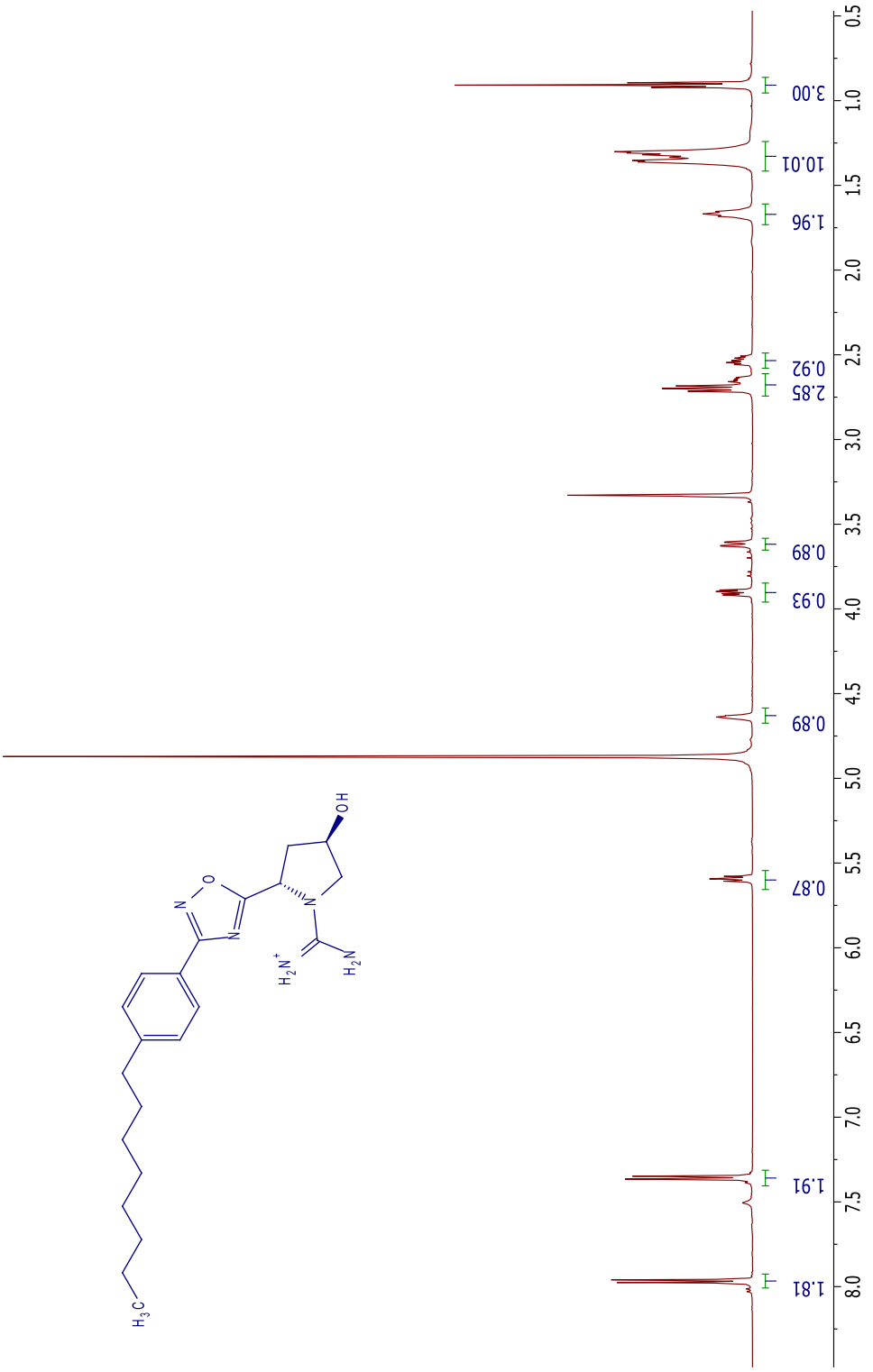

^{13}C NMR spectrum of **33b**